

PRINCIPLES OF  
YACHT DESIGN

SECOND EDITION



PRINCIPLES OF  
YACHT DESIGN  
SECOND EDITION

LARS LARSSON and ROLF E ELIASSON



INTERNATIONAL MARINE  
Camden • Maine

**International Marine**  
**A Division of The McGraw-Hill Companies**

First published in Great Britain in 1994, revised 2000

10 9 8 7 6 5 3 2 1

Copyright © Lars Larsson and Rolf E Eliasson 2000

All rights reserved. No part of this publication may be reproduced in any form or by any means – graphic, electronic or mechanical, including photocopying, recording, taping or information storage and retrieval systems – without the prior permission in writing of the publisher. The name ‘International Marine’ and the International Marine logo are trademarks of The McGraw-Hill Companies.

A CIP catalogue record for this book is available from the Library of Congress

ISBN 0-07-135393-3

Questions regarding the ordering of this book should be addressed to:

The McGraw-Hill Companies  
Customer Service Department  
P O Box 547  
Blacklick, OH 43004

Retail customers: 1-800-262-4729  
Bookstores: 1-800-722-4726  
[www.internationalmarine.com](http://www.internationalmarine.com)

Printed and bound in Great Britain

# CONTENTS

---

<b>Preface to the Second Edition</b>	ix
<b>List of Symbols</b>	x
<b>Introduction</b>	1
<b>1. Design Methodology</b>	<b>5</b>
The design spiral	5
Computer aided design (CAD)	7
<b>2. Preliminary Considerations</b>	<b>10</b>
Choice of boat-type	10
Intended use	10
Main dimensions	11
Cost	13
Checklist of considerations	15
Checklist for the YD-40	15
<b>3. Hull Geometry</b>	<b>16</b>
Definitions	16
Lines drawing	20
Tools	22
Work plan	26
Computer aided design of hulls	27
<b>4. Hydrostatics and Stability</b>	<b>30</b>
Calculation of areas	30
Wetted surface	32
Displacement	32
Centre of buoyancy	34
Water plane area	38
Transverse and longitudinal stability at small angles	40
Transverse stability at large angles of heel	42
Curve of static stability	44
Rolling	46
Influence of waves on the righting moment	49
Stability statistics	52
Assessment of seaworthiness	53

---

<b>5. Hull Design</b>	<b>56</b>
Forces and moments on a sailing yacht	56
Resistance components	58
Viscous resistance, basic concepts	60
Frictional resistance	61
Viscous pressure resistance	64
Roughness	66
Wave resistance, basic concepts	69
Influence of hull shape on wave resistance	73
Heel resistance	83
Added resistance in waves	83
Other seakeeping aspects	88
Hull statistics	90
<b>6. Keel and Rudder Design</b>	<b>96</b>
Flow around a wing	96
Definition of the keel planform	99
Classical wing theory	100
Tip shape	105
Advanced planform design	107
Evaluation of some planform concepts	113
Definition of the section	115
Three useful NACA sections	116
Influence of shape on section characteristics	118
Some practical conclusions regarding section shape	124
Influence of deviations from the theoretical section shape	125
Advanced section design	128
Statistics on keel and rudder area	130
The YD-40	130
<b>7. Sail and Rig Design</b>	<b>132</b>
Flow around sails	132
Planform	134
Sail camber	139
Mast interference	142
Means for reducing mast disturbances	143
Streamlining	146
A practical model for sail and rig aerodynamics	147
Sail statistics	153
<b>8. Balance</b>	<b>155</b>
Effect of heel	155
Good balance	157
Centre of effort of the underwater body	157
Centre of effort of the sails	160
Lead	162
Rudder balance	162

---

<b>9. Propeller and Engine</b>	<b>164</b>
Resistance in calm and rough weather	165
Propeller characteristics	169
Design of an optimum propeller	171
Performance of the non-optimum propeller	174
Check of blade area	179
Propeller resistance	181
<b>10. High Speed Hydrodynamics</b>	<b>183</b>
Planing	183
Deadrise	187
Forces on a planing hull	188
Spray rails, stepped bottoms and transom flaps	193
Dynamic stability	197
Alternative propulsion devices	199
An example	200
<b>11. Rig Construction</b>	<b>205</b>
Definitions and scope of the standard	205
Forces on the shrouds	208
Forces on the stays	212
Comparison between wire and rod	214
Transverse mast stiffness	218
Longitudinal mast stiffness	218
Fractional mast top	218
Boom	218
Spreaders	220
Holes in the mast	222
The YD-40 rig	222
<b>12. Hull Construction</b>	<b>226</b>
Concepts in structural mechanics	227
Global loads	228
Local hydrostatic loads	234
Local hydrodynamic loads	234
Transverse load distribution	237
Local deformations	237
Forces from the keel	239
Forces from grounding	241
Forces from the rudder	243
Summary of loadings	245
<b>13. Materials</b>	<b>250</b>
Glass reinforcement	251
Wet laminates	256
Fatigue	256
Exotic laminates	257
Sandwich	260

---

Typical sandwich buckling	263
Sandwich bending	264
Sandwich in practice	265
Final remarks	267
<b>14. Scantling Determination</b>	<b>269</b>
Structure of the ISO Standard	269
Hull definitions	272
Basic laminate	274
Design loads for the bottom	275
Design loads for the topsides	280
Design loads for the decks and bulkheads	280
Design loads for the internals	280
Longitudinal impact distribution factor	280
Area reduction factor	282
Panel calculation	284
Stiffener calculation	286
Spade rudder stock	287
Chainplates and keelbolts	290
Sandwich construction	290
The YD-40 scantlings	293
<b>15. Layout</b>	<b>297</b>
Generic space requirements	297
Accommodation	298
Deck layout	305
<b>16. Design Evaluation</b>	<b>311</b>
Non-dimensional parameters	312
The Velocity Prediction Program (VPP)	313
Towing tank testing	316
Computational Fluid Dynamics (CFD)	318
<b>Appendix 1</b>	
Main particulars of the YD-40	322
<b>Appendix 2</b>	
Weight calculation	323
<b>Appendix 3</b>	
STIX calculation	329
<b>References</b>	<b>330</b>
<b>Index</b>	<b>332</b>



# PREFACE

---

## SECOND EDITION

Since this book was first published we have received many comments and suggestions from interested readers, and we have tried to incorporate as much as possible of this valuable advice in the second edition. One major change has been the inclusion of more material relevant to power boats. Although the emphasis in the book has been on sailing yachts, many power boat enthusiasts have found it interesting and requested more information related to this area. In the new edition we have tried to accomplish this. There is an entirely new chapter on high speed hydrodynamics with special reference to power boats, and in an updated chapter on scantling determination, both types of boats are considered. Since most of the other material is also useful, we feel confident that power boat designers and owners may benefit from reading this book.

Another important task has been to update the material related to international standards. The ISO/TC188 Working Group 22 has delivered a final proposal for the seaworthiness of sailing craft between 6 m and 24 m. This draft, which is most likely to be approved, differs from the one presented in the first edition of the book, and the new approach is described here, with the permission of the chairman, Mr Andrew Blyth. The ISO/TC Working Group 18 dealing with scantlings has not yet arrived at a final proposal, but with the permission of the chairman, Mr Fritz Hartz, their main ideas are included in the updated chapter on scantlings. Previously this chapter was based entirely on the ABS rule.

Minor changes and corrections have been made throughout the book and, for clarity, the original chapter on hull construction has been divided into two, one dealing with loads and the other with materials.

We would like to express our gratitude to all readers who have taken the time to suggest improvements. In particular we would like to thank the following (in alphabetical order): H Barkla, B Beck, P K Coles, G Dyne, F Eldridge, G Heyman, H Liljenberg, N Newland, P Schwarzel and C Voghera.

Lars Larsson & Rolf E Eliasson  
Gothenburg 1999

# LIST OF SYMBOLS

---

In general, the symbols used in this book are those recommended by the International Towing Tank Conference (ITTC). However, in the chapters on scantling determination (hull dimensioning) and the Nordic Boat Standard (rig dimensioning) other symbols have been used. This is to simplify the later use of these standards by readers.

$A, A_{(i)}$	area, general
$a$	elongation
$a_{(i)}$	distance from neutral axis to centre of area
$A_0$	area of propeller disk
$a_1$	distance from $L_{WL}$ to $T_1$
$a_2$	distance from $L_{WL}$ to $T_2$
ABS	American Bureau of Shipping
$A_D$	propeller blade area, developed
$A_F$	fore triangle area
$A_f$	flange area
$A_{ir}$	projected rudder area
$A_M$	mainsail area, or midship section area below designed waterline
$A_{min}$	keel/hull area
AP	aft perpendicular
$A_R$	aerodynamic driving force
AR, $\Delta AR$	aspect ratio and change in aspect ratio, respectively
$AR_e$	effective aspect ratio
$A_S$	sail area (main + fore triangle) or aerodynamic side force
$A_W$	area of water plane
$A_X$	maximum section area below designed waterline
$b$	half beam
B	beam of hull amidships, or centre of buoyancy, hull upright
B'	centre of buoyancy, hull heeled
BD	boom height above deck
BG	distance between centre of buoyancy and gravity
BM	metacentric radius
$B_{MAX}$	maximum beam of hull
$B_u$	Taylor thrust coefficient
$B_{WL}$	beam of waterline

---

$C$	chord length, or crown width of stiffener, or compressive strength (see also list of Indices)
$C_{1,2}$	spreader compression force
$C_B$	block coefficient
$C_D$	drag coefficient
$C_{DI}$	induced drag coefficient
$C_{D0}$	drag coefficient at zero angle of attack, or drag coefficient of mast, rig and topsides
$C_{DP}$	viscous (parasitic) drag coefficient of sails
$CE$	aerodynamic centre of effort
$C_F$	skin friction coefficient
$CFD$	Computational Fluid Dynamics
$C_H$	heel resistance coefficient
$C_L, C_{Lmax}$	lift coefficient and maximum lift coefficient, respectively
$C_{Lr}$	rudder lift coefficient
$CLR$	hydrodynamic centre of lateral resistance
$C_P$	prismatic coefficient, or pressure coefficient
$C_R$	residuary resistance coefficient
$C_S$	aerodynamic side force coefficient
$D$	depth of yacht, or drag, or propeller diameter
$D_{1,2,3}$	diagonal shrouds
$d_{kb}$	core diameter of keelbolt
$DWL$	designed waterline
$E$	modulus of elasticity, or base of mainsail (IOR)
$E_C$	compressive modulus of elasticity
$E_F$	flexural modulus of elasticity
$E_T$	tensile modulus of elasticity
$E_{TC}$	average modulus of elasticity
$F$	flat factor of sails, or flexural strength, or flange width of stiffener, or design head reduction factor
$F_{1,2,3}$	dimensioning transverse rig forces
$F_a$	freeboard aft
$F_f$	freeboard forward
$F_h$	horizontal boom force
$F_i$	impact force
$F_n$	Froude number
$FP$	forward perpendicular
$F_r$	rudder side force
$F_s$	design head reduction factor
$F_S$	freeboard at mast
$F_v$	vertical boom force
$FRP$	fibre reinforced plastic
$g$	acceleration of gravity, or girth length, or ballast weight
$\overline{G}$	centre of gravity, or empty weight of yacht
$\overline{GM}$	metacentric height
$\overline{GRP}$	glass reinforced plastic
$\overline{GZ}$	righting arm

---

$h$	roughness height, or rudder height, or design head, or height of stiffener, or mast height above deck or superstructure to the highest sail-carrying forestay
$H$	floor height
$H_{1/3}$	significant wave height
$h_a$	distance between rudder bearings
$HA$	heeling arm
$h_b$	distance from bottom of rudder to lowest bearing
$I$	height of fore triangle (IOR), or moment of inertia
$I_L$	longitudinal moment of inertia of water plane area
IMS	International Measurement System
IOR	International Offshore Rule
ISO	International Standards Organization
$I_T$	transverse moment of inertia of water plane area
$I_{yy}$	mass moment of inertia around a transverse axis through G
$I_x$	transverse moment of inertia for the mast
$I_y$	longitudinal moment of inertia for the mast
$J$	base of fore triangle (IOR)
$k$	gyradius in pitch, or aspect ratio factor
$k_1$	mast panel factor, or aspect ratio factor
$k_2$	mast staying factor
$k_3$	mast step factor
$K_Q$	torque coefficient
$K_T$	thrust coefficient
$l$	horizontal length of rudder at centre of effort, or long span of panel, or stiffener length
$L$	length, general, or length rated, or lift
$L_f$	floor length
$l_{1,2,3}$	rig panel lengths
$l_a$	distance from $L_{WL}$ to top of aft stay
$l_c$	distance from leading edge to centre of effort
LCB	longitudinal centre of buoyancy
$L_{OA}$	length overall
$L_{pp}$	length between perpendiculars
$L_{WL}$	length of waterline
$m$	mass displacement, mass (general), or mast material factor
$M$	bending moment, or metacentre
$M_{b_{hull}}$	hull bending moment
$M_{fl}$	floor bending moment
$M_{kl}$	floor bending moment, from grounding
$M_{kt}$	transverse moment from keel
$M_r$	rudder bending moment
$M_s$	spreader bending moment
$N$	rudder force factor
NBS	Nordic boat standard
$n$	number of persons on board, or rate of revolutions, or number of floors in way of keel
$n_{kb}$	number of keelbolts

---

$OF_{\text{bolt}}$	keel bolt offset
$O_x$	transverse fractional mast top length
$O_y$	longitudinal fractional mast top length
$P$	height of mainsail (IOR), or propeller pitch, or load, general
$P_a$	dimensioning aft stay load
$P_{ah}$	horizontal part of aft stay load
$P_{av}$	vertical part of aft stay load
$P_b$	bottom pressure
$P_c$	composite property
$P_{\text{crit}}$	critical load
$P_D$	delivered power, or design pressure
$P_{\text{deck}}$	compression force in deck
$P_{Dv}$	dimensioning shroud load
$P_{fh}$	horizontal part of forestay load
$P_{fi}$	dimensioning inner forestay load
$P_{fo}$	dimensioning outer forestay load
$P_{fv}$	vertical part of forestay load
$P_{hd}$	horizontal component of stay forces
$P_{kb}$	keel bolt load tension
$P_{kt}$	total keel bolt load
$P_m$	mat property
$P_{\text{mast}}$	mast pressure
$PT$	dimensioning mast load
$P_r$	grounding load
$Q$	torque
$R$	resistance, general, or reef factor of sails
$R_A$	windage
$R_{AW}$	added resistance in waves
$R_F$	frictional resistance
$R_H$	heel resistance
$RM$	righting moment
$RM_1$	righting moment at 1 deg heel
$RM_{30}$	righting moment at 30 deg heel
$RM_{90}$	righting moment at 90 deg heel
$R_n$	Reynolds number
$RORC$	Royal Ocean Racing Club
$R_R$	residuary resistance
$r_t$	nose radius
$R_{vc}$	rudder centre of effort, vertical distance from top
$RYA$	Royal Yachting Association
$s$	short span of panel, stiffener spacing
$S_{(n)}$	length of spreader
$SA$	total triangular sail area
$SAF$	sail area, fore triangle (IOR)
$SAM$	sail area, mainsail, triangular (IOR)
$SL$	length of spinnaker leech (IOR)
$SM$	section modulus

---

$SM_{fl}$	floor section modulus
$SM_{hull}$	hull girder section modulus
$SM_i$	section modulus to inside of panel
$SM_k$	section modulus increase in way of keel
$SM_o$	section modulus to outside of panel
$SMW$	spinnaker width (IOR)
$S_w$	wetted surface area
$S_{wc}$	wetted surface area with 'c' indice
$t, t_{max}$	thickness and maximum thickness, respectively
$T$	draft of yacht, or propeller thrust, or tensile strength
$T_1$	wave period, or transverse foresail force
$T_2$	transverse mainsail force
$T_{boom}$	transverse force at foot of mainsail
$T_{bu}$	upper boom force
$t_c$	core thickness
$TCG$	transverse centre of gravity
$t_f$	face thickness
$T_{head}$	transverse force at top of mainsail
$T_{hl}$	lower shroud force
$T_{hu}$	upper shroud force
$T_r$	rudder torsional moment
$T_s$	time to stop
$V$	volume displacement, or yacht speed
$V_{1,2}$	vertical shroud
$V_{AW}$	apparent wind speed
$V_{AWe}$	effective apparent wind speed, yacht heeled
$VCB$	vertical centre of buoyancy
$VPP$	Velocity Prediction Program
$V_s$	yacht speed (m/s)
$W$	weight displacement, or effective width of panel, or fibre angle
$Wf$	fibre content by weight
$W_k$	weight of ballast
$X_0$	position of neutral axis
$x_{lc}$	distance from leading edge to centre of rudderstock
$X_m$	ratio of mat in a composite
$X, Y, Z$	Cartesian coordinates. Origin at FP, X aftwards, Y to starboard, Z vertically upwards
$y$	deflection
$Y_k$	distance from keel centre of gravity to $L_{WL}$
$\alpha$	angle of attack, or scale factor
$\alpha_u$	aft stay angle to mast
$\alpha_f$	forestay angle to mast
$\beta$	leeway angle
$\beta_{1,2,3}$	diagonal shroud angle to mast
$\beta_{AW}$	apparent wind angle

---

$\gamma_{1,2}$	vertical shroud angle
$\delta$	Taylor parameter, or horizontal angle of spreader
$\delta_{RM}$	additional righting moment from crew to windward
$\eta$	safety factor
$\eta_0$	propeller efficiency
$\Theta$	trim angle
$\lambda$	wavelength, or taper ratio
$\Lambda$	sweep angle
$\nu$	kinematic viscosity
$\rho$	density
$\sigma$	normal stress, or cavitation number
$\sigma_{0.2}$	yield stress
$\sigma_d$	design stress
$\sigma_c$	design stress for rudder stock
$\sigma_f$	normal stress in sandwich face
$\sigma_u$	ultimate stress
$\sigma_y$	yield stress
$\tau$	Burrill parameter, or shear stress
$\Phi$	heel angle
$\omega_\phi$	natural frequency (in roll)
$\omega_c$	frequency of wave encounter
$\nabla$	volume displacement

### Indices

c	canoe body
k	keel
r	rudder
u	upper
l	lower

**Conversion factors**

To convert *metric* measures into *imperial* measures, multiply by *x*

To convert *imperial* measures into *metric* measures, multiply by *y*

<i>Metric</i>	<i>Imperial</i>	<i>x</i>	<i>y</i>
<b>Length</b>			
Millimetres (mm)	Inches	0.039	25.40
Centimetres (cm)	Inches	0.394	2.540
Metres (m)	Inches	39.37	0.025
Metres (m)	Feet	3.281	0.305
Metres (m)	Yards	0.914	1.094
Kilometres (km)	Geographic miles	0.621	1.609
Kilometres (km)	Nautical miles	0.5397	1.8532
<b>Area</b>			
Square millimetres (mm <sup>2</sup> )	Square inches	0.0016	645.10
Square centimetres (cm <sup>2</sup> )	Square inches	0.155	6.452
Square metres (m <sup>2</sup> )	Square inches	1600.0	0.00063
Square metres (m <sup>2</sup> )	Square feet	10.764	0.0929
Square metres (m <sup>2</sup> )	Square yards	0.8355	1.1968
<b>Volume</b>			
Cubic centimetres (cm <sup>3</sup> )	Cubic inches	0.0610	645.10
Cubic metres (m <sup>3</sup> )	Cubic feet	35.315	0.0283
Cubic metres (m <sup>3</sup> )	Cubic yards	0.764	1.309
Litres (L)	Cubic inches	61.024	0.0164
Litres (L)	Cubic feet	28.317	0.0353
Litres (L)	US gallons	0.264	3.785
Litres (L)	Imp gallons	0.220	4.546
<b>Mass and Weight</b>			
Grams (g)	Ounces	0.0353	28.350
Kilograms (kg)	Pounds	2.2046	0.4536
Tonnes, metric (T)	Pounds	2204.6	0.00045
Tonnes, metric (T)	Tons, long	0.9843	1.0160
Newton (N)	Pounds	0.2247	4.450
Kilonewton (kN)	Pounds	224.73	0.0044
<b>Density</b>			
Kilograms/m <sup>3</sup> (kg/m <sup>3</sup> )	Pounds/cubic foot	0.0624	16.026
<b>Pressure, stress, work, energy</b>			
Newton/mm <sup>2</sup> (N/mm <sup>2</sup> )	Pounds/sq inch	144.95	0.0069
Kilonewton/mm <sup>2</sup> (kN/mm <sup>2</sup> )	Pounds/sq inch	144950	0.0000069
Pascal (Pa) (= 1 N/m <sup>2</sup> )	Pounds/sq inch	0.00014	6899
Kilopascal (kPa) (= 1 kN/m <sup>2</sup> )	Pounds/sq inch	0.14495	6.899
Megapascal (MPa) (= 1 N/mm <sup>2</sup> )	Pounds/sq inch	144.95	0.0069
Gigapascal (GPa) (= 1 kN/mm <sup>2</sup> )	Pounds/sq inch	144950	0.0000069
Newton-metres (Nm)	Foot-pounds	0.7370	1.3568
Kilonewton-metres (kNm)	Foot-pounds	737.00	0.0136
Horsepower (metric)	Horsepower (imp)	1.0142	0.9860
Kilowatts (kW)	Horsepower (imp)	0.7463	1.3400
<b>Speed</b>			
Metres per second (m/s)	Feet per second	3.2808	0.3048
Metres per second (m/s)	Knots	1.9425	0.5148
Kilometres per hour (km/h)	Miles per hour	0.6214	1.6093
Kilometres per hour (km/h)	Knots	0.5397	1.8532



# INTRODUCTION

---

During the past 30 years yachting has expanded from being, generally speaking, a minority sport – too expensive for the large majority of people – into a major recreational activity practised by millions all over the world. In the 1960s, many attractive coastal areas were still relatively free from pleasure boats; today it can be difficult to find a suitable mooring place for the night. The interest in racing has increased correspondingly at all levels, from dinghy racing to the America's Cup and around the world races.

During this period, many new yacht designs have appeared and the number of professional, as well as amateur designers has increased steadily. In fact most yachtsmen have a keen interest in the principles behind the design of their yacht and the theory of sailing. Most yachting magazines have design sections, and articles on design principles feature regularly.

At the same time, yacht research has boomed. The total expenditure in one round of the America's Cup is now in the region of £150–200 million, about one tenth of which is spent on research and development. Yacht research is presented regularly at several series of conferences, such as the HISWA Symposium in Holland, the SNAME/AIAA Symposium on the US West Coast and the Chesapeake Symposium on the East Coast. Papers on sailing theory are frequently found in scientific journals on hydrodynamics and fluid mechanics.

With this background, it is surprising that there is no good up to date book on yacht design available. More than 100 years ago, Skene wrote his now classic *Elements of Yacht Design*, which was revised several times by Kinney. This work is still used at design offices all over the world and by many amateur designers, but while several of the methods explained in the book are still useful, many sections dealing with building materials, design principles etc, are obsolete.

Two other, more or less classic books on the same topic are *Sailing Yacht Design* by D Phillips-Birt and *Sailing Yacht Design – An Appreciation of a Fine Art* by R G Henry and R T Miller. These books were first published in the 1950s and early 1960s, respectively. They are now out of print and do not seem to be widely used any longer. However, the latter was updated in an interesting paper: *Sailing Yacht Design – A New Appreciation of a Fine Art* by R T Miller and K L Kirkman at the Annual Meeting of the Society of Naval Architects and Marine Engineers in 1990.

The most well-known books on sailing theory are the excellent ones by C A Marchaj: *Sailing Theory and Practice*, first published in 1964,

*The Aero-Hydrodynamics of Sailing* in 1979 and *Seaworthiness – the Forgotten Factor* in 1986. Other books in the same category are *The Science of Yachts, Wind and Water* by H F Kay and *Technical Yacht Design* by A G Hammitt, both published in the early 1970s. However, neither one of these is useful for the designer, since they do not cover methodology, statistical data for existing yachts or design evaluation techniques. Furthermore, these books concentrate on the hydro and aerodynamic aspects of the problem, while, for instance, loading, strength and structural problems for example, as well as practical design considerations, are either not mentioned, or are treated very briefly.

Two more recent books on the topic are *Modern Developments in Yacht Design* by D Connell & J Leather and *The Design of Sailing Yachts* by P Gutelle, both out of print. The former is not very useful as a textbook, since only a few selected aspects of the subject are covered, and the latter falls in the same category as those in the previous paragraph. Gutelle, however, refers to a future second volume of his book, where the more practical aspects of design will be treated. Comprehensive reviews of the literature and research in sailing theory may be found in L Larsson's 'Scientific Methods in Yacht Design' and J Milgram's 'Fluid Mechanics for Sailing Vessel Design', published in the *Annual Review of Fluid Mechanics* 1990 and 1998, respectively.

There is thus no modern textbook comparable to Skene's as a guide for the yacht designer. Trying to replace this classic text with a modern one is an exciting challenge, and a successful result would satisfy a deeply-felt need among professional and amateur yacht designers all over the world. With the present book the challenge has been taken up.

For a book of this kind to be successful, two conditions must be satisfied:

- It must cover all aspects of yacht design
- Although it must be comprehensible for amateurs, it must be advanced enough to be of interest also to professional designers.

There follows a short presentation of this book and an explanation of the strategy adopted for satisfying these two requirements.

The book begins with a description of the methodology recommended in the design process. Specifications of the yacht and the design concept are discussed in Chapter 2, and Chapters 3 and 4 cover the geometric description of the hull and the hydrostatics and stability in calm water and waves. The hydrodynamic design of the hull, keel and rudder, and the aerodynamics of the sails are explained in Chapters 5, 6 and 7, and methods are introduced for finding the balance of the yacht in Chapter 8. Chapter 9 deals with the selection of the correct propeller and engine.

Structural aspects of design are treated in Chapters 11, 12, 13 and 14. Loads acting on the rig and hull are identified and methods for computing them introduced. Dimensioning according to the ISO Standard is explained and complete calculations carried out for one example. There is also a discussion on different FRP (fibre reinforced plastics) materials,

including sandwich laminates. Practical matters, such as the layout of cockpit, deck and cabin are discussed in Chapter 15, and Chapter 16 presents different means for evaluating the design. A complete weight calculation is carried out in Appendix 2.

The different aspects of the design process are therefore well covered. To satisfy the second requirement above, the material must be well presented, and we have tried to accomplish this in a number of ways.

Yacht design is by its nature a quantitative process. A designer, professional or amateur, is not much helped by qualitative reasoning. It is not enough to know that the hull can withstand a greater load if the skin is made thicker, or that stability is increased by more lead in the keel. What he needs to know, as exactly as possible, is the *minimum* skin thickness and the *least* amount of lead needed in the keel for the yacht to be safe under all possible conditions. If he is not able to compute these quantities the yacht may be slower and more expensive than necessary and, worst of all, it may be unsafe. Therefore, a basic principle of this book has been to provide formulae or diagrams for all aspects of the design process. The reader should be able to evaluate quantitatively every step in the design procedure.

We are fully aware that many potential readers may be intimidated by a text loaded with formulae, and would reject the book as being too technical. To avoid this, the equations have been removed from the text and inserted into the figures. A serious designer will need to work through the formulae himself for the reasons just explained, but we believe that the book could also be of interest to yachtsmen in general, since many may have a keen interest in the basic physics of sailing. They will be able to read the text without digging too deeply into the quantitative aspects.

On the other hand, the equations are not very complicated from a mathematical point of view. They are numerous, and they may be lengthy, but they are all of the algebraic type. Higher mathematics, such as integral or differential calculus, have been completely avoided, and everyone with a basic mathematical background from, say, secondary school should be able to understand them.

To help the reader understand the practical application of the principles and formulae presented, the design of a new yacht, called YD-40 (Yacht Design 40 footer) is followed throughout the book. Thus, after most of the formulae the computed value for the YD-40 is given, and all drawings (like lines plan, interior and exterior layout, rig plan and general arrangement) are for this modern cruiser/racer. This does not mean, of course, that the book is limited to this type of yacht. The material covers other cruisers and racers, traditional or modern designs and different rig types. To a certain extent dinghies are also included, but there is not much discussion on multihulls, and reference to power boats is made only occasionally. Power boats are addressed specifically in the chapters on high speed hydrodynamics and scantlings, but much of the other material in the book is applicable to this type of craft as well.

The YD-40 is specified in detail in Appendix 1, where all the data is given. There are two different sets of data. One is for the cruising condition, with all the necessary equipment and the tanks half full, while the other is for the light version, without cruising equipment. The latter version, or an even lighter one, is normally used in advertising material for new yachts. The weight calculation in Appendix 2 is for the YD-40 in the half loaded condition, including crew.

To evaluate a new design and its qualities it is important to compare it with other yachts. Sections with statistical data are therefore included in many of the chapters. Median values for existing yachts are given and the spread, within which approximately 95% of all yachts lie, is indicated. There is also a discussion on the effects of deviating from the median, which will enable the designer to create a yacht with special qualities. The position of the YD-40 within the statistical data is also shown and a motivation for this position is given in the light of the yacht specification in Chapter 2 and Appendix 1

In order to satisfy the more qualified readers of the book there are sections on advanced design, where the methods and tools described are not normally available to non-professionals. Also, throughout the book, the results of the most recent research in yacht design are presented. Much of this is not discussed in yachting literature.

Finally, some general remarks on the principles and style of the book must be made. With few exceptions the SI system of units is adopted. Unfortunately, the ABS rule does not follow this standard, so in the chapter on scantlings we have had to adopt other systems. Otherwise it is only the yacht speed that does not follow in the SI system; it is given in knots. At the present time it is probably premature to give the speed in metres per second (m/s). A conversion table between the SI and English units may be found on page xvi.

Another standard adopted is the nomenclature specified by the International Towing Tank Conference (ITTC). This has been developed over a very long period of time and is agreed by all members of the ITTC, which include all reasonably sized towing tanks in the world, as well as most universities teaching Naval Architecture. The symbols in this system are listed separately at the beginning of the book.

A References section may be found at the end of the book. The list is arranged in alphabetical order by the first author's surname. No reference numbers are given in the text, but contributions from different individuals or groups are identified by the author's name, and it should be easy to find the relevant publication in the list. It should be noted that there are more references in the list than are specifically referred to in the text.

# 1

# DESIGN METHODOLOGY

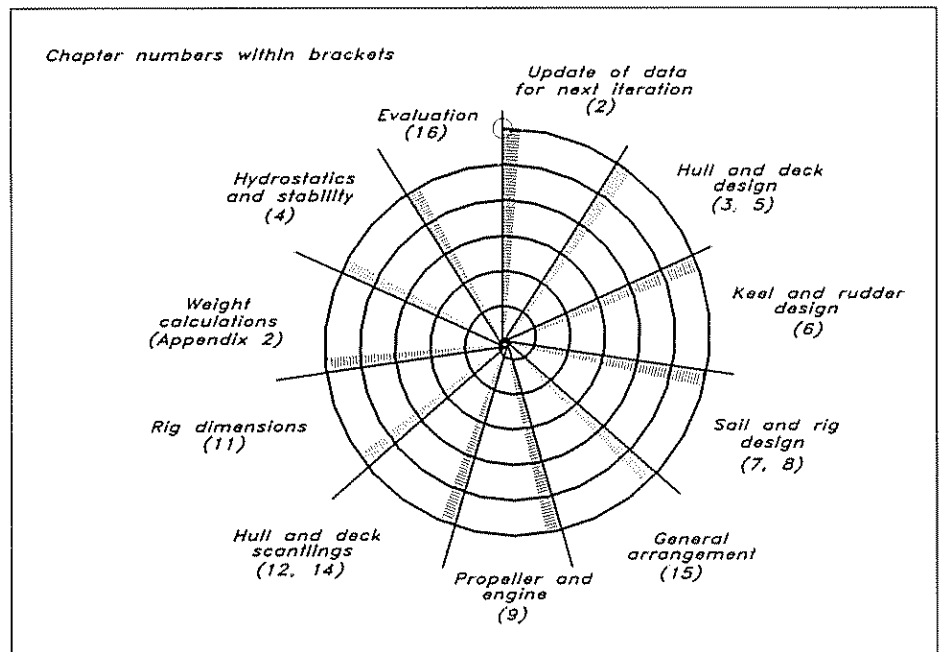
Yacht design is an iterative, 'trial and error' procedure where the final result has to satisfy certain requirements, specified beforehand. To achieve this the designer has to start with a number of assumptions and work through the design to see if, at the end, it satisfies the requirements. This will most certainly not be the case in the first iteration, so he will have to change some assumptions and repeat the process, normally several times. The sequence of operations is often referred to as a spiral, where the designer runs through all the design steps and then returns to the starting point, whereupon a new 'turn' begins. After several turns the process may have produced the desired result. We will describe the design spiral in more detail below.

If all steps are taken manually the procedure can be very time consuming, and it is tempting to stop the iterations before the initial specifications have been fully met. A huge saving in time and accuracy is possible if modern computer aided design (CAD) techniques are adopted, and we will discuss this possibility in the second part of the chapter.

## The design spiral

In Fig 1.1 the design spiral is shown. Eleven different segments may be identified, and each segment corresponds to an operation by the

Fig 1.1 *The design spiral*



designer. Not all operations have to be carried out in each turn, and the tools used in each operation may vary from turn to turn. In principle, more and more segments are included, and better and better tools are used, as the process converges towards the final solution. The figure shows that each sector corresponds to a chapter (or possibly two) in this book.

From the start the designer has only the specifications of the yacht, ie its requested capabilities. Based on his experience, or data from other yachts, he assumes the main data of the hull. Non-dimensional parameters such as displacement/length ratio, sail area/wetted area ratio, heeling arm and metacentric height may thus be computed, and a rough check of the performance may be made based on statistics from other yachts. The procedure is summarized in Chapters 2 and 16. In this first spiral turn the designer jumps from the first to the last segment directly, and the evaluation is very rough.

In the second turn, after having adjusted the main parameters, it may be time to begin the actual design of the hull, keel, rudder and sail plan. The theory for this is given in Chapters 3, 5, 6, 7 and 8. A rough layout of the interior and exterior design (see Chapter 15) may be made too, to give an initial weight estimate, needed for the stability calculation (see Chapter 4). It is likely that neither the weight, nor the stability will be correct, so several turns may be required to satisfy these requirements reasonably. Of course, not all previous operations may have to be redone in each turn. Having found a reasonable weight and stability for the yacht, the next turn may include the detailed hull scantling calculations and the dimensioning of the rig, as well as the choice of the engine (see Chapters 9–14). Only at this stage can an exact weight calculation be carried out, as shown in Appendix 2.

As the designer approaches the final solution he may want to evaluate the design more carefully, and to do this a Velocity Prediction Program (VPP) is required. Such programs are described in Chapter 16, where other, even more accurate, techniques are also presented. The amateur designer may not have access to either of these tools, however, so his evaluation of the current design will have to be based on experience.

It should be pointed out that in some segments internal iterations are required. This is particularly the case in the hull design area. Here, requirements for volume and its distribution are probably specified beforehand, and it may take several iterations to satisfy them. If the process is manual, iterations between the different views to fair the lines are also required, as will be described in Chapter 3. In the hydrostatics and stability segment iterations are required to find the proper sinkage and trim when the hull heels at large angles.

**Computer Aided Design (CAD)**

Thanks to the rapid development in recent years, computer aided design (CAD) may be carried out efficiently on PC or Macintosh computers. It is important to have a high resolution screen and special graphics software speeds up the process. A laser printer will produce reasonably good small-scale graphical output, but professional designers use pen plotters of various sizes to produce drawings up to full scale.

The most important module of a CAD system for yacht design is a powerful program for generating the hull lines, and such programs have been available since the early 1980s. The hull is represented mathematically, either by two families of lines, one running longitudinally and the other transversely on the surface, or by surface patches matched at the intersections by some conditions of fairness. In either case, any point on the surface may be found from the mathematical representation, or more precisely, if two coordinates of a point are given, the program computes the third one. Thus, if the user provides the distance from the bow,  $X$ , and the distance above the waterline,  $Z$ , the program computes the local beam,  $Y$ , at this location. By specifying several points, any cut through the surface may be obtained, for instance, any station or waterline.

There are principally two different problems in connection with the surface representation. The task can be either to generate a new hull, or to duplicate, as accurately as possible, an existing one. The latter problem is more difficult. It is certainly possible in an iterative process to approach a given shape, but it can be time consuming. Fortunately, the designer is normally interested in the first task: creating a new hull. To achieve this he has to work with a set of master curves close to, but not normally exactly on the surface. Each master curve is defined by a set of points (vertices) lying on the curve. The number of curves and vertices varies from case to case, but are often in the range 5–15. By moving one vertex the master curve changes and the hull surface is locally deformed in such a way that it is still smooth. In most programs the curvature of the surface may be plotted, thus enabling the designer to generate fair lines even on a small scale, and with the relatively low resolution of the screen. Some programs use points on the hull itself for defining its shape, but all the major programs on the international market use master curves. There seems to be a consensus among yacht designers that this approach is very effective for creating fair lines. In Chapter 3 we will show how the hull is generated by the master curves.

Most hull geometry programs have the capability to rotate the hull and show it in different perspectives on the screen. The possibility of showing a perspective plot of the hull is important and is a major improvement compared with the manual approach, where only three standard views are employed (see Chapter 3). For example the shape of the sheer line may look quite different in perspective compared with the side view, since the line that meets the eye is influenced also by the beam distribution along the hull. Hulls that look good in a side view may look quite ugly in reality.

Some of the more advanced programs include the deck and superstructure as for the hull model, ie these parts of the yacht are represented in three dimensions and may be displayed in perspective. In other programs they are treated separately. To compute stability at large angles of heel the deck, cabin and cockpit need to be modelled, and this is frequently done in a separate module where these parts are added relatively crudely, section by section.

A keel/rudder module is often available in yacht CAD systems. The designer may choose between a number of different profiles for the cross-section and specify the planform of the keel/rudder. The code computes the volume, weight of the keel, centre of gravity and centre of effort of the hydrodynamic force. The latter is required in the balancing of the yacht, as explained in Chapter 8. For this the sail plan is also required, and some systems have a simple sail module which computes sail areas and centres, given the sail corner coordinates.

The total weight and centre of gravity location (in three directions) are computed in a weight schedule monitor, which accepts the weight and position relative to a given reference point of all items on board. Appendix 2 presents the input and output from such a monitor.

Very important modules of the yacht CAD system are the hydrostatics and stability programs. These compute all the quantities discussed in Chapter 4, including stability at small and large heel angles, weight per mm of sinkage, and moment per degree of trim. In the stability calculation the correct sinkage and trim are found for each heel angle – a very time consuming procedure if carried out manually.

The Velocity Prediction Program (VPP), mentioned earlier, may also be regarded as a module of the CAD system. As explained above, this program computes the speed, heel angle and leeway angle at all wind speeds and directions of interest, based on a set of dimensions for the hull, keel, rudder and sails. The very simple performance estimator, based on a few main parameters and used in the first iteration of the design spiral, may also be a module of the system.

Finally, more or less advanced programs for the structural design of the yacht may be included. Such programs can be based on the rules given by the classification societies: the American Bureau of Shipping, (ABS), Lloyd's Register of Shipping (LR) and others or the ISO Scantling Standard 12215. The ISO Standard will be described in Chapter 14. Other methods employed in the rig and scantling calculations may be based on basic strength theory or finite element techniques.

Computer aided design may be extended to computer aided manufacturing, which can be used in the production of the yacht. For example, the very time consuming lofting process, where the builder produces full-scale templates, may be eliminated. Traditionally, the builder receives offset tables from the designer. Based on these offsets the templates are drawn at full scale with a reduction in dimension for the skin thickness of the hull. This is necessary, since the templates are used internally during the building process. If the hull has been CAD



---

designed, however, the full-scale templates with the proper reduction may be plotted directly, provided a sufficiently large plotter is available. Plate expansions may also be obtained from the CAD system, simplifying the production of steel and aluminium hulls.

# 2

# PRELIMINARY CONSIDERATIONS

---

**B**efore actually starting the design work, we must have a clear picture of the yacht's purpose: what are the requirements, limitations and objectives of the design? In this chapter we will list the considerations that form the starting point of the design.

## **Choice of boat-type**

Regardless of whether the client is an individual owner or a boatbuilding firm, he will have definite ideas as to the type of boat he wants. Most people have a particular yacht in mind which, with changes in dimensions, style, arrangement, rig or hull form, satisfies their demands. These preferences are often modified by other considerations, such as local conditions, economic considerations and the intended use. Personal opinion often governs the choice of type to such an extent that the more logical and scientific arguments may become of secondary concern, if not set aside entirely.

## **Intended use**

The intended use of the yacht is a matter that comes first on the list of considerations. The first distinction is that between racing and cruising.

For the racer we must naturally decide to which rule the boat should be designed, and in which class it will be racing. This gives us a good starting point regarding the size of boat and crew, rig size and type, by comparing it with existing successful designs. Having established the type and size of boat, we can proceed with the design process described in the following chapters, making adjustments so as to conform to the rule we are following.

For the cruiser the primary requirement influencing the type of design to adopt regarding hull, deck, accommodation and rig, is the yacht's intended use in broad terms ie unlimited ocean passagemaking, open or restricted offshore use, or coastal or sheltered use. Obviously, it is easier to reach high standards of safety, stability and performance with a big yacht, provided there is sufficient crew to handle the vessel.

This brings us to the question of the need for compromise. The requirements of speed, seaworthiness, dryness, weatherliness, ease of handling, comfort and other qualities often conflict, but the fewer the compromises the better the design will be. We must decide at an early stage what particular qualities we desire most, or require to the greatest extent. By getting our priorities right from the start we know where compromises can be made with the least harm. Too many yachts are designed on the assumption that it is possible to achieve all of the qualities of the perfect yacht without regard to the limitations of the chosen type and its intended use. To achieve a good design it is crucial

to define the intended use, weigh the requirements that these impose on the yacht and choose a type of yacht whose design elements fulfil that need. When the type of yacht is chosen we must stick to it throughout the whole design process. Of course there will be alterations along the way, but if we find that many major changes are necessary it will probably be best to start the design work from square one.

The intended use is not only about sailing area, performance and range, but also about who is going to use the boat and under what circumstances. If we take a design intended for charter use, the requirement will usually be a large number of berths and a roomy cockpit to accommodate everyone when sailing. The time at sea will be restricted, most sleeping will be in harbour or at anchor and the handling systems must be understood by novices. By contrast, an experienced owner who wishes to make extended passages with a small crew will have the opposite requirements.

### Main dimensions

It is generally agreed that increasing the size of the boat will produce a better design in terms of performance and comfort; on the other hand the boat might be more difficult to handle by a small crew. Size is also linked to the intended area of use: unlimited ocean use naturally places greater demands on a boat compared with sheltered water use. Not only will it need to withstand strong winds and heavy seas, but it will also need to carry more fuel, water and stores – all of which point to the bigger yacht. However, it is not self-evident that size in this respect means length; a better measure would perhaps be displacement, since this describes the volume of the boat. Take two boats of similar displacement: the longer one will usually have better performance but its carrying capabilities will be roughly the same as for the shorter one.

The requirements of engine, rig and deck equipment depend largely on size, weight and length as well as beam. To reach a certain speed under power with a limited power source the length-weight ratio is of vital importance, while the stability required to carry enough sail is more dependent on the beam and weight. In this context it is noticeable that the heeling forces increase with size to the power of 3, while the stability increases with size to the power of 4. So scaling a boat up linearly does not produce a design compatible with good performance and stability.

The changes in proportions with increasing size have been calculated for an allometric series of yachts from  $L_{OA} = 7\text{m}$  to  $L_{OA} = 19\text{m}$  by H M Barkla of the University of St Andrews, Scotland (see Fig 2.1). As we can clearly see, different dimensions and parameters scale differently with length. The scaling factors shown in the figure produce boats of similar behaviour regarding performance and ‘feel’ when scaled in either direction from a base model. The ‘L’ in Fig 2.1 refers to the length relation between the base model and the derivative. For example, if we increase the length of the boat by 50%, ie 1.5 times L, the beam, depth and freeboard will be increased by  $1.5^{0.7} = 1.33$  times the original value to keep the boat within the same performance-family.

Fig 2 1 Proportions versus size (Barkla)

PRIMARY RELATIONS – Independent of basic model	Scale Factor
Assumed:	L
Sail area	$L^{1.85}$
Beam, depth, freeboard	$L^{0.70}$
Keel & rudder span, chord, thickness	$L^{0.70}$
Derived:	
areas – section	$L^{1.40}$
– wetted – hull	$L^{1.70}$
– keel & rudder	$L^{1.40}$
– lateral – hull	$L^{1.70}$
– keel & rudder	$L^{1.40}$
volumes – hull	$L^{2.40}$
– keel	$L^{2.10}$
ratios – $L_{WL}/\nabla^{1/3}$ (ex-keel)	$L^{0.20}$
– $SA/\nabla^{2/3}$ (ex-keel)	$L^{0.25}$
Second moments of waterplane – lateral	$L^{3.10}$
– longitudinal	$L^{3.70}$
SECONDARY RELATIONS – dependent to some extent on basic model	
Total volume of displacement	$L^{2.38}$
Total wetted area	$L^{1.63}$
Sail area / wetted area	$L^{0.22}$
Sail area / $\nabla^{2/3}$ (incl-keel)	$L^{0.26}$
Distance of VCB below $L_{WL}$	$L^{0.64}$
BM	$L^{0.72}$
GM	$L^{0.45}$
Initial righting moment	$L^{2.83}$
Separation of centres of effort (lead)	$L^{0.86}$

Fig 2 2 Preliminary design parameters

Design	LOA	LWL	BMAX	T	$\nabla$	SA	DLR	LDR	SDR	SA/SW	STIX
YD-40	12.05	10.02	3.71	2.07	7.3	75.4	205	5.2	20.0	2.79	46
40' Yacht on Market	12.27	9.88	3.93	2.15	7.8	78.4	229	5.0	19.9	2.88	47

LOA = Length overall [m]

LWL = Length in waterline [m]

BMAX = Maximum beam [m]

T = Maximum depth from waterline [m]

 $\nabla$  = Light load volume displacement [ $m^3$ ]SA = Nominal sail area, main + 100% fore triangle [ $m^2$ ]SW = Wetted area of hull and appendages [ $m^2$ ]DLR = Displacement Length Ratio [ $28300 \cdot \nabla / L_{WL}^3$ ]LDR = Slenderness Ratio [ $L_{WL} / \nabla^{1/3}$ ]SDR = Sail area Displacement Ratio [ $SA^{2/3} / \nabla^{1/3}$ ]

STIX = Stability Index, described in Chapter 4

A very good way of establishing dimensions for the hull and rig of a new design before there are any drawings or calculations, is to decide on some vital dimensionless ratios that can be checked against known designs. Chapter 5 deals in more detail with this, and explains what factors are involved. Fig 2.2 shows, for the YD-40, the values of the ratios derived from first estimates of the main dimensions. Comparison is made with an existing yacht of the same size. Once we are satisfied with the numbers we have a good starting point for the design.

## Cost

No one is interested in having a boat built more expensively than necessary. Taking only that prerequisite into account, the obvious answer seems to be to build the boat as small as possible, since building costs relate directly to size (or rather weight). However, in going for light weight we might be forced to use exotic materials and advanced building methods which in turn might increase the cost compared with using heavier materials and a more conventional building technique. At the other end of the scale are the heavy building methods needed for steel and ferrocement, for instance, which certainly provide cheap materials but produce heavy boats that need much power (sail and engine) to drive them, and robust deck equipment for handling them, all of which cost money.

A common pitfall when designing a boat in the smaller size range to keep costs down, is to miniaturize. Everything might look well proportioned on paper, but in practice the design may not work because the human being cannot be scaled down. Moreover, trying to squeeze too much into a small volume would not produce a cost-effective design, not only because everything found in a bigger yacht would be there, but also because it would be so much harder to fit in, due to lack of space.

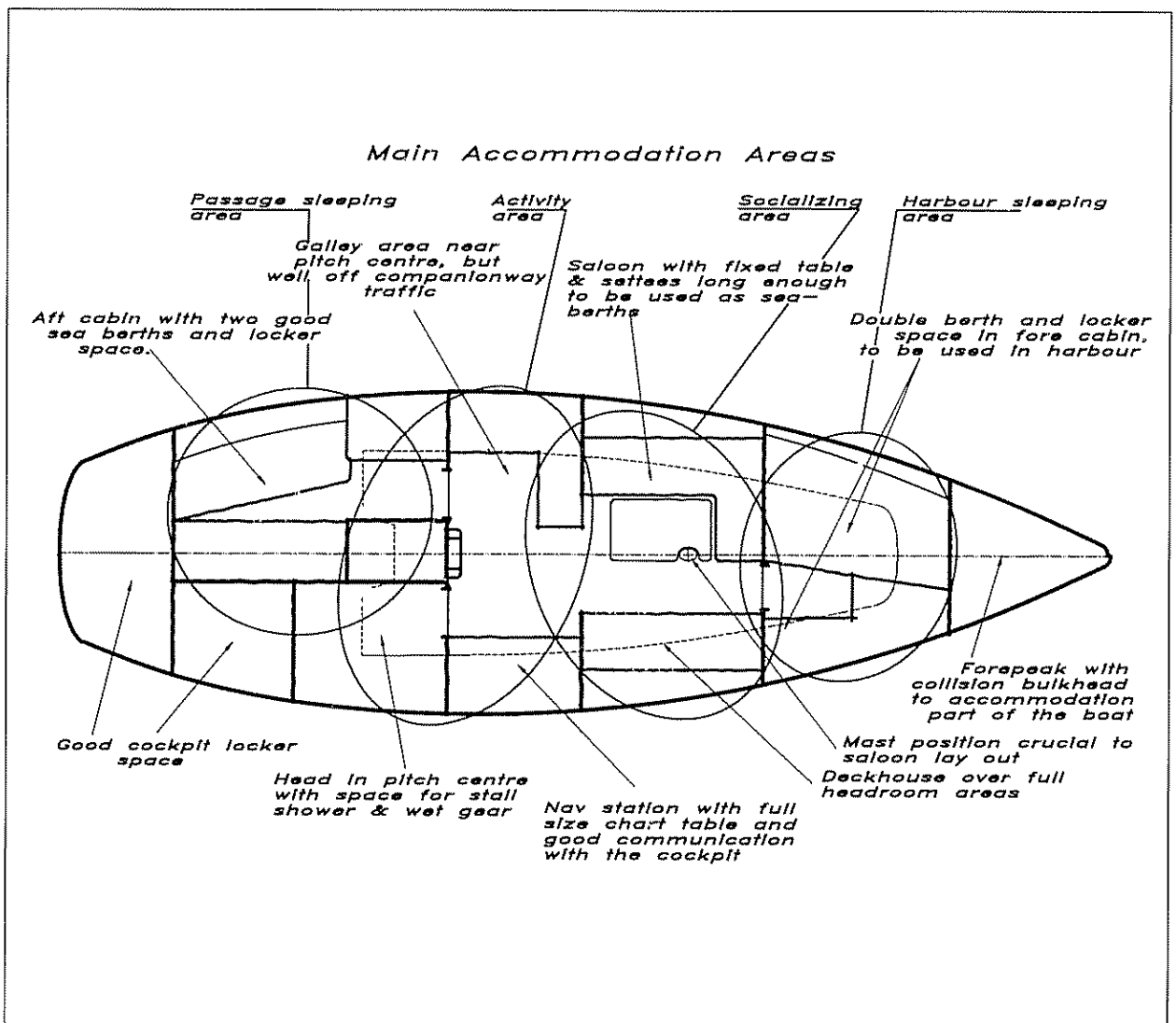
The hull form is basically derived from hydrodynamic and hydrostatic requirements, while the form of the deck is more open to the whim of the designer, to fashions and trends, and to what 'character' the design is intended to radiate. A deck with lots of angles and sharp turning points is much more difficult to build (FRP construction) compared with one with smooth areas and large radii in the corners. Here we have a choice that most definitely will affect the construction cost. Designing decks or parts of decks that require multiple moulds to make mould-release possible, will also make the costs higher. We have to be quite sure that the benefits of such a design outweigh the increased cost that goes along with it.

To some extent the same reasoning can be applied to the accommodation. Obviously, a flat panel attached to another at a square angle is much cheaper to produce than a curved one attached at an oblique angle. On the other hand, rounded panels and oblique angles can be used to achieve better space utilization which, in the end, will make the boat so much better that the increased building costs can be justified. Another way of increasing usable space is to let areas and compartments overlap one another. It is not always necessary to have

the full cabin height over the full length of the boat. For example a toilet can be under a cockpit seat with the rest of the head area under the superstructure. Instead of thinking of the accommodation as a two-dimensional jigsaw puzzle, it might be fruitful to think of it as a three-dimensional puzzle so as to utilize the space available in the best way. A word of warning though: complicating things too much might raise the cost out of all proportion, so a better way might be to make the whole boat bigger and simpler in order to fulfil the requirements.

The amount of standard equipment also plays an important role in the overall cost of the boat, regardless of whether she is light or heavy. By this we mean whether to have an airconditioner/heater, running hot and cold water, a watermaker, a freezer/refrigerator, electric winches, full electronics with radar, a chartplotter and auto pilot, self furling sails and so on. All these items can almost equal the cost of the rest of the boat.

Fig 2 3 Preliminary layout – YD-40



## Checklist of considerations

---

To summarize the above considerations the following list can be applied:

- |  |   |
|--|---|
| <ol style="list-style-type: none"> <li>1 Define the intended use and limits.</li> <li>2 Collect information about similar boats.</li> <li>3 Decide on the main dimensions and ratios.</li> <li>4 Decide on the preliminary layout and exterior.</li> </ol> | <ol style="list-style-type: none"> <li>5 Make a first approximation of weights and form parameters.</li> <li>6 Check against 3 and correct if necessary.</li> <li>7 Produce a preliminary design to work from.</li> </ol> |
|--|---|

## Checklist for the YD-40

---

Having considered these points we are now ready to lay down a preliminary design. To make that meaningful we must decide on a specific one, and in this book we will use the YD-40. The design brief for this yacht is as follows:

- |  |  |
|--|--|
| <ol style="list-style-type: none"> <li>1 An ocean-going yacht, with long-term accommodation for four, to be capable of being handled by a crew of two. The performance shall be good enough for it to be successfully entered in club level racing. The ocean-going requirement demands carrying capabilities for water and stores for up to a month without reprovisioning.</li> <li>2 See Fig 2.2 for comparison with a similar yacht.</li> <li>3 The main dimensions and ratios are also derived from the comparison in Fig 2.2.</li> <li>4 Figure 2.3 (see opposite) is a first sketch of</li> </ol> | <p>the yacht showing the principal areas of accommodation. Basically they are designed around the assumption that they will be functional under way with a crew of four. This means four good sea berths, two in the aft cabin and two in the saloon, a galley, head and navigation area in the pitch centre of the boat. The saloon shall be big enough to accommodate the occasional racing crew, and other social entertaining in harbour, and the forward cabin shall be used as an in-harbour master cabin. The accommodation shall not be pressed into the ends of the boat to enhance performance, and judged on a length-only basis this will reduce the building costs.</p> |
|--|--|

Having established the main dimensions, type of boat and area of use we can proceed with the more precise design work. Comparing with Fig 2.2 we can see that the design brief is met quite well, with the main dimensions and their connected ratios chosen.

# 3

# HULL GEOMETRY

---

The hull of a yacht is a complex three-dimensional shape, which cannot be defined by any simple mathematical expression. Gross features of the hull can be described by dimensional quantities such as length, beam and draft, or non-dimensional ones like prismatic coefficient or slenderness (length/displacement) ratio. For an accurate definition of the hull the traditional lines drawing is still a common tool, although most professional yacht designers now take advantage of the rapid developments in CAD introduced in Chapter 1.

In this chapter we start by defining a number of quantities, frequently referred to in yachting literature, describing the general features of the yacht. Thereafter, we will explain the principles of the traditional drawing and the tools required to produce it. We recommend a certain work plan for the accurate production of the drawings and, finally, we show briefly how the hull lines are generated in a modern CAD program.

## Definitions

The list of definitions below includes the basic geometrical quantities used in defining a yacht hull. Many more quantities are used in general ship hydrodynamics, but they are not usually referred to in the yachting field. A complete list may be found in the International Towing Tank Conference (ITTC) *Dictionary of Ship Hydrodynamics*.

### *Length overall ( $L_{OA}$ )*

The maximum length of the hull from the forwardmost point on the stem to the extreme after end (see Fig 3.1). According to common practice, spars or fittings, like bowsprits, pulpits etc are not included and neither is the rudder.

### *Length of waterline ( $L_{WL}$ )*

The length of the designed waterline (often referred to as the DWL).

### *Length between perpendiculars ( $L_{PP}$ )*

This length is not much used in yachting but is quite important for ships. The forward perpendicular (FP) is the forward end of the designed waterline, while the aft perpendicular (AP) is the centre of the rudder stock.

### *Rated length*

The single most important parameter in any rating rule. Usually  $L$  is obtained by considering the fullness of the bow and stern sections in a more or less complex way.

### *Beam ( $B$ or $B_{MAX}$ )*

The maximum beam of the hull excluding fittings, like rubbing strakes.



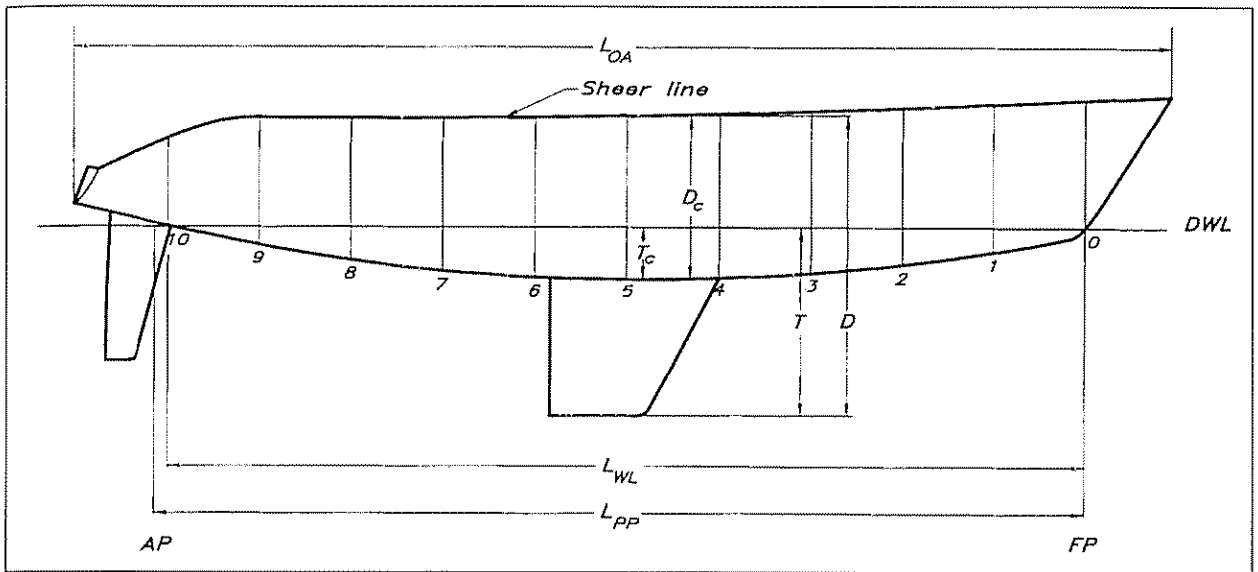


Fig 3 1 Definitions of the main dimensions

- Beam of waterline ( $B_{WL}$ )** The maximum beam at the designed waterline.
- Draft ( $T$ )** The maximum draft of the yacht when floating on the designed waterline.  $T_c$  is the draft of the hull without the keel (the 'canoe' body).
- Depth ( $D$ )** The vertical distance from the deepest point of the keel to the sheer line (see below).  $D_c$  is without the keel.
- Displacement** Could be either mass displacement ( $m$ ) ie the mass of the yacht, or volume displacement ( $V$  or  $\nabla$ ), the volume of the immersed part of the yacht.  $m_c$ ,  $V_c$  and  $\nabla_c$  are the corresponding notations without the keel.
- Midship section** For ships, this section is located midway between the fore and aft perpendiculars. For yachts it is more common to put it midway between the fore and aft ends of the waterline. The area of the midship section (submerged part) is denoted  $A_M$ , with an index 'c' indicating that the keel is not included.
- Maximum area section** For yachts the maximum area section is usually located behind the midship section. Its area is denoted  $A_X$  ( $A_{Xc}$ ).
- Prismatic coefficient ( $C_p$ )** This is the ratio of the volume displacement and the maximum section area multiplied by the waterline length, ie  $C_p = \nabla / (A_X \cdot L_{WL})$ . This value is very much influenced by the keel and in most yacht applications only the canoe body is considered:  $C_{pc} = \nabla_c / (A_{Xc} \cdot L_{WL})$ . See Fig 3.2. The prismatic coefficient is representative of the fullness of the yacht. The

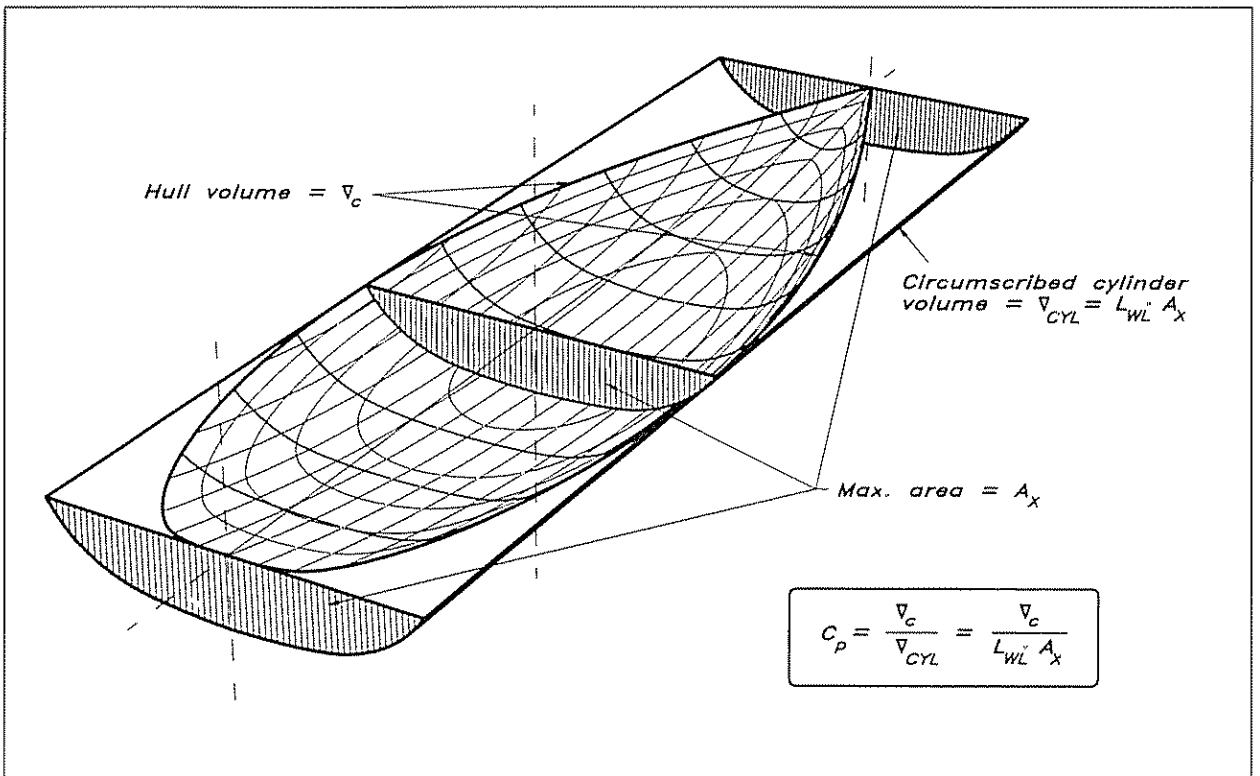


Fig 3.2 The prismatic coefficient

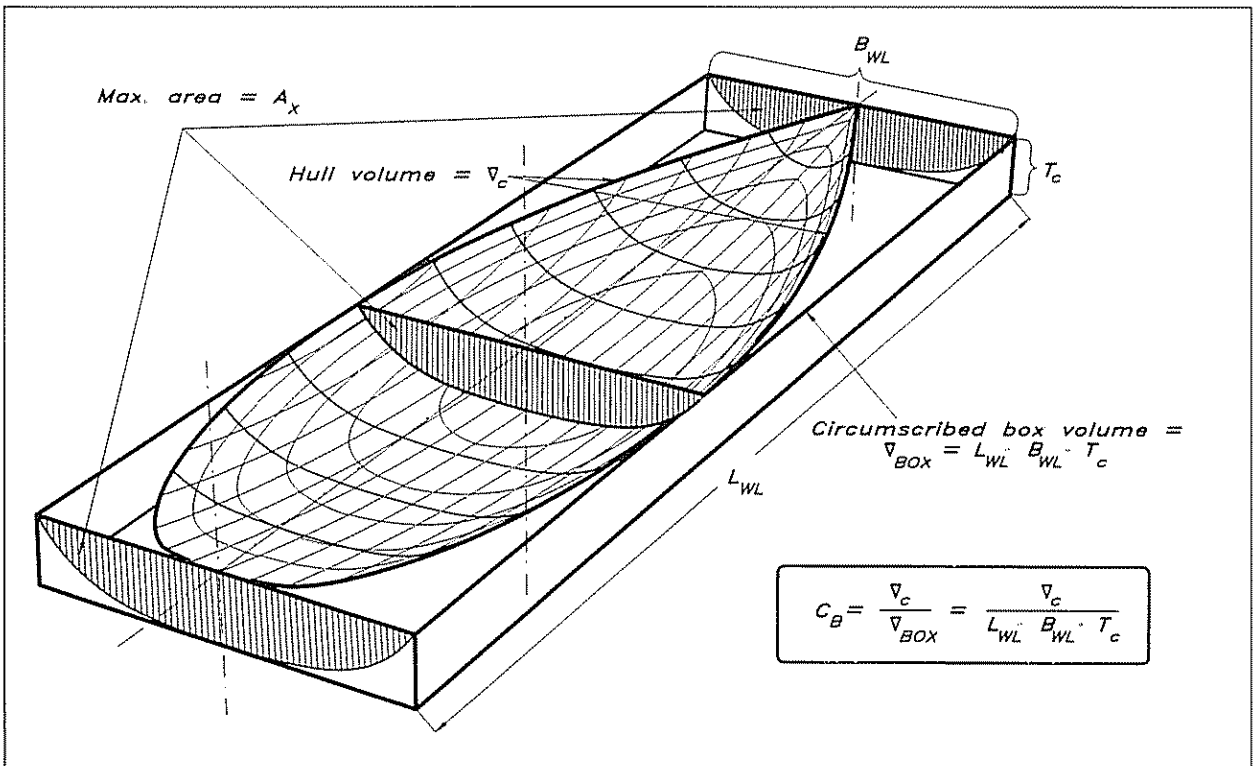
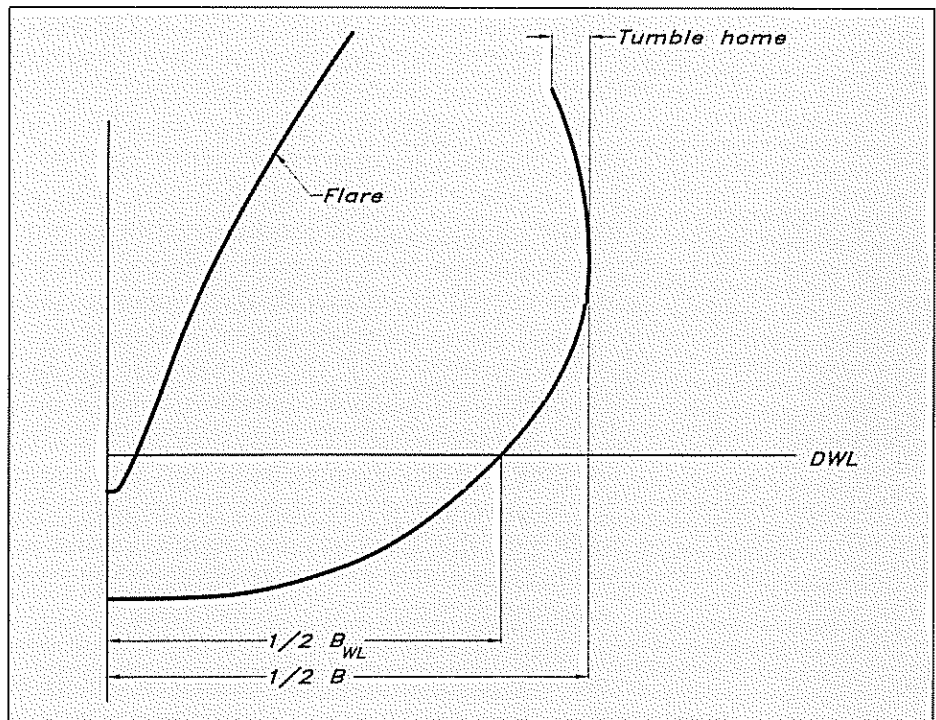


Fig 3.3 The block coefficient

fuller the ends, the larger the  $C_p$ . Its optimum value depends on the speed, as explained in Chapter 5.

- Block coefficient ( $C_B$ )** Although quite important in general ship hydrodynamics this coefficient is not so commonly used in yacht design. The volume displacement is now divided by the volume of a circumscribed block (only the canoe body value is of any relevance)  $C_{Bc} = \nabla_c / (L_{WL} \cdot B_{WL} \cdot T_c)$ . See Fig 3.3.
- Centre of buoyancy (B)** The centre of gravity of the displaced volume of water. Its longitudinal and vertical positions are denoted by LCB and VCB respectively
- Centre of gravity (G)** The centre of gravity of the yacht must be on the same vertical line as the centre of buoyancy. In drawings G is often marked with a special symbol created by a circle and a cross. This is used also for marking geometric centres of gravity. See, for instance, Figs 5.27 or 8.2.
- Sheer line** The intersection between the deck and the topside. Traditionally, the projection of this line on the symmetry plane is concave, the 'sheer' is positive. Zero and negative sheer may be found on some extreme racing yachts and powerboats.
- Freeboard** The vertical distance between the sheer line and the waterline.
- Tumble home** When the maximum beam is below the sheer line the upper part of the topsides will bend inwards (see Fig 3.4). To some extent this reduces the weight at deck level, but it also reduces the righting moment of the

Fig 3.4 Definition of tumble home and flare



crew on the windward rail. Further, the hull becomes more vulnerable to outer skin damage in harbours.

### *Flare*

The opposite of tumble home. On the forebody in particular, the sections may bend outwards to reduce excessive pitching of the yacht and to keep it more dry when beating to windward.

### *Scale factor ( $\alpha$ )*

This is not a geometrical parameter of the hull, but it is very important when designing a yacht. The scale factor is simply the ratio of a length (for instance the  $L_{WL}$ ) at full scale to the corresponding length at model scale. Note that the ratio of corresponding areas (like the wetted area) is  $\alpha^2$  and of corresponding volumes (like displacement)  $\alpha^3$ .

### *Lines drawing*

A complete lines drawing of the YD-40 is presented in Fig 3.5. The hull is shown in three views: the profile plan (top left), the body plan (top right) and half breadth plan (bottom). Note that the bow is to the right.

In principle, the hull can be defined by its intersection with two different families of planes, and these are usually taken as horizontal ones (waterlines) and vertical ones at right angles to the longitudinal axis of the hull (sections). While the number of waterlines is chosen rather arbitrarily, there are standard rules for the positioning of the sections. In yacht architecture the designed waterline is usually divided into ten equal parts and the corresponding sections are numbered from the forward perpendicular (section 0) backwards. At the ends, other equidistant sections, like # 11 and # -1 may be added, and to define rapid changes in the geometry, half or quarter sections may be introduced as well. In Fig 3.5 half sections are used throughout.

The profile is very important for the appearance of the yacht, showing the shapes of the bow and stern and the sheer line. When drawing the waterlines, displayed in the half breadth plan, it is most helpful if the lines end in a geometrically well defined way. Therefore a 'ghost' stem and a 'ghost' transom may be added. The ghost stem is the imagined sharp leading edge of the hull, which in practice often has a rounded stem, and the ghost transom is introduced because the real transom is often curved and inclined. If an imagined vertical transom is put near the real one at some convenient station, it will facilitate the fairing of the lines. The drawing of Fig 3.5 has been produced on a CAD system and no ghost stem is shown. However, a ghost transom is included.

In the body plan, the cross sections of the hull are displayed. Since the hull is usually symmetrical port and starboard, only one half needs to be shown, and this makes it possible to present the forebody to the right and the afterbody to the left. In this way mixing of the lines is avoided and the picture is clearer. Note that in the figure the half stations are drawn using thinner lines.

The above cuts through the hull are sufficient for defining the shape, but another two families of cuts are usually added, to aid in the visual perception of the body. Buttocks are introduced in the profile plan,

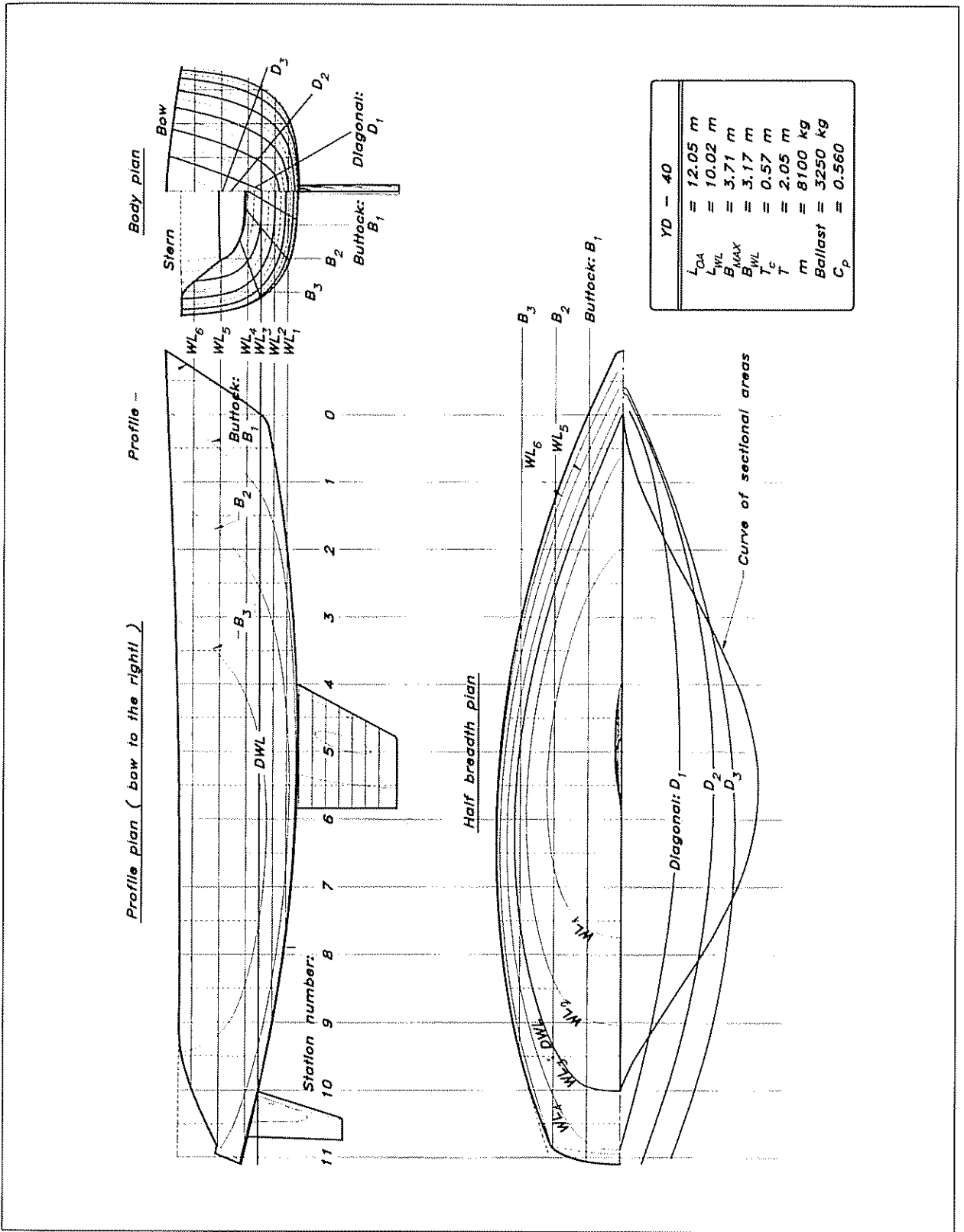


Fig 3.5 The lines drawing

showing vertical, longitudinal cuts through the hull at positions indicated in the half breadth plan. The diagonals in the lower part of the half breadth plan are also quite important. They are obtained by cutting the hull longitudinally in different inclined planes, as indicated in the body plan. The planes should be as much as possible at right angles to the surface of the hull, thus representing its longitudinal smoothness. In practice, the flow tends to follow the diagonals, at least approximately, so that they are representative of the hull shape as 'seen' by the water. Special attention should be paid to the after end of the diagonals, where knuckles, not noticed in the other cuts, may be found, particularly on IOR yachts from the 1970s and the 1980s. Almost certainly, such unevenness increases the resistance and reduces the speed of the yacht.

The other line in the lower part of the half breadth plan is the curve of sectional areas, representing the longitudinal distribution of the submerged volume of the yacht. The value at each section is proportional to the submerged area of that section, while the total area under the curve represents the displacement (volume). A more detailed description of the construction of the curve of sectional areas will be given in Chapter 4.

In order to define exactly the shape of the hull a table of offsets is usually provided by the designer. This is to enable the builder to lay out the lines at full size and produce his templates. Offsets are always provided for the waterlines, but the same information may be given for diagonals and/or buttocks also. Note that all measurements are to the outside of the shell.

## Tools

The drawing should be made on a special plastic film, available in different thicknesses. The film is robust and will not be damaged by

Photo 3.6 *Tools (triangle, plastic film, straight edge, brush, pens, pencil, erasing shield and eraser)*

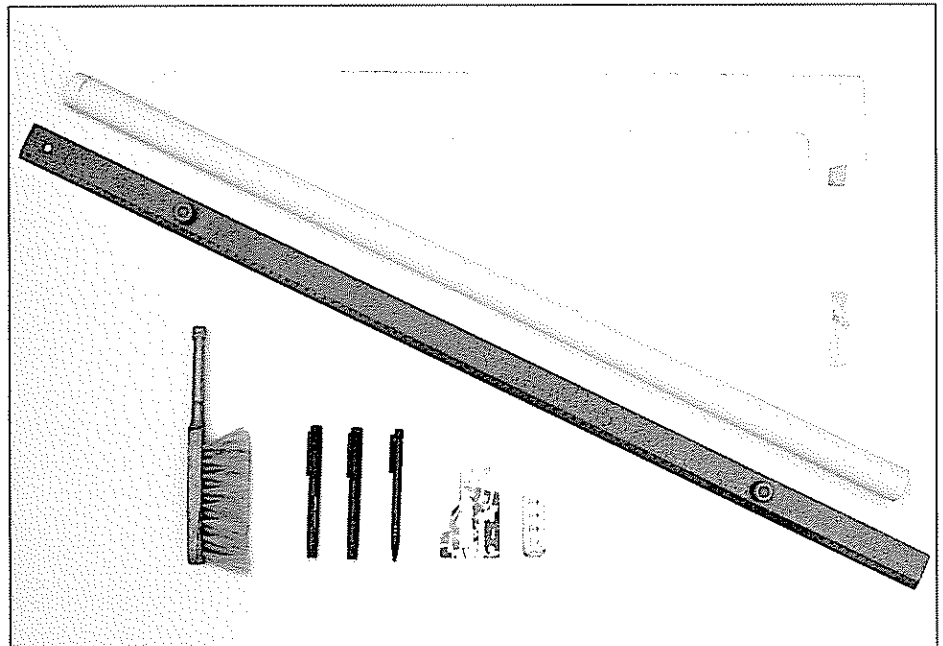
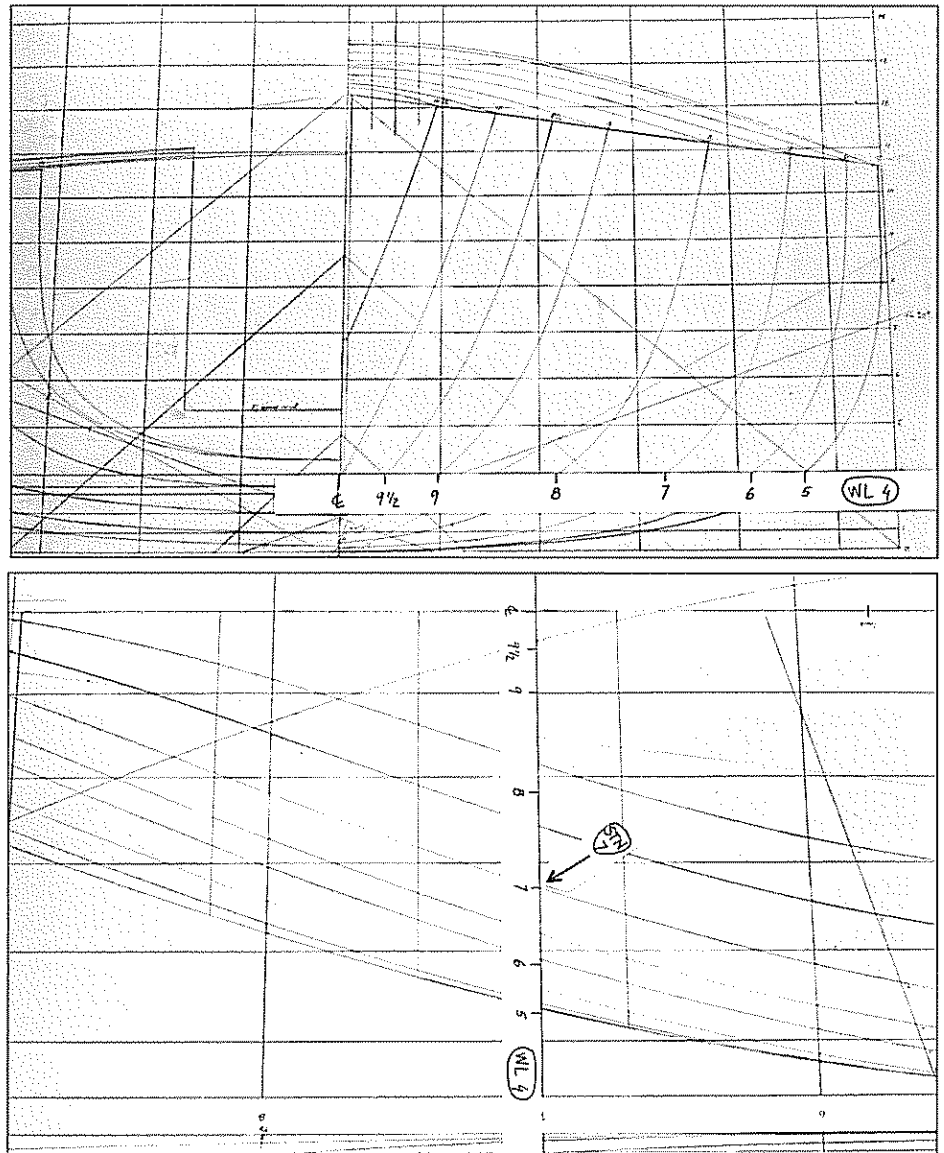


Photo 3 7 Transfer of measures from body plan (TOP) to half breadth plan (BOTTOM) using a paper ribbon



erasing. Furthermore, it is unaffected by the humidity of the air, which may shrink ordinary paper.

Since the film is transparent the grid for the lines drawing is drawn on the back so that it will remain, even after erasing the hull lines on the front many times. Great care must be exercised when drawing the grid, making sure that the alignment and spacing are correct and that all angles are exactly  $90^\circ$ . In Fig 3.5 the grid is shown as thin horizontal and vertical lines, representing waterlines, buttocks and stations.

Black ink should be used when drawing the grid and preferably when finishing the hull lines also. However, when working on the lines a pencil and an eraser are needed. There are, in fact, special pencils and erasers for this type of work on plastic film. An erasing shield and a brush are also most useful (see Photo 3.6).

For creating the grid a long straight edge is required, together with a

Photo 3.8 *Ducks and a spline used for drawing a waterline*

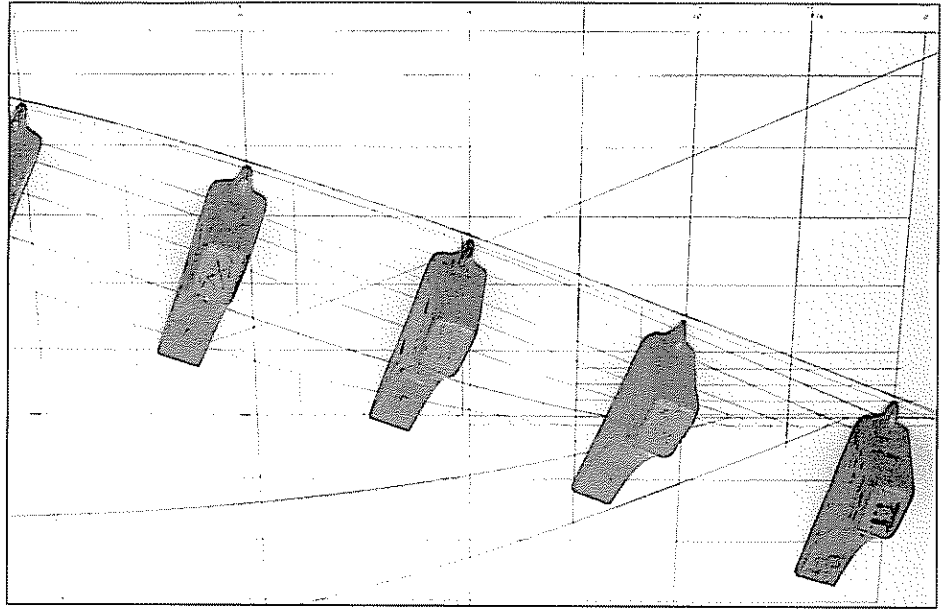
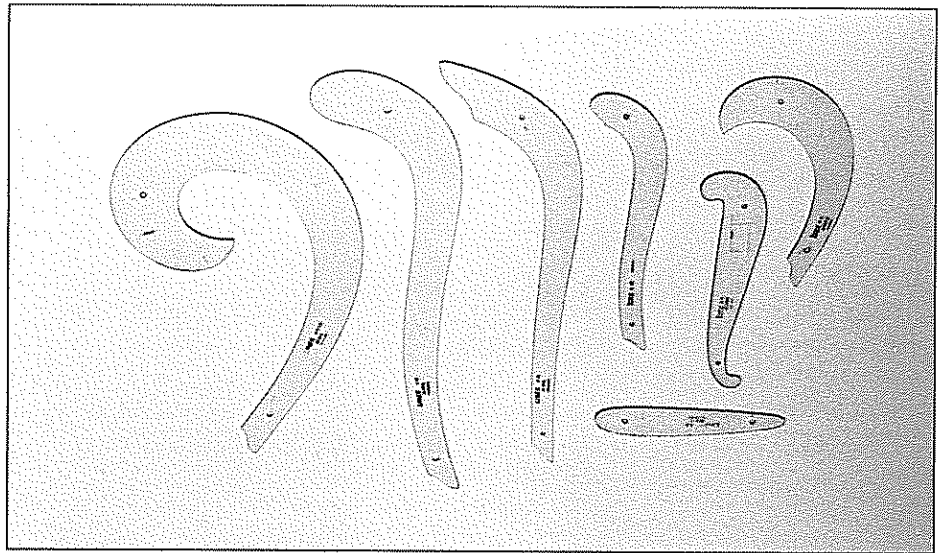


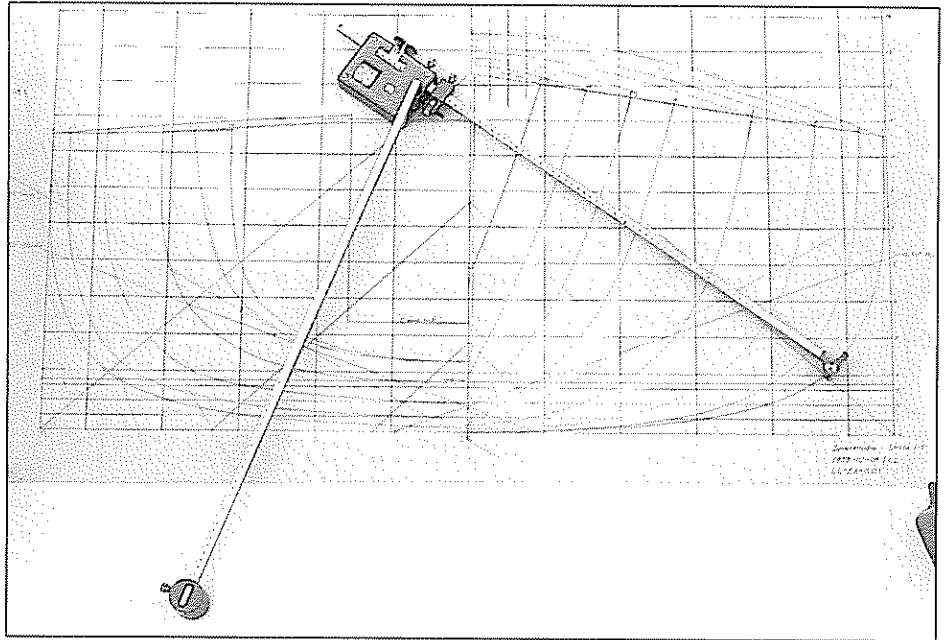
Photo 3.9 *Templates used for drawing lines with large curvature*



large 90° set square. It is very convenient to have a bunch of paper ribbons, which can be used for transferring different measures from one plan to the other. For example, when drawing a waterline the offsets of this line may be marked on the ribbon directly from the body plan and moved to the half breadth plan (Photo 3.7).

To draw the hull lines it is necessary to have a set of splines and weights or ducks. Long, smooth arcs can be created when bending the splines and supporting them by the ducks at certain intervals. Photo 3.8 shows how these tools are used when drawing a waterline. The splines should be made of plastic, somewhat longer than the hull on the drawing, and with a cross-section of about 2.5 mm<sup>2</sup>. Many different types of ducks can be found, some of them home made. Preferably,



Photo 3.10 *Planimeter*

they should be made of lead, and the weight should be between 1.5 and 2.5 kg. To be able to support the spline, they should have a pointed nose, as shown in Photo 3.8.

The splines are needed when drawing the lines in the profile and half breadth plans. However, the lines of the body plan are usually too curved for the splines, so it is necessary to make use of a set of templates especially developed for this purpose. The most well known ones are the so called Copenhagen ship curves, the most frequently used of which are shown in Photo 3.9.

A very convenient instrument, well known in naval architecture, is the planimeter, used for measuring areas (see Photo 3.10). The pointer of the planimeter is moved around the area to be measured, and the change in the reading of the scale when returning to the point of departure gives the area enclosed by the path followed. Considering the difficulty in following exactly any given line the accuracy is surprisingly high, more than adequate for the present purposes. The need for measuring areas will be explained in the next chapter.

Since many calculations have to be carried out when preparing the drawings, and indeed in the whole design process, an electronic calculator is essential. A simple one would be sufficient in most cases, but a programmable calculator would simplify some of the calculations, particularly if a planimeter is not available. Most scientific calculators have programs for calculating areas with acceptable accuracy, and programs are available for most of the calculations described in the next chapter.

## WORK PLAN

Designing the hull is a complex process, and many requirements have to be considered. One difficulty is that important parameters, such as the displacement, cannot be determined until the lines have been fixed. This calls for an iterative method. Such a method is also required in the fairing of the lines. The problem is to make the lines in one projection correspond to smooth lines in the other two projections. For an inexperienced draftsman this problem is a serious one, and many trials may be needed to produce a smooth hull.

While the preferred sequence of operations may differ slightly between yacht designers the main steps should be taken in a certain order. In the following, we propose a work plan, which has been found effective in many cases. It should be pointed out that the plan does not take into account any restrictions from measurement rules.

**Step 1: Fix the main dimensions** These should be based on the general considerations discussed in Chapter 2, using information on other yachts of a similar size, designed for similar purposes. This way of working is classical in naval architecture, where the development proceeds relatively slowly by evolution of previous designs. It is therefore very important, after deciding on the size of the yacht, to find as much information as possible on other similar designs. Drawings of new yachts may be found in many of the leading yachting magazines from all over the world.

The dimensions to fix at this stage are: length overall, length of the waterline, maximum beam, draft, displacement, sail area, ballast ratio, prismatic coefficient and longitudinal centre of buoyancy. One of the aims of this book is to help in the choice of these parameters and to enable the reader to evaluate older designs when trying to find the optimum for his own special demands.

**Step 2: Draw the profile** As pointed out above, this step takes much consideration, since the aesthetics of the yacht are, to a large extent, determined by the profile.

**Step 3: Draw the midship section** The midship section can be drawn at this stage, or, alternatively, the maximum section if it is supposed to be much different. This may occur if the centre of buoyancy is far aft. The shape of the first section drawn is important, since it determines the character of the other sections.

**Step 4: Check the displacement** To find the hull displacement calculate (or measure) the submerged area of the section just drawn and multiply by the waterline length and the prismatic coefficient chosen for the hull. From the ballast ratio, the keel mass can be computed and the volume can be found, dividing by the density of the material (about 7200 kg/m<sup>3</sup> for iron and 11 300 kg/m<sup>3</sup> for lead). Assume that the rudder displacement is 10% of that of the keel and add all three volumes. If the displacement thus obtained is different from the prescribed one, return to step 3 and change accordingly.

The procedure described is for a fin-keel yacht. For a hull with an integrated keel, as on more traditional yachts, the prismatic coefficient usually includes both the keel and the rudder.

**Step 5: Draw the designed waterline** One point at or near the midship station is now known, together with the two end points from the profile, so now a first attempt can be made to draw the designed waterline.

**Step 6: Draw stations 3, 7 and the transom** The waterline breadth is now known, as well as the hull draft, and the sections should have a family resemblance to the midship section. Often it is helpful to draw a ghost transom behind the hull.

**Step 7: Draw new waterlines** Two or three waterlines can now be drawn above and below the DWL. If the appearance is not satisfactory, go back to step 6 and change.

**Steps 8 and 9: Add new sections and waterlines** Once this is done, sections 1–9 should be completed as well as 7–10 waterlines. Constant adjustments have to be made in order to create smooth lines in the body plan, as well as in the half breadth plan.

**Step 10: Recheck the displacement and the longitudinal centre of buoyancy** The curve of sectional areas can now be constructed. Its area gives the displacement (excluding that of keel and rudder) and its centre of gravity corresponds to the longitudinal position of the centre of buoyancy. If not correct, adjustments have to be made from steps 5 or 6.

**Step 11: Draw diagonals** Inspect the smoothness, particularly near the stern. Adjust if necessary.

**Step 12: Draw buttocks** This is the final check on the smoothness. Usually only very minor corrections have to be made at this stage.

### Computer aided design of hulls

As mentioned in Chapter 1, most CAD programs use master curves for generating the hull surface. Each curve is defined by a number of points, called vertices. Photo 3.11 shows, in a plan view, the grid of master curves used for generating the YD-40 hull. One of the transverse curves has been selected in Photo 3.12 and it can be seen how the smooth hull surface is generated inside the curve, which is shown as piece-wise linear between the vertices.

Photo 3.11 Grid of master curves used for the YD-40 (the vertical line to the right marks the origin of the coordinate system)

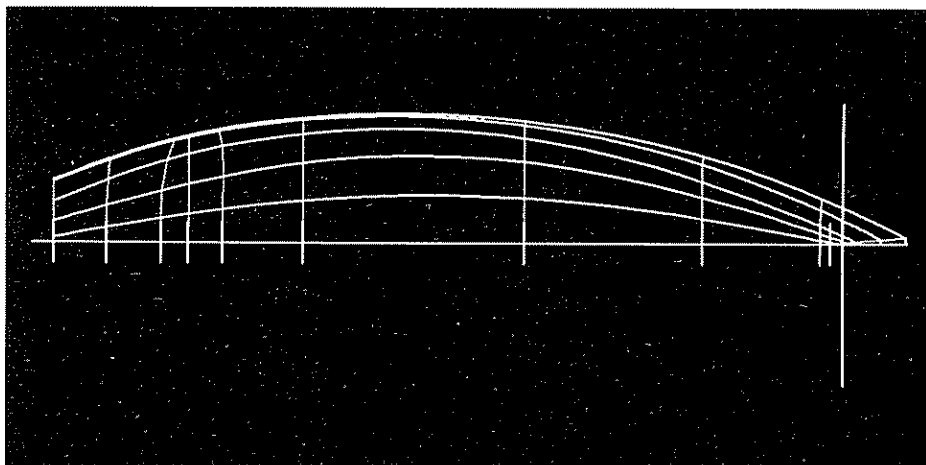
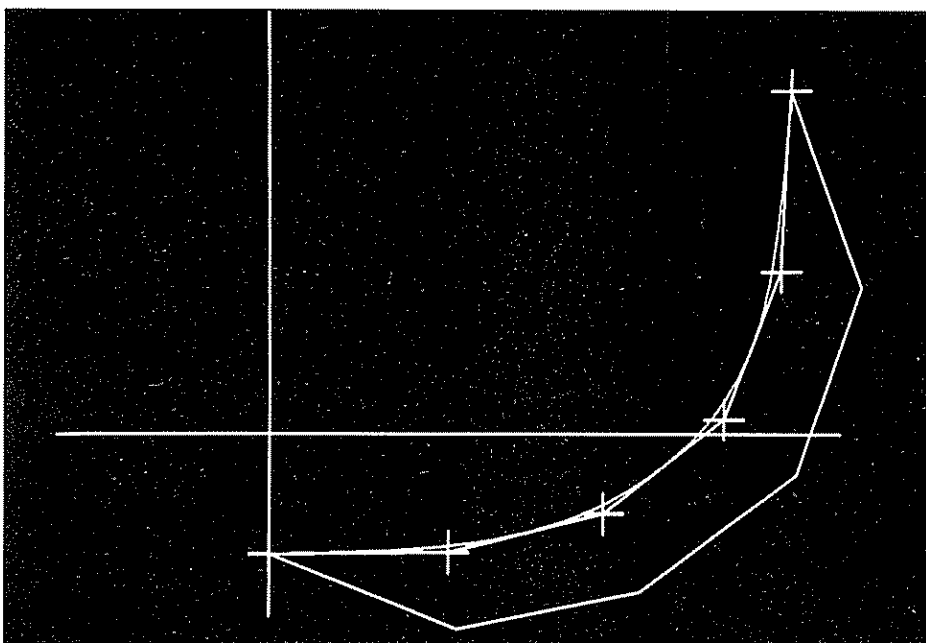


Photo 3.12 A section with vertices (crosses), master curve (between the crosses), hull surface and curvature (outermost line)



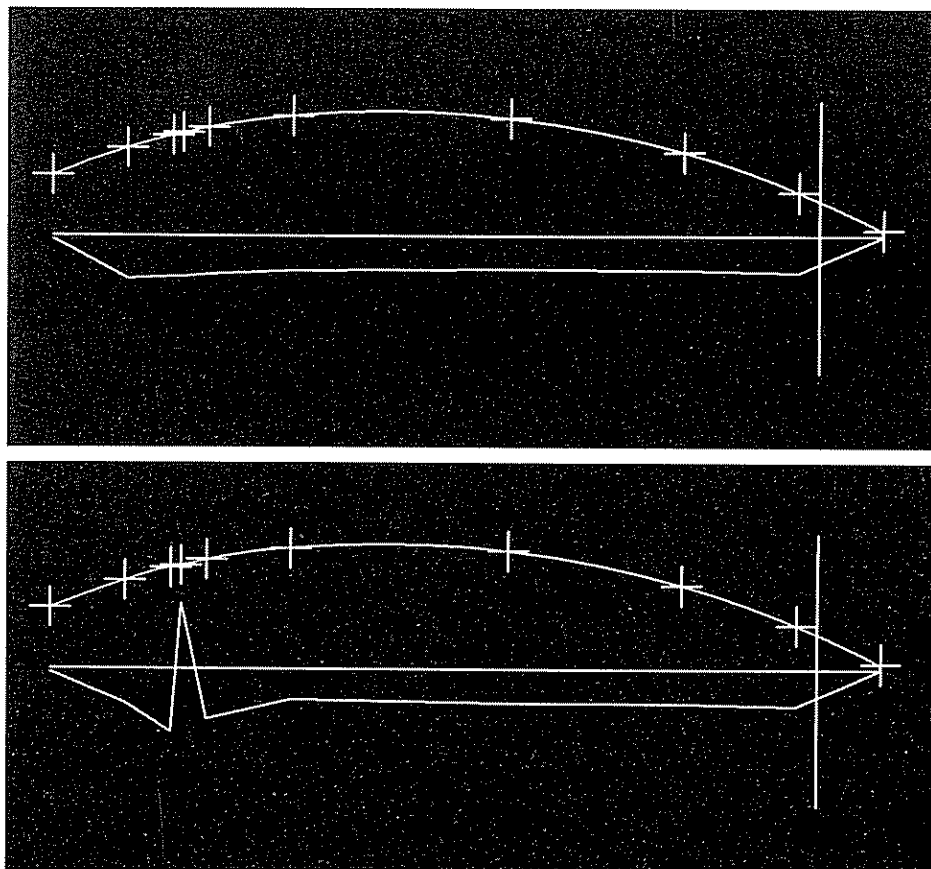
The task of the designer is to specify the vertices in such a way that the desired hull shape is created. There are different ways of achieving this. Some programs start from a long cylindrical body or a box, while others start from a flat rectangular patch, defined by an orthogonal grid. These original shapes are then distorted by moving the vertices around, and it is relatively easy to produce a yacht-like body. However, it takes experience and experimentation to obtain a shape that satisfies criteria

set up beforehand. In practice, designers very seldom start from scratch, but work from earlier designs, which already have a desirable shape and a known grid of master curves surrounding it. Since most new designs are evolutions of previous ones this approach is very natural.

A problem encountered when the first CAD programs for yachts appeared was that the scale on the screen was too small, and the resolution too low to enable the designer to create fair lines. Small bumps on the surface could not be detected on the screen, and it sometimes happened that the bumps were noticed only after the start of the hull construction. Therefore the CAD program developers introduced plots of the curvature of lines on the hull. Such a plot is shown in Photo 3.12. The curvature of the line, which essentially corresponds to a section, is almost constant, except at the ends where it goes to zero.

Photo 3.13 illustrates the sensitivity of the curvature to small changes of the surface. The sheer line is shown in a plan view. In the top photo (the real design) the curvature is smooth and relatively constant along the hull. In the bottom photo one vertex point has been moved 10 mm at full scale perpendicular to the surface. The resulting change in the sheer line is so small that it cannot be detected by eye, but the curvature exhibits a considerable bump and some smaller fluctuations, showing that the line is not smooth. By looking at the curvature, lines may thus be generated that look fair even at full scale.

Photo 3.13 Sheer line with vertices and curvature  
(TOP) Real design.  
(BOTTOM) One vertex point moved 10 mm



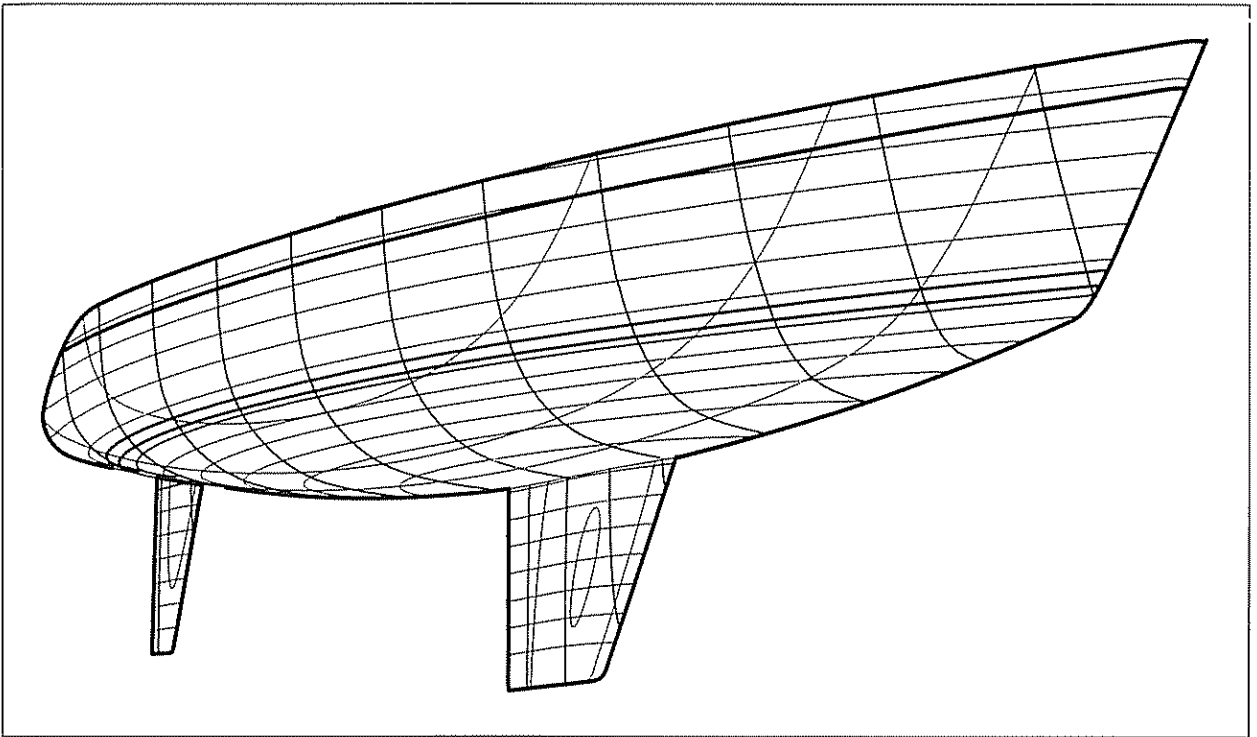


Photo 3.14 *Perspective view of the YD-40*

A great advantage of most CAD programs is that the hull may be shown in perspective. As pointed out in Chapter 1 it is important to study the sheer line in particular from different angles, since the impression of the hull contour in reality is also influenced by the beam distribution, which is not visible if only the profile view is studied. Fig 3.14 shows the YD-40 in perspective, and a good impression can be obtained of the shape.

By using a CAD program a fair hull can be produced rapidly and different requirements may be satisfied without too much work, such as a given prismatic coefficient or longitudinal centre of buoyancy. Meeting such requirements accurately in a manual process is extremely time consuming, so it is understandable that CAD techniques are always used nowadays by professional designers. However, due to the considerable cost of a CAD system, most amateur designers will still have to use the manual approach described above.

# 4

# HYDROSTATICS AND STABILITY

---

Looking back at hull development in the history of yachting, it is obvious that opinion about the optimum shape of a yacht has changed many times. This is due in part to the changing rules, but more recently the changes in design trends reflect the increasing knowledge about the physical laws governing the behaviour of sailing yachts. The aim of this book is to present the state of the art in yacht design. While current knowledge does not provide explanations for all phenomena, there is one area where the basic laws have been known for a long time, and where the methods have been in use by designers for centuries. This is the area of hydrostatics and stability.

Hydrostatics and stability represent perhaps the most important aspects of a design since the properties of a yacht in these respects reflect its ability to carry the required weight and to withstand the heeling moment from the sails. It should be stressed that the exact knowledge of stability is restricted to the static case, with no waves on the water surface. We have, however, chosen to include also dynamic stability in this chapter, although the laws are quite different.

We begin this chapter by introducing some simple ways of computing areas. This knowledge is required in subsequent paragraphs dealing with calculations of the wetted surface, displacement and its centre of gravity, the prismatic coefficient, the water plane area and the related mass per mm of immersion as well as the moment per degree of heel and trim. The discussion of dynamic stability includes stability in waves, methods for reducing roll, requirements for offshore yachts and some statistical information on the righting moment of existing yachts.

## Calculation of areas

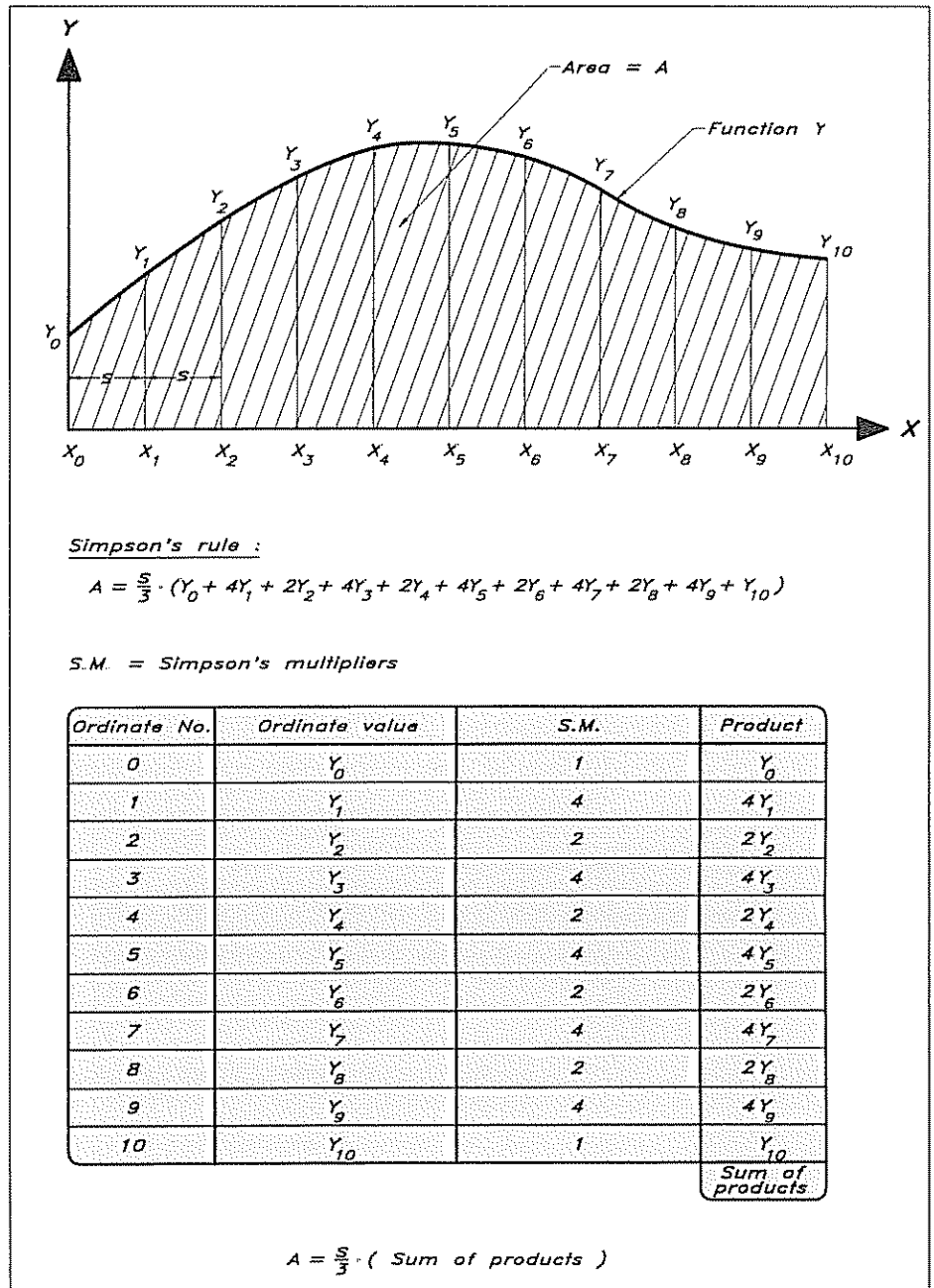
For the amateur designer, one way to obtain the area of a closed curve might be to draw it on a square grid and just count the number of squares. In most cases this method is accurate enough, but it is tedious and would hardly be used by professionals.

Another convenient way is to make use of the planimeter, as explained in the previous chapter. This method is fast and accurate but few amateur designers have access to this handy instrument.

The best choice for many designers is to compute the area using a simple numerical method, based on the ordinates (y-values) of the curve at certain intervals. Such methods are often included in the subroutine package of electronic calculators, but if this option is not available it is simple to apply the method from first principles.

Fig 4.1 introduces the most common numerical method for computing

Fig 4.1 Simpson's rule



areas. It is called Simpson's rule, and is quite popular in naval architecture. Since the sequence of operations is always the same when applying Simpson's rule a special scheme, shown in Fig 4.1, may be employed. The distance between the end points of the interval, in this case  $X_0$  and  $X_{10}$ , is divided into an even number of equidistant steps, in this case 10. The step size is denoted  $S$ . Values of the function  $Y$  are computed for all  $X$ -values and may be inserted into the table in the column 'ordinate value'. By multiplying each value by its Simpson multiplier, 1 for the end values and 4 and 2 alternating for the others,

and adding all the products the 'sum of products' is obtained. The area  $A$  under the curve  $Y$  is then simply obtained as this sum multiplied by the step size divided by 3.

Of course, the number of steps may be other than 10, but the number has to be even in Simpson's rule. In many applications within yacht design the number of steps is indeed 10, due to the standard division of the waterline from station 0 to station 10, but sometimes a higher accuracy is needed near the ends, where half stations may be introduced. The principle of Simpson's rule may still be used, by considering end intervals as pairs of halves, but the number of full intervals must always be even, so normally two or four intervals have to be divided. Fig 4.3 shows the change caused by dividing an interval into two halves. In the following discussion, we will always refer to Simpson's rule for area calculations. However, the other methods mentioned above may be used as alternatives.

### Wetted surface

Due to the three-dimensional nature of the hull an exact calculation of the wetted surface is complicated, but a good approximation may be obtained as explained in Fig 4.2. If the girth length  $g$  along the surface from the keel to the waterline is measured at each station, and plotted against the longitudinal position on the hull from bow to stern, the area  $A$  under the curve is a reasonably good representation of the wetted surface of one half of the hull. The computation of this area is also shown in Fig 4.2. The values for the YD-40 are given in brackets.

The problem with the computed area is that the longitudinal slope of the hull, as seen in the waterlines or the diagonals, is not considered. The effect of this is small, but a more accurate result is obtained by adding 2–4%, ie by multiplying by a 'bilge factor'  $c$ , which is in the range 1.02–1.04. The bilge factor can be estimated by comparing the length of a typical diagonal with the straight line distance between the end points of the waterline.

To simplify the presentation as much as possible, we have chosen to use full-scale entries for all formulae. Measures obtained from the drawings therefore have to be converted to full scale before being used in the calculations. In this way the somewhat confusing exercise with scale factors of various powers can be avoided in the different formulae. Note also that many calculations, like the present one, are made for only one half of the hull. Where this is the case the final value is therefore obtained only after multiplying by 2.

A very fast, but somewhat more approximate method to find the wetted surface is to make use of an empirical formula based on the length, beam, draft, displacement and prismatic coefficient of the canoe body (as shown in Fig 4.2). For smooth hulls this formula is surprisingly accurate, but if a drawing of the hull is available the method above is recommended.

### Displacement

According to Archimedes' principle the mass of a floating body is equal to the mass of the displaced volume of water. Thus the volume displacement of the yacht,  $\nabla$ , multiplied by the density of water,  $\rho$  (ie the weight





displacement  $m$ ), has to be equal to the total mass of the yacht.

In this chapter we will deal with the calculation of the volume displacement, while the mass of the yacht will be discussed in Appendix 2. It should be noted, that  $\rho$  is equal to  $1000 \text{ kg/m}^3$  for fresh water, but varies for salt water, depending on the salinity. As an average value for salt water  $1025 \text{ kg/m}^3$  may be used.

To obtain the volume, the curve of sectional areas has to be determined first. This is obtained by plotting the area of each section (the submerged part) at a suitable scale in the half breadth plan, as explained in Chapter 3. A difficulty encountered when applying Simpson's rule to compute the area  $A_s$  of a section is that the ordinates are not known at suitable intervals, so each section has to be properly divided (see Fig 4.3).

The ordinates in Fig 4.3 are the half breadths arranged in such a way that the depth *at that section* is divided into five parts. Half spacing is used in the lowest interval, since the ordinates vary rapidly in that region. The Simpson multipliers are thus changed in this interval, but otherwise the normal scheme may be used.

Having obtained all the areas of the sections and had them plotted to obtain the curve of sectional areas (as in the lines plan of Fig 3.5), the displacement is obtained as the area under the curve. Fig 4.4 shows how this is computed using Simpson's rule. Note again that full-scale values are used throughout and that the values for the YD-40 are given in brackets.

**Centre of buoyancy**

The moment created by a force with respect to a perpendicular axis is

Fig 4.3 Calculation of the sectional area

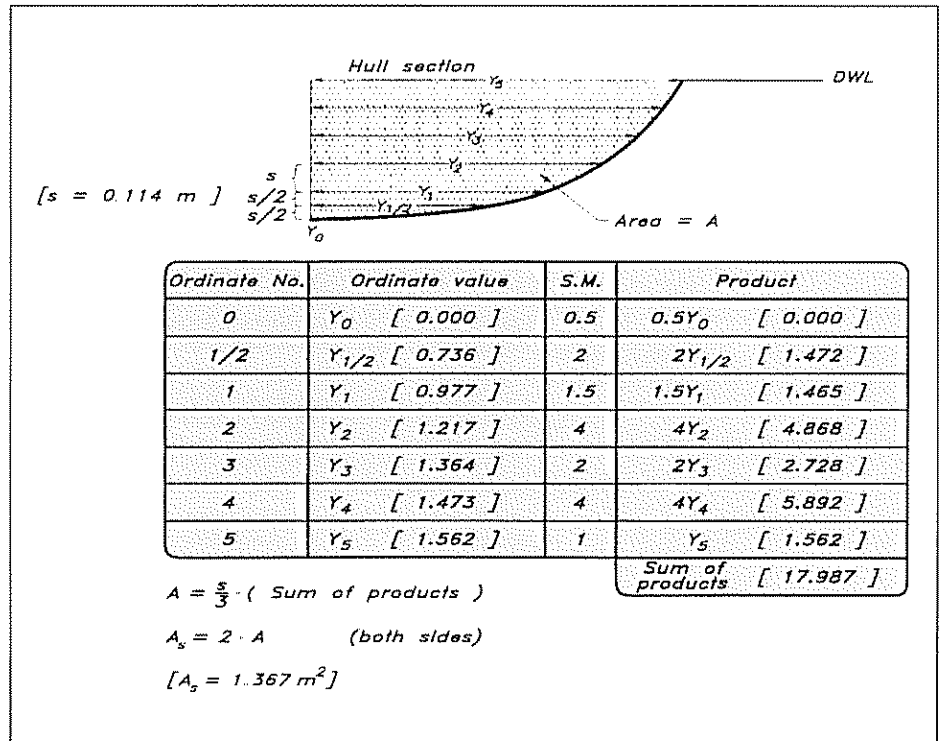
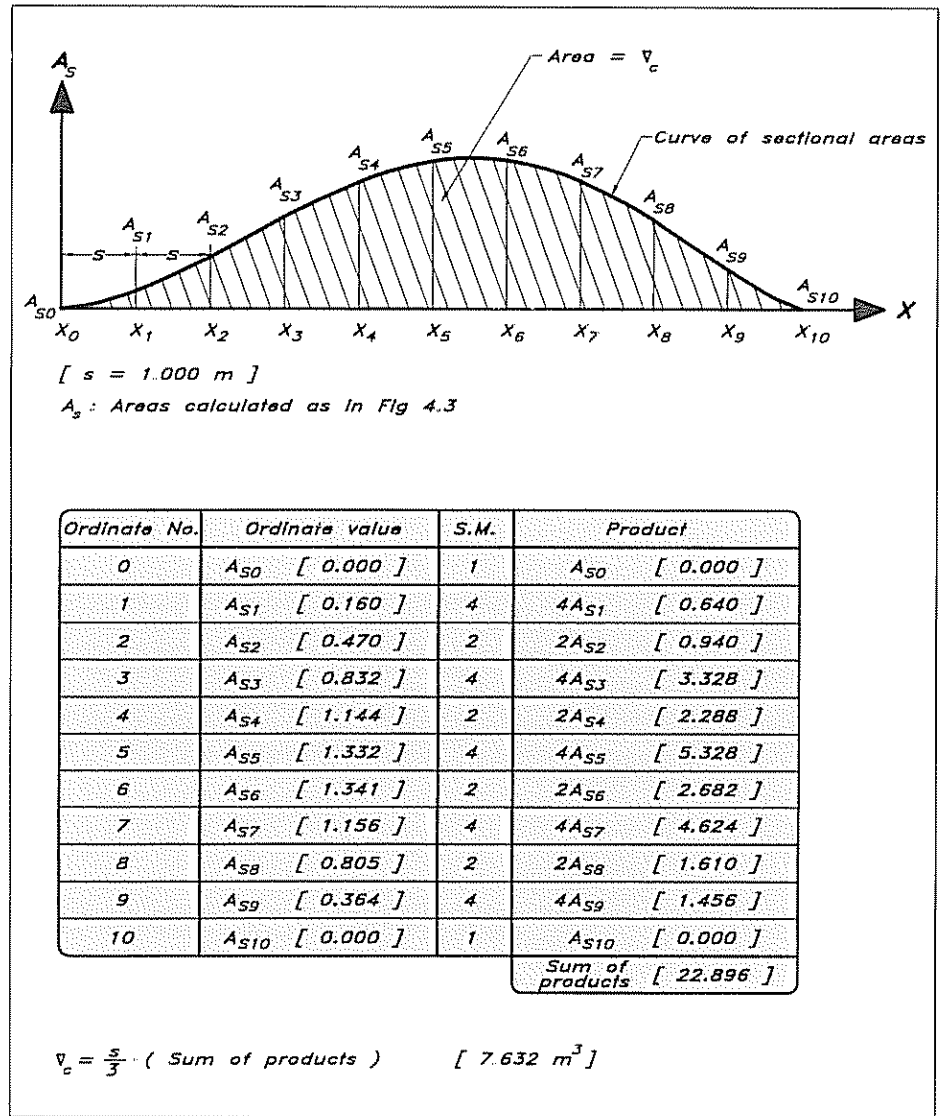


Fig 4.4 Calculation of the volume displacement

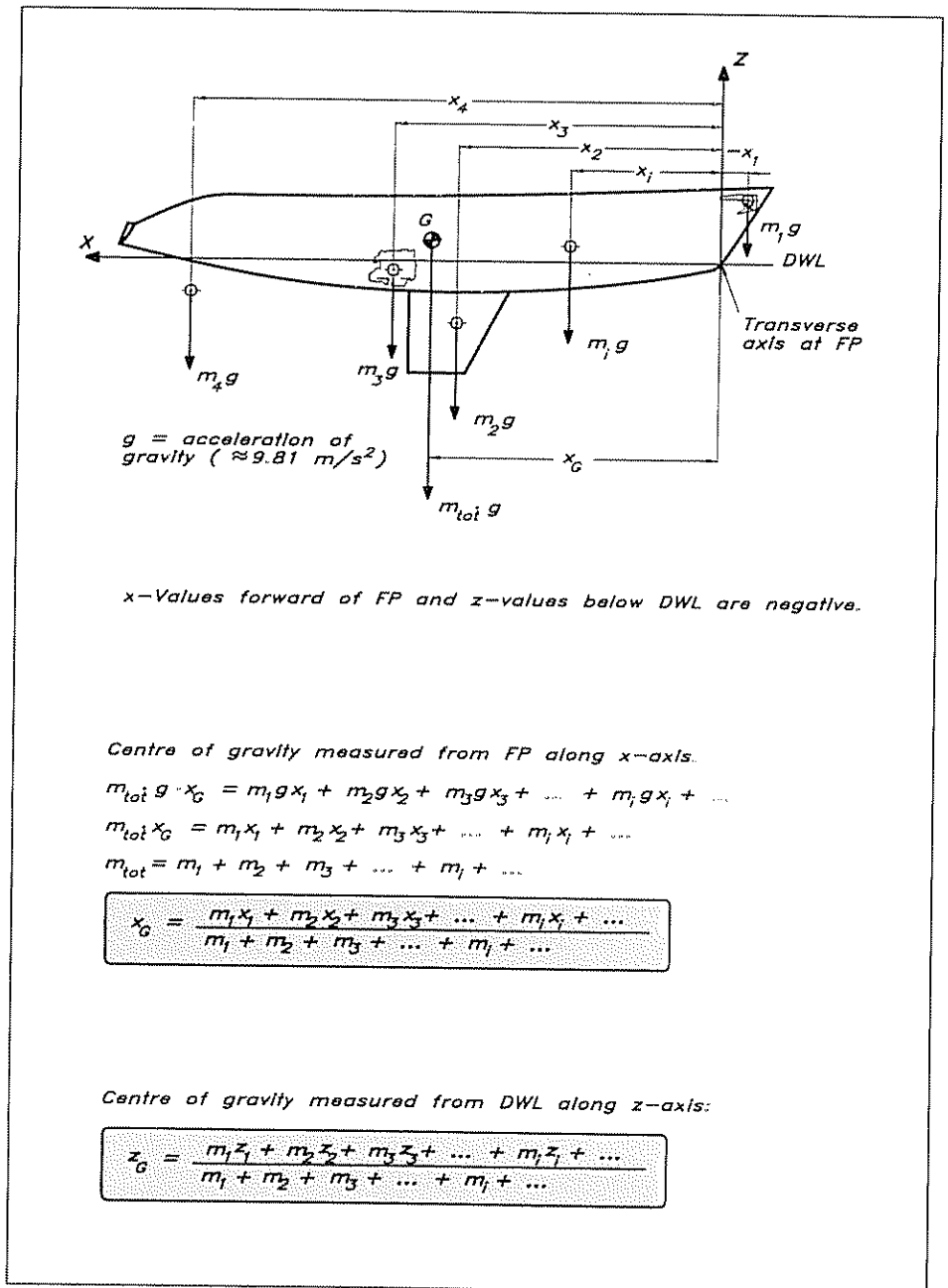


the product of the force and the distance to the axis (the lever arm). This concept can be used for finding the centre of gravity of a body. By definition, the centre of gravity is the point where the mass of the body may be assumed concentrated. The gravitational force may be assumed acting at this point.

One way to calculate the distance to the centre of gravity from an arbitrary axis, is to add the moments of the different parts of the body with respect to this axis. This gives a resulting moment, which must be equal to that of the concentrated mass at the centre of gravity. This method is explained in Fig 4.5, where the axis chosen is located athwartships at the FP.

A corresponding computation can be performed for the centre of gravity of the displaced volume of water, ie the centre of buoyancy. Let us first compute the longitudinal position, LCB, using the same axis as

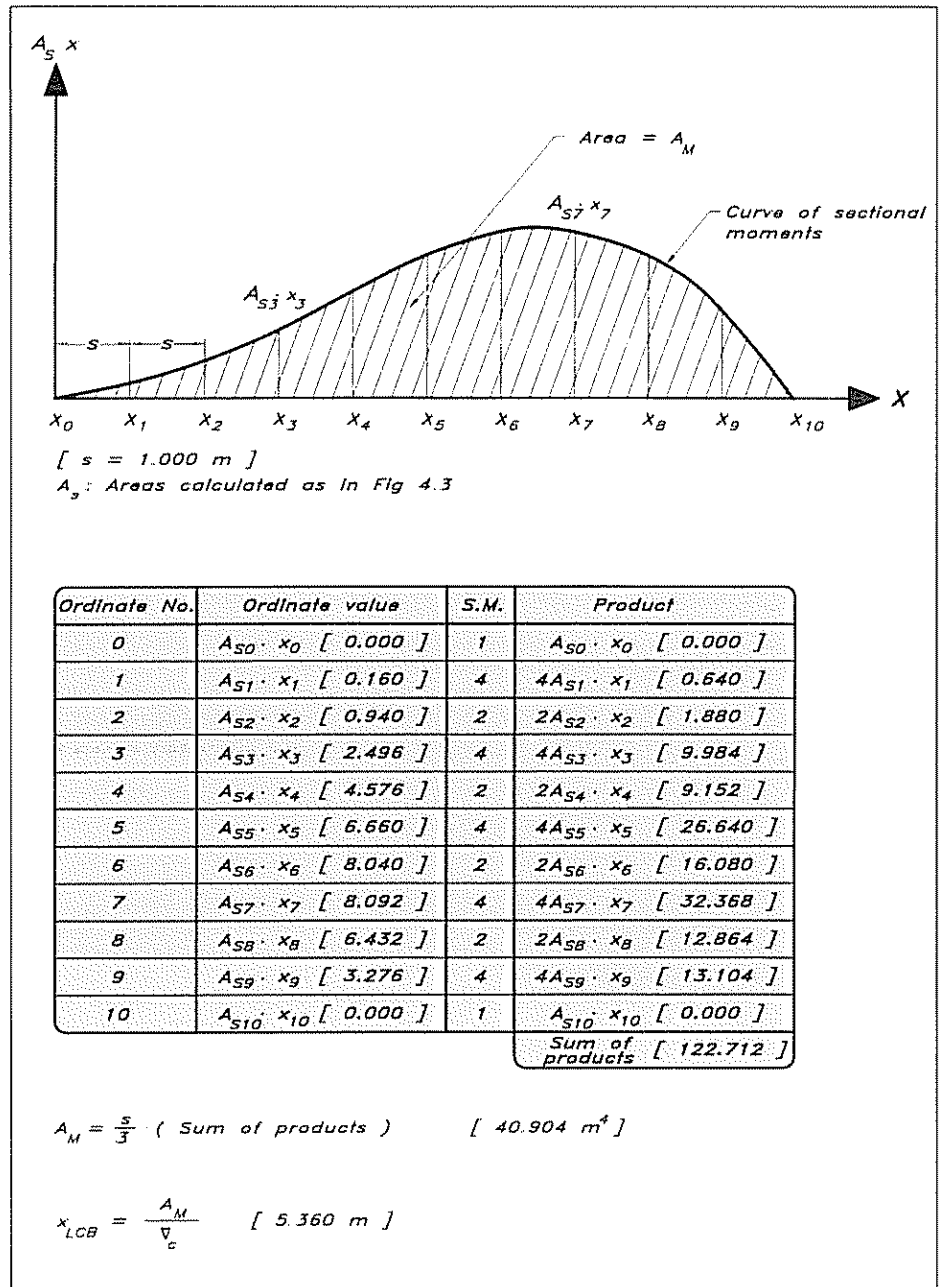
Fig 4.5 Methods of finding the centre of gravity



before. Each section of the hull may now be considered as contributing to the moment by an amount proportional to its area multiplied by its distance from the FP. Thus a 'curve of sectional moments' can be constructed in a similar way to the curve of sectional areas. The area under the new curve represents the total moment, from which the position of the centre of buoyancy can be obtained as explained in Fig 4.6.

There is a simple alternative method, which is used frequently for determining the LCB. If carefully employed, this method is probably as accurate as the numerical one. The sectional area curve is simply cut out in a piece of cardboard and the cut out part is balanced on the edge

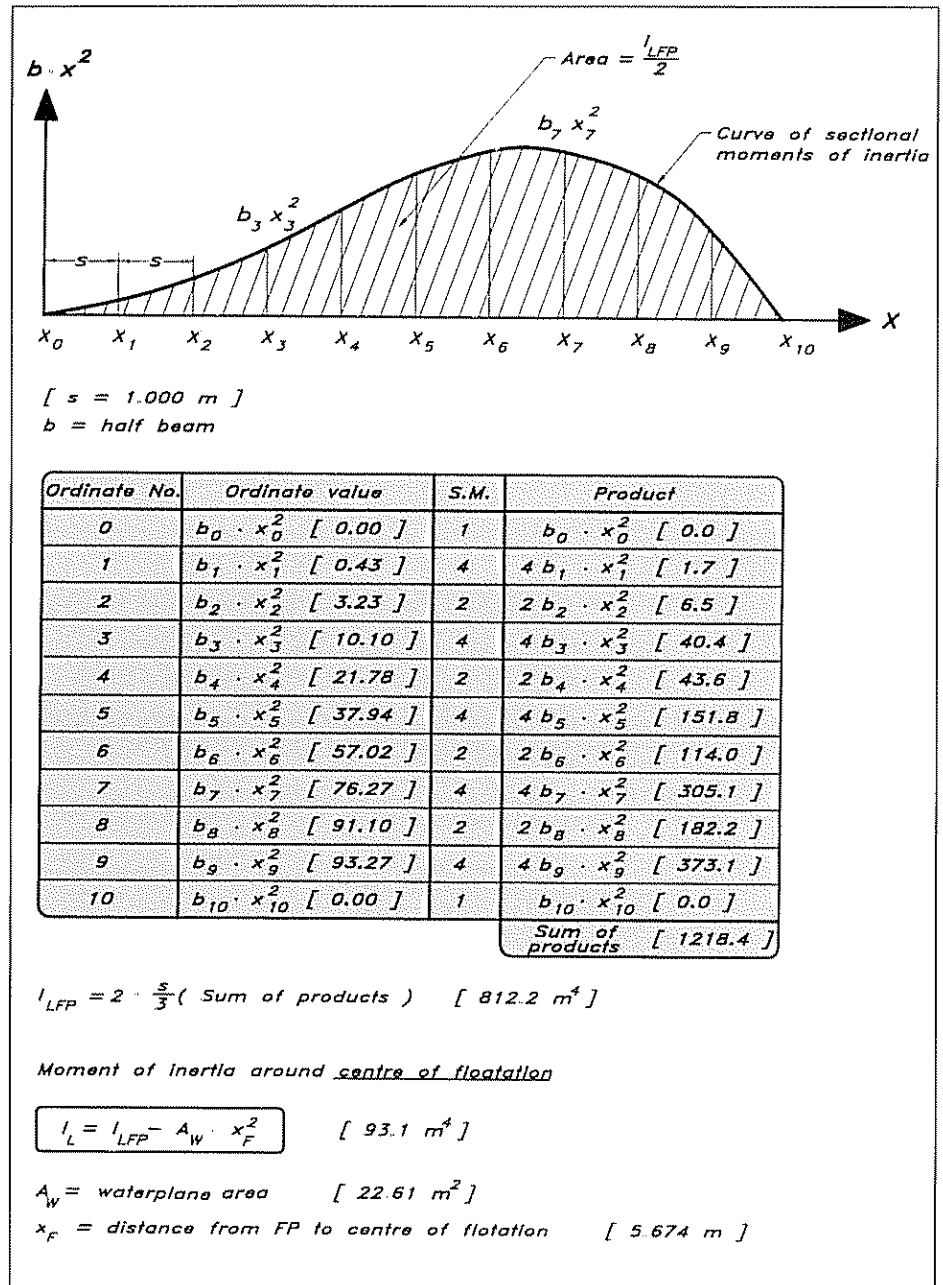
Fig 4.6 Calculation of the longitudinal centre of buoyancy of the canoe body



of a knife at right angles to the longitudinal axis. When the cardboard is balanced, its centre of gravity is on the edge of the knife. This is also the position of the LCB. If the piece is hung on a needle and allowed to rotate, the vertical line through the needle crosses the centre of gravity. By hanging the piece at two positions and using a plumb bob to mark the vertical lines, the centre of gravity is found at their intersection.

For the determination of the vertical position of the centre of buoyancy (VCB), the vertical distribution of sectional moments must be considered. If the areas of several waterlines are known, the vertical distribution of the volume can be plotted in the form of a curve. This curve can then be

Fig 4 7 Calculation of the longitudinal moment of inertia

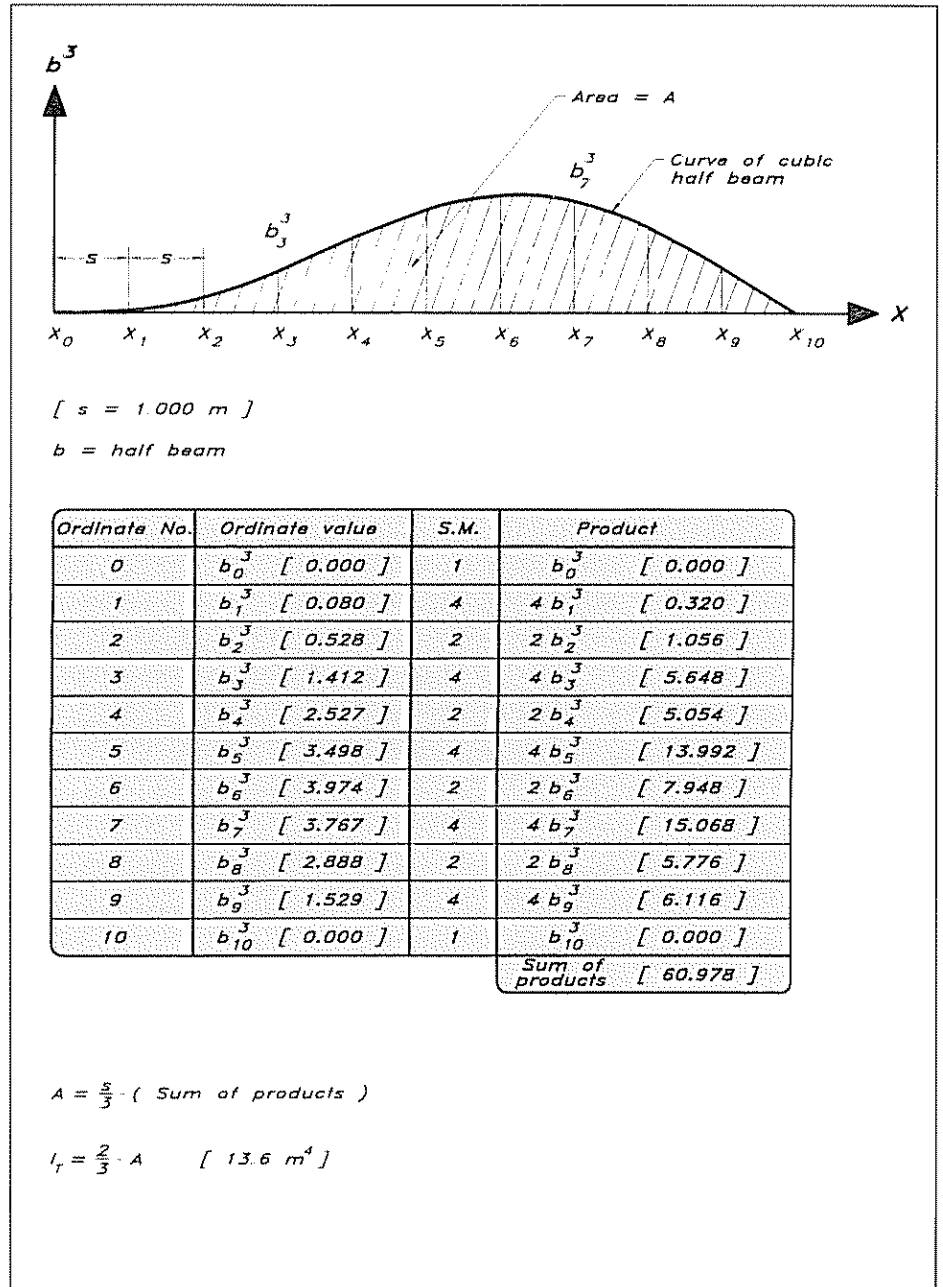


treated in the same way as the sectional area curve and the location of the VCB can be found. However, the areas of the waterlines might not be known, since they are not normally required for other purposes. Another possibility is to cut out all sections of the hull from a piece of paper and glue them together just as in the body plan. The vertical position of the centre of gravity for this paper body is the desired VCB.

### Water plane area

The water plane area, ie the area inside the designed waterline (DWL), is important in several respects: first, its size determines 'the weight per mm immersion', ie the additional weight required to sink the hull a

Fig 4.8 Calculation of the transverse moment of inertia



certain distance; secondly, its centre of gravity is located on the axis around which the hull is trimmed, when moving a weight longitudinally on board; thirdly, the so-called moment of inertia (sometimes called the second moment of area) around a longitudinal axis determines the stability at small angles of heel; and fourthly, the moment of inertia around a transverse axis through the centre of gravity (of the area) yields the longitudinal stability, ie the moment required to trim the hull a certain angle.

The calculation of the area is straightforward, using Simpson's rule exactly as shown in Fig 4.1. If the area is denoted  $A_{DWL}$  (full-scale value),

the additional displacement when sinking the hull 1 mm is  $0.001 \cdot A_{DWL}$  m<sup>3</sup>. The mass of this volume, corresponding to the applied mass on the hull, is  $\rho \cdot 0.001 \cdot A_{DWL}$ , where  $\rho$  is the water density. The mass per mm immersion is thus calculated from this simple formula.

As appears from the previous paragraphs the centre of buoyancy is determined from the geometrical centre of gravity of the sectional area curve. Either a numerical method, like Simpson's, or the simple 'cardboard' method can be used for the calculation. To obtain the geometrical centre of gravity of the water plane area, usually called the 'centre of flotation', the same techniques can be employed.

No simple method is available for finding the moment of inertia, but the numerical calculation is similar to that of the centre of gravity. Let us first calculate the longitudinal moment of inertia  $I_{LFP}$  about a transverse axis at the FP. A 'curve of sectional moments of inertia' can now be constructed, where each ordinate is the product of the waterline half-width and the *square* of the distance from the FP. The area of this curve can be used for finding the full-scale moment of inertia (both sides) in the usual way (see Fig 4.7).

In the formula for longitudinal stability, to be presented in the next section, the moment of inertia  $I_L$  is taken about an axis, not through the FP, but through the centre of flotation. The calculated value  $I_{LFP}$  may, however, be converted to  $I_L$  quite simply, as shown in Fig 4.7.

In principle, the transverse moment of inertia  $I_T$  around the longitudinal axis, needed for the transverse stability, could be computed in a similar way, but then the water plane area would have to be divided into a set of longitudinal strips, which could be treated like the transverse ones above. This division is impractical, however, since it is not used in any other calculation. An alternative method is therefore shown in Fig 4.8. Note that, for reasons of symmetry the longitudinal axis has to pass through the centre of flotation, so no correction need be applied.

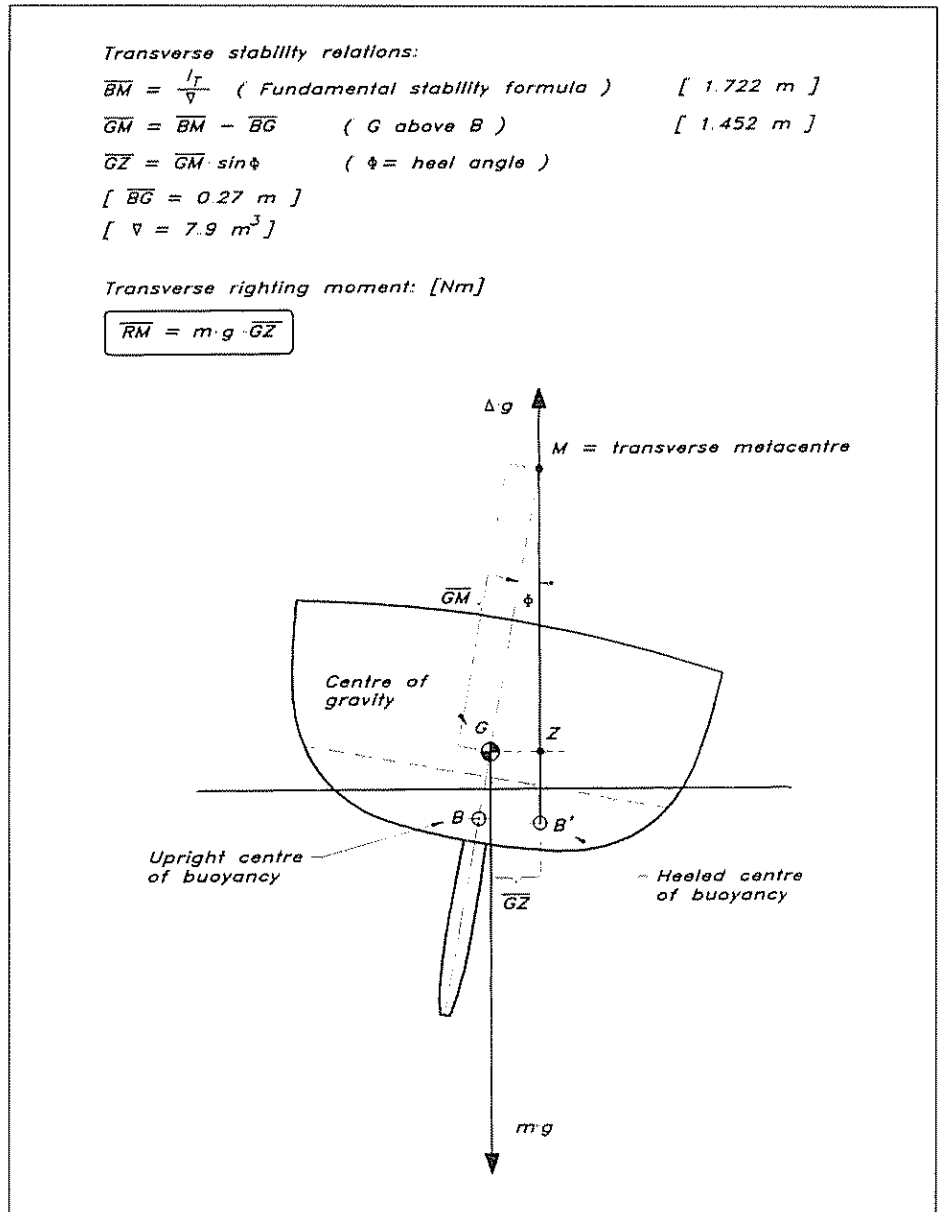
### Transverse and longitudinal stability at small angles

The transverse stability of a yacht may be explained with reference to Fig 4.9. When the yacht is heeled the centre of buoyancy moves to leeward from B to B'. The buoyancy force, upwards, then creates a couple with the equally large gravity force acting downwards at G. The lever arm is usually called  $\overline{GZ}$  and the righting moment is  $m \cdot g \cdot \overline{GZ}$ , since the gravity force is the mass, m, times the acceleration of gravity, g (9.81 m/s<sup>2</sup>).

There is another important point marked in the figure: the transverse metacentre, M. This is the intersection between the vertical line through B' and the symmetry plane of the yacht. For small angles of heel this point may be assumed fixed, which simplifies the calculations considerably. The distance between G and M,  $\overline{GM}$ , is called the metacentric height and  $\overline{BM}$  is the metacentric radius. A fundamental stability formula (which will not be proven here) says that the metacentric radius is equal to the ratio of the transverse moment of



Fig 4.9 Transverse stability



inertia  $I_T$  and the volume displacement  $\nabla$ . Using this formula and some simple geometric relations the righting moment may be obtained as explained in Fig 4.9.

Since the stability of the yacht is proportional to  $\overline{GM}$  there are two principal ways of increasing it. Either  $G$  may be lowered or  $M$  may be raised. A low  $G$  is found on narrow, heavy yachts with a large ballast ratio, like the 12 m and other R yachts. They have weight stability. Modern racing yachts, on the other hand, are wide and shallow, which raises  $M$ . They have form stability.

The method of calculating the longitudinal stability corresponds exactly to that of the transverse stability. Thus, the restoring moment when the hull gets a trim angle, may be computed from the formulae of

Fig 4.10 Longitudinal stability

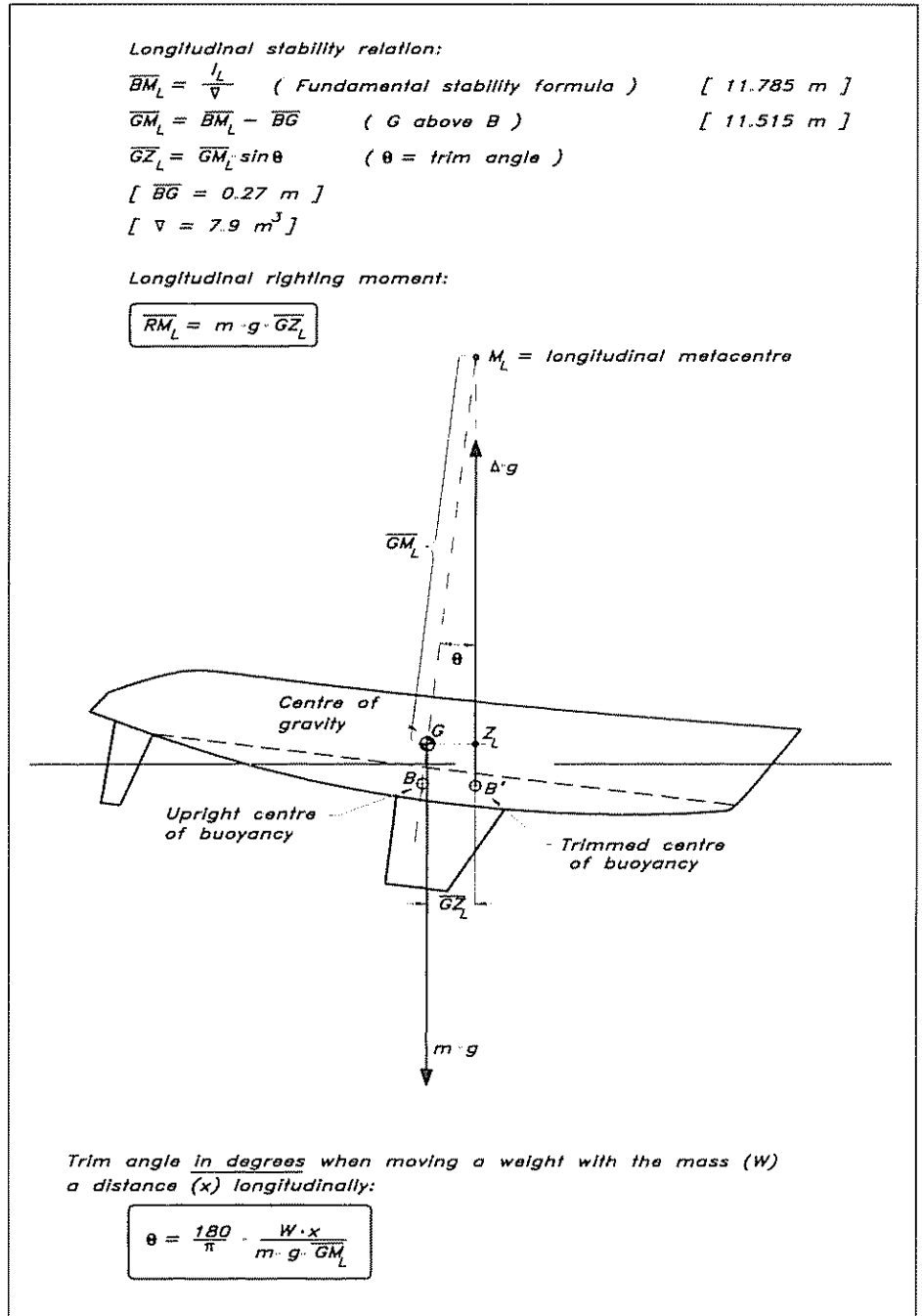


Fig 4.10, which correspond to those of the previous figure. There is also a formula for computing the trim angle obtained when moving a weight longitudinally on board the yacht.

### Transverse stability at large angles of heel

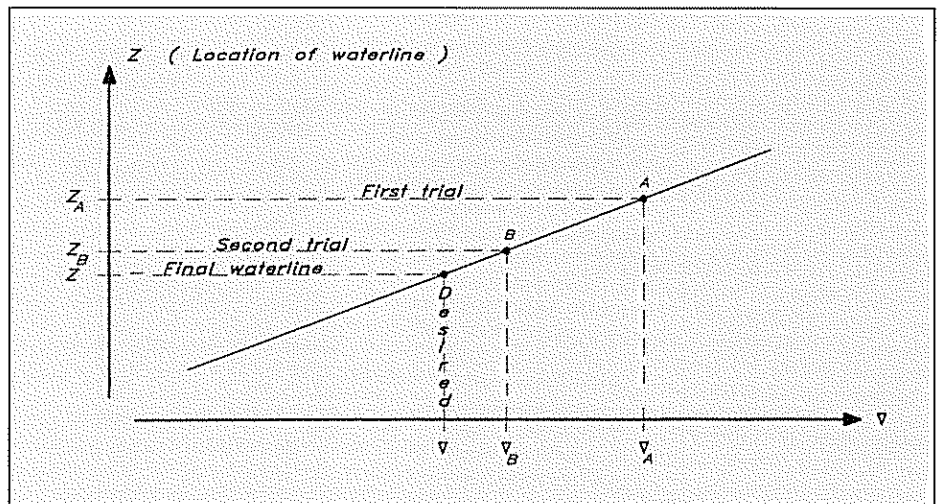
The calculation of the righting moment at large heel angles is considerably more complicated than that for small angles. One difficulty arises from the fact that the positioning of the heeled hull with respect to the water surface is not known. If the hull is just rotated about the

centreline (at the level of the DWL), the displacement will generally become too large and a trimming moment will develop. The only way to overcome this difficulty is by trial and error, ie by trying several attitudes, varying the sinkage and trim systematically, in order to find a position where the displacement and LCB correspond to the original ones.

After finding the right attitude a considerable amount of calculation is needed to find the righting moment, since no simple formulae, like those for small heel angles, are available. In practice, these calculations have seldom been carried out manually even for ships, because before the computer era naval architects made use of a special instrument, called an integrator, a development of the planimeter. Such an instrument is, however, rarely available to the yacht designer, so we will propose a slightly more approximate method, which is often accurate enough. The method is illustrated in Fig 4.11. Special care must be taken, however, with very beamy yachts with large fore and aft asymmetry. Such hulls will develop a considerable trim when heeling, and this effect is not considered here.

To find the attitude of the hull, rotate it first around the centreline at DWL to the desired angle. Then calculate the displacement  $\nabla_A$  up to this waterline located at  $Z_A$ . This cannot be done, however, without knowing the shape of the sections on both sides of the symmetry plane, so the body plan has first to be completed to include both sides of the hull.

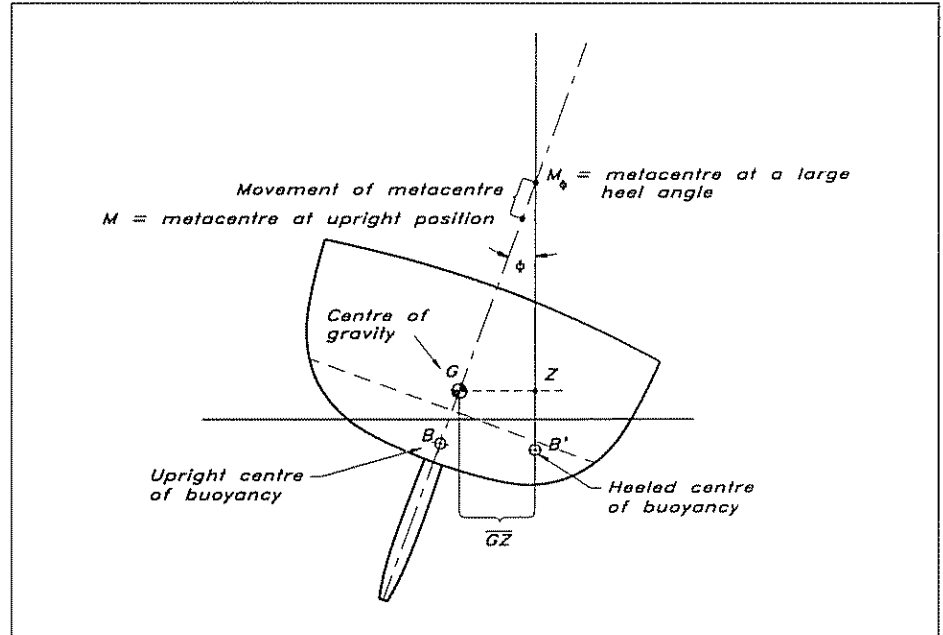
Fig 4.11 Procedure to find the heeled waterline



The displacement  $\nabla_A$  is bound to be too large, so a new waterline at  $Z_B$  has to be found. A first estimate of this line can be made by dividing the excess displacement by the area of the original DWL. This gives the approximate distance to the new waterline at  $Z_B$ , for which the displacement  $\nabla_B$  is also computed. Not even this is likely to be very accurate, but the final position  $Z$  of the waterline can be found by interpolation or extrapolation to the right  $\nabla$ , as explained in the figure. In this way the displacement will be quite accurate, although all effects of trim are neglected.

Having found the waterline, the 'cardboard method' is used to find the transverse position of the centre of buoyancy,  $B'$  in Fig 4.12. All heeled sections below the waterline are cut out in cardboard and glued together in their correct positions. The centre of gravity can then be found from the intersection of two lines, obtained using a plumb bob, as explained above.

Fig 4.12 Stability at large angles of heel



Knowing  $B'$ , the location of the point where the vertical through  $B'$  hits the centre plane  $M_\phi$  can be found, see Fig 4.12.  $\overline{BM}$  may then be measured from the figure and the remaining formulae for small angles applied.

### Curve of static stability

The curve of static stability represents the righting moment at varying angles of heel. An example of this is given in Fig 4.13. Since the moment differs from the lever arm only with respect to the constant  $\Delta g$ , the vertical scale could equally well represent  $\overline{GZ}$ .

For small angles  $\overline{GM}$  is constant and  $\sin \Phi \approx \Phi$  (in radians), so  $\overline{GZ}$  is proportional to the heel angle, ie  $\overline{GZ} = \overline{GM} \cdot \sin \Phi \approx \overline{GM} \cdot \Phi$ . The slope of the  $\overline{GZ}$  curve at the origin may thus be obtained by noting that the tangent should pass through the point  $\overline{GZ} = \overline{GM}$  for  $\Phi = 1$  radian, ie at  $57.3^\circ$ .

Another important aspect of the  $\overline{GZ}$  curve is the maximum, which represents the largest possible righting moment of the hull. Obviously the yacht will capsize if the heeling moment exceeds this level.

Of great interest is the so-called stability range, which is the range of angles for which a positive righting moment is developed. For larger angles the hull is stable upside-down.

It is also of interest to note that the area under the RM curve up to

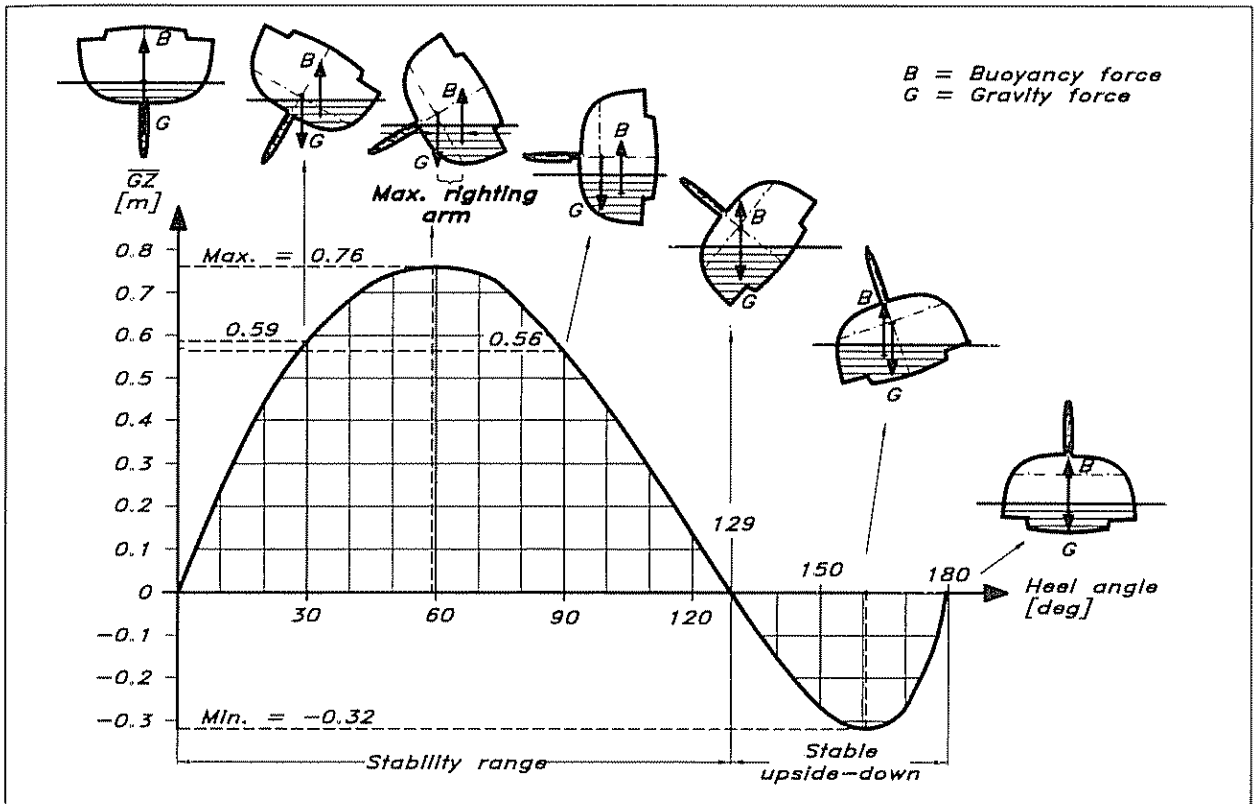


Fig 4.13 The curve of static stability – YD-40

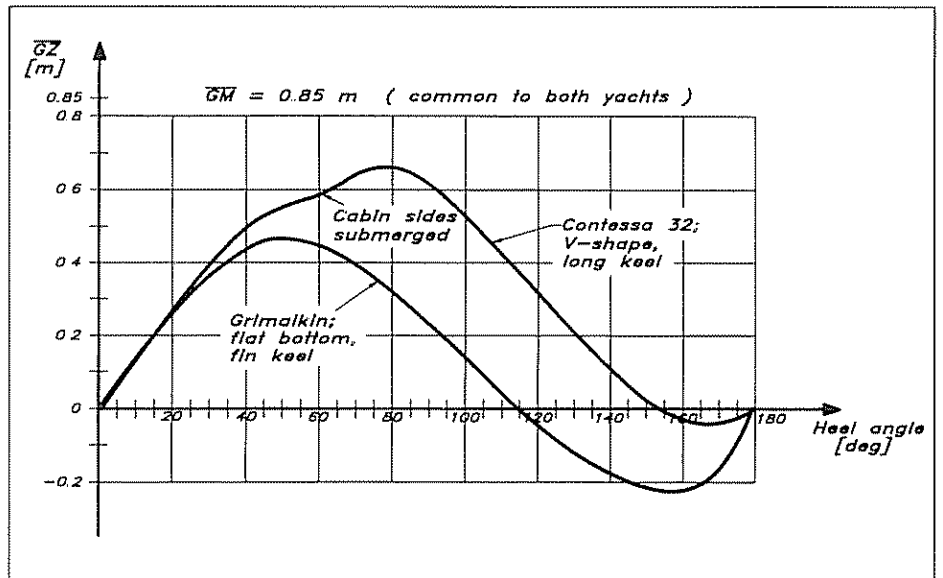


Fig 4.14  $\overline{GZ}$  – Curves for Grimalkin and the Contessa 32

a certain angle represents the work, by waves for instance, needed to heel the hull to this angle.

Large differences are found in the stability curves for modern fin-keel yachts and traditional V-shaped long keel ones. After the Fastnet Race disaster in 1979, a study was carried out at Southampton University, in which two yachts of similar size were compared. Both raced in Class V.

One was a cruiser-racer, the Contessa 32, while the other one was an extreme racer, *Grimalkin*, 30 foot LOA.

Interestingly enough both yachts have the same  $\overline{GM} = 0.85$  m (as appears from Fig 4.14, which shows the  $\overline{GZ}$ -curves). This does not mean, however, that RM is exactly the same for small angles, since the mass differs: 4600 kg for the Contessa 32 and 3800 kg for *Grimalkin*. At  $1^\circ$  of heel RM is 670 Nm (Newton-metres) and 550 Nm, respectively. It should be noted that the sail area is almost exactly the same for both yachts.

A larger difference is found in the maximum  $\overline{GZ}$ , which is about 40% higher for the Contessa 32. Converted into righting moment the difference is even larger. For the Contessa 32  $RM_{\max}$  occurs at about  $80^\circ$  and is equal to 30200 Nm, while for *Grimalkin*  $RM_{\max}$  is only 17900 Nm at about  $50^\circ$ .

A more significant difference is also found in the stability range. The Contessa 32 is stable up to about  $155^\circ$  while zero righting moment occurs already at about  $115^\circ$  for *Grimalkin*. There is thus a very small range of angles,  $25^\circ$ , where the Contessa 32 is stable upside down, and the area between the RM curve and the horizontal axis is very small in this range. For *Grimalkin* the corresponding range is about  $65^\circ$  and the area is significant. This means that it is considerably more difficult to put the latter yacht into the upright position once it has capsized. The amount of work required by wind and waves is large, so this yacht may be expected to stay upside down for some time, perhaps a few minutes, while the Contessa 32 would return to the upright position almost immediately after a knockdown.

From this discussion it is clear that the traditional yacht is safer under rough conditions than the more modern one. In the following paragraphs we will elaborate further on the effects of waves on stability, before we present some statistics and criteria for the seaworthiness of ocean-racing yachts.

## Rolling

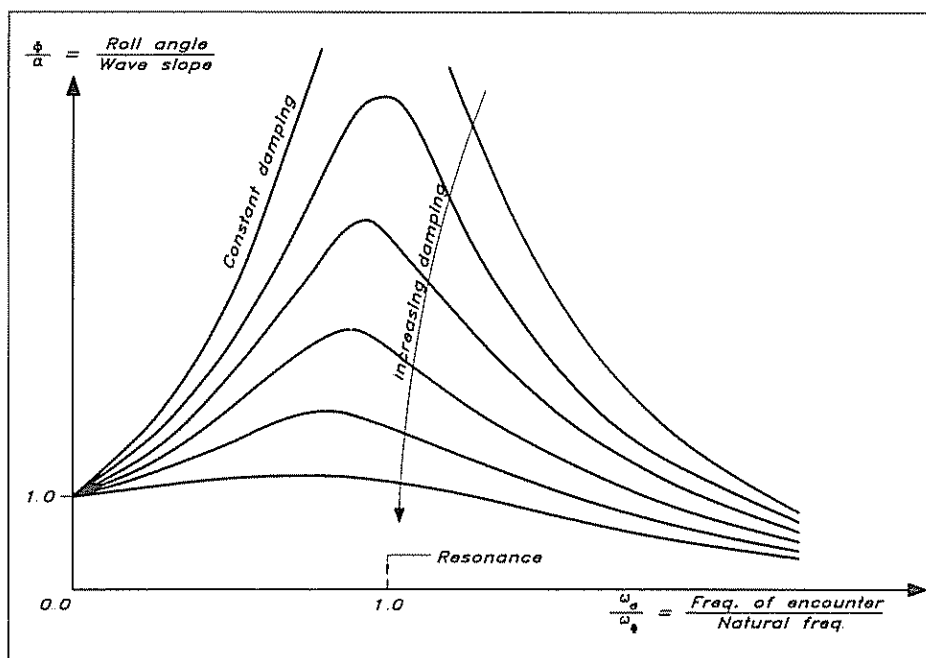
A sailing yacht in a seaway moves in all six degrees of freedom, ie surge, sway, heave, roll, pitch and yaw. The first three are linear motions in the longitudinal, transverse and vertical directions, while the remaining three are rotations around a longitudinal, transverse and vertical axis, respectively. From a safety point of view, rolling is the most important motion, and it will be dealt with in this and the following section. More important for the added resistance in waves are the pitching and heaving motions, and these will be discussed in Chapter 5, in connection with hull design.

If a hull is given a heel angle in still water and is then suddenly released, the righting moment will immediately tend to put the hull upright. The hull starts rolling back to its upright position, but due to its inertia it will not stop when the heel angle is zero. Rather, it will continue to roll over to the other side, where an opposing righting moment develops. The hull then rolls back and forth, until the motion is damped out. In fact, for a sailing yacht, the damping is very large, so the motion dies rapidly.

This example contains many of the important features in connection with rolling excited by a seaway. Of great importance is the frequency with which the hull rolls in the still water test; the so-called natural frequency. The higher the stability, and the lower the inertia, the larger the natural frequency. It can easily be imagined that if the frequency of the waves hitting the hull in rough water is the same as the natural frequency (resonance), very large motions may result, at least if the damping is small.

This phenomenon is clearly borne out in Fig 4.15. The horizontal scale is the frequency of encounter of the waves divided by the natural frequency of the hull, and the vertical scale is the roll angle divided by the wave slope. Several curves are shown in the diagram, each one with a constant damping. Note that the lowest curves represent the largest damping.

Fig 4.15 Roll amplitude for varying frequencies and damping



If the frequency of encounter is low or the natural frequency high, small values are obtained on the horizontal axis. This is where all curves converge into a value of one on the vertical axis. The roll angle is then the same as the wave slope. This may happen for long ocean waves after a gale, where most hulls will follow the wave contour. A liferaft, with a very small inertia, ie high natural frequency, will follow the wave contour for much shorter waves of higher frequency also, since the value on the horizontal scale is still very low. At the other end of the spectrum all curves tend to zero. This is where the waves hit the hull at such a high frequency that it does not have the time to react, an unlikely situation for waves of any significant height.

A dangerous condition is when the frequency of encounter is close to the natural frequency, ie close to resonance. As appears from Fig 4.15

the roll angle may then be several times larger than the wave slope and the yacht may capsize. We will now discuss the various means of avoiding this situation.

If the yacht approaches resonance, ie the frequency of encounter gets close to the natural frequency, one of these frequencies must be changed. The most straightforward way of doing this is to change the course. Since the frequency of encounter depends both on the wave speed (and length) and the speed component of the yacht in the direction of wave propagation, changing the course will change this frequency. If the yacht beats to windward many more waves are met per minute than if it runs downwind with the waves. This technique of avoiding excessive roll is used also on large ships under severe conditions. Speed reductions are also possible, of course.

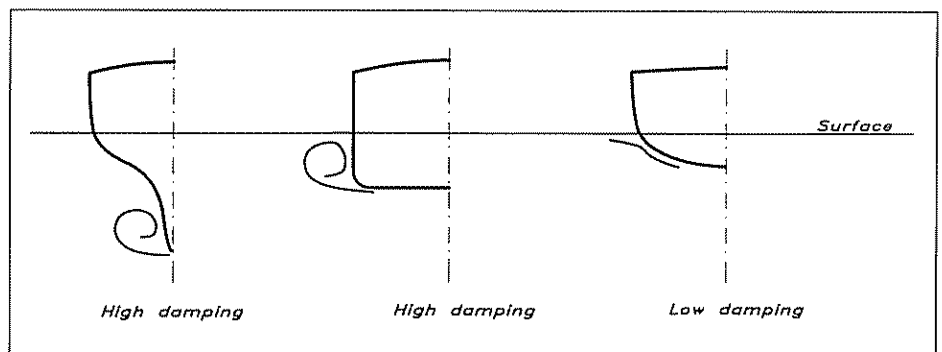
From a theoretical point of view the natural frequency may be changed by increasing or reducing either the stability or the inertia (or more precisely, the mass moment of inertia around a longitudinal axis). To avoid the resonance situation the natural frequency can be either increased or reduced. However, in conditions where the problem occurs it is better to move to the left in Fig 4.15, either by increasing stability or reducing inertia. If weights located at a high position are moved down to the bottom of the hull (which is probably closer to the centre of gravity) both these effects are accomplished.

The technique of avoiding resonance is closely related to the operation of the yacht, while the other way to reduce roll, namely to increase damping, is the designer's task. Damping may be caused by three things:

- Friction between the water and the yacht.
  - Generation of waves on the water surface.
  - Generation of vortices from the keel, rudder, sharp bilges and sails.
- This factor is by far the most important for sailing yachts.

Vortex generation depends partly on the shape of the sections (see Fig 4.16), but mainly on the size of the lateral area. Excessive rolling combined with low speed creates large angles of attack of the flow approaching the keel and rudder, which then get overloaded and stall. These phenomena will be dealt with at some length in Chapter 6. For

Fig 4.16 Influence of section shape on damping

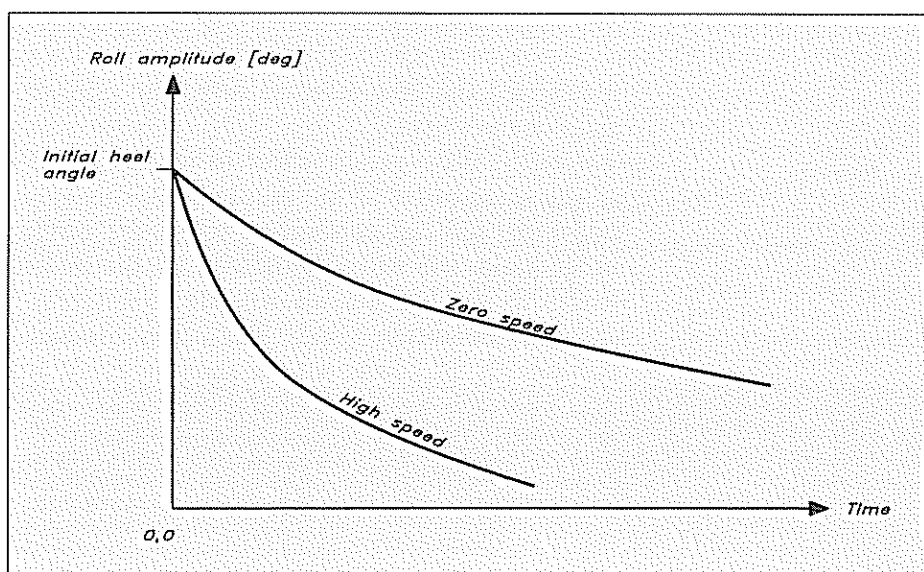




the forces on the stalled surfaces the area is much more important than other geometrical properties, so a long keel yacht will have more damping than a fin-keel one. This is an important conclusion, which speaks in favour of traditional designs and against more modern ones with a small lateral area.

It should be pointed out also, that forward speed increases damping considerably, particularly for fin-keel yachts. If the speed is high enough the keel starts working properly and the forces get much larger. Fig 4.17 shows how the roll amplitude decays with time for *Grimalkin* in still water. At zero speed the decay is much smaller than at high speed, where the rolling is rapidly damped. It is therefore important, especially for fin-keel yachts, to keep the speed up under critical conditions.

Fig 4.17 Influence of speed on roll damping – fin-keel yacht



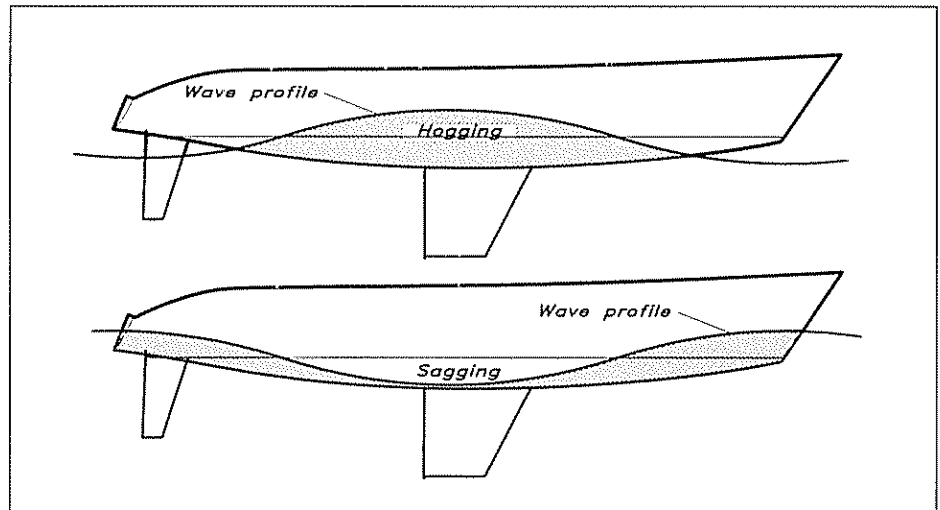
### Influence of waves on the righting moment

The righting moment is influenced by waves in two ways:

- The wave profile along the hull changes the waterline shape
- The centrifugal forces on the water particles change the pressure in the wave

As regards the wave profile, two typical cases may be distinguished. These are shown in Fig 4.18. Hogging is when the wave crest is at midship, and sagging when the trough is at this position. For a sailing yacht, with some flare at all sections, hogging means that the submerged part of the hull gets thinner at the ends and beamier at midship. Since the water plane moment of inertia and the metacentric radius depend on beam cubed (Figs 4.8 and 4.9), this results in an increase in stability. In sagging the opposite occurs, with an increase in beam at the ends and a reduction at midship, ie a more even distribution of beam, which causes a reduction in stability. (It may be

Fig 4.18 *Hogging and sagging*



mentioned that the effect is often the opposite for a ship with vertical sides at midship.)

For the wave profile effect to be significant the wavelength has to be of the same order as the hull length. This is not the case at sea, at least not under difficult conditions, where the waves are much longer. On the other hand, the waves generated by the hull itself often have the same length as the hull (as we will see in Chapter 5). The hull is then in a sagging condition and this may reduce stability considerably, particularly for hulls with a shallow draft, where the maximum beam may be much reduced in the wave trough. A formula for this effect will be given in the final section in this chapter.

To understand the effect of centrifugal forces some knowledge is required about the particle motion in the waves. This is explained in Fig 4.19. When the wave passes a certain point on the surface the water particles exhibit an orbital motion. Thus, when the particle is in a wave crest it moves with the wave, while the opposite is true in a wave trough. It is easy to compute the orbital speed, since the diameter of the circle is equal to the wave height, and the time to complete one full turn is equal to the wave period. For ocean waves this speed may be several metres per second.

The centrifugal effect on the water particles is explained in the lower part of Fig 4.19. In a crest the centrifugal force is directed upwards, ie opposite to the gravitational force; while in a trough the two forces are in the same direction. An extreme case is when the two forces are equally large, which may happen for short and steep waves. Gravitation is then cancelled in the wave crest and the water will no longer be continuous, but break down into droplets. A hull in this position will lose all its stability. A relevant question is whether it will still stay afloat, and the answer is yes (provided it does not capsize). It will, in fact, float at the original waterline. This is because the hull loses as much weight as the water due to the circular motion.

Complete loss of stability is, fortunately, very rare, but significant

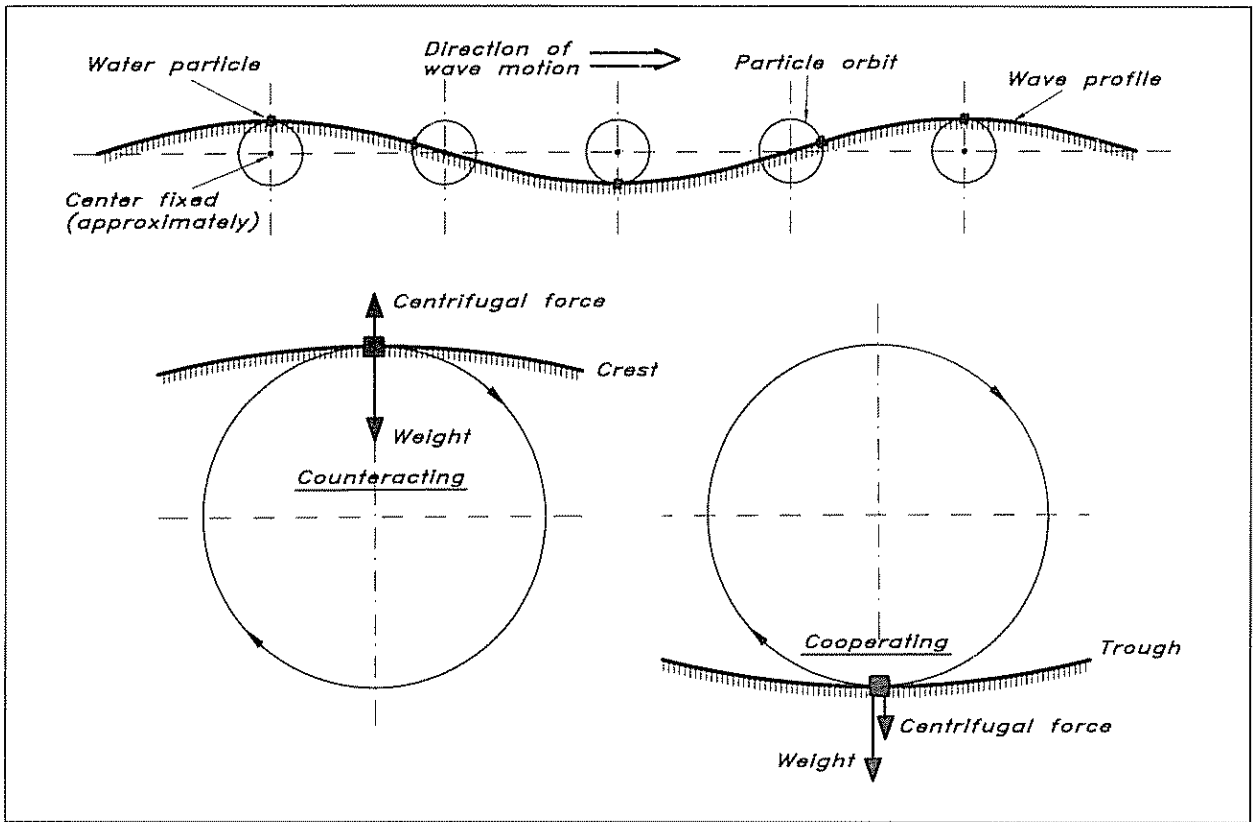


Fig 4.19 Particle motion in a wave

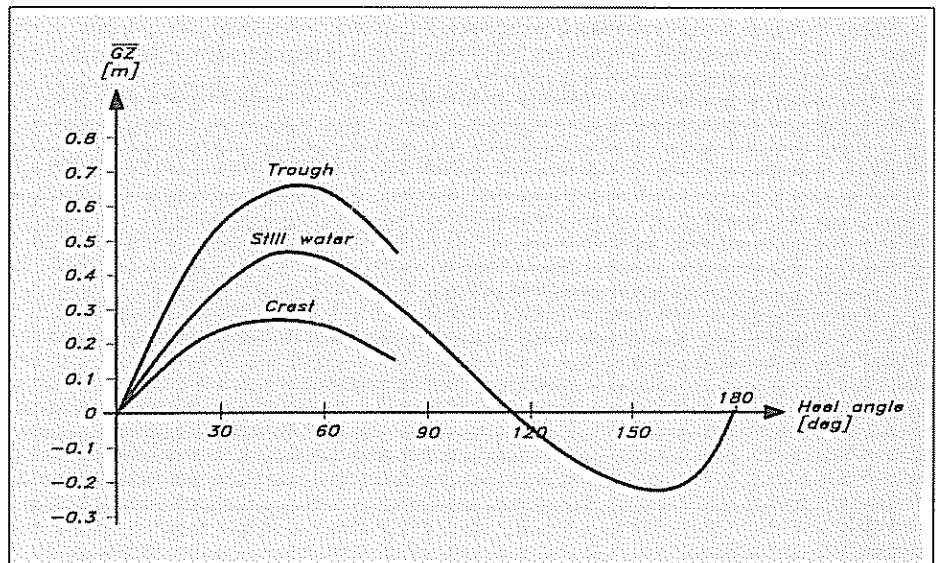


Fig 4.20 Influence of wave on the stability curve – Grimalkin

reductions may occur, as shown in Fig 4.20. *Grimalkin's* stability curve is shown for a wave height of 12 metres and a wave period of 9 seconds. These extreme conditions were actually measured in the *Fastnet* disaster in 1979. It is seen that on a wave crest the stability is almost halved, and this is at a position when the yacht is most exposed to the wind.

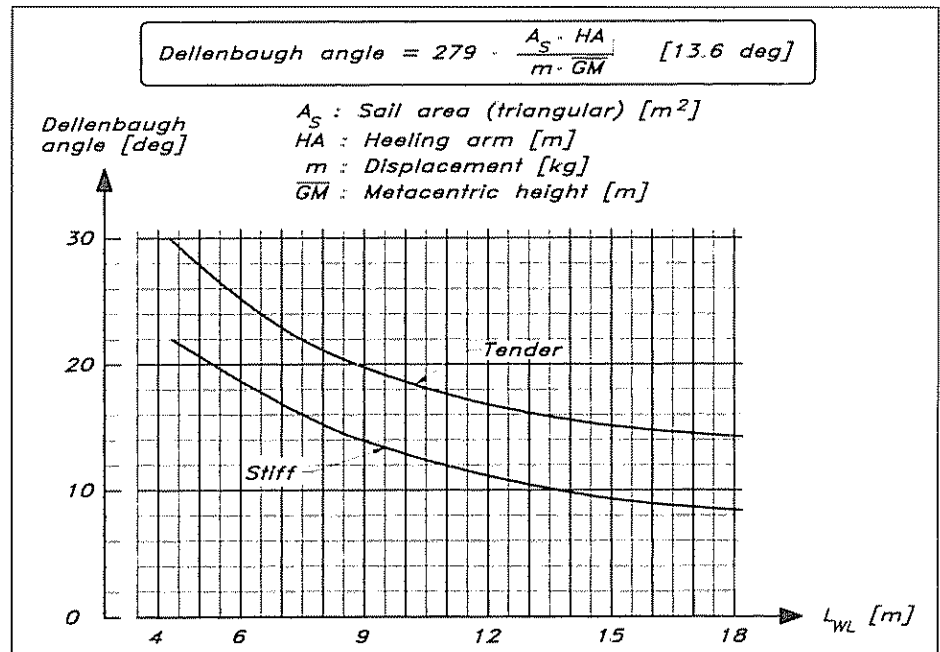
## Stability statistics

In general, modern yachts have larger  $\overline{GM}$ s than traditional ones due to their larger beam/draft ratio. The scatter is very large, however. In a survey of American IMS yachts around 1990 the lowest value was 0.67 m and the highest 2.1 m. Contrary to what could be anticipated, there was no definite trend of increasing  $\overline{GM}$ s with length. This is an effect of the reduction in relative beam for larger yachts (to be discussed in Chapter 5). The vast majority of yachts had a  $\overline{GM}$  in the range 0.75 – 1.5 m. As appears from Fig 4.9 the YD-40 has a  $\overline{GM}$  of 1.45 m and is thus relatively stiff.

As for the stability range, several yachts in the IMS fleet had a positive righting moment up to 180° while there were other yachts which developed negative stability at 100° of heel. The average was 122°, which, as we have seen above, must be considered a relatively low value from a safety point of view.

A rapid way of judging the stability of the yacht is to compute the so-called Dellenbaugh angle. This is approximately the heel angle the hull will attain when sailing to windward in a 8 m/s breeze. The angle is computed from a simple formula (given in Fig 4.21), containing the sail area, heeling arm,  $\overline{GM}$  and displacement. The heeling arm is defined as the vertical distance between the centre of effort of the sails and the centre of lateral pressure of the underwater body. (Both will be discussed later, particularly in Chapter 8.) Most modern yachts fall within the band of Fig 4.21, which gives the Dellenbaugh angle versus the waterline length. The difference between stiff and tender yachts is about 6° for all lengths. For a 10 m  $L_{WL}$  yacht the angle is therefore between 13° and 19°, and the value for the YD-40 is 13.6°, which confirms the finding above that the yacht is quite stiff. Note that the Dellenbaugh angle says nothing about the stability at large angles of heel.

Fig 4.21 Dellenbaugh angle



<b>Assessment of seaworthiness</b>	<p>It is extremely difficult to find rigorous criteria for the safety of offshore yachts. We have touched upon several factors of importance in previous sections, but when it comes to dynamic effects in a seaway little quantitative information has been given. Nevertheless, the problem is of great importance and work is under way to develop criteria for yachts of 6 m up to and including 24 m length, endorsed by the International Standards Organization (ISO).</p> <p>The general idea is to define a 'stability index', STIX, obtainable from the main dimensions of the yacht and its righting moment curve. Different qualities of the design, of importance from a seakeeping and safety point of view, are identified and expressed in the form of factors, which are multiplied to obtain the STIX. The factors are explained below. In Fig 4.22 the exact formulae are given.</p>
<b>Base length factor (<math>L_{BS}</math>)</b>	<p>The size of the yacht is the single most important parameter, when assessing safety at sea, since it defines a scale with which to measure the waves. The larger the yacht the smaller the relative size of the waves. In this approach the size is simply taken as a weighted average of the length overall and the waterline length.</p>
<b>Displacement length factor (FDL)</b>	<p>A light displacement relative to the size of the yacht may be considered a disadvantage from a control point of view and is therefore penalized, as appears from Fig 4.22. The formula is designed to yield a value of 1.0 for a 'normal' yacht, and the minimum and maximum values used in the STIX computation are 0.75 and 1.25, even though the actual value may be outside this range. Similar principles apply also to the other factors below.</p>
<b>Beam displacement factor (FBD)</b>	<p>Based on research carried out in both England (Wolfson Unit, Southampton) and the USA (Society of Naval Architects and Marine Engineers) after the Fastnet disaster, it has been concluded that a large beam in combination with light displacement accentuates the risk of wave-induced capsizes. The hull also gets more stable upside-down, which is undesirable. On the other hand, a very small beam to displacement ratio may have a negative effect on the form stability, so large deviations in both directions from the norm are penalized.</p>
<b>Knockdown recovery factor (FKR)</b>	<p>This refers to the ability of the yacht to spill water out of the sails after a knockdown.</p>
<b>Inversion recovery factor (FIR)</b>	<p>A measure of the yacht's ability to recover unaided after an inversion.</p>
<b>Dynamic stability factor (FDS)</b>	<p>As shown in Fig 4.13, the area under the righting moment curve up to a certain heel angle represents the work needed by external forces (from wind and waves) to heel the yacht to this angle. This is utilized in the dynamic stability factor, which is proportional to the area under the righting moment curve over the whole stability range, ie up to the angle of vanishing stability. However, if the first downflooding angle is</p>

Determination of monohull stability index (STIX) : [46]

$$STIX = (14 + 0.16 \cdot L_{BS}^2) \cdot (FDL \cdot FBD \cdot FKR \cdot FIR \cdot FDS \cdot FWM \cdot FDF)^{0.5} + \delta \quad \text{when } L_{BS} < 10$$

$$STIX = (8 + 2.2 \cdot L_{BS}) \cdot (FDL \cdot FBD \cdot FKR \cdot FIR \cdot FDS \cdot FWM \cdot FDF)^{0.5} + \delta \quad \text{when } L_{BS} \geq 10$$

$\delta = 5$  if, when the boat is fully flooded with water, it has a reserve buoyancy, and also has  $GZ_{90} > 0$ ,  $\delta = 0$  in all other cases.

$L_H$  = hull length (m) excluding bolted on extensions (bowsprit, stern roller etc.)

$B_H$  = hull width (m) excluding bolted on extensions (cap rails, rub rails etc.)

$m_{MSC}$  = displacement (kg) in minimum sailing condition (including two crew, basic standard equipment but no payload)

$h_{CE}$  = height of centre of sailarea above the waterline when the boat is upright

$h_{LP}$  = height of centre of lateral area below the waterline when the boat is upright

$GZ_{90}$  = righting arm at 90° heel

$GZ_D$  = righting arm at  $\phi_D^*$  heel

$\phi_V$  = angle of vanishing stability

$\phi_D$  = first occurring downflooding angle (For details see ISO 12217-2 standard)

Base Length Factor : [10.66]

$$L_{BS} = (L_H + 2L_{WL})/3$$

Displacement Length Factor : [0.99]

$$FDL = \left[ 0.6 + \frac{15 \cdot m_{MSC} \cdot F_L}{L_{BS}^3 \cdot (333 - B \cdot L_{BS})} \right]^{0.5} \quad 0.75 < FDL < 1.25$$

$$F_L = (L_{BS}/11)^{0.2}$$

Beam Displacement Factor : [1.03]

$$F_B = \frac{3.3 \cdot B_H}{(0.03 \cdot m_{MSC})^{1/3}} \quad 0.75 < FBD < 1.25$$

$$FBD = \left[ \frac{13.31 \cdot B_{WL}}{B_H \cdot F_B^3} \right]^{0.5} \quad \text{if } F_B > 2.2$$

$$FBD = \left[ \frac{B_{WL} \cdot F_B^2}{1.682 \cdot B_H} \right]^{0.5} \quad \text{if } F_B < 1.45$$

$$FBD = 1.118 \cdot (B_{WL}/B_H)^{0.5} \quad \text{if } 1.45 \leq F_B \leq 2.2$$

Knockdown Recovery Factor : [1.22]

$$F_R = GZ_{90} \cdot m_{MSC} / (2 \cdot A_S \cdot h_{CE}) \quad 0.5 < FKR < 1.5$$

$$FKR = 0.875 + 0.0883 \cdot F_R \quad \text{if } F_R \geq 1.5$$

$$FKR = 0.5 + 0.333 \cdot F_R \quad \text{if } F_R < 1.5$$

$$FKR = 0.5 \quad \text{if } \phi_V < 90^\circ$$

Inversion Recovery Factor : [1.07]

$$FIR = \phi_V / (125 - m_{MSC}/1600) \quad \text{if } m_{MSC} < 40000 \quad 0.4 < FIR < 1.5$$

$$FIR = \phi_V / 100 \quad \text{if } m_{MSC} \geq 40000$$

Dynamic Stability Factor : [1.27]

$$FDS = A_{GZ} / (15.81 \cdot \sqrt{L_H}) \quad 0.5 < FDS < 1.5$$

$A_{GZ}$  = the positive area under the GZ-curve (m.deg.) as follows:

from upright to  $\phi_V$  if  $\phi_D \geq \phi_V$

from upright to  $\phi_D$  if  $\phi_D < \phi_V$

Wind Moment Factor : [1.00]

$$FWM = 1.0 \quad \text{if } \phi_D > 90^\circ \quad 0.5 < FWM < 1.0$$

$$FWM = V_{AW} / 17 \quad \text{if } \phi_D < 90^\circ$$

$V_{AW}$  = the steady apparent windspeed to heel the vessel to  $\phi_D$  when carrying

full sail =  $(13 \cdot m_{MSC} \cdot GZ_D / (A_S \cdot (h_{CE} \cdot h_{LP}) \cdot \cos \phi_D^{1.3}))^{0.5}$

Downflooding Factor : [1.25]

$$FDF = \phi_D / 90 \quad 0.5 < FDF < 1.25$$

Design Categories :	A	B	C	D
STIX Lower Limits :	32	23	14	5

Fig 4.22 STIX stability index (Ossanen, Dolto, Eliasson & Moon)

smaller, the area should be computed up to this angle. The downflooding angle is defined as the heel angle at which a downflooding opening becomes immersed. The opening may be to either a main hatch or to a recess which is not quick-draining.

*Wind moment factor  
(FWM)*

For hulls with a downflooding angle smaller than  $90^\circ$  this factor represents the risk of downflooding due to a gust heeling the unreefed boat.

*Downflooding factor  
(FDF)*

This factor represents the risk of downflooding in a knockdown.

STIX is obtained from the formulae at the top of Fig 4.22. Different relations are used for base lengths below and above 10 m. Based on the STIX number, the yachts are classified in four different categories, A–D. The limits for the different categories are given in Fig 4.22. A yacht in category A is considered very seaworthy and should be fit for ocean passages, while a yacht in category D should be used only in sheltered waters.

As appears from the figure, the YD-40 has a STIX of 46 and is thus very well qualified for category A. Only the displacement length factor is below 1.0 and even this is very close (0.99). The strongest points are related to the righting moment (FKR and FDS) and the downflooding angle (FDF). In Appendix 3 the complete STIX calculation for the YD-40 is presented. Note that the calculations shall be carried out for the so called 'minimum sailing condition', which is the 'light yacht' plus two crew, a liferaft and some standard equipment. The light yacht corresponds to the light displacement of Appendix 1. The values for the hull dimensions in Appendix 3 have been interpolated to the minimum sailing condition between the two conditions in Appendix 1.

The stability index has been developed by van Oossanen, Dolto, Eliasson and Moon in an ISO working group ISO/TC/ 188/SC WG 22 under the chairmanship of A G Blyth. The work is presented here by permission of the ISO. It should be stressed that the standard has not yet been approved (January 1999), although it is in its final form for approval.

# 5

# HULL DESIGN

---

In this chapter we describe the theories behind the hydrodynamic design of the hull. We start by introducing the various forces acting on a sailing yacht, and explain how the forces are created by the flow around the hull. Formulae will be given for the force components, and the trade-offs in the hull design process will be dealt with at some length. Finally, there is a section on hull statistics, which may be used as a guide for selecting the main dimensions of a new design.

## Forces and moments on a sailing yacht

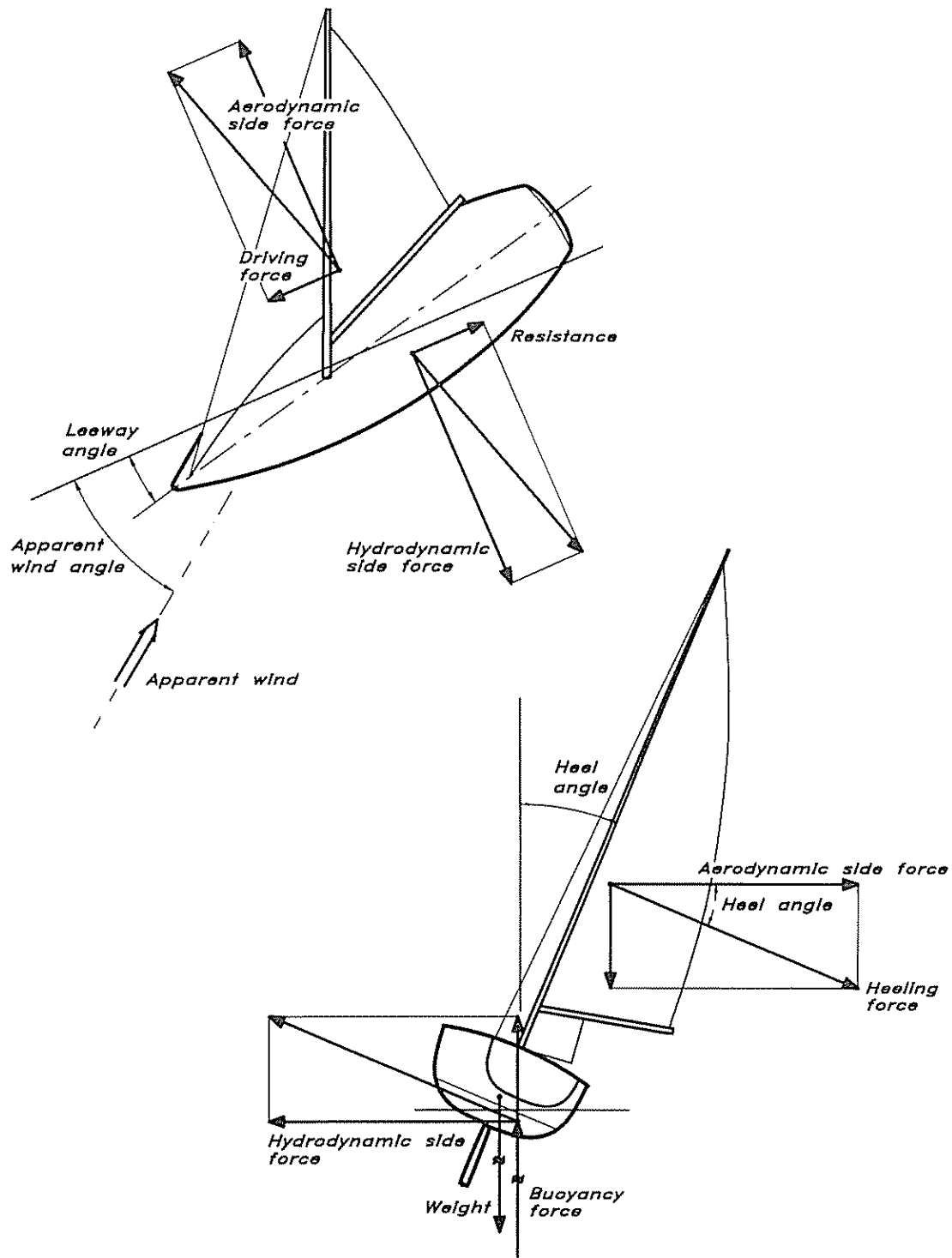
Fig 5.1 shows the different forces acting on a sailing yacht. In the plan view the horizontal components of the forces are displayed. When the hull is driven through the water a resistance is developed. Under equilibrium conditions, when the yacht is sailing at constant speed in a given direction, the resistance has to be balanced by a driving force from the sails. Unfortunately, this cannot be created without at the same time obtaining a side force, which in turn has to be balanced by a hydrodynamic side force. The latter is developed by the underwater body when sliding slightly sideways, ie when the yacht has a leeway angle. Since the turning moment under equilibrium conditions must be zero, the resulting hydro- and aerodynamic forces (in the horizontal plane) must act along the same line.

The view at the bottom of Fig 5.1 is along the direction of motion. It is seen that the resulting hydro- and aerodynamic forces are at right angles to the mast. This is not necessarily exactly true, but it is an approximation that is always made in sailing yacht theory. The heeling moment from the aerodynamic force is balanced by the righting moment from the buoyancy force and the weight.

In Fig 5.1 the apparent wind direction is marked by a fat arrow. This is not the true wind direction, since the wind felt onboard the yacht is influenced by its speed through the air. Fig 5.2 illustrates the relations between the true and apparent wind speeds and directions, the so-called velocity triangle. Note that the wind created by the yacht speed (which must be used when adding the wind vectors) is opposite to the arrow shown as yacht speed in the figure.

This chapter will deal mainly with the resistance force and its components, and how it can be minimized by proper design. The side force will be considered in the next chapter in connection with the discussion of keels and rudders, since these have primary responsibility for the side force production.

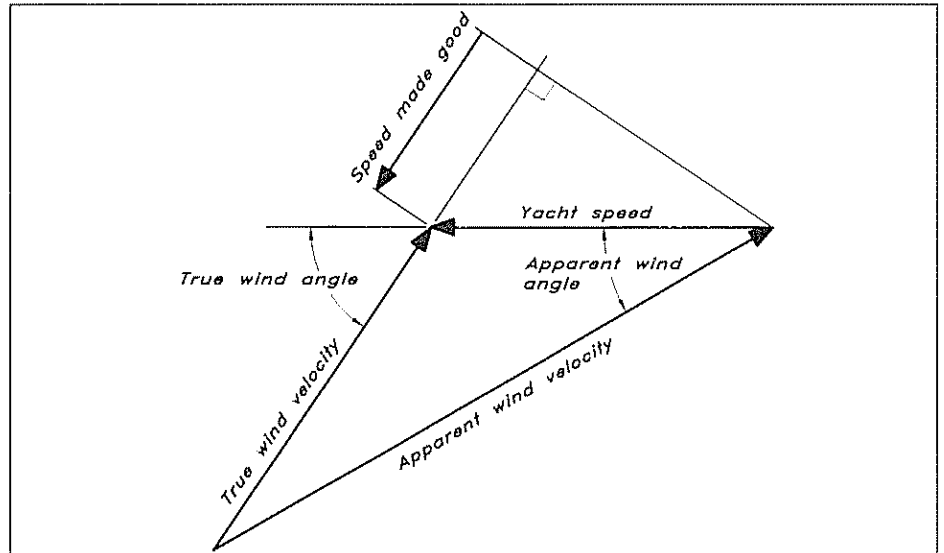
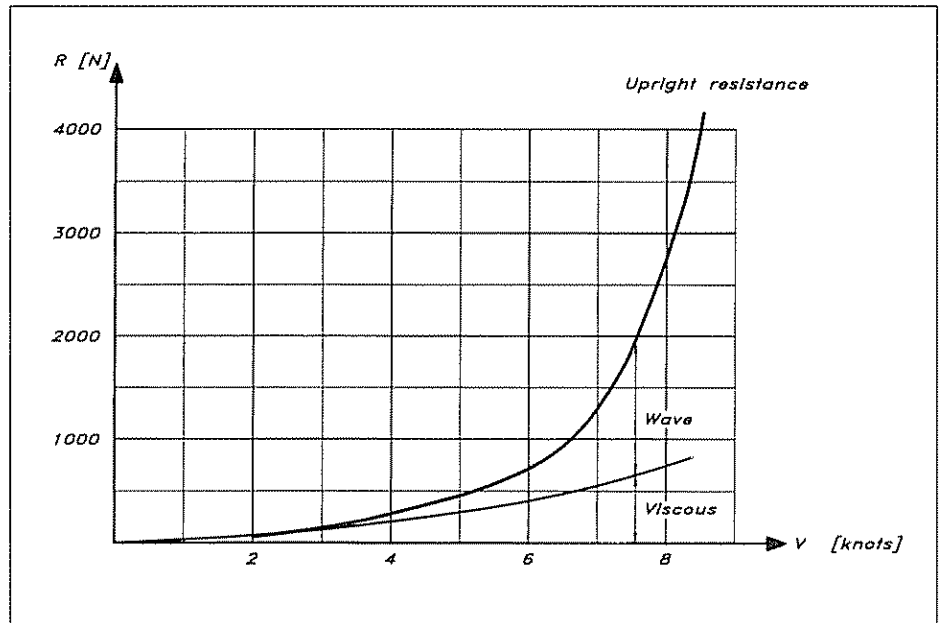




**FIG. 5-1** Forces on a Sailing Yacht

Fig 5.1 Forces on a sailing yacht

Fig 5.2 Velocity triangle

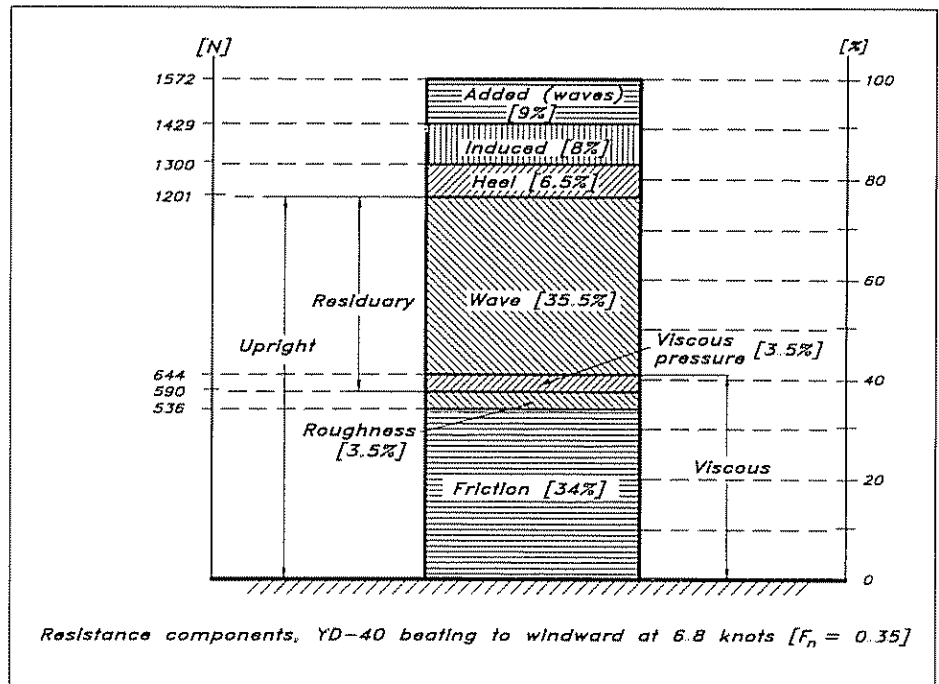
Fig 5.3 Upright resistance  
YD-40

### Resistance components

Fig 5.3 shows the resistance curve for the YD-40 if it were to be towed upright in smooth water. At low speeds the dominating component is the viscous resistance due to frictional forces between the hull and the water. The friction gives rise to eddies of different sizes, which contain energy left behind the hull in the wake. This component increases relatively slowly with speed, as opposed to the second component, the wave resistance, which occurs because the hull generates waves, transferring energy away. The sum of the viscous and wave resistance components is often referred to as the upright resistance.

In a real sailing situation the picture is more complicated, particularly upwind in a seaway. Fig 5.4 shows a breakdown of the total resistance of the YD-40 beating to windward offshore at 6.8 knots in a fresh

Fig 5.4 Breakdown of total resistance, YD-40



breeze. The values of the resistance components are shown to the left as computed by the formulae to be given in this chapter. All components are also given in % of the total force. We will refer extensively to this figure in the following discussion.

The viscous resistance has been subdivided into components, to be discussed later. As well as the viscous and wave components we have three new forces: heel, induced and added resistance. The heel resistance is the sum of the changes in the viscous and wave resistance due to heel. This component is introduced in sailing theory for convenience. Since methods for obtaining the two resistance components for upright hulls are well established in ship hydrodynamics it is an advantage to consider the effects of heel separately.

The induced resistance is caused by the leeway. When the yacht is moving slightly sideways, water flows from the higher pressure on the leeward side, below the tip of the keel and rudder, and also below the bottom of the hull, to the lower pressure on the windward side. Longitudinal vortices are then created. Most sailors have probably seen the vortex from the keel tip at large heel angles. When the vortex gets close to the surface, air is sucked down into its centre, which makes it visible. The vortices contain rotational energy left behind the hull.

In a seaway all the calm water resistance components are increased, due to the unsteady motions of the yacht. However, it is an advantage to lump all the changes together into one component, called the added resistance in waves. This component is represented at the top of the bar in Fig 5.4.

To sum up, we have five major resistance components: the viscous resistance, the wave resistance, the heel resistance, the induced resistance

and the added resistance in waves. We will now discuss them in turn and show how they are affected by the shape of the hull.

### Viscous resistance, basic concepts

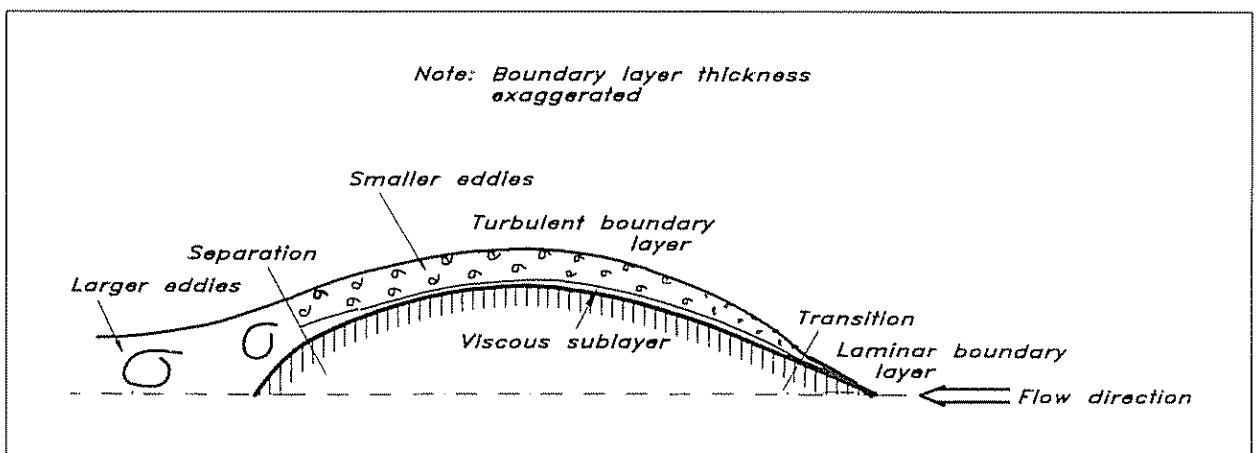
Viscous resistance derives its name from the fact that it is the viscosity of the water that gives rise, directly or indirectly, to this resistance component. The water viscosity (kinematic), denoted  $\nu$ , depends on the water temperature. At 20° Celsius it is  $1.0 \cdot 10^{-6} \text{ m}^2/\text{s}$ . We will use this value in the following discussion. Viscosities for other temperatures may be found in standard tables. For estimates of the viscous resistance the present value is good enough.

To understand the nature of viscous resistance certain concepts of fluid mechanics must be known. The most important ones from this perspective are explained in Fig 5.5.

Whoever has looked down the side of a ship moving in reasonably calm water must have seen that the water close to the hull is entrained and moves with the hull. It looks as if the water particles closest to the hull were stuck to the surface. This is in fact the case. The molecular forces between the hull and the water are strong enough to stop the relative motion in the innermost water layer. Viewed from the hull the water velocity increases gradually from zero at the surface to approximately the ship speed a certain distance away. The part of the flow within this distance, normally less than 1 m for a large ship, is called the boundary layer. On a smaller scale, the same phenomenon occurs with a sailing yacht. At the bow the boundary layer is very thin, but grows backwards, attaining a thickness of the order of 0.1 m near the stern. The boundary layer of Fig 5.5 is thus grossly exaggerated for clarity.

Near the bow the flow within the boundary layer is smooth. The velocity in one layer is slightly larger than in the layer just inside. This is the laminar part of the boundary layer. After a certain distance from the bow disturbances start to occur, and shortly thereafter the flow structure breaks down into a seemingly chaotic state: turbulence. The boundary layer is now characterized by eddies of different sizes and frequencies. The fluctuating velocities caused by the eddies are, however,

Fig 5.5 *Different regions in the flow around the hull*



considerably smaller than the mean velocity at all points in the boundary layer, so the flow is always moving backwards.

A special region can be distinguished in the inner part of the turbulent boundary layer. This region is extremely thin. If the total boundary layer thickness over the main part of the yacht is of the order of a few centimetres, the inner region, called the viscous sublayer, is of the order of 0.1 mm. Nevertheless it plays quite an important role, particularly in connection with surface roughness, as we will see. In the viscous sublayer the flow is mainly laminar, but is sometimes disturbed by turbulent bursts, located at isolated spots, moving downstream with the flow.

The region where the flow changes from laminar to turbulent is called the transition region and is normally very short. In Fig 5.5 it is marked as a point.

Close to the stern another flow phenomenon, called separation, may occur. If the stern is very full, the flow cannot follow the surface and bend inwards as rapidly as the hull. In fact, the flow closest to the surface stops and forces the flow further out to proceed in a direction more straight backwards. Large eddies develop, as indicated in the figure. It should be stressed that these eddies are much stronger than the ones in the turbulent boundary layer. The mean flow may now move forwards. While it is impossible in practice to avoid transition to turbulence in the boundary layer on a sailing yacht, separation should definitely be avoided, since it increases the resistance considerably. During one period of the IOR era very uneven stern lines were used to 'cheat the rule', ie to reduce the rating, but the price paid was a slower yacht, and after some corrections had been introduced into the rule this type of stern disappeared.

The viscous resistance may be subdivided into three components: the direct friction on the smooth surface, the pressure imbalance between the fore and afterbodies due to the boundary layer, and the increase in friction due to surface roughness. We will now deal with these components individually.

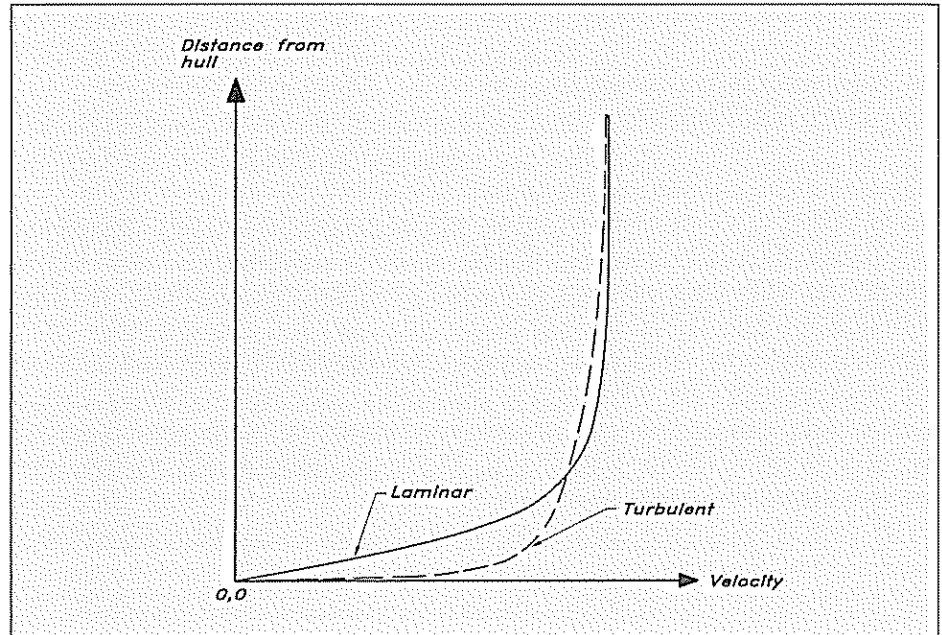
### **Frictional resistance**

Having introduced some important concepts related to viscous resistance we are now ready to discuss the first and most important component, due to the direct friction between the water and the hull surface. Although the water does not slip along the surface, a resistance force is developed, because the layer of water closest to the hull is influenced by the next layer, which is moving backwards. This in turn is affected by another adjacent layer, and so on. The frictional force is in fact proportional to the rate at which the speed of water increases with the distance from the surface.

Some conclusions as to the frictional resistance may now be drawn. First, since the friction acts on the hull surface, minimizing the wetted surface area must be advantageous. This improvement is responsible for the increase in speed of new designs in the 1960s, when the fin keel was introduced, marking a considerable reduction in the wetted surface.

Secondly, since the velocity distribution in the laminar part of the boundary layer is different from that in the turbulent part, the friction is different. In the laminar case, the thin water layers affect each other only by molecular forces, which are relatively weak, while in the turbulent case adjacent layers are more strongly connected due to the 'stirring' effect of the eddies. Typical velocity distributions in the two types of boundary layers are shown in Fig 5.6.

Fig 5.6 Velocity distribution in the laminar and turbulent boundary layer



Since the velocity increases much more rapidly with the distance from the surface in the turbulent case, the friction is much larger. The laminar flow should thus be maintained as far back as possible. This effect is very important in the design of keels, rudders and other appendices, like bulbs, where the shape can be chosen freely. However, many other effects have to be considered for the hull, so not much can be done in this respect. The technique employed in appendage design will be described in the next chapter. Here it suffices to say that straight lines on the forebody are likely to increase the laminar length, but in any case the area covered by a laminar boundary layer will be only a small fraction of the total wetted surface of the hull.

As an example, the boundary layer and friction (often called skin friction) distributions on a 7.6 m traditional yacht, for which flow calculations have been made, are given in Fig 5.7. The quantities are given along one streamline from bow to stern. It may be seen that the boundary layer thickness increases slowly in the laminar part, but after transition the increase is much faster, particularly near the stern. The scale to the left gives the thickness in mm. The friction drops rapidly in the laminar part to a very small value, but increases abruptly at transition. After transition it drops again to almost zero at the stern.

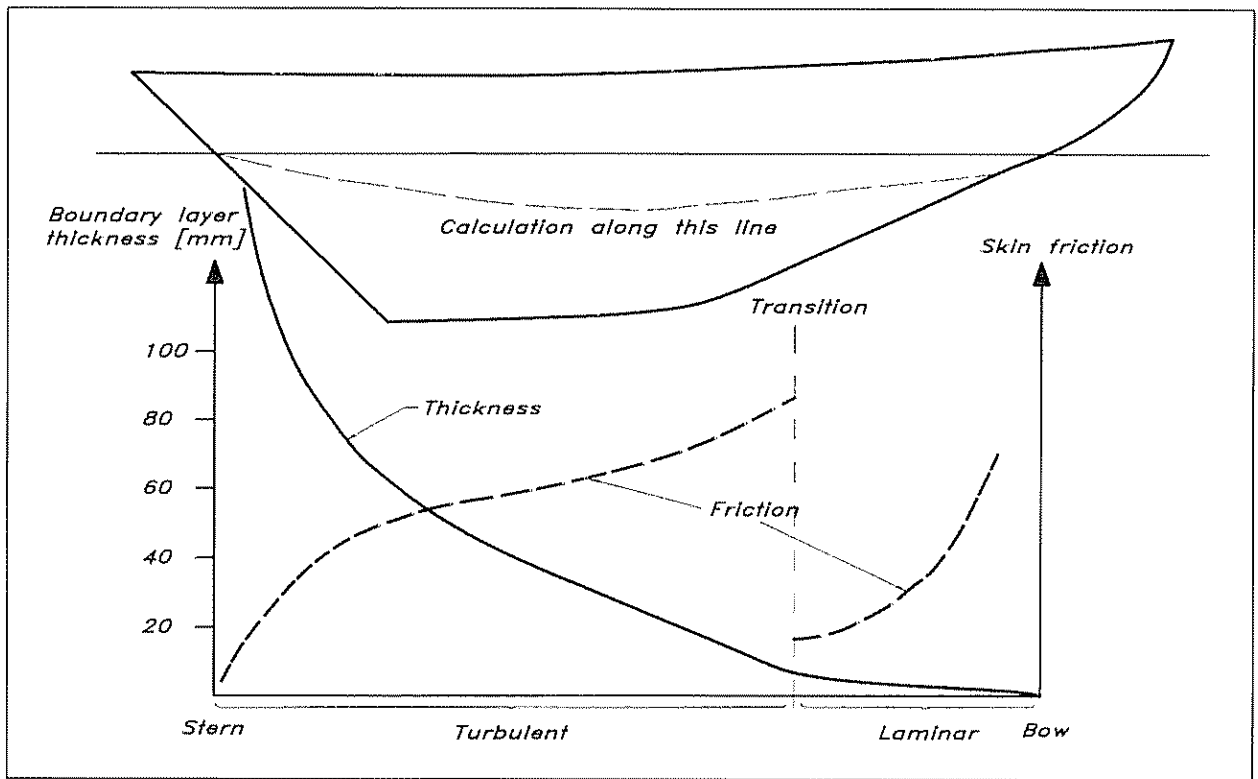


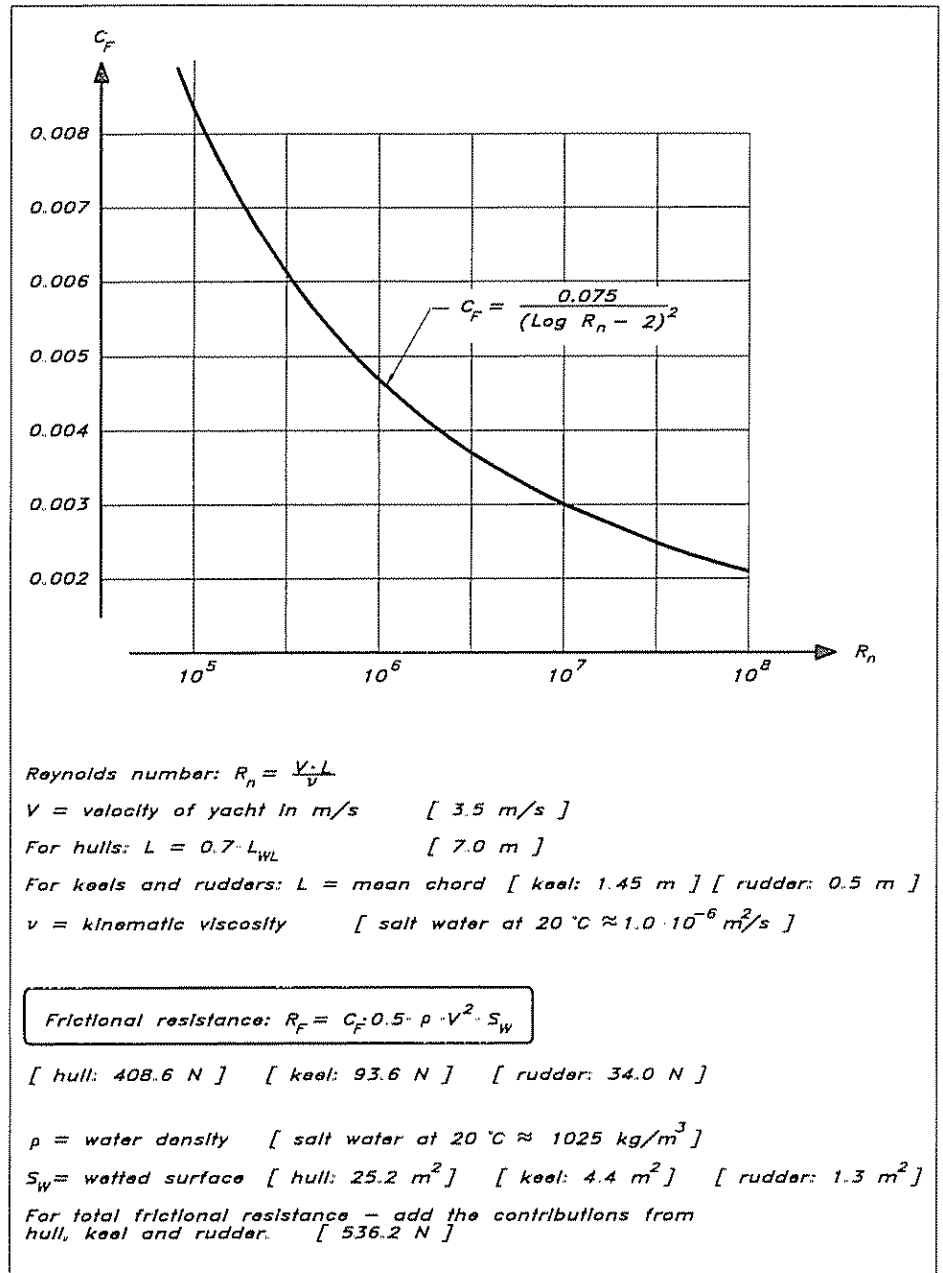
Fig 5.7 Boundary layer and skin friction distribution on a 7.6 m traditional yacht

This hull has a relatively long laminar part due to the straight hull lines on the forebody.

The data for Fig 5.7 were obtained by a computer program (SHIPFLOW), for the flow around ships and other bodies. This program, which will be described in Chapter 16, is used in advanced yacht design, mostly in connection with the America's Cup, but it is too complex and expensive for the amateur yacht designer. There are, however, simple formulae valid for flat plates, which can be used for estimates of the boundary layer thickness and skin friction. Like all quantities related to the viscous resistance they depend on a dimensionless number, called the Reynolds number,  $R_n$ . This is the product of the plate velocity  $V$  and length  $L$ , divided by the kinematic viscosity of the water  $\nu$ ,  $R_n = V \cdot L / \nu$ . Fig 5.8 shows how the friction varies with the Reynolds number, and the relevant formulae for estimating the friction of the different parts of the underwater body are also given. Note that, when the friction of the hull is computed, only 70% of the waterline length is used for defining the Reynolds number. This is because water particles do not generally follow the entire length of the bottom. For instance, those hitting the hull near maximum beam will follow the hull only a short distance before leaving it for the wake behind the hull. Values within brackets in Fig 5.8 are for the YD-40.

The diagram in the figure gives the total skin friction coefficient,  $C_F$ , which may be converted into the frictional resistance force  $R_F$ , using the formula inside the box. This way of representing forces by a coefficient  $C$  with an index is very common in fluid mechanics, and the force may

Fig 5.8 Calculation of the frictional resistance



always be obtained by multiplying by the so-called dynamic pressure  $0.5 \cdot \rho \cdot V^2$  and a representative area, here normally the wetted surface  $S_W$ .

The values computed for the YD-40 are at 3.5 m/s, or 6.8 knots, the same speed as in Fig 5.4. By adding the contributions from the hull, keel and rudder the total friction is obtained as 536 N, also given in the bar of Fig 5.4.

### Viscous pressure resistance

Fig 5.9 shows a typical pressure distribution on the hull at a given depth, ie along a certain waterline. It is seen that the bow and stern pressures are higher than in the undisturbed water at this depth, while



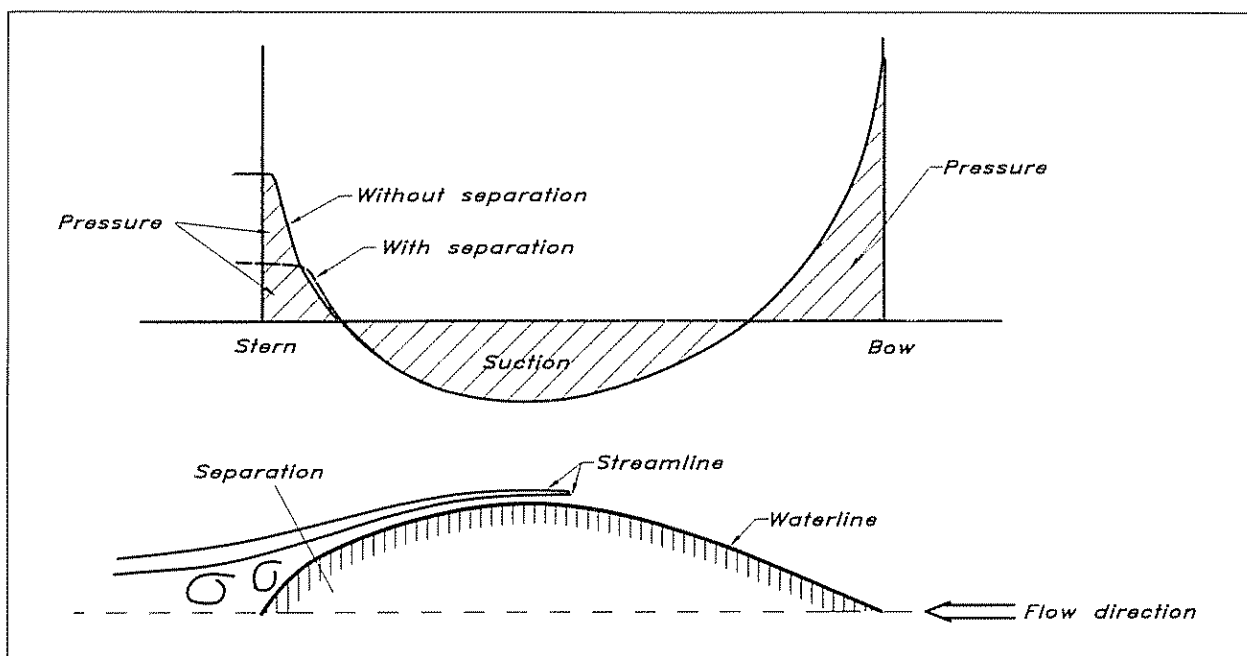


Fig 5.9 Pressure distribution with and without separation

the pressure in the middle part of the hull is lower. Had there been no boundary layer, the pressure forces over the bow would have balanced those over the stern exactly and there would have been no resulting force (neglecting for a moment the effect of the waves, which also have an influence on the pressure). The boundary layer does, however, modify the pressure distribution, and, since the layer is considerably thicker around the stern than at the bow, the stern pressure is affected most. A slightly lower pressure is found at the stern, giving rise to the resistance component, which is indirectly caused by friction, through the boundary layer. For a sailing yacht it is in the range 5–10% of the direct frictional force.

The pressure resistance just described is unavoidable, but it can be minimized by proper design of the stern. Thus, the blunter the stern the larger the pressure drop. As long as separation is avoided the effects are small, but if the flow separates a large reduction in pressure will occur, and the pressure resistance may be considerably larger than the 5–10% mentioned. When judging the bluntness of the stern, the shape of the diagonals should be studied, since these are closer to the flow direction than the waterlines. Maximum slopes of the diagonals have been suggested in the literature, but the values vary considerably between the different authors, ranging from about 22° to about 30°. Most likely the upper limit is too high, and to be safe it is better not to exceed the lower value.

It should be pointed out that the viscous pressure resistance is influenced by the prismatic coefficient and the location of the longitudinal centre of buoyancy. The larger the  $C_p$ , the fuller the ends of the hull, and the more aft the position of the LCB the fuller the stern. In order to minimize the viscous resistance the hull should have a shape

like a cod, but very slender. The  $C_p$  should be less than 0.5 and the LCB should be positioned in front of the midship section. This would be a good design were it not for the wave resistance. As will be seen later, bluff forebodies tend to increase the waves, while in fact bluff afterbodies tend to decrease them. A thick stern boundary layer (on a bluff afterbody) makes the hull appear longer than it really is, and this effect is even more pronounced if separation occurs. Some designers have therefore produced very bluff sterns with some separation, just to decrease the wave resistance. This is not likely to pay off, however, unless there are important gains, from a measuring point of view in a rating rule. Obviously, the stern design, as well as  $C_p$  and LCB, must be optimized considering the speed for which the yacht is designed (ie for which wind conditions it is optimized). The higher the speed the more important the wave resistance and the bluffer the stern. Optimum values of  $C_p$  and LCB will be given later, in the discussion of wave resistance.

While the frictional resistance is set mainly by the wetted surface, the viscous pressure resistance depends on the shape of the hull. This is also the case for the wave resistance, and both appear due to pressure imbalances, so it is very common to lump both together into one component: the residuary resistance. We will not give any formula here for the viscous pressure resistance itself, but follow general practice and give the formula only for the residuary resistance. This will be presented later. In Fig 5.4 we have simply assumed that the viscous pressure resistance is 10% of the friction, which is a reasonable figure.

### Roughness

The third component of the viscous resistance, due to surface roughness, might not be too important from a design point of view, but it is certainly of interest for the practising yachtsman, and should, therefore, be discussed.

According to a large number of experiments with flows over rough surfaces, the effect of roughness disappears if the roughness elements are embedded in the viscous sublayer, introduced above. There is thus a limit, below which the surface may be considered smooth from a resistance point of view: 'hydraulically smooth' in fluid mechanics terminology. We have already noted that the thickness of the viscous sublayer is very small, normally of the order of 0.1 mm. Let us look at this in more detail, using the boundary layer calculation for the 7.6 m traditional yacht as an example. In Fig 5.10 the thickness of the viscous sublayer, ie the permissible roughness height, is given for three different speeds. One branch of the curves represents the hull, while the other is for the keel. At the forward end of the hull the boundary layer is laminar and, although the theories for this part are less well developed, it is safe to assume, as has been done in the figure, that the permissible roughness in this region is the same as in the most forward part of the turbulent boundary layer.

Several observations may be made concerning Fig 5.10. First, there is a strong dependence on speed: secondly, there is an increase in the permissible roughness aftwards. Thirdly, the increase is not as large on

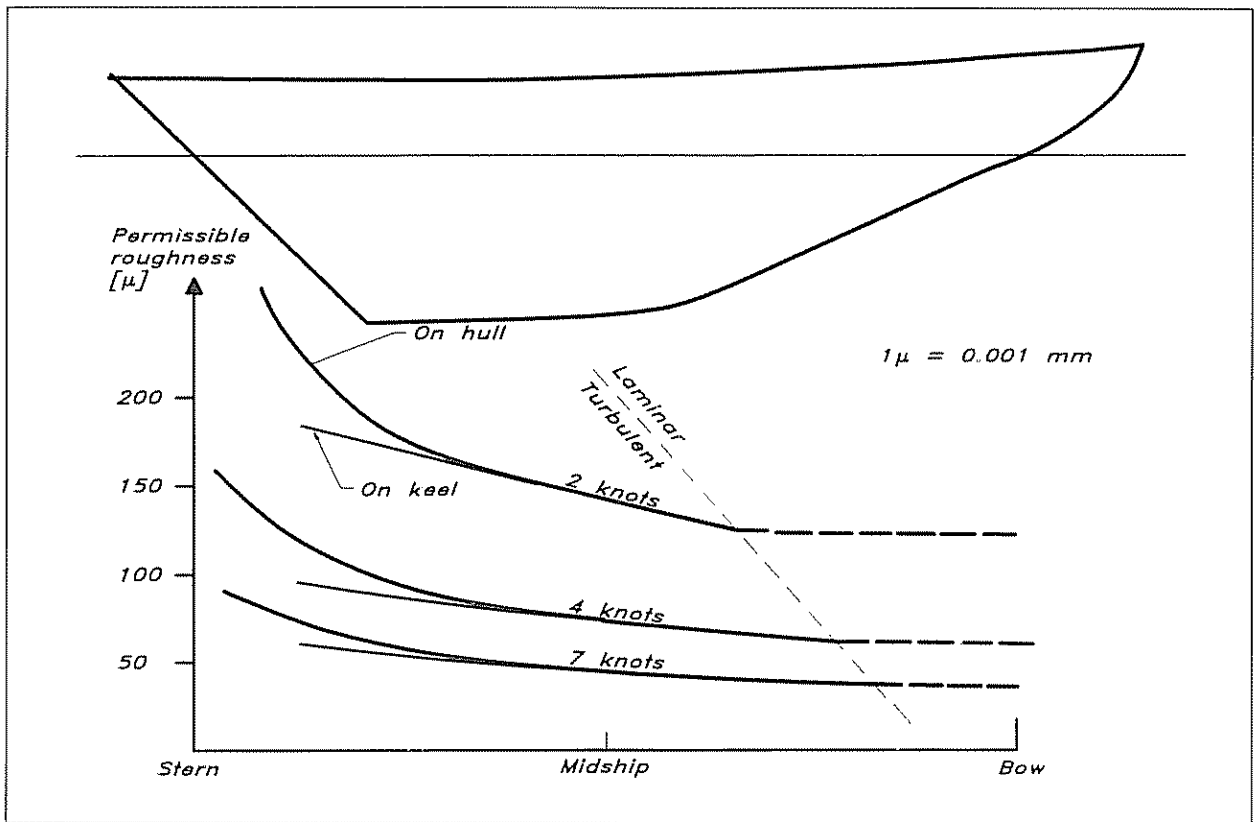


Fig 5.10 Permissible roughness. Traditional yacht

the keel as on the hull near the stern. We may also note that the most strict requirement is 0.03 mm, or 30  $\mu$ m for the highest speed on the forward half of the hull. To get a feeling for this small value we may note that a sandpaper of number 400 has a grain size of 25  $\mu$ m. This does not mean that the surface should be sanded with this paper. A considerably rougher one would yield the required smoothness, since the grooves left after the paper are much smaller than the grains.

There is a very simple relation which can be used for estimating the permissible roughness on the forward part of the hull. This relation is given in numerical and graphical form in Fig 5.11. Note that the roughness is given in microns and that it is inversely proportional to the speed.

An appropriate question now is how much the viscous resistance is increased if the requirement for a hydraulically smooth surface is not met. To answer this, we may return again to the calculations for the traditional yacht. In Fig 5.12 the increase in viscous resistance for varying roughness heights and speeds is given. It is seen that the increase is considerable, particularly at higher speeds. Fig 5.12 was computed based on measurements for flat plates, where the surface was densely covered with sand grains. This is not the case for a sailing yacht, so the values given must be considered as an upper limit. In any case, it is obvious that roughness heights above the limit for a hydraulically smooth surface cannot be tolerated for racing yachts. It

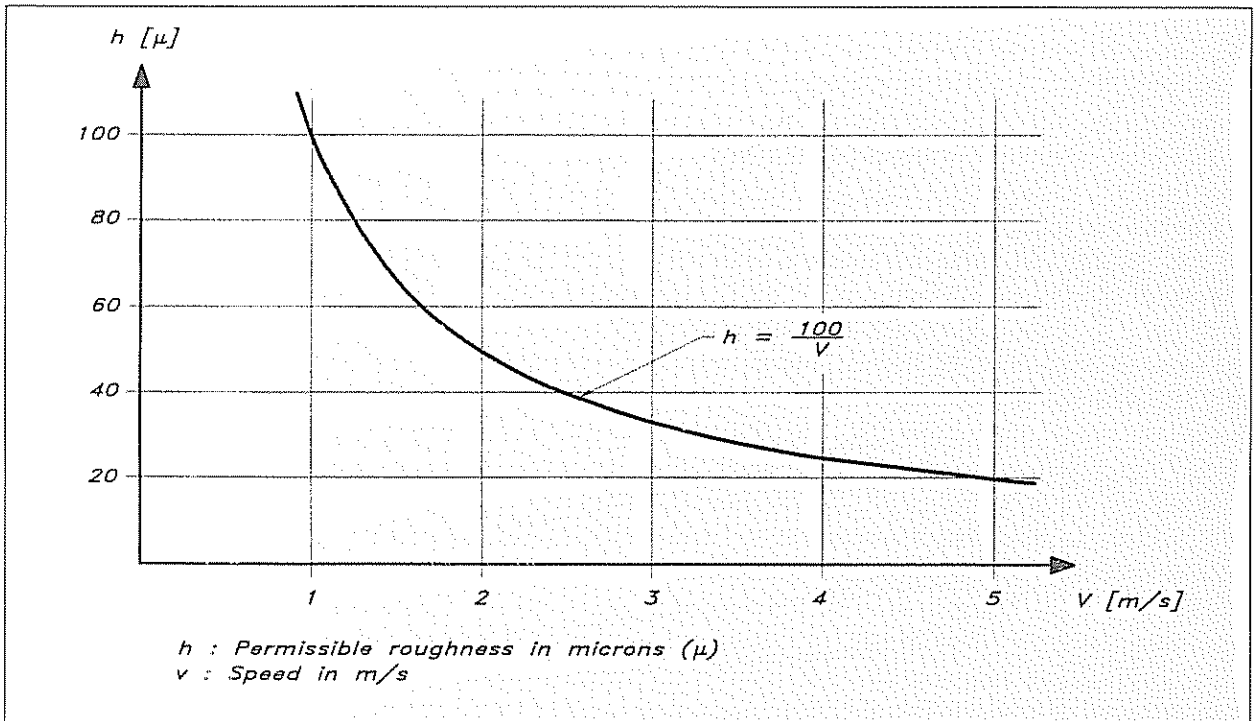


Fig 5.11 Estimation of the permissible roughness at different speeds

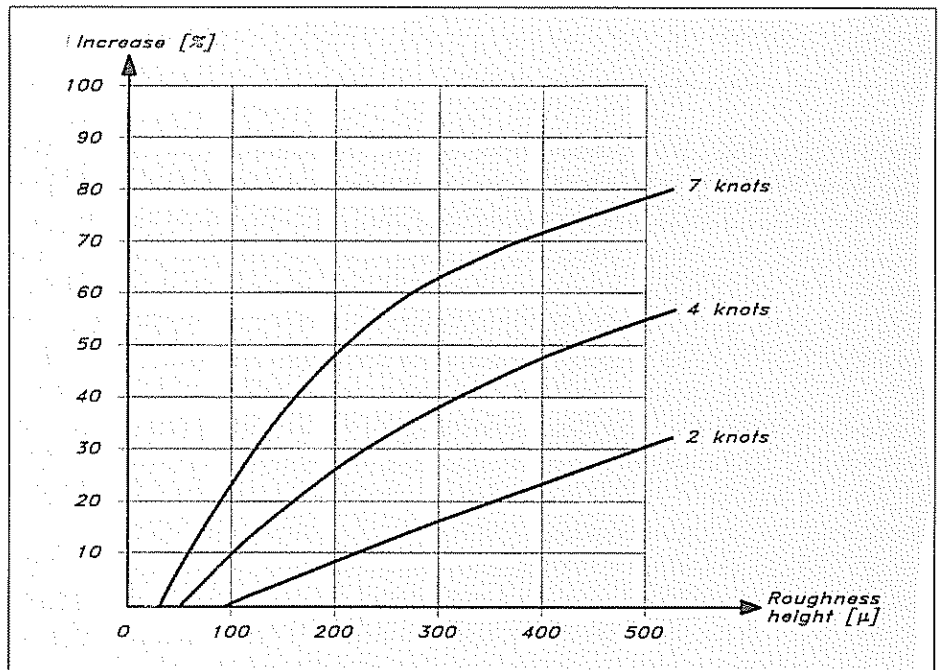


Fig 5.12 Increase in viscous resistance due to roughness – traditional yacht

should be pointed out that barnacle growth results in much larger increases in resistance than indicated here. Two or even threefold increases in the viscous resistance have been noted for densely packed barnacles, several millimetres in height.

The YD-40 has a maximum speed of about 8.5 knots, ie slightly more than 4 m/s. According to Fig 5.11 the permissible roughness is

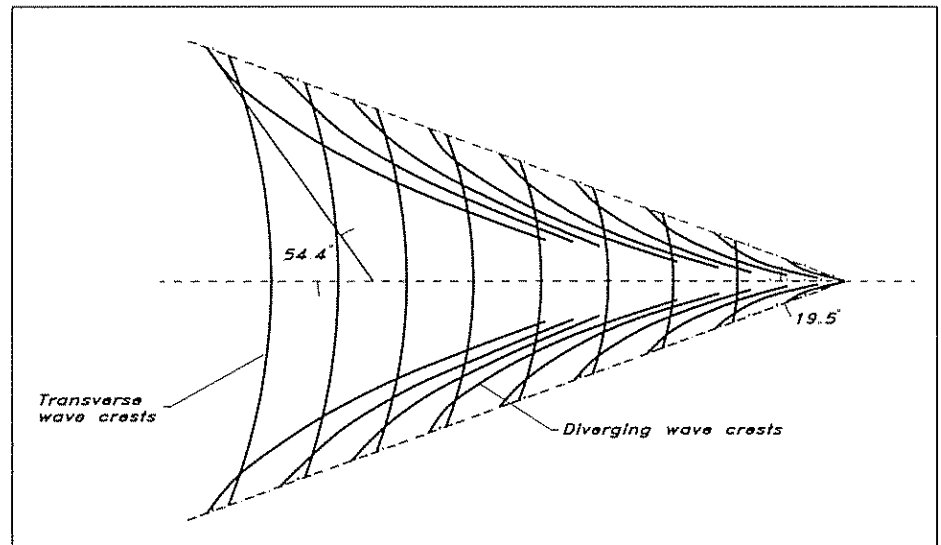
then about  $20\mu$ . Normally, a brush-painted surface has grooves  $50 - 100\mu$  in height, so there is a significant resistance increase as compared to the hydraulically smooth surface. In Fig 5.4 the roughness component is 10% of the friction and the speed is 6.8 knots. This is reasonable, judging from Fig 5.12, where the 7 knot curve yields 8–23% increase for heights between 50 and  $100\mu$ . As pointed out above this is probably somewhat high for normal roughness types. The fact that the curves of the figure are for a different hull is not too important, since the speed is the most significant factor.

### Wave resistance, basic concepts

We will now turn to the second major resistance component of Fig 5.4: wave resistance. Like the viscous resistance it could be split into sub-components, but they are of interest only under certain conditions, for instance when the bow wave breaks or is transformed into spray. We will neglect these phenomena here. As in the case of viscous resistance we will start by introducing some basic concepts.

If one throws a stone into a pond, circular, concentric waves originate from the point where the stone hits the surface. If one were to throw several stones in a row along a straight line the circular waves would interfere with one another and create a wave system very similar to that far behind a yacht. This is a system with well-defined properties, called the Kelvin wave system, and is due to a travelling point disturbance on the water surface. The same system is found far behind large ships, and in fact behind all objects moving along the surface. The reason why the same system is created is that if the waves have travelled a sufficiently large distance, and occupy a large area compared to the dimensions of the object, the latter may always be considered as a point. For instance, if a ship moving in calm water is viewed from an aeroplane, the ship itself is very small as compared with the area covered by the wave system, and the latter has the typical Kelvin structure. Fig 5.13 is an illustration of this phenomenon. It may be seen that two types of waves

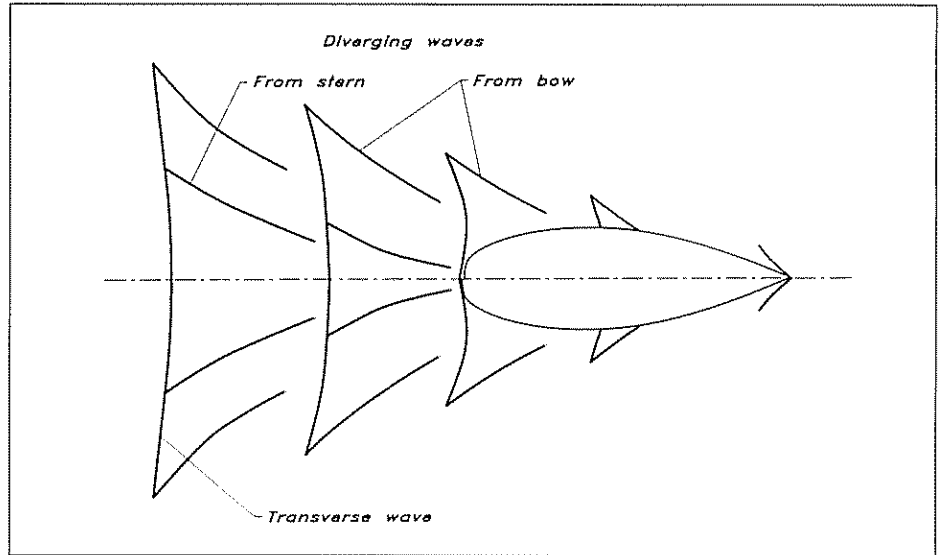
Fig 5.13 *The Kelvin wave system*



exist: diverging waves moving sideways and transverse waves at right angles to the direction of motion, moving with the ship.

Locally, the situation is quite different and the waves are highly dependent on the shape of the hull. Within distances of a few hull lengths, waves from all points on the hull surface will in theory contribute to the wave system. Some of the points are, however, more important than others, since the disturbance is larger. For a sailing yacht the high pressure regions at the bow and stern are dominant, and it is usually assumed that only two wave systems exist (see Fig 5.14).

Fig 5.14 Local bow and stern wave systems

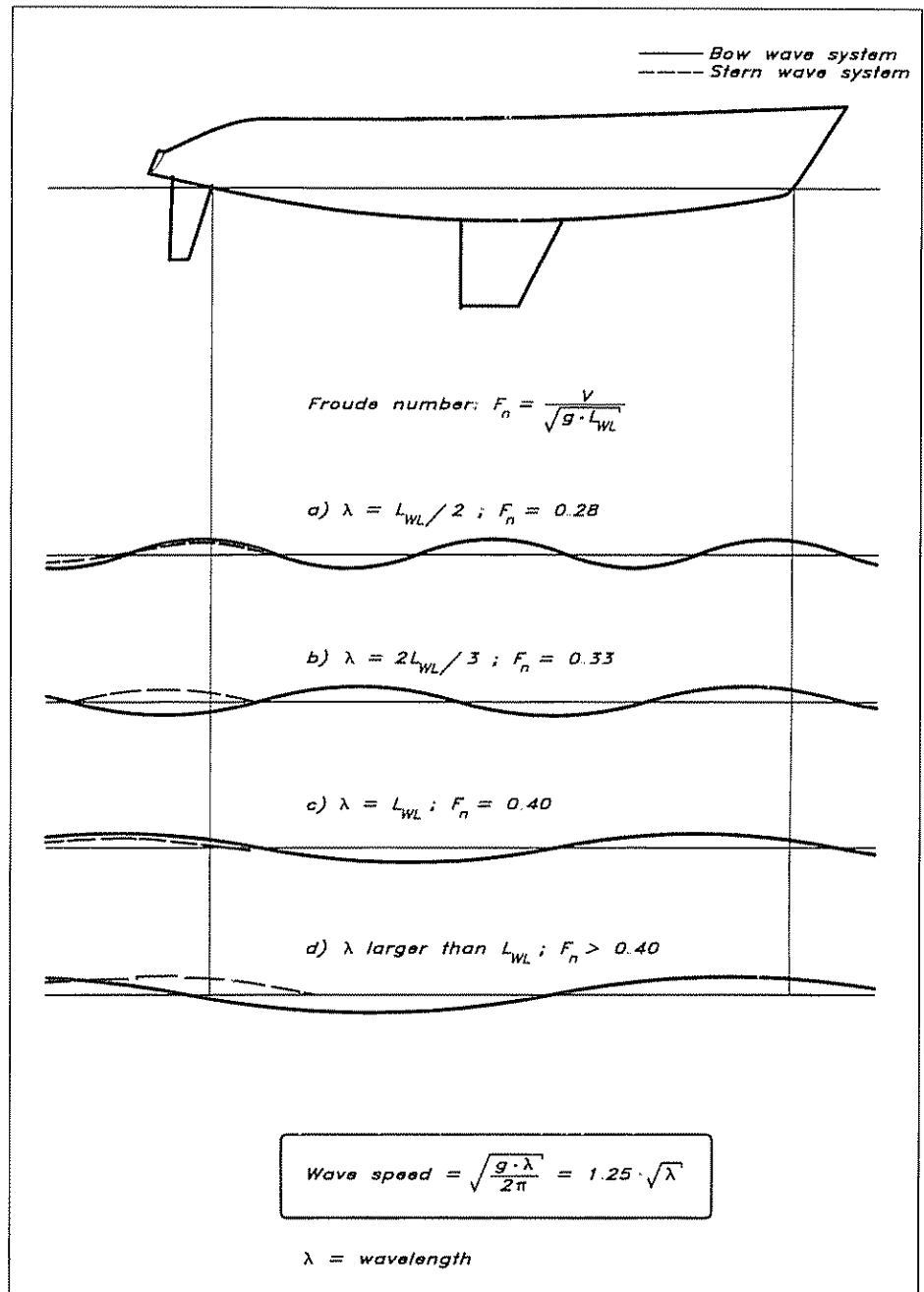


There is a very simple relation between wavelength and travelling speed for surface waves. As can be seen in Fig 5.15 the speed is equal to 1.25 times the square root of the length. For example, a 7 m long wave will have a speed of 3.3 m/s.

Since the wave system travels with the yacht, at the same speed in the longitudinal direction, the length of the generated waves will depend on the yacht speed. If, for instance, the speed is 1.25 times the square root of the waterline length, the length of the wave is the same as the waterline length. A yacht with an  $L_{WL}$  of 7 m will thus have one wave crest at the bow and the next one at the stern if the speed is 3.3 m/s.

The speed dependence of the waves gives rise to an important phenomenon: interference. An illustration of this is given in Fig 5.15. If the wave crests from the bow system coincide with those from the stern, large waves will be created. On the other hand, if the bow wave crests coincide with troughs in the stern waves, the result is an attenuated wave. The first case is illustrated in (a) and (c), where the wavelength is half and equal to the waterline length, respectively. In (b) the wavelength is  $\frac{2}{3}$  of  $L_{WL}$ , and the waves are attenuated. In the last figure (d) the wavelength is larger than the  $L_{WL}$ . The second wave crest then occurs aft of the stern, which, when the speed increases, will move into a trough, giving the hull a large trim angle.

Fig 5.15 Interference between the bow and stern waves

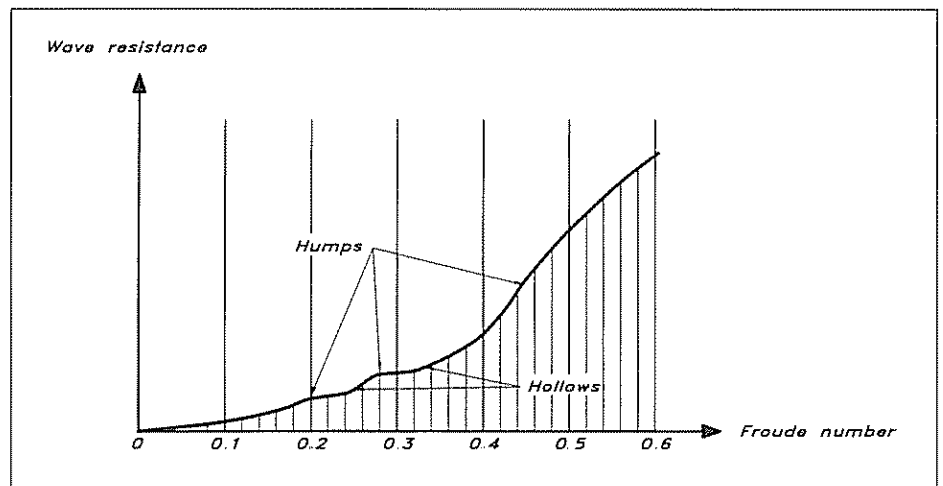


In each of the cases (a)–(d) a quantity  $F_n$  is given. This is the so called Froude number, which plays a similar role for the wave resistance as the Reynolds number does for viscous resistance. The Froude number is a dimensionless speed, where the velocity in metres per second is divided by the square root of the waterline length times the acceleration of gravity (see Fig 5.15). It is the Froude number that determines how many waves there are along the hull. For instance, at  $F_n = 0.40$  there is one wave, at 0.28 there are two, etc. The properties of the wave resistance curve are highly dependent on the Froude number,

as we will see below. The Froude number is therefore a very important quantity and we use it extensively in the following discussion, rather than the velocity in knots or metres per second. Using the simple definition, the Froude number can always be converted easily into these dimensional quantities.

Since the wave resistance occurs because energy is transported away in the waves, the amplification and attenuation due to interference between the wave systems must have some effect on the wave resistance curve. Thus, at speeds where there is an amplification of the waves the resistance must be relatively large, while the opposite must be true at speeds where there is an attenuation. The wave resistance curve thus exhibits what is normally referred to as humps and hollows (see Fig 5.16). It may be assumed that wave resistance increases with speed to the sixth power, but in addition there are the fluctuations due to interference.

Fig 5.16 *Humps and hollows on the wave resistance curve*



Humps and hollows may be more or less pronounced, depending on the hull shape. For many sailing yachts they are very small in the lower speed range, but the last hump is still important. The slope of the curve gets very large just below this speed and to get over the hump is difficult. If this can be achieved, however, the increase in resistance becomes more gradual, and the hull enters the semi-planing speed range. Catamarans and extremely light canoes and dinghies may accomplish this even beating to windward, while the lightest displacement hulls, like the America's Cup yachts enter the semi-planing range in the downwind legs. Most displacement hulls cannot, however, pass the barrier at the last hump.

According to the discussion above, the largest hump in the resistance curve should occur when the wavelength is equal to the waterline length, at  $F_n = 0.40$ , but in practice it occurs at a higher Froude number, ie at a higher speed. This is because the overhangs at the bow and stern cause the distance between the bow and stern waves to be larger than the nominal waterline length. The last hump thus occurs



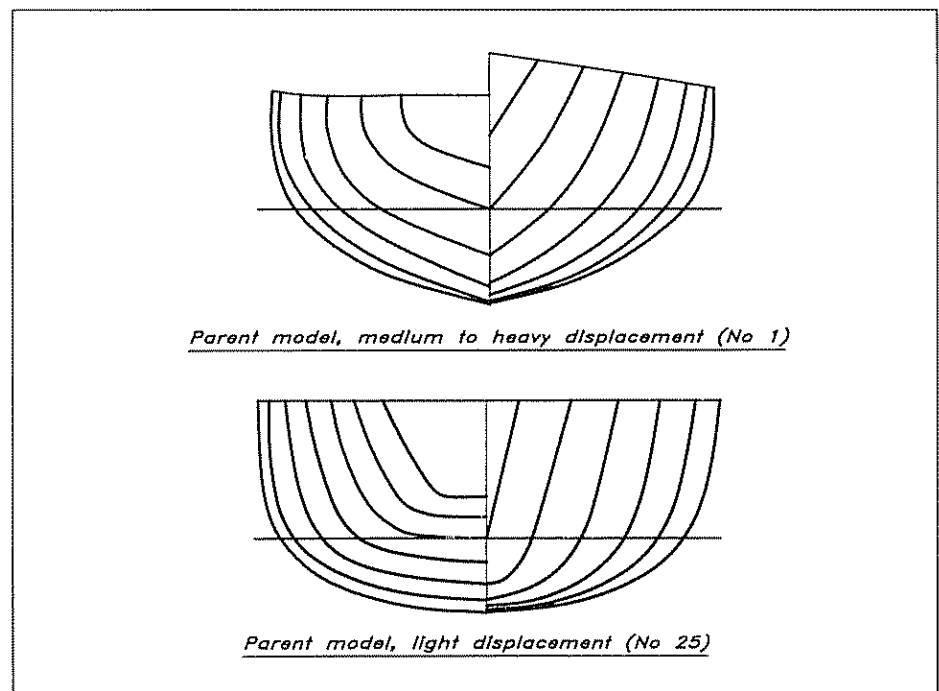
normally at a Froude number of about 0.5. Heavy displacement hulls cannot reach this value, except under special conditions, as when sailing in heavy following seas. Normally, it is difficult to reach higher Froude numbers than 0.45 for this kind of hull. The YD-40 has a waterline length of 10 m, so it is difficult to reach higher speeds than  $0.45 \sqrt{10 g} = 4.5$  m/s, corresponding to 8.7 knots. This is also apparent from the resistance curve of Fig 5.3. A hull twice as long would reach a speed of  $0.45 \sqrt{20 g} = 6.3$  m/s (12.2 knots). The speed has thus increased by a factor of  $\sqrt{2}$ .

It should be mentioned that in most literature on sailing theory an older quantity, the so-called 'speed length ratio' is used instead of the Froude number. This is defined as the speed in knots, divided by the square root of the waterline length in feet. In fact it differs only by a constant from the Froude number, but its disadvantages are that it is not dimensionless and that it is not based on metric quantities. Conversion between the two numbers can be made easily using the formula: Froude number =  $0.30 \cdot (\text{speed length ratio})$ .

### Influence of hull shape on wave resistance

Very extensive series of tests with models of sailing yachts have been carried out by Professor J Gerritsma and his co-workers at the Delft University of Technology in the Netherlands. The first series was run during the 1970s and comprised 22 models with a systematic variation of five different hull parameters:  $L_{WL}/B_{WL}$ ,  $B_{WL}/T_c$ ,  $C_p$ , LCB and  $L_{WL}/\nabla_c^{1/3}$ . All hulls were derived from a Frans Maas designed parent model, a medium displacement, contemporary ocean racer. Its body plan is shown in Fig 5.17(top). During the 1980s it became apparent, however, that an extension of the series to lighter displacements was

Fig 5.17 Body plans of the two Delft parent models



required, and a new parent model was designed by van de Stadt & Partners, see Fig 5.17 (bottom). Seventeen hulls based on this design were tested. The full range of variations in the five hull parameters for all 39 models is given in Table 5.1.

**Table 5.1**  
**Range of hull form parameters in the Delft series**

$L_{WL}/B_{WL}$	2.76 – 5.00
$B_{WL}/T_c$	2.46 – 19.32
$L_{WL}/\nabla_c^{1/3}$	4.34 – 8.50
LCB	0.0 – -6.0
$C_p$	0.52 – 0.60

(LCB in % of LWL forward of midship.)

From the Delft series several important empirical relations were derived. The formula for the wetted surface was presented in Fig 4.2. Now, however, we are concerned with resistance. Rather than presenting the wave resistance separately the scientists chose to give the sum of the wave and viscous pressure resistance, ie the residuary resistance. Since the hulls were smooth the only component missing in the total upright resistance is the friction (see Fig 5.4). As mentioned above, there is a good reason for lumping together the wave and viscous pressure resistance, since they are both dependent on the three-dimensional shape of the hull. When optimizing the hull for a certain speed, the combined effect on the wave and viscous pressure components must be considered.

The residuary resistance based on a statistical analysis of all 39 hulls may be computed from the formulae of Figs 5.18 and 5.19. To better fit the measured results the speed range has been split into two parts, one for the typical displacement speeds up to a Froude number of 0.45, Fig 5.18, and one for the semi-planing range 0.475–0.75 (Fig 5.19). The low speed formula contains four parameters:  $B_{WL}/T_c$ ,  $L_{WL}/\nabla_c^{1/3}$ , LCB and  $C_p$ , while the high speed formula contains only three:  $L_{WL}/B_{WL}$ , LCB and a special parameter  $A_w/\nabla_c^{2/3}$ . The latter parameter was chosen for the high speed range rather than the length/displacement ratio since it may better represent the ability of the hull to create a lifting force, the quantity  $A_w$  being the water plane area.  $A_w/\nabla_c^{2/3}$  is thus a kind of loading parameter for the water plane. Note that the total upright resistance is obtained by adding the friction, computed as in Fig 5.8.

The interested reader with access to a programmable calculator may program the formulae and use the coefficients of the tables to compute the residuary resistance of yachts of varying shapes. An accurate and effective optimization of a design may then be carried out, by

$$F_n = [0.125 - 0.450]$$

$$\begin{aligned} \frac{R_R}{g \cdot m_c} \cdot 10^3 &= a0 + a1 \cdot C_p + a2 \cdot LCB + a3 \cdot B_{WL} / T_c + \\ &+ a4 \cdot L_{WL} / \sqrt{v_c}^{1/3} + a5 \cdot C_p^2 + \\ &+ a6 \cdot C_p \cdot L_{WL} / \sqrt{v_c}^{1/3} + a7 \cdot (LCB)^2 + \\ &+ a8 \cdot (L_{WL} / \sqrt{v_c}^{1/3})^2 + a9 \cdot (L_{WL} / \sqrt{v_c}^{1/3})^3 \\ [ \frac{R_R}{g \cdot m_c} \cdot 10^3 &= 7.971 \text{ at } F_n = 0.35 ] \end{aligned}$$

LCB in % of  $L_{WL}$  from midship, positive forward.

$F_n$	a0 a5	a1 a6	a2 a7	a3 a8	a4 a9
0.125	-6.735654 -38.86081	+38.36831 +0.956591	-0.008193 -0.002171	+0.055234 +0.272895	-1.997242 -0.017516
0.150	-0.382870 -39.55032	+38.17290 +1.219563	+0.007243 +0.000052	+0.026644 +0.824568	-5.295332 -0.047842
0.175	-1.503526 -31.91370	+24.40803 +2.216098	+0.012200 +0.000074	+0.067221 +0.244345	-2.448582 -0.015887
0.200	+11.29218 -11.41819	-14.51947 +5.654065	+0.047182 +0.007021	+0.085176 -0.094934	-2.673016 +0.006325
0.225	+22.17867 +7.167049	-49.16784 +8.600272	+0.085998 +0.012981	+0.150725 -0.327085	-2.878624 +0.018271
0.250	+25.90867 +24.12137	-74.75668 +10.48516	+0.153521 +0.025348	+0.188568 -0.854940	-0.889467 +0.048449
0.275	+40.97559 +53.01570	-114.2855 +13.02177	+0.207226 +0.035934	+0.250827 -0.715457	-3.072662 +0.039874
0.300	+45.83759 +132.2568	-184.7646 +10.86054	+0.357031 +0.066809	+0.338343 -1.719215	+3.871658 +0.095977
0.325	+89.20382 +331.1197	-393.0127 +8.598136	+0.617466 +0.104073	+0.460472 -2.815203	+11.54327 +0.155960
0.350	+212.6788 +667.6445	-801.7908 +12.39815	+1.087307 +0.166473	+0.538938 -3.026131	+10.80273 +0.165055
0.375	+336.2354 +831.1445	-1085.134 +26.18321	+1.644191 +0.238795	+0.532702 -2.450470	-1.224173 +0.139154
0.400	+566.5476 +1154.091	-1609.632 +51.46175	+2.016090 +0.288046	+0.265722 -0.178354	-29.24412 +0.018446
0.425	+743.4107 +937.4014	-1708.263 +115.6006	+2.435809 +0.365071	+0.013553 +1.838967	-81.16189 -0.062023
0.450	+1200.620 +1489.269	-2751.715 +196.3406	+3.208577 +0.528225	+0.254920 +1.379102	-132.0424 +0.013577

$$[ R_R = 611 \text{ N at } F_n = 0.35 ]$$

Fig 5.18 Residuary resistance in the low speed range

$$F_n = [0.475 - 0.750]$$

$$\frac{R_R}{g \cdot m_c} \cdot 10^3 = c0 + c1 \cdot L_{WL}/B_{WL} + c2 \cdot A_W/\nabla_c^{2/3} + c3 \cdot LCB +$$

$$+ c4 \cdot (L_{WL}/B_{WL})^2 + c5 \cdot (L_{WL}/B_{WL}) \cdot (A_W/\nabla_c^{2/3})^3$$

(  $A_W$  = waterplane area )

$F_n$	$c0$	$c1$	$c2$	$c3$	$c4$	$c5$
0.475	+180.1004	-31.50257	-7.451141	+2.195042	+2.689623	+0.006480
0.500	+243.9994	-44.52551	-11.15456	+2.179046	+3.857403	+0.009676
0.525	+282.9873	-51.51953	-12.97310	+2.274505	+4.343662	+0.011066
0.550	+313.4109	-56.58257	-14.41978	+2.326117	+4.690432	+0.012147
0.575	+337.0038	-59.19029	-16.06975	+2.419156	+4.766793	+0.014147
0.600	+356.4572	-62.85395	-16.85112	+2.437056	+5.078768	+0.014980
0.625	+324.7357	-51.31252	-15.34595	+2.334146	+3.855368	+0.013695
0.650	+301.1268	-39.79631	-15.02299	+2.059657	+2.545676	+0.013588
0.675	+292.0571	-31.85303	-15.58548	+1.847926	+1.569917	+0.014014
0.700	+284.4641	-25.14558	-16.15423	+1.703981	+0.817912	+0.014575
0.725	+256.6367	-19.31922	-13.08450	+2.152824	+0.348305	+0.011343
0.750	+304.1803	-30.11512	-15.85429	+2.863173	+1.524379	+0.014031

Fig 5.19 Residuary resistance in the high speed range

investigating different alternatives. This approach is more quantitative than the traditional one, where the designer has to rely on experience and rules of thumb.

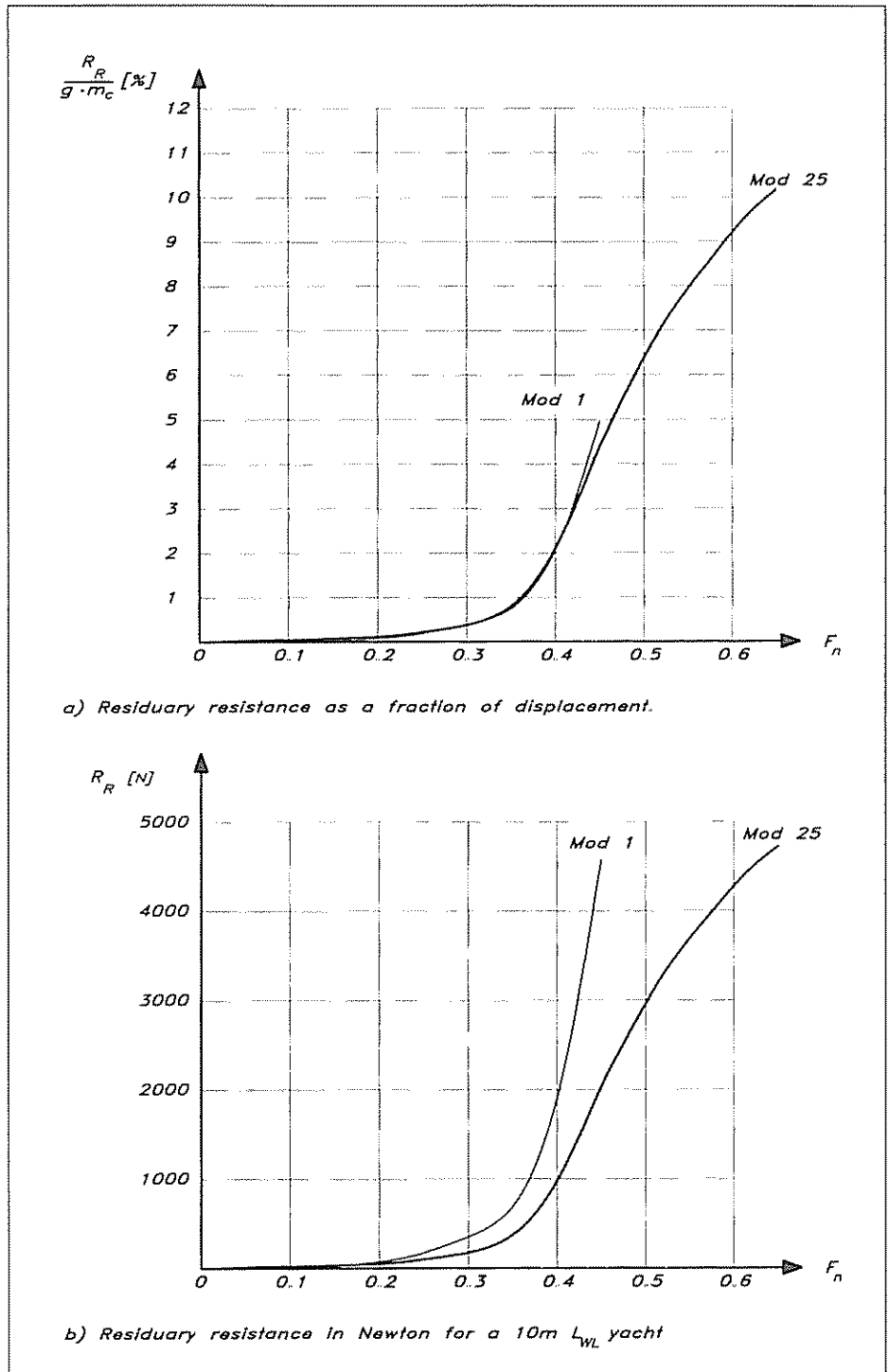
In the following we shall also use the formulae to draw some general conclusions on the influence of the hull shape on the residuary resistance.

### Displacement

In the formulae of Figs 5.18 and 5.19 the residuary resistance is expressed as a fraction of the hull weight. This fraction is in the range 0–10% for hull speeds of practical interest. As an example, the resistance curves for the two parent models of Fig 5.17 are shown in Fig 5.20. These hulls are typical representatives of the medium/high displacement series (models 1–22) and the light displacement series (23–39), respectively. The resistance as a fraction of hull weight (top figure) is very similar up to a Froude number of around 0.4, but thereafter the curve for model 1 bends upwards, while that of model 25 exhibits an inflexion after which the slope is reduced.

A quite different picture is seen in the bottom part of Fig 5.18, which shows the residuary resistance in Newtons for the two hulls at full scale, assuming an  $L_{WL}$  of 10 m. The displacement of hull no 1 is 9.18 tons, while that of no 25 is only 4.62 tons, so there is approximately a factor of two between the heavy and the light hull displacements. This is reflected in an approximately equally large difference in resistance for

Fig 5.20 Residuary resistance of the two Delft parent models



the low speed range. Due to the very sharp increase in resistance for the heavy hull above  $F_n = 0.45$  this yacht will not reach higher Froude numbers than that, while the light hull can reach 0.60 or higher, since the slope of the curve is small.

From Fig 5.20 we learn that the displacement is a very important

parameter for the residuary resistance. In the displacement speed range, up to about  $F_n = 0.45$ , the resistance is roughly proportional to the displacement. At a certain Froude number the residuary resistance is more or less the same, expressed as a fraction of the displacement, regardless of the shape of the yacht, ie whether it is small or large, light or heavy, narrow or beamy, etc. For example, at  $F_n = 0.3$  the residuary resistance is normally 0.3–0.4% of the hull weight, at  $F_n = 0.35$  0.7–0.8%, at 0.40 2.0–2.5% and at 0.45 4.5–5.5%. Note that the resistance is given versus Froude number. If yachts of different sizes are compared the larger yacht will have a larger speed at the Froude number in question.

While the displacement, or hull weight, rather, is the major factor determining the residuary resistance, the form parameters of Fig 5.18 may change the resistance within the limits given above for a given displacement. Variations of 10–20 % in the residuary resistance may thus occur due to changes in these form parameters, and at least three of them ( $L_{WL}/\nabla_c^{1/3}$ ,  $C_p$  and LCB) need to be considered if the hull is to be optimized. In the following we will consider all five parameters, ie  $L_{WL}/B_{WL}$  and  $B_{WL}/T_c$  also.

### *Length/displacement ratio*

A high length/displacement ratio has a somewhat unfavourable effect on the resistance per unit weight in the low speed range. It is barely visible in Fig 5.20(a) due to the limited resolution, but the lighter hull with a larger length/displacement ratio has a slightly larger resistance per kg of displacement in this speed range. However, the major effect is in the high speed range, which can only be reached if the length/displacement ratio is large enough. Exactly how large the ratio has to be is impossible to say, since the other parameters, as well as section shape, stability, etc also play a role. However, values around 5.7 are often quoted in the literature. Hulls with lower values are likely to run into the ‘barrier’ at around  $F_n = 0.45$ , while those with a larger ratio may pass the hump and reach higher speeds. The larger the ratio the higher the speed possible. Unfortunately, it is very difficult to build standard yachts with a length/displacement ratio larger than about 5.2, due to structural problems. Extreme racers such as the America’s Cup yachts may, however, reach values up to 7.5, and such values are often found for racing dinghies like the 5-o-5 and the Flying Dutchman. It is difficult to beat the International Canoe with a value of 8.8. Further information on length/displacement ratios is given in the section on hull statistics.

An older parameter, often used in the sailing literature, is the displacement/length ratio, defined as  $\Delta_c/(L/100)^3$ , where  $L$  is the waterline length in feet and  $\Delta_c$  is given in tons. To facilitate the comparison between the two ratios Fig 5.21 has been prepared. The planing limit expressed in displacement/length ratio is about 150, while the practical lower limit for standard hulls is about 200.

### *Prismatic coefficient*

The optimum value of  $C_p$  for heavy to medium displacement hulls may be derived from the formula of Fig 5.18 for each given speed, and the

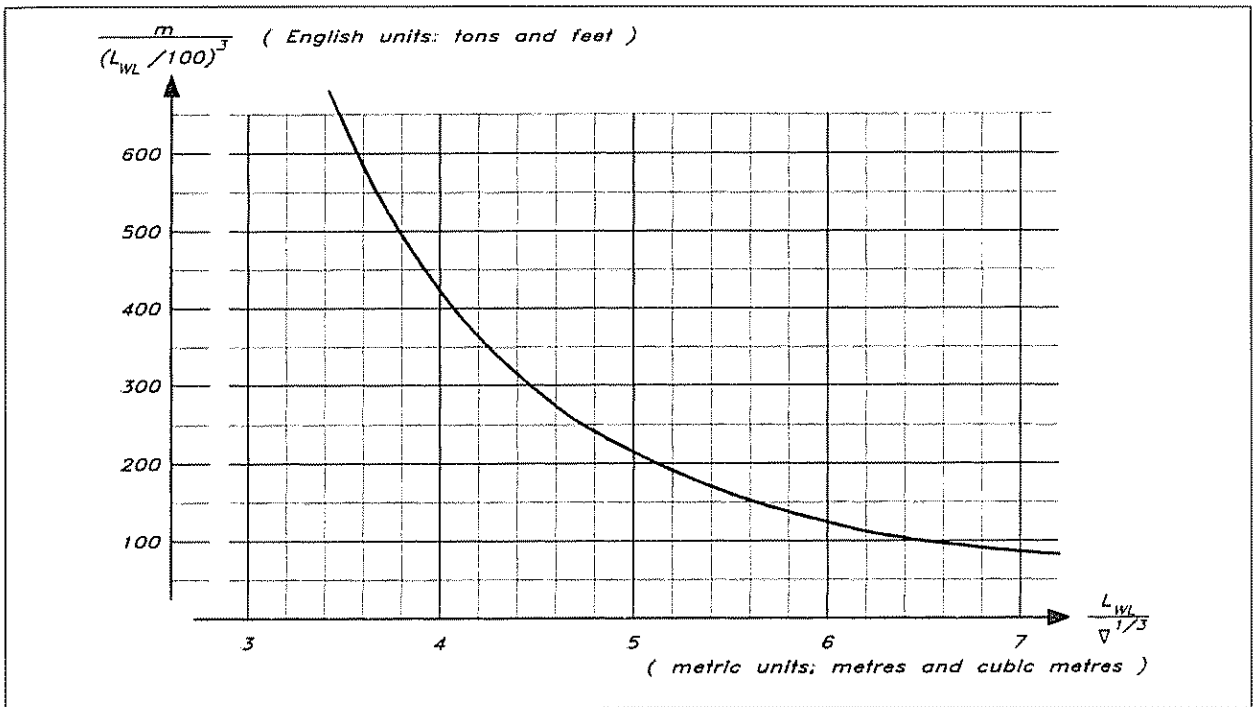


Fig 5.21 Displacement/length against length/displacement ratio

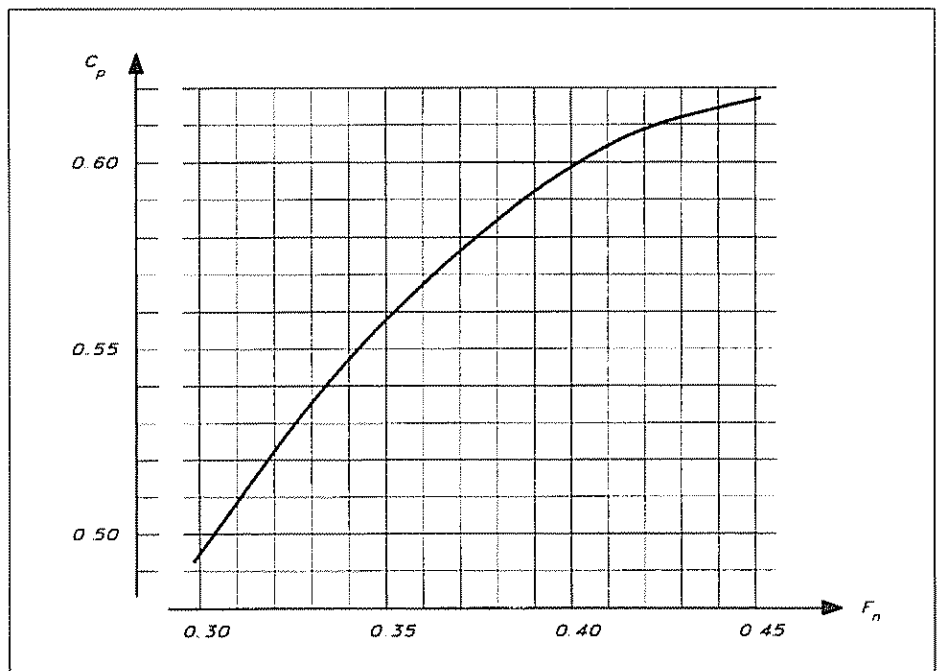
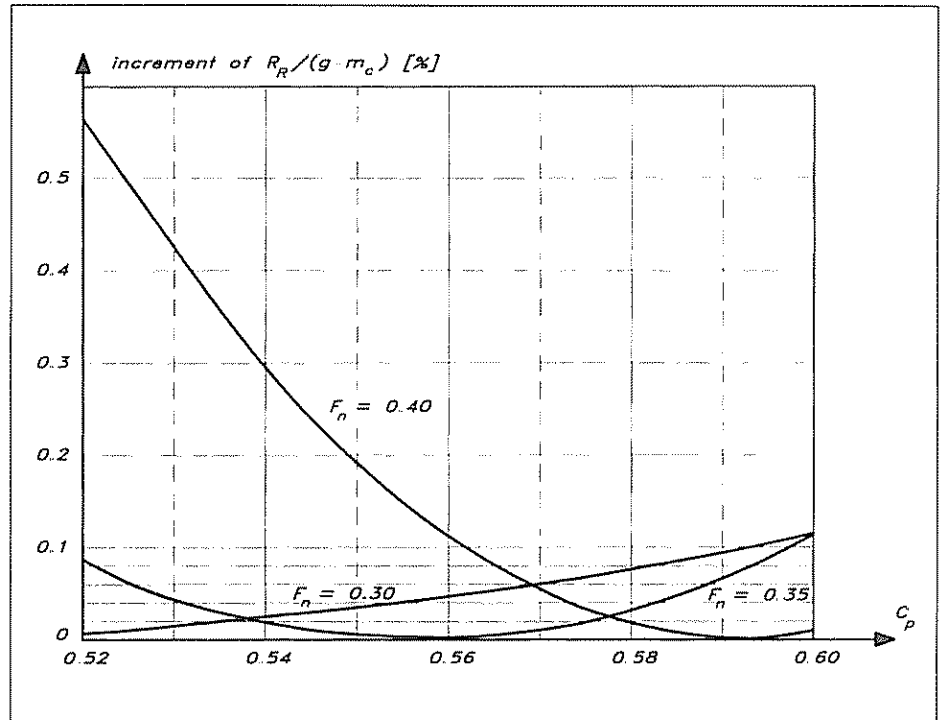


Fig 5.22 Optimum prismatic coefficient

result is given in Fig 5.22. The designer has to decide at what speed his yacht shall have its optimum performance. Upwind in light wind the prismatic coefficient should be 0.5 or even lower, while downwind in more wind the coefficient should be 0.6 or slightly higher, if the hull is of the traditional heavy or medium displacement type. Normally, hulls are designed for maximum performance beating upwind in a breeze. The Froude number is then around 0.35, which gives a prismatic of 0.56.

The increase in residuary resistance, if  $C_p$  differs from the optimum, may also be obtained from the formula. In Fig 5.23 the increase is given for three different Froude numbers: 0.30, 0.35 and 0.40. These cover the upwind speed range for most yachts. It can be seen that the largest increases occur if  $C_p$  is too small and the speed is relatively high.

Fig 5.23 Resistance increase (in % of displacement) due to non-optimum prismatic coefficient



For lightweight hulls, which can reach the semi-planing region at Froude numbers above 0.45, the situation is more complicated. To attain high downwind speeds and surfing capabilities the aft part of the bottom has to be flat and relatively horizontal. The best solution is in fact to have a submerged transom, as on power boats, but this is hardly possible for a sailing yacht, which has to operate in a wide speed range. The low speed characteristics of this solution are not acceptable. For transom stern hulls the optimum prismatic increases to about 0.70 at Froude numbers of 1.0, due to the fact that the transom should become larger as the speed increases, but if a transom has to be avoided the requirement of a flat horizontal bottom automatically means a small prismatic. No optimum value can be derived from the high speed formula of Fig 5.19, since  $C_p$  is not even included. Neither is it possible to derive useful relations from the general hydrodynamics literature, since submerged transoms are always assumed in this speed range. In practice, the designer has to some extent to sacrifice the upwind characteristics in the low speed range and use a somewhat smaller prismatic than the optimum from Fig 5.22 to obtain better downwind performance.



*Centre of buoyancy*

Fig 5.24 gives the optimum location of the centre of buoyancy, LCB. Again this is for the medium to high displacement hulls. Obviously, the variation is very small over the speed range. Note that a negative sign means aft of midship, and that the numbers given represent the distance from this section in percentage of  $L_{WL}$ . As in the case of  $C_p$  the increase due to a non-optimum LCB has been computed and the result is given in Fig 5.25.

Fig 5.24 Optimum location of centre of buoyancy

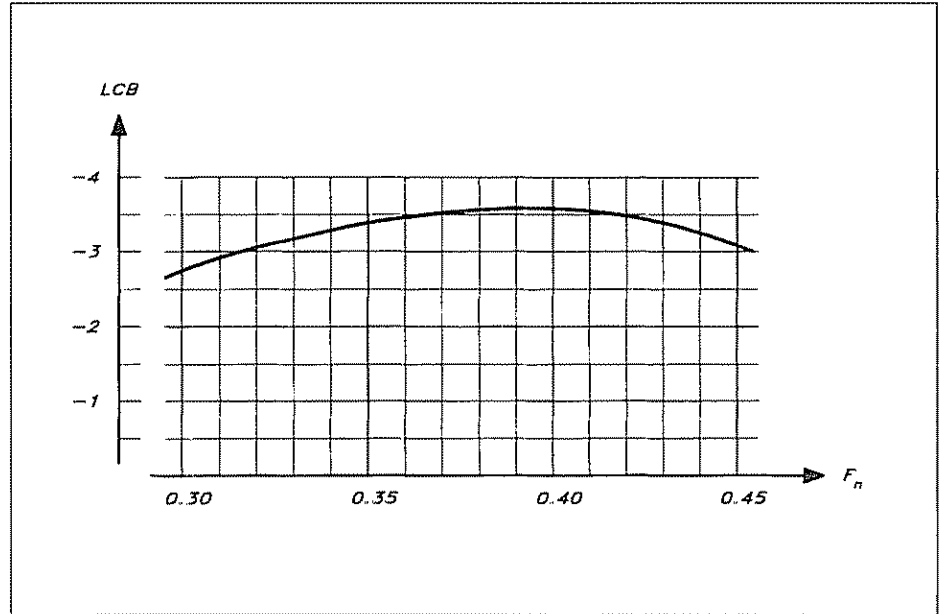
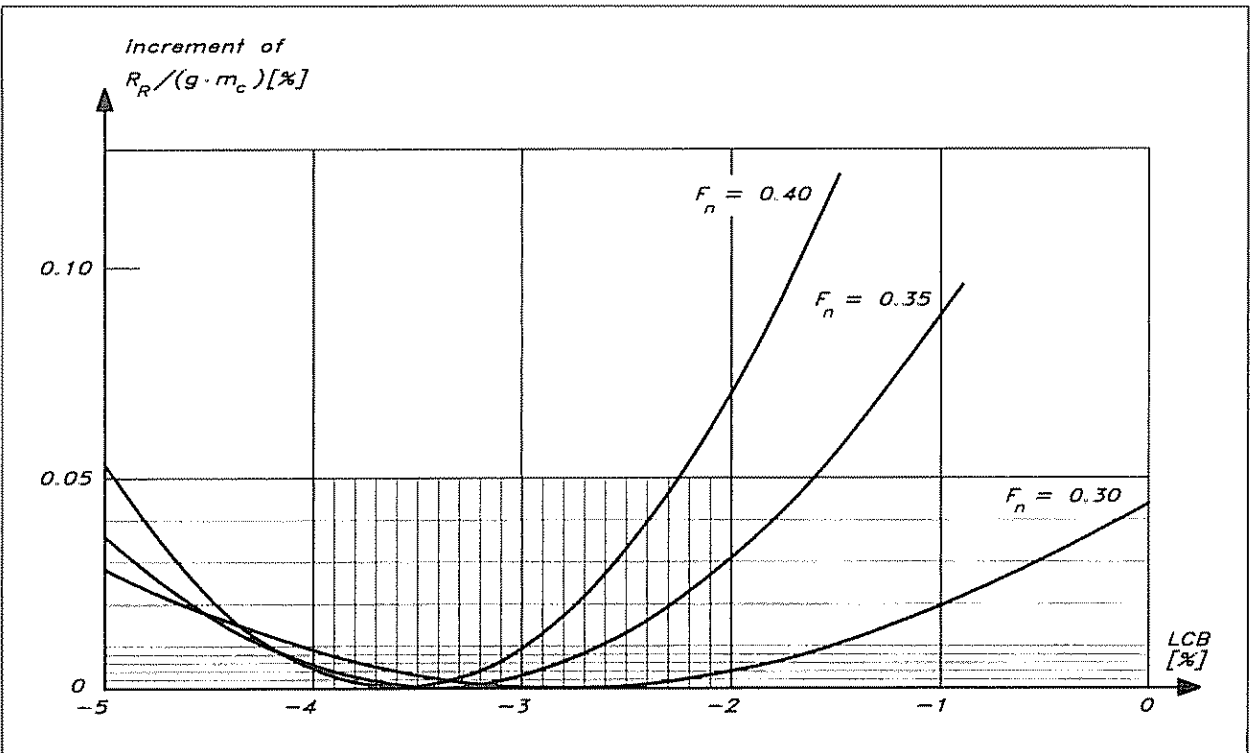


Fig 5.25 Resistance increase (in % of displacement) due to non-optimum LCB location



The reasons why  $C_p$  should be increased and LCB moved aft when the speed increases in the low speed range have been mentioned in connection with the viscous pressure resistance. A full stern increases this component, while the wave resistance is reduced, due to the fact that the thick boundary layer and possible separation makes the effective hull longer. At speeds corresponding to Froude numbers in the range 0.40–0.45 wave resistance dominates, and a full stern is better, while the opposite is true at lower speeds where the waves are small.

As in the case of  $C_p$  the optimum LCB value in the high speed range depends on whether or not a submerged transom can be accepted. If so, the LCB should move aft to about 6% of  $L_{WL}$  from the midship at a Froude number of 1.0. This is also related to the fact that the transom should increase with speed. However, if a transom cannot be accepted, the LCB automatically moves forward relative to the locations given in Fig 5.24, since the stern region has to be flat.

A problem occurs when applying the above results to hulls with an integrated keel, since the measurements were made with fin-keel type of yachts. The quantities above are for the hull alone. It is therefore necessary to make an artificial separation of the hull and keel and compute the parameters for this new hull.

### *Length/beam and beam/draft ratio*

The effect of these parameters is very small. A beam variation was made between the first three models in the Delft series, keeping all of the above parameters constant. Naturally, this variation caused changes both in the length/beam and beam/draft ratios, but the result showed that the narrow boat ( $B_{WL}/T_c = 3.0$ ) had the smallest residuary resistance up to a Froude number of 0.375. Thereafter, the medium boat ( $B_{WL}/T_c = 4.0$ ) was the best. The beamiest boat ( $B_{WL}/T_c = 5.35$ ) was worse than the others in all but the highest speeds above  $F_n = 0.4$ , where it became better than the narrow one.

It is possible to extract the effect of  $B_{WL}/T_c$  alone from the low speed formula. Since the coefficient  $A_3$  is positive an increase in this ratio should result in a slight increase in residuary resistance. Unfortunately, conclusions cannot be drawn on the influence of  $L_{WL}/B_{WL}$  alone, since it is not included in the low speed formula. Neither is it possible to draw any general conclusions on this parameter alone from the high speed formula, where the parameter occurs in several terms.

Often, the effect on the wetted surface, and hence the frictional resistance, is as large or larger than the effect on the residuary resistance when beam is changed. There are also other aspects on beam variations, above all the hull stability, which increases with beam to the third power. The effect on the added resistance in waves is also quite important, and a large beam, or large fullness in the bow region in particular, increases this resistance component considerably. Finally, there is an important effect on the resistance due to heel, as will be seen below.

The YD-40 has been designed to have its best performance upwind in a fresh breeze, when the Froude number is about 0.35. As appears from Figs 5.22 and 5.24, the prismatic coefficient should then be 0.56

and the longitudinal centre of buoyancy should be located 3.5% behind midship. Both these requirements are met. The choice of other shape parameters will be discussed in connection with hull statistics in a later section.

### Heel resistance

When the hull heels due to the side force from the sails, two resistance components develop, as explained in the first section of this chapter. The induced resistance is by far the most important one, but it will not be discussed here, since it is mainly caused by the keel and rudder, which generate the major part of the hydrodynamic sideforce. Less important is the heel resistance, which represents the change in upright (viscous plus wave) resistance due to the heel angle. One way to obtain this component would be to compute the hull parameters for the heeled hull and use them in the formulae above. By comparing with the unheeled results the effect of heel could be obtained. However, if this technique were to be used, there is no need to treat the heeled resistance as a separate component.

Fig 5.26 Heel resistance

*Heel resistance coefficient:*

$$C_H = [6.747 \cdot (T_c/T) + 2.517 \cdot (B_{WL}/T_c) + 3.710 \cdot (B_{WL}/T_c) \cdot (T_c/T)] \cdot 10^{-3}$$

$[ 21.611 \cdot 10^{-3} ]$

*Heel resistance:*

$$R_H = 0.5 \cdot \rho \cdot V^2 \cdot S_W \cdot C_H \cdot F_n^2 \cdot \phi \quad [ 99 \text{ N} ]$$

$\rho$  : Density of water [1025 kg/m<sup>3</sup>]  
 $V$  : Boat speed [3.5 m/s]  
 $S_W$  : Wetted surface of hull in upright position [ 25.2 m<sup>2</sup> ]  
 $\phi$  : Heel angle [rad] =  $\frac{\pi \cdot \phi}{180}$  [deg] [ 13.6 deg ]

A more common technique, simpler, but more approximate, is to use an entirely empirical correction to the upright resistance. From the Delft series the formulae of Fig 5.26 may be obtained. It may be seen that the two geometrical quantities of interest are the hull draft to the total draft,  $T_c/T$ , and the beam to hull draft ratio,  $B_{WL}/T_c$ , as mentioned above. The resistance increases with Froude number squared and is proportional to the heel angle.

When computing the heel resistance of the YD-40 in Fig 5.4 the heel angle, which should be appropriate for about 8 m/s of wind, has been taken as the Dellenbaugh angle (defined in the previous chapter). This angle is 13.6°, and yields a heel resistance of 99 N, 6.5% of the total. Note that the angle shall be given in radians (degrees/ 57.3) in the formula.

### Added resistance in waves

Chapter 4 introduced some basic safety factors when sailing in waves, and presented and discussed the solution of the equation for the rolling

motion. It was pointed out that similar equations hold for the other types of motion, provided the coupling between them can be neglected. Here we shall deal with a special aspect of seakeeping, namely the added resistance caused by the waves. As pointed out in Chapter 4, the theory of seakeeping is quite complex and cannot be treated comprehensively in this book. We will explain only some fundamental concepts related to the added resistance, and give some guidelines on how to reduce it.

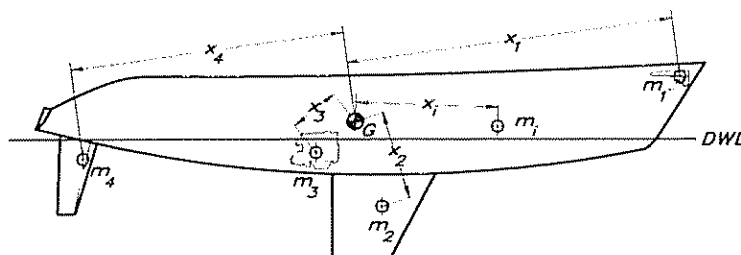
When a yacht moves in a seaway, the waves impose motions of all kinds on the hull. The most important ones, from a resistance point of view, are the heave and pitch motions, which are usually strongly coupled. When the hull heaves and pitches it generates its own wave system, which carries energy away in much the same way as the still water wave pattern, thereby creating a resistance force.

Of some importance for a sailing yacht is also the rolling motion, which, as we have seen, creates vortices at the tip of the keel and rudder, ie a kind of induced resistance, similar to the one created by the tip vortices when the yacht is sailing in smooth water (see Chapter 6). In the following we will concentrate on heave and pitch.

As in the case of rolling the yacht has natural frequencies in heave and pitch. When the frequency of encounter of the waves is equal to the natural frequency of one of these motions resonance occurs, and the corresponding motion amplitude gets very large. The added resistance is particularly serious if resonance occurs in pitch, since the resistance may then increase considerably. Ocean waves are normally considerably longer than the yacht, and the frequency of encounter is much smaller than the natural frequency, so resonance is unlikely to occur offshore. In sheltered waters, however, it may happen. To move away as far as possible from resonance, the natural frequency should be increased when the frequency of encounter is smaller and vice versa, so practically it is always beneficial to have as high a natural frequency as possible. This means that the hull will follow better the contour of the waves.

The most important quantity in connection with the natural

Fig 5.27 Calculation of the mass moment of inertia –  $I_{YY}$



Mass moment of Inertia:

$$I_{YY} = m_1 x_1^2 + m_2 x_2^2 + m_3 x_3^2 + \dots + m_i x_i^2 + \dots$$

$$\text{Gyradius: } k = \sqrt{\frac{I_{YY}}{m}} \quad ; \quad ( I_{YY} = m \cdot k^2 )$$

frequency in pitch is the mass moment of inertia of the yacht around a transverse axis through the centre of gravity. This quantity may be computed, considering all weights on board, as described in Fig 5.27. Note that all parts of the yacht, including the mast, keel and hull skin, have to be considered. To make the calculation, all large components have to be divided into smaller pieces, each one with a certain mass and distance from the centre of gravity. The calculation of the mass moment of inertia could be made in connection with the weight calculation, presented in Appendix 2, but this is seldom done, simply because there are no guidelines for its maximum value. We will, however, elaborate on this quantity and look at an example, showing the importance of minimizing it.

Since every object contributes to the moment of inertia not only by its mass, but also by the distance to the centre of gravity squared, objects positioned far away will have a large influence. Such objects include, for instance, lights, wind gauges or antennas at the top of the mast, or tanks, anchors and other mooring gear stowed at the ends of the yacht.

For convenience, another quantity, namely the gyradius, which is related to the moment of inertia, is defined in Fig 5.27. This is the length which, squared and multiplied by the hull mass, gives the moment of inertia. For ships the gyradius is usually assumed to be one quarter of the hull length, and this seems to be a reasonable assumption for a sailing yacht also. The mass moment of inertia may thus be approximated as one quarter of the overall hull length squared times the hull mass.

To obtain a more exact value of the gyradius, and to study its effect, careful calculations were carried out for a three-quarter tonner,

Table 5.2 (a)

**Mass moment of inertia for *Sunshine*, cruising version**

<i>Object</i>	<i>Mass (kg)</i>	<i>% of total mass</i>	<i>Moment of inertia (moi)</i>	<i>% of total moi</i>
Rig	104	3.2	6798	42.0
Hull	597	18.3	3631	22.4
Deck	300	9.2	1867	11.5
Keel	1200	36.8	1296	8.0
Rudder	30	0.9	471	2.9
Motor	230	7.1	345	2.1
Others	800	24.5	1774	11.0
<b>Total</b>	<b>3261</b>	<b>100.0</b>	<b>16182</b>	<b>100.0</b>

Table 5.2 (b)  
**Mass moment of inertia for *Sunshine*, racing version**

<i>Object</i>	<i>Mass (kg)</i>	<i>% of total mass</i>	<i>Moment of inertia (moi)</i>	<i>% of total moi</i>
Rig	73	2.2	4759	43.1
Hull	299	9.2	1816	16.4
Deck	150	4.6	933	8.4
Keel	1200	36.8	1296	11.7
Rudder	30	0.9	471	4.3
Motor	230	7.1	0	0.0
Others	1279	39.2	1774	16.1
<b>Total</b>	<b>3261</b>	<b>100.0</b>	<b>11049</b>	<b>100.0</b>

*Sunshine*, built in the early 1980s. In Table 5.2 the contribution to the mass moment of inertia of all parts of the yacht is given. Table 5.2(a) gives the values relevant for a cruising version, while the corresponding values for an extreme racing version are given in 5.2(b). The masses are also given, and it should be noted that, for rating reasons, the total mass is the same. Note also the very large contribution from the rig in both tables. It is twice as important as the hull and four to five times as important as the keel for the moment of inertia. The cruising version had a gyradius of 2.22 m, while it was only 1.85 m for the racer.

The effect of varying the gyradius was investigated by computing the motions and added resistance using a ship motions computer program, and introducing the resistance into a Velocity Prediction Program (VPP) for sailing yachts. (An introduction to VPPs will be given in Chapter 16.) The result of the calculations is presented in Figs 5.28 and 5.29. In the first figure the variation in speed made good to windward (the velocity component opposite the wind direction) is given for four wind speeds from 6 to 18 m/s, with a gyradius varying from 1.5 to 2.5 m. A significant drop in speed is noted between the two extremes. On the other hand, as we have seen, the range in gyradius is probably too wide. Introducing the two values computed for *Sunshine*, 2.22 m and 1.85 m respectively, it is seen that the speed of the cruiser is roughly 0.1 knots lower than that of the racer. This is a reduction in speed by 2.2%, and would render the cruiser chanceless in a race. The corresponding results computed as an average over all wind directions are given in Fig 5.29. It should be pointed out that no effect of the sails on the motions was considered in these calculations. Since only pitch and heave are taken into account, this approximation is reasonable. In rolling, the sails certainly have a large damping effect.

No general method for computing the added resistance in waves has

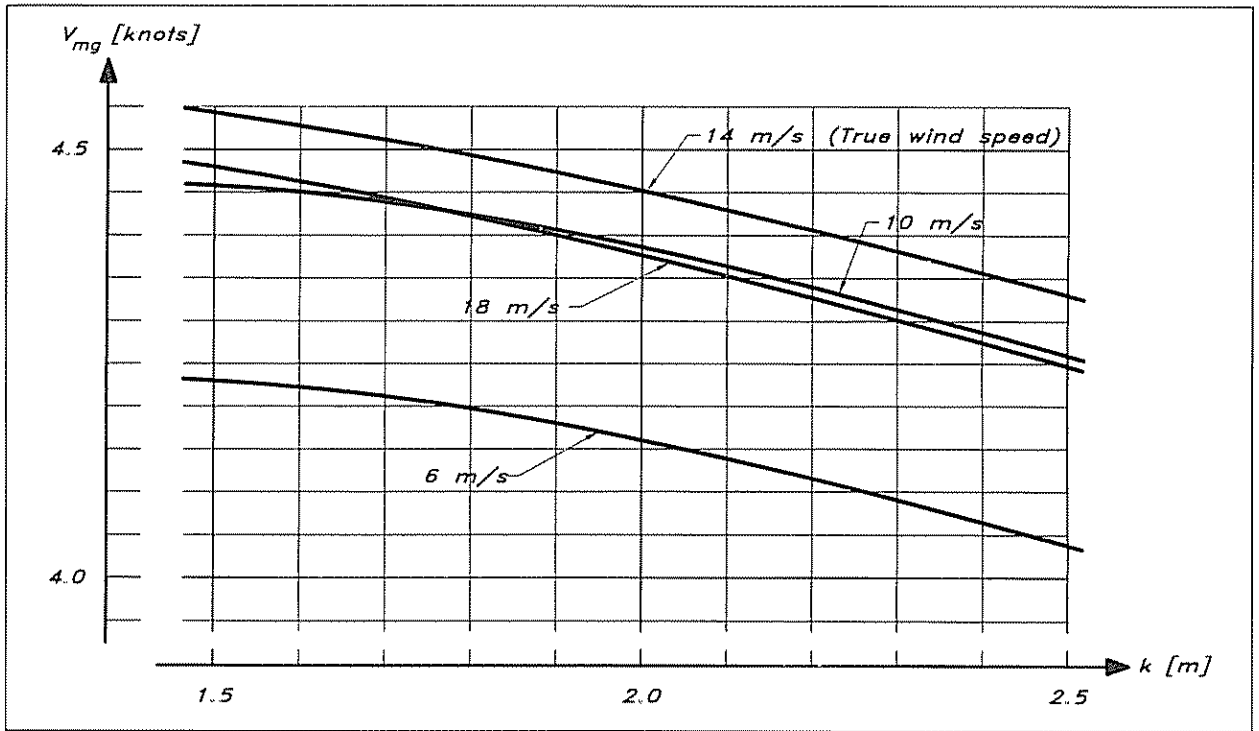


Fig 5 28 Influence of gyradius on speed made good – Sunshine

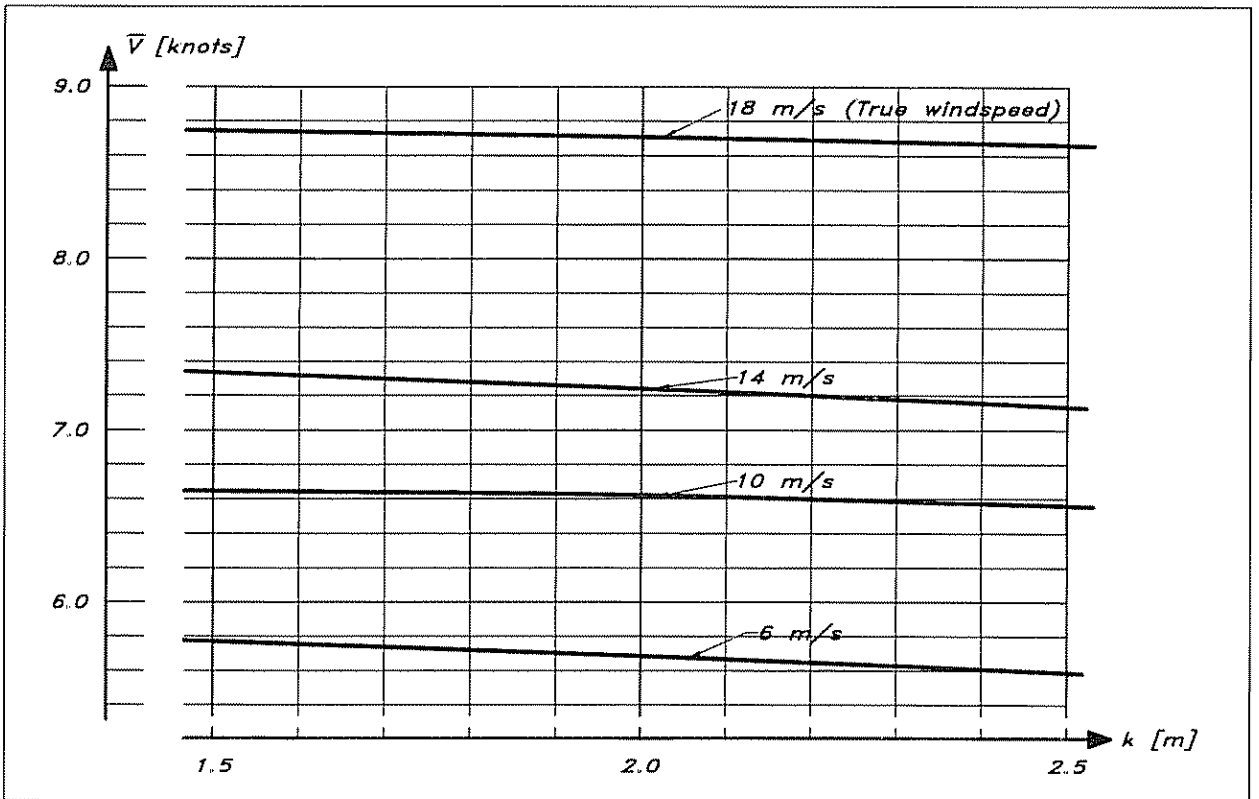


Fig 5 29 Influence of gyradius on average speed – Sunshine

been presented in the literature, so individual calculations using a ship motions program for each hull has to be made, as in the above example. However, Professor Gerritsma and his co-workers at the Delft University of Technology have carried out very extensive calculations for systematically varied hull forms. Their aim has been to provide a statistical formula, like those presented for the residuary resistance, also for the added resistance in waves. The complete results of the study are not yet available, but some useful information has been released, and we will present two diagrams based on that information.

Fig 5.30 gives the added resistance for 10 m  $L_{WL}$  yachts of varying length/displacement ratio moving at an angle of  $135^\circ$  relative to the direction of wave propagation. The waves thus hit the hull at an angle of  $45^\circ$  from ahead. It is seen that resonance occurs at a wave period between three and four seconds, where the resistance is at its maximum. The waves used for the calculation are relevant to unsheltered waters of the size of the North Sea. The relation between wave height and wave period for this water area is given in Fig 5.31. Since the waves are irregular, the exact meaning of height and period is not obvious, but as in common practice, we mean the so-called significant wave height and the mean period. The significant wave height is the mean value of the largest one third of the waves, and that is what is normally estimated as the wave height by experienced sailors. Fig 5.31 also gives the relation between wavelength and period, valid for all deep water waves. We will use the results of Figs 5.30 and 5.31 in the resistance estimation for the propeller and engine selection in Chapter 9.

### Other seakeeping aspects

The two most important requirements on a sailing yacht in a seaway are that it is stable enough to avoid capsizing even under severe conditions, and that the hull can withstand the loads exerted by the

Fig 5.30 Added resistance in waves for a 10 m  $L_{WL}$  yacht

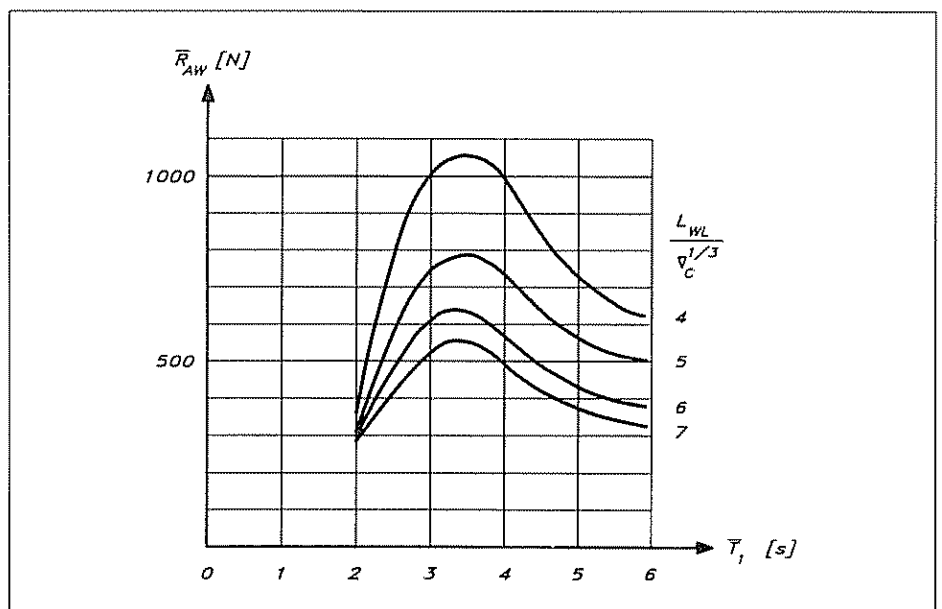
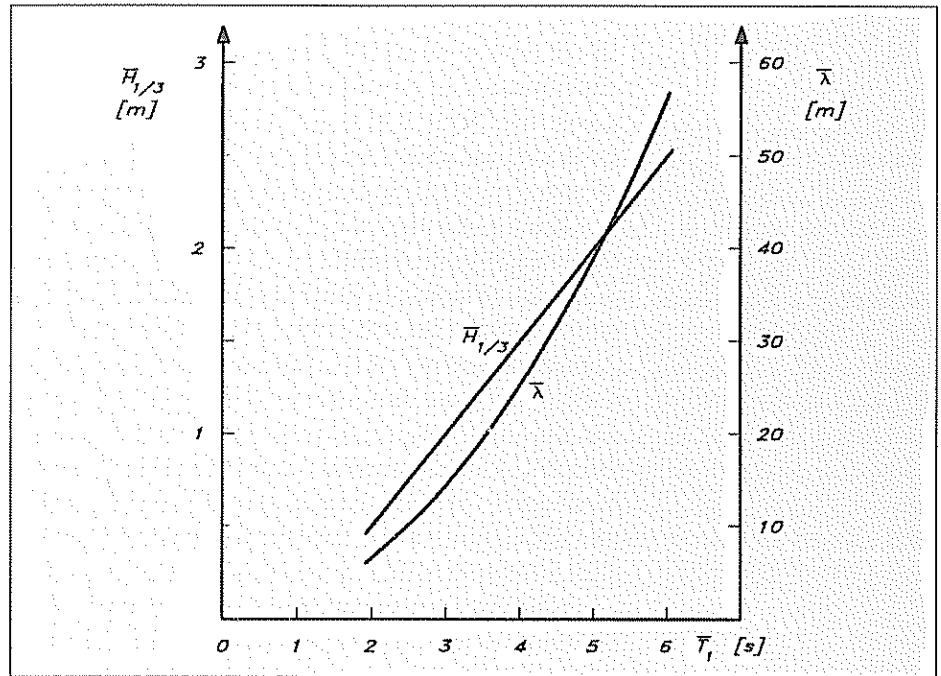




Fig 5.31 Relation between wave period, height and length



waves. These aspects are dealt with in Chapters 4 and 12 respectively. For a racing yacht the added resistance comes next in order of importance, and it was therefore dealt with at some length in the previous section. However, for a cruising yacht other aspects of the design may be equally important. In fact, what might be termed 'seakindness' may be more valuable for a crew, which has to spend months on board the yacht during long ocean crossings. A yacht that is seakind is easy to live on even under relatively difficult conditions. By its very nature this property is more difficult to quantify, but it is clear that the motions of a seakind yacht must be soft enough to enable the crew to work without problems and to relax after work.

As explained in Chapter 4, the motions of the yacht depend on its inertia, its stability and its damping. Since pitch, roll and heave are the most important motions, the most important inertial quantities are the mass moments of inertia around a transverse and a longitudinal axis (or the corresponding gyradii), as well as the hull mass. The stability depends on the shape of the waterline area and its moment of inertia around two axes. Finally, the damping depends on the size of the keel.

Most modern designers strive for small gyradii, a light hull, large stability and a small keel. All these features tend to increase the accelerations onboard the yacht, thus making it less seakind. For a cruising yacht this is unlikely to be the optimum solution. A very severe problem of this kind was experienced when the first large ships for carrying ore were taken into service. When the ore was loaded on the bottom of the hull, its stability became so large that excessive accelerations were created. In fact, some fatal accidents occurred when people were thrown towards the bulkheads in heavy seas. Modern ore

carriers have the ore in a cradle lifted from the bottom of the hull, and much softer motions are obtained. Another ship type for which soft motions are important is the fishing boat, where the fishermen have to carry out their work on deck, often in heavy seas. To cope with this problem some boats have an increased transverse gyradius from weights of iron or concrete put as far sideways as possible inside the hull.

Other quantities which affect the hull's seakeeping capabilities are the overhangs fore and aft, the freeboard height and the bow flare. A large forward overhang is likely to increase pitching, since large pitching moments are created when a wave hits this part of the hull far from the centre of gravity. Aft overhangs may, of course, have a similar effect in following seas, but the frequency of encounter is then much lower so the problem is small. On the contrary, the stern overhang may be beneficial, since it may damp the pitch motions in head seas. A high freeboard forward, and a flared one in particular, prevents green water on deck, and spray hitting the cockpit is effectively avoided also. The hull thus gets much dryer.

A final point to mention is the balance between the forward and aft halves of the hull. Many yachts of the 1980s had very full stern sections, while the forward sections were very sharp. This may be good for the surfing abilities of the hull, but it is not good for the course stability when rolling. When the hull heels over, the centre of buoyancy moves much more sideways in the stern than in the bow. The force required to move the volume of water sideways comes from the hull, which by the law of action and reaction is affected by the same force from the water, but in the opposite direction. The stern is thus affected much more than the bow, and the hull changes its course in the heeling direction. This happens, of course, both to starboard and port, and the hull becomes difficult to keep on course.

### Hull statistics

To aid the designer in his choice of main proportions for the yacht, a compilation of hull statistics for the most important quantities is presented in this section. The data come from several hundred yachts of both European and American design.

Statistics will be given for the main hull dimensionless ratios: length overall/max beam, length of waterline/draft, length of waterline/canoe body draft and length of waterline/(volume displacement)<sup>1/3</sup>. Two ratios important for the above-water appearance of the hull will be presented also: freeboard forward/length of waterline and freeboard forward/freeboard aft. Finally, statistics for the ballast ratio will be discussed.

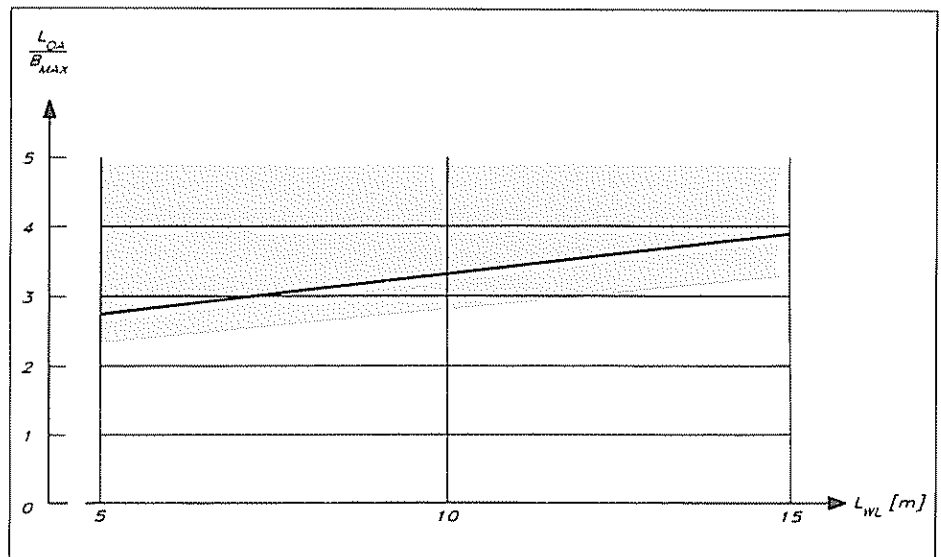
It should be pointed out that the data used in the statistical evaluation are for the light condition, ie without crew, stores, water and fuel. This condition corresponds best to the official data for a yacht and is used for rating purposes and in class rules. A fully equipped cruising yacht with the crew on board may be up to 20% heavier. In the computations for the YD-40 in this book we have assumed a half-loaded condition with the crew, which reflects reality more closely. To compare with other yachts in this section, we will,

however, use the light condition. The differences are shown in Appendix I.

**Length overall/max  
beam ( $L_{OA}/B_{MAX}$ )**

As seen in Chapter 2 most dimensionless hull ratios exhibit a dependence on the size of the yacht. This is true also for  $L_{OA}/B_{MAX}$ . The larger the yacht the larger the ratio, ie large yachts are less beamy, relatively speaking. The reason for this is that if a given hull is simply scaled to a larger size its stability will increase faster than its heeling moment from the sails. The hull will thus become unnecessarily stable and a somewhat narrower yacht would suffice. It may be shown that, everything else being scaled properly, beam should be scaled as  $(\text{length})^{2/3}$ . This means that  $L_{OA}/B_{MAX}$  will be scaled as  $(\text{length})^{1/3}$ , ie the ratio will increase slightly with length. For example, if the length is doubled the ratio will increase by 25%. The assumption that everything else is scaled properly, like ballast ratio, position of ballast, mast height etc, may seem an oversimplification, but the simple scaling rule above seems to fit the hull statistics over all hull lengths from 5 to 15 m  $L_{WL}$  very well. In Fig 5.32  $L_{OA}/B_{MAX}$  is given for this range of hull sizes.

Fig 5.32 Length/beam ratio



The line of Fig 5.32 represents the median, ie there are approximately as many yachts above as below the line. In this case the median differs from the average, since there is a considerably larger spread upwards than downwards, as can be seen from the shaded area, representing the scatter of the data. As in the graphs that follow the limits are adjusted in such a way that about 95% of all yachts fall within the shaded area. A design close to a limit is thus quite extreme. The spread downwards here is about 15%, while the upper limit is at a constant value of 5.0.

It may be seen from the figure that a 7 m ( $L_{WL}$ ) yacht typically has a length/beam ratio of 3.0, while a hull twice as long has a ratio of 3.75, ie an increase by 25%.

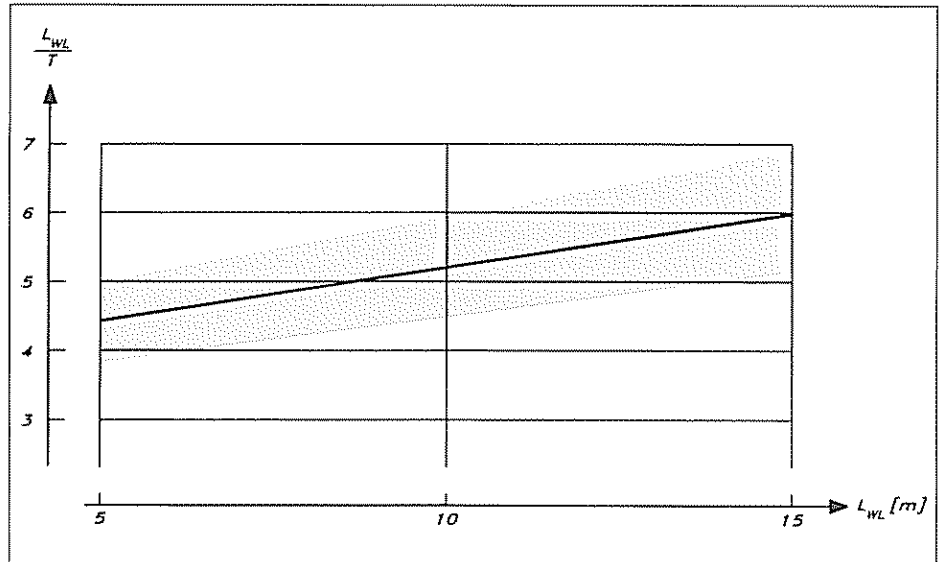
The YD-40 has an overall length of 12.05 m and a beam of 3.71 m.

Its  $L_{OA}/B_{MAX}$  is thus 3.25. For an  $L_{WL}$  in the light condition of 9.85 m this corresponds very well with the median line of Fig 5.32. In fact, for a new design the hull is slightly narrow, since new hulls are often a bit beamier than the median according to the figure. The data in the statistical analysis of this section may be considered representative of the yacht fleets in Europe and the United States in the early 1990s, and may therefore represent an average of design trends in the 1980s and to some extent in the 1970s also.

**Length of  
waterline/draft  
( $L_{WL}/T$ )**

$L_{WL}/T$  is plotted versus  $L_{WL}$  in Fig 5.33. Obviously, this ratio increases with length as well. A larger yacht has a larger ratio, i.e. a smaller relative draft. In fact, beam is a better scaling factor than length for the draft of a sailing yacht, and a good approximation is  $B_{MAX} = 1.6 \cdot T$ , which is valid more or less for all lengths. This relation corresponds very well to the median line in Fig 5.33. The upper and lower limits in this case are 15% from the median line.

Fig 5.33 Length/draft ratio



The choice of draft for a cruising yacht is a trade-off between performance and practical advantages, like the possibilities of entering more shallow water areas, ease of handling ashore etc, while for a racing yacht draft is penalized to cancel the performance advantage. The YD-40 has an  $L_{WL}$  of 9.85 m and a draft of 2.04 m in the light condition. This yields an  $L_{WL}/T$  of 4.83. According to Fig 5.33, the median for this size is 5.2, which yields a draft of 1.89. The extra 0.15 m will give the YD-40 an edge upwind, consistent with the desire to create a fast cruiser/racer.

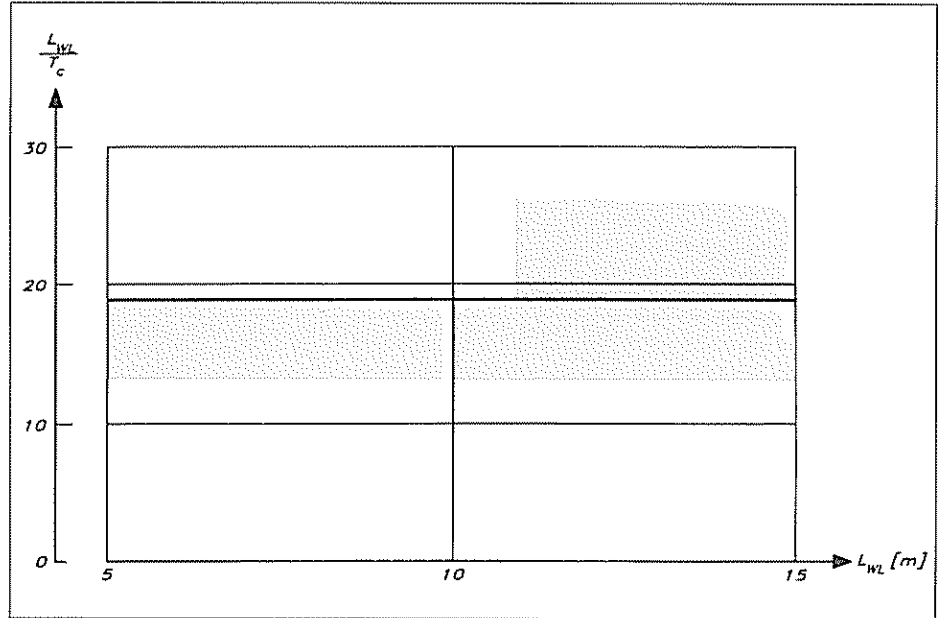
**Length of  
waterline/canoe body  
draft ( $L_{WL}/T_c$ )**

Since most modern yachts have fin keels it is possible in most cases to define the canoe body draft. This seems to scale very well with length, as can be seen in Fig 5.34. A typical value of  $L_{WL}/T_c$  is 18 for a medium displacement yacht. The ultra light dinghy type racing

machines may reach values up to 26, while heavy displacement, narrow hulls may have as small an  $L_{WL}/T_c$  as 12. For the ultra light hulls data are available only for large waterline lengths. The YD-40 has an  $L_{WL}/T_c$  of 18.2, close to the medium.

As explained above the length/displacement ratio is a very important

Fig 5 34 Length/hull draft ratio

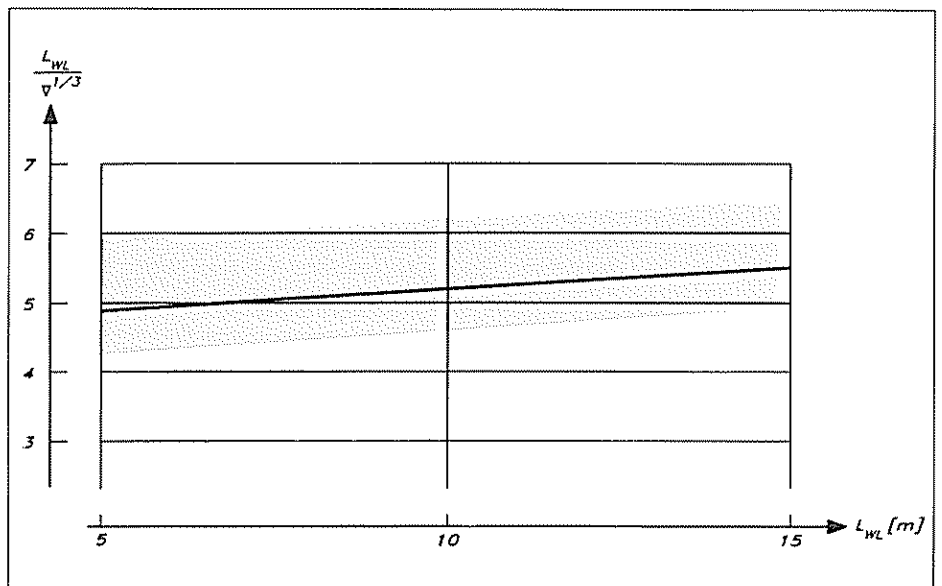


**Length/displacement ratio ( $L_{WL}/\nabla^{1/3}$ )**

quantity for the resistance of the yacht at high speeds. To enable the yacht to exceed a Froude number of about 0.45, ratios above about 5.7 are required. In Fig 5.35 the length/displacement ratio is plotted versus waterline length.

Since beam and draft do not increase linearly with length, displacement

Fig 5 35 Length/displacement ratio



increases slightly slower than length cubed. In fact, with the same assumptions as above, the displacement increases as  $(\text{length})^{7/3}$ , which means that the length/displacement ratio increases as  $(\text{length})^{2/3}$ . Increasing the length by a factor of two increases the ratio by 17%. The increase is not quite as fast in the statistical data, as may be seen in Fig 5.35.

As was the case in the length/beam ratio the spread is asymmetric. The lower limit in this case is some 12% below the median line, while the upper limit is put 20% above the median. There are, however, certain kinds of hulls outside the limits. Thus, some extreme ultra light yachts have considerably higher ratios, and since the statistics are based mainly on yachts which may participate in some kind of racing (performance handicapping system, IMS or IOR), some heavy cruising yachts may have been missed.

The length/displacement ratio is, of course, quite different between a racer and a cruiser, since the equipment required for comfortable living on board is rather heavy. In the case of the YD-40 we have tried to create a cruiser/racer with full comfort. Its length/displacement ratio is 5.16, which is close to the median for a 10 m  $L_{WL}$  yacht.

***Length overall/length  
of waterline  
( $L_{OA}/L_{WL}$ )***

The overhangs of modern hulls have decreased as compared to hulls designed before the 1960s. To a certain extent this is a matter of fashion, but there is also an attempt to reduce the longitudinal gyradius as much as possible for a given (effective) waterline length. The inverse slope of the transom is another effect of this effort.

A medium value of  $L_{OA}/L_{WL}$  for modern yachts is 1.23 with a spread of 0.15 up and down. There is no discernible trend with hull length. The YD-40 is very close to the median:  $L_{OA}/L_{WL}$  is 1.22.

***Freeboard height***

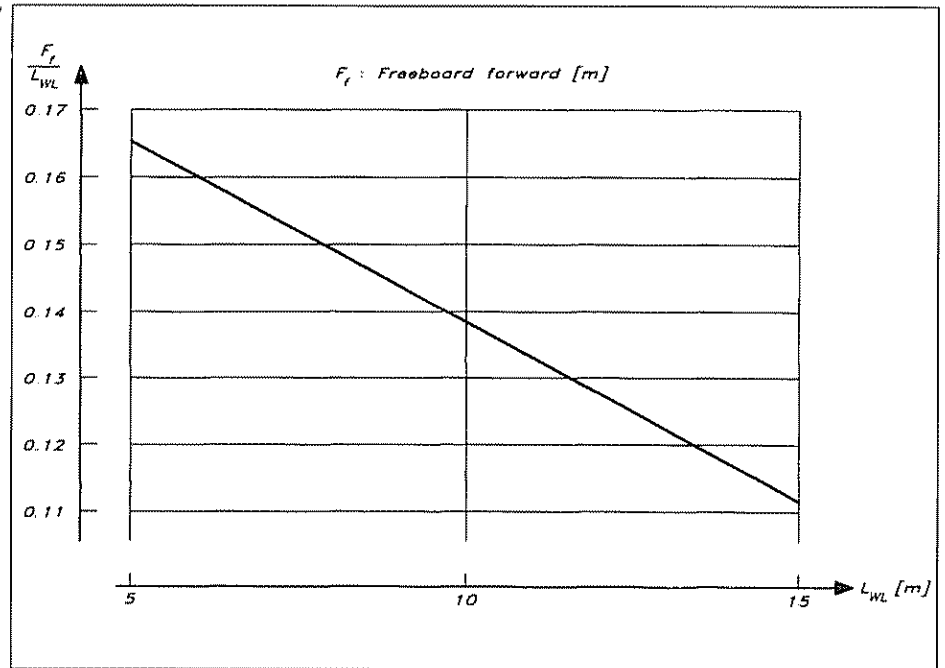
It is a well-known fact that the relative freeboard height decreases with hull length. Obviously this is due to the requirements of the accommodation. Even on very small yachts headroom for moderately tall people is required. The trend is shown in Fig 5.36, which shows the freeboard forward versus the waterline length. No upper and lower limits are given, since the statistical basis for this graph is smaller than for the others above (only about 50 yachts).

A typical value of freeboard forward/freeboard aft is 1.3. As compared to older yachts this is lower, so modern yachts have a more horizontal sheer line. Both the forward and aft freeboards are higher however, and the camber of the sheer line, the 'spring', is smaller. The YD-40 is representative of modern cruiser/racers and has somewhat higher freeboards than the statistical mean value, which is influenced to a certain extent by some older designs. The freeboard forward/waterline length is 0.144, while the mean value is 0.138 for this size of hull, and the ratio of the two freeboards is 1.22.

***Ballast ratio***

The ballast ratio, ie the ratio of keel weight to total weight, varies considerably on modern yachts. A good average value is 0.45 and most yachts lie within the range 0.35–0.55 (see Fig 5.37). There does not seem

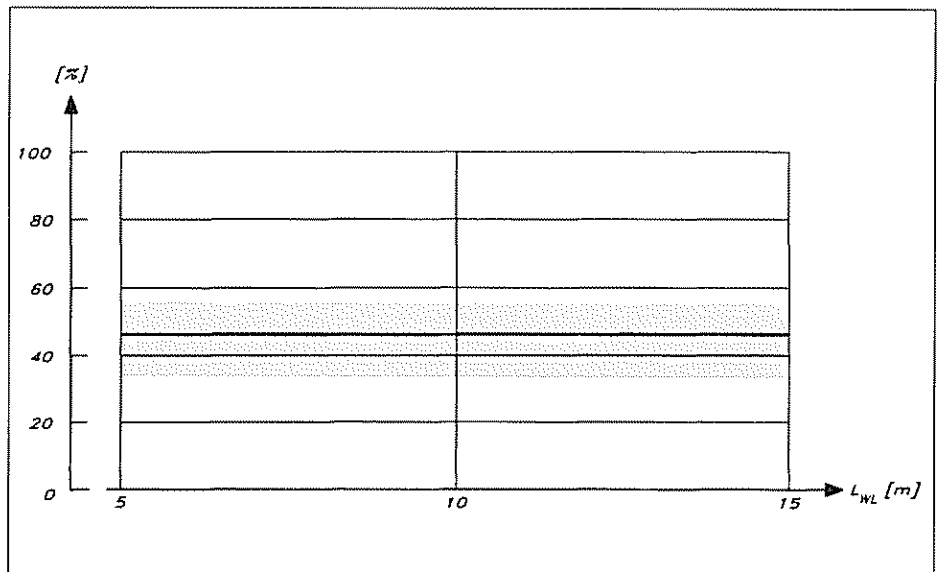
Fig 5.36 Freeboard forward/length ratio



to be any particular variation with length, at least not below 12 m ( $L_{WL}$ ), which is the upper limit for the data used for evaluating these numbers. Our YD-40 represents the average with a ballast ratio of 0.45. The keel mass is 3250 kg and the light displacement 7250 kg.

It should be mentioned, finally, that the official displacements used in the statistics may be slightly low, due to optimistic weight calculations even for the light condition. In reality, the length/displacement ratio and the ballast ratio are probably somewhat lower than the official ones. The values given for the YD-40 should, however, be realistic.

Fig 5.37 Ballast ratio



# 6

# KEEL AND RUDDER DESIGN

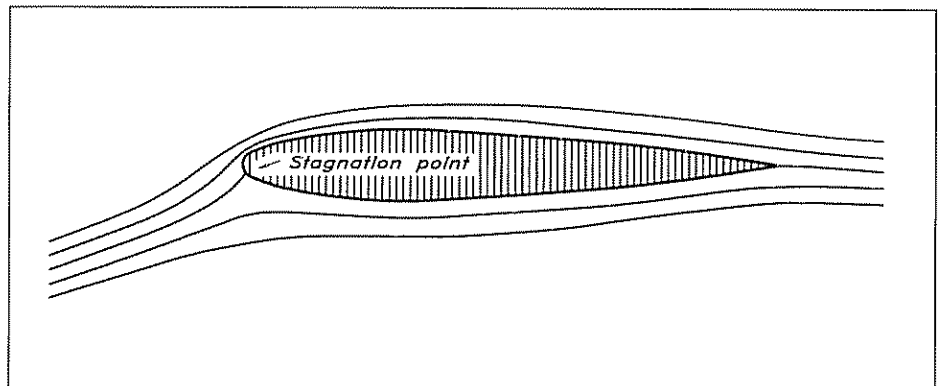
---

In the design of keels and rudders well established principles from aircraft aerodynamics may be employed. Although most aircraft today fly at speeds at which the compressibility of the air is important (more than 100 m/s), much information may be gleaned also for the incompressible water flow, partly due to the early aerodynamic research carried out more than 50 years ago. In this chapter we will first give a short introduction to the basic principles of the flow around a wing (keel or rudder) at an angle of attack, and the corresponding force generation. The remaining part of the chapter deals with the two main aspects of wing design: the planform and the wing section. As in the previous chapter we also provide statistics, enabling the designer to select a suitable size for the keel and rudder.

## Flow around a wing

When a wing works properly the flow on both sides is attached. No separation occurs, and the streamlines around a section of the wing resemble those in Fig 6.1. If we assume for a moment that the wing is infinitely long with a constant cross-section and that the flow is at right angles to the span, there is a stagnation point close to the leading edge (nose), where the flow is divided into two parts, following the upper and lower surfaces of the section, respectively. At the stagnation point itself there is no flow in either direction along the surface, and since the fluid does not penetrate the wing there is no velocity at right angles to the surface either. A similar point with zero velocity is found at the trailing edge (tail) of the section. This is the so called two-dimensional case, where the properties at all cross-sections are the same. In practice this is accomplished by putting the wing between two walls at right angles to the span, for instance in a wind tunnel. The properties of the section (profile) may then be investigated.

Fig 6.1 *Flow around a wing section*





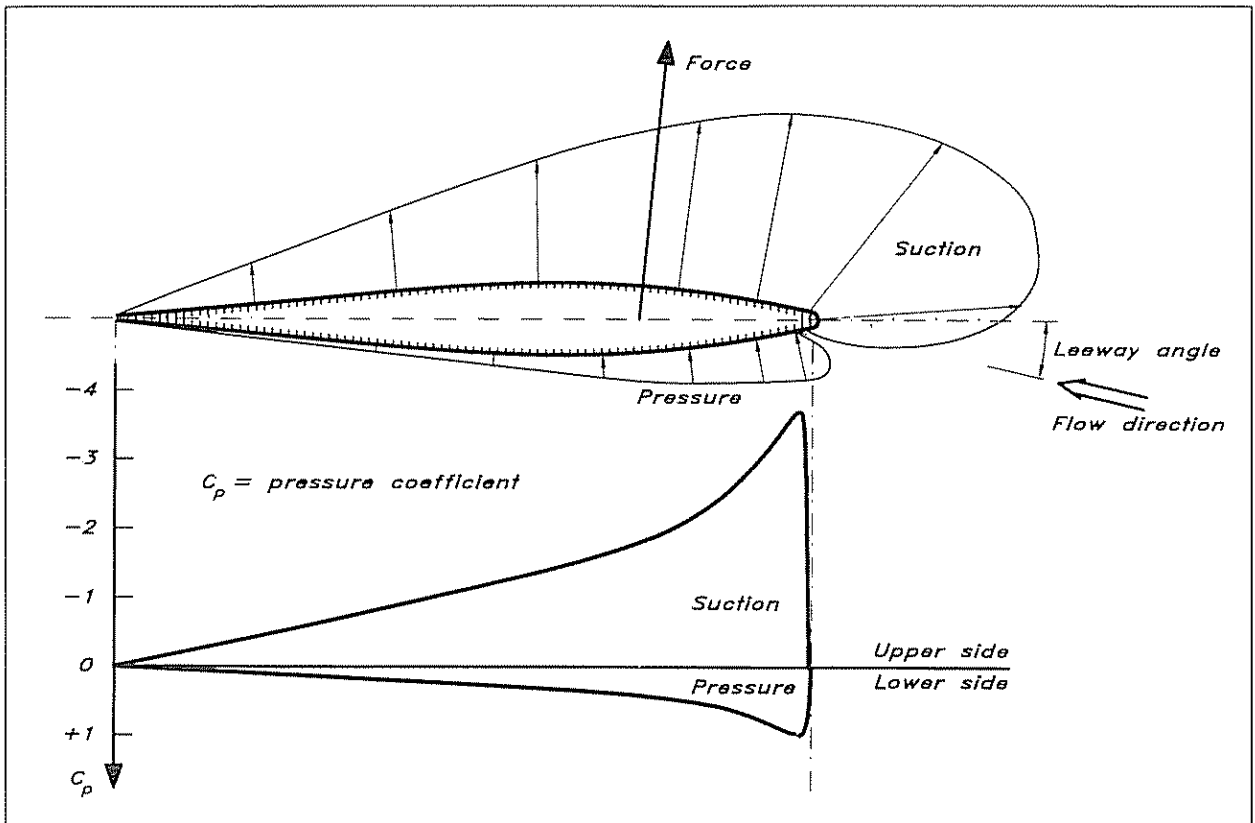


Fig 6.2 Pressure distribution around a wing section

Most of the wing sections of interest in sailing yacht design are symmetric, as in Fig 6.1, since they have to work equally well on both tacks. At zero angle of attack the pressure distribution along the section looks in principle like the one along a waterline (see Fig 5.9), ie there is high pressure at the nose and tail, and lower pressure in between. However, at non-zero angle of attack (as in Fig 6.1), the flow becomes highly asymmetric. In particular, there is a large difference between the flow that has to move from the stagnation point past the nose on to the upper side and the one moving backwards from the stagnation point. While the former flow passes a region of very large curvature, the latter moves more or less straight back. There is also a difference in speed between the two sides, the upper speed being higher than the undisturbed one, and the lower speed slower. Quite different pressures are then created as shown in Fig 6.2, and it is particularly noteworthy that there is a large suction peak at the nose. Further back on the top side the suction is gradually reduced. On the lower side the pressure is positive, but its absolute value is lower than on the other side. If all the pressure forces on the section are added, a resulting force (shown as an arrow) is obtained. The angle between the undisturbed flow and the resulting force depends on the efficiency of the wing. For a two-dimensional case without friction the angle would be  $90^\circ$ . In a real situation it is always smaller than  $90^\circ$  (pointing more backwards). The designer's task is to make the angle as close to  $90^\circ$  as

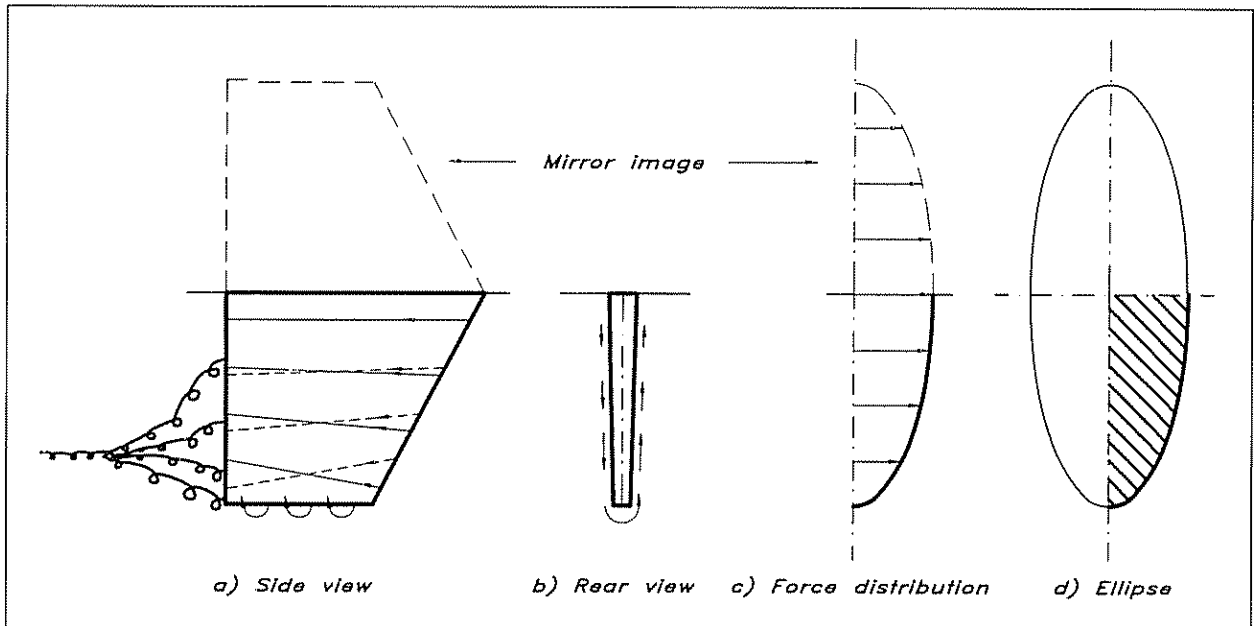
possible, and in the following we will explain how this may be accomplished.

Since the pressure and suction forces are much larger in the front part of the wing, the centre of effort of the resulting force is located in the forward part. In fact, it may be shown theoretically that the centre of effort is at one quarter of the distance from nose to tail for a symmetric section in a two-dimensional frictionless fluid. The lower part of Fig 6.2 shows a diagram, where the pressure is plotted in the more normal way, ie with the pressure on the vertical scale and the position along the section on the horizontal scale. Note, however, that negative pressures are plotted upwards. In this way the upper side of the wing corresponds to the upper part of the diagram, and conversely for the lower side. The distance between the upper and lower curves is representative of the vertical force being generated at that position, and the total vertical force is proportional to the area between the two curves.

Real wings are not, of course, infinitely long, nor are they mounted between the walls of a tunnel. They therefore have free ends in the flow, and that creates some new phenomena. This is the three-dimensional case.

In Fig 6.3 a keel is shown from the side (a) and from behind (b). Since the pressure is higher on the leeward side of the keel than on the windward side, the flow will tend to move around the tip from the leeward to the windward side. This creates a downward motion on the leeward side, gradually increasing from zero at the root to a maximum at the tip. A corresponding motion upwards is created to windward. Streamlines on the two sides of the keel therefore have different directions, and when they meet at the trailing edge vortices are created. This is particularly so at the tip, where a strong vortex is left behind the keel. Sometimes, when the yacht heels strongly this vortex can be seen,

Fig 6.3 Force and vortex distribution on a wing



since air is sucked into the low pressure core of the vortex when it gets close to the surface. As appears from the figure, all the vortices created at the trailing edge tend to roll up into a single one left behind the yacht. Since this vortex contains rotational energy it gives rise to a resistance component, the induced resistance, discussed in the previous chapter.

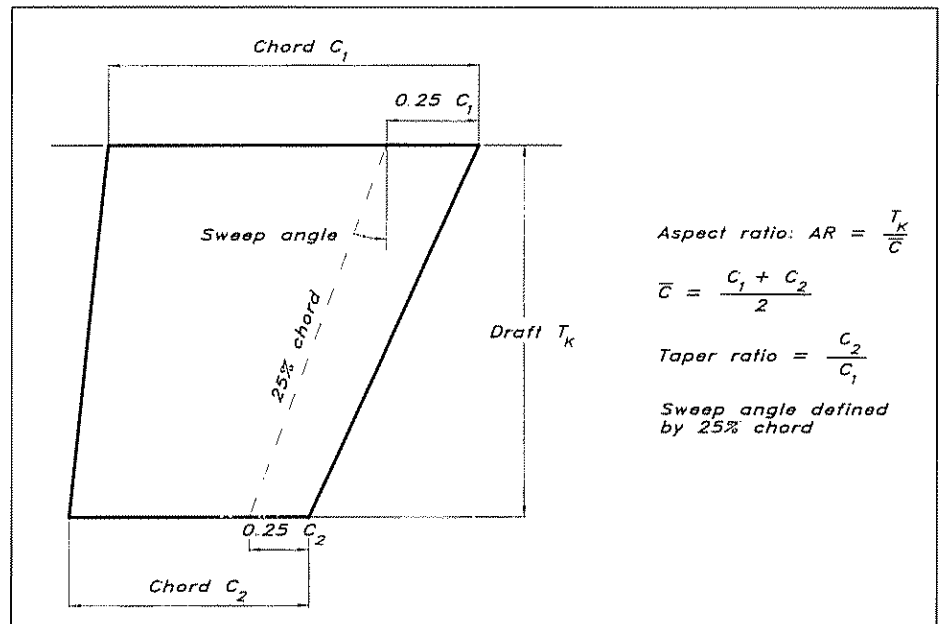
At the tip the side force generated must go to zero, since no pressure jump between the two sides can exist in the flow at the tip. Near the root, on the other hand, the flow is uninfluenced by the tip and a large force may be generated, since the bottom acts as a wall, preventing the overflow. The variation between root and tip depends on the shape of the keel, and it may be shown that the best distribution of the force is an elliptical one. With this distribution the minimum amount of vertical energy is left behind, which means that the induced resistance is minimized. In Fig 6.3 (c) an elliptical distribution is shown. This may be imagined as one quarter of a full ellipse, as shown in (d). The simplest way to obtain an elliptical distribution of the side force is to make the keel planform elliptic. This has some disadvantages, however, and we will return shortly to the optimization of the planform.

An interesting phenomenon is indicated in Fig 6.3 (a) and (c). If the bottom of the hull may be considered as a flat plate of infinite extension, the flow around the keel would be the same as if the plate had been replaced by the mirror image of the keel in the plate. A flat wall parallel to the flow thus acts as a symmetry plane. Now, the bottom is neither flat nor infinite in reality, but for modern shallow hulls this is a reasonable approximation.

### Definition of the keel planform

The definition of the planform of a trapezoidal keel is given in Fig 6.4. First, it should be mentioned that the horizontal distance from nose to tail at all depths is called the chord. Two chords are specified in the

Fig 6.4 Definition of the planform



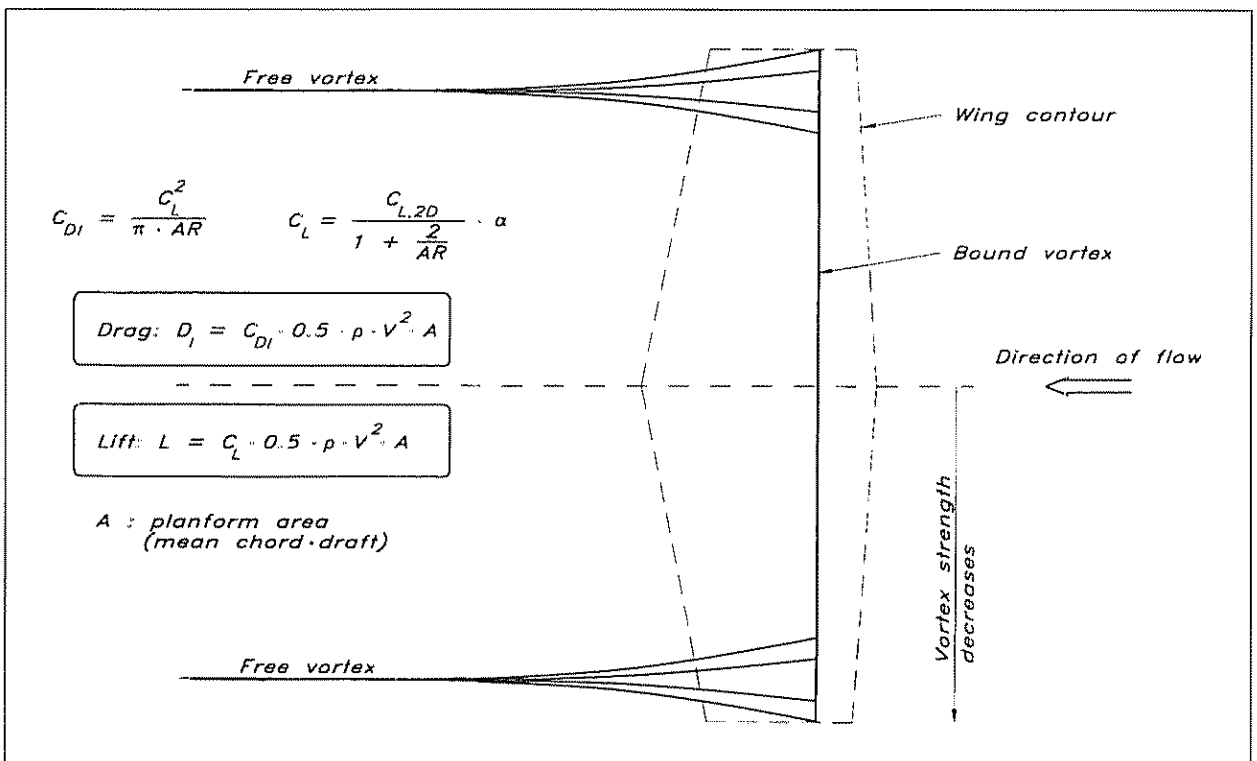
figure, namely the root and tip chords,  $C_1$  and  $C_2$ . These can be used to define a mean chord  $C = (C_1 + C_2)/2$ . The most important parameter for the efficiency of the keel is the aspect ratio, AR, defined as  $AR = T_k/C$ , ie the keel depth divided by the mean chord. This is the geometric aspect ratio. As explained above, the effective aspect ratio  $AR_e$  is twice as large, if the keel is attached to a large flat surface. The second parameter to be defined is the taper ratio,  $\lambda$ , which is simply the ratio of the tip chord to the root chord, ie  $\lambda = C_2/C_1$ .

Most keels are not exactly vertical, but sweep backwards to some extent. It is not obvious, however, how to define this sweep angle. The leading or trailing edges might be used for defining the angle, or perhaps the mid-line between the two, but the most appropriate choice turns out to be the line 25% of the chord length from the leading edge. As pointed out above, under certain ideal conditions, the centre of effort at every section lies along this line. Even though this is not exactly true in a real case, it is still a good approximation for fin keels and rudders of normal aspect ratios. We will return to the location of the centre of effort in Chapter 8, in connection with the balance of the yacht.

**Classical wing theory**

One of the most well known and useful theories in aerodynamics is the so-called lifting line theory for computing the lift and induced resistance (drag) of wings. Without going deeply into the mathematics, the basics of the theory may be explained with reference to Fig 6.5, which shows a wing with two free ends, symmetric about the centreline. It could also be interpreted as a keel with its image reflected in the hull bottom. The wing is

Fig 6.5 *Lifting line theory*



dashed in the figure, since in the theory it is replaced by a set of vortices. There is thus one vortex along the span of the wing (from tip to tip). This is called the bound vortex, since it is fixed to the wing. However, as we have seen, vortices are shed backwards from the wing, particularly close to the tip. These are the free vortices, which align themselves with the local flow direction. There is a theorem stating that a vortex cannot have a free end in the flow. Thus, when a vortex filament bends backwards and leaves the bound part, the vortex strength of the latter is reduced by the strength of the filament. At the tip, all the vorticity has been shed backwards, and the bound vorticity is zero. Behind the wing, all the free vortex filaments roll up into one concentrated free vortex on each side. These two in turn are connected through the starting vortex (not shown in the figure), created when the wing started its motion.

The local force created by the vortex system is proportional to the component of the vortex at right angles to the local flow direction. Since the free vortices are parallel to the flow they do not create any force, but the bound vortices on the wing generate a force that is proportional to the vortex strength. The theory also shows that the best distribution of vorticity, and hence force, on the wing is the elliptical one. In this case, the drag and lift coefficients,  $C_D$  and  $C_L$  of the wing, and the corresponding forces, can be obtained easily, as shown in Fig 6.5.  $C_{L2D}$  is the lift coefficient per degree in the two-dimensional case. For a symmetrical section in a frictionless fluid this coefficient may be obtained theoretically as  $\pi^2/90 = 0.11$ . In a real flow it is slightly smaller due to viscosity, and 0.10 is a good approximation for all symmetrical sections.

If the force distribution on the wing is not elliptic, the *effective* aspect ratio should be used in the formula. This is always smaller than the elliptical one, but the difference is normally not very large, so the actual aspect ratio may be used for good estimates for non-elliptical loadings also. We may summarize the most important results as follows:

- the lift and induced drag coefficients can be estimated in most cases from the formulae of Fig 6.5
- the aspect ratio is the most important parameter for the lift and drag of a wing
- the elliptical force distribution is the best one

The effect of the aspect ratio appears again in Fig 6.6, which is based on wind-tunnel experiments with wings of different aspect ratios. Lift and drag coefficients are given for varying angles of attack. In the lefthand diagram very different curves are obtained depending on  $AR_c$ . For instance, at  $5^\circ$ , which is a typical leeway angle and hence angle of attack for a keel, the square wing with  $AR_c = 1$  produces less than one third of the lift coefficient of the two-dimensional wing, which has  $AR_c = \text{infinity}$ . An effective  $AR_c = 3$  is relatively common for keels. It may be seen that this produces about twice as much lift as the square wing.

In the range of practical  $AR_c$  the drag is relatively unchanged, but it should be kept in mind that this is for a given angle of attack, while in

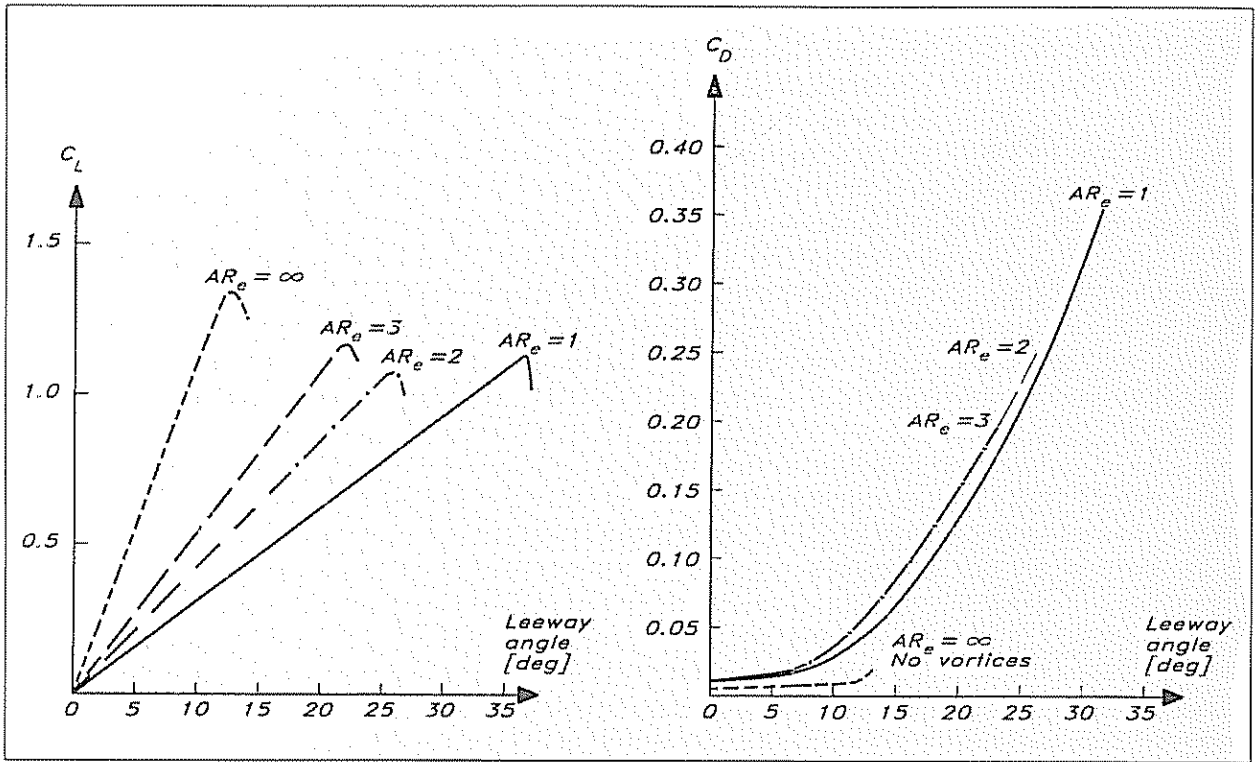


Fig 6.6 Influence of aspect ratio on lift and drag

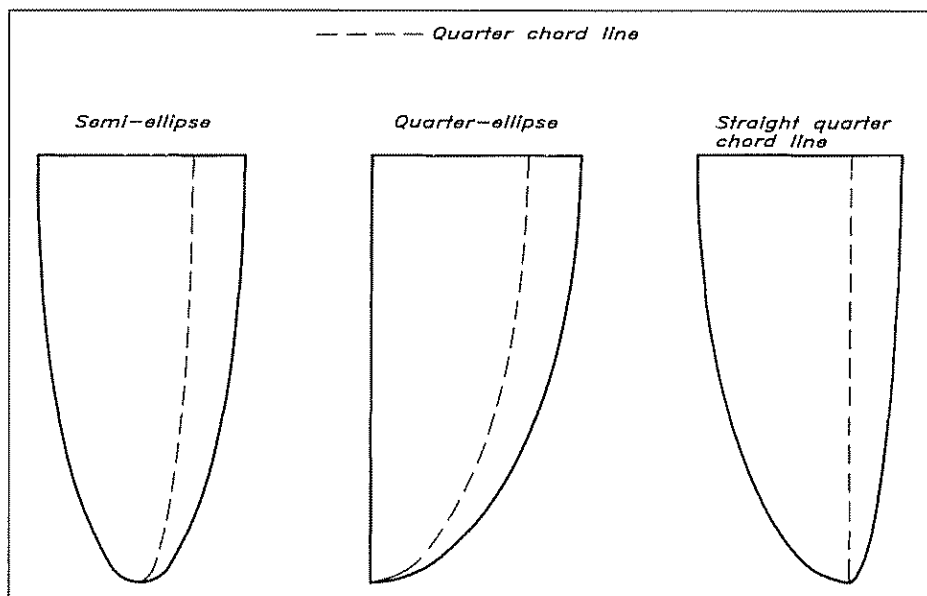
reality a more interesting question is how much drag is produced for a given side force. As pointed out in Chapter 5 the task of the keel is to balance the given side force from the sails at the expense of the smallest possible drag. With this in mind the lift diagram could be interpreted in a different way. For a given side force the leeway for the two-dimensional keel would be less than one third, and for the  $AR_e = 3$  keel less than half that of the  $AR_e = 1$  keel. Quite different drags would then be obtained as the righthand drag diagram suggests. Note that  $C_D$  in Fig 6.6 represents the total drag, ie also the viscous components, as presented in Fig 5.4. This is why  $C_D$  is not zero at zero leeway angle.

The differences between traditional long keels and fin-keels are now obvious. While the long keels have an effective aspect ratio considerably smaller than one, the modern fin-keel  $AR_e$ s are usually larger than three. Large performance differences are therefore to be expected. However, there are also disadvantages to the fin-keel. One of these was discussed in Chapter 3 in connection with roll damping, and it was shown that a long keel is considerably more effective in this respect. Another disadvantage occurs at low speeds. As appears from the lift equation of Fig 6.5, the lift is proportional to the lift coefficient, the speed squared and the keel area. Since fin-keels have a smaller area they operate at higher lift coefficients (which are easily obtained since they are more effective) However, the maximum  $C_L$  is about the same for all aspect ratios and it is reached much faster for a fin-keel yacht when the speed drops, if the side force is still required. This may happen when berthing, or at the start of a race when there may be a considerable side force

from the sails, but the speed is low. The keel then stalls and the yacht starts moving sideways. The difference between long keels and fin-keels is quite significant, and many owners of modern yachts have experienced problems when manoeuvring in harbours.

To obtain the advantageous elliptical distribution of the side force the keel may be designed with an elliptical plan form. This means that the chord length must vary elliptically from tip to root. Two geometries that would satisfy these requirements are the half ellipse and the quarter ellipse (see Fig 6.7), but in both cases the important quarter chord line would be bent, so the force distribution would not be exactly elliptical. In the third alternative the design has started from a straight quarter chord line and the chord lengths have been distributed elliptically in the vertical direction, always keeping the 25% point on each chord on the line.

Fig 6.7 Different elliptical keels



The elliptical planform has certain disadvantages, not least from a practical point of view, so trapezoidal keels are much more common. It is, in fact, possible to obtain a force distribution which is very nearly elliptic for this kind of keel also, provided the taper ratio is chosen to fit the sweep angle according to Fig 6.8. As can be seen in the figure, a small taper ratio requires a large sweep back and vice versa. At zero angle the taper ratio should be around 0.45, and for large ratios the keel should actually point forwards, since the angle is negative. Most keels have a sweep angle of 20–30 degrees, which should call for a taper ratio of about 0.1. This is not practical, however, since the centre of gravity would then be too high up, and the stability poor. There is another disadvantage of small taper ratios. If the keel is unswept, and either elliptic or has a taper ratio of 0.45, the area distribution in the vertical direction corresponds to the force distribution. If smaller chords near the tip are compensated by sweepback to get large enough forces in the area, this part will be more highly loaded than the rest of the

Fig 6.8 Optimum relation between sweep angle and taper ratio

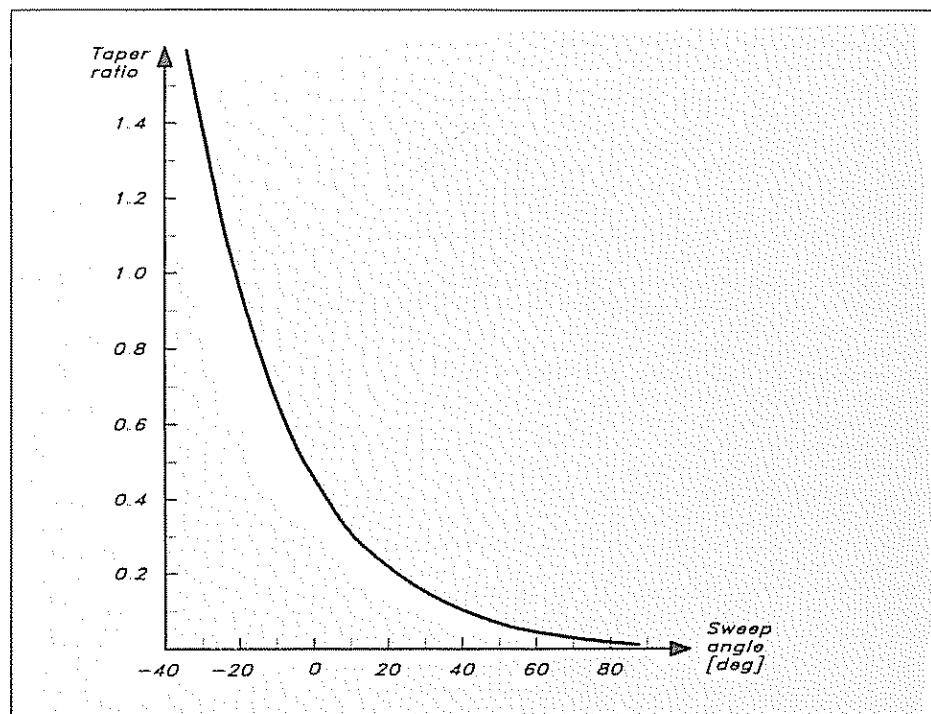
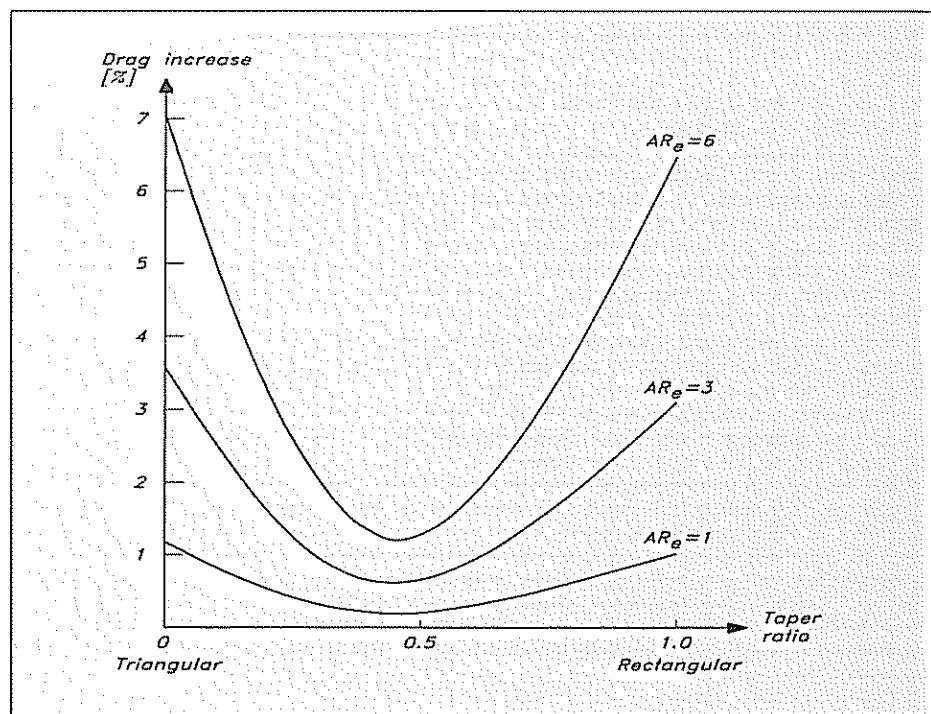


Fig 6.9 Increase in induced drag due to non-optimum taper ratio



keel. The local lift coefficient will be higher and this part will stall earlier. In practice, lower taper ratios than 0.2 are not recommended. As a matter of fact, most designers use much larger ratios, 0.4–0.6, for stability reasons. Note that, if a given thickness ratio is used, the cross-sectional area of the keel increases as chord squared, which means that



the amount of ballast carried near the tip is highly dependent on the tip chord.

Fig 6.8 is obtained from the lifting line theory, as is Fig 6.9, which shows the penalty if the force distribution is not elliptical. Only the zero sweep angle case is presented. The vertical axis shows the percentage increase in drag for the trapezoidal keel as compared to the elliptic one. It may be seen that the penalty is smallest at a taper ratio of about 0.45, as expected. In this case very small drag increases are noted, for practical aspect ratios less than 1%. If the taper is far from the optimum the increase may be up to 3–4%. It is interesting to note that the importance of a correct force distribution is quite dependent on the aspect ratio. For long keels with  $AR_c$  smaller than 1.0 the penalty is practically insignificant.

### Tip shape

The lifting line theory is a useful tool in explaining the most important features of planform design. The most important conclusion to be drawn is that the primary parameter is the aspect ratio, whose influence on the forces can be computed with good accuracy using the formulae above. Sweep angle and taper may contribute a few per cent to the efficiency of the keel, but there are other factors not included in the theory which could also have some influence. We discuss one of them here, namely, the shape of the tip.

In the theory the wing is replaced by a vortex system, which is appropriate for the major features of the flow. However, in reality, the detailed shape of the wing tip will have some influence on the velocity distribution. One effect is that the trailing, free vortices, which are aligned with the local flow, may be positioned slightly differently, depending on the tip shape. This is important, since the effective span of the wing in Fig 6.5 is determined from the distance between the two trailing vortices far behind the wing. For a sailing yacht this means that it is the depth of the trailing vortex that defines the effective aspect ratio, rather than the actual keel depth.

Fig 6.10 shows the measured results of a series of tips. Both the planform view and a front view are shown, and the change in aspect ratio relative to the theory is given for each configuration. The location of the tip vortex is also indicated. It may be seen that the best design is the simplest one with a square cut off in both views. The worst one is a tip that is rounded in both directions. In the former case the geometric aspect ratio is reduced by 0.04, while in the latter case the reduction is 0.20.

The reason why the square tip is better, considering first the planform view, is that the flow along the tip is guided backwards by the flat ending. It will not tend to move upwards as much as it would if the tip had been rounded. So the vortex stays further down. In fact, it would be possible to improve the tip shape even further by rounding the forward part in such a way that the flow approaches the tip smoothly, but the important thing is to keep the aft part straight.

The square shape in the front view is better than the rounded one,

Fig 6.10 Influence of tip shape and aspect ratio

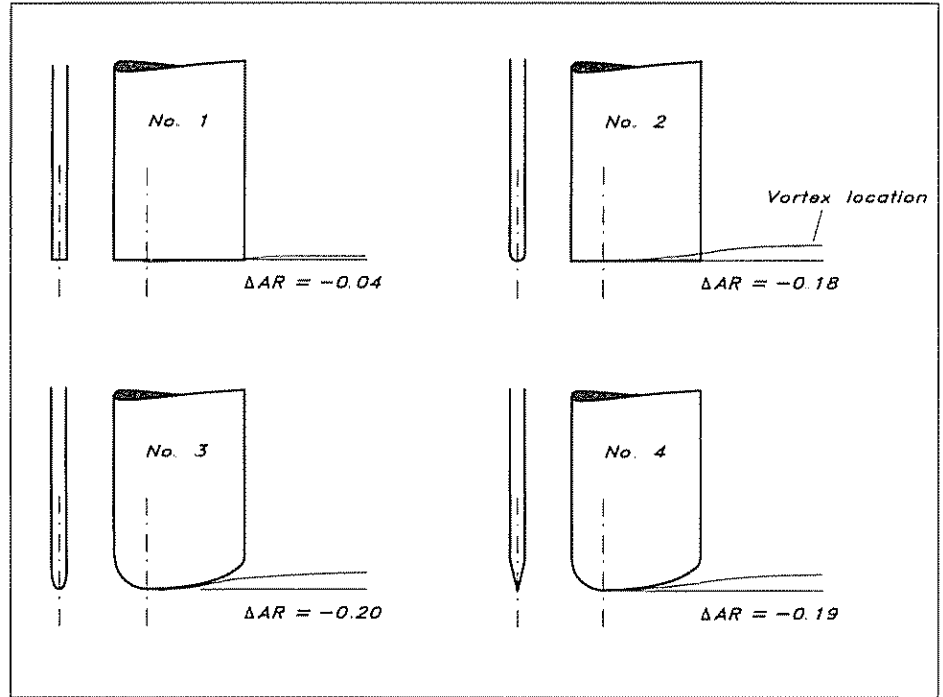
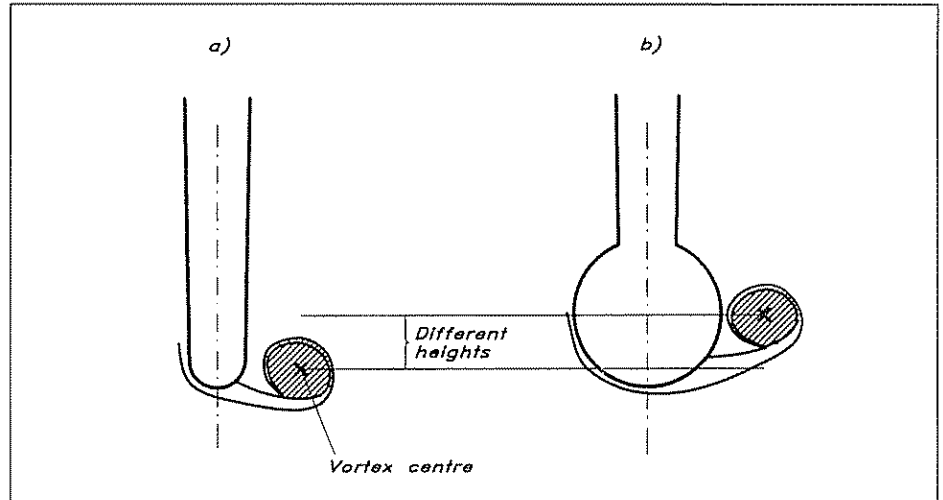


Fig 6.11 Location of tip vortex



since the downward flow on the leeward side separates at the edge and the vortex is moved below the tip. A rounded shape permits the flow to move around to the windward side before it separates. The vortex may then be found on the windward side, not at maximum depth. Fig 6.11 shows that this effect could be even larger for a bulbous keel. A disadvantage of the square ending is that separation will also occur at the corners under conditions when lift is not required. In downwind sailing an extra drag component will then appear. This disadvantage may be partly eliminated if the tip is made V-shaped and if the corners where the V meets the vertical part are rounded off.

A water-tunnel investigation of four different tip shapes (round, square, V and bulb) revealed that the best shape overall was the V, while

the round shape was the best downwind. The effect of the bulb is a bit uncertain. As we have seen in Fig 6.11 the large radius may help the flow pass the tip and move up on the other side, but this does not happen for all bulbs. A way to avoid this is to put a small riblet at maximum draft, thereby promoting separation of the vortex. Disadvantages of the bulb are that the wetted area increases greatly and that some interference drag is created in the corners between the bulb and the keel. These negative aspects may, however, be well compensated by the large increase in stability. Whether or not the total effect is positive depends on the stability of the hull itself. For instance, the America's Cup class yachts would not be able to carry their huge sail area without a very large bulb. The bulbs of this class have been the subject of extensive optimization studies, where the shape and fairing to the keel have been perfected. It should be remembered that heavy weights far from the total centre of gravity increases the gyradius, and have a negative effect on the performance of the yacht in a seaway.

### **Advanced planform design**

In this section we will describe some more advanced concepts used recently in the keel planform design for racing yachts. In most cases a relatively detailed knowledge of the flow around the hull and keel is required, and this calls for tank testing or Computational Fluid Dynamics (CFD) methods, not normally available to the amateur designer. It may, however, still be of interest to understand the principles behind the different concepts. A similar presentation will be made in connection with section design.

### ***Winged keels***

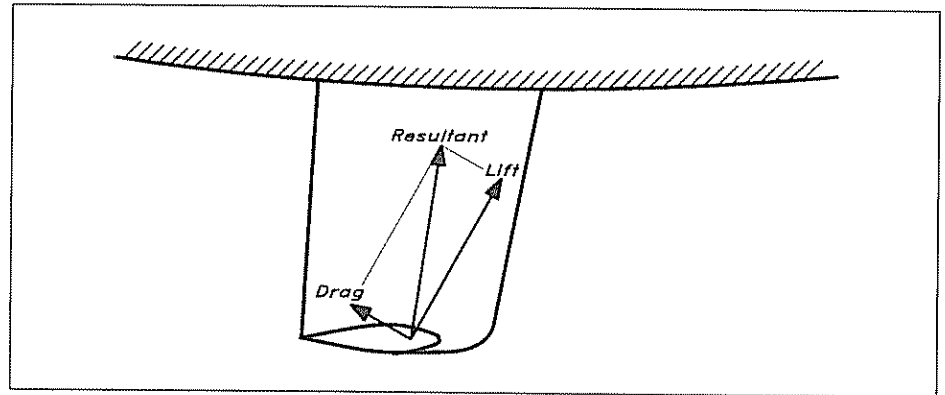
The most spectacular development in planform design in recent years is the keel wing used on many 12 metre yachts in the 1980s. This technique is slowly making its way into cruising. The basic idea is to increase the effective aspect ratio of the keel, without making it deeper, and thereby reduce the induced resistance. Alternatively, the keel could be made shallower for a given resistance, an attractive option for cruising yachts.

The idea of manipulating the tip flow with some kind of device is not new. Even in the 1940s experiments were made with end plates on keels at the Davidson Laboratory in New York. By putting a plate perpendicular to the keel plane at the tip, the overflow from the pressure to the suction side was reduced, and the effective aspect ratio increased. However, this was only at the expense of a large increase in viscous resistance due to the plates, so the total effect was unfavourable. It was not until the late 1960s that more effective devices with a streamlined wing shape were wind-tunnel tested by the aerodynamicist S O Ridder, and used on racing yachts. The real breakthrough came after the victory of the Australian 12 metre *Australia II* in the 1983 America's Cup races.

If the tip device is to reduce the overflow it obviously has to have an angle of attack relative to the local flow direction. A device following the local streamlines would not alter the direction of the flow. With this in mind it is easy to understand why the simple plates did not work. A

flat plate at an angle of attack produces a large drag, because the flow separates at the leading edge. It is therefore necessary to use well designed foils with a minimum of viscous resistance to obtain a net positive result. Since the foils will not be aligned with the flow a lift force will develop. On the leeward side of the keel the flow is directed downwards and the wing generates a downward force. The opposite is true on the windward side, where the force points upwards. If the foil is effective enough both forces may have a component forwards. The wing then pulls the yacht along. Fig 6.12 demonstrates that this occurs only if the drag is small enough relative to the lift. If this condition is not satisfied the wings will generate a drag force. It should now be apparent why the proper design of the wings is of the utmost importance.

Fig 6.12 Keel wing force on windward side



Another way of looking at the effect of the wings is to consider the trailing vorticity left behind the keel. Without the wings a strong vortex is formed near the tip due to the overflow. The wing takes advantage of the vortical energy and reduces it, so that less is left in the wake, thereby reducing resistance. It should be pointed out that new vortices (of less strength) are now left behind the tips of the wings, where some overflow occurs.

Points to consider in the design of keel wings are:

- root chord
- span
- taper
- twist
- longitudinal position at keel tip
- cant angle
- junction angle
- junction fairing
- section characteristics

In the early days of keel wing design, attempts were made to exploit the lowering of the centre of gravity of the yacht made possible by fattening the wings. Therefore, the weight of the wings could have been added to the list above, but in modern designs it has been realized that it is better to put this weight in the lower part of the keel or in a bulb, used in connection with the wings.

As to the root chord, there is a trade-off between frictional and induced resistance. In a frictionless fluid the root of the wing should be

as large as the tip of the keel in order to avoid discontinuities in the load carried over from the keel to the wing. Such discontinuities mean shed vorticity and hence induced resistance. On the other hand, to minimize wetted surface and friction the chord should be as short as possible.

A similar situation exists for the span. In principle, the vortices shed at the wing tips are smaller for large spans, but the wetted surface is larger. Another important aspect of span size is the variation in local flow direction along the span. The larger the span the stronger the variation. In the inner part of the wing the flow is mostly governed by the displacement of the hull, while further out the flow direction is determined by the waves. Obviously, heel angle and speed will alter these conditions. It is thus more complicated to design large span wings.

The taper and twist of the sections determine the loading and shedding of vorticity spanwise, and have to be optimized together.

If the chord of the wing root is smaller than that of the keel tip, the position of the wing along the tip has to be considered. A forward position may be advantageous, since this part of the keel carries the largest load. On the other hand, the wing has been shown to have a very positive effect on the keel lift/drag characteristics when using the trim tab, if it is positioned below the tab. This speaks in favour of an aft position.

The cant angle has caused some debate in the yachting literature. This is the angle between the wing viewed from behind and the horizontal (hull upright). In our explanation above, the wings get their loading from the keel, due to the overflow from the pressure to the suction side. This is likely to be the major effect, but when the yacht heels and yaws the leeway itself causes an angle of attack on the wings, in such a way that the leeward wing becomes more heavily loaded, and the windward wing carries a reduced load. For instance, if the hull heels  $45^\circ$  and the cant angle is  $45^\circ$  the leeward wing will be vertical and exposed to the full leeway angle. The other wing will be horizontal and more lightly loaded. In this situation the largest vortex will be shed at the tip of the leeward wing which is at a draft that is probably larger than the nominal one. This is certainly an advantage. On the other hand, it is advantageous to equalize the vortices from the two wing tips, as will be explained below, and also, in fact, to spread them apart as much as possible. These latter effects speak in favour of small cant angles.

The junction angle is defined as the angle of the wing root relative to the horizontal, viewed from the side. This has to be adjusted, as well as the angle of all sections, to the local flow direction. A common practice is to carry out the adjustment for the upright condition (where the wings are not needed) in such a way that the drag of the wings is minimized. In the early days of the winged keels this was accomplished by measuring the force on the wing and adjusting its angle in the towing tank to obtain minimum wing drag. The disadvantage of this approach is that the effect of the variation in the spanwise direction is

not accounted for. It is now possible to compute the flow direction locally, and to unload each section of the wing by proper twisting.

At the junction between the keel and the wing a vortex is normally created. This vortex gives rise to a resistance component. The same phenomenon, in fact, occurs also in the junction between the keel and the hull. To alleviate the problem a special fairing, called a fillet, may be introduced. The classic design of the fillet is to start at the leading edge and increase the radius along the intersection backwards to the trailing edge, where the fairing radius should be of the order of the (largest) boundary layer thickness. In the keel/hull junction the hull boundary layer is normally a few centimetres, for a 40 footer like the YD-40 around 5 cm. In the keel/wing junction the keel boundary layer is thinner, and a radius of about 1 cm seems appropriate. It is very important that the fillet is tapered off smoothly behind the trailing edge. Other ideas for fillet design have been suggested recently, but they do not seem to work at an angle of attack, and are therefore of little use in yacht design.

Considering all the trade-offs and the detailed knowledge of the flow required, it is very unlikely that other than experienced fluid dynamicists can design effective wings. If wings are just added without the above considerations, the chances that they will have a negative effect, rather than a positive one, are quite high.

### *Inverse taper*

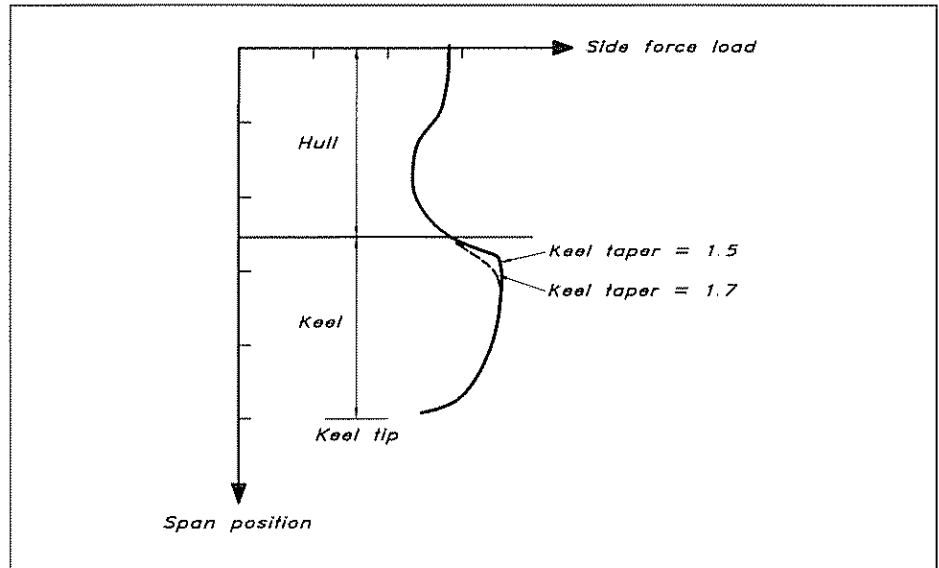
Inverse taper, or taper ratios larger than one, were investigated by the *Australia II* team in the early 1980s, even before they decided to go for the winged keel. This taper, in itself, caused an increase in performance, but not as large as in combination with the wings. The reason why inverse taper may be advantageous for a very heavy yacht like a 12 metre (apart from the obvious stability improvement) is that the deep hull will carry a substantial part of the side force, ie the keel plus the hull must be considered a wing, albeit with a very strange planform and with a huge thickness in the upper part.

The load distribution for two taper ratios larger than one is shown in Fig 6.13. Obviously, it is very different from the optimum elliptical distribution from the tip of the keel to the waterline. A particularly harmful feature is the rapid drop in load at the junction between the keel and the hull, where much vorticity is shed. A way to alleviate this problem is to reduce the keel chord at the intersection with the hull, thereby reducing the difference between the keel and the hull loadings. As can be seen in the figure the smaller chord for the larger taper gives a somewhat smoother load distribution, and hence smaller vorticity and induced resistance.

Another important effect of the inverse taper is that the load will be moved away from the water surface, which may have a positive effect on the wave resistance. This advantage is, of course, even larger if wings are added.

An important condition for the use of inverse taper is that the hull is deep. For modern fin-keel yachts the hulls are shallow and act more or

Fig 6.13 Side force distribution – inverse taper



less as a flat wall attached to the top of the keel, as we have seen above. The simple theory presented in Fig 6.5 may be used for designs without wings. If wings are added, the load distribution will be completely changed, and a more complicated optimization procedure is required.

#### *Forward rudders (canard wings)*

In the America's Cup races of 1987 the American yacht *USA* featured a radical underwater design, where the two normal tasks of the keel (to lower the centre of gravity and to produce a side force), were split on different devices. The ballast was put into a large bulb, kept in position below the hull by a streamlined strut, and the side force production was left for a forward and an aft rudder.

The effect of splitting the side force between two surfaces may be investigated using biplane theory. The principle is straightforward: by reducing the lift on each one of the surfaces, keeping the span unchanged, the sum of the induced resistances becomes smaller than for one surface alone. This is so because, as we have seen in the lifting line theory, the induced resistance is proportional to the lift squared. If there were no interference between the two surfaces, splitting the lift into two halves would result in a resistance of each surface of only one quarter of the original one, ie the total resistance would be halved. Unfortunately, the interference effects cannot be ignored, unless the trailing vortex systems are several span lengths apart. There is thus no point in putting the aft wing in the wake of the forward one. The vortex systems would then coincide and co-operate to generate the same resistance as if there had been only one wing. If the wings, or lifting surfaces, are put side by side, there is a gain. For instance, on sailing catamarans the two centreboards are several span lengths apart and may be considered independent.

At first glance, the forward and aft rudder configuration may seem a useless idea, since the rudders are located behind one another. However,

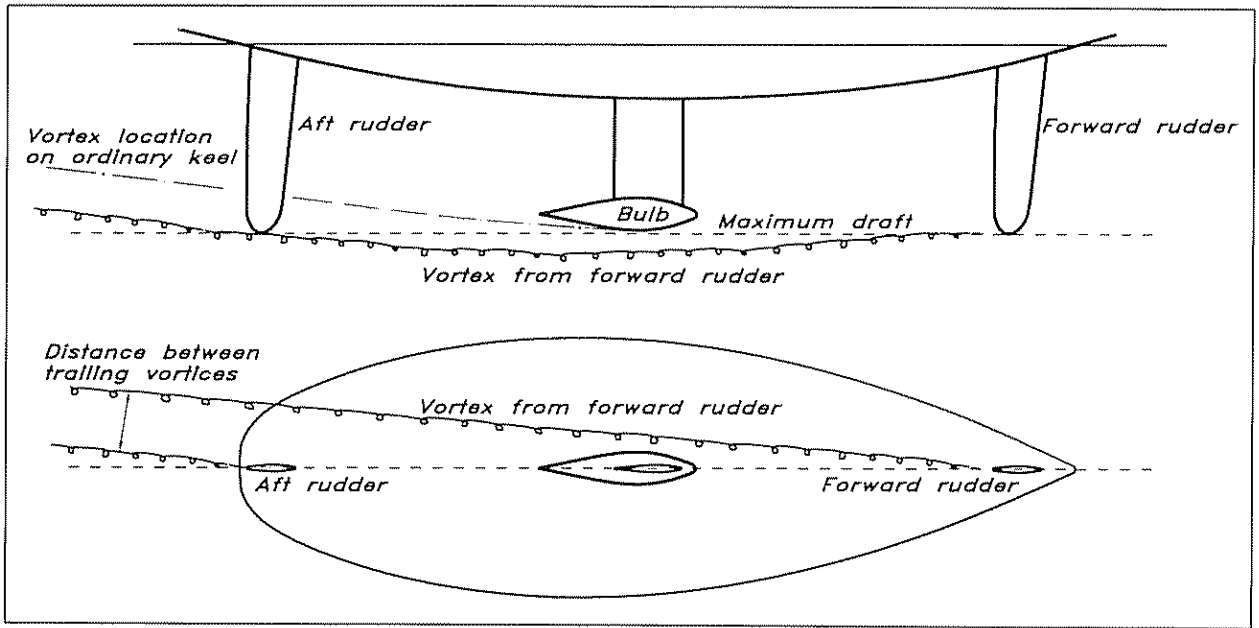


Fig 6.14 Forward and aft rudder configuration

because the hull has a leeway angle and the rudders are far apart the distance between the trailing vortex systems may be significant, if not large (see the bottom part of Fig 6.14). A leeway angle of  $4^\circ$  with the rudders separated 15 metres would result in a trailing vortex separation of approximately 1 metre, which is about 40% of the draft. This should be enough for a noticeable drag reduction.

Fig 6.14 illustrates another interesting effect of the positioning of the rudders at the ends of the relatively deep hull. The trailing vortex systems are influenced by the flow around the hull, as can be seen in the top figure. The ultimate location in the wake will be further down than for an ordinary keel positioned approximately at the maximum draft of the canoe body. Since it is the location of the vortex far behind that determines the effective draft, the rudder arrangement is better, given the maximum geometric draft of the configuration.

A third possible advantage of the forward and aft rudder configuration is the effect on the wave system. While an ordinary keel has an unfavourable effect on the waves, the opposite may be true for the rudders. When the hull sails upwind at full speed, the Froude number is around 0.35 and the wavelength is slightly smaller than the waterline length. There is thus a wave trough at midship. If the hull heels significantly the suction side of the keel will be close to the water surface, thus deepening the trough. The rudders, on the other hand, will apply their suction in regions where there are wave crests, which should reduce their height.

There are several practical aspects of the forward and aft rudder configuration. In principle manoeuvrability will be increased, but that requires a good control system for the co-operation between the rudders. Another aspect is the risk of ventilation when the rudders are lifted due to the heeling of the yacht. Beamy yachts may lift the rudders

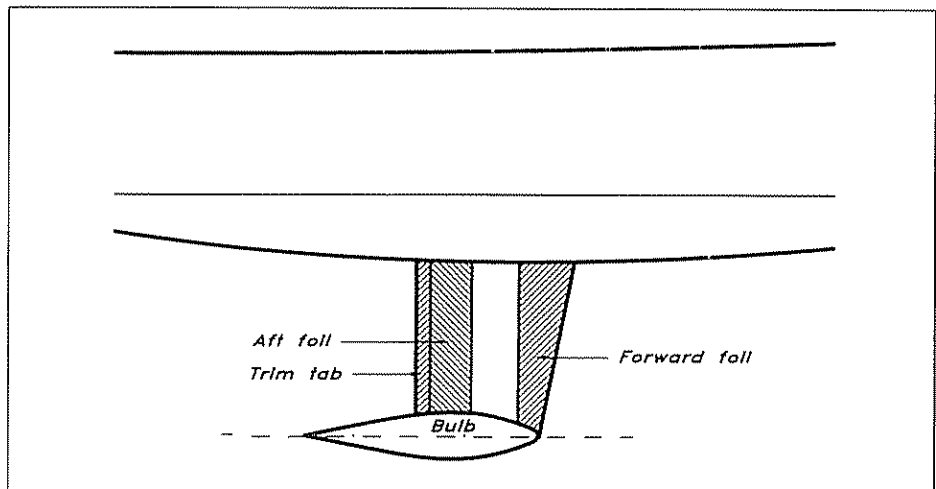


too much to be effective. In any case, the forward and aft rudder configuration is interesting and will probably appear more frequently on fast racing yachts in the future.

### *Tandem keels*

As for the forward and aft rudders, the side force on a tandem keel is split on two foils, but much closer together. Normally they are also linked through a horizontal fin or a bulb (see Fig 6.15, where there is also a trim tab on the aft foil). There is now a strong interaction between the two foils in much the same way as between the jib and the mainsail, which will be described in the next chapter. The reader is referred to the theoretical explanation given there.

Fig 6.15 *Tandem keel with trim tab*



The two major positive effects of the tandem configuration are the increased maximum lift coefficient obtainable before stall, and the possibility of obtaining laminar flow over a larger area. The latter may seem surprising, but according to experiments the turbulence in the wake of the forward foil is swept sideways fast enough not to disturb the aft foil, so laminar flow may be exploited even there. The increased maximum lift coefficient means that a smaller lateral area is required, so both effects mean smaller friction. A further step in this direction might be taken by dropping the rudder altogether and steering the yacht with the trim tab.

### **Evaluation of some planform concepts**

An evaluation of seven different keel concepts was made at the Delft University of Technology in the early 1980s. All keels were tested on the same hull, a 3.2 m model of a 63 ft fast cruising yacht. To isolate the hydrodynamic effects from the stability, which varied somewhat between the keels, all evaluations were made with the same righting moment of the yacht.

The seven keels are shown in Fig 6.16. Since the emphasis was placed on minimizing the draft of the yacht without compromising performance too much, most of the keels had a very small span: only 1.39 m. This was true for nos 2, 3, 4, 5 and 6, while 1 and 7 had a more

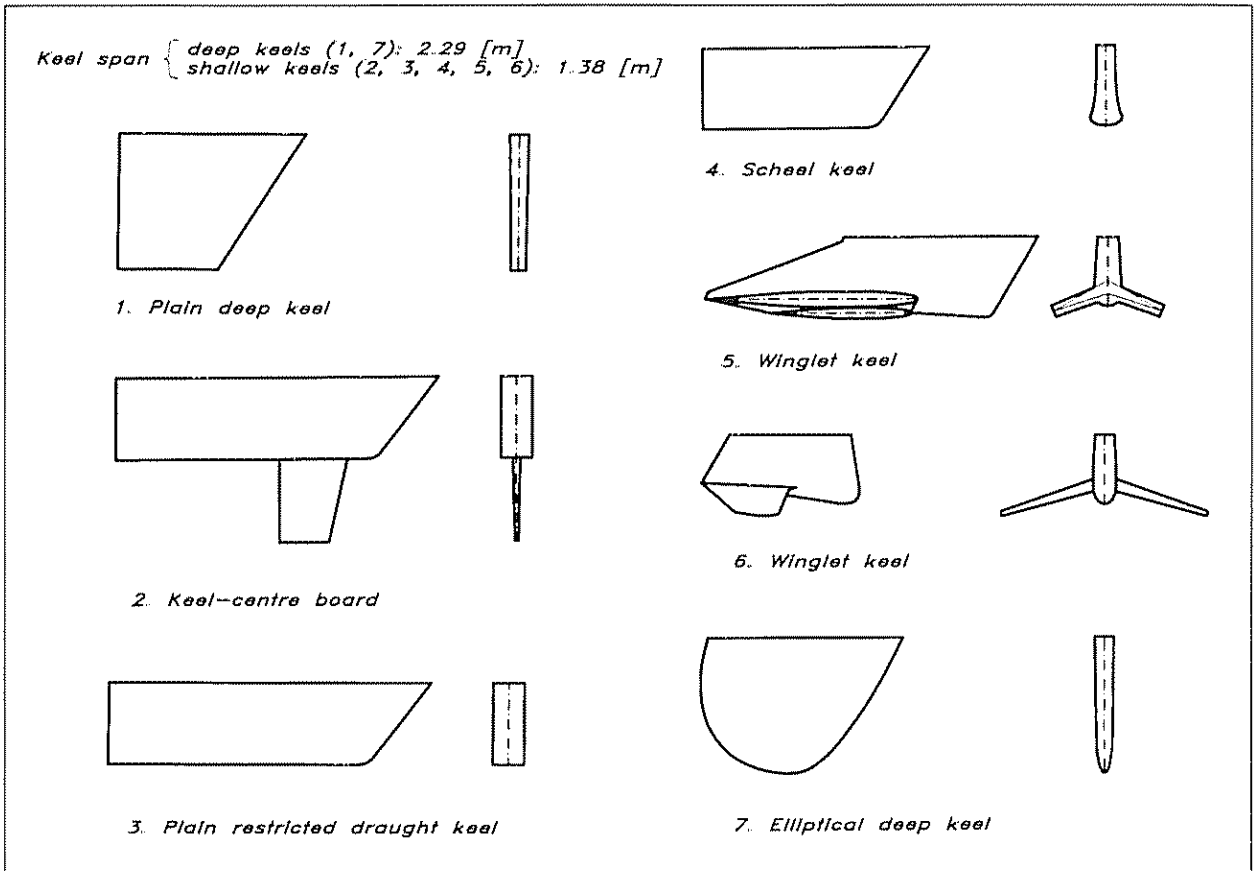


Fig 6.16 Keels tested by Prof. Gerritsma et al

normal span of 2.29 m. No 1 was a standard trapezoidal keel, with which to compare all the others, and no 7 was elliptic. Among the shallow draft keels, no 3 was just a trapezoidal reference case, while the others exploited some kind of device at the tip. No 2 had a centreboard, which increased the draft by 1.41 m, no 4 was a so-called Scheel keel and nos 5 and 6 had wings of different spans. A Scheel keel has very thick sections near the tip, as can be seen from the figure. This is to try to reduce the overflow by means of the 'corners' seen in the front view near the bottom of the keel.

Tests were made and evaluated using a Velocity Prediction Program (VPP), as explained in Chapter 16. Sailing speeds at all wind speeds and directions of interest were thus obtained, and Table 6.1 presents the final outcome, namely the elapsed time on an Olympic course at two wind speeds. It may be seen that the elliptic and the basic trapezoidal keels are the best, and virtually identical. The fact that they are the best is not, of course, surprising, since they have the largest draft. More interesting perhaps is the fact that keel no 6, which is much shallower, is almost equally good in the strong wind. It is thus possible to reduce the draft by introducing wings without much loss in performance. In fact, if the draft difference had been smaller the winged keel might have been equal, or even better. The winglet keel with the small span, the Scheel keel and the shallow trapezoidal keel were 2%, 3.5% and 5%, respectively, slower than

the best on the Olympic course. A somewhat disappointing result is the performance of the centreboard keel, which had the largest draft including the board, but was 2% slower than the best. It should be noted, however, that the board was left down under all conditions, while in reality it would have been raised downwind.

**Table 6.1**  
Elapsed time (hours, with decimals) on an Olympic course  
for the Delft keels

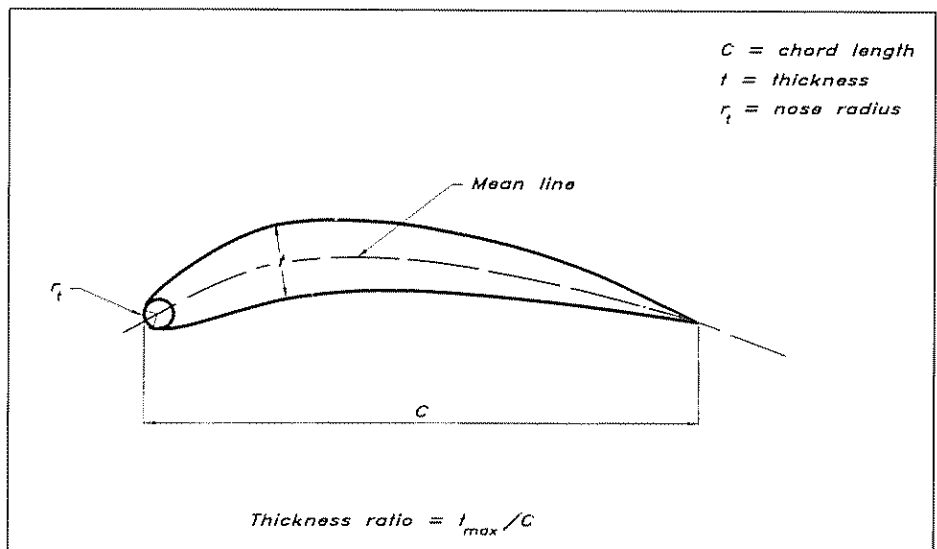
Wind speed (knots)	Keel no						
	1	2	3	4	5	6	7
15	3.96	4.06	4.13	4.10	4.04	4.01	3.96
25	3.52	3.60	3.72	3.64	3.60	3.53	3.52

### Definition of the section

The sectional shape of the keel does not have such a significant effect on its characteristics as the planform, but on the other hand the most important planform parameter, the aspect ratio, is fixed in most class rules and heavily penalized in rating rules. A study of the influence of the sectional characteristics may therefore be worthwhile.

In Fig 6.17 the geometrical parameters defining a foil section are presented. The section of the figure is asymmetric, ie the mean line, defined as the line midway between the upper and lower surface contours, is bent. As pointed out above, asymmetric sections are rarely used for sailing yachts, since they have to perform equally well on both tacks. We will limit most of the following discussion to symmetric

Fig 6.17 Definition of section shape



sections, where the mean line is straight. The thickness  $t$  is measured at right angles to the mean line, and the maximum thickness is denoted  $t_{\max}$ . The thickness ratio of the section is  $t_{\max}/C$ , where  $C$  is the chord length. An important parameter for the section characteristics is the nose radius,  $r_n$ , which is defined as the radius of curvature at the leading edge. This definition is not very practical, but as a rule of thumb the nose radius defines a circle, which follows the nose contour upwards and downwards about  $45^\circ$ .

### Three useful NACA sections

Unfortunately, many sailing yachts use foil sections that are not well designed. As a general rule the designer should not attempt to develop his own section, unless he is an experienced fluid dynamicist. There are several books listing useful sections available, and these can be used in most cases. The most well-known publication in this area is Abbott & von Doenhoff's *Theory of Wing Sections*. This book contains not only theories of wings and wing sections, but also an extensive presentation of the geometry and characteristics of a large number of sections.

In Table 6.2 the geometries of three useful sections are presented. The first belongs to the so-called four digit series, where the last two digits represent the thickness ratio and the first two give information about the mean line. For a symmetric section only the last two digits are of interest. The other two sections belong to the six-series, which may be considered more modern, even though it was designed in the 1940s. The six-series contains five different groups, denoted 63, 64, 65, 66 and 67, where the second digit gives the position of minimum pressure along the chord. The 63-series thus has its minimum at 30% of the chord from the leading edge, the 64-series at 40%, etc. This information is quite important, as we will see. After the dash in the number the first digit concerns the mean line, while the last two give the thickness ratio in per cent. All three sections of Table 6.2 have a thickness ratio of 10%. The

Fig 6.18 Nose radius

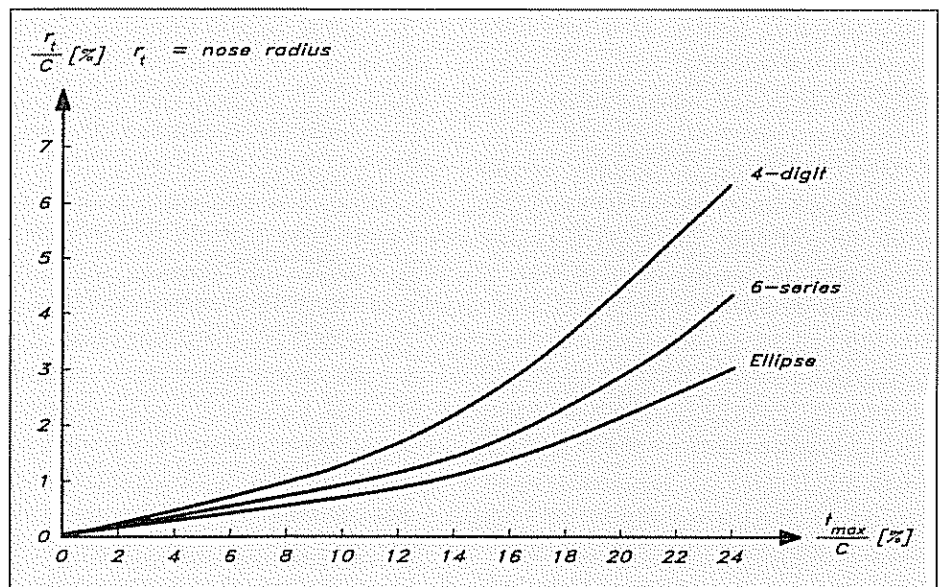


**Table 6.2**  
**Three useful NACA sections**

x	y 0010	y 63-010	y 65-010
0	0	0	0
0.5		0.829	0.772
0.75		1.004	0.932
1.25	1.578	1.275	1.169
2.5	2.178	1.756	1.574
5.0	2.962	2.440	2.177
7.5	3.500	2.950	2.647
10	3.902	3.362	3.040
15	4.455	3.994	3.666
20	4.782	4.445	4.143
25	4.952	4.753	4.503
30	5.002	4.938	4.760
35		5.000	4.924
40	4.837	4.938	4.996
45		4.766	4.963
50	4.412	4.496	4.812
55		4.140	4.530
60	3.803	3.715	4.146
65		3.234	3.682
70	3.053	2.712	3.156
75		2.166	2.584
80	2.187	1.618	1.987
85		1.088	1.385
90	1.207	0.604	0.810
95	0.672	0.214	0.306
100	0.105	0	0

four-digit series can be scaled to any other thickness by multiplying all y-values by the thickness desired divided by the given 10%. This is not precisely true for the six-series, but it is a good approximation if the thickness ratios are not too far from 10%

The sections are specified in the table by a set of x-y values, where x is along the chord, measured from the nose and y is at right angles to x. Note that both coordinates are given in per cent of the chord length and that only one half of the (symmetric) section is defined. To be able to describe the most important part of the section, namely the nose region, the nose radius is required. This varies quadratically with the thickness ratio, as appears from Fig 6.18, which gives the radius, not only for the two series, but also for an ellipse. It is seen that the six-series is relatively close

to the ellipse, while the nose radius for the four-digit series is much larger.

### **Influence of shape on section characteristics**

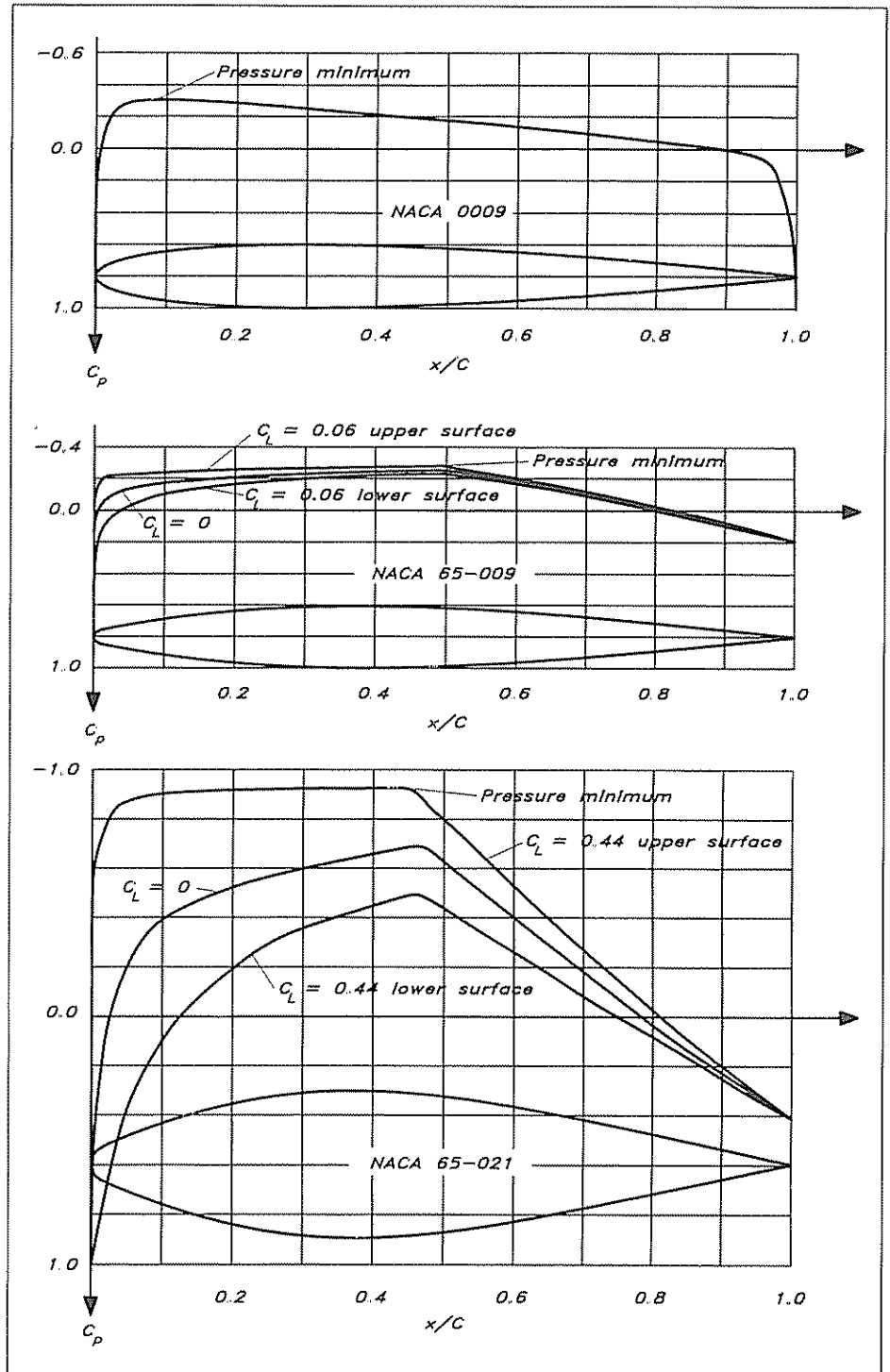
In order to understand the influence of the shape of the section on its performance, reference should be made to Fig 5.5, which shows the boundary layer around a hull. In principle, the same picture may represent the flow around an airfoil section. There is a laminar boundary layer developing backwards from the leading edge. After a certain distance the flow becomes unstable, and shortly thereafter the boundary layer undergoes transition to the turbulent state. Under certain conditions the flow may separate and recirculation may occur. When compared to the case of Fig 5.5, which is symmetric, one difference is that for an airfoil at an angle of attack the flow picture is not the same on the two sides. We recall from the discussion in Chapter 5 that the boundary layer development is determined from the pressure distribution, which in turn depends on the shape. A favourable pressure distribution with diminishing pressure stabilizes the flow, which is then sucked backwards. An increasing pressure works in the opposite direction and destabilizes the flow in such a way that transition moves upstream and separation occurs more easily.

With these considerations in mind it is of interest to examine the pressure distribution on the three typical sections shown in Fig 6.19. The first is a conventional four digit NACA section with a thickness ratio of 9%, while the other two belong to the 65-series, with 9% and 21% thickness ratios, respectively. As before, negative pressure is upwards on the vertical scale. It may be seen that the four-digit section has its pressure minimum very far forward, close to 10% of the chord from the leading edge. This means that a favourable pressure distribution exists on only 10% of the chord, and that transition is likely to occur far forward. On the two other sections the maximum thickness and hence the pressure minimum, occurs further back, and a much larger laminar zone can be anticipated, resulting in a considerable drag reduction.

For the 65-series two extra pressure distributions are given. These show the pressure on the upper and lower sides of the section at the maximum angle (ie maximum lift coefficient) for which it works properly. It can be seen that a favourable pressure distribution is maintained even on the suction side up to a lift coefficient of 0.06 for the thin section and 0.44 for the thick one. At higher lifts, ie larger angles of attack, the suction peak moves very far forward on the suction side, transition occurs close to the leading edge and the drag increases. A typical lift coefficient sailing upwind is 0.2, while it is almost zero downwind. The differences between the three sections may now be summarized as follows:

- the four-digit series has its pressure minimum further forward and has consequently a smaller region of laminar flow as compared to the 65-series;
- the thin section works well only in a small range of angles of attack, while the thick section accepts larger angles.

Fig 6.19 Influence of shape on pressure distribution



We will now turn to a more quantitative discussion of the differences in lift and drag. First the difference between the series will be presented. In Fig 6.20 two sections of the same thickness (9%), are shown, together with the corresponding drag curves. The four-digit and 63-series are compared, since the 65-series, shown in Fig 6.19, is rarely used for such small

thicknesses. It appears that the 63-section has about 20% smaller drag up to about 2° of angle of attack, while for larger angles the four-digit section is superior. It should be pointed out that the angle is for a two-dimensional wing, ie with AR = infinity. For more practical ARs the angle is about twice as large, given the lift coefficient (cf Fig 6.6).

The influence of the thickness and its distribution for the same type of sections, all belonging to the 6-series, is exemplified in Fig 6.21. Two 9% and two 21% sections are shown. The sections of the same thickness

Fig 6.20 Comparison between two profiles

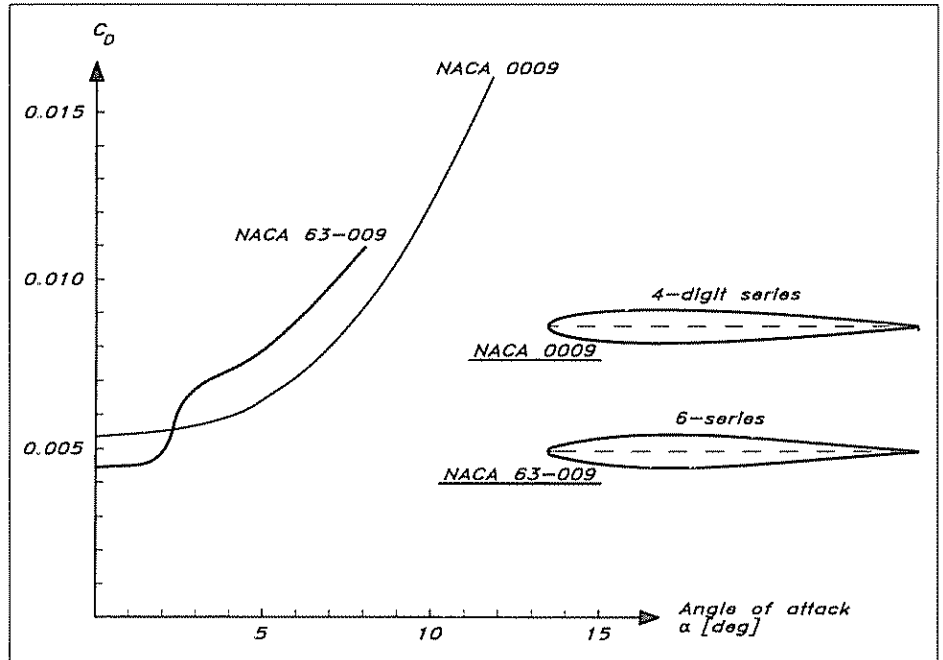
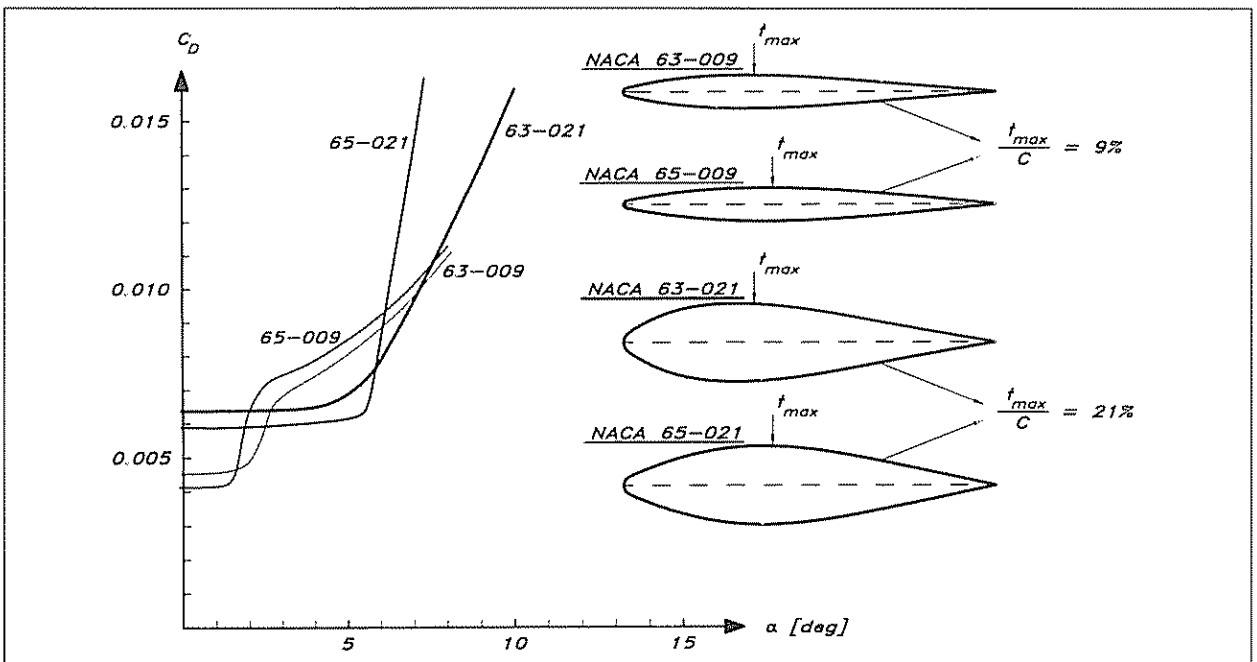


Fig 6.21 Influence of section shape on drag





differ, since they are from the 63 and 65-series, respectively. The location of the maximum thickness (and the pressure minimum) is different. It can be seen that the thin sections have the smallest drag at small angles of attack, while the so-called 'drag bucket' is much wider for the thick ones. Furthermore, the 65-sections give smaller drag than the 63-sections, but the drag bucket is slightly narrower

To simplify the comparison at zero angle of attack Fig 6.22 has been prepared. The drag coefficient for varying thickness ratios is given for the four-digit, as well as the 63 and 65-series. There is obviously quite a large difference, particularly between the four-digit series and the others.

The difference between the lift coefficients is much smaller, as can be seen from Fig 6.23. For the range of angles of interest ( $2-3^\circ$ ,

Fig 6.22 Influence of thickness on drag at zero angle of attack

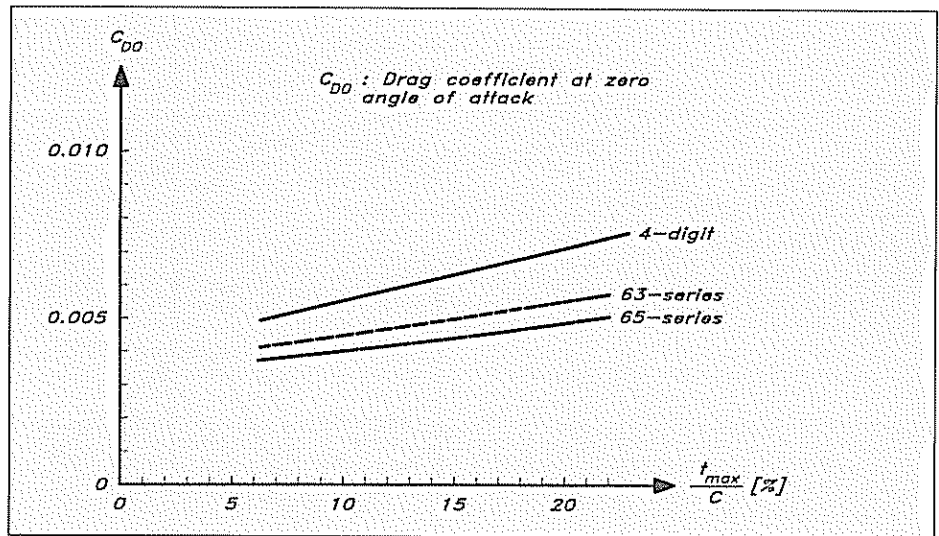
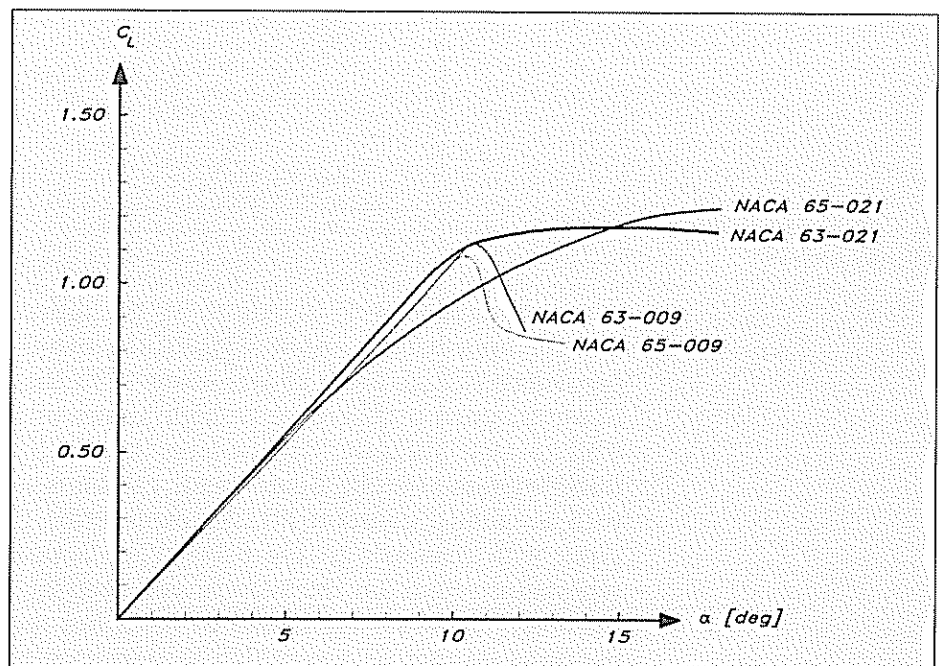


Fig 6.23 Influence of section shape on lift



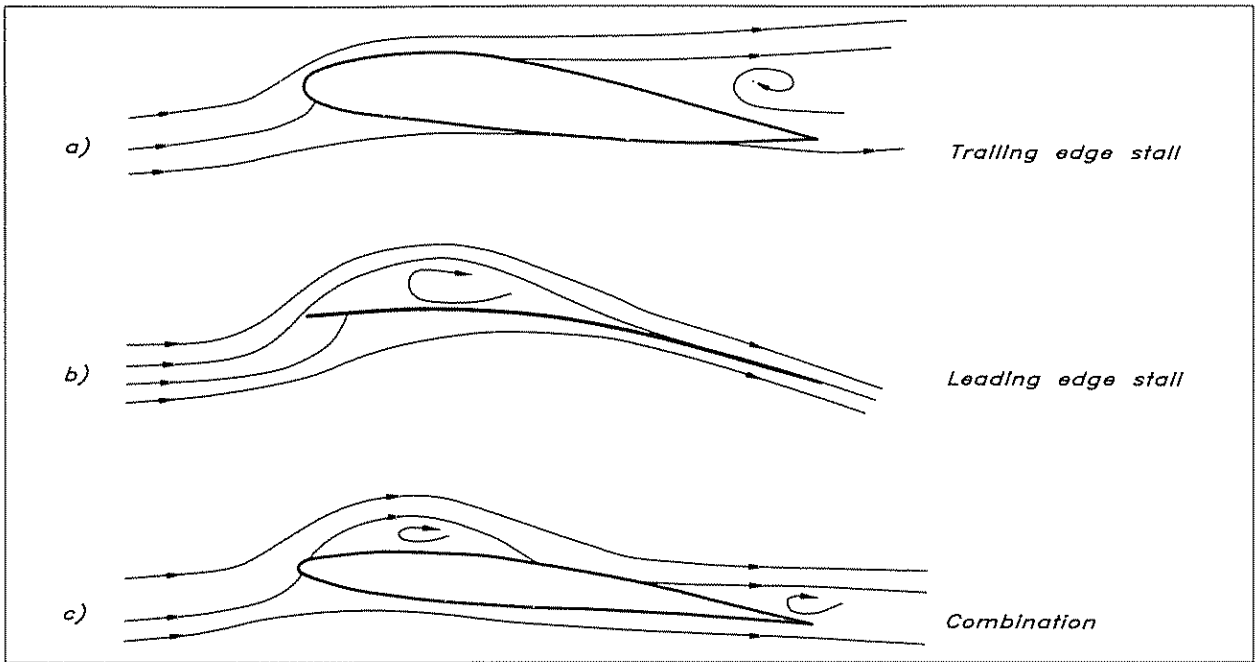


Fig 6.24 Different types of stall

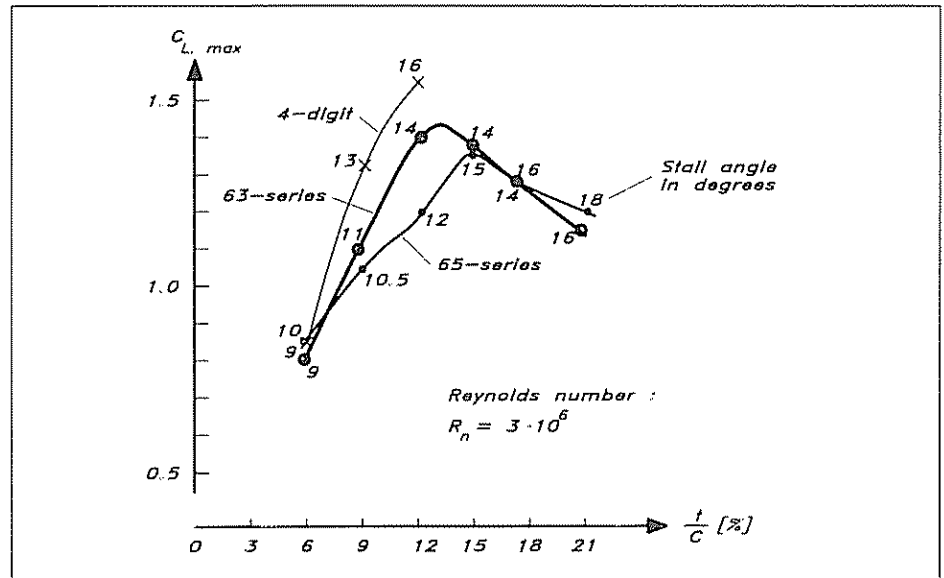
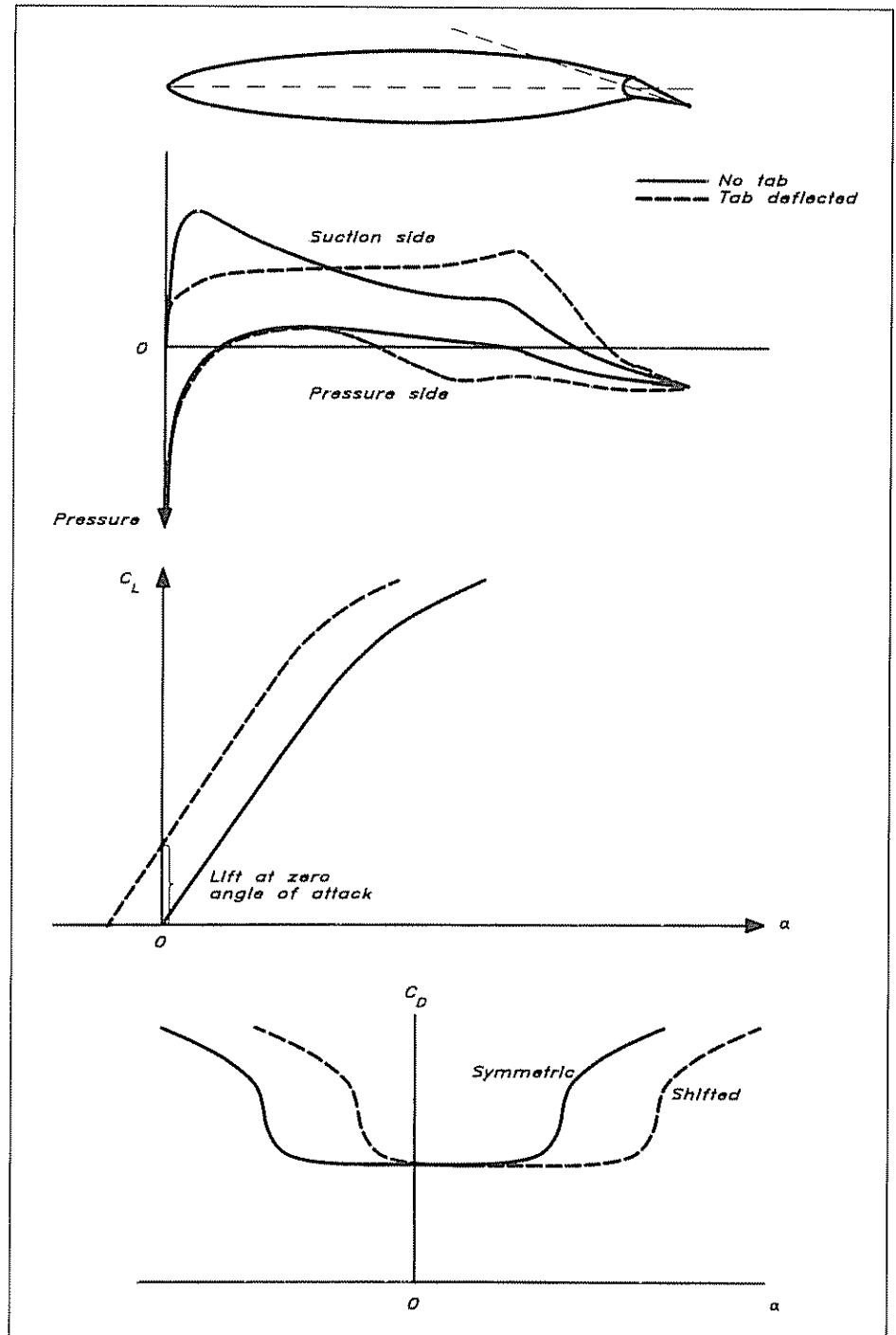


Fig 6.25 Maximum lift for different profiles

corresponding to  $4-6^\circ$  at  $AR = 3$ ), the difference is hardly noticeable and the approximate value, 0.10, of the two-dimensional lift coefficient per degree ( $C_{L,2D}$ ), given above, seems to fit the data quite well. There is, however, quite a difference at high angles of attack. The thin sections tend to stall abruptly, with a large loss in lift as a consequence. The thick sections, on the other hand, exhibit a much more gradual stall, with an almost constant lift. An explanation of the differences may be given with reference to Fig 6.24. When a thick section (case a) stalls, separation occurs on the suction side near the trailing edge. The larger the angle the larger the separated zone, but the changes are smooth. In the opposite case, ie a very thin section (case b), the flow cannot follow

the sharp bend around the nose even for small angles of attack, so a separation bubble develops at the nose. When the angle is increased the bubble grows smoothly until it reaches the trailing edge and the maximum lift is developed. No jump in lift occurs, but the drag is large for all angles. On a section of medium thickness, 9–12% (case c), both types of separation start to develop at relatively high angles of attack.

Fig 6 26 *Effect of trim tab*



The catastrophic drop in lift occurs when the separation bubbles meet and the entire suction side suddenly becomes separated.

The maximum lift coefficient for the four-digit and the 63 and 65-series sections is given as a function of thickness ratio in Fig 6.25. It can be seen that the highest lift may be achieved by sections with a thickness ratio in the range 12–15%, and that the four-digit series is the best one in this respect. The angle at which the maximum occurs for each section is also indicated. Note again that this angle is approximately twice as large for keels of normal aspect ratio.

A possibility not discussed earlier is to divide the section into one fixed and one movable part. The mean line is then no longer straight, but exhibits a sharp corner at the hinge. This design may have several advantages, provided it is well done. An example of such a configuration is the trim tab behind a fixed keel. Fig 6.26 shows the principal effect of a deflection of the tab on the pressure distribution, as well as on the lift and drag. The stagnation point moves from its asymmetric position at the nose closer to the original symmetry line of the section, and therefore the large suction peak created by the sharp bend around the nose is reduced or even eliminated. The pressure distributions on both sides become closer to the one at zero angle of attack, and the favourable pressure decrease can be maintained at higher angles of attack. This effect is substantiated by the shift of the drag bucket to the right in the lower part of the figure. Another important effect is that the lift curve is moved to the left, giving a lift force even at zero angle of attack. By proper adjustment of the trim tab enough side force to balance the sails may be generated without leeway, which is an advantage, since the hull will then move straight through the water and thus produce minimum resistance.

When the tab is deflected there is normally a knuckle in the section at the hinge, which causes pressure spikes on both sides. This inevitably causes a drag increase, which to some extent reduces the positive effect of the tab. A way to alleviate this problem was pointed out by the yacht designer G Heyman. Since the suction side is the most sensitive one, it is advantageous to design this to be smooth *with the tab deflected*. The suction sides of the tab and the main part of the section are thus integrated to yield a smooth curve from nose to tail, at the tab angle of interest. Of course, this means that when the tab is set to zero angle the section will not be smooth, but this may not be so serious, since the section is then normally unloaded.

### Some practical conclusions regarding section shape

We are now in a position to draw some practical conclusions from the discussion above. We will have to consider the keel and the rudder separately, since their function and operating conditions are different. Thus the keel normally operates at small angles of attack and the speed of the yacht depends on the drag produced at these small angles. The rudder, on the other hand, may help the keel to produce the necessary side force, but its main task is to provide enough moment to manoeuvre the yacht under all conditions. Therefore the rudder has to be designed with emphasis on the maximum side force required.

Since the lift and angle of attack for the keel are small, sections of the six-series are preferable. The 63 or 65-series may be used, but the thickness ratio should not be too small to keep the drag bucket wide enough for upwind sailing. 12% for the 63 and 15% for the 65-series may be considered as suitable lower limits. A thick section is, of course, favourable from a ballast point of view, but there are reasons for keeping the thickness limited. Thus, the drag at zero angle of attack increases with thickness (as seen in Fig 6.22), and experience has shown that a thick keel at the root produces unnecessary waves when the yacht heels. A good compromise is to use a relatively thick section, 15–18% say, at the tip and gradually decrease the thickness ratio to 12%, say, at the root, at the same time gradually changing from the 65 to the 63-series.

The rudder has to be designed for the maximum side force required, and this force is proportional to the product of the maximum lift coefficient and the plan form area. A large  $C_{L_{max}}$  means that the area can be small, and the total wetted surface reduced. On the other hand, a larger wetted surface can be tolerated if it has an extensive area of laminar flow. Furthermore, the rudder operates most of the time at higher angles than the keel, particularly if the yacht is sailing in a seaway, and corrections to the course have to be made continuously. With all this in mind it is obvious that the more extreme laminar sections, such as the 65-series should be avoided, since they have a lower  $C_{L_{max}}$  and higher resistance at larger angles than the two other types of section discussed above. For light and fast hulls such as catamarans, dinghies and lightweight displacement hulls, relatively small rudder angles are required, which would speak in favour of the 63-series, while for heavier yachts with larger rudder angles the four-digit series might be preferable. A suitable thickness for most yachts is 12–15%, since the maximum  $C_{L_{max}}$  is obtained in this range. Very fast hulls with surface piercing rudders should use thinner sections, however, since the spray generated at the nose is proportional to the thickness squared.

#### **Influence of deviations from the theoretical section shape**

The most sensitive part of the section is the nose, where the flow has to pass a region of very high curvature on its way from the stagnation point on to the suction side when the section has an angle of attack. Therefore, the nose radius as presented in Fig 6.18 should be used as closely as possible. In Marchaj's *Sailing Theory and Practice* two investigations are reported, where the influence of imperfections at the nose was tested. First, the bluntness was altered, as indicated on the left in Fig 6.27. The figure shows that the drag increased considerably, regardless of whether the nose was made blunter or sharper, as compared with the ideal shape. A more careful variation was made in the second investigation, where the nose radius was varied for a 12% section. Special emphasis was placed on the high lift properties, and a lower  $C_{L_{max}}$  was obtained both for larger and smaller radii, compared to the correct one (see Fig 6.27, right).

In Chapter 5 the influence of surface roughness on the viscous resistance of the hull was discussed in some detail. The importance of a

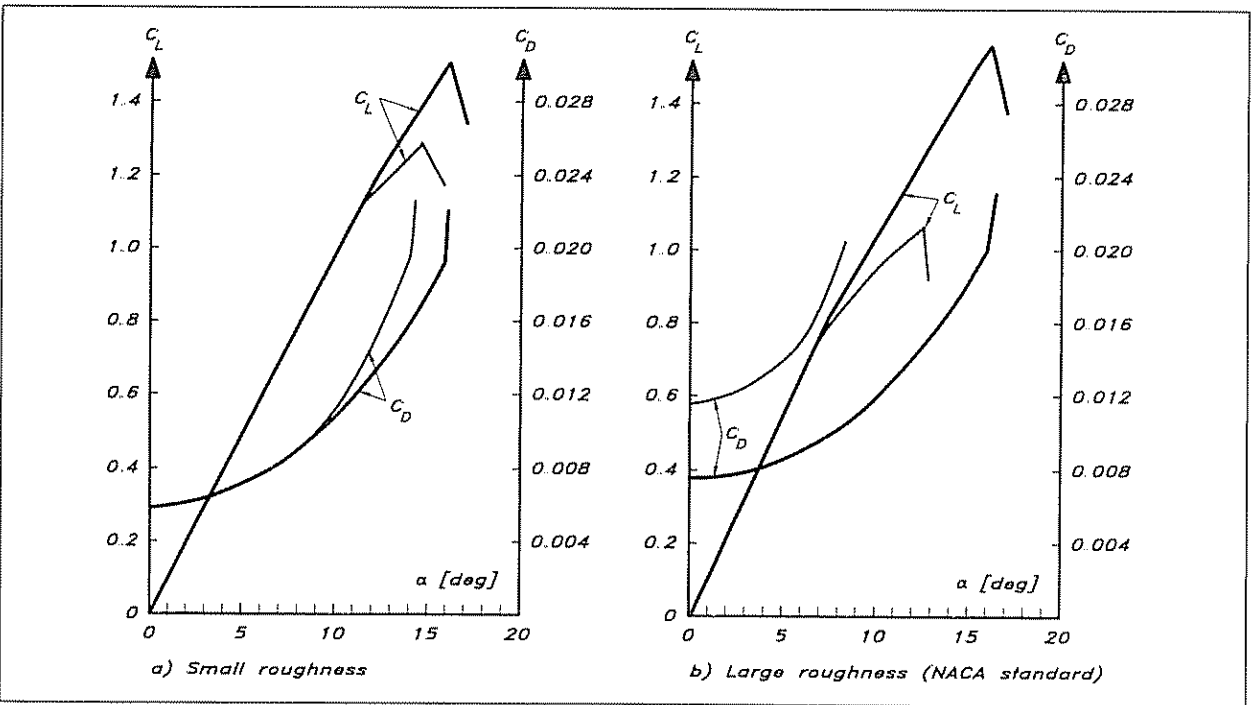
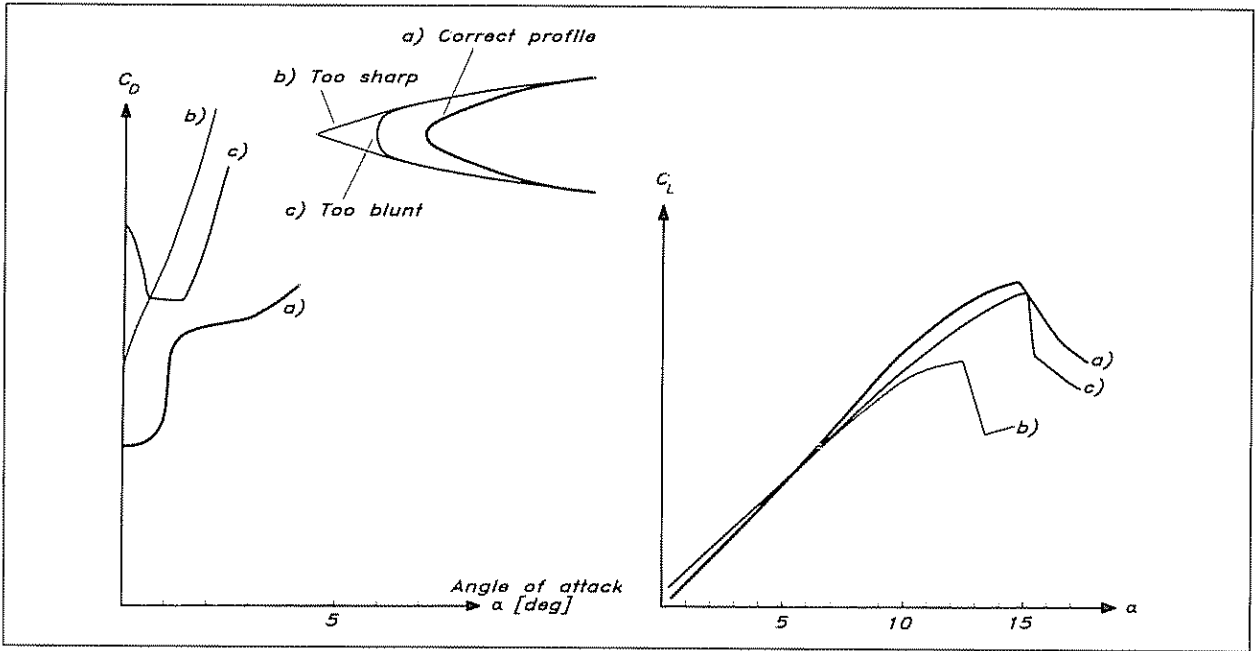


Fig 6.27 (Top) Influence of nose shape on drag and lift

Fig 6.28 Influence of roughness on drag and lift

smooth surface is even greater for the keel and rudder, particularly if laminar sections are used. Small imperfections may cause premature transition, making the favourable characteristics deteriorate more than for a less advanced section from the four-digit series. However, even a section of this kind may be affected negatively. Fig 6.28, (left) shows the influence of a very small roughness element, of the order of 10  $\mu\text{m}$ , on a NACA 0012 section. It may be seen that the drag is not greatly affected for small angles, but stall occurs much earlier. To the right in

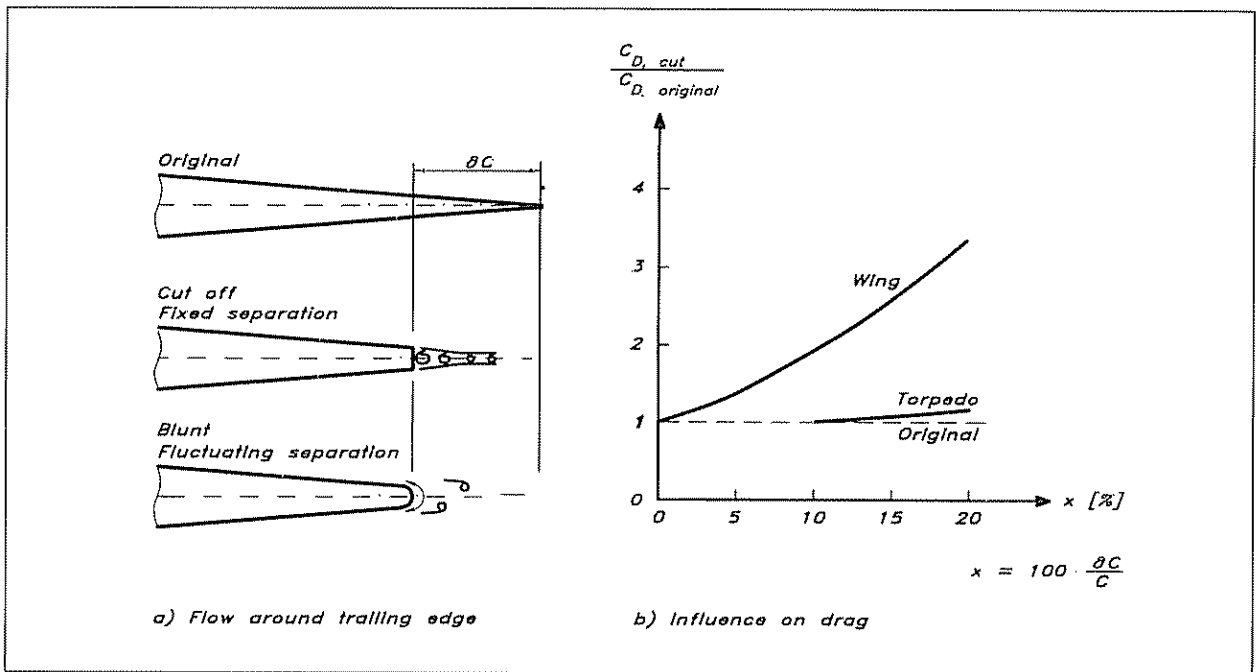










Fig 6.29 Influence of trailing edge shape

the same figure the influence of NACA's standard roughness on the same section is shown. This roughness is relatively large: 0.04% of the chord length, corresponding to a height of 0.4 mm on a one metre chord, and the effect is dramatic, with a large drag increase at small angles and a very early stall. As pointed out in Chapter 5, the influence of roughness increases with speed, so for planing boats, great care should be taken to keep the foils (centreboard and rudder) free from surface imperfections. This is particularly important on the forward one third of the chord.

For practical reasons the trailing edge of a keel or rudder section cannot be razor-sharp. It is therefore interesting to investigate the effect of various endings of the section. Reference should be made first to Fig 6.29, which shows the effect of cutting off part of the tail. For a wing the drag starts increasing immediately, even for very small cut-offs. This is in contrast to the effect on an axisymmetric body, like a torpedo or a keel bulb, where relatively large cut-offs are permitted without a drag penalty. Therefore, the cut-off on a wing should be kept to a minimum. The way the cutting is done is also of importance. Fig 6.30 shows some alternatives. An interesting phenomenon is the vibration that occurs for certain shapes. The figure shows the amplitude of the vibrations at resonance for each case relative to those of a square cut-off. It can be seen that if the edge is symmetric and wedge-shaped (cases 2–5), the total wedge angle has to be  $30^\circ$  or smaller. For  $90^\circ$  and  $60^\circ$  much larger vibrations occur than for the square ending. This is also the case if the ending is rounded in some way, which it normally is, if the trailing edge of the keel or rudder is left without attention. An asymmetric cut-off is somewhat more forgiving, and a  $45^\circ$  cut-off is acceptable, provided the corner on the cut-off side is smoothed. The vibrations are not only of

Fig 6.30 Influence of trailing edge geometry on vibration level

<i>Case</i>	<i>Geometry</i>	<i>Relative vibration amplitude</i>
1		1
2		1.9
3		3.8
4		0.43
5		0
6		0.38
7		0.03
8		0

academic interest. On the contrary, they may cause severe vibrations and noise in the entire hull at speeds where resonance occurs. Using the information in Fig 6.30 these problems can be solved.

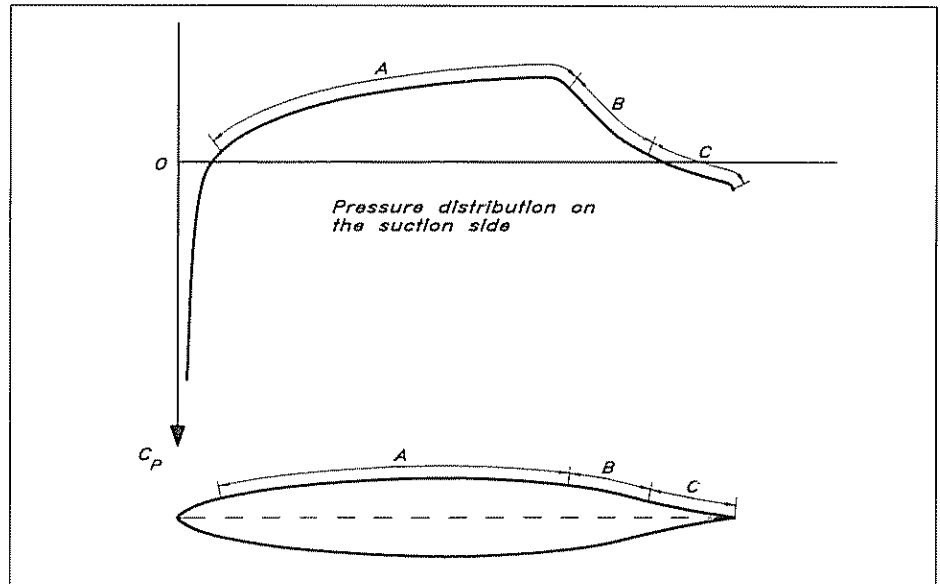
### Advanced section design

The NACA sections presented above are quite efficient and useful for most sailing yachts. However, under certain conditions more advanced sections have been used. This is so in connection with the America's Cup and other races, where large amounts of money are invested to squeeze out the last tenths of a percentage point in performance. Computer programs are then used to obtain sections that are optimized, not only for the lift to be carried, but also for the Reynolds number in question. In this chapter we have not, so far, included any discussion of the Reynolds number effects, but as indicated in the previous chapter, this number has an influence on the boundary layer development and hence the drag.



When designing an optimum section the designer starts from the pressure distribution on the suction side at the design lift coefficient (angle of attack). The distribution may be divided into three zones (see Fig 6.31). To keep the boundary layer laminar the pressure must decrease, and this is what happens in zone A, where the thickness of the section increases. At some position this increase obviously has to stop, since the thickness has to go to zero at the trailing edge. This also means that the pressure has to start increasing at some position along the chord. The required slope of the pressure distribution in zone A depends on the Reynolds number and the ambient turbulence level. A higher Reynolds number and a higher turbulence level give a more unstable flow, and hence a larger slope of the pressure distribution is required to maintain the laminar boundary layer. The possible slope is set by the magnitude of the suction at the peak value and the length of zone A. Since the latter should be long the peak must be high, ie the maximum thickness should be as large as possible, without causing problems in the other two zones, where the pressure has to rise again.

Fig 6.31 *Distribution of the three zones of interest in advanced section design*



The pressure recovery zone is split into two parts, B and C, since different strategies should be used in the early and later parts of the recovery. The problem is to avoid separation. In principle, the thicker the boundary layer and the faster the pressure increase the larger the risk of separation. At the suction peak, where transition is assumed to occur, the boundary layer is relatively thin, and can withstand a rapid pressure increase. Approaching the tail, however, the boundary layer thickens rapidly and a much more gentle increase in pressure is required. Thus, in zone B, the pressure increase should be fast, which calls for a rapid thinning of the section. In zone C, on the other hand, the pressure should increase slowly, so the tail must taper off in a smooth manner. This gives optimized sections the typical concave appearance at the tail.

Obviously, the design of sections in the manner described takes considerable experience, and access to accurate computer programs for the computation of the pressure distribution and of the boundary layer development, including both transition and separation. Neither of these conditions is likely to be satisfied for the amateur designer, who will have to rely on standard sections, for instance from the NACA series described above.

### Statistics on keel and rudder area

Since the task of the keel is to produce the major part of the hydrodynamic side force to balance the aerodynamic side force from the sails, it is reasonable to look at the keel area as a fraction of the sail area. We will simplify the calculation of the latter by referring to the sum of the main and fore triangles.

A good average of keel area to sail area for fin-keel, cruiser/racer yachts is 3.5%, and the spread is approximately 0.75%. Percentages below 2.75% are found only on pure racing yachts, and even for these problems may start to occur in the region 2–2.5% when the keel is heavily loaded, as when sailing to windward in heavy seas. The smaller the area the higher the minimum speed at all wind conditions, so yachts with a small keel have to keep the speed up all the time. Very extreme and fast designs like the America's Cup or Whitbread yachts may have keel blades as small as 1.5% of the sail area, but they also have a bulb that may contribute somewhat to the side force.

While keels seem to have become smaller in recent years, at least for racing yachts, rudders may have become somewhat larger. For more or less over-canvassed racers in particular a relatively large rudder is required to avoid broaching problems downwind under severe conditions. An average value of rudder area to sail area on modern cruiser/racers is 1.4%. This includes a possible skeg in front of the rudder. The lower limit seems to be around 1% and the upper 2%.

Since larger yachts move at higher speeds for all wind strengths, smaller relative keel and rudder areas could be anticipated. No such trend has been detected, however, in the statistical material, at least in the range up to about 12 m  $L_{WL}$  in which the majority of the yachts lie.

### The YD-40

The keel area of the YD-40 is 2.18 m<sup>2</sup>, while the sum of the main and fore triangles is 71.8 m<sup>2</sup>. This keel is thus 3% of the triangle area, somewhat on the low side, but reasonable for this well-performing cruiser/racer.

For the keel the sweep angle is 21°, which calls for a taper ratio of about 0.2 to give the optimum load distribution, according to Fig 6.8. This would, however, give a very unfavourable volume distribution of the keel, with a high centre of gravity. As for most other designs a slight loss in hydrodynamic performance is accepted to lower the centre of gravity and thereby increase the stability. The tip chord of the keel is 1.05 m and the root 1.85 m, which gives a taper ratio of 0.57. With a span of 1.50 m this gives a geometric aspect ratio of 1.0 and an effective ratio of 2.0, assuming the bottom to be a flat wall. At this aspect ratio

the increase in induced resistance is around 1% for taper ratio deviations of 0.4 from the optimum (as appears from Fig 6.9). Since the induced resistance is only 8% of the total in upwind sailing (and less downwind), according to Fig 5.4, the increase in total resistance due to the too high taper ratio is less than 0.1%. This is certainly compensated for by the stability increase.

Thin sections at the root and fat ones at the tip are favourable for several reasons. Most importantly, this lowers the centre of gravity, thereby increasing stability, but furthermore, as pointed out above, a thick section near the hull seems to increase the waves due to the keel at large heel angles. The third reason to keep the root chord thin is that the interference drag in the junction is reduced. In fact, experiments indicate that this drag component is negative below 8%, and increases quadratically with thickness ratio above that level. For structural reasons, however, the root should not be made too thin, as explained in Chapter 11.

For the YD-40 we have chosen a 10.5% NACA 63-section at the root and a 17.5% 65-section at the tip. The section type is changed linearly between the two extremes, while the thickness ratio has a break point 0.65 m below the root, where the ratio is 14%. There is thus a linear variation between 10.5% and 14% in the upper part, and between 14% and 17.5% in the lower part. This gives slightly more volume in the lower part as compared to a linear variation from root to tip.

Since the stability aspect is irrelevant for rudders, there is no need to depart from the optimum taper, at least not if the rudder is well submerged even under heel. Beamy yachts, and yachts which are very unbalanced fore-and-aft, tend to lift the rudder when heeling, and this calls for larger chords in the lower part of the rudder. The YD-40 is quite slender, however, and well balanced fore-and-aft, so these problems should not occur.

It is advantageous if the rudder shaft is at right angles to the bottom, where it exits, since the gap between the hull and the rudder may then be sealed for all rudder angles. This is the case for the YD-40, and since the 25% line approximately coincides with the shaft axis, this line is approximately at right angles too. In the upper part of the rudder the flow follows the bottom, so the sweep angle is zero. Further down the flow direction is more horizontal, so there is a small sweep. We have neglected this and chosen a taper ratio of 0.46. The root chord is thus 0.688 m and the tip chord 0.320 m. A rudder span of 1.47 m gives a high geometric aspect ratio of 2.9 and an area of 0.74 m<sup>2</sup>. The latter is 1.03% of the sail area and is thus relatively small. There are two reasons for this. First, the slenderness and the fore-and-aft symmetry of the hull will make the yacht well balanced, and secondly, we have chosen the section with the largest  $C_{Lmax}$  for the rudder, namely the NACA 0012. Since the rudder shall be designed for the maximum side force required, and since this is proportional to the product of the area and  $C_{Lmax}$  this choice may help reduce the area required.

# 7

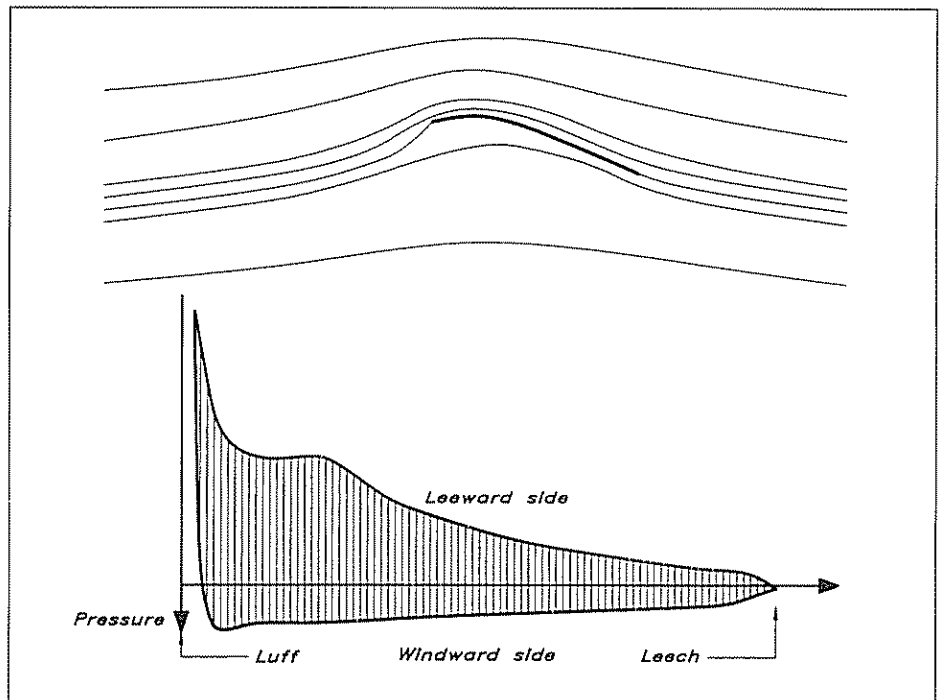
# SAIL AND RIG DESIGN

A sail is a wing, which differs in some important respects from the wings of the previous chapter. Thus, the sail has virtually no thickness, but it has a camber which is quite large. It often works in the disturbed flow from a mast. Nevertheless, most of the principles described above still apply, and we will discuss them in connection with the design of sails and sailplan in this chapter.

## Flow around sails

Fig 7.1 shows the flow around a single sail without a mast, together with the pressure distribution on the two sides. It can be seen that the negative pressures (upwards, cf Fig 6.2) on the suction side are much larger than the positive ones on the pressure side. Since it is the difference in pressure between the two sides (ie the vertical distance between the two curves) that gives the force, it is obvious that the major contribution to the sail force comes from the suction on the leeward side of the sail.

Fig 7.1 Flow around a sail



The flow around two sails close together is shown schematically in Fig 7.2. Streamlines for the two sails in combination are shown as thick lines, while streamlines for the single mainsail are shown as thin lines.

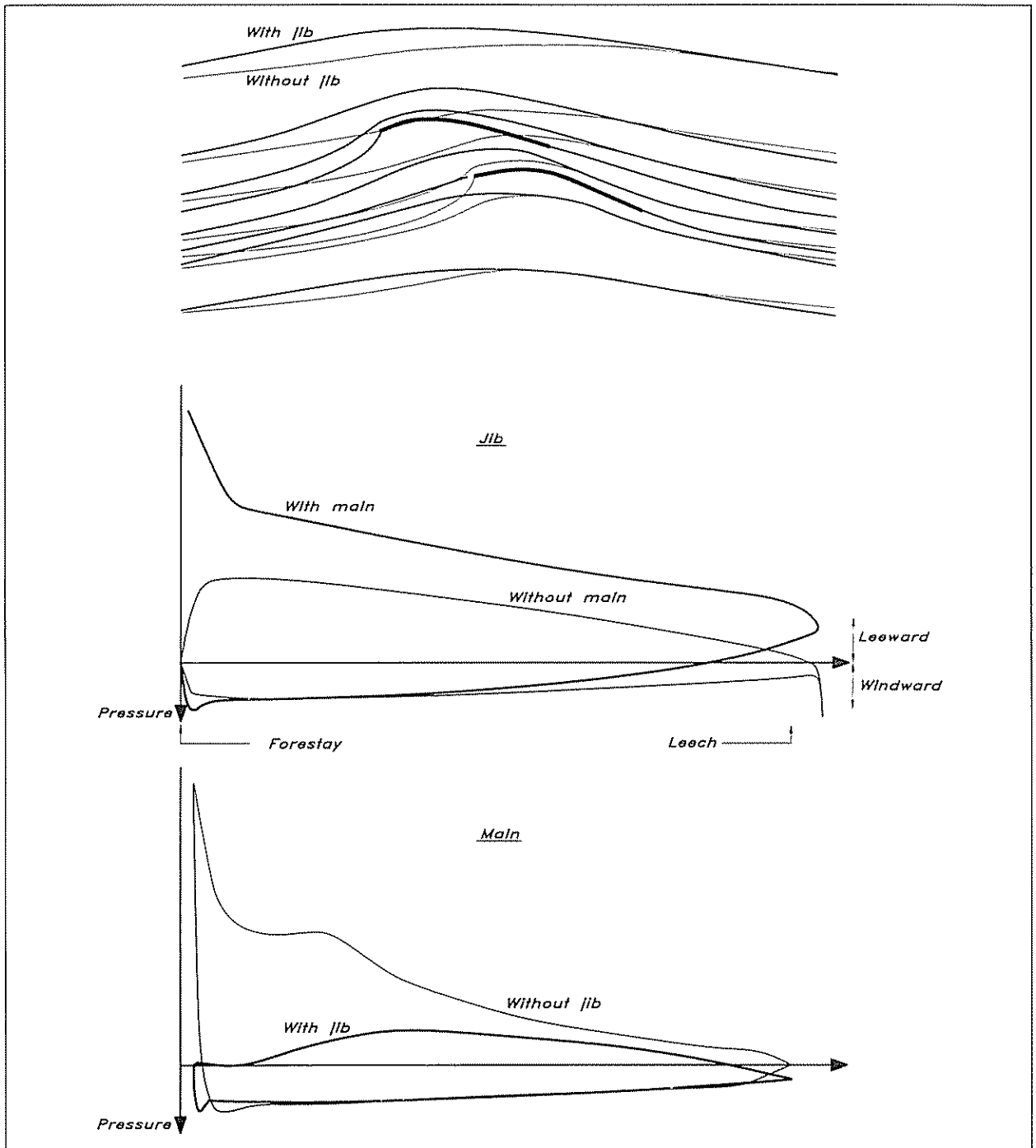


Fig 7.2 Flow around a mainsail/jib combination

The latter are in principle the same as in the previous figure. Mast disturbances are neglected. There is a very interesting difference in the upstream flow between the two cases. Approaching the sails the thick lines bend much further apart than the thin ones. This means that the air approaches the mainsail at a smaller angle than in the single sail case, while the opposite is true for the jib. Thus, as compared to the single sail case, the main gets unloaded, while the jib gets more load.

This is reflected in the pressure plots in the lower part of the figure. Most of the suction over the forward half of the main has disappeared and the total force, represented by the area between the pressure curves on the two sides, has dropped considerably. On the other hand, the suction on the leeward side of the jib has increased from the leading to the trailing edge and the force is much larger.

This interpretation of the slot effect was presented by the American aerodynamicist A E Gentry in the 1970s, and it represented a radical departure from the common belief that the suction behind the mainsail is increased by the presence of the jib. This opinion stems from an erroneous interpretation of the so-called Venturi effect. When the flow in a tube passes a restriction, ie a reduction in the cross-sectional area, the speed increases and the pressure drops. This is an indisputable fact, but the situation is different between the two sails. Unlike the flow in the tube the air approaching the sails has the freedom to avoid the restriction. Rather than going between the sails some of it may bend sideways and pass outside the jib/mainsail combination, ie to leeward of the jib and to windward of the main. As we have already noted, this is exactly what happens. Less air passes near the leeward side of the main if a jib is introduced in front of it.

Gentry's explanation is based on an idealized model of the flow, where viscosity is neglected. This does not alter the main conclusion, but if viscosity is considered, some further conclusions may be drawn. Thus, the boundary layer on the suction side of the mainsail experiences a much smoother pressure distribution than for the single sail. The flow in the boundary layer does not have to make its way against a rapidly increasing pressure, so the risk of separation is very much reduced. This means that the sail can be sheeted at a larger angle to the main flow, at midship or even, in fact, somewhat to windward.

## Planform

At the top of the sail and at the boom the lift force goes to zero and vortices are shed, giving rise to an induced resistance. The larger the height of the sail the smaller the effect of the vortices. As for the keel, the most important efficiency parameter for the sail is the aspect ratio. We define it here as the luff length ( $P$  or  $I$ ) divided by half the foot length ( $E$  or  $J$  in the IOR notation) so neglecting the roach it corresponds to the definition of the previous chapter. It should be mentioned that in some sailing literature the foot length is not divided by two in the definition, so the aspect ratio is half as large.

Very interesting studies of different planforms have been carried out computationally by Professor J H Milgram at Massachusetts Institute of Technology (MIT). For a masthead rig he varied systematically the aspect ratios of the main and fore triangles by changing the foot lengths. The calculations were for the upwind condition, and the computed force was resolved into its driving component  $R$  and side force  $S$ . These forces are given in coefficient form:  $C_R$  and  $C_S$  respectively, in Figs 7.3 and 7.4. Note that the coefficients are obtained by dividing by a sail area, which is either the real one (thick line) or the

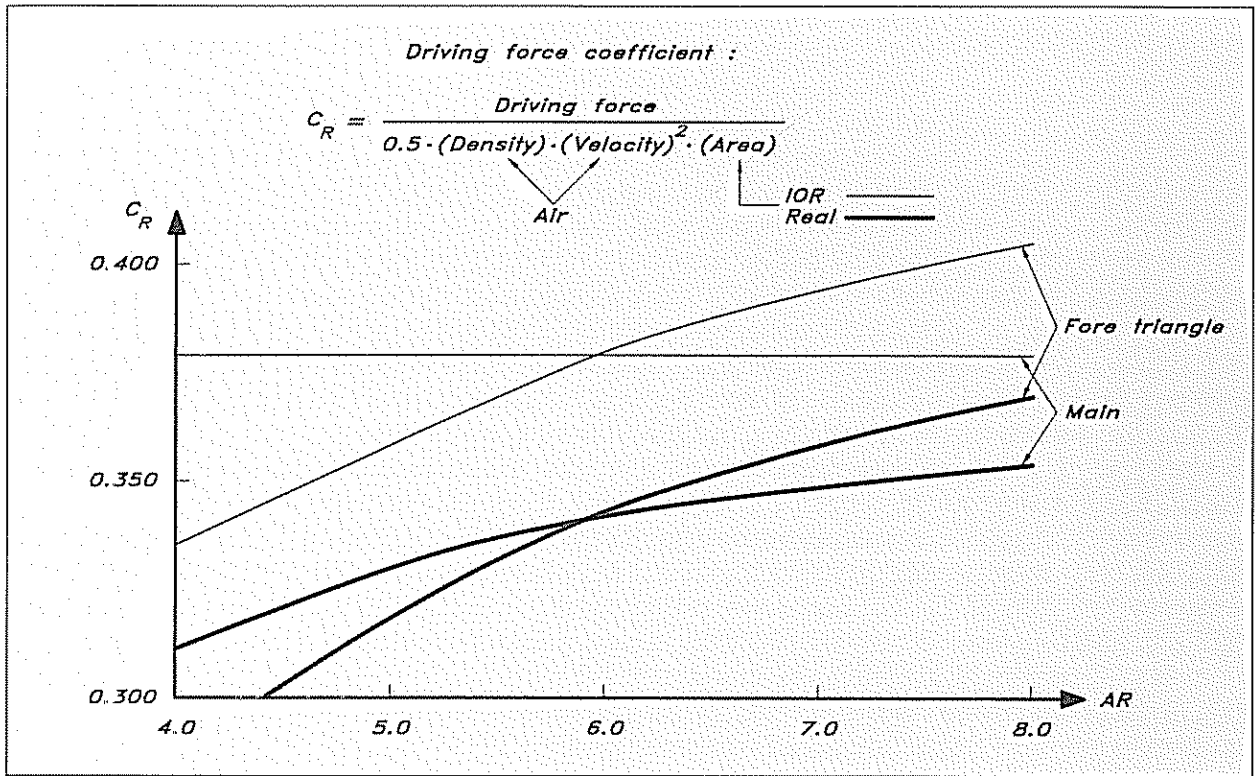


Fig 7.3 Computed influence of aspect ratio on driving force

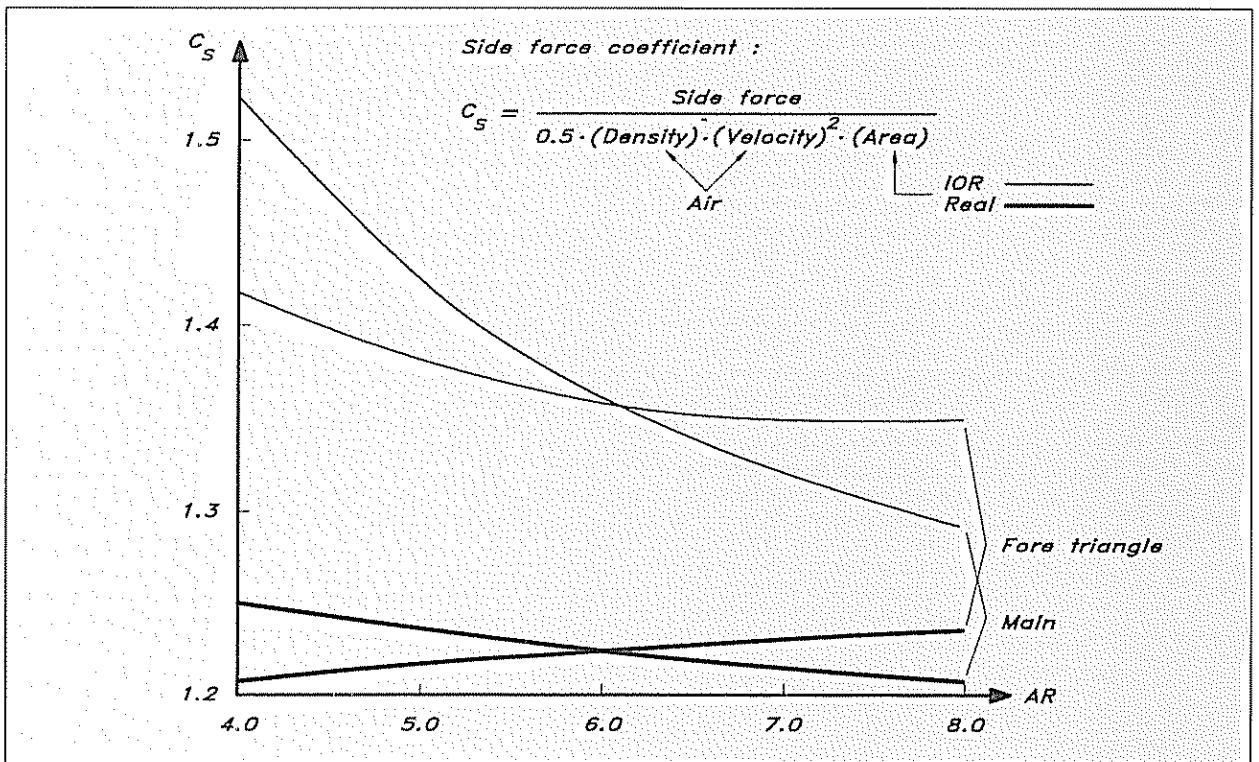


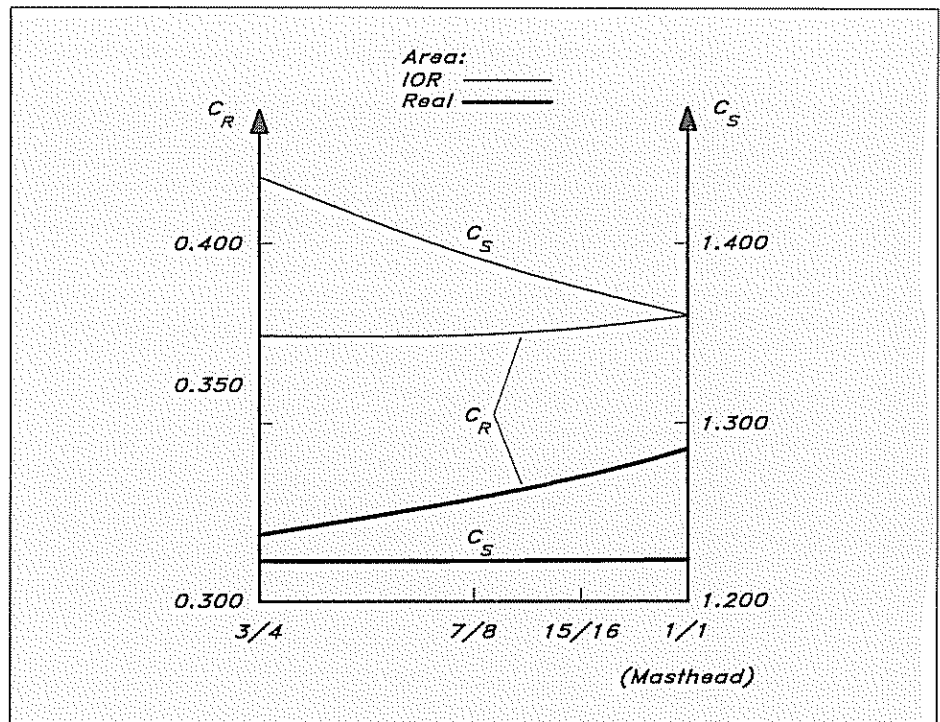
Fig 7.4 Computed influence of aspect ratio on side force

measured one according to the IOR (thin line). Although this rule is not much used today, it is interesting to see how the penalties imposed affect the efficiency. The coefficients may thus be considered representative of the force for a given area, either real or measured.

The graphs for the mainsail have been obtained keeping the fore triangle aspect ratio constant ( $AR = 6$ ) and vice versa. In Fig 7.3 it can be seen that the driving force increases considerably with increasing  $AR$ . To a certain extent the advantage is offset by the penalties of the rule, but for the fore triangle there is still a great advantage in a high aspect ratio. The side forces of Fig 7.4 decrease greatly with aspect ratio if the IOR area is kept constant. This is because the real area is reduced due to the penalties. If the real area is used as a reference, the side force is relatively constant.

In another interesting series of calculations Professor Milgram varied the point of attachment of the forestay to the mast. Four rigs were computed, where the attachment point was at  $3/4$ ,  $7/8$ ,  $15/16$  and  $1/1$  of the full mast height, respectively. The results may be seen in Fig 7.5. There is a significant gain in driving force for the real sail, when the fore triangle height is increased, while the side force is almost constant. For the IOR sail the gain in driving force is not so large, but the side force is reduced.

Fig 7 5 Computed influence of fore triangle height on driving and side force



The results of the previous figures seem to indicate clearly that the aspect ratio of the sails should be as large as possible. This is not true under all circumstances, however. Considerations which have to be made in a real case include:



- points of sailing other than upwind
- the effect of the mast on the mainsail flow
- the increase in heeling moment with aspect ratio.

The latter disadvantage is fairly obvious and its importance depends on the wind strength and the stability of the boat. We will not discuss this any further, but consider the other two points in some more detail.

C A Marchaj has reported wind-tunnel tests for sails of varying aspect ratios. All points of sailing were considered. Fig 7.6 shows the driving force and Fig 7.7 the side force for three aspect ratios: 6, 3 and 1. The latter is an almost square gaff sail. It can be seen that for small apparent wind angles, ie upwind, Milgram's conclusions are confirmed. Around  $30^\circ$  the high aspect ratio sail develops more than twice the driving force of the square sail. However, at large wind angles the situation is different. Around  $120^\circ$  the square sail is superior, and develops 50% more thrust than the narrow sail. At  $70^\circ$  the thrusts are almost equal. The side force of Fig 7.7 increases somewhat with aspect ratio at  $30^\circ$ , but the opposite is true above  $45^\circ$ . The general conclusion is that the positive effect of a high aspect ratio is reduced if all points of sailing are of interest.

The mast reduces the positive effect of a high aspect ratio mainsail even further. For a given sail area, the higher the aspect ratio the thicker the mast required, and the smaller the average chord length of the mainsail. Both effects tend to increase the proportion of the sail which is ineffective due to the mast disturbance. Marchaj found in wind-tunnel measurements

Fig 7.6 Measured influence of aspect ratio on driving force

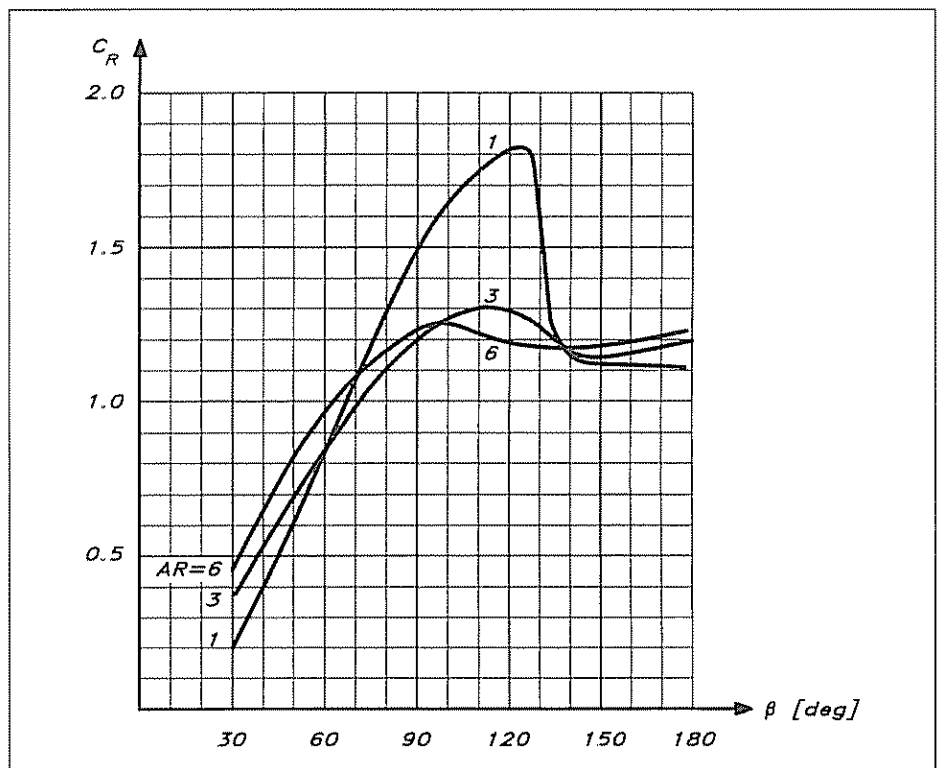
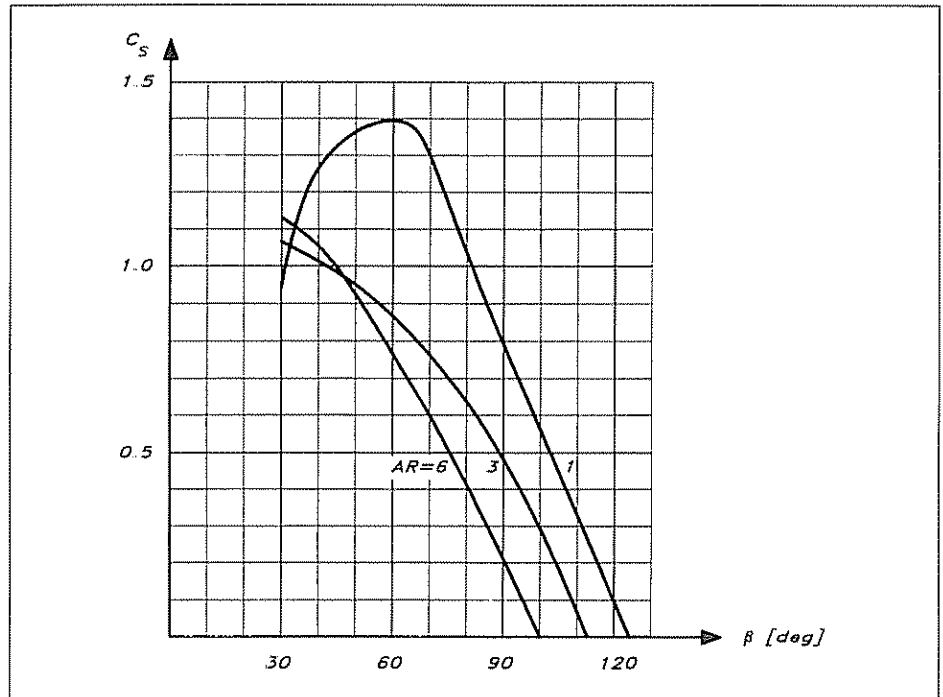


Fig 7.7 Measured influence of aspect ratio on side force

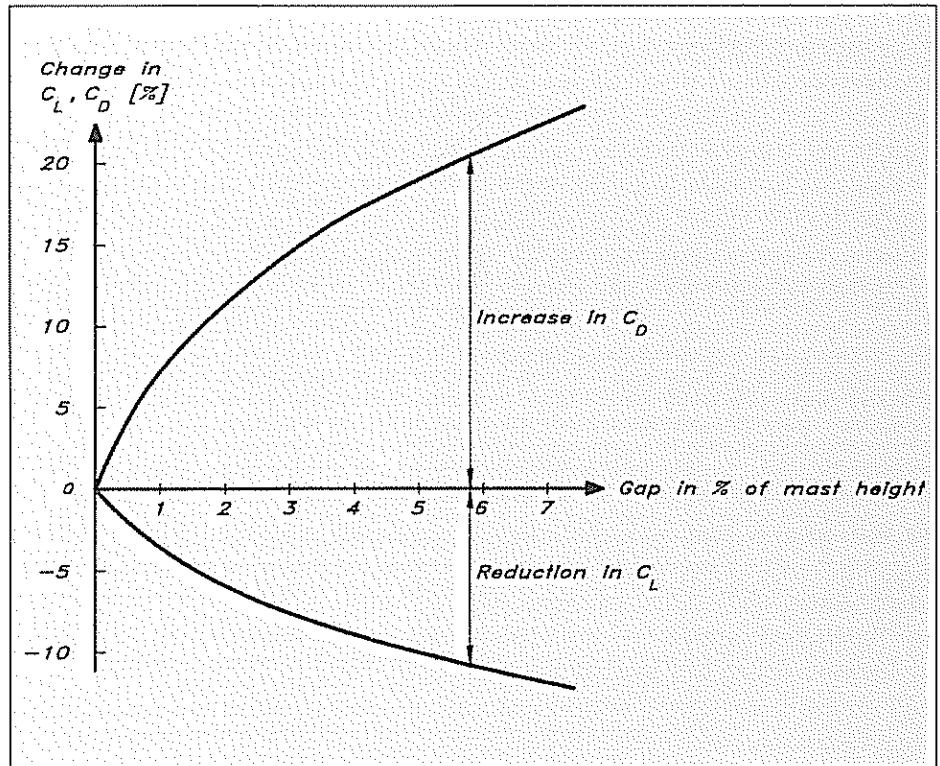


that a 6.0 aspect ratio sail was less effective, even upwind, than a 4.6 aspect ratio sail, and this was attributed to the mast disturbance. In these tests the mast diameter was 8% of the average chord length of the high aspect ratio sail. This seems to be a bit more than is used today, so the effect was probably somewhat exaggerated, but it shows that there is a limit for the positive effect of the aspect ratio of the mainsail.

A high aspect ratio is not the only way to reduce the induced resistance of the sails. A very effective way is to try to seal the gap between the sail and the deck of the yacht. In Fig 7.8 some results of wind-tunnel measurements by Bergstrom and Ranzén at the Royal Institute of Technology in Stockholm are presented. The change in lift and drag coefficients of the sails is given as a function of the gap size in per cent of the mast height. It may be seen that the lift is decreased and the drag increased by an increasing gap. For instance, a gap of 0.1 m and a mast height of 10 m gives a drag increase of 7% and a lift decrease of 4% compared to the fully sealed case. Of course, it is impossible to seal the gap fully between the boom and the hull, so the figures should be relevant for the foresail only. Note that the drag and lift are the force components parallel to, and at right angles to, the apparent wind. They can easily be converted into the driving and side forces parallel to, and at right angles to, the direction of motion of the yacht (see Fig 7.21).

For the YD-40 we have chosen a masthead rig with a very high aspect ratio of the fore triangle: 7.8. This should give a high aerodynamic efficiency of the genoa. For the mainsail the aspect ratio is 6.4, which is likely to be close to the upper limit, considering mast interference. The mast diameter here is 6% of the mid-chord of the main, and we will employ the devices explained below for reducing the

Fig 7.8 Effect of gap between sail and deck



disturbances. A disadvantage of the masthead rig, which is often referred to for smaller boats, is the difficulty in trimming the mast properly. Longitudinal bending can only be achieved by the lower shrouds (see Chapter 11), so it is true that it is more difficult to reduce the camber of the mainsail. The high-quality sailcloth produced today makes this drawback less serious, but it is still a factor to consider.

The genoa of the YD-40 allows a small gap to the deck. This is a deliberate performance reduction so as to increase cruising comfort, and should not occur on a pure racer. By lifting the clew a little, two handling advantages are obtained: visibility is increased and the use of the jib roller is facilitated. If the clew is right on the deck the block normally has to be moved if the jib is reefed by rolling around the head foil. With the present design the sheet is at right angles to the forestay, so the sheeting angle will not change when using the roller.

### Sail camber

Since the sail is a wing of practically zero thickness the only characteristic feature of the section is the camber. We will now look at the effect of camber size and position. Figs 7.9 and 7.10 are obtained from measurements with plate sails without a mast reported by Marchaj. Three different cambers were investigated:  $\frac{1}{7}$ ,  $\frac{1}{10}$  and  $\frac{1}{20}$  of the chord length. It is seen immediately that the larger the camber the larger the forces in both directions. There is a particularly large difference between the  $\frac{1}{10}$  and  $\frac{1}{20}$  sails. In fact, the latter sail is quite extreme. Sails that flat are rarely used in practice, but it is of interest to include it, since the trends then become more clear.

Fig 7.9 Influence of camber on driving force

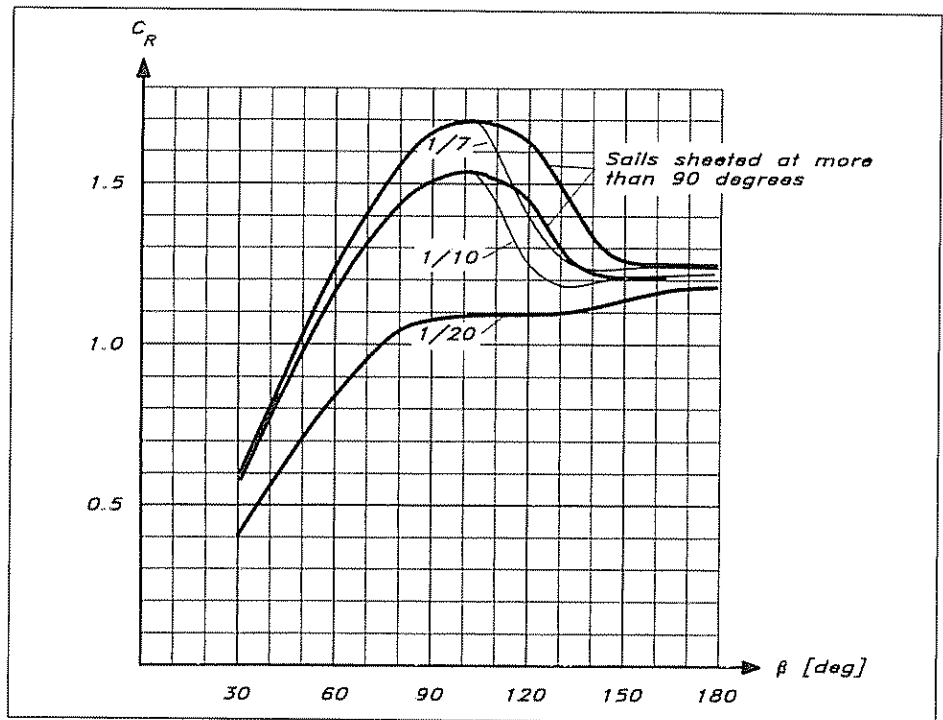
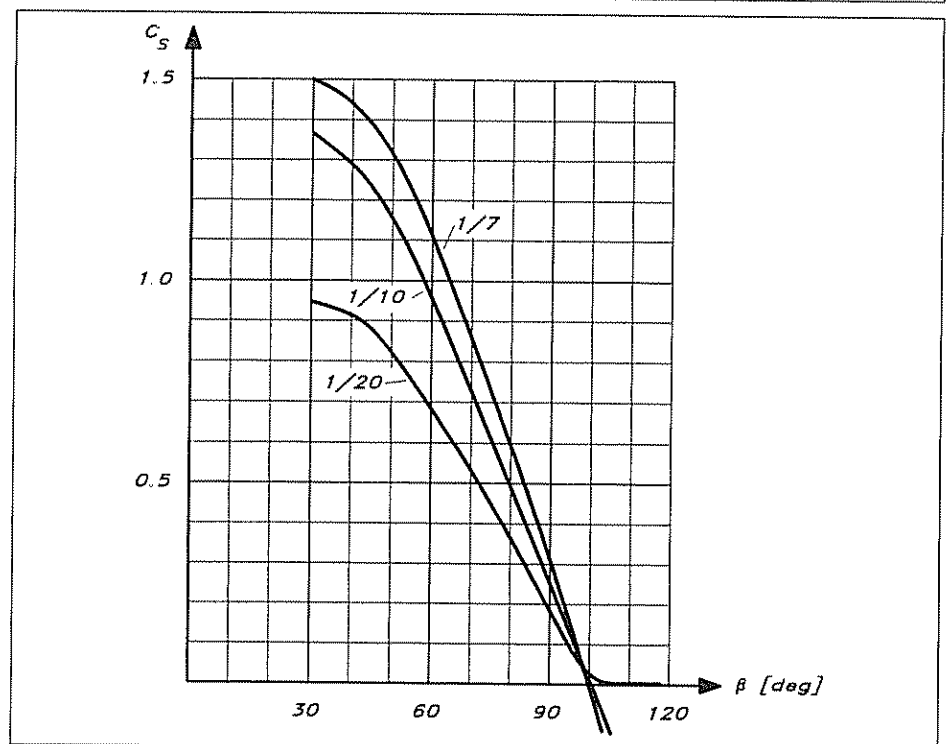


Fig 7.10 Influence of camber on side force



For the upwind case, at  $30^\circ$  and below, there is a very small difference in driving force between the two deepest sails, but the deepest one has a slight advantage. The difference in side force is somewhat larger: approximately 10%. Which sail is the best is hard to say, since it depends on the ability of the underwater body to balance the side force

without producing too much induced resistance. The problem can be resolved in a complete equilibrium calculation for the yacht, such as in a VPP program (see Chapter 16), but the result is not obvious without such a calculation, unless heeling is a problem. In stronger winds the 10% smaller side force of the  $\frac{1}{10}$  sail has to be compensated by reefing of the  $\frac{1}{7}$  sail. Considering the fact that the centre of effort of the sails is then lowered, the area has to be reduced some 7%, which would reduce the driving force by an equal amount. This force would then be smaller than the  $\frac{1}{10}$  sail. It is thus better to flatten the sail than to reef it to reduce heeling, a fact well known by most sailors.

From Figures 7.9 and 7.10 it is obvious that for larger apparent wind angles the full sail is the best. At the maximum driving force around  $100^\circ$  there is a difference of about 10% between the  $\frac{1}{7}$  and  $\frac{1}{10}$  sails, while the side force is zero. An interesting feature of the measured results is that it is advantageous to develop a negative side force, ie to windward, for angles in the range  $100$  to  $150^\circ$ . The sails should thus be sheeted at more than  $90^\circ$  giving an angle of incidence of the sail small enough to avoid separation on the leeward side. The total force developed is then so large that, although it points somewhat to windward, the driving component is larger than if the sail is sheeted in the normal way. This possibility does not normally exist in practice, due to the shrouds, but it could be of interest for dinghies.

The effect of the position of the maximum camber is shown in Figs 7.11 and 7.12. These figures are based on wind-tunnel measurements for sails with a mast, and are thus applicable to the mainsail. It can be seen that this effect is much smaller than that of the camber size. Interesting

Fig 7.11 Influence of maximum camber position on driving force

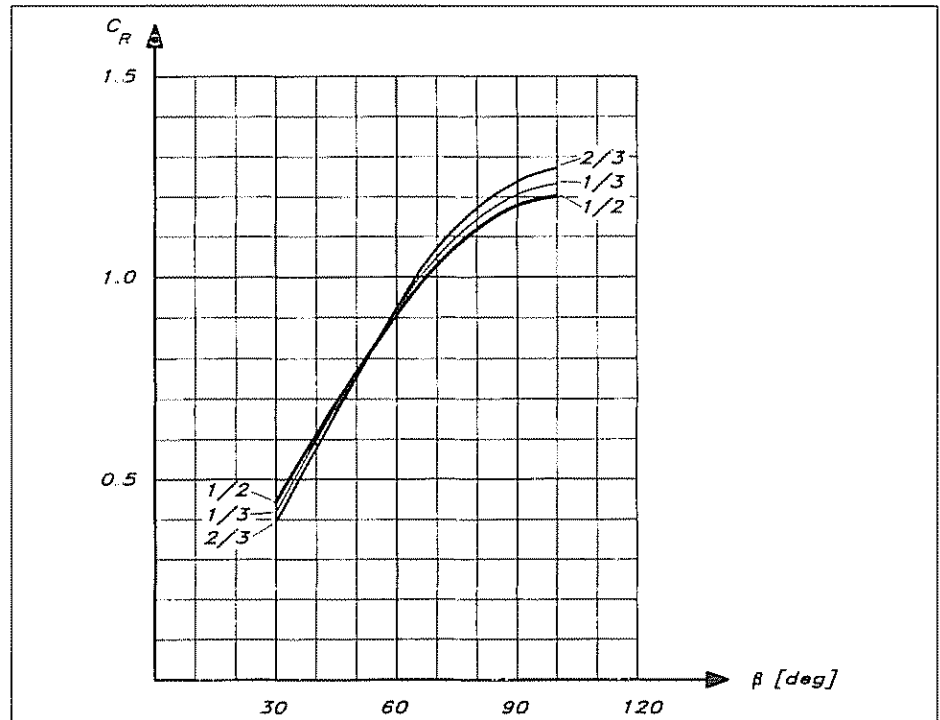
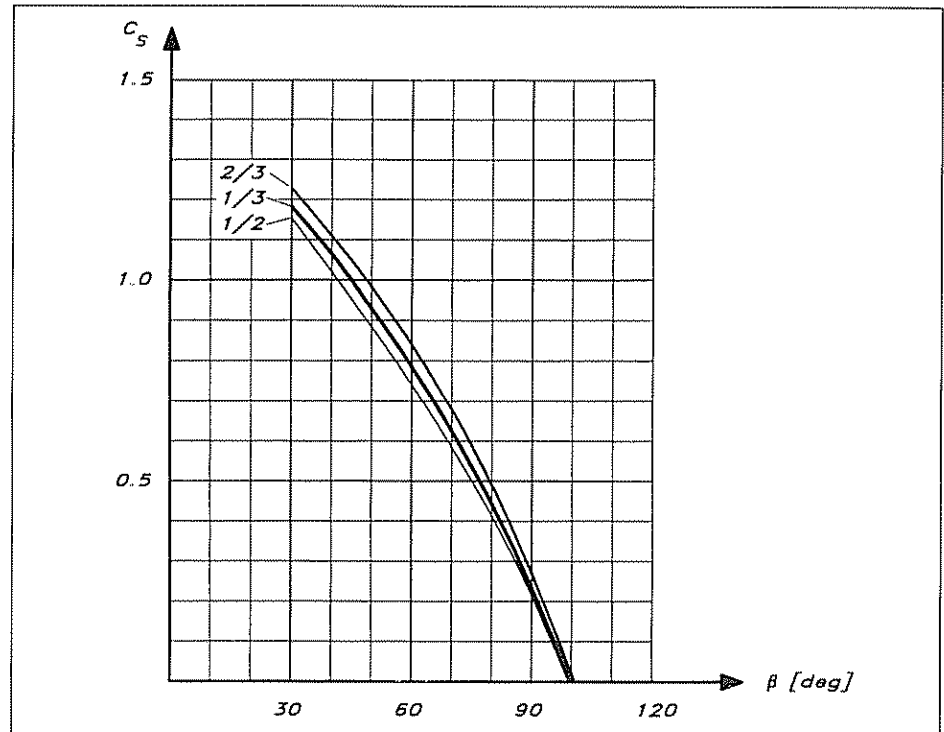


Fig 7.12 Influence of maximum camber position on side force



differences, however, are noted in the figures, which show results for three sails with the maximum camber at  $\frac{1}{3}$ ,  $\frac{1}{2}$  and  $\frac{2}{3}$  of the chord. At small angles the  $\frac{1}{2}$  sail develops the largest driving force, followed by the  $\frac{1}{3}$  and  $\frac{2}{3}$  sails. Around  $55^\circ$  they are all equal, while at the maximum driving force around  $100^\circ$  the  $\frac{2}{3}$  sail is the best, followed by the  $\frac{1}{3}$  and  $\frac{1}{2}$  sails. The side force is smallest for the  $\frac{1}{2}$  sail and largest for the  $\frac{2}{3}$  sail in the range of angles up to maximum thrust. The results indicate that the sail with the maximum camber at mid-chord is the best upwind, while on broad reaches the maximum camber should be further aft. Note that these conclusions are for the mainsail. A more forward position of the camber is likely to be better for the foresail. The aft position should be avoided, since the flow approaching the mainsail might then be too disturbed.

### Mast interference

The flow around a sail behind a mast in upwind sailing is shown schematically in Fig 7.13. As can be seen in the figure the flow is not attached to the sail all the way. Three zones of separation can often be distinguished. Two are immediately behind the mast, to windward and leeward, respectively, while the third zone is on the aft part of the leeward side. The separation behind the mast can be minimized by proper shaping of the mast section and by introducing turbulence stimulators. The aft separation zone depends, in fact, to some extent on the forward one, since a massive separation forward causes a thick boundary layer to develop in the attached part of the flow. This layer separates more easily than a thin one. To a large extent the aft separation depends also on the loading of the sail. By proper sheeting and a good mast design this zone can be very small or even eliminated.

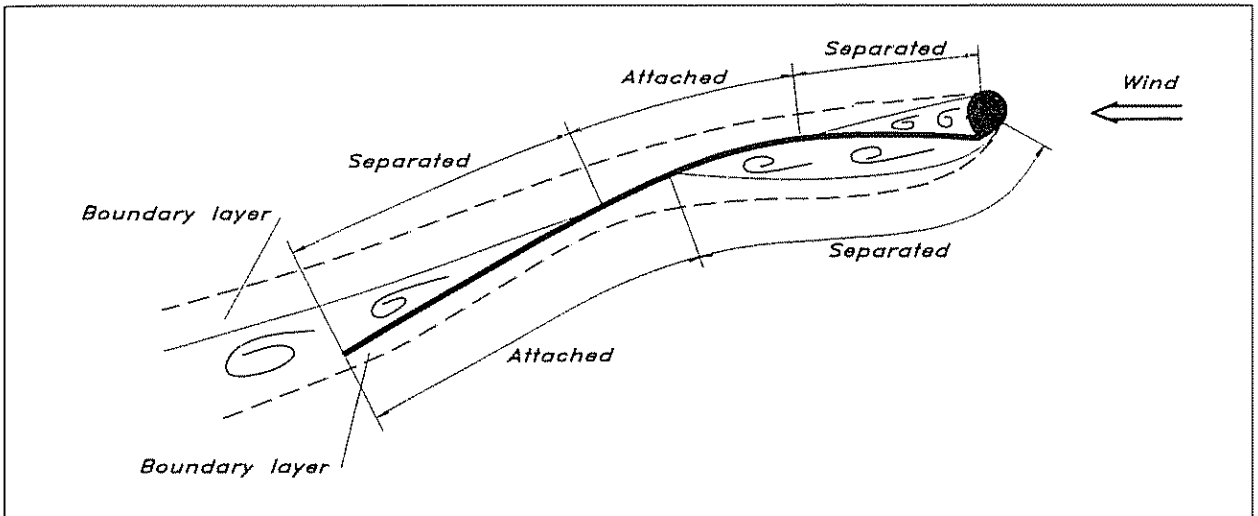


Fig 7.13 Flow around a mast/sail combination

There are two reasons why separation has to be avoided. First, the pressure distribution on the sail is disturbed, essentially in such a way that pressure differences between the two sides of the sail are reduced. This causes a reduction in lift and driving force. Secondly, separation itself causes a drag increase. Experiments at Southampton University with a mast/sail combination indicated large effects of mast disturbance. Thus, when a circular mast with a diameter of 7.5% of the sail chord was put in front of the sail the driving force upwind was reduced by about 20%, as compared to the case without a mast. A thicker mast of 12.5% was also tested and the driving force was almost halved. It was, however, possible to regain almost half of the loss by turning the mast in such a way that the leeward side of the mast/sail junction became smooth.

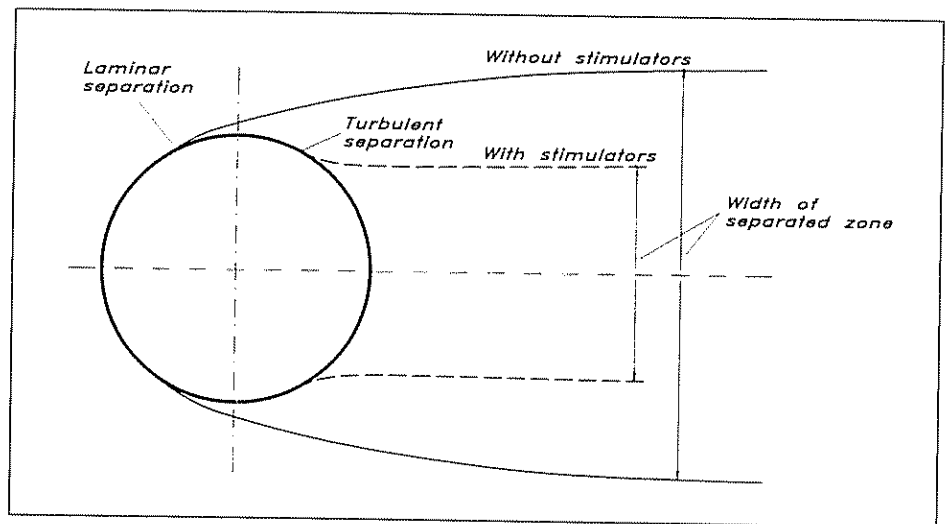
The YD-40 has a relatively robust mast. Being a cruiser/racer it should have a simple rig, manageable by a family on a cruise. Therefore, running backstays and inner forestays have been avoided, at the expense of a thicker section in the longitudinal direction. The dimensions (obtained from the rig calculation in Chapter 11), are 206 mm by 139 mm. The average is 173 mm, which is about 6% of the average chord length of the sail, considering the roach. This is not much, so the major part of the sail should work properly, especially as we will employ the technique described in the next section to reduce the mast disturbance. There is no doubt, however, that the top part of the sail will be significantly disturbed.

#### Means for reducing mast disturbances

A well-known, but seemingly paradoxical phenomenon in fluid dynamics is the reduction in drag of bluff bodies when their surface is changed from smooth to rough. As we have seen in Chapter 5 a rough bottom of a yacht causes a considerable resistance increase. The reason for the different behaviour is that the viscous resistance of the hull, which is a slender body, is essentially due to direct friction (see Fig 5.4), while the resistance of a bluff body to a large extent is due to pressure losses in the wake (viscous pressure resistance).

Let us return to Fig 5.5, showing the different regions in the flow around the hull. It can be seen that the boundary layer is laminar at the bow, but undergoes transition relatively quickly. Thereafter it is turbulent, and may, in rare cases, separate from the hull at a separation point near the stern. The same flow regions may exist around the cylinder, but not always. If the Reynolds number (ie the product of diameter and velocity, divided by viscosity, cf Fig 5.8) is small, the boundary layer never gets turbulent, but separates directly in the laminar part. This happens, in fact, before the maximum thickness (as shown in Fig 7.14). The wake then becomes quite wide and the drag is high. On the other hand, if the boundary layer gets turbulent before separation, the latter is delayed to a point well aft of the maximum thickness (see Fig 7.14). The wake is then narrower and the drag smaller. The reason why turbulence delays separation is that it has a stirring effect on the flow. High speed fluid from outside the boundary layer is convected inwards and energizes the flow that is about to stop moving along the surface.

Fig 7.14 Effect of stimulators on the flow around a cylinder



With this explanation in mind it is not difficult to understand why a rough cylinder may have a smaller resistance than a smooth one. If the Reynolds number is in the subcritical region, and laminar separation occurs, introducing roughness causes the boundary layer to turn turbulent earlier, maybe before separation. This is then delayed, as just explained, and the drag gets smaller. Now a mast is normally in the subcritical region and has a high drag, but it is close enough to the low drag region to make the roughness trick work. Fig 7.15 shows the drag coefficient of circular cylinders of around 0.1 m diameter with different roughness heights. The height is given as a percentage of the diameter. It may be seen that at 11 m/s the drag is reduced by 50% if the roughness height is 0.5% of the diameter. The more narrow wake also disturbs the sail much less, so there is a double gain. Unfortunately, the optimum roughness height varies with the wind velocity, but a height of 1% covers most of the interesting velocities quite well. Note that it is the apparent wind that is of interest.



Fig 7.15 Drag of circular cylinders with sand roughness

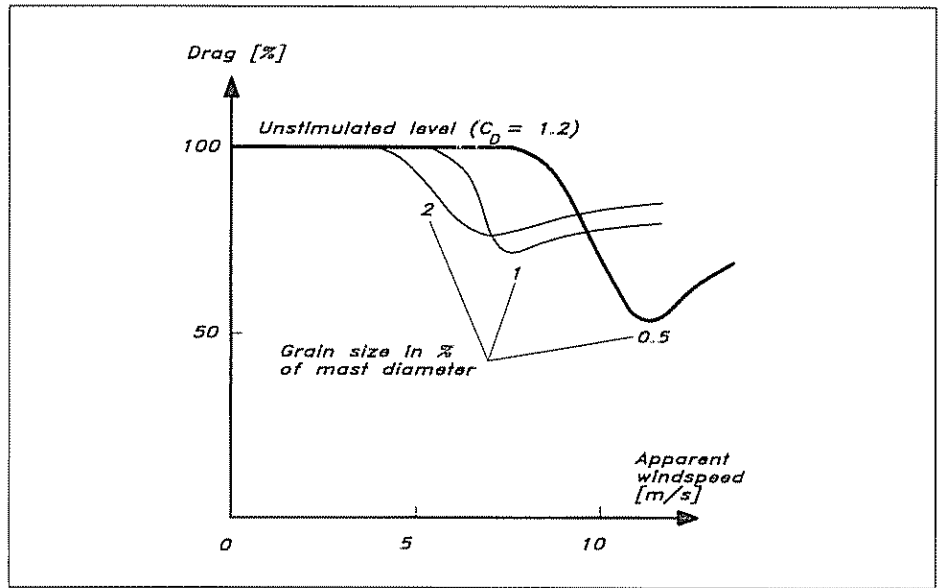


Fig 7.16 Position of trailing edge separation on a sail with three different masts

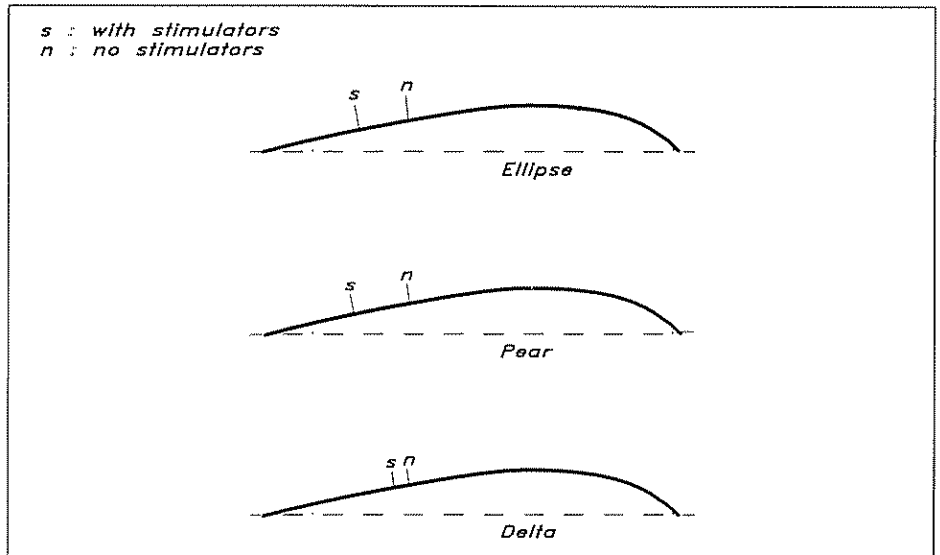


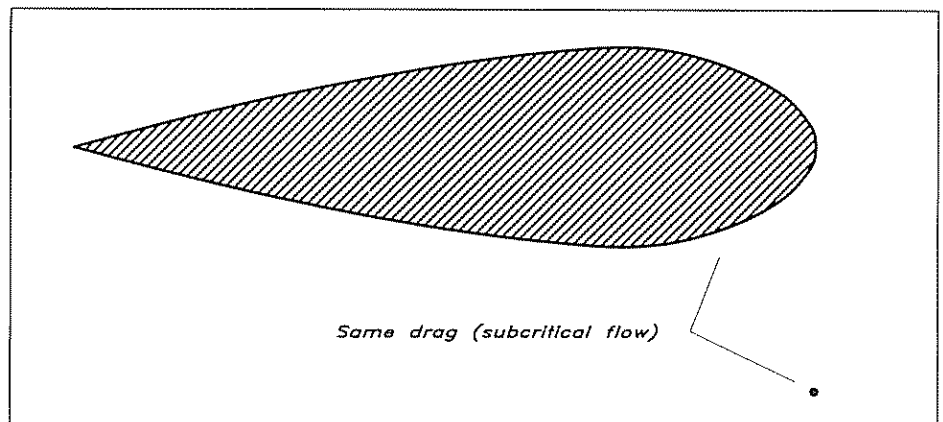
Fig 7.16 shows results from measurements made by one of the authors and his students. A plate sail with different masts, with and without roughness, was tested in a wind tunnel, and the position of the rear separation point was measured. The mast sections were the most common ones: ellipse, pear and delta. Practically no difference could be detected in the separation location for the three smooth masts, while the positive effect of the roughness was largest for the ellipse and pear masts. It can be seen in the figure that a considerable increase in the effective length of the sail is obtained in all cases. The roughness in this test was 1% of the mast diameter and was created by sand grains of uniform size glued to the front half of the mast. Later tests have indicated that much less disturbance is required. In fact, a small riblet of the same height put at the leading edge of the mast produced the same effect. Note that when the sail is working, the stagnation point on

the mast is always on the windward side, so the flow entering the leeward side of the sail has to pass the riblet, even if it is in the symmetry plane of the mast. There is no effect, however, on the flow on the windward side, so a better solution might be to put one riblet on each side of the mast, at  $45^\circ$ , say, on each side of the symmetry plane.

### Streamlining

The windage of the mast and rig is considerable, as we will see in Chapter 9, and all means of streamlining different components, such as spreaders and shrouds, are valuable. A striking figure is that of Fig 7.17, which shows two 2-dimensional bodies with the same drag. The upper one is a streamlined foil, where most of the drag comes from friction, and the lower one is a round bar, for which pressure drag dominates. The drag coefficient for the bar is around 1.0, while it is only about 0.03 for the foil, based on the front area. The diameter of the bar thus has to be more than 30 times smaller than the foil thickness for the same drag.

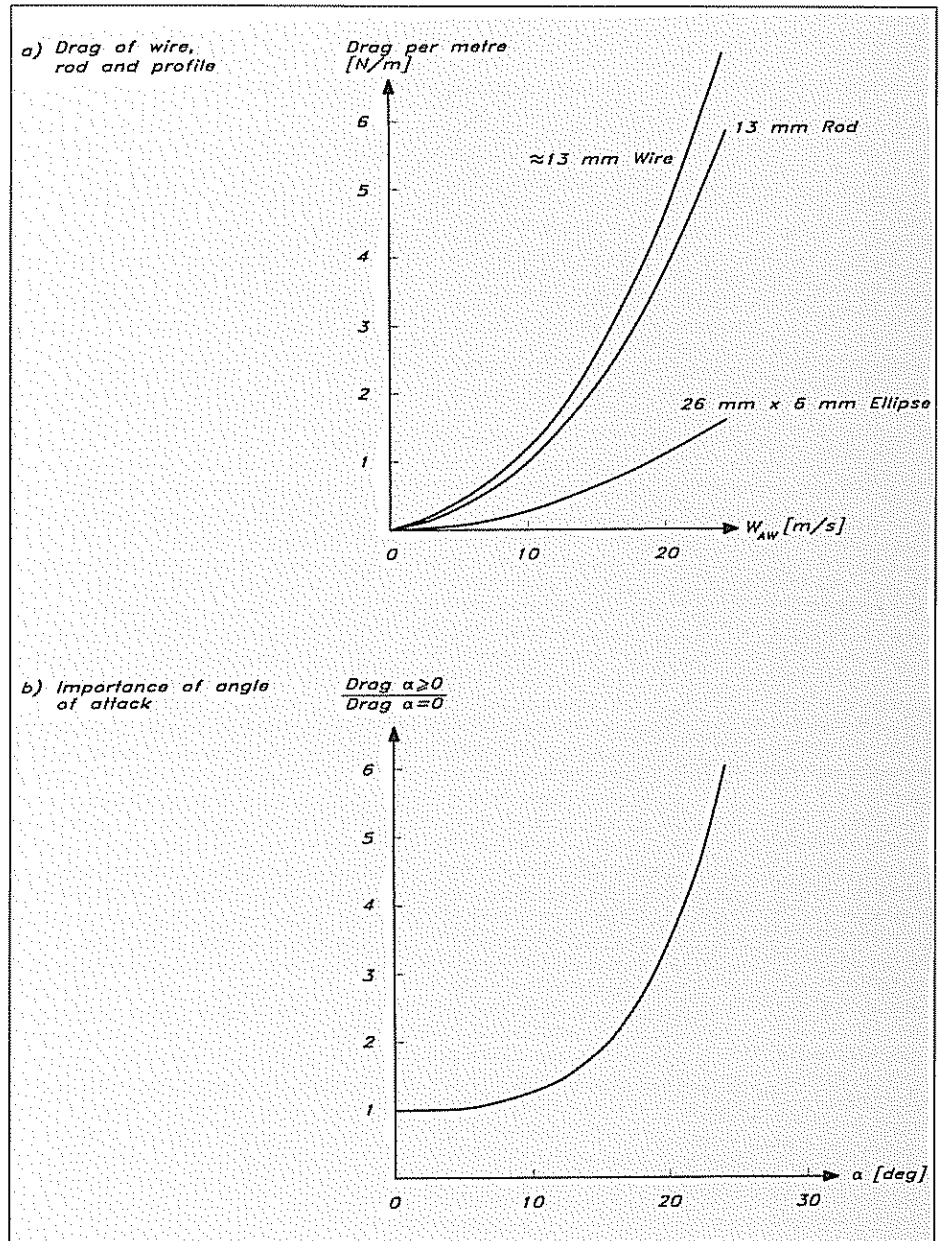
Fig 7.17 Effect of streamlining



In Fig 7.18 results are presented from wind-tunnel tests at the Davidson Laboratory in New York. Drag measurements were made for three different types of shroud: a wire, a circular rod and an elliptic rod. It may be seen that the wire has the highest drag, somewhat higher than that of the rod. At first sight this might seem contrary to the findings above (that a rough mast has a smaller drag than a smooth one), but the difference is that the wire has such a small Reynolds number (due to the small diameter) that the turbulent boundary layer never appears, even if the surface is rough.

The ellipse is outstanding with a drag that is only  $\frac{1}{4}$  of that of the wire. This is so in spite of the fact that the ellipse was tested at an angle of attack of  $19^\circ$ . Small as this may seem, it is probably realistic upwind, considering the fact that the sails guide the flow more in the longitudinal direction than the apparent wind. It is quite important that the angle of attack does not get too large for the ellipse, as can be seen in Fig 7.18(b). This diagram shows the relative increase in resistance when the angle increases from zero. Up to  $10^\circ$  the additional drag is small, but at  $20^\circ$  the drag is three times larger than the minimum. Thereafter, the increase is still faster.

Fig 7.18 Drag of shrouds and stays



### A practical model for sail and rig aerodynamics

A model for the aerodynamics of sailing yachts was presented in 1980 by G Hazen. This model is used, with minor modifications, in many Velocity Prediction Programs (VPPs), for instance in the IMS handicap system. We will describe the original model first and then introduce the later improvements.

In Hazen's model the lift and viscous drag of each sail are prescribed as functions of the apparent wind angle. The corresponding coefficients are given in Table 7.1. Only five angles are given in the original model:  $27^\circ$ ,  $50^\circ$ ,  $80^\circ$ ,  $100^\circ$  and  $180^\circ$ . Interpolation between these angles is supposed to be done using spline functions. Manual fairing, for instance

	<u>Area</u>	<u>Centre of effort</u>
<i>Sail area and height of centre of effort above sheer</i>	Main: $A_M = 0.5 \cdot P \cdot E$	$CE_M = 0.39 \cdot P + BAD$
	Jib: $A_J = 0.5 \cdot \sqrt{I^2 + J^2} \cdot LPG$	$CE_J = 0.39 \cdot I$
	Spinnaker: $A_S = 1.15 \cdot SL \cdot J$	$CE_S = 0.59 \cdot I$
	Mizzen: $A_Y = 0.5 \cdot PY \cdot EY$	$CE_Y = 0.39 \cdot PY + BADY$
	Mizzen staysail: $A_{YS} = 0.5 \cdot YSD \cdot (YSMG + YSF)$	$CE_{YS} = 0.39 \cdot PY + BADY$
	Foretriangle: $A_F = 0.5 \cdot I \cdot J$	
Nominal area	$A_N = A_F + A_M + A_Y$	
Lift	$C_L = \frac{C_{LM} \cdot A_M + C_{LJ} \cdot A_J + C_{LS} \cdot A_S + C_{LY} \cdot A_Y + C_{LYS} \cdot A_{YS}}{A_N}$	
Viscous/parasitic drag	$C_{DP} = \frac{C_{DPM} \cdot A_M + C_{DPJ} \cdot A_J + C_{DPS} \cdot A_S + C_{DPY} \cdot A_Y + C_{DPYS} \cdot A_{YS}}{A_N}$	
Induced drag	$C_{DI} = C_L^2 \cdot \left( \frac{1}{\pi \cdot AR} + 0.005 \right)$ <div style="display: inline-block; vertical-align: middle; margin-left: 20px;"> <math>\left\{ \begin{array}{l} \text{close hauled: } AR = \frac{(1.1 \cdot (EHM + FA))^2}{A_N} \\ \text{other courses: } AR = \frac{(1.1 \cdot EHM)^2}{A_N} \end{array} \right.</math> </div>	
Drag of mast and topsides	$C_{DD} = 1.13 \cdot \frac{(BMAX \cdot FA) + (EHM \cdot EMDC)}{A_N}$	
Total drag	$C_D = C_{DP} + C_{DI} + C_{DD}$	
Flattening: Multiply $C_L$ by flat factor $F$		
Reefing: Multiply $C_L$ and $C_{DP}$ by reef factor $R$ squared Multiply height of CE by $R$		
Standard IOR notation:		
$P$ : Mainsail hoist	$YSD$ : Mizzen staysail depth	
$E$ : Foot of mainsail	$YSMG$ : Mizzen staysail mid-girth	
$I$ : Height of foretriangle	$YSF$ : Mizzen staysail foot	
$J$ : Base of foretriangle	$BMAX$ : Max beam of yacht	
$LPG$ : Perpendicular of longest jib	$FA$ : Average freeboard	
$SL$ : Spinnaker leech length	$EHM$ : Mast height above sheer	
$PY$ : Mizzen hoist	$EMDC$ : Average mast diameter	
$EY$ : Foot of mizzen	$BAD$ : Height of main boom above sheer	
	$BADY$ : Height of mizzen boom above sheer	
Newer additions:		
Full length battens: Increase lift of main by 15% for angles up to 60 degrees		
Blanketing and fractional rig exposed mast correction, see paper by C.L. Poor on IMS.		

Fig 7.19 Hazen's model for rig and sail aerodynamics

using physical splines, is also possible of course, but linear interpolation is too approximate.

Coefficients are given for five sails: main, jib, spinnaker, mizzen and mizzen staysail. To obtain the total lift or viscous drag (sometimes called the parasitic drag, which explains the index 'P') the area of each sail is to be multiplied by the corresponding coefficient and all sails added. The final coefficient is obtained by dividing by a nominal sail area, which is the sum of the foretriangle, main and mizzen areas. All areas are computed as triangular, ie the roach is neglected. In Fig 7.19 the relevant equations are given. There is no explicit interaction between the sails, but the blanketing of the mainsail by the mizzen is taken into account in the mizzen coefficients. In view of the previous discussion on interaction the method is quite crude, but it has proved to be useful nevertheless.

**Table 7.1(a)**  
**Sail coefficients, lift**

Angle	Main	Jib	Spinnaker	Mizzen	Mizz. stays
27	1.5	1.5	0.0	1.3	0.0
50	1.5	0.5	1.5	1.4	0.75
80	0.95	0.3	1.0	1.0	1.0
100	0.85	0.0	0.85	0.8	0.8
180	0.0	0.0	0.0	0.0	0.0

**Table 7.1 (b)**  
**Sail coefficients, viscous drag**

Angle	Main	Jib	Spinnaker	Mizzen	Mizz. stays
27	0.02	0.02	0.0	0.02	0.0
50	0.15	0.25	0.25	0.15	0.1
80	0.8	0.15	0.9	0.75	0.75
100	1.0	0.0	1.2	1.0	1.0
180	0.9	0.0	0.66	0.8	0.0

The induced drag, which is more important than the viscous drag for upwind sailing, is computed from the simple wing theory presented in Chapter 6, Fig 6.5 in particular. The induced drag coefficient is thus proportional to the square of the lift coefficient, and inversely proportional to the aspect ratio. In the present method the entire nominal sail plan is considered when computing the aspect ratio, and the induced drag is computed for all the sails together.

The aspect ratio of a wing was defined in Chapter 6 as the span divided by the average chord. This may be expressed in another way. Since the projected area is equal to the span times the average chord, the aspect ratio may be defined also as the span squared divided by the area. In the present model this definition is used. However, due to some mirror effect of the water surface the effective span is taken to be 110% of the height of the masthead above the water, if the yacht is close-hauled. When the jib is eased and the gap to the deck opens up, only the mast height above deck level should be considered, and 110% of this height is used in the aspect ratio definition (see Fig 7.19).

Hazen argues that some of the viscous drag, originating from the separation on the leeward side of the sail, is proportional to the lift squared as well, so he introduces an addition to the induced drag to account for this effect. It appears as a constant, 0.005, in the expression for the induced drag.

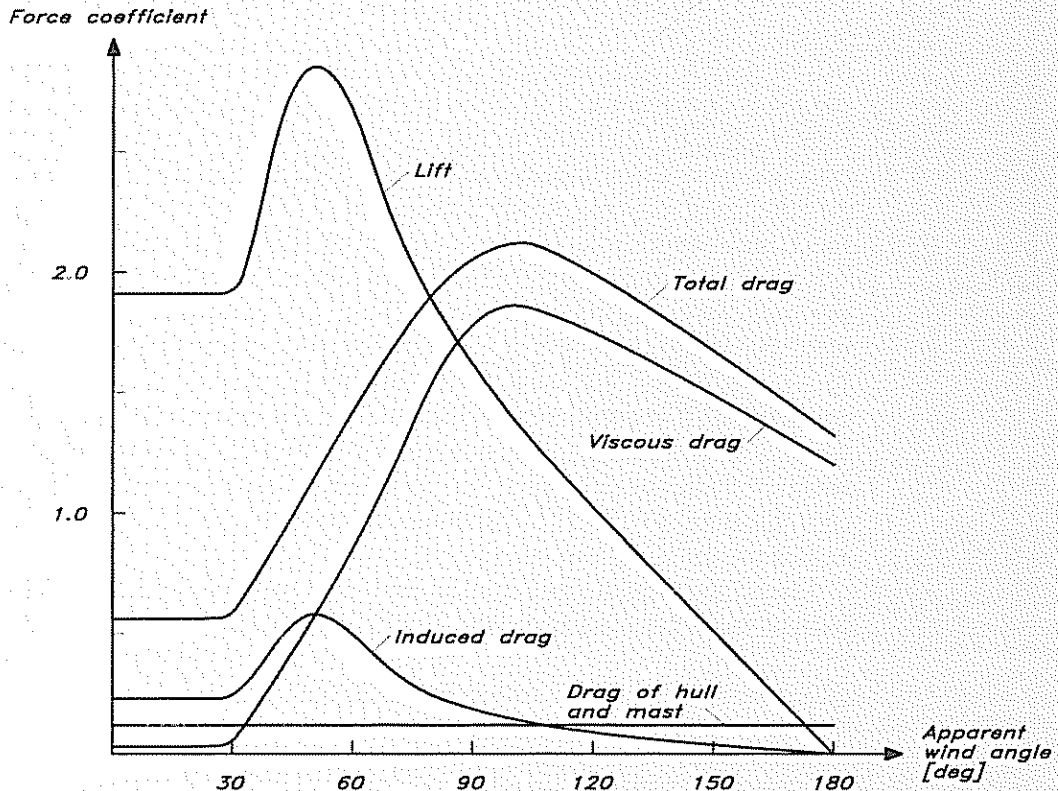
In this model the drag of mast and topsides are included as well. The frontal area of the topsides is taken as the average freeboard times the maximum beam, while that of the mast is computed as the mean diameter times the mast height above deck. The drag coefficient is assumed to be 1.13. In Chapter 9 we will discuss this drag component in more detail. The total drag is found as the sum of the viscous, induced and mast/topsides components.

The height of the centre of effort of each individual sail is given in Fig 7.19. For the main, mizzen and mizzen staysail it is taken to be at 39% of the luff length above the boom. For the jib and spinnaker it is at 39% and 59% of the fore triangle height, respectively, above the sheer line.

Sail coefficients computed for the YD-40 are presented in Fig 7.20 for apparent wind angles from 0° to 180°. The curves were obtained from the tabulated values above, so only five points were computed on each curve. Splines were therefore used to find the intermediate points. As is common practice, the curves have been drawn horizontal below 27°. Angles smaller than about 20° will not be reached, since the driving force then becomes too small.

An interesting feature of the sail model is the possibility of considering reefing and flattening of the sails. The effect of these two actions is quite different. Reefing is specified by a factor  $R$  which defines the reduction in sail height.  $R$  is equal to 1 for the unreefed sail. The new height of the centre of effort is thus obtained as  $R$  times the original height, while the new area is found by multiplying by  $R^2$ . This means that both lift and drag (excluding mast/topsides) are reduced with  $R^2$ , while the major part of the heeling arm is reduced with  $R$ .

The flattening factor  $F$  specifies the reduction in lift due to the flattening of the sails. This factor, which is equal to 1 for the normal sail, cannot be directly related to the sail geometry, but the smaller the camber the smaller the factor. Note that  $F$  has no effect on the heeling arm, and that it has different effects on the lift and drag. Since the lift is proportional to  $F$ , the induced drag is proportional to  $F^2$ . This means



$$\text{Main: } A_M = 0.5 \cdot 15.1 \cdot 4.7 = 35.5$$

$$\text{Jib: } A_J = 0.5 \cdot \sqrt{16.9^2 + 4.3^2} \cdot 6.45 = 56.2$$

$$\text{Spinnaker: } A_S = 1.15 \cdot 16.6 \cdot 4.3 = 82.0$$

$$\text{Foretriangle: } A_F = 0.5 \cdot 16.9 \cdot 4.3 = 36.3$$

$$\text{Nominal sail area: } A_N = 36.3 + 35.5 = 71.8$$

$$\text{Aspect ratio, close hauled: } AR = \frac{(1.1 \cdot (16.9 + 1.30))^2}{71.8} = 5.58$$

$$\text{Aspect ratio, other courses: } AR = \frac{(1.1 \cdot 16.9)^2}{71.8} = 4.81$$

$$\text{Drag of hull and mast: } C_{D0} = 1.13 \cdot \frac{(3.71 \cdot 1.30) + (16.9 \cdot 0.173)}{71.8} = 0.121$$

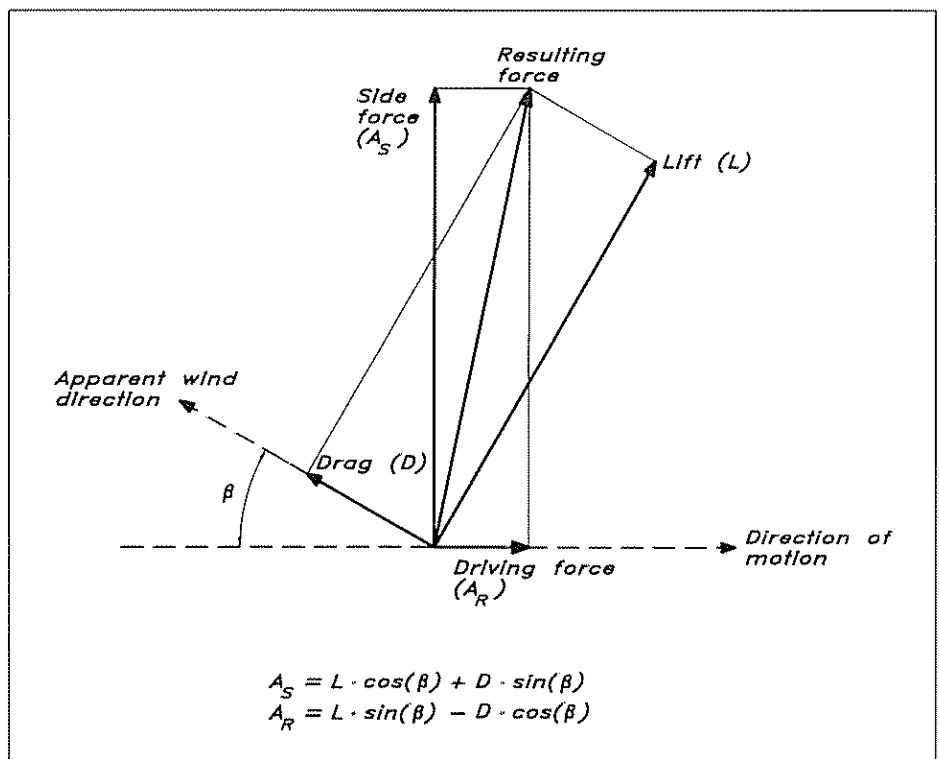
Fig 7 20 Sail coefficients – YD-40

that flattening reduces drag more than lift, ie the resulting force rotates forwards. It is therefore better to flatten the sails before reefing, as pointed out above. In most VPPs optimum values of R and F are found for all conditions, thereby providing information on the best sail setting.

The sail forces provided by the model are the lift and drag components. To be useful for predictions the components parallel to, and at right angles to, the direction of motion are required. Fig 7.21 explains how lift and drag can be converted to driving force and side force. Another geometrical transformation has to be made to obtain forces for the heeled condition. As has been seen above, no account has been taken of the effects of heel. This is done separately, in a somewhat unusual way. Rather than modifying all coefficients, the apparent windspeed and direction are computed in a plane that heels with the yacht. This can be done quite easily, as shown in Fig 7.22. The component of the apparent velocity along the hull is unchanged by heel, while the component at right angles thereto is proportional to the cosine of the heel angle. For simplicity, leeway is neglected in this computation, so the two directions to consider are along, and at right angles to, the direction of motion.

Since the original presentation of this aerodynamic model, full-length battens have become popular. This is now accounted for by increasing the lift by 15% for upwind sailing. Blanketing functions have been introduced, as well as a correction for fractional rigs. Finally, the size of the mainsail is now computed more exactly. By using the chord length

Fig 7.21 Relation between aerodynamic force components





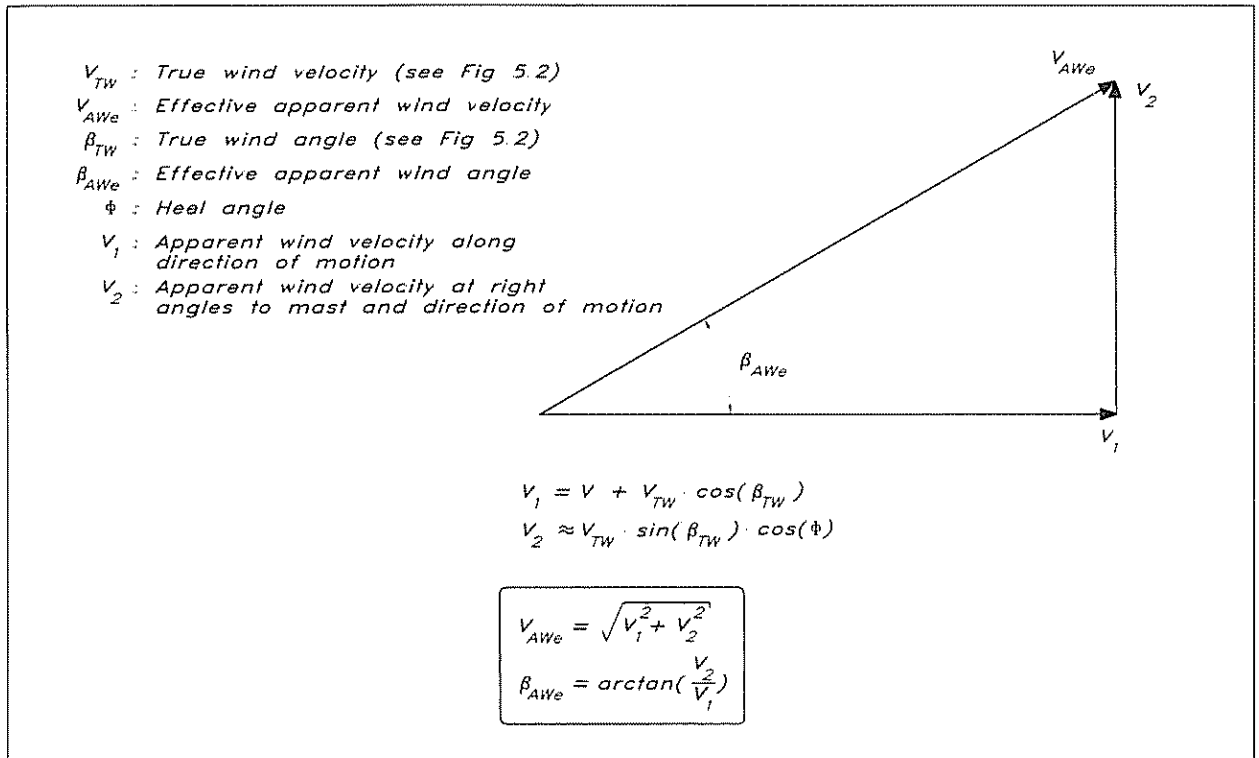


Fig 7 22 Effective apparent wind at non-zero heel angle

at different heights the roach may be accounted for. On the other hand, the mainsail area is now divided by 1.16, so for normal roaches the net effect is negligible. Descriptions of the new features are given in two papers by C L Poor on the IMS system (see the list of References). It should be pointed out that already in the original model some corrections to the IOR measures were used to account for extra long spinnaker poles, head foils etc, but for the sake of simplicity we have neglected these here.

### Sail statistics

The sail area is obviously a measure of the driving force obtainable for a sailing yacht. To judge whether the area is large enough it must in some way be compared with the resistance producing properties of the yacht. As we have seen in Chapter 5 these are the wetted surface and the displacement. While the former determines the friction, which is dominant at low speed, the latter is the most important property for the wave resistance, the largest component at high speeds. Suitable non-dimensional parameters are therefore: sail area/wetted surface and sail area/(volume displacement)<sup>2/3</sup>

Statistics presented by R T Miller and K L Kirkman, based on the IMS fleet in the USA, show that practically all boats have a sail area/wetted surface ratio between 2.0 and 2.5. The mean value is 2.25. There does not seem to be any discernible influence of yacht size. (Dinghies may have somewhat larger numbers, since they are balanced by the crew.) The sail area/displacement ratio, defined above, is within 15 and 22 for the vast majority of yachts and the mean value is 19. It

should also be mentioned that the sail area is defined as the sum of the fore and main triangles.

As for the distribution between the two triangles, the average is in fact 50/50. The minimum main is 27% and the maximum one 58% of the total area. The typical yawl has a distribution between the fore triangle, main and mizzen of 43/47/10, while this distribution for a typical ketch is 46/39/15. Data are also available for the mainsail aspect ratio. The average is 5.9 and the minimum and maximum are 4.2 and 7.0, respectively.

The YD-40 has a sail area/wetted surface ratio of 2.4 and a sail area/(volume displacement)<sup>2/3</sup> ratio of 19.7 (light displacement). It is therefore above the average for both, and should be particularly fast in light air, since the sail area/wetted surface is quite high. The distribution between the triangular areas is close to the average: 49/51, while, as we have seen, the aspect ratio of the main is high: 6.4. This fact, in combination with the high aspect ratio genoa, shows that we have favoured upwind sailing.

# 8

## BALANCE

---

One of the more difficult problems in the design of a sailing yacht is to find the best longitudinal position of the sail plan relative to the underwater body. If the sails are too far aft the yacht will require a considerable weather helm to go on a straight course, while lee helm will be required with the sails too far forward. The problem is complicated by the fact that neither the aerodynamic nor the hydrodynamic centres of effort are known, and that the yacht should behave reasonably well at all heel angles. An entirely theoretical solution to the problem has never been presented, but several semi-empirical methods have been proposed. Most of them, however, have the disadvantage of being less well tested, so in this chapter we will describe some simple rules of thumb used by designers to find the balance of the yacht. These methods work reasonably well for most hulls that are not too different from the common trend, but sometimes corrections have to be made after the first sailing tests.

The chapter starts with an explanation of the effect of heel on balance and continues with a discussion on the location of the centre of effort, first of the underwater body and thereafter of the sails. The rule of thumb for selecting the 'lead' of the sails is then described, and, finally, some guidelines for balancing the rudder are given.

### Effect of heel

In Chapter 5 the forces and moments acting on a sailing yacht were described. It was shown in Fig 5.1 that under equilibrium conditions the hydro and aerodynamic resulting forces must act along the same line, viewed from above. This situation is depicted in Fig 8.1(a), where the hull heels only a few degrees. If this yacht heels more (as in Fig 8.1(b)), the centre of effort of the sails moves to leeward, while the opposite is true for the centre of effort of the underwater body. Since the hull rotates essentially around a fore-and-aft line, which is not at right angles to the hydro and aerodynamic forces, the motion of the two centres will cause the forces to act along different lines. The aerodynamic force will act behind the hydrodynamic one, and the yacht will tend to luff up. To counteract this the helmsman has to give some weather helm, which will bring the hydrodynamic force astern until it hits the same line as the aerodynamic force.

Of course, if the heel is even smaller than in Fig 8.1(a), the opposite situation occurs, ie the yacht will tend to bear away. These effects are caused by the mere rotation of the hull, which will move the centres apart. However, there is also a second effect of the heel on the hydrodynamics of the underwater body. Due to its asymmetric shape

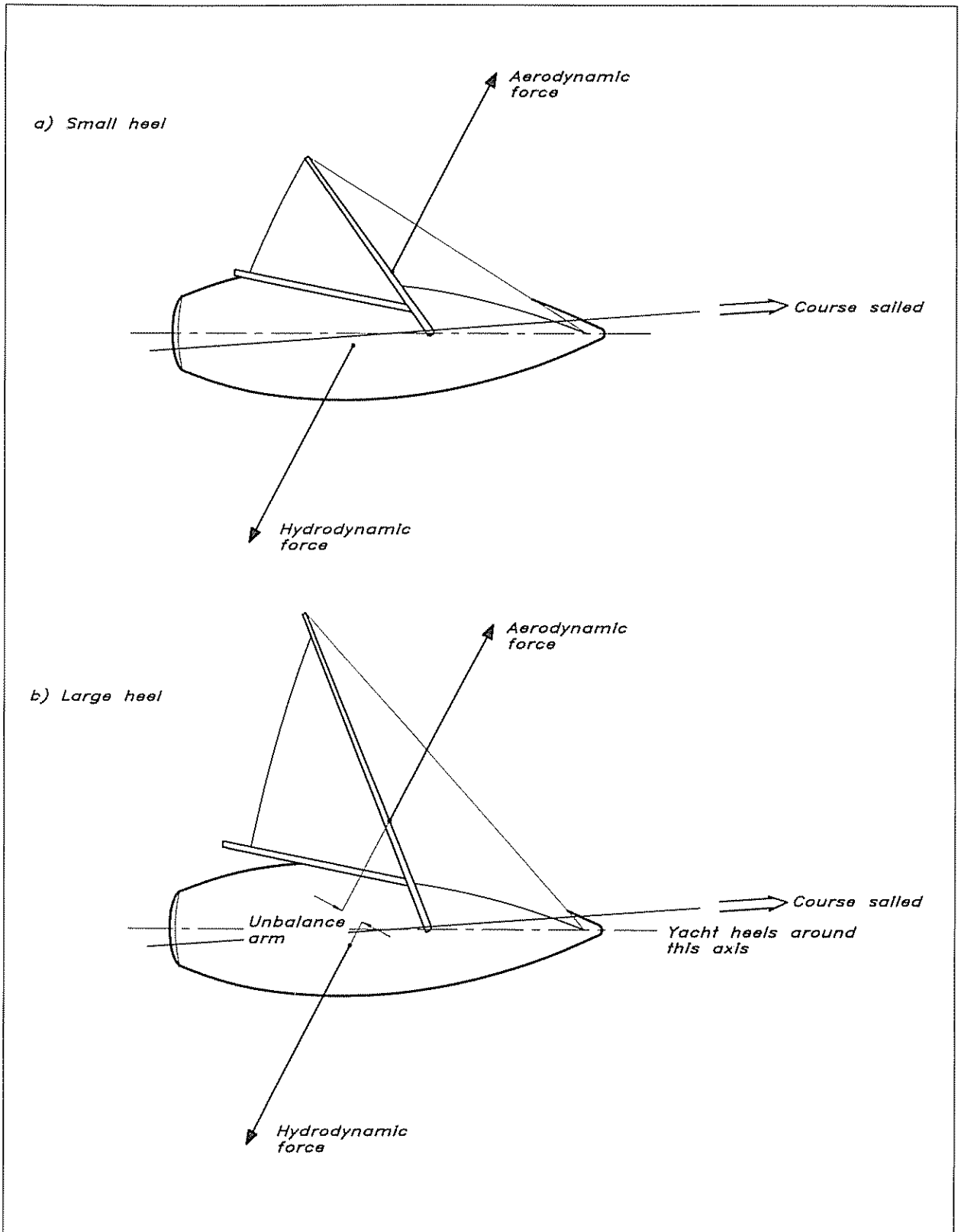


Fig 8.1 Imbalance due to non-alignment of hydro and aerodynamic forces

under heel the hydrodynamic centre will move slightly forwards, thus increasing the imbalance. This effect depends very much on the shape of the hull and may be insignificant for slender yachts with fore-and-aft symmetry. For beamy yachts with flat stern sections it could be quite important, however.

This discussion points at the major difficulty in designing a balanced yacht. It is impossible to position the sail plan in such a way that the yacht is balanced at all angles of heel. Normally, the emphasis is placed on small angles, for which a good balance is sought. Larger weather helms are then tolerated under more heel.

### Good balance

So far we have not defined what we mean by a well-balanced yacht. For several reasons this is *not* a yacht for which zero helm is required to steer it on a straight course. As we have seen in Chapter 6, the rudder normally contributes to the side force, ie it unloads the keel to a certain extent. The larger the weather helm the larger the side force produced by the rudder. Experience shows, however, that there is a limit to the angle at which the total effect is positive. For a certain angle the total resistance of the yacht is minimum, and if this angle is exceeded the resistance grows larger.

From the discussion of Canard wings in Chapter 6 we know that the keel/rudder combination may be analysed using biplane theory, and this shows that, since the wakes of the keel and rudder are separated due to the leeway, there is an advantage in distributing the load between the two lifting surfaces (see Fig 6.14). The rudder, however, is less effective due to the smaller draft (normally), and should therefore carry the smaller load. Theoretical optimization is possible, but complicated. For extreme racing yachts the optimum rudder angle has traditionally been found from towing tank testing, but for most yachts the simple rule of thumb is to assume 5° of weather helm to be optimum.

Apart from the possible resistance reduction, there are other reasons for having a certain weather helm. From a safety point of view there is an advantage in having a yacht that automatically tends to luff up in a gust, thus unloading the sails and reducing the risk of excessive heel. Also from a steering point of view it is an advantage to feel the effect of the gust as an increased force on the tiller or wheel. This helps the helmsman to react and makes the yacht feel more lively. Since the apparent wind angle instantaneously gets larger in the gust, due to the relatively smaller effect of the yacht speed on the apparent wind (see Fig 5.2), the yacht should luff up to take advantage of the gust, and this is more or less automatic for a well-balanced yacht.

### Centre of effort of the underwater body

The centre of effort of the underwater body for three hulls tested by Professor K Nomoto and his co-workers at the Osaka University Ship Experiment Tank is shown in Fig 8.2. In the yachting literature this point is normally referred to as the Centre of Lateral Resistance (CLR). It is denoted 'hydrodynamic CLR' in the figure. The three hulls are quite different, the first being a traditional long keel rescue vessel, the

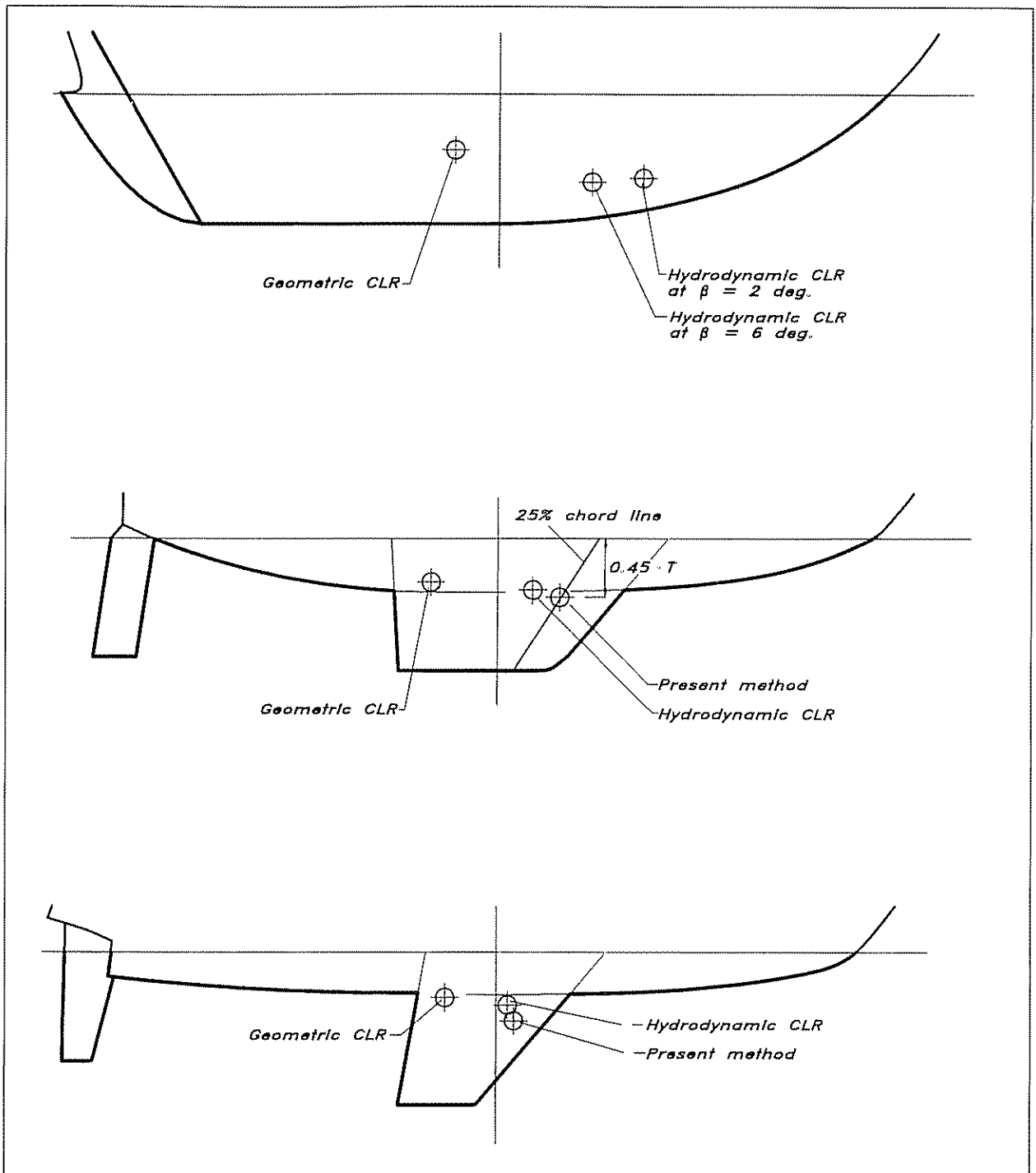


Fig 8.2 Hydrodynamic centre of effort for three hulls (Nomoto and Tatano)

second a heavy fin-keel cruising yacht and the third a typical IOR racer of the 1970s. It is seen that the hydrodynamic CLR is quite far away from the 'geometric CLR', which is simply the geometric centre of gravity of the underwater profile, including hull, keel and rudder. This is not surprising, in view of the fact that the centre of effort of a plane wing of large aspect ratio is at 25% of the chord from the nose, not at

50% where the centre of gravity lies. Certainly, the underwater body is a wing of a very peculiar shape and thickness distribution, and the aspect ratio is small, but wing theory at least shows that there is no reason to assume that the hydrodynamic CLR should coincide with the geometric one.

Various ways to find an approximate position of the hydrodynamic CLR have been proposed. Professor J Gerritsma suggested a method for fin-keel yachts in which only the keel and rudder are considered. To some extent the effect of the hull is taken into account by extending the keel and rudder to the waterline, as can be seen in Fig 8.2 (only the keel needs to be extended in these cases). To find the side force and the CLR, the wing theory described in Chapter 6 is employed. This gives a good estimate of the side force, but the CLR is too far aft, if the keel and rudder are treated independently. A better estimate is obtained (as proposed by Gerritsma) if the force from the rudder is multiplied by a factor of 0.4. The physical justification for this is the change in inflow angle to the rudder caused by the keel, which reduces the lift to about 40% for zero helm. Even with this modification Gerritsma's method tends to predict CLR too far aft, and the reason for this is that the forebody of the hull contributes somewhat to the position, even though the contribution to the force is very small. This is so, since the centre of pressure on the hull is very far forward.

An improvement of Gerritsma's method was suggested by Professor Nomoto and his co-workers in which the force on the forebody is computed from a theory for slender bodies. Using Gerritsma's method, with a rudder reduction factor of 0.4, quite good results were obtained. Neither one of the two methods is very complicated, but they have the disadvantage that very little empirical data exists for linking the computed CLR to the centre of effort of the sails. We have therefore not presented the details of Nomoto's method. Instead, we propose a simplification for which empirical data are available.

It turns out that for most fin-keel yachts the effect of the rudder and the forebody cancel each other reasonably well, so as a first approximation they may both be neglected in the CLR prediction. We thus use only the extended keel and compute the location of the centre of pressure on this, assuming that it lies on the 25% chord, at 45% draft. Inherently, we thus assume that the keel has a large aspect ratio and that the loading is nearly elliptical, but these approximations are not very important in the present context. In this method, CLR is easily found by connecting the points at 25% of the local chord at the waterline and at the tip of the keel by a straight line, and finding the point at 45% of the draft on this line. The procedure is shown in Fig 8.2.

The obvious disadvantage of the proposed method is that it should be used only for fin-keel yachts. In principle, it could be tried also for long keels considering the whole lateral plane as a wing, but we lack experience of how to relate the CLR thus obtained to the centre of effort of the sails, and therefore do not want to propose this approach. For long keels the only feasible method is to use the

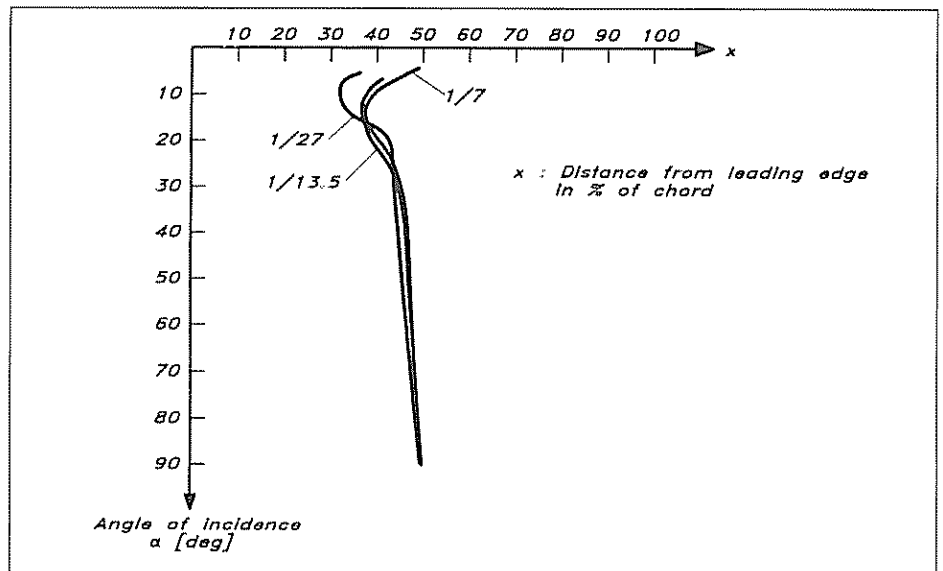
geometric CLR and relate this empirically to the sail plan. This is the standard rule of thumb used for centuries and there is considerable experience available.

### Centre of effort of the sails

When the wind is at  $90^\circ$  angle of attack to a sail the flow behind it is completely separated. The centre of effort (or CE, as it is normally denoted) is then at the geometric centre of gravity of the sail. This is what happens on a run. For other courses the angle of attack is usually considerably smaller and the CE further forward. As pointed out above, this centre is at the 25% chord for a plane wing of large aspect ratio. Now, the sail is not a plane, so even if it works like a wing at smaller angles of attack, the CE will not normally be located that far forward.

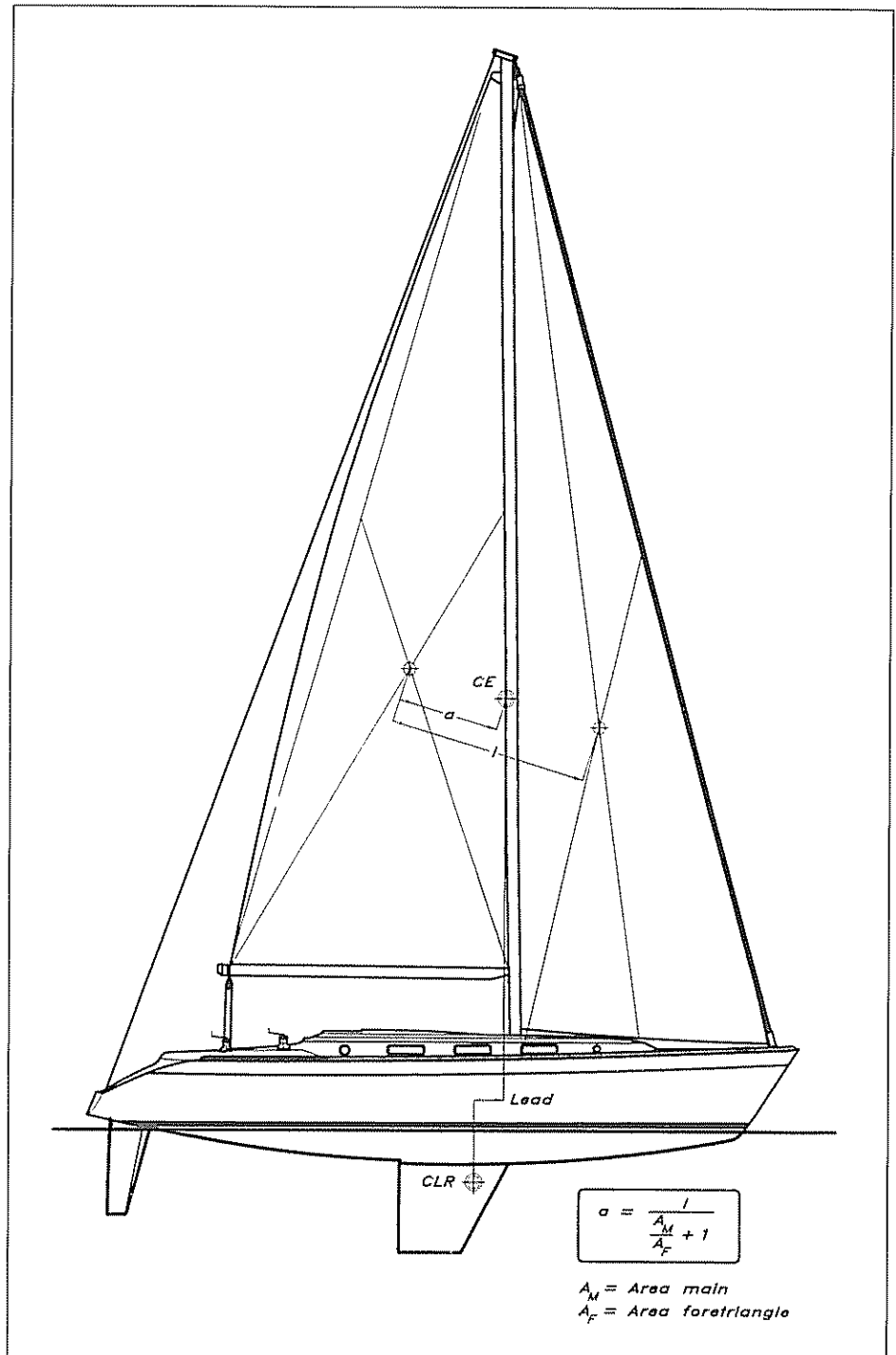
Fig 8.3 shows how the CE moves with the angle of attack for different sail cambers. This is for a sail of aspect ratio 5.0. It may be seen that the flattest sail with a camber ratio of  $1/27$  has its CE at about 30% of the chord at small angles, while this point has moved back to 37% for the full sail with the camber  $1/7$ . A practical implication of this is the change in balance caused by changing from a flat to a full sail. More weather helm will be required for the latter.

Fig 8.3 Centre of effort for sails at varying angles of attack (Marchaj)



Another implication of Fig 8.3 is that there is normally a considerable distance between the geometric CE (corresponding to 50% of the chord) and the aerodynamic CE. In principle, it should be possible to determine a centre of the total sail plan based on, for example, 35% of the chord, but this approach is not normally used. Instead, only the geometric centre is employed. Fig 8.4 shows how this is found for a sloop rig. The centre for each sail is found first, as the intersection between straight lines from two corners to the mid-point of the opposite side. The fore and main triangles are used in this method. Having found the individual centres they are connected by a straight



Fig 8 4 *Definition of lead*

line, and the total CE is obtained as a point on the line, located as shown in the figure. If the yacht has a mizzen, only 50% of its area should be counted (cf the rudder efficiency above). The common centre for the main and jib then has to be found as shown in the figure, and then the main plus jib area at this point is combined with the reduced mizzen area at the mizzen CE, in the same way.

**Lead**

It is obvious from the above discussion that the positioning of the sail plan relative to the underwater body is too complex to be handled entirely theoretically. Regardless of which method is used for finding CE and CLR their relative location has to be based on experience, if the yacht is to be as well balanced as possible under all conditions. In all the methods used CE is in front of CLR, and the horizontal distance between them is called 'lead' (see Fig 8.4). The amount of lead depends, first, on which method is used for finding CLR and secondly on the type of yacht under consideration. In principle the following will increase the lead:

- A large beam. The beamy hull gets more asymmetric under heel, thereby creating a moment to windward.
- A long keel. The real CLR is at, or in front of, the 25% chord and this moves more and more forwards on the hull the longer the keel.
- A large aspect ratio of the sails. The leeward displacement of the CE with heel angle is larger for a high sail.
- A low stability. Hulls with low stability obviously heel more and cause a larger displacement to leeward of the CE.

We recommend the geometric method for finding the CLR of long keel yachts. The lead, in percentage of  $L_{WL}$  should then be as follows:

- Masthead sloops: 12–16%
- Sloops with a fractional rig: 10–14%
- Ketches: 11–15%

For fin-keel yachts the extended keel method proposed here (Fig 8.2) should be used. The following leads are then recommended:

- Masthead sloops: 5–9%
- Sloops with a fractional rig: 3–7%

**Rudder balance**

Since the yacht should have a certain weather helm, it could be quite tiresome to steer it for long periods of time if the rudder is not properly balanced. The moment on the rudder stock is equal to the side force developed, multiplied by the distance between the centre of the stock and the centre of pressure (see Fig 8.5). The position of the centre of pressure may be obtained from Fig 8.6 for the actual aspect ratio. Note

Fig 8.5 Rudder balance

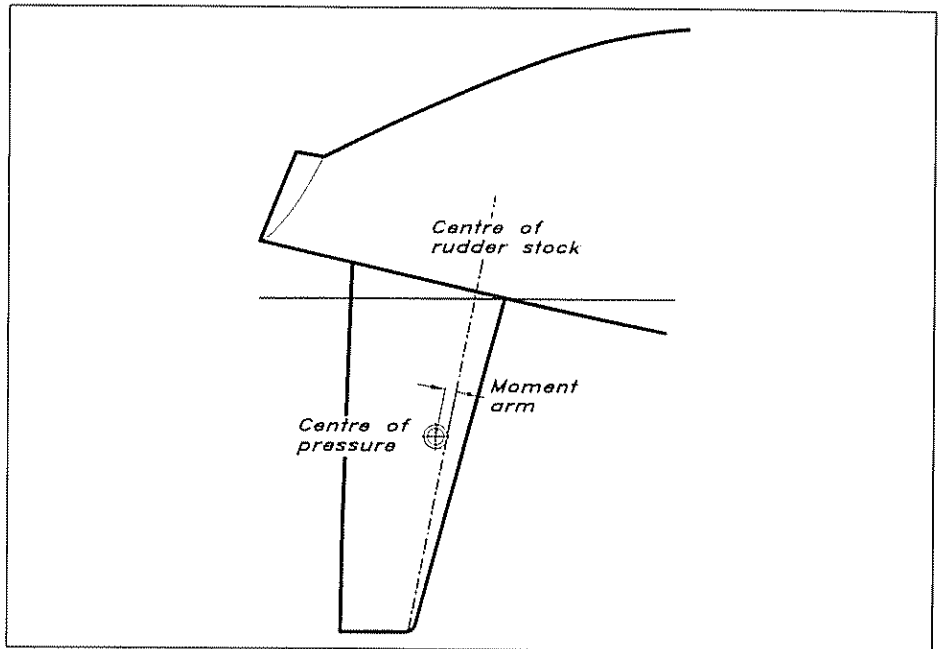
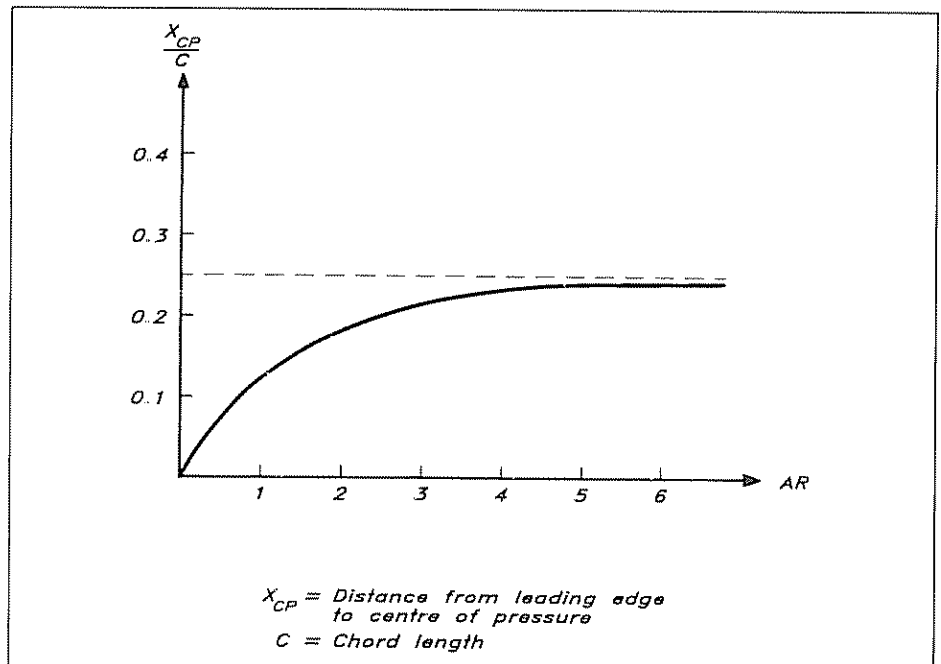


Fig 8.6 Position of centre of pressure for plane wings of varying aspect ratio



that for a rudder hung below the bottom of the hull the effective aspect ratio is twice the geometric one (as explained in Chapter 6). It is seen in the figure that the centre of pressure moves towards the leading edge when the aspect ratio goes to zero.

It is of the utmost importance that the rudder is not over-balanced (ie has its centre of pressure forward of the rudder stock centre), since it will then become unstable. A suitable location is 50 mm behind the centre of the stock. This will give a good feeling for the rudder force, without tiring the helmsman.

# 9

## PROPELLER AND ENGINE

---

Since most sailing yachts today have auxiliary power, it is important to consider the design of the propeller and the power required under different circumstances. There may be three reasons for having an engine in a sailing yacht. First, yacht harbours are often crowded, and it is difficult to manoeuvre under sail in the limited space available. In some harbours it is not even permitted for safety reasons. Secondly, if sailing conditions are not perfect, many cruising skippers prefer to use the engine, particularly if they are short of time. Thirdly, the engine may be a life-saver under critical conditions in rough weather.

The first case does not put any major demands on the engine-propeller design, since only very limited power is required. It is important, however, that the propeller works reasonably well when going astern. In the second case, speed is an important factor, while in the third case enough thrust should be developed to escape from dangerous situations even against strong winds and heavy seas. These two latter cases put different demands on the propeller, and it is important to find a good compromise to achieve a reasonable performance in both situations. Perhaps the most important requirement is that the propeller allows the engine to work close to its optimum under severe weather conditions.

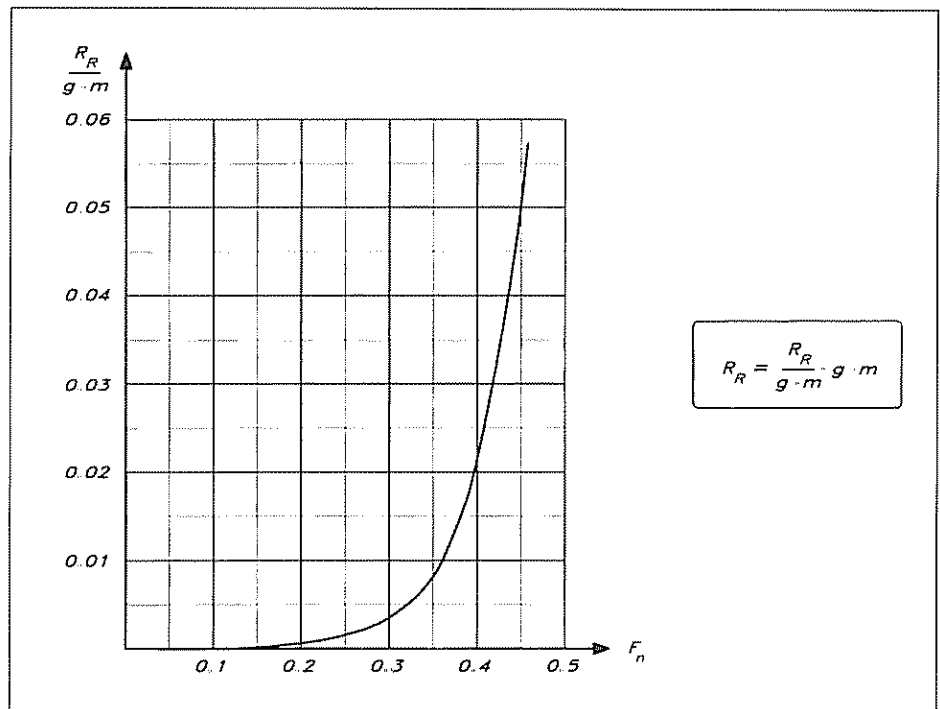
In the first part of this chapter we will consider the total resistance of the yacht based on our discussion in Chapter 5. This will serve as a basis for the propeller design in calm weather, while for the rough weather case we will also introduce the added resistance in waves, and the windage from the above-water part of the yacht. Having found the resistance under the two conditions we will show how the optimum propeller and the required power may be obtained under each condition. The final choice of the propeller has to be a compromise between the two requirements, and we must also consider what is available from manufacturers, both as to the propeller and the engine. After selecting a suitable combination we will investigate its performance. Finally, we will discuss the added resistance due to the propeller when sailing.

It should be pointed out that the calculations in the present chapter will be more approximate than those of Chapters 5 and 6, in which the fine tuning of the yacht and appendages was discussed. To obtain a suitable propeller/engine combination this accuracy is not needed, and it is also very difficult to obtain, since many of the influencing factors are not known with great accuracy.

### Resistance in calm and rough weather

The resistance was discussed extensively in Chapter 5 (see Fig 5.4 in particular). Since we are now interested in the upright case we can forget about the heel and induced resistance, and if the hull is not too fouled we can also forget about the roughness drag. What is left in calm water is then the friction and the residuary resistance. How the friction is computed was explained in detail in Fig 5.8 and the residuary resistance calculation was presented in Figs 5.18 and 5.19. However, the formulae of the latter figures are quite complex and we could do with a more approximate estimate for the present case. As was pointed out in Chapter 5, the residuary resistance, in percentage of the displacement, is more or less the same for all yachts at a given relative speed (Froude number), and we have plotted this approximate relation in Fig 9.1. From Figs 5.8 and 9.1 the reader can thus obtain an estimate of the resistance in calm weather.

Fig 9.1 Estimation of residuary resistance



In rough weather we also have the added resistance in waves (mentioned in Chapter 5), and the windage (discussed in Chapter 7). Let us start with the latter.

Fig 9.2 gives the appropriate formulae for calculating the windage of the hull, mast and rig separately. In principle they have already been given in Chapter 7, but they are repeated here for clarity and some missing coefficients are also included. The frontal area of the hull and superstructure may be taken simply as the maximum beam times the freeboard forward, and the drag coefficient is assumed to be 0.5. Often, somewhat higher values are used, but considering the fact that the windspeed at the level of the hull is significantly smaller than at 10 m height, where observations are made, this should be accurate enough.

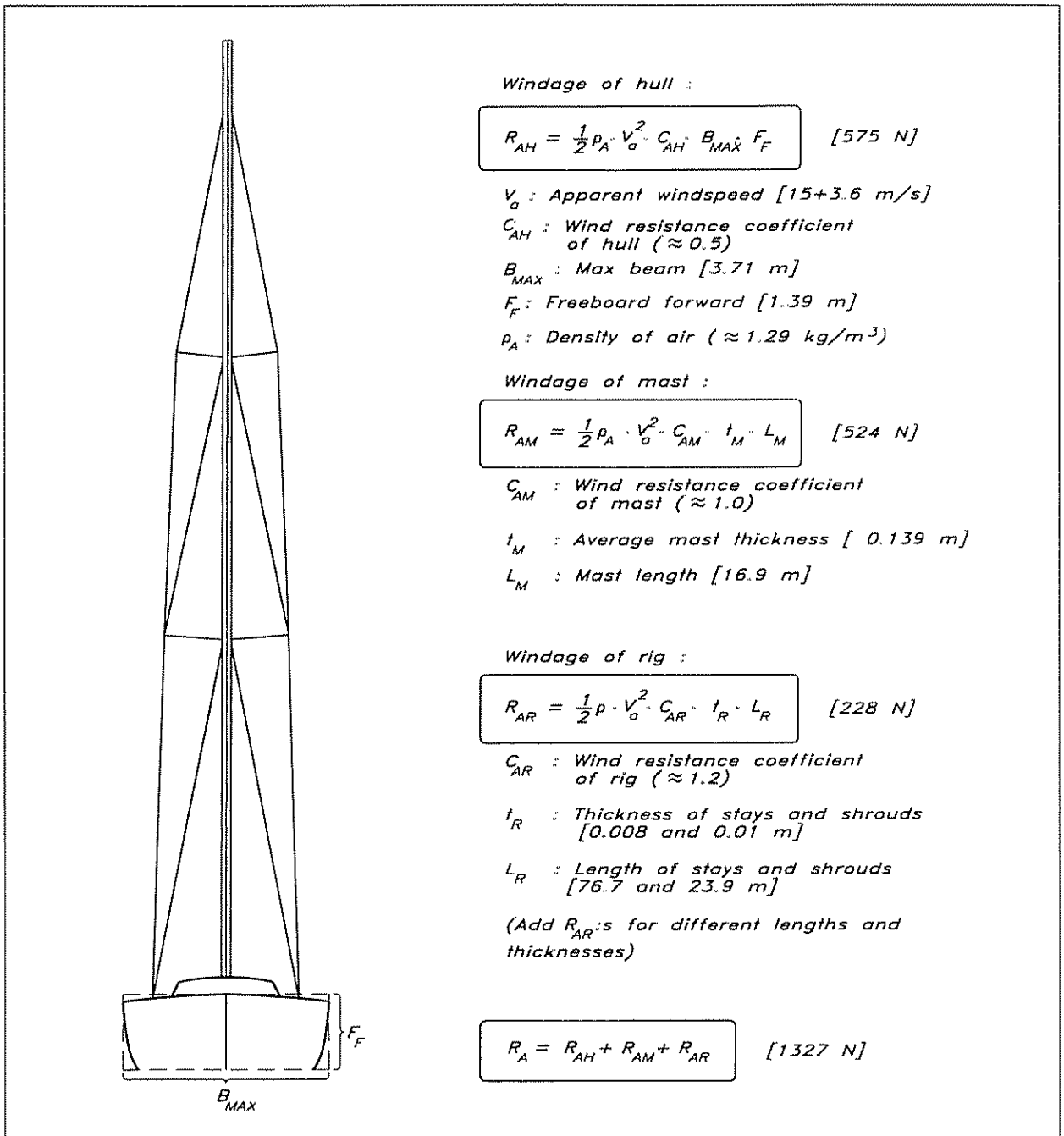


Fig 9.2 Estimation of windage

For the mast the frontal area is taken as the mean thickness times the height, and the drag coefficient is set to 1.0, somewhat lower than the undisturbed value of 1.2 used for the stays. This is reasonable, considering disturbances from spinnaker halyards etc, which act as turbulence stimulators. The drag of stays and shrouds may have to be added over components with different diameters. Geometrical values for the YD-40 are given within square brackets, as usual, but no drag values are given, since the windspeed will vary in the example below.

The most difficult quantity to estimate is the added resistance in waves. In Fig 5.4 it was assumed to be 10% of the sum of the other components, which may be reasonable for the conditions in question. However, now we will have to consider much worse conditions for the rough weather case. We will make use of the added resistance curves of Fig 5.30 computed by Prof Gerritsma et al. These were obtained for 10 m  $L_{WL}$  yachts at a Froude number of 0.35 and a wave angle of  $135^\circ$  measured between the directions of motion of the waves and the yacht. The waves were thus  $45^\circ$  from head seas. To make use of the results some assumptions must be made. First, a dimensionless resistance is obtained by dividing by the weight (mass displacement times acceleration of gravity). This can be done for each curve of Fig 5.30, since the length/displacement ratio is known, as well as the length (10 m). Note that we only know the values for the canoe body. If the waves and yacht were geometrically scaled, and the Froude number was the same at two scales, the dimensionless resistance could be used for all scales. This is not quite true, since the shorter waves are comparatively higher, ie steeper, but if we restrict the discussion to yachts with an  $L_{WL}$  between 5 and 15 m we can adopt this approximation for the present purposes.

The second approximation is related to the Froude number. Although 0.35 corresponds to a reasonable speed by engine, we do not know whether we will obtain that speed exactly. However, we are only interested in the maximum value of the added resistance, ie the peaks of Fig 5.30, and these are likely to be about the same for other speeds (although they will be obtained at different wave periods).

Finally, we assume that the *maximum* added resistance is the same in head seas as in the computed  $135^\circ$  seas. This is reasonable, since the possible coupling between roll and pitch is not considered in the calculations, which take into account only heave and pitch.

It should be mentioned that if the computation is to be carried out for other waves than those of Fig 5.31, a good approximation is obtained by multiplying the values presented in Fig 9.3 by the square of the ratio between the actual wave height and the present one. The specification of the waves is the most uncertain part of this computation. The waves of Fig 5.31 are typical for unsheltered waters off the coast in many sailing areas of interest. However, on the oceans the waves are longer, and in certain other cases (such as in a shallow area or a narrow passage with head seas), the waves could be considerably steeper.

The result of the above discussion is shown in Fig 9.3. The estimated maximum added resistance in dimensionless form is plotted versus length/displacement ratio. This figure may be used for yachts of different sizes and slenderness. Numbers for the YD-40 are included, and it can be seen that the maximum added resistance for this hull is 730 N. This value has been used in Fig 9.4, which shows the total resistance of the YD-40 in calm and rough weather. The different contributions at 7, 8 and 8.5 knots are given in the table. To be on the safe side we have here assumed a wind speed of 15 m/s, which is somewhat higher than the speed for which the maximum added resistance occurs.

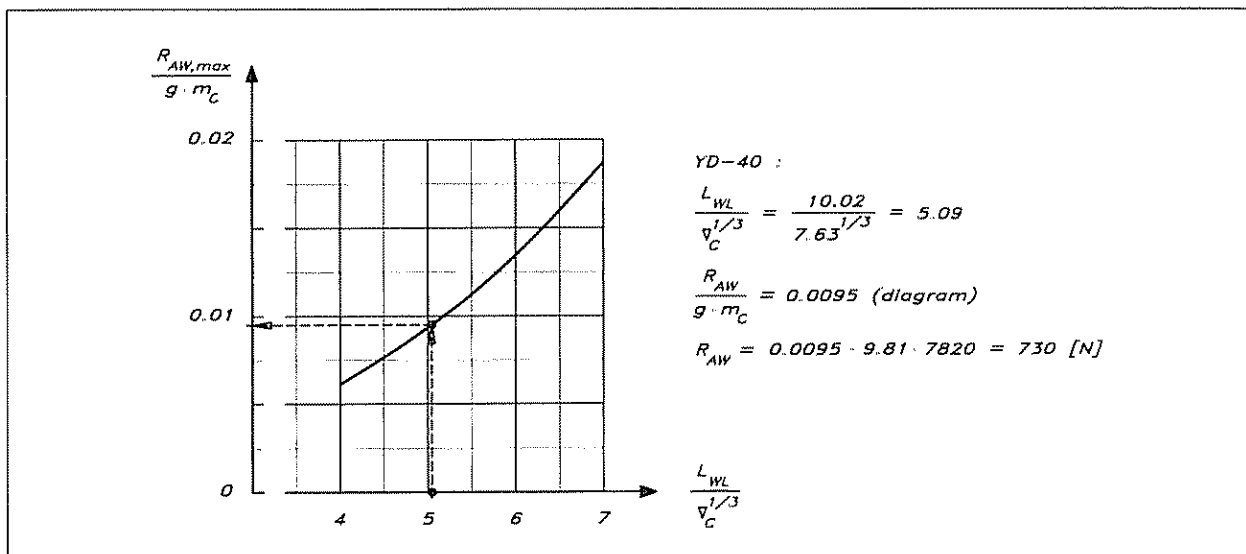


Fig 9.3 Estimation of maximum added resistance in waves

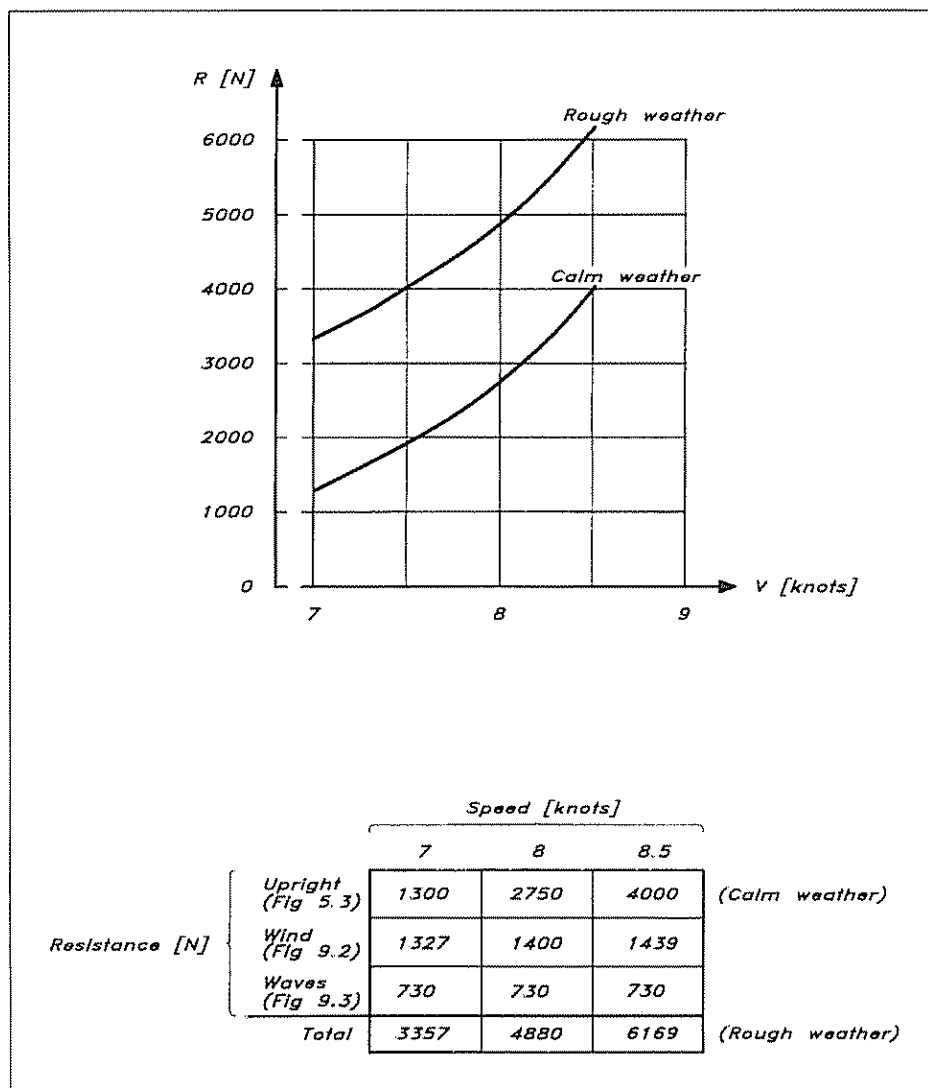


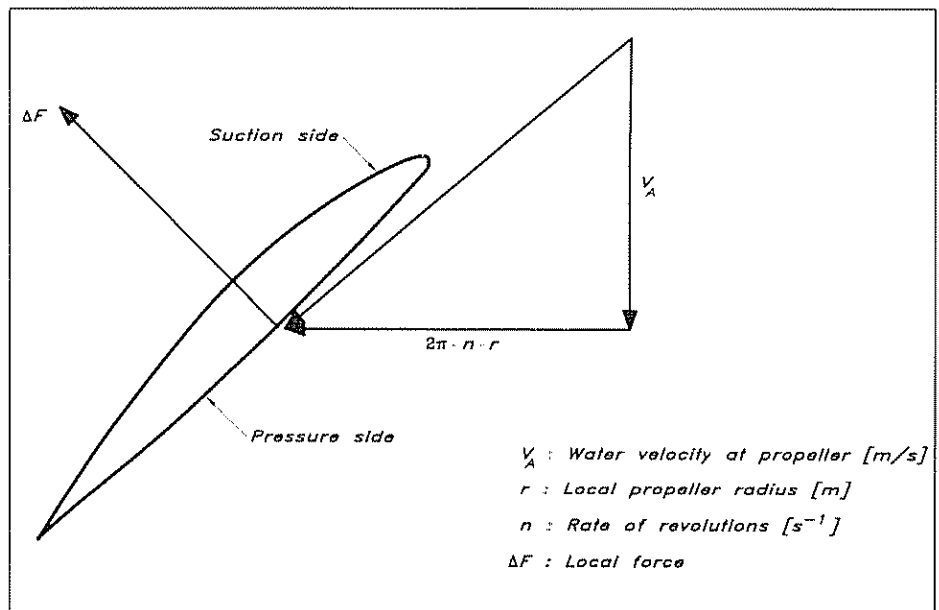
Fig 9.4 Resistance in calm and rough weather – YD-40



### Propeller characteristics

Propeller blades act as wings when the propeller rotates and advances through the water. A section of a blade at a certain radius is shown in Fig 9.5. It can be seen that the resulting velocity, to which the blade is exposed, is composed of the axial component (due to the forward motion) and the tangential component (due to the rotation). The former is normally not exactly equal to the yacht speed, but somewhat lower, since the propeller operates in the wake behind the hull. This effect can be quite significant for bluff ships, but for a sailing yacht with the propeller below the bottom of the hull it should be less than 10%, so we will neglect it in the following. The tangential component is proportional to the local radius and the rate of revolutions. It thus increases linearly with the radius, which means that the angle of the approaching flow gets smaller and smaller towards the tip. Therefore, the blades have to be twisted to become more and more at right angles to the propeller shaft further out. In fact, the propeller is normally designed so that the sections at all radii would advance the same distance for one turn of the propeller, had they been free from the others and cutting through a solid body. This distance is called the pitch, and is, together with the diameter, the most significant property of the propeller.

Fig 9.5 Cut through a propeller blade



The pitch should be large enough to create a suitable angle of attack between the section and the approaching flow (as can be seen in Fig 9.5). A resulting force, more or less at right angles to the flow is then developed. Had there been no resistance the angle would have been exactly  $90^\circ$ , but, since we have both induced and viscous resistance, the resulting force points more backwards (as explained in Chapter 6). The force has one component in the axial direction, the useful thrust, and one in the tangential direction, giving rise to an

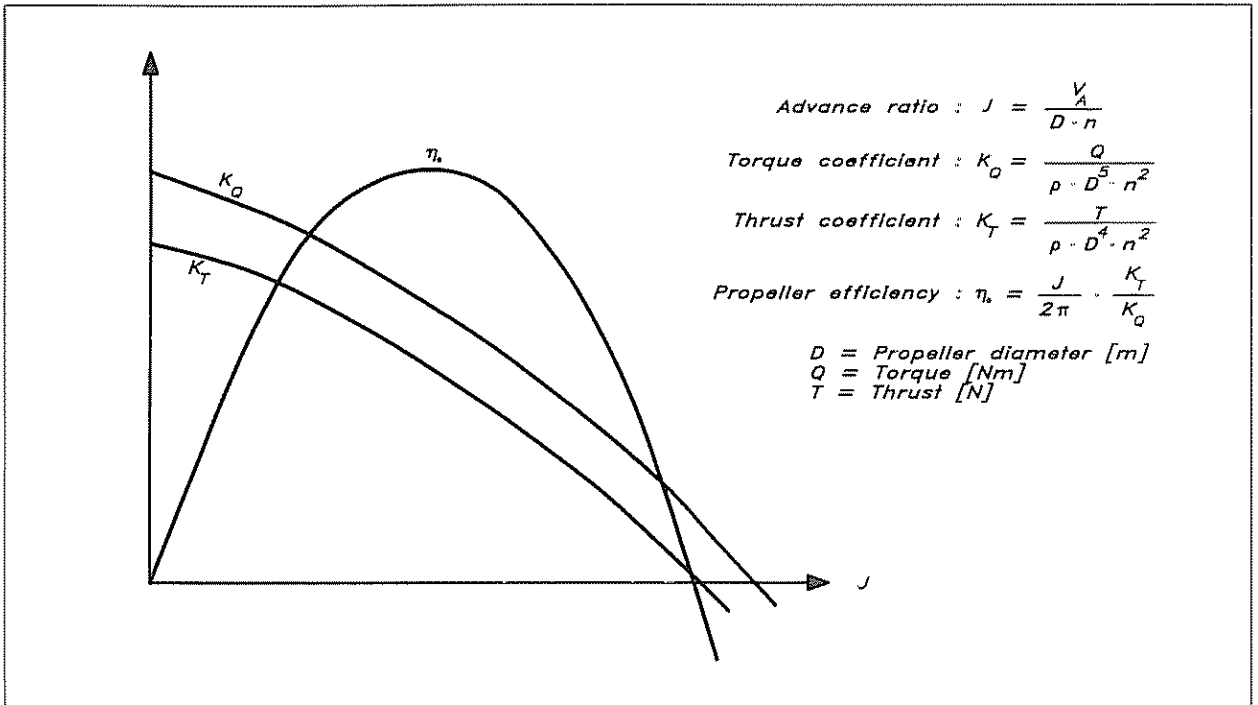


Fig 9.6 Propeller characteristics

unwanted torque. These components may be made dimensionless in a similar way as described earlier for the various resistance components and the lift. However, a typical velocity in the present case is the diameter times the rate of revolutions, and a typical area is the diameter squared. If these replace the normal velocity and area a thrust coefficient may be defined as in Fig 9.6. To make the torque dimensionless another diameter has to be included in the denominator. The advance ratio, defined in the figure, is a measure of the angle of the approaching flow. By dividing the effective power (thrust times axial velocity) by the delivered power (torque times angular frequency), the efficiency of the propeller can be found. It may be expressed as seen in the figure.

The thrust and torque coefficients and the efficiency are called the propeller characteristics and they are normally given as functions of the advance ratio (see Fig 9.6). To obtain this diagram the propeller is run in free water, often on a long shaft in front of a very slender hull containing the measuring equipment. Systematic variations in advance ratio are made either by varying the speed for a given rate of revolutions or vice versa. At zero speed a large thrust and torque are developed, but the efficiency is zero, since the propeller does not move forwards. At high speeds both the thrust and the torque go to zero, since the angle of attack of the blades goes to zero. At still higher speeds the propeller works as a turbine and negative thrusts and torques are developed. When the thrust is zero the efficiency is also zero. At some intermediate speed the efficiency reaches its maximum, and it is important to design the propeller for this condition.

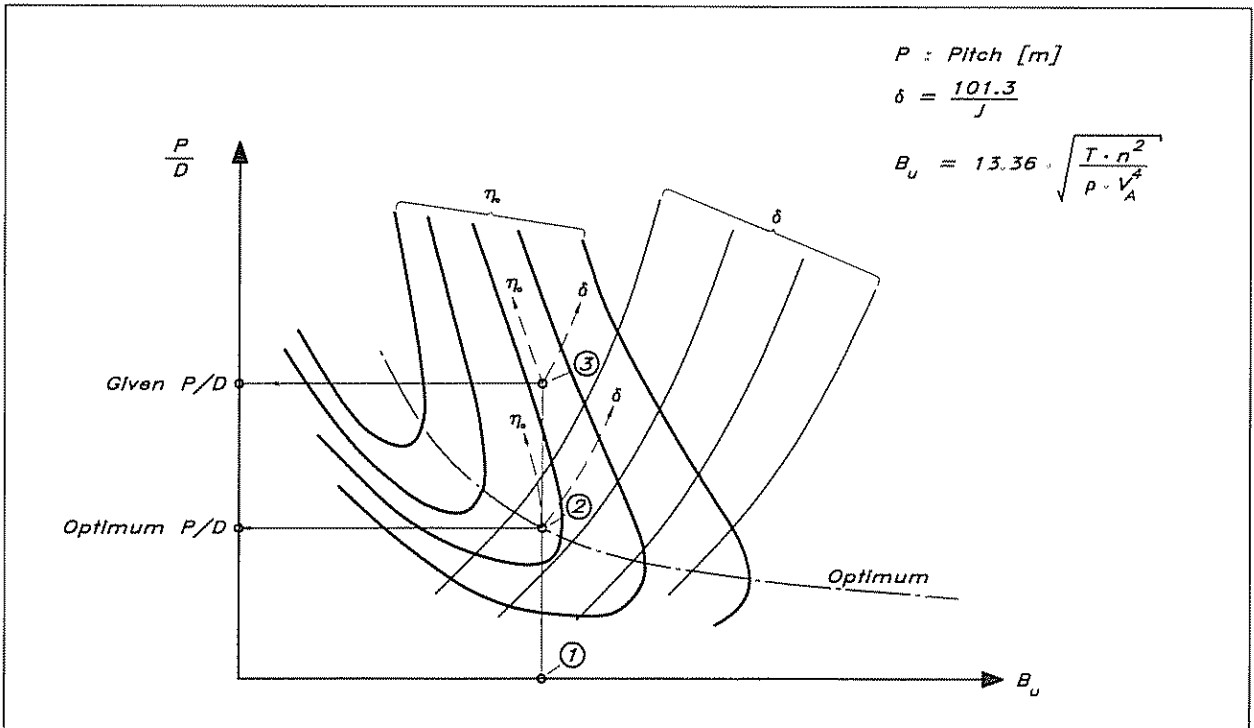
A final remark should be made about Fig 9.5. Propeller specialists normally deal with the induced resistance in a way different to ours, as described in Chapter 6. In their approach, induced velocities from the trailing (helical) vortices are employed. If these were introduced, Fig 9.5 would be slightly more complicated. The methods are, however, equivalent and the following discussion is valid for both.

**Design of an optimum propeller**

To design the optimum propeller we need to know the advance velocity of the propeller, the thrust (or power) and the rate of revolutions. As we have already noted, the advance velocity is normally smaller than the speed of the yacht, due to the fact that the propeller operates in a wake. Considering the other approximations we will neglect this effect, which is small for a sailing yacht. Another approximation we will adopt is the assumption that the thrust of the propeller is equal to the total resistance of the yacht. This is not exactly true, since the propeller itself reduces the pressure around the stern, thereby increasing the resistance, but this effect should be very small for a yacht with the propeller below the hull and well in front of the stern.

There are several systematic series of propellers documented, but only a few of them include two-bladed propellers, which are of interest in connection with yachts. One series which does have two blades is the so-called Troost propeller series, developed and tested at the Netherlands Ship Model Basin (presently MARIN, Wageningen). The results are presented in the form of  $B_u - \delta$  diagrams, where  $B_u$  is a thrust coefficient and  $\delta$  is an inverted advance ratio. Both are defined in

Fig 9.7 Principles for using the  $B_u - \delta$  diagram



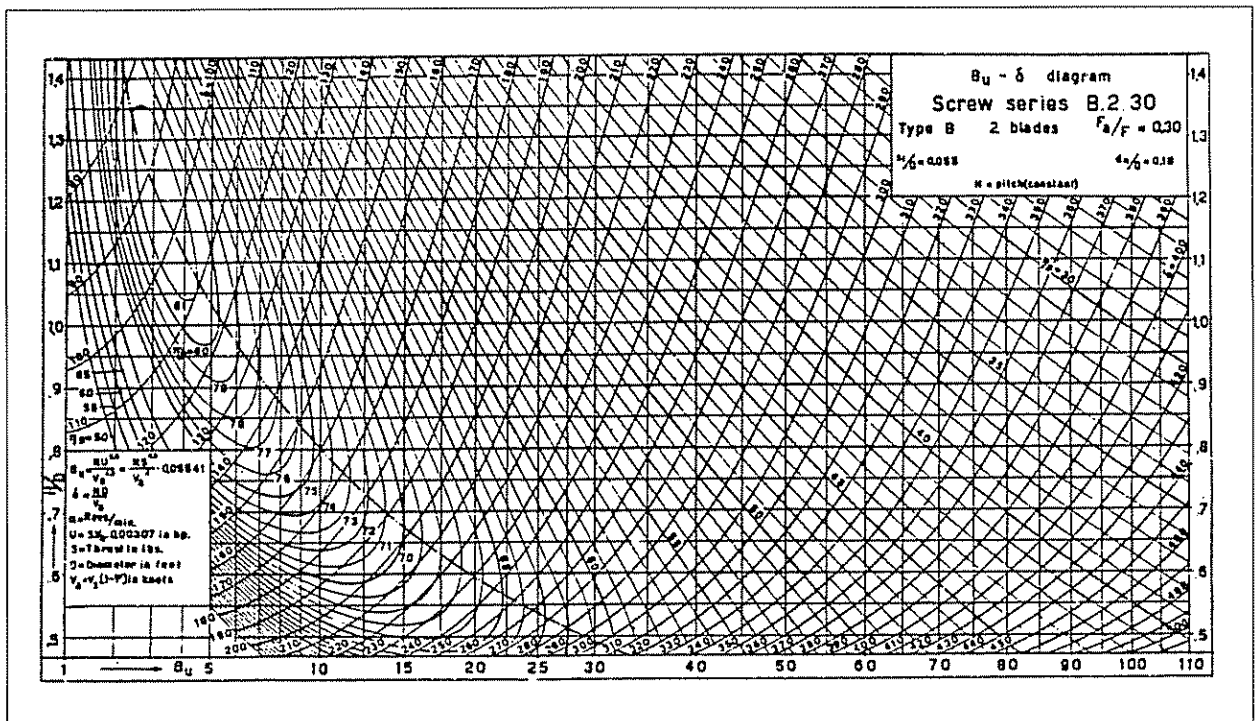


Fig 9.8  $B_u - \delta$  diagram, 2-bladed Troost propellers (Courtesy of MARIN)

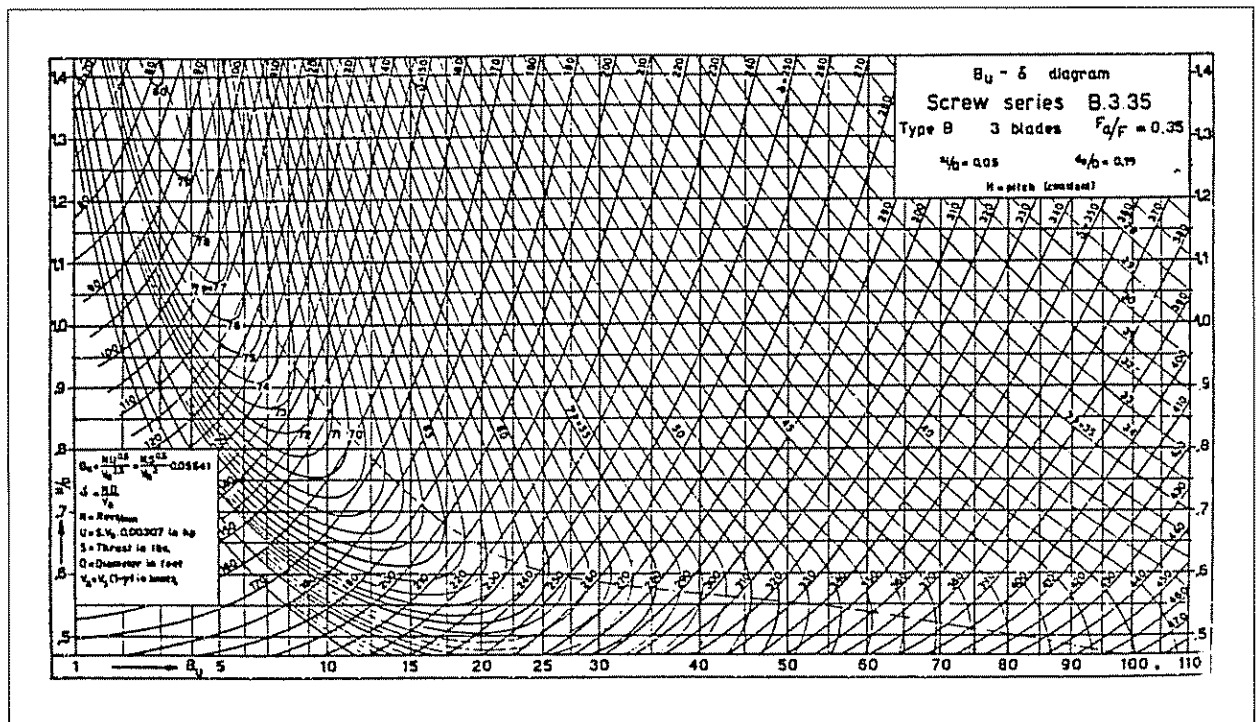


Fig 9.9  $B_u - \delta$  diagram, 3-bladed Troost propellers (Courtesy of MARIN)

### Principles for using the $B_u - \delta$ diagram

- 1 Compute  $B_u$  to obtain point 1 in the Fig 9.7.
- 2 If optimum efficiency is requested, go to point 2 on the optimum curve.
- 3 Alternatively, if the propeller is already available, go to point 3, corresponding to the known pitch ratio  $P/D$ .
- 4 From point 2, go to the vertical axis and read the optimum pitch ratio.
- 5 Interpolate the efficiency between the  $\eta_0$  - curves at point 2 or 3.
- 6 Interpolate in a similar way between the  $\delta$  - curves.
- 7 Knowing  $\delta$  the advance ratio may be obtained from the definition of  $\delta$ , and from the advance ratio the diameter may be computed.
- 8 Finally, the delivered power may be found from the effective power (resistance  $\cdot$  speed) and efficiency. Note that this is the power available at the propeller. This is somewhat smaller than the nominal power of the engine, due to transmission losses. A 10% reduction is reasonable.

Fig 9.7, which also explains the way to use the diagrams presented in Figs 9.8 (two blades) and 9.9 (three blades). (If the power is known, similar so called  $B_p - \delta$  diagrams may be used)

A suitable engine has to be selected from the product catalogue of an engine manufacturer. As a rough estimate 3 kW per ton of displacement may be used for pure sailing yachts, while 44.5 kW/ton is appropriate for motor sailers. In the case of the YD-40, with a displacement of 8.12 tons the engine should have a power of around 24 kW. It is seldom possible to find an engine that exactly fits this requirement and we will assume in the following that the closest choice in our case delivers 26 kW at the shaft. The nominal power of the engine is thus somewhat higher. We will also assume that this power is delivered at 3000 rpm and that the gear ratio is 2.5:1. This gives 20 revolutions per second of the propeller.

By computing the optimum propeller for different speeds it is possible to find the speed corresponding to the power available. Such a calculation is presented for the YD-40 in Fig 9.10. The speeds are 7, 8 and 8.5 knots, and the calculations are carried out for both the calm weather and the rough weather cases. The results are shown in Fig 9.11, where (a) gives the delivered power and (b) the optimum diameter and pitch. In both diagrams curves are given for calm and rough weather cases. It is seen from the power diagrams that the speed will be 7.5 knots and 8.4 knots respectively under the two conditions. This yields optimum diameters of 0.62 m and 0.58 m respectively, while the optimum pitches are 0.29 m

	Calm weather			Rough weather		
$V_A = [\text{knots}]$	7	8	8.5	7	8	8.5
$V_A = [\text{m/s}]$	3.60	4.11	4.37	3.60	4.11	4.37
$T = [\text{N}]$	1300	2750	4000	3357	4880	6169
$B_u$	23.2	25.9	27.6	37.3	34.5	34.3
$\delta$ [diagram]	250	270	280	330	320	320
$D$ [m]	0.44	0.55	0.60	0.59	0.65	0.69
$P/D$ [diagram]	0.55	0.53	0.51	0.47	0.47	0.47
$P$ [m]	0.24	0.29	0.31	0.28	0.31	0.32
$\eta_b$ [diagram]	0.64	0.63	0.62	0.58	0.59	0.59
$P_D$ [kW]	7.3	17.9	28.2	20.8	34.0	45.6

Engine max :  $P_D = 26$  [kW] at  $n = 3000$  [rpm]

Gear ratio 2.5:1

$$n = \frac{3000}{2.5 \cdot 60} = 20 \text{ [rps]}$$

$$B_u = 13.36 \cdot \sqrt{\frac{T \cdot n^2}{P \cdot V_A^4}} = 8.35 \cdot \frac{\sqrt{T}}{V_A^2}$$

$$D = \frac{\delta \cdot V_A}{101.3 \cdot n} = \frac{\delta \cdot V_A}{2026}$$

$$P_D = \frac{T \cdot V_A}{\eta_b}$$

Fig 9.10 Design of optimum propeller – YD-40

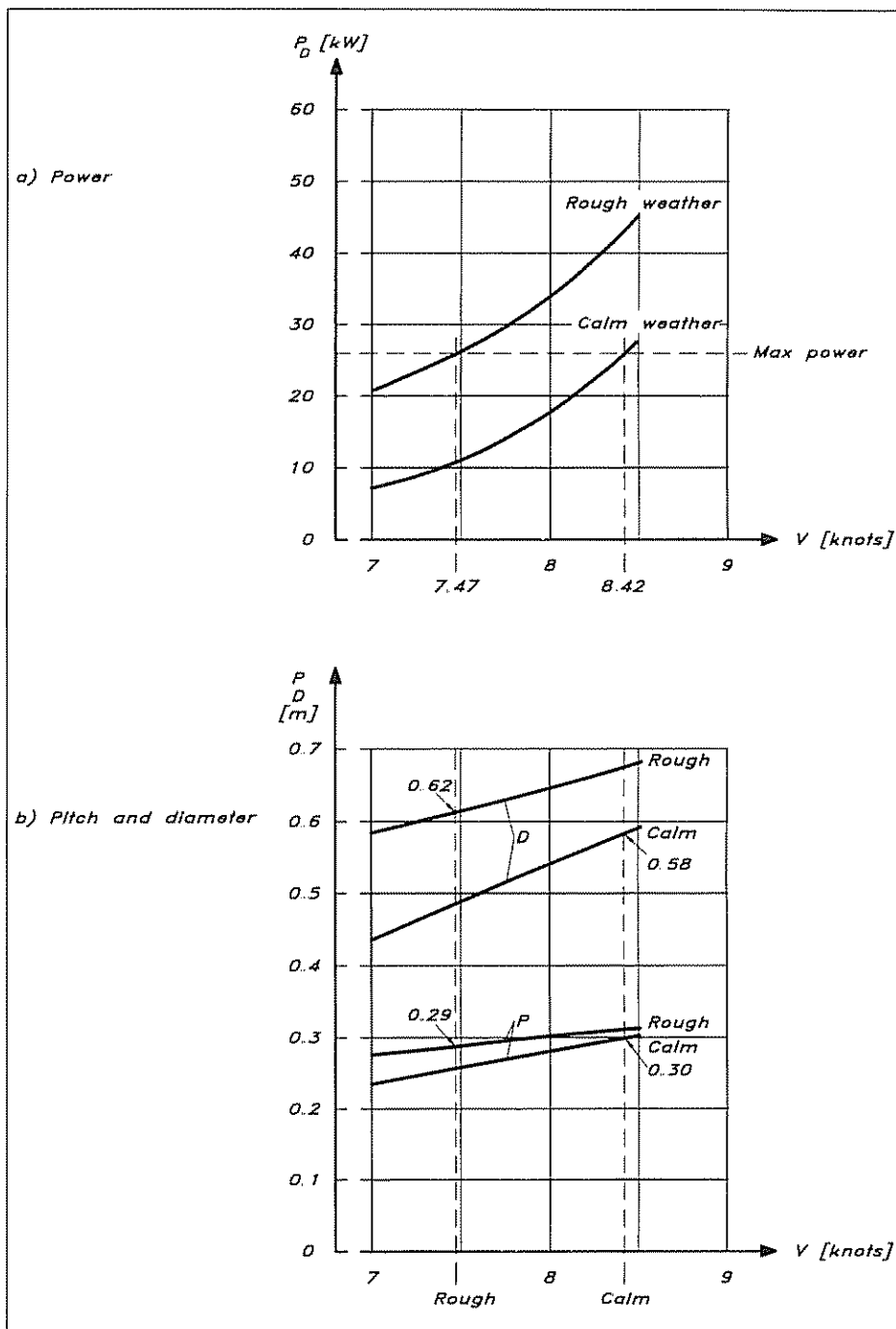
and 0.30 m. The difference between the two propellers is thus relatively small, and it should be possible to find a propeller that works well under both conditions.

Now we have to look again at what is available, in this case from the propeller manufacturers. There are three principally different types of propeller for sailing yachts: fixed, folding and vaning. As will be seen later, the folding propeller has superior drag properties when not in use, and it seems to be the most popular choice today. However, the only diagrams for propeller design that are available are for the fixed case, and we will have to use them even though we chose a folding propeller. The computed optimum diameter for the YD-40, around 0.6 m, is relatively large for this type and there is not much choice for this size from most manufacturers. As a general rule, the best compromise from an efficiency point of view is to select the propeller which comes closest to the requested one in terms of pitch times diameter, since that will load the engine approximately as much as computed for the optimum propeller. In our case we will assume that the best propeller we can find has a diameter of 0.53 m and a pitch of 0.33 m. The pitch ratio is thus 0.62. We will now see how this non-optimum propeller performs.

### Performance of the non-optimum propeller

The propeller characteristics of two-bladed Troost propellers are given in Fig 9.12. This diagram is for a blade area ratio of 0.3, as was also the case for Fig 9.8. The blade area ratio is defined as the area of all

Fig 9.11 Optimum propeller - YD-40



blades together divided by the propeller disk area. We will return to the importance of this ratio later.

To find the characteristics of the chosen propeller with a pitch ratio of 0.62, interpolation must be made between the curves of Fig 9.12. The characteristics thus obtained have been plotted in Fig 9.14. This diagram shall now be used to find the rate of revolutions and the power required for the propeller in question at different yacht speeds. These two

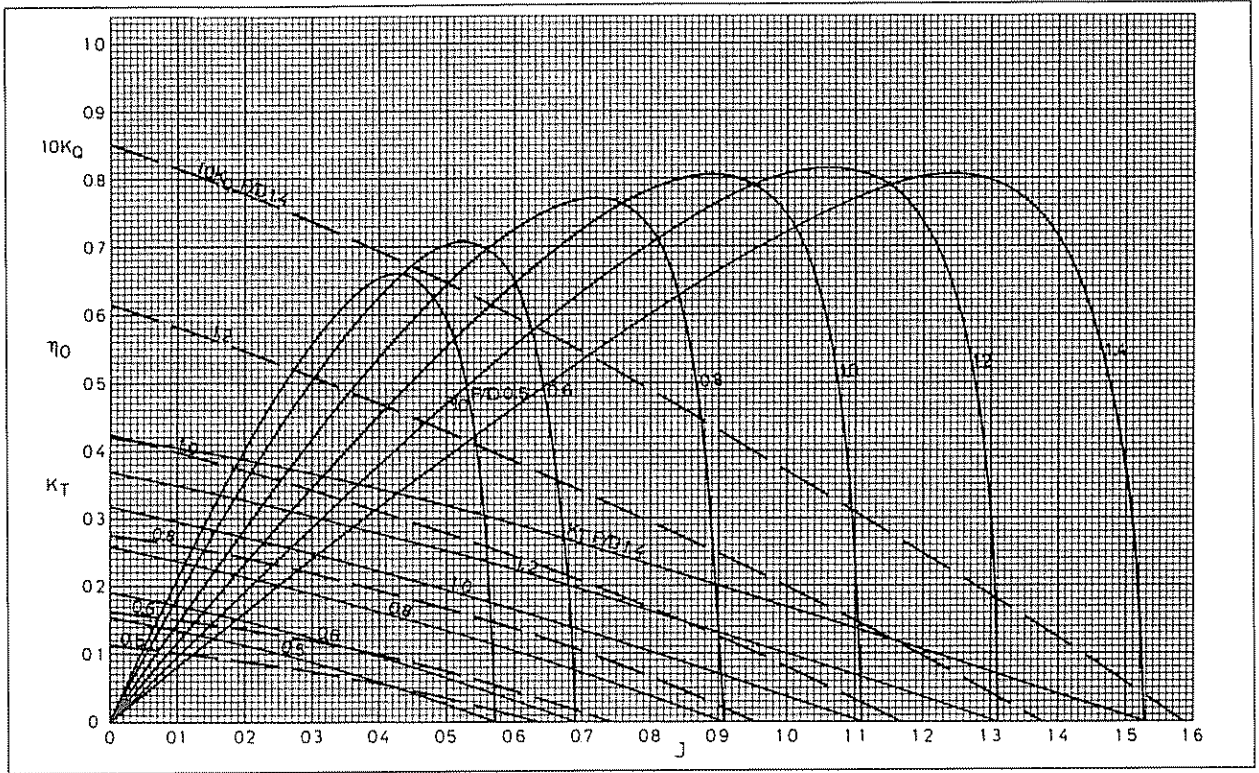


Fig 9.12 Propeller characteristics, 2-bladed Troost propellers (Courtesy of MARIN)

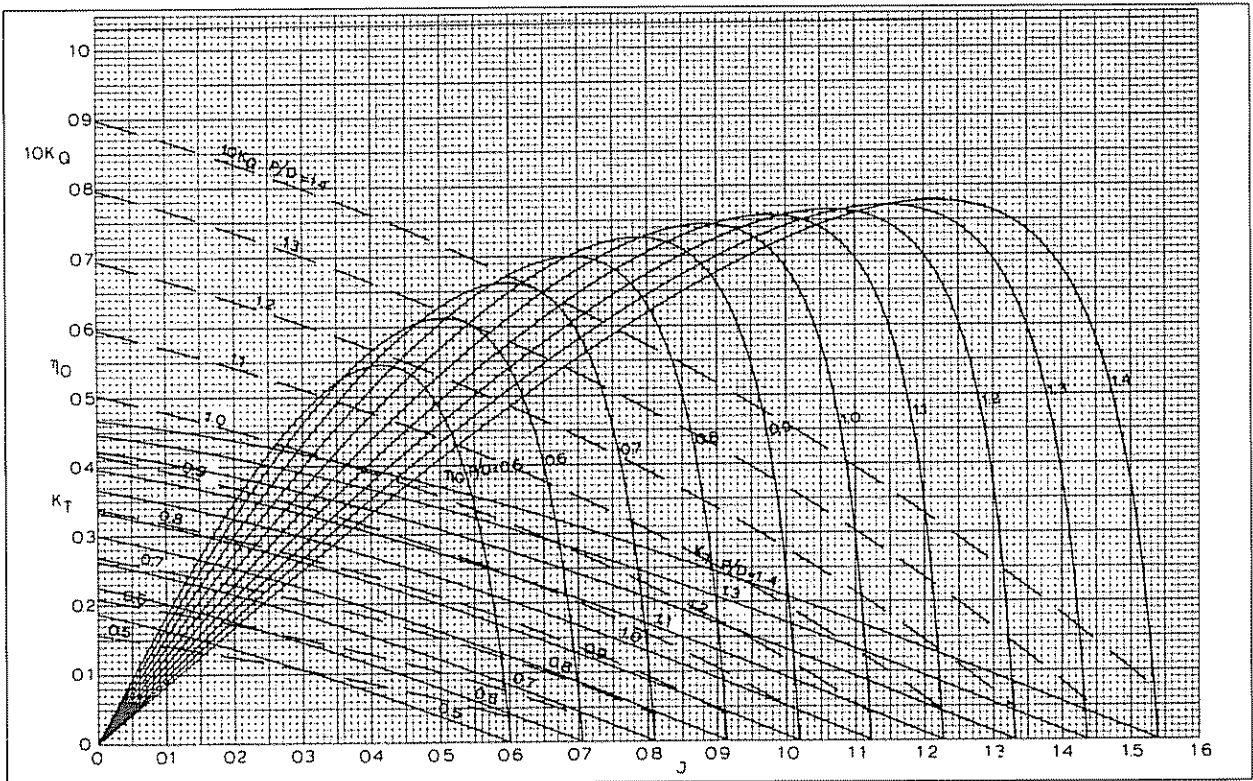
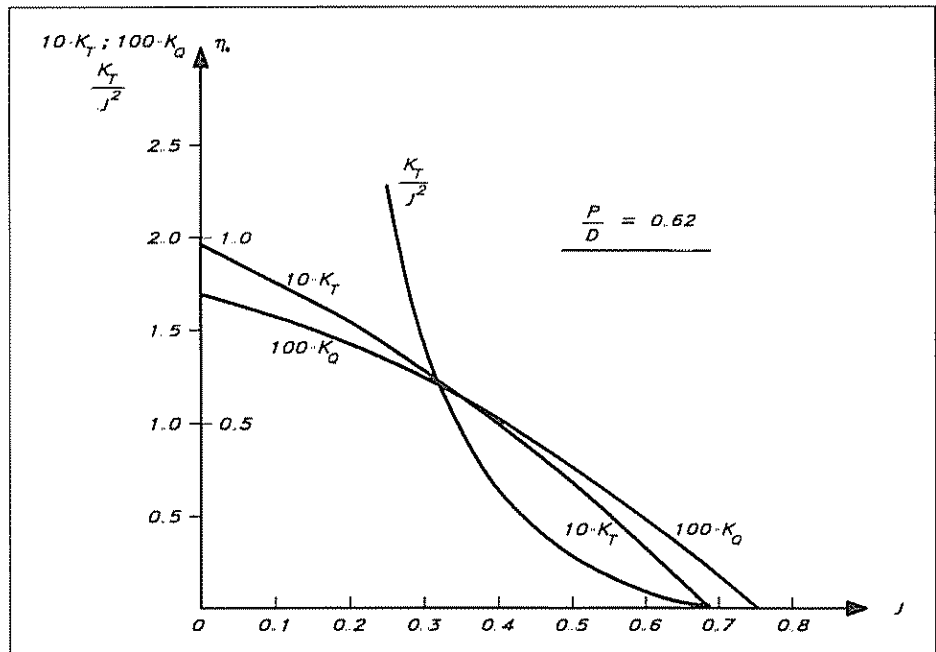


Fig 9.13 Propeller characteristics, 3-bladed Troost propellers (Courtesy of MARIN)



- 1 Assume that the velocity at the propeller is equal to the yacht speed, as before.
- 2 Compute the total resistance and assume that this is equal to the thrust, as before.
- 3 Compute the propeller loading,  $K_T/J^2$ .
- 4 Find the point on the loading curve in Fig 9.14 that corresponds to the computed value, and read the advance ratio and the torque coefficient on the same vertical line.
- 5 Compute the rate of revolutions from the definition of the advance ratio and the power from the torque and the angular frequency.

Fig 9 14 Interpolated  
2-bladed propeller  
characteristics



quantities must match the output curve of the engine, as we will see.

If the thrust coefficient is divided by the advance ratio squared, a quantity independent of the rate of revolutions is obtained. This quantity,  $K_T/J^2$ , is often referred to as the propeller loading, and it can be computed from the characteristics. This has been done in Fig 9.13. The computation may now proceed as follows:

All formulae required are given in Fig 9.15, which also presents calculations for the YD-40 at the three speeds used above. The results are plotted in the form of power versus rate of revolutions in Fig 9.16. Two curves are given, corresponding to the calm and rough weather cases. The limits for the engine are also indicated, representing the maximum engine output and the maximum rate of revolutions,

Fig 9.15 Computation of power required for non-optimum propeller – YD-40

	Calm weather			Rough weather		
	7	8	8.5	7	8	8.5
$V_A = V$ [knots]						
$V_A = V$ [m/s]	3.60	4.11	4.37	3.60	4.11	4.37
$T = R$ [N]	1300	2750	4000	3357	4880	6169
$D$ (given) [m]	0.53	0.53	0.53	0.53	0.53	0.53
Coefficient	0.347	0.563	0.724	0.896	1.000	1.118
$J$ (diagram)	0.475	0.415	0.385	0.355	0.340	0.330
$K_O$ (diagram)	0.0084	0.0100	0.0107	0.0114	0.0118	0.0122
$n$ [rps]	14.3	18.7	21.4	19.1	22.8	25.0
$P_D$ [kW]	6.60	17.5	28.2	21.4	37.6	51.2

$$\text{Coefficient} = \frac{K_T}{J^2} = \frac{T}{\rho \cdot D^2 \cdot V_A^2} = \frac{T}{289 \cdot V_A^2}$$

$$n = \frac{V_A}{D \cdot J}$$

$$P_D = 2\pi \cdot K_O \cdot \rho \cdot D^5 \cdot n^3 = 0.269 \cdot K_O \cdot n^3$$

respectively. The top corner of the 'allowable region' is the point for which the optimum propeller was designed, ie 26 kW and 20 rps. Due to the fact that the chosen propeller is not optimum this corner is not reached. At the maximum rate of revolutions the engine develops 22 kW with this propeller and the speed is about 8.2 knots in calm weather. As we have seen above, 8.4 knots would be reached with the optimum propeller. In rough weather we will use 25 kW at maximum rps and the speed will be around 7.2 knots, a reduction by about 0.3 knots, as compared to the optimum. This is very reasonable, however, and we are on the right side of the corner.

There are two reasons for being to the right of the corner. First, if the resistance for some reason gets larger than expected in rough weather, more power is required at all rates of revolution and we will move in the direction of the corner. There is thus a certain 'spare power' available for extra difficult situations. Had we been on the other side of the maximum, the power would have dropped under extra load. Secondly, we have used diagrams for fixed propellers in the design process, and they are certainly more efficient than the folding ones, so the actual power required is higher than that computed. The difference is hard to estimate, since characteristics for folding propellers are not available, but it could well be 20% in terms of efficiency, which would move the power curve to the other side of the corner. The efficiency would then be around 0.5 rather than around 0.6, as in the calculations above. For lack of better information we will consider the propeller designed as adequate.

**Check of blade area**

If the propeller is very highly loaded the pressure on the suction side may get so low that the water evaporates, ie bubbles of vapour are created. If these are large the thrust is influenced and noise and erosion of the propeller blades occur. This is called cavitation. To avoid this problem the area of the blades carrying the thrust must be large enough. A simple check may be made using a method proposed by Burrill. We will describe this in the following discussion.

Fig 9.16 Engine and propeller power

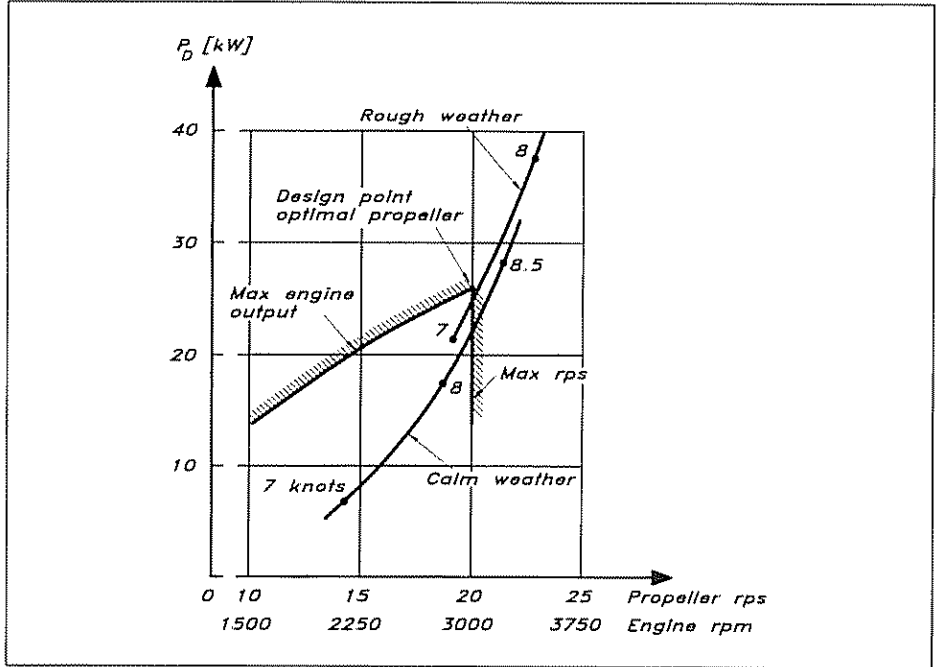


Fig 9.17 Burrill diagram

**Pressure at propeller shaft:**  
 $P_p = P_{atm} + \rho \cdot g \cdot h_p$   
 $P_{atm}$  : Atmospheric pressure  
 $h_p$  : Depth at propeller shaft

**Cavitation number :**  

$$\sigma = \frac{P_p - P_v}{\frac{1}{2} \rho \cdot V_A^2 \cdot [1 + (\frac{Q_A Z \pi}{J})^2]}$$
 $P_v$  : Vaporization pressure

**Blade area :**  

$$\frac{A_D}{A_0} = \frac{T}{\tau \cdot \frac{1}{2} \rho \cdot V_A^2 \cdot [1 + (\frac{Q_A Z \pi}{J})^2] \cdot (1.067 - 0.229 \frac{P_D}{D}) \cdot \frac{\pi}{4} \cdot D^2}$$

$A_D$  : Developed blade area  
 $A_0$  : Area of propeller disk

The Burrill diagram plots the risk of cavitation  $\tau$  on the y-axis (0.1 to 0.3) against the cavitation number  $\sigma$  on the x-axis (0 to 0.6). A diagonal line represents the 'Upper limit according to Burrill'. The area above the line is shaded and labeled 'Risk of cavitation', while the area below is labeled 'No cavitation'.

The relevant formulae are given in Fig 9.17. First, a cavitation number is defined. This is the 'margin' to cavitation at the propeller shaft in dimensionless form. The nominator thus contains the difference between the static pressure at the shaft and the vaporization pressure at the temperature in question, while the denominator is the dynamic pressure at 70% of the propeller radius. The static pressure at the shaft is the sum of the atmospheric and hydrostatic pressures at this depth, as shown in the Fig 9.17.

Having computed the cavitation number the diagram in Fig 9.17 may be used for finding the maximum value of the quantity  $\tau$  for non-cavitating conditions. This value is simply read from the line and used in the formula for the minimum blade area ratio. Note that this ratio is defined by the developed area, ie the sum of the areas of the blades considered 'flattened out and untwisted' and the area of the propeller disk.

In Fig 9.18 the blade area is checked for the YD-40. The worst case is the one having the largest loading  $K_T/J^2$ . In the calculations of Fig 9.15, this is the 7 knots heavy weather case. The 8 and 8.5 knots will not be reached, as we have seen. Using the values of the table in Fig 9.15 and a propeller depth of 0.48 m, the minimum blade area ratio becomes 0.285. As we have already noted, the Troost propeller designed had a ratio of 0.3, so this is large enough. Had the area been too small a larger diameter would have helped. Three-bladed propellers have larger blade area ratios, but they cannot be folded and have a very large drag when sailing.

Fig 9.18 Computation of blade area required – YD-40

Calculation according to Fig 9.17

$$h_p = 0.48 \text{ [m]}$$

$$P_{atm} = 101300 \text{ [Pa]}$$

$$P_p = 101300 + 1025 \cdot 9.81 \cdot 0.48 = 106127 \text{ [Pa]}$$

$$P_v = 2300 \text{ [Pa], at } 20^\circ\text{C}$$

$$\frac{P}{D} = 0.62$$

$$D = 0.53 \text{ [m]}$$

Worst case – rough weather, 7 knots (see Fig 9.15):

$$V_A = 3.60 \text{ [m/s]}$$

$$J = 0.355$$

$$T = 3357 \text{ [N]}$$

$$\sigma = \frac{106127 - 2300}{0.5 \cdot 1025 \cdot 3.60^2 \cdot [1 + (\frac{0.7\pi}{0.355})^2]} = 0.40$$

$$\tau = 0.220 \text{ (diagram Fig 9.17)}$$

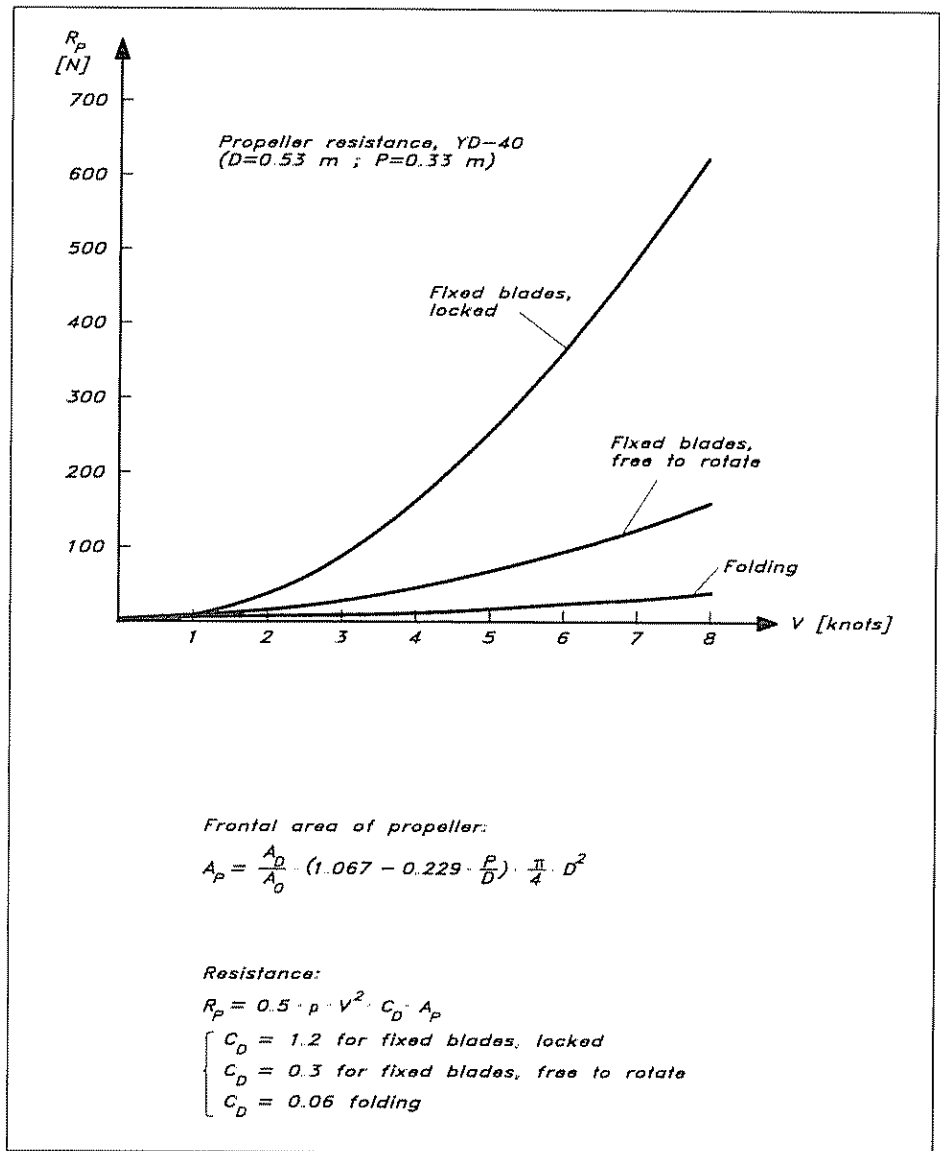
$$\frac{A_D}{A_0} = \frac{3357}{0.220 \cdot 0.5 \cdot 1025 \cdot 3.60^2 \cdot [1 + (\frac{0.7\pi}{0.355})^2] \cdot (1.067 - 0.229 \cdot 0.62) \cdot 0.25 \cdot \pi \cdot 0.53^2} = 0.285$$

**Propeller resistance**

The propeller resistance when sailing may be estimated using the frontal area of the propeller and some suitable drag coefficient. To obtain the area an approximate relation shown in Fig 9.19 may be used, and the drag coefficient for a fixed propeller, locked in position and outside the wake of the keel, may be set to 1.2. The resistance is then obtained easily as shown in the figure. If the propeller is completely free to rotate, its resistance is reduced to only about one fourth of that of a locked propeller. This is, however, an ideal situation. In practice the clutch and the friction will slow down the rotation. Outstanding from a resistance point of view is the folding propeller with a resistance that is normally less than 5% of that of the fixed and locked one.

In Fig 9.19 the resistance of the YD-40 propeller has been plotted for varying speeds. If a propeller with fixed blades and locked in position was to be used, the resistance at the typical upwind sailing

Fig 9.19 Propeller resistance when sailing



speed of 6.8 knots used in Fig 5.4 would be 460 N. This is 29% of the total resistance without propeller, and it would reduce the speed by about 0.8 knots for a given driving force. If the propeller were completely free to rotate the effect would be four times smaller, ie a 0.2 knots speed reduction. Most yachtsmen prefer to reduce the speed loss even more and use a folding propeller, for which the loss in our case would be less than 0.04 knots.

# 10

# HIGH SPEED HYDRODYNAMICS

---

Although the emphasis of this book is on sailing yachts, much of the theory presented is the same for power boats. There is no difference in the hull geometry definition or the principles for producing a drawing, manually or using a CAD system. The displacement of the yacht, as well as its static and dynamic stability properties, are computed in exactly the same way as for the sailing yacht. Neither is there any basic difference in the flow around the hull nor in the associated viscous and wave resistance components. The upright resistance may thus be obtained by the formulae presented in Chapter 5 up to a Froude number of about 0.7 and the same is true for the added resistance in waves. Heel resistance is obviously irrelevant, but induced resistance as well as lift is of importance in the design of efficient power boat rudders. Both planform and profile need to be considered. A reader only interested in power boats can safely skip the two chapters on sails and balance, but he should pay keen interest to the preceding chapter on propellers and engines.

An area not covered in the foregoing is the special hydrodynamics of high speed craft, ie craft operating in the planing mode. Few sailing yachts reach this speed range, although some very special sailing craft like windsurfers or extremely light dinghies may be fast enough. Planing power boats are, however, becoming more and more popular, and to satisfy the interested power boat enthusiasts the present chapter on high speed hydrodynamics has been included.

## Planing

According to Archimedes, the buoyancy of a body wholly or partly submerged in a fluid is equal to the weight of the displaced volume of fluid. The buoyancy, which is caused by the hydrostatic pressure in the fluid, was dealt with in Chapter 4. At zero speed this force balances exactly the weight of a floating body. However, as soon as the body starts moving, the hull puts water particles into motion by exerting a force on each particle. The same force, but in the opposite direction, is exerted on the hull. This force per unit area may be called the hydrodynamic pressure. Although not distinguished in this way, we have seen this pressure in Fig 5.4, and we have found in Chapter 5 that it is responsible for both the viscous pressure resistance and the wave resistance. These two resistance components are caused by the longitudinal component of the pressure force over the hull surface. In the vertical direction the hydrodynamic pressure causes the hull to sink (or rise) and trim. At high speed this vertical pressure force may be considerably larger than the buoyancy, lifting the hull more or less

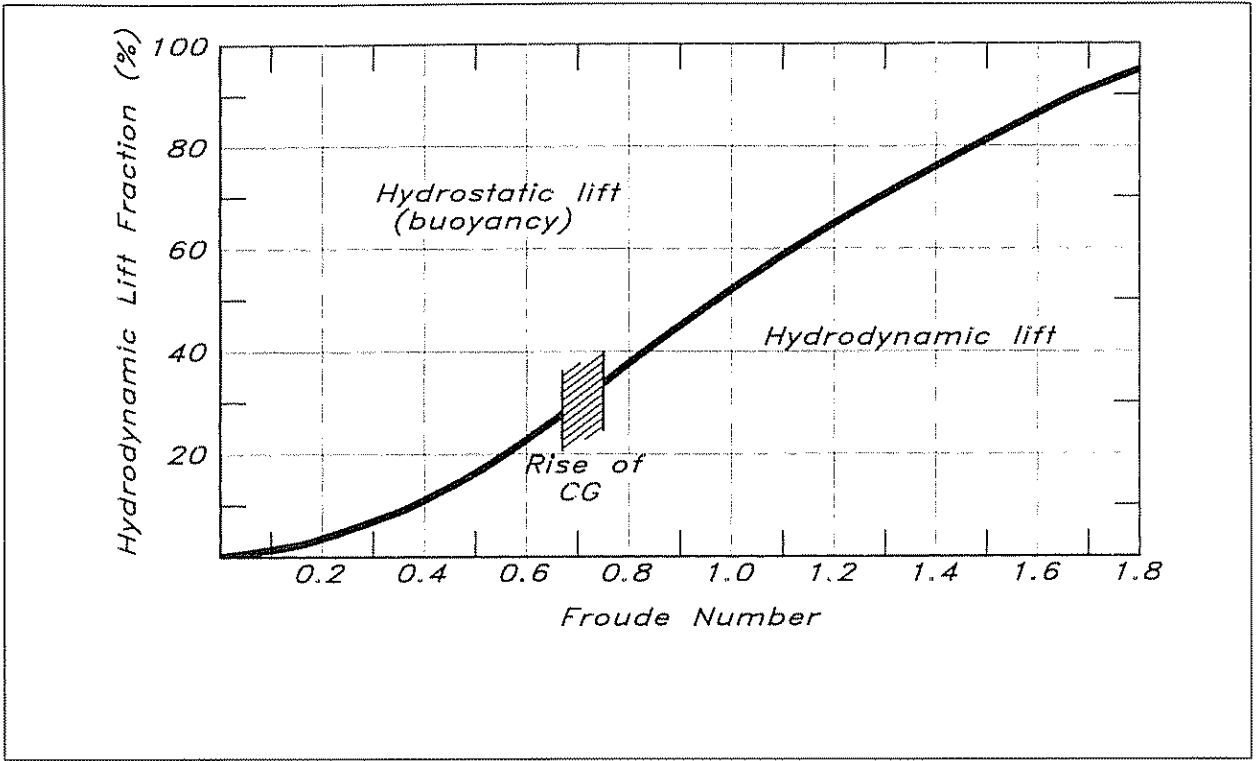


Fig 10.1 Distribution of hydrostatic and hydrodynamic lift components at varying Froude numbers (example)

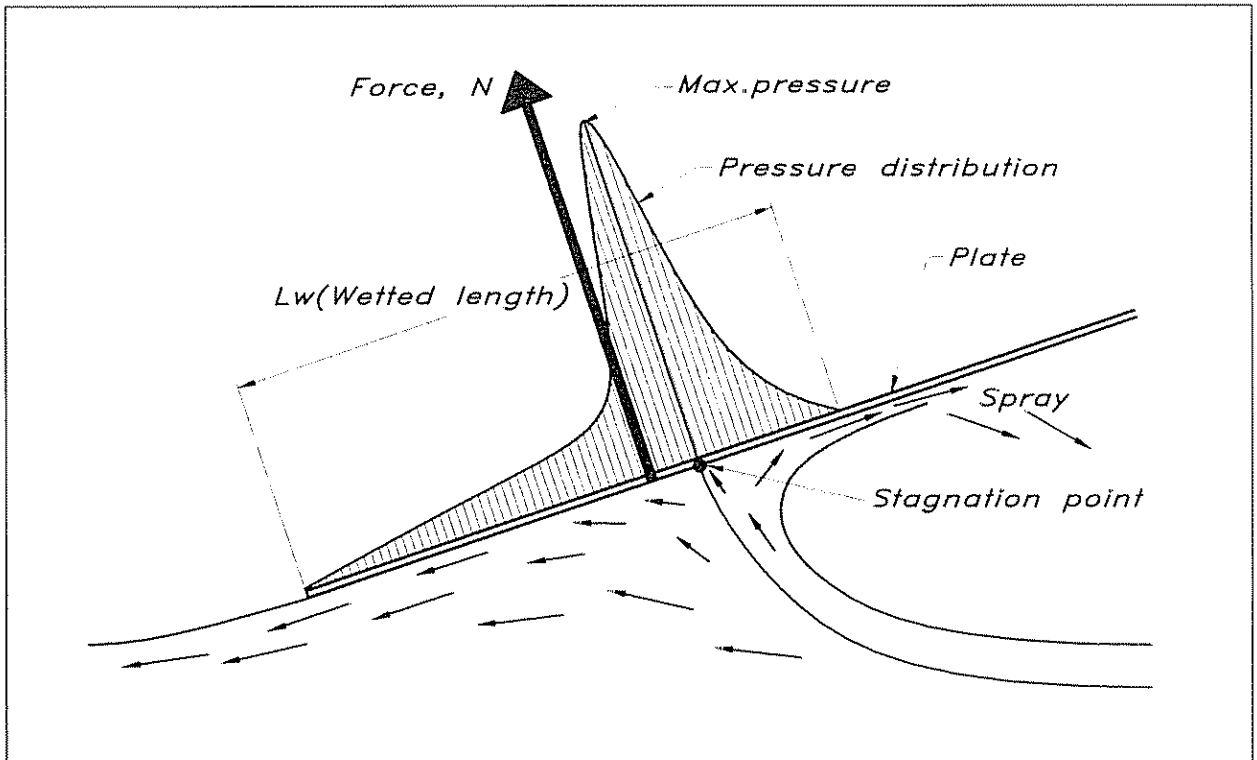


Fig 10.2 Pressure and velocity distribution beneath a planing flat plate (principle)



completely out of the water. A hull predominantly supported by the hydrodynamic pressure is considered to be planing. Note that not all hulls may reach speeds high enough for this to occur. Fig 10.1 shows the hydrodynamic and the hydrostatic lift components for a typical high speed hull at varying Froude numbers.

The basic principles of planing may be explained with reference to Fig 10.2, which shows the flow beneath a flat plate skimming along the water surface. Velocity vectors are displayed to show the direction of the flow relative to the plate. It is seen that at one point the flow hits the plate at right angles. This is the stagnation point, where the flow is divided into two parts, one going backwards and one forwards. At the stagnation point the pressure (hydrodynamic) is very high, since all the kinematic energy has been converted into pressure. There is no flow relative to the plate at this position. On both sides of the stagnation point the pressure is reduced and eventually it drops to zero. This happens at the trailing edge and at the forward location where the velocity has become parallel to the plate. Further forward the thin water sheet breaks down into spray, which drops down onto the water surface.

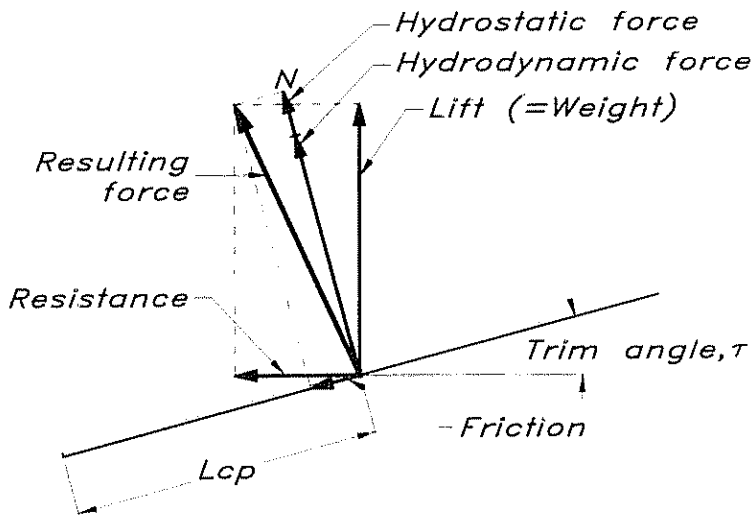
The high pressure creates a force at right angles to the plate, i.e. a force tilted backwards from the vertical the same angle as the pitch angle of the plate. The vertical component is the lift which has to balance the weight of the boat, while the horizontal component is the total pressure resistance, essentially the wave resistance.

In reality, the idealized picture above is somewhat more complicated. First, there is always some hydrostatic pressure present. Obviously this component is also at right angles to the plate and it adds to the pressure of Fig 10.2. As appears from Fig 10.3, this means an increase in both lift and drag. There is thus a resistance component caused by the hydrostatic pressure. For a displacement hull the hydrostatic pressure forces acting backwards on the forebody are more or less balanced by those on the afterbody acting forwards. The latter forces are almost entirely missing on a planing hull where the transom is dry.

A second complicating factor is friction, which is parallel to the plate. Although there is some component in the forward direction in front of the stagnation point, the resulting frictional force points essentially backwards and increases resistance. There is also a small reduction in the lift force. It is interesting to note that if it were not for the friction the resistance of the plate would be uniquely defined by its weight (which is equal to the total lift) and the trim angle.

If the weight of the plate is changed the lift has to change correspondingly. A weight increase may thus be compensated by an increase in trim or wetted surface. In the latter case the plate is sunk a little deeper into the water and the friction is increased. To increase the trim angle the centre of gravity has to be moved backwards.

Savitsky at the Davidson Laboratory carried out a large series of systematic experiments for planing surfaces and proposed several general relations which are frequently used by designers of high speed hulls. In Fig 10.3 a formula is found for computing the lift force, given the length



Lift according to Savitsky (neglecting friction):

$\lambda$  : Wetted length-beam ratio  $\frac{L_w}{b}$

$\tau$  : Trim angle [°]

$C_v$  : speed coefficient  $\frac{V}{\sqrt{g \cdot B}}$  (Beam Froude number)

$V$  : Speed [m/s]

$C_{L_0}$  : Lift coefficient =  $\frac{m \cdot g}{0.5 \cdot \rho \cdot V^2 \cdot b^2}$

$$C_{L_0} = \tau^{1.1} \cdot \left( 0.012 \cdot \lambda^{0.5} + 0.0055 \cdot \frac{\lambda^{2.5}}{C_v^2} \right)$$

Centre of pressure:

$L_{cp}$  : Distance from centre of pressure to trailing edge [m]

$$\frac{L_{cp}}{L_w} = 0.75 - \frac{1}{\frac{5.21 \cdot C_v^2}{\lambda^2} + 2.39}$$

Fig 10.3 Forces on a flat planing surface

to beam ratio of the wetted surface and the trim angle. Note that the beam is used as a reference length in the speed coefficient (corresponding to the Froude number) and the lift coefficient. The first term in the lift formula is the contribution from the hydrostatic contribution, while the second one is the hydrodynamic pressure.

At first glance it may appear as if both contributions to the lift would increase with an increasing length to beam ratio. However, this holds only for a lift coefficient which has been obtained by dividing by beam squared. Had this coefficient been defined in the usual way by the wetted surface the first term would have decreased with length to beam ratio. A wide and short planing surface is thus more efficient in generating dynamic lift than a long and narrow one. As we know from Chapter 6, this is also the case for wings. Wide hulls do, however, generate a much larger added resistance in waves, and in reality this puts a restriction on the beam.

Fig 10.3 also gives Savitsky's formula for the location of the centre of pressure of the planing surface. This location is important when determining the trim angle of a power boat, as will be seen below.

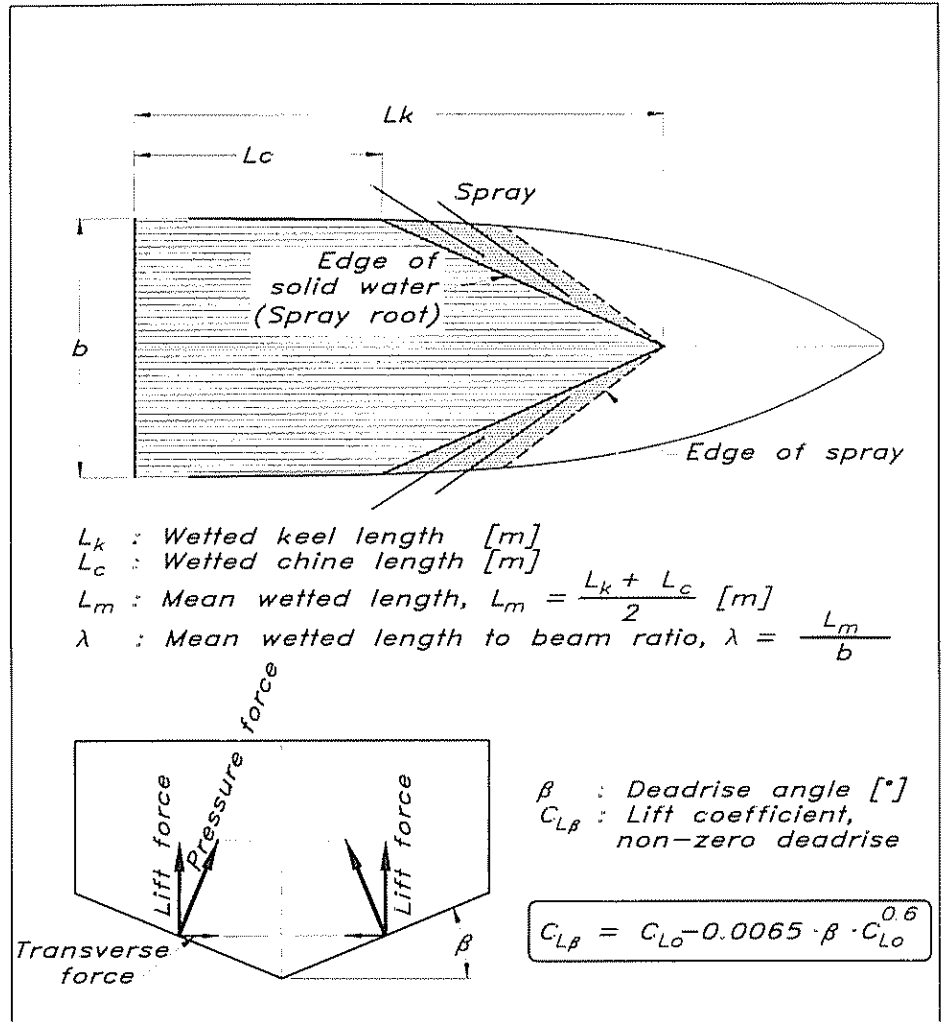
## Deadrise

A flat plate skimming along a water surface may be useful for explaining the basic principles of planing, and it may be of interest for surfboards and water skis, but power boat hulls almost inevitably have V-shaped sections, ie a so-called deadrise. The reason for this is the seakeeping qualities of the hull. A completely flat bottom would be impossible in a seaway, since the vertical accelerations would be too large. The ride would be extremely bumpy and put people on board in danger. V-shaped sections reduce the problem considerably; the deeper the V, the smaller the accelerations. However, the deadrise reduces the lift, so a larger wetted surface or trim angle is required, which both increase resistance.

The reason why deadrise reduces the lift force is that the water that hits the bottom of the boat may now be deflected sideways. In fact, for a normal deadrise angle most of the spray goes this way. As explained above, the hydrodynamic pressure that lifts the boat is caused by the reaction forces from the water particles which have been forced to change their direction when approaching the hull. For a flat plate the change in direction is almost  $180^\circ$  in the part of the flow in front of the stagnation point (see Fig 10.2). This results in high pressure. If the spray goes out sideways, however, the change in direction is much smaller and so is the reaction force. Further, this force is now tilted inwards, so a useless transverse component appears; see Fig 10.4, which also provides a formula for the change in lift due to the deadrise.

To understand the advantageous effects of the deadrise when it comes to seakeeping accelerations, compare the impact of a wedge hitting the free surface with that of a flat plate. In the latter case the entire surface of the plate hits the water simultaneously, while the wedge surface gets immersed gradually. The reaction force thus builds up much more slowly for the wedge.

Fig 10.4 The influence of deadrise on spray and pressure forces

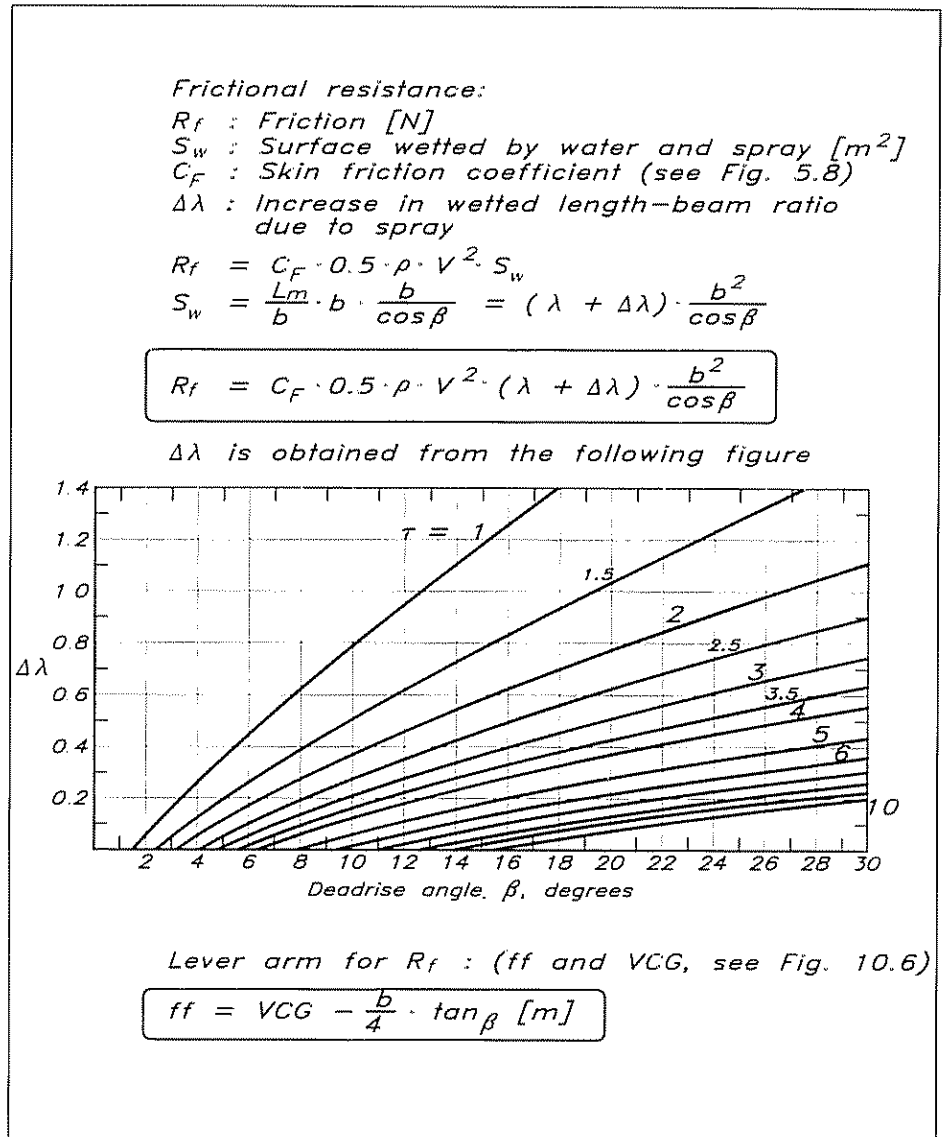


The spray from a bottom with deadrise normally increases the frictional resistance, since most of the spray actually goes backwards. Savitsky measured this effect and devised a spray correction to the wetted length to beam ratio. This correction is shown graphically for different deadrise and trim angles in Fig 10.5, which also gives the appropriate formulae for computing the frictional resistance.

**Forces on a planing hull**

Fig 10.6 shows a planing hull with the most important forces acting on the hull displayed. N corresponds to the pressure force in Fig 10.3 (hydrostatic and hydrodynamic contributions) and  $R_f$  is the friction. There is also the propeller thrust T and the resistance of the propeller drive, denoted  $R_a$ , where the index 'a' stands for appendage. For a hull with a propeller on a shaft the resistance from all appendages like the shaft, shaft brackets and rudder must be considered. Useful formulae for streamlined shapes and inclined circular cylinders are given in Fig 10.7. The direction of the appendage forces vary somewhat, but without too much loss in generality they may be assumed parallel to the keel

Fig 10.5 Calculation of the frictional resistance of the hull

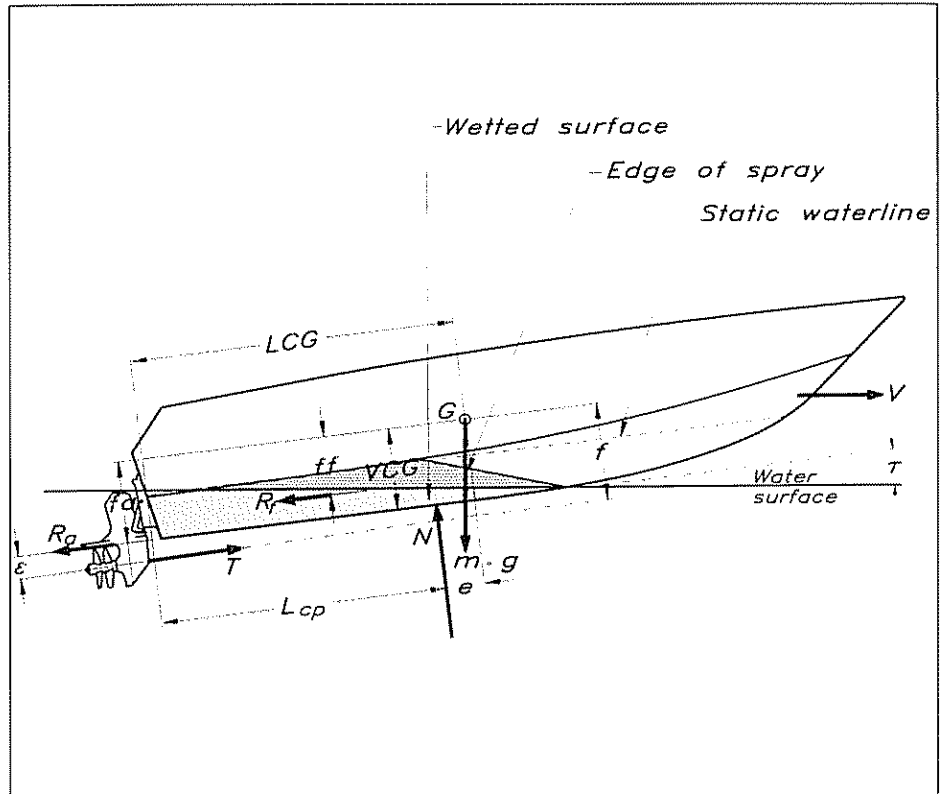


line. Some lift may be generated by the appendages, particularly the shaft, but this is neglected in the following.

The weight is shown as a force  $mg$  acting vertically through the centre of gravity  $G$ . To compute the moments this point may be taken as the origin. It is seen that  $N$ ,  $R_f$  and  $R_a$  create a moment to trim the boat by the bow and that their respective lever arms are  $e$ ,  $ff$  and  $fa$ . The propeller thrust, on the other hand, creates a bow-up moment with the arm  $f$ . The hull automatically attains a trim angle where the moments cancel, ie the net moment is zero. Thus, for example, if there is a net moment to trim the boat by the bow the trim will become smaller and the force  $N$  moved forwards until balance is achieved.

If a bow-down moment is applied to a hull originally at an optimum trim angle, the new smaller trim means that the hydrodynamic pressure is reduced. On the other hand, the wetted surface is increased, so it may

Fig 10.6 Forces on a planing hull



Resistance of rudders and brackets:

- $R_r$  : Rudder or bracket resistance [N]
- $S_r$  : Wetted surface [m<sup>2</sup>]
- $C_{Fr}$  : Skin friction coefficient (see Fig. 5.8)
- $\frac{t}{c}$  : Thickness to chord length ratio

$$R_r = 0.5 \cdot \rho \cdot V^2 \cdot S_r \cdot C_{Fr} \cdot \left[ 1 + 2 \cdot \frac{t}{c} + 60 \cdot \left( \frac{t}{c} \right)^4 \right]$$

Resistance of propeller shaft:

- $R_{sh}$  : Shaft resistance [N]
- $l$  : Shaft length in water [m]
- $d$  : Shaft diameter [m]
- $\epsilon$  : Shaft angle relative to flow [°]
- $C_{Fsh}$  : Skin friction coefficient based on shaft length

$$R_{Fsh} = 0.5 \cdot \rho \cdot V^2 \cdot l \cdot d \cdot (1.1 \cdot \sin^3 \epsilon + \pi \cdot C_{Fsh})$$

Fig 10.7 Appendage resistance

Fig 10.8 Moments, trim and resistance

*Bow-down moment (M):*

$$M_h = g \cdot m \cdot \left[ \frac{e \cdot \cos(\tau + \varepsilon)}{\cos \varepsilon} - f \cdot \frac{\sin \tau}{\cos \varepsilon} \right]$$

$$M_f = R_f \cdot \left[ f_f - e \cdot \tan \varepsilon - \frac{f}{\cos \varepsilon} \right]$$

$$M_a = R_a \cdot \left[ f_a - e \cdot \tan \varepsilon - \frac{f}{\cos \varepsilon} \right]$$

$$M = M_h + M_f + M_a \quad [Nm]$$

*Linear interpolation between two computed moments,  $M_1$  and  $M_2$ , at two trims,  $\tau_1$  and  $\tau_2$ , to find  $\tau_0$ , giving zero moment:*

$$\tau_0 = \tau_1 - \frac{M_1 \cdot (\tau_2 - \tau_1)}{M_2 - M_1}$$

*Linear interpolation between two computed frictional resistance values  $R_{f1}$  and  $R_{f2}$  to find  $R_{f0}$  corresponding to the trim angle  $\tau_0$*

$$R_{f0} = R_{f1} + \frac{R_{f2} - R_{f1}}{\tau_2 - \tau_1} \cdot (\tau_0 - \tau_1)$$

*Resistance:*

$$R = [g \cdot m \cdot \sin \tau_0 + R_f] \cdot \frac{\cos(\tau_0 + \varepsilon)}{\cos \varepsilon} \quad [N]$$

*Effective power*

$$P_E = V \cdot R \quad [W]$$

be that the lift is still large enough. If it is not, the hull will sink down until the increased hydrostatic buoyancy will make up for the loss in hydrodynamic lift. In both cases there is an increase in friction which outweighs the advantage of having the force  $N$  pointing less backwards. This situation occurs if the centre of gravity is too far forward.

If the centre of gravity is too far aft, a net moment to trim the boat by the stern will increase the trim, thereby increasing the pressure and reducing the wetted surface. The hull rides higher, which is good, since friction is reduced, but the larger drag component of the force  $N$  makes the total resistance larger. When the centre of gravity is too far aft, often an instability occurs. Increasing the trim, the force  $N$  moves too far aft, causing a bow-down moment. The bow falls down, and the process is repeated. We have a porpoising boat, a phenomenon not that uncommon.

It is thus very important to design the boat to achieve equilibrium at the reasonable trim angle, and a procedure for calculating trim and resistance is described overleaf. This scheme is a simplification of a procedure proposed by Hadler, based on Savitsky's previous work. Hadler's original paper (*Trans. Society of Naval Architects and Marine Engineers*, Vol. 74, 1966) includes the effect of the propeller on the pressure forces on the hull and a procedure for correcting the propeller characteristics for the shaft inclination relative to the flow. Some lift

## Procedure for finding the equilibrium trim angle and the corresponding resistance and power

- 1** First determine the following quantities:  
 $m$ : Mass displacement  
 $LCG$ : Distance from transom to centre of gravity  
 $VCG$ : Distance from baseline (keel) to centre of gravity  
 $b$ : Maximum beam between chines (or between spray rails, see the next section)  
 $\epsilon$ : Propeller shaft inclination relative to baseline  
 $\beta$ : Deadrise angle (take the average of the angles at the transom and at the CG)  
 $f$ : Distance between shaftline and centre of gravity  
 $V$ : Speed
- 2** Compute the speed coefficient  $C_V$  (Fig 10.3).
- 3** Compute the lift coefficient from its definition in Fig 10.3 (ie use the formula including  $m$  and  $g$ ). In Fig 10.3, which is for flat plates, this gives  $C_{L0}$  but for a hull with a deadrise it will give  $C_{L\beta}$ .
- 4** Compute the corresponding  $C_{L0}$  from formula for  $C_{L\beta}$  (Fig 10.4) by trial and error, ie try to find the  $C_{L0}$  that gives the  $C_{L\beta}$  computed in step 3.
- 5** Assume a trim angle  $\tau$ , say  $4^\circ$ .
- 6** Compute the wetted length to beam ratio  $\lambda$  from the framed formula for  $C_{L0}$  in Fig 10.3 by trial and error, ie try to find the  $\lambda$  that gives the  $C_{L0}$  obtained in step 4.
- 7** Compute the mean wetted length  $L_m$  from  $\lambda$  (Fig 10.4) and calculate the Reynolds number.
- 8** Compute the skin friction coefficient  $C_f$  using the ITTC formula (Fig 5.8).
- 9** Find the increase in  $\lambda$  due to spray,  $\Delta\lambda$ , and compute  $R_f$  (Fig 10.5).
- 10** Compute the lever arm  $ff$  for  $R_f$  relative to the centre of gravity (Fig 10.5).
- 11** Compute the resistance  $R_a$  for all appendages according to the formulae of Fig 10.7.
- 12** Compute the lever arm's  $f_a$  relative to the centre of gravity of the hull. Assume that the force acts on the centroid of the wetted surface for each appendage and is parallel to the baseline.
- 13** Compute the distance of the centre of pressure from the transom,  $L_{cp}$ , from formula in Fig 10.3 ( $L_w$  is equal to  $L_m$  for a bottom with deadrise).
- 14** Compute the lever arm for the pressure force,  $e$ , as the difference between  $LCG$  and  $L_{cp}$ .
- 15** Compute the resulting bow-down moment  $M$  from the formula of Fig 10.8. This equation is derived in Hadler's paper considering the horizontal and vertical force balance.
- 16** Most likely, the computed moment will be different from zero, so the trim angle has to be changed to obtain balance. Go back to step 5 and repeat the calculations with another trim. (If the computed bow-down moment is positive, reduce the trim angle and vice versa.)
- 17** Compute the trim angle for zero moment by linear interpolation (extrapolation) between the two computed moments. Use the formula of Fig 10.8.
- 18** Compute the frictional resistance at this trim angle by linear interpolation between the two computed values (Fig 10.8).
- 19** Compute the resistance from the formula of Fig 10.8.
- 20** Compute the effective power from the formula of Fig 10.8.



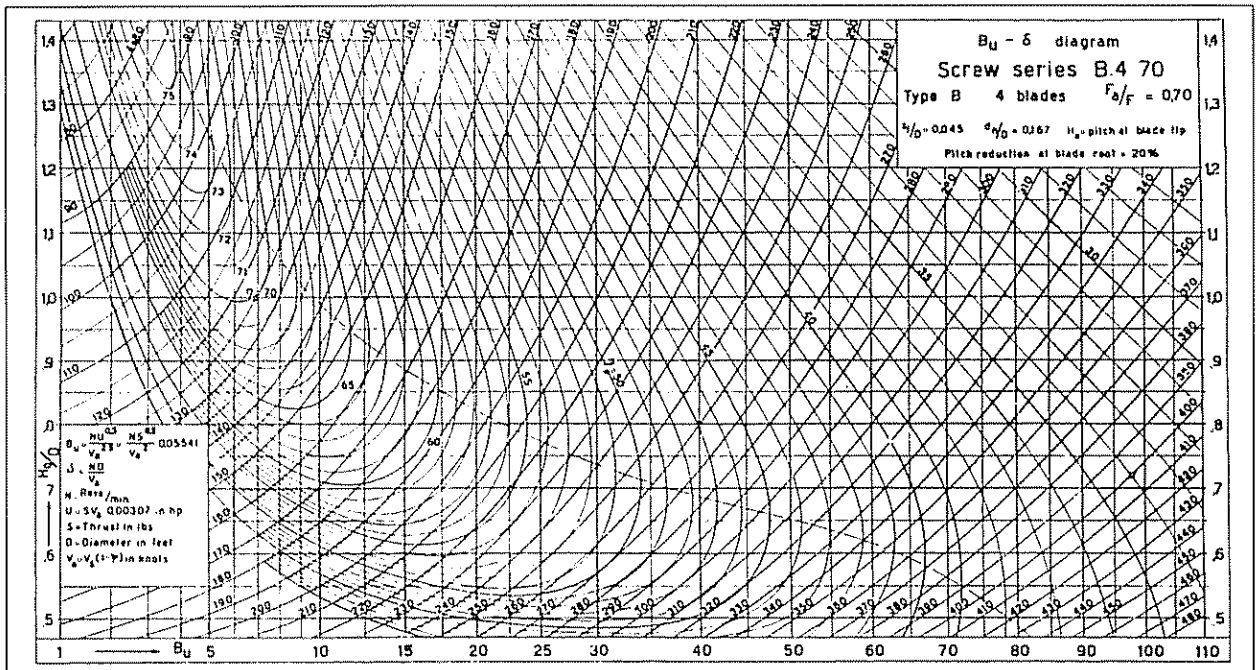


Fig 10 9  $B_u-\delta$  diagram, 4-bladed propellers with an area ratio of 0.70 (By courtesy of MARIN)

forces on the appendages are also included. These effects are neglected here, as well as the air resistance. Although Hadler’s work is old it still seems to be the most accepted procedure for planing hull predictions.

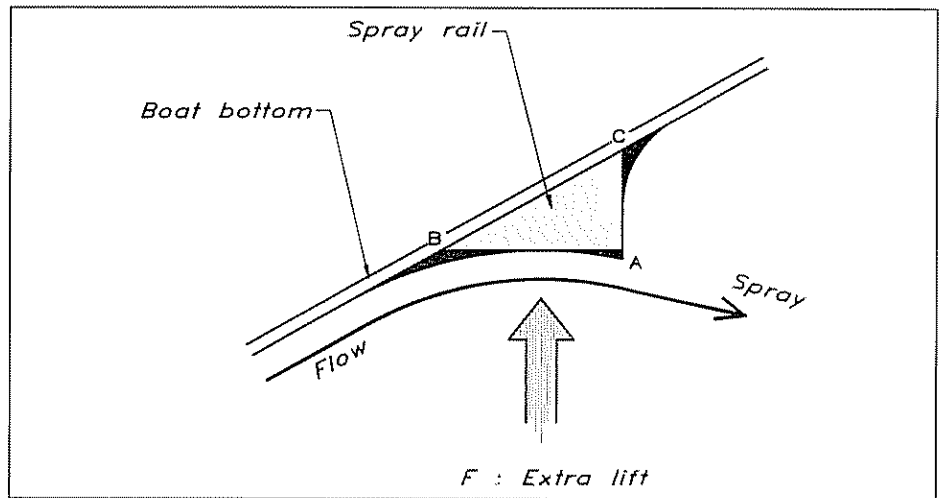
The effective power  $P_E$  is the power made good when driving the boat. To obtain the real power required to turn the propeller (the delivered power  $P_D$ ),  $P_E$  must be divided by the propulsive efficiency. In Chapter 9 the total propulsive efficiency was assumed to be equal to the propeller efficiency, which can be read from diagrams of the type presented in Figs 9.8 and 9.9. The same approximation may be adopted here. However, a more appropriate diagram in this case is that of Fig 10.9, which is for four-bladed propellers with an area ratio of 0.70. The procedure for designing an optimum propeller described in Chapter 9 may now be used, assuming that the resistance obtained above is equal to the propeller thrust. Note that we have now neglected the resistance increase in rough weather. This is permissible, since the boat cannot normally drive at full speed in rough weather anyhow.

Although the procedure described in this section includes several simplifications it should be useful for optimizing the trim angle and the corresponding location of the centre of gravity, as well as for estimating the required power. Normally a good target for the trim angle is  $4^\circ$ . Readers interested in more details are referred to Hadler’s original paper.

**Spray rails, stepped bottoms and transom flaps**

As we have seen above, a deep V-shape is good for seakeeping performance, but not very efficient in generating lift. One way to improve the lift production is to add spray rails along the hull. A typical cross section of such a rail is shown in Fig 10.10. When the water flows sideways, as shown in Fig 10.4, it is forced to turn downwards by the rail. This creates a lift. The rail should be as sharp as possible at point

Fig 10 10 Cross section of a spray rail



A, where the water leaves the hull, but it should be smoothly blended into the main hull at point B to reduce resistance. In order not to create a larger resistance than necessary at speeds where the rail does not work, a smooth junction at C is also recommended. To increase the lift further, the surface between B and A may be inclined downwards.

Since the water runs sideways mainly on the forebody, the rails are most efficient in this region. Further back, where the flow is more or less parallel to the keel, they may be cut. Keeping them in this region may increase the resistance, but can be justified as anti-rolling devices.

Spray rails on a planing hull are shown Fig 10.11. The wetted surface at two speeds is also indicated. If the speed will not exceed 25 knots it may be wise to cut the outer rail at D, since it will be useless further aft. However, if the hull may attain a speed of 40 knots the wetted surface must be reduced. Had the outer rail been cut, the water would have continued to clear the hull at the chine and the centre of pressure would have been moved too far aft. This would have caused the bow to fall, resulting in a larger resistance and also possibly steering problems. If the rail is kept all the way to the stern the wetted beam (between rails) becomes smaller, which means that the wetted length is not so much reduced when the speed increases. The centre of effort thus does not move that far backward and the hull maintains its trim better. Note that the beam used in the calculations above is now the distance between the rails. There is no accurate procedure developed for the extra rail lift, but their effect may be roughly included by measuring the deadrise angle from the keel to the outer edge of the active rail. This angle is smaller than that measured along the surface and so yields a higher lift.

Spray rails should not be too effective on the forebody of the hull. If high lift is developed when the forebody hits a wave, large accelerations will occur, reducing the positive effect of the V-shape. Therefore, the rails should be made smaller in this region and the bottom side should be inclined upwards rather than downwards.

Stepped bottoms have been used for a very long time to improve performance. A very famous design was *Maple Leaf*, built in wood in

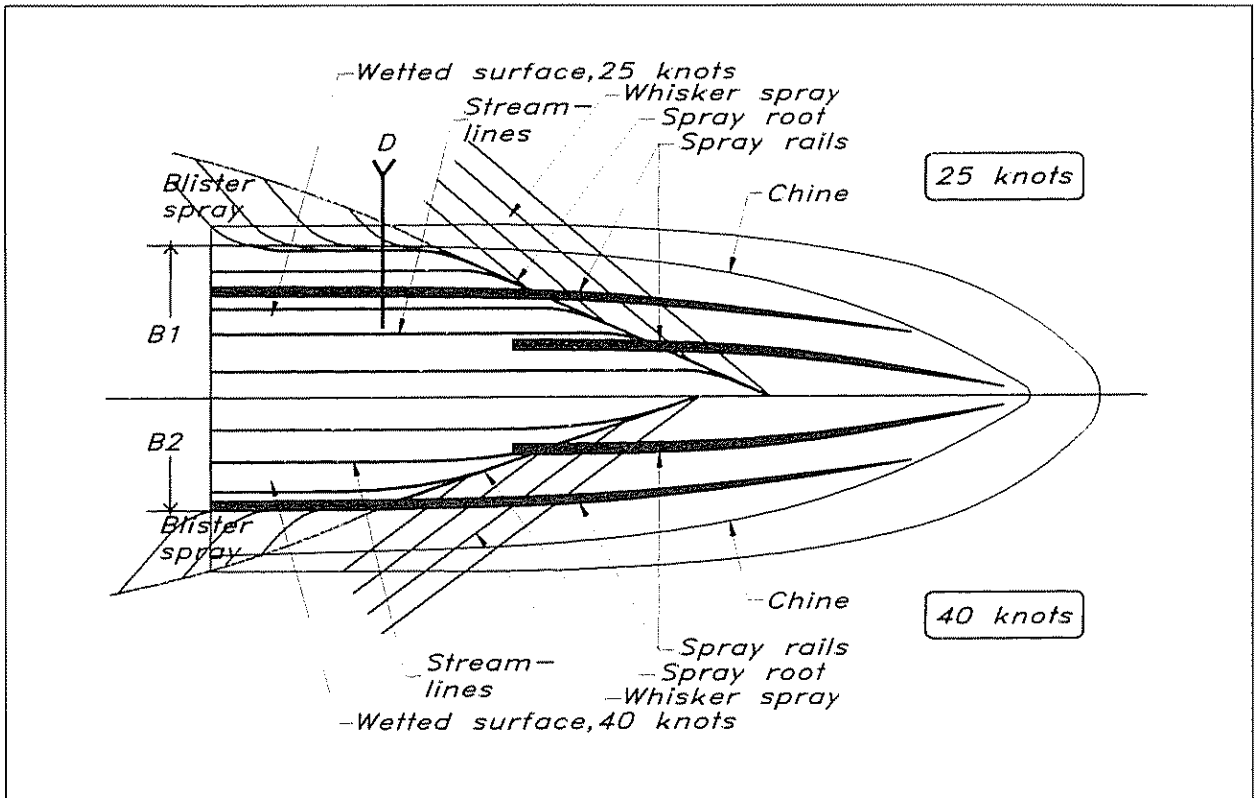
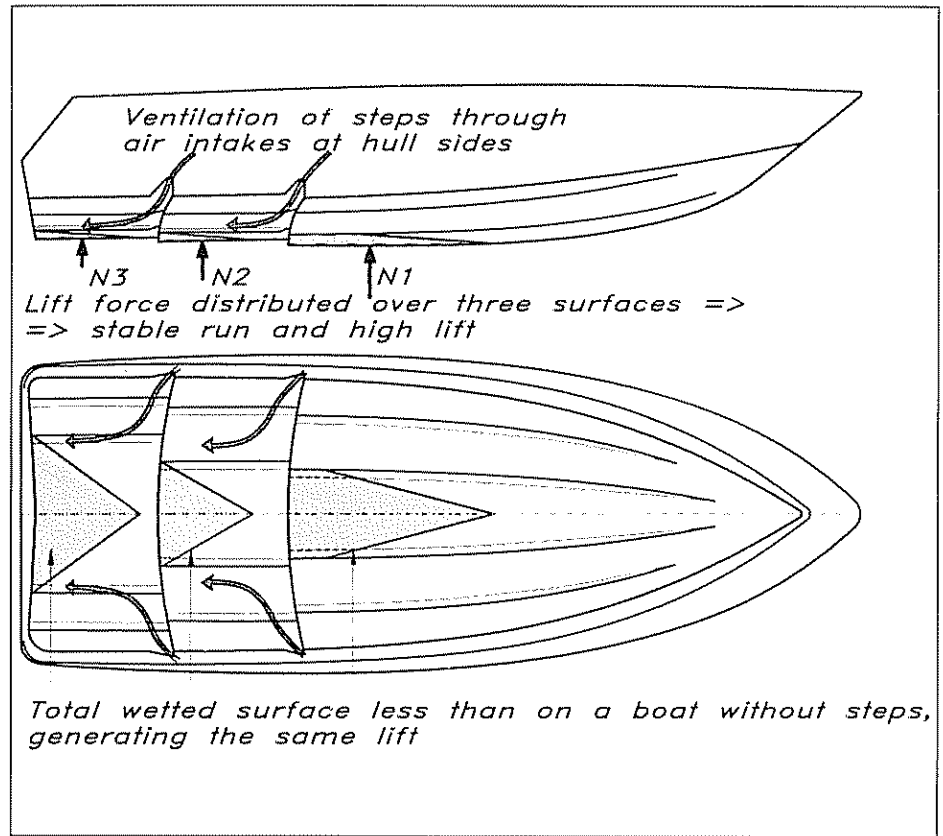


Fig 10.11 Spray rails on a planing hull

1912, and since then many successful racing hulls have had this type of bottom. The reason why the stepped hulls are more effective is that the wetted area is divided into several smaller areas each with a large beam compared to the length; see Fig 10.12. As we have seen above, the lift production is more efficient for a surface with a small length to beam ratio. (The planing bottom is different from a wing, where it usually does not help splitting the surface into several tandem wings.) The increased lift generation capability means that the total wetted surface may be reduced, as well as the friction.

Fig 10.12 shows that the region behind each step has to be ventilated. Air thus has to be sucked into this region in sufficient quantities. Normally this is not a problem since the pressure is very low, but it is extremely important that the air supply is not cut. New air is continuously needed since the water entrains the air behind each step. This may be achieved most simply by extending the step sideways to the open air at the hull's side. However, this principle is somewhat dangerous, since these openings may be closed temporarily (and momentarily!) by waves. When the air supply is lost, a backflow occurs behind the step causing an excessive increase in resistance. The speed thus drops momentarily – a dangerous situation, which may even cause injuries to the crew. If the supply is cut only on one side the hull will turn abruptly, and possibly even capsize. To avoid this problem, air is often sucked through openings well above the waterline, or it may be supplied through tubes from deck level. Another possibility is to

Fig 10.12 *Hull with steps*

discharge the exhaust gases through the step. In this way the gases will be sucked out, improving the efficiency of the engine.

Since the lift is now spread to several surfaces along the hull (see Fig 10.12) the longitudinal stability becomes very large. It is difficult to change the trim. This is no problem in smooth water, but in a seaway the hull may tend to follow the contour of the waves. Larger hulls may acquire a tendency to bump into the next wave, making the ride very uncomfortable. Smaller boats, which tend to jump between the waves, are not so affected by this problem.

Another effect of spreading the lift to several efficient surfaces, one after the other, is that the transverse stability may be put in jeopardy. The hull rides high on a very narrow set of wetted surfaces. At very high speeds some designers have chosen to take advantage of the aerodynamics of the above-water part of the hull, using wing-like devices to keep the hull upright.

Transom flaps may be fitted to the hull to control the trim. Temporary adjustments for correcting changes in the centre of gravity may thus be made easily. The flaps may also be used to adjust the trim when the hull is running at off-design speeds, for instance in restricted waters or when the hull is under acceleration. This reduces the fuel consumption and, even more importantly, the generated waves, which may be excessive at these speeds. It is also possible to use the flaps for adjusting the trim in a seaway to reduce the bumpiness.

**Dynamic stability**

There are two important dynamic stability phenomena for high speed hulls. One is caused by the large centrifugal forces generated when a hull at high speed changes its direction. The other occurs due to the suction forces which may be generated near the chines due to convexity of the hull buttocks. We will deal with both in the following.

When the rudder is given an angle of attack a force is generated sideways. This causes the hull to start moving in this direction and, since the force is aft of the centre of gravity, the hull also starts to rotate. After a short while the hull has obtained an angle of attack to the flow and a side force opposing the rudder force develops, mostly on the forebody. Now the direction of motion has started to change; the path is curved. A centrifugal force directed 'outwards', ie in the same direction as the rudder force, is now gradually built up. (See Fig 10.13.)

It is seen that the pressure force on the 'outer' side is larger than that on the 'inner' side. The difference in their horizontal components is the side force mentioned above. There is, however, also a vertical component, which is larger on the outer side and the resulting pressure force creates a moment (around the centre of gravity) that tends to heel the hull inwards. This moment is amplified by the rudder force. Taking the centre of gravity as the origin for the moment means that neither the gravity nor the centrifugal force contribute, so the total effect is a moment that will heel the hull inwards.

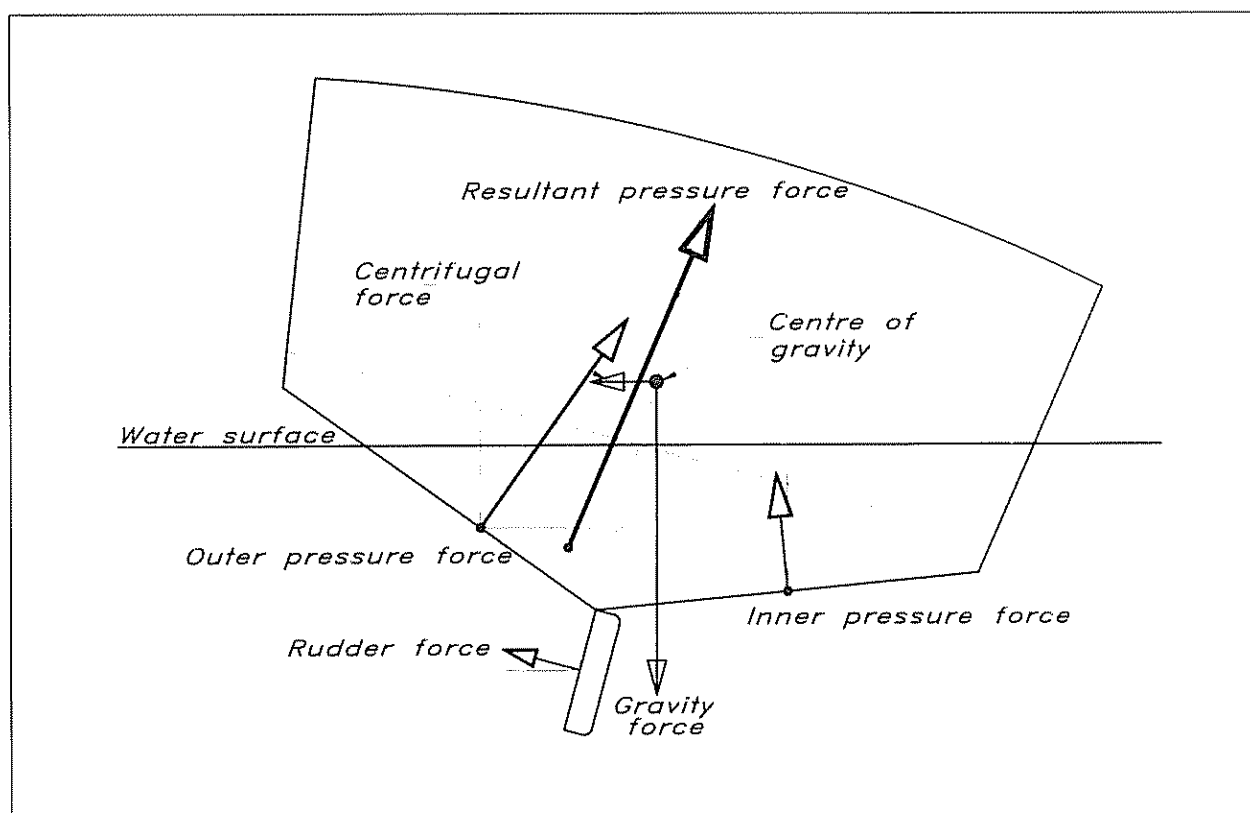


Fig 10.13 Forces on a turning hull

If the centre of gravity is moved upwards the resulting hull pressure force will soon pass through this point, thus creating no moment. At this stage, the rudder force still heels the hull inwards, but if the centre of gravity is moved still higher, the hull pressure forces will start heeling the hull outwards and at one position the moment from these forces will exactly balance the moment from the rudder. Now the hull does not heel at all. For any higher position of the centre of gravity the hull heels outwards.

Whether the hull is going to heel outwards or inwards thus depends on the height of the centre of gravity. Most planing hulls have their centre low enough to heel inwards, but some pleasure craft with a high flybridge may have it high enough to heel outwards, even dangerously so. For displacement hulls the pressure forces on the two sides are almost exclusively due to buoyancy, which is the same on the two sides (hull upright), thus creating no moment. The change in pressure force due to the turn is more or less horizontal and thus practically always directed below the centre of gravity. Even though the corresponding moment is to some degree compensated by the rudder, the result is a hull heeling outwards.

The other type of dynamic instability, often called 'chine walking', occurs due to convexity of the buttocks. When a flow passes over a convex surface the pressure is reduced, and the larger the curvature, the lower the pressure. If the buttocks are too curved near the chine a suction force may develop. Of course, as long as the hull is exactly upright the effects from the two sides cancel, but if the hull gets a small heel angle the side that is most submerged will generate the largest suction, and the more submerged it gets the larger the suction. The situation is thus unstable; the heel tends to increase all the time, until hopefully the static righting moment gets large enough to compensate the heeling moment. Now, any disturbance may reduce the suction, which means that the large righting moment will roll the boat back, and due to its inertia it will roll over to the other side, where the process is repeated. The hull thus rolls from side to side and may in fact eventually capsize. Further, it is very difficult to steer the boat when it is rolling in this way.

Normally, the buttocks on the wetted part of the hull are kept relatively straight, but it is very difficult to avoid convex buttocks on the forebody. The problem therefore normally occurs when the trim gets too small, ie when the forebody goes into the water at high speed. Situations when this may happen are:

- if the boat is overloaded
- if the load is put too far forward
- if the engine power has been increased without moving the centre of gravity backwards
- if the trimplanes generate too large a bow-down moment.

The control of the trim is thus very important.

**Alternative propulsion devices**

Today, the most important alternative to the conventional propeller is the water jet. This device works like an aircraft jet engine, deriving its thrust from the reaction force when the fluid is accelerated. In the water jet the acceleration is achieved by an impeller. Water enters through an intake, normally in the bottom of the boat, and is ejected through a duct at the stern. Note that it is the acceleration of the water that creates the force, so it does not matter whether the water is ejected above or below the water surface.

The basic principle for obtaining the thrust is the same as for a propeller, and the requirements for efficiency are the same. To optimize propulsion, as much water as possible should be accelerated but the speed increase should be as small as possible. For a propeller this speaks in favour of a large diameter and a low rpm. Unfortunately this is hard to achieve in a water jet, where the flow has to pass a channel inside the hull and the space is limited. The water jet has been less popular in the past, although the basic principles have been known for a long time. In fact, a patent on water jet propulsion was granted in England in 1661!

The reason why water jets have gained in popularity for high speed propulsion is the fact that no outside appendages are required. The higher the speed of a planing hull the smaller the wetted surface to lift it. Appendages, such as brackets and open shafts, obviously have a constant wetted surface, and thus account for an increasing proportion of the resistance as the speed goes up. Although it is hard to claim that there are no corresponding losses in a water jet intake and channel they are normally smaller, particularly as the need for rudders is relaxed. There is thus an advantage from a frictional point of view, and the advantage gets larger and larger as the speed increases. An example of a water jet driven hull will be given below. For more information on water jet efficiency, see the paper by Dyne and Widmark in the References section.

The concept of cavitation was introduced in Chapter 9. When the pressure at any point in the flow gets below the vapour pressure, the water evaporates. Bubbles of vapour and air dissolved in the water are created and these interfere with the flow and solid surfaces. Particular problems occur when the bubbles reach regions of high pressure where they may implode abruptly, causing large pressure pulses. Such pulses create vibrations and may erode the surface of, for example, a propeller. Further, the thrust of a cavitating propeller is often reduced.

When the speed goes up, the rate of revolutions of the propeller is increased, and both effects contribute to high velocities around the propeller blades. High velocities mean low pressures, so the risk of cavitation gets larger and larger with increasing speed. To avoid cavitation, large blade area ratios, as in Fig 10.9, are required for high speed boats. At speeds above 40 knots this may not help, however, and the problems with thrust reduction, vibrations and erosion may get large enough to prevent the use of conventional propellers. A possible alternative is then the so-called super-cavitating propellers. These are designed to have a steady cavitation bubble covering the entire suction

side, thus effectively eliminating the problems due to cavitation.

The disadvantage of the super-cavitating propellers is the reduced thrust and efficiency. Once the blade speed is high enough to generate a bubble covering the whole back side of the blade, the suction force cannot be increased any further. Higher speeds will only result in higher pressure side forces, so the increase in thrust is slower than normal. On the other hand, there is no friction on the suction side which reduces the torque to some extent.

Since the back side of the blade is no longer in contact with the water it may be designed without the usual constraints on shape. It is, however, important to ensure that the water separates at the leading edge, so in contrast to conventional blade sections the super-cavitation one should have a sharp nose. This gives the section a wedge-like shape, designed to withstand the considerable forces generated at these speeds. Design methods for super-cavitating propellers are available. For references, see the propeller chapter in the *Principles of Naval Architecture* (SNAME, 1988. A new edition is under way.)

Another typical high speed propulsion device is the surface piercing propeller. This is usually placed behind the transom, with only part of the propeller disk in the water. Its main advantage is the same as for the water jet: no submerged appendages are needed. The shaft may stick out directly from the transom. In this case the restrictions on propeller diameter, normally imposed on a propeller behind the hull, are somewhat relaxed, thus increasing efficiency. Both super-cavitating and conventional blade sections are used, and since much air is entrained at the water impact of each blade the collapse of cavitation bubbles (now partly filled with air) is smoother.

The main disadvantage of surface-piercing propellers is the large variation in blade loading. At the top position, when the blade is in the air, the loading is zero, while it is maximum when the blade points downwards. Apart from generating vibrations, this pulsating load causes fatigue which needs to be considered in the design. An exhaustive investigation of the problems may be found in a thesis by Olofsson (see the References section).

### **An example**

As an example of a contemporary high speed boat, a rescue vessel for the Swedish Rescue Society, designed by one of the authors (Eliasson), will now be introduced. Fig 10.14 shows a picture of the 12 m craft landing after a jump in a 4 m wave. The hull is also shown in Fig 10.15, together with its main particulars. It is designed for an operating speed of 40 knots in smooth water and with good rough water capabilities.

To balance the hull at such a high speed the centre of gravity has to be relatively far aft. With a more forward location the trim would have been smaller with a risk of chine walking and broaching. In general, the craft would have been more difficult to steer in a seaway. For a pleasure craft it may be difficult to move the weight this far back, since the accommodation area and most of the equipment will be in the forward half of the hull.





Fig 10 14 *Rescue boat in rough seas (Photo: Dan Ljungsvik)*

The disadvantage of having the weight this far aft is that the ride may be bumpy in a head sea. Rather than hitting the next wave by the bow the hull will land on the afterbody after a jump. A remedy is to trim the hull slightly more by the bow using the trim flaps. Another disadvantage is the non-optimum low speed performance. At lower speeds a larger wetted surface is required, which means that the pressure force is moved forwards and the hull trimmed by the stern. This creates large waves and resistance, but again the trim flaps may be used to reduce the problem.

The particular features of the design are described and keyed to Fig 10 15 overleaf.

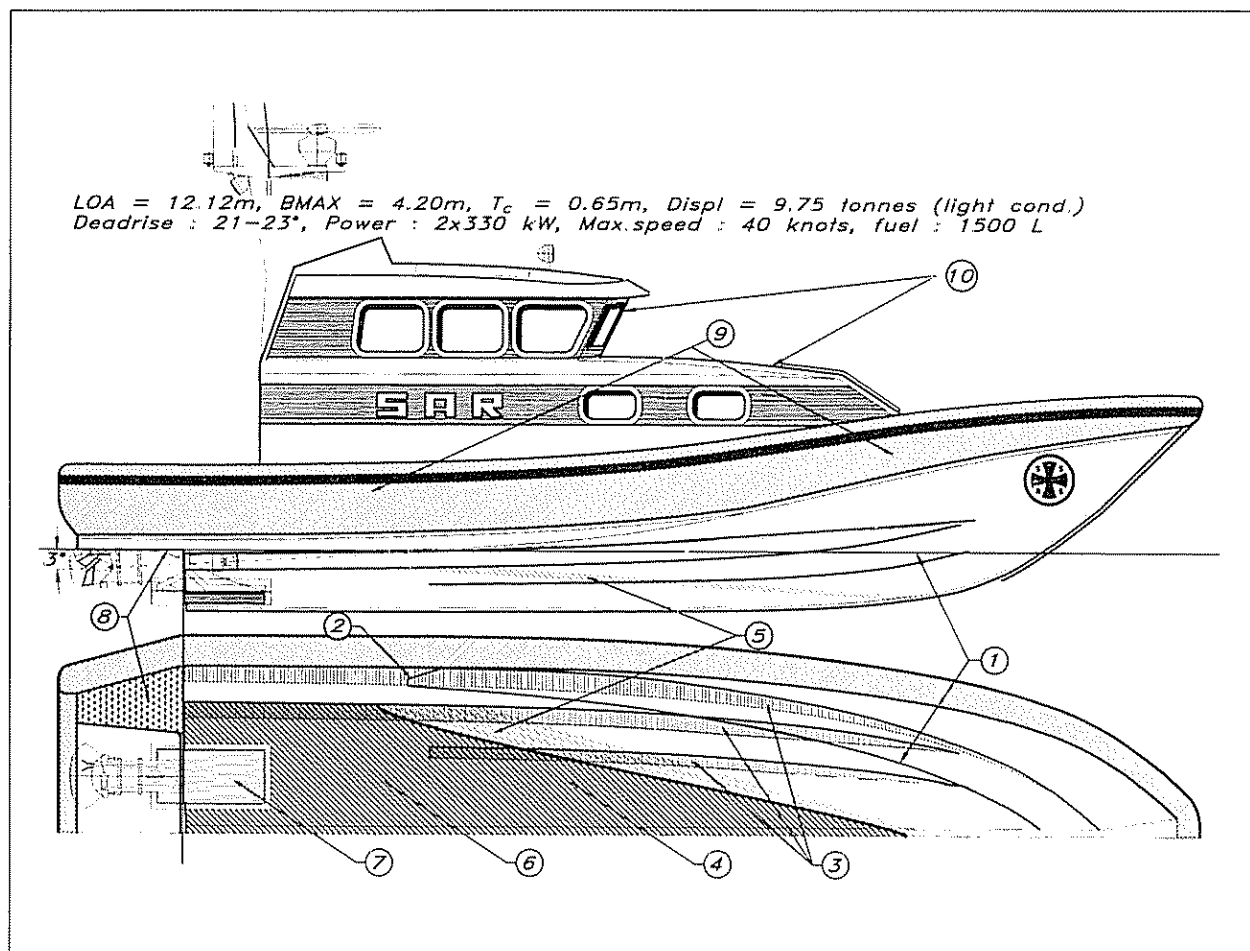


Fig 10.15 Main features of the rescue vessel

### Key to Fig 10.15.

- 1 This is the still waterline. It has no relation to the waterline at full speed, as can be seen in the photo, but it gives an idea about the shape of the forebody. The bow is not particularly fine; a certain fullness is required to avoid problems with broaching in a following sea. On the other hand, it should not be too full, since this would hamper the performance in head seas and may lead to chine walking if the forward buttocks are too convex.
- 2 The waterline bends forwards at this position, showing that the bottom close to the chine has a negative deadrise. This is to generate a lift and to deflect the spray downwards. The hull runs dry, as can be seen in the picture.
- 3 The spray rails also have a negative deadrise as explained above. The inner one is cut off before the transom.
- 4 This is the boundary of the wetted surface (spray root) at 40 knots. There is no reason to extend the spray rails very far into this region. A certain overlap is desirable, however, since the spray root may move back and forth in a seaway.
- 5 In this area the spray should be deflected by the rails.

- |   |   |
|---|---|
| <p>6 The wetted surface is not large at 40 knots! Compare with the waterline area at zero speed.</p> <p>7 Modern water jets are used for propulsion. This is the intake, which is large enough to handle the enormous flow rate. As the flow into the intake should be as clean as possible, there should be no rails, keels or other devices ahead that can lead air into the jets.</p> <p>8 The aftmost part of the bottom is raised over the full beam. This is to encompass the two water jets and to enable proper operation in reverse. Note that this part</p> | <p>of the bottom is above the water at high speed. The trim flaps are hinged on the transom below the jets.</p> <p>9 The collar is of a modified RIB type. It is not filled with air, but with an elastic polyurethane foam, covered with a skin of tough polyurethane and Kevlar. Tapering of the collar forwards is very important since otherwise too much buoyancy might be developed when the hull runs into a head wave, capsizing the boat backwards.</p> <p>10 For stability reasons the deckhouse is relatively large.</p> |
|---|---|

The rescue vessel may be used as an example for the performance prediction above. Results are shown in Fig 10 16, where the numbering of the steps corresponds to that in the proposed procedure. The deadrise angle varies between  $21^\circ$  and  $23^\circ$ , but, as explained above, the angle used in the computations is measured to the edge of the spray rails and is the average of the angles at the transom and at the centre of gravity. A trim of  $4^\circ$  caused a bow-up moment of 41.4 kNm (kilonewton metres), while the moment at  $5^\circ$  was 69.4 kNm bow-down. It is thus clear that the trim angle for zero moment is between the two computed values and the linear interpolation formula yielded a trim of  $4.37^\circ$ . In turn, this resulted in a resistance of 14.4 kN, corresponding to an effective power of 296 kW at 20.6 m/s (40 knots).

Now, the question is what engine power is required to achieve this. Since the vessel is equipped with water jets the propeller diagram cannot be used. An optimally designed propeller for this vessel would most likely have had an efficiency of at least 65% and so would an optimum water jet unit. This is a high efficiency, which is attainable due to the light loading of the propulsor at this high Froude number. At smaller Froude numbers the efficiency of the water jet deteriorates more than for a conventional propeller, but on the other hand the resistance is smaller due to the lack of external appendages, so it would be competitive also at somewhat lower speeds.

The water jet for the rescue vessel is designed to produce a high thrust also at very low speed (so called bollard pull), since the vessel must be capable of towing larger vessels. Therefore, the efficiency at full speed is reduced, and 50% may be a reasonable assumption for this case. Note that the deviation from the optimum may be important also for other cases. To obtain the optimum efficiency a specialist design of the water jet is required.

Assuming an efficiency of 50%, the delivered power must be 592 kW.

Fig 10.16 Summary of rescue vessel calculation

Step No	Variable	Computed value	Computed value	Computed value
1	$m$	9750 kg		
	LCG	3.550 m		
	VCG	1.145 m		
	$b$	2.740 m		
	$\varepsilon$	3°		
	$\beta$	17.9°		
	$f$	0.490 m		
	$V$	20.6 m/s		
2	$C_V$	3.970		
3	$CL_\beta$	0.060		
4	$CL_\alpha$	0.087		
5	$\tau$	4.0°	5.0°	
6	$\lambda$	2.00	1.40	
7	$L_m$	5.480 m	3.840 m	
	$R_n$	$113 \cdot 10^6$	$79 \cdot 10^6$	
8	$C_F$	$2.05 \cdot 10^{-3}$	$2.16 \cdot 10^{-3}$	
9	$\Delta x$	0.32	0.24	
	$R_F$	7.96 kN	5.93 kN	
10	$ff$	0.920 m	0.920 m	
11	—	—	—	
12	—	—	—	
13	$L_{cp}$	3.890 m	2.800 m	
14	$e$	-0.44 m	0.75 m	
15	$M$	-41.4 kNm	69.4 kNm	
16	—	—	—	
17	$\tau_o$	—	—	4.37°
18	$R_{Fo}$	—	—	7.2 kN
19	$R$	—	—	14.4 kN
20	$P_E$	—	—	296 kW
21	$P_D$	—	—	592 kW

This is the power at the impeller shaft. Due to mechanical losses in the gearbox and shaft bearings another 5% may be added, which would give approximately 630 kW. The most suitable engines found for this vessel have a power of 2 x 330 kW, so there should be some spare power if needed.

# 11

# RIG CONSTRUCTION

---

This chapter deals with the dimensioning and construction of the rig. Over the years different methods have evolved, ranging from old rules of thumb for solid wooden spars to sophisticated computer models for exotic composite materials. We will take a middle line, using accepted standard engineering practices as they are used in the Nordic Boat Standard (NBS). The reason for using this NBS standard instead of ABS or Lloyd's Register is the simple fact that NBS is one of the few yacht scantling standards that takes the rig into consideration. At the end of the chapter we will dimension the rig of the YD-40.

## Definitions and scope of the standard

The standard is valid for normal masthead and fractional rigs, with one or two pairs of spreaders. In Fig 11.1 the required data for the calculations is defined. Other limits to this standard are, first, that the area of the fore triangle is not greater than 1.6 times the area of the mainsail  $\{I \cdot J / (E \cdot P) < 1.6\}$ , and secondly that the sail area is greater than the righting moment divided by 128 times the heeling arm. If this is not the case then the boat is classified as a motorboat with a steady sail.

The starting point when dimensioning the rig is to calculate the righting moment. It is commonly agreed that a heel angle of  $30^\circ$  is a good design angle. This corresponds to a reasonably high wind strength with the sails still generating high loads and the boat making good speed through the water. Letting the boat heel over more (ie using a higher righting moment), in reality means a slower boat owing to increased resistance, with a correspondingly smaller dynamic force.

As can be seen from the box in Fig 11.1 there are basically two ways of calculating the righting moment. We can start with calculating the moment for  $30^\circ$  of heel, or with the moment for  $1^\circ$  of heel. Calculating the  $RM_{30}$  means that we will have to make a calculation of the hull's heeled centre of buoyancy and the position of the centre of gravity in order to establish the righting arm. By using the  $RM_1$  instead, which we can get from the hull's upright hydrostatics (see Chapter 4), we need only estimate the centre of gravity of the vessel. Either way, the moment we get is to be that of the empty boat, which is then modified to represent the fully laden boat including crew to windward, as shown in the box in the figure.

Fig 11.2 shows the different types of rig that this standard covers. The stability of the mast athwartship is dependent on the number of spreaders and the location of the mast foot, ie on deck or keel-stepped.

- $G$  Empty weight of boat [kg]
- $\Delta$  Full load weight of boat [kg]
- $g$  Ballast weight [kg]
- $B$  Maximum beam [m]
- $LOA$  Length overall [m]
- $A_S$  Sail area [m<sup>2</sup>]
- $RM$  Dimensioning righting moment [Nm]
- $RM_{30}$  Righting moment at 30 degrees heeling with empty weight of the boat [Nm]
- $RM_1$  Righting moment at 1 degree heeling with empty weight of the boat [Nm]
- $n$  Number of persons on board
- $F_S$  Freeboard at mast [m]
- $\delta_{RM}$  Additional moment from crew to windward [Nm]
- $HA$  Heeling arm [m]

$$A_M = E \cdot P / 2$$

$$A_F = J \cdot I / 2$$

$$A_S = A_M + A_F$$

If  $A_S > RM / (12B \cdot HA)$   
the boat is considered to be a sailing boat, and the rig is to be dimensioned accordingly.

$$\delta_{RM} = 75 \cdot n \cdot (3.4B - 4.9F_S)$$

$$RM = RM_{30} \cdot \Delta / G + \delta_{RM}$$

or

$$RM = 27 \cdot RM_1 \cdot \Delta / G + \delta_{RM}$$

$$RM_{min} = 29 \cdot RM_1$$

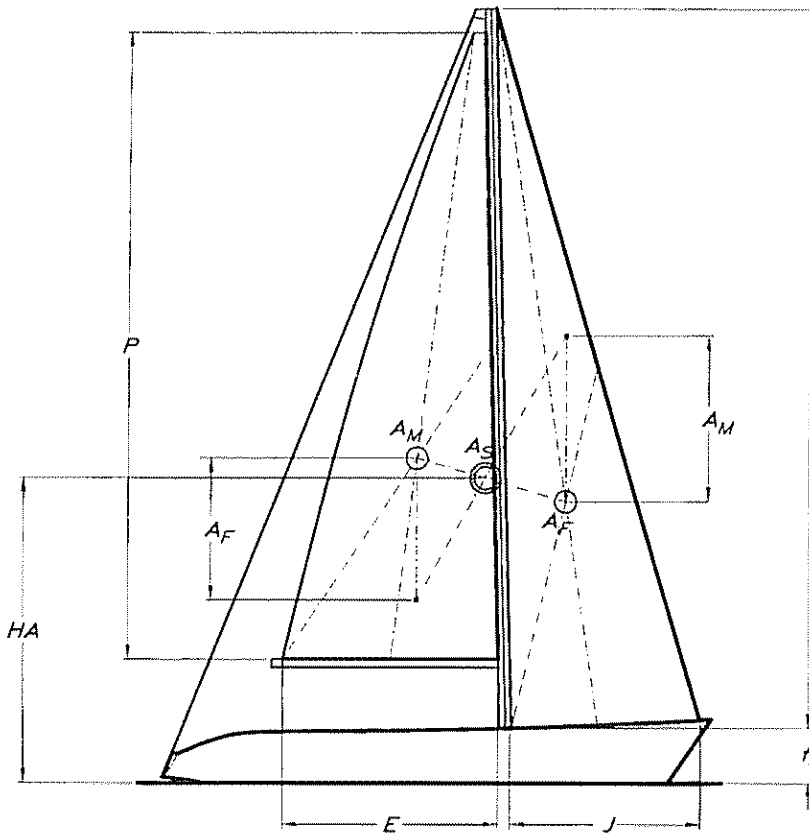


Fig 11.1 Definitions and righting moments

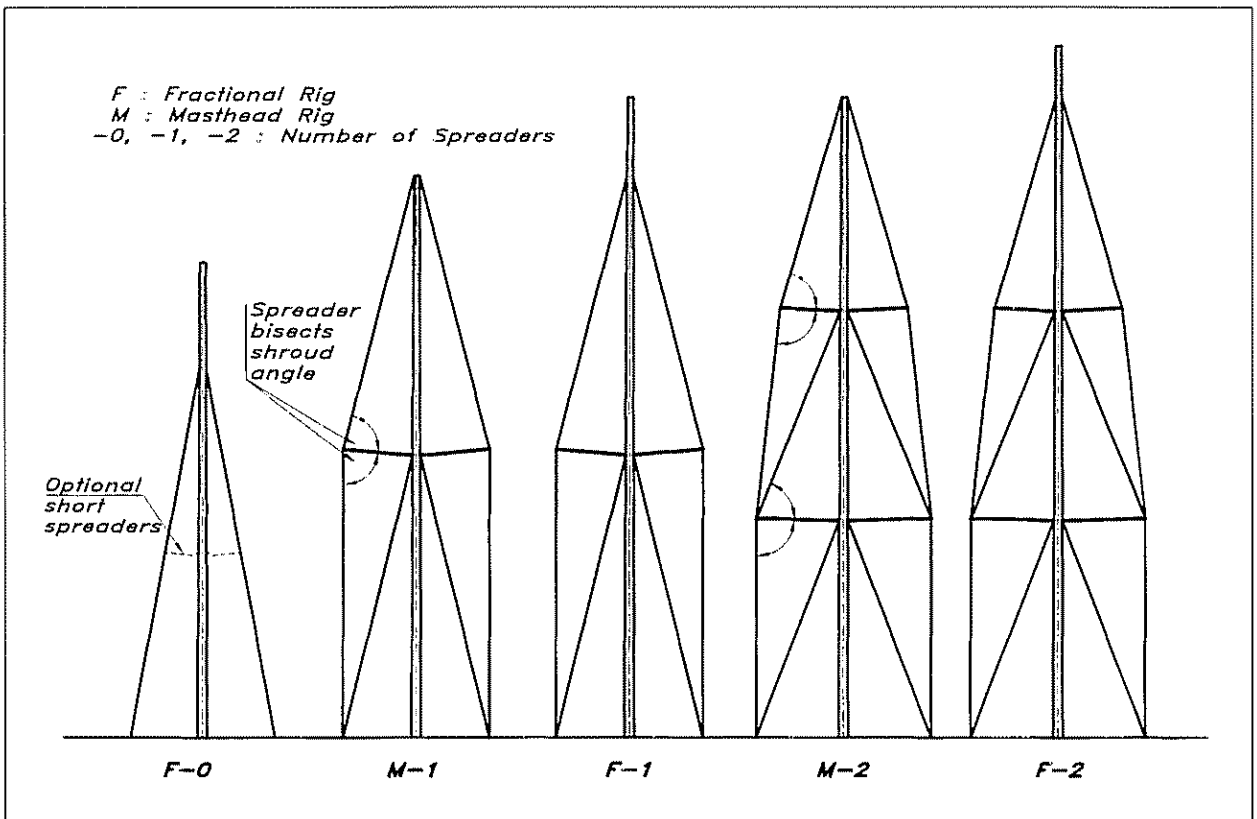


Fig 11 2 Types of rigs

The longitudinal stability of the mast depends on the spread of lower shrouds, runners, inner forestay and location of the mast foot. It is common practice that the transverse and longitudinal stability are studied separately. Compared to a single-spreader, deck-stepped mast, we can increase overall mast stability by increasing the number of spreaders and/or bringing the mast down to the keel. At the same time we get the following pros and cons:

#### Increased number of spreaders

- + Thinner mast which gives better mainsail efficiency.
- + Smaller outer dimensions/wall thickness give a lighter mast.
- + Smaller foresail sheet angles are possible.
- More difficult to trim.
- Often special measures must be made to take care of the longitudinal stability, ie runners, inner forestay, high longitudinal moment of inertia.
- Higher cost.

### Mast through deck

- + Thinner mast which gives better mainsail efficiency.
- + Smaller outer dimensions/wall thickness give a lighter mast.
- + Smaller foresail sheet angles are possible.
- More difficult to trim, especially lengthwise.
- High horizontal forces in deck level.
- Risk of heat and water leakage.

### Forces on the shrouds

The forces come from the wind pressure on the sails and dynamic additions from wind and sea. Two load cases are considered in Fig 11.3: in case 1 the rig is loaded by only a foresail, and in case 2 the rig is loaded by a deep reefed mainsail. In case 1 the transverse force  $T_1$  is simply the righting moment divided by the distance from the waterline to the uppermost shroud, as illustrated in Fig 11.3(A). It does not matter what kind of foresail is carried, since the dimensioning force comes from the righting moment

In case 2, with the reefed mainsail, the transverse force  $T_2$  is calculated by dividing the righting moment by the distance from the waterline to the geometric centre of the mainsail, approximately  $\frac{1}{3}$  of the luff up from the boom. This force is then distributed between the head of the sail,  $T_{\text{head}}$ , and the boom,  $T_{\text{boom}}$ , according to Fig 11.3(B). When  $T_{\text{head}}$  lies between two shrouds, the force shall be distributed between the two shrouds proportionally to the distances from the shrouds' attachment points to the location of the force, Fig 11.3(C), and the resulting forces are  $T_{\text{hu}}$ , acting on the upper shrouds, and  $T_{\text{hl}}$ , on the lower shrouds. The boom force is working on the deck and on the lower shrouds, where we are interested to know the load on the shrouds. This load,  $T_{\text{bu}}$ , is a fraction of the boom force proportioned as the ratio of the boom height above deck to the distance of the shroud to the deck, Fig 11.3(D).

We now have all the components forming the transverse loads on the rig. Regardless of rig type, the dimensioning force is  $T_1$  in load case 1. In case 2 the dimensioning force is different combinations of  $T_{\text{hu}}$ ,  $T_{\text{hl}}$  and  $T_{\text{bu}}$ , depending on rig type according to Fig 11.4. Rig type F-0 only has  $F_1$  as a dimensioning force, type M-1 and F-1 have  $F_1$  and  $F_2$ , and type M-2 and F-2 include force  $F_3$  as well. For the dimensioning of the shrouds we use the maximum forces  $F_1$ ,  $F_2$  or  $F_3$  from load case 1 or case 2. Note that there is no  $F_3$  force on a double-spreader rig in case 2, if the reefed mainsail does not reach the upper spreaders (see notes 1 and 2 in Fig 11.4).

When calculating the shroud forces in the following figures, 11.5 to 11.8, it is essential to calculate the two above mentioned load cases



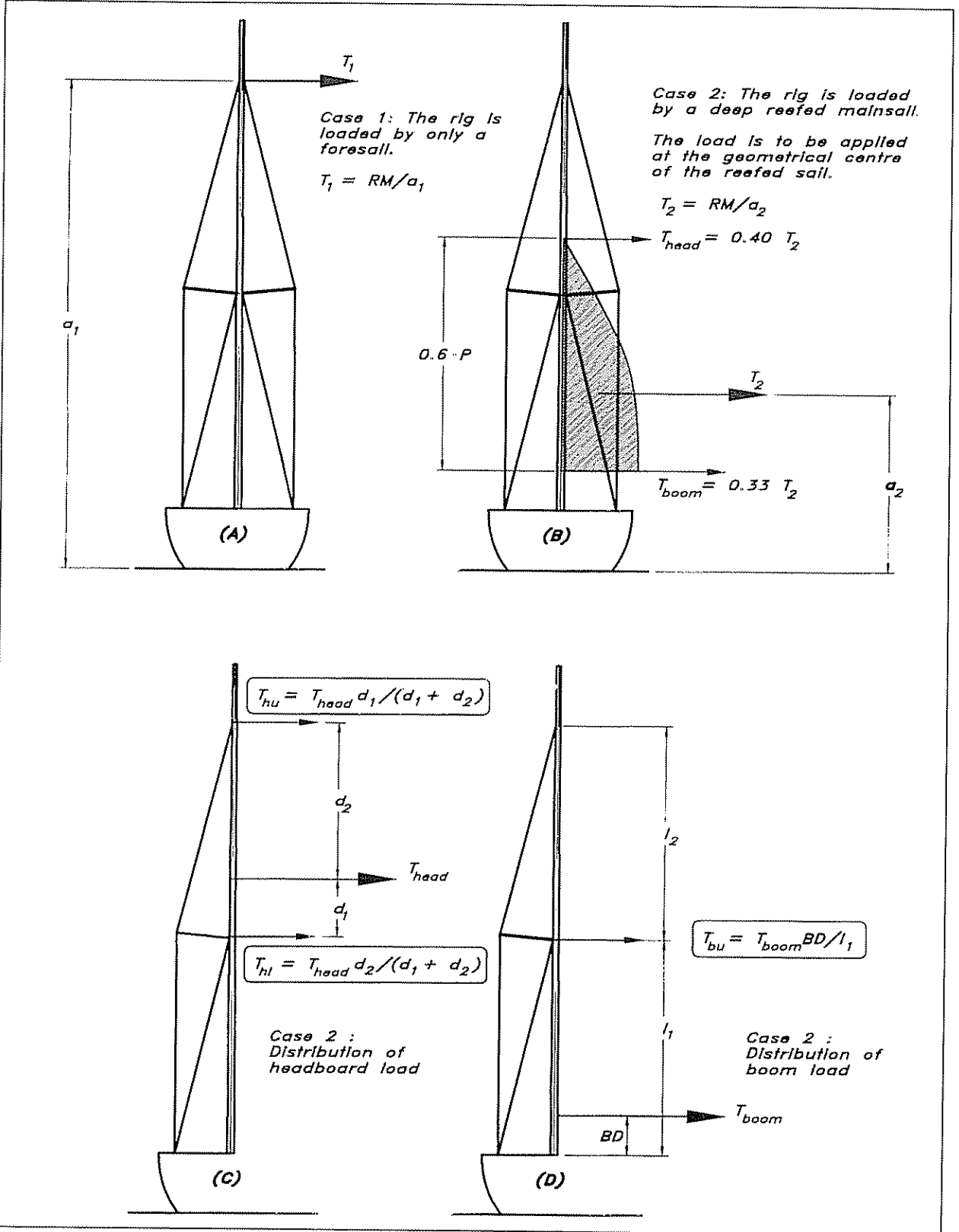
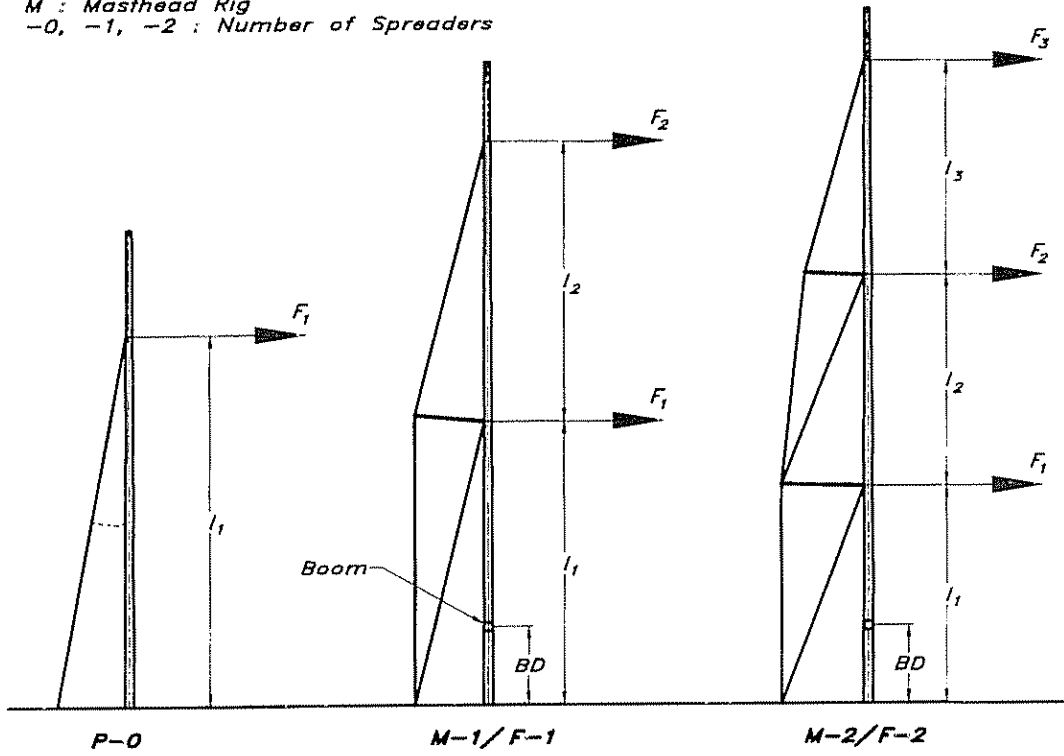


Fig 11.3 Transverse loads

*F* : Fractional Rig  
*M* : Masthead Rig  
 -0, -1, -2 : Number of Spreaders



Dimensioning Forces $F_1, F_2, F_3$						
Type of Rig	Load Case 1 (Fig 10.3A)			Load Case 2 (Fig 10.3B)		
	$F_1$	$F_2$	$F_3$	$F_1$	$F_2$	$F_3$
<i>F</i> -0	$T_1$	0	0	$T_{hu}+T_{bu}$	0	0
<i>M</i> -1/ <i>F</i> -1	0	$T_1$	0	$T_{hl}+T_{bu}$	$T_{hu}$	0
<i>M</i> -2/ <i>F</i> -2 <sup>1)</sup>	0	0	$T_1$	$T_{bu}$	$T_{hl}$	$T_{hu}$
<i>M</i> -2/ <i>F</i> -2 <sup>2)</sup>	0	0	$T_1$	$T_{hl}+T_{bu}$	$T_{hu}$	0

1) If  $BD+0.6P > l_1+l_2$   
 2) If  $BD+0.6P < l_1+l_2$

Fig 11.4 Dimensioning forces for shrouds

Fig 11.5 Shroud load  
- rig F-0

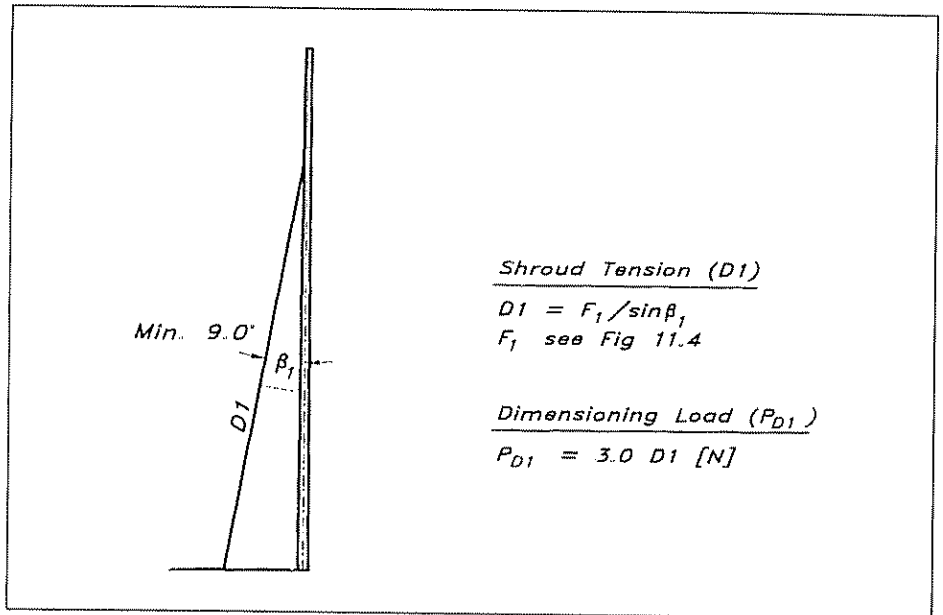
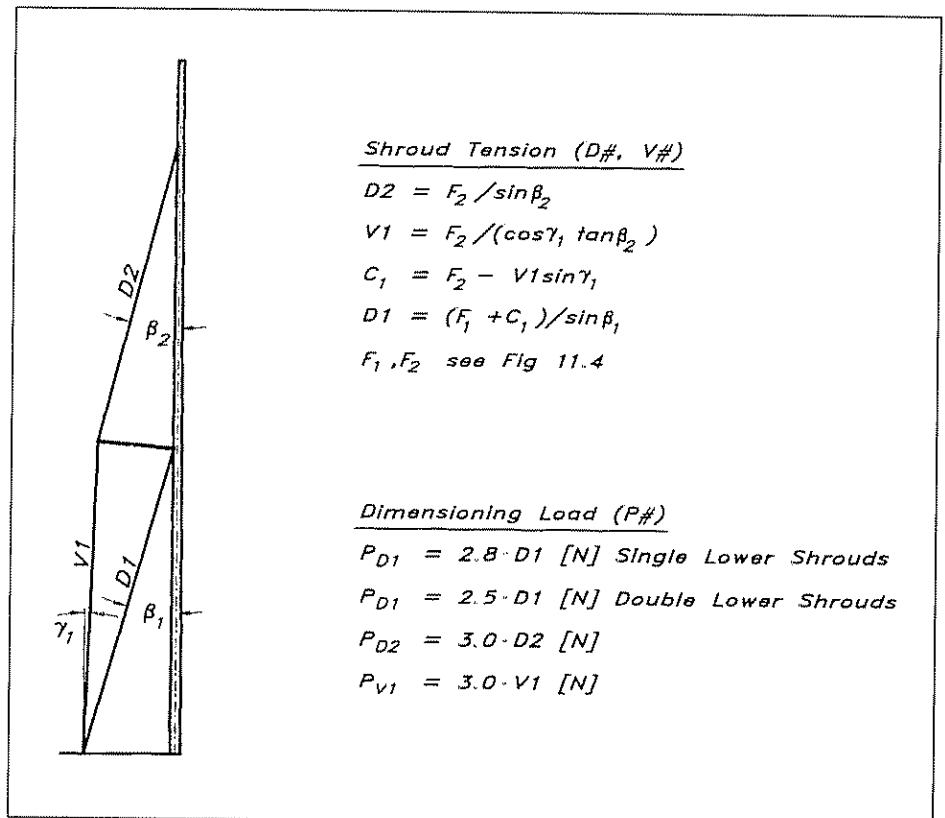


Fig 11.6 Shroud load  
- rig M-1, F-1

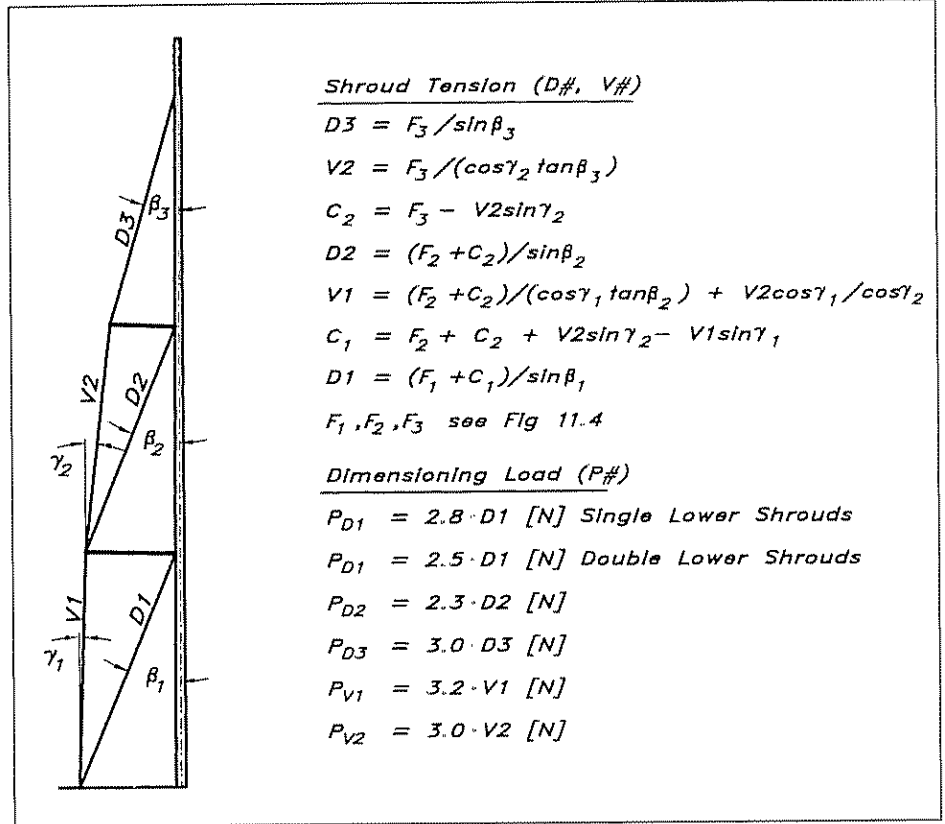


separately, and then compare the results and choose the worse case, ie the highest load for each shroud.

Fig 11.5 gives the dimensioning load of the shrouds on an F-0 type rig. As can be seen it is the shroud tension multiplied by 3, and the smallest permissible shroud angle is 9°.

Fig 11.6 shows the same thing for a single-spreader rig. Depending

Fig 11.7 Shroud load – rig  
M-2, F-2

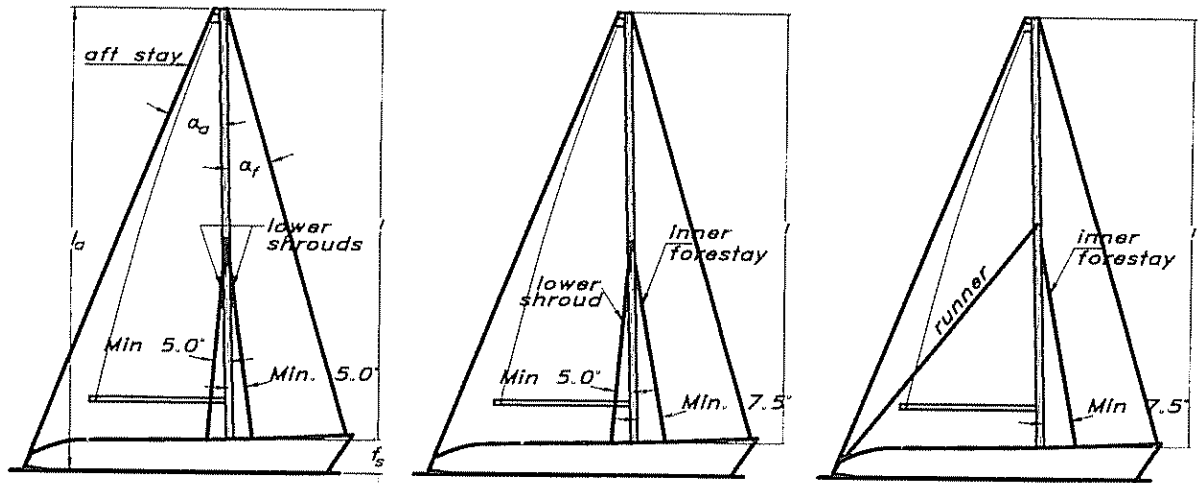


on whether we have single or double lower shrouds the dimensioning load is the shroud tension multiplied by 2.8 or 2.5. The upper shrouds are dimensioned from the shroud tension multiplied by 3 though, and the smallest permissible athwartship's angle is still 9°.

Fig 11.7 deals with the double-spreader rig. The method of calculation follows the same pattern as on the previous rigs. After calculating the shroud forces according to the formulae, we apply safety factors to the different parts and get the shroud loads. Basically, the safety factor distribution follows the one for the single-spreader rig, apart from the V1-position shroud, where the safety factor is 3.2. If we have separately coupled intermediate and upper shrouds to a common lower shroud, this shroud has to take the combined pull from the intermediate and upper shroud, that is the reason for the increased factor of safety. If, on the other hand, the intermediates and uppers run all the way down to the deck, their combined strength must at least equal V1.

**Forces on the stays**

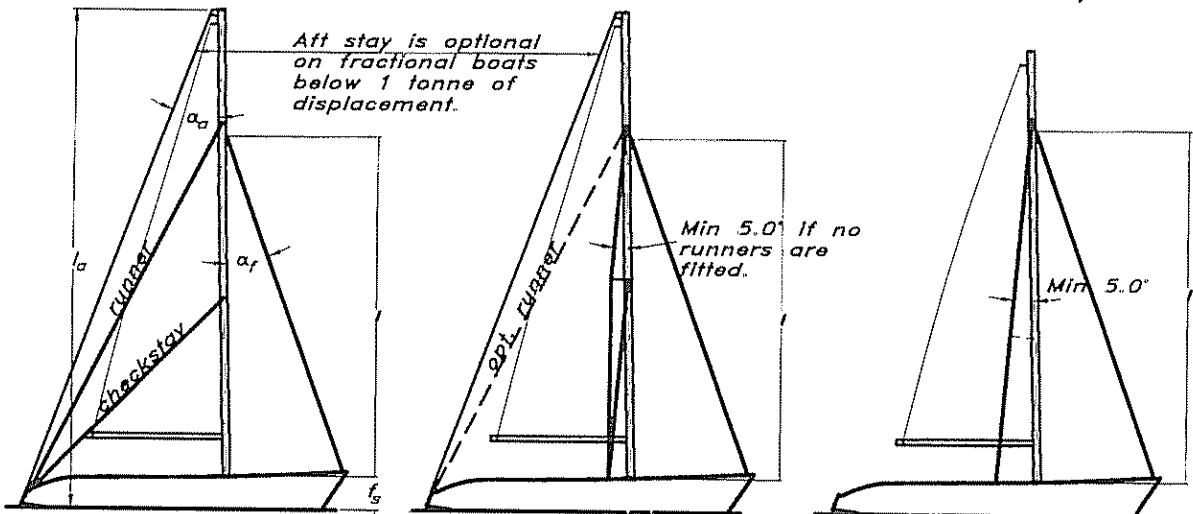
The longitudinal loads are primarily dependent on what tensioning devices there are on the boat: winches, tackles, hydraulics etc. The NBS-standard recognizes six different types of rig. Each basic type, masthead or fractional, is divided into three sub groups, according to Fig 11.8. For the masthead rig they are: (1) Double lowers, (2) Single lowers with inner forestay and (3) Runners with inner forestay. The fractional rig is divided into (4) Runners with checkstay, (5) Single lowers with swept



1) Double Lowers

2) Single Lowers with Inner Forestay

3) Runners with inner Forestay



4) Runners with Checkstay (Only on Fractional Rig)

5) Single Lowers with swept Spreaders (Only on Fractional Rig)

6) Simple Rig with no or short Spreaders

The foremost sail carrying forestay shall have a breaking strength ( $P_{fo}$ ) of at least:

$$P_{fo} = 15 \cdot RM / (l + f_s) \text{ [N]}$$

The inner forestay shall have a breaking strength ( $P_{fi}$ ) of at least:

$$P_{fi} = 12 \cdot RM / (l + f_s) \text{ [N]}$$

The aft stay shall have a breaking strength ( $P_a$ ) of at least:

$$P_a = P_{fo} \cdot \sin \alpha_f / \sin \alpha_a \text{ [N] Masthead rigs}$$

$$P_a = 2.8 \cdot RM / (l_a \sin \alpha_a) \text{ [N] Fractional rigs}$$

Fig 11 8 Loads on longitudinal stays

spreaders and (6) Simple rig with no spreaders or short spreaders. The different staying types induce different loads on the mast itself which have to be accounted for when dimensioning the mast. This will be discussed later.

As for the shrouds, the dimensioning force for the stays is derived from the righting moment at 30° of heel. The foremost sail carrying stay is required to have a breaking strength ( $P_{fo}$ ) of the righting moment multiplied by 15 divided by the distance of the stay above the deck plus the freeboard height at the mast. The inner forestay's load ( $P_{fi}$ ) is calculated accordingly, but using the righting moment multiplied by 12 instead.

The strength requirements for the aft stay ( $P_a$ ) differs between masthead and fractional rigs. For the masthead rig the aft stay is to have the same strength as the forestay, modified by a factor, depending on the angles that the aft stay and forestay make to the mast. The aft stay breaking strength for the fractional rig is calculated by taking the righting moment multiplied by 2.8 and dividing it by the mast height above the water multiplied by the sine of the aft stay angle to the mast. Runners on a fractional rig are dimensioned in the same way as the aft stay of a masthead rig.

The strength requirements calculated above include safety factors and consequently the breaking strength of the wires can be used. When it comes to turnbuckles, though, it is wise to increase the dimensioning forces by 25% to ensure that if anything breaks it will be the standing rigging and not the attachment. For the same reason it is prudent to allow for an equal increase in the loads for the chainplates.

### Comparison between wire and rod

In the following we will compare the two most common types of standing rigging, ie 19-strand stainless steel wire and solid rod of stainless steel. When choosing between wire or rod the following comparisons should be made:

- |                           |                   |
|---------------------------|-------------------|
| • Breaking strength       | • Weight          |
| • Fatigue                 | • Wind resistance |
| • Resistance to corrosion | • Handling        |
| • Elongation              | • Price           |

### *Breaking strength*

Breaking strength is the maximum load a wire/rod can carry without breaking. For every shroud and stay the breaking force is calculated and a proper wire/rod dimension is picked that can absorb the actual load. Depending on available sizes, the wire and rod form different stepped curves for breaking strength. Therefore, it is unlikely that there will be the same relationship between wire and rod dimensions for every shroud/stay. For a certain stay, a wire dimension might fit well while the rod becomes over-strong. Normally, a rod is 20% stronger than a wire of the same diameter.

***Fatigue***

Fatigue is normally regarded as the number of loads that can be applied before the wire/rod breaks. There are very few investigations regarding fatigue strength of 19-strand wire and rod.

Generally speaking, if the attachment points for the shrouds/stays are made in such a way that changes of angles can take place, wire is slightly more sensitive to fatigue because the individual strands rub against each other. Rod, on the other hand, is sensitive to surface damage which can lead to fatigue-cracking. The wire has the advantage that the strands, when fatigued, break one at a time, and thereby give a warning that a change of wire is needed (providing, of course, that we regularly inspect the standing rigging). In a rod, a fatigue break comes without warning, and the beginning of cracking is almost impossible to detect by visual inspection.

***Resistance to corrosion***

Resistance to corrosion is similar since the material is the same for both wire and the rod (AISI 316). This alloy might be discoloured, especially in the pockets between the strands of a wire, but this does not affect the strength.

***Elongation***

Elongation ( $a$ ) of a loaded wire/rod increases proportionally to the load ( $P$ ) and length ( $L$ ), and inversely to the cross-sectional area ( $A$ ) and modulus of elasticity ( $E$ ):  $a = (P L) / (A E)$ .

As long as the load is within 70% of the ultimate breaking load (slightly more for rod) the wire/rod regains its original length when the load is released. A properly dimensioned rig should never get working loads greater than 50% of the breaking strength, ie there will be no plastic (permanent) deformations in the rig. The permanent deformations that can be measured come from first-time deformations of the attachment points and deformations of the hull girder. We will look more into this last item in the next chapter on hull construction.

In this comparison we assume the rod and the wire to be made of the same material. Due to the fact that the wire is constructed of strands that 'compress' and 'straighten' under load, the actual modulus of elasticity for the wire is approximately 20% less than for the solid rod. Comparing the cross-sectional area, the rod's area is approximately 30% greater than the wire's, due to air between the wire strands, rod and wire having the same diameter.

The following relations are valid with constant length and force:

- Same weight: rod elongation = 80% of the wire
- Same size: rod elongation = 60% of the wire

The smallest elongation that it is possible to obtain by using rod gives two advantages when used in shrouds:

- 1 When loaded, the mast falls off to leeward, this, together with the heeling, puts the centre of effort of the sails outboard of the centre of lateral resistance, which tends to turn the boat into the wind (weather helm). With a stiffer rig the mast will not fall off as much to leeward, and the weather helm moment decreases, though not very much – normally 2–3%.
- 2 The lesser the mast top falls off to leeward, the straighter it is, and this makes it more resistant to bending and able to absorb greater loads.

The stiffer rod rig has one disadvantage though. A hull that becomes deformed is putting the ends of a shroud or stay closer to each other, and since the elongation of the rod is smaller than that of the wire at the same amount of pre-tensioning, the rod is losing more of its pre-tension compared to the more flexible wire.

To get a good pointing ability the forestay should be as straight as possible. This is achieved by tensioning the backstay or runners. When subjected to a wind load the forestay takes a curve; the smaller the curve, the stiffer a stay and/or boat. At temporary increases in the wind-load by 60% the depth of the curve of the wire forestay increases by 55% and for the rod forestay by 50%. The rod gives a slightly straighter forestay, but no account has been taken of the hull girder stiffness. The hull's flexibility makes the differences smaller, or, to put it another way, to really be able to utilize the rod rig, higher demands are put on the hull girder stiffness.

### *Weight*

The boat's total displacement, stiffness and mass moment of inertia is influenced by the weight of different rigs. As we have shown earlier the latter is of the utmost importance when sailing in a seaway.

Just as for the breaking strength, the weights of wire and rod form two different 'step-functions' which varies the result of the comparison for different rigs, although the same basis for the evaluation is used.

### *Wind resistance*

Wind resistance of the shrouds and stays increases with increasing diameter. Since a rod of equal strength to a wire is thinner, the resistance is less, and since the surface of the rod is smoother the resistance, especially in low wind strengths, is still less than that for a wire. This latter effect (due to smoothness) diminishes with increasing wind strength.

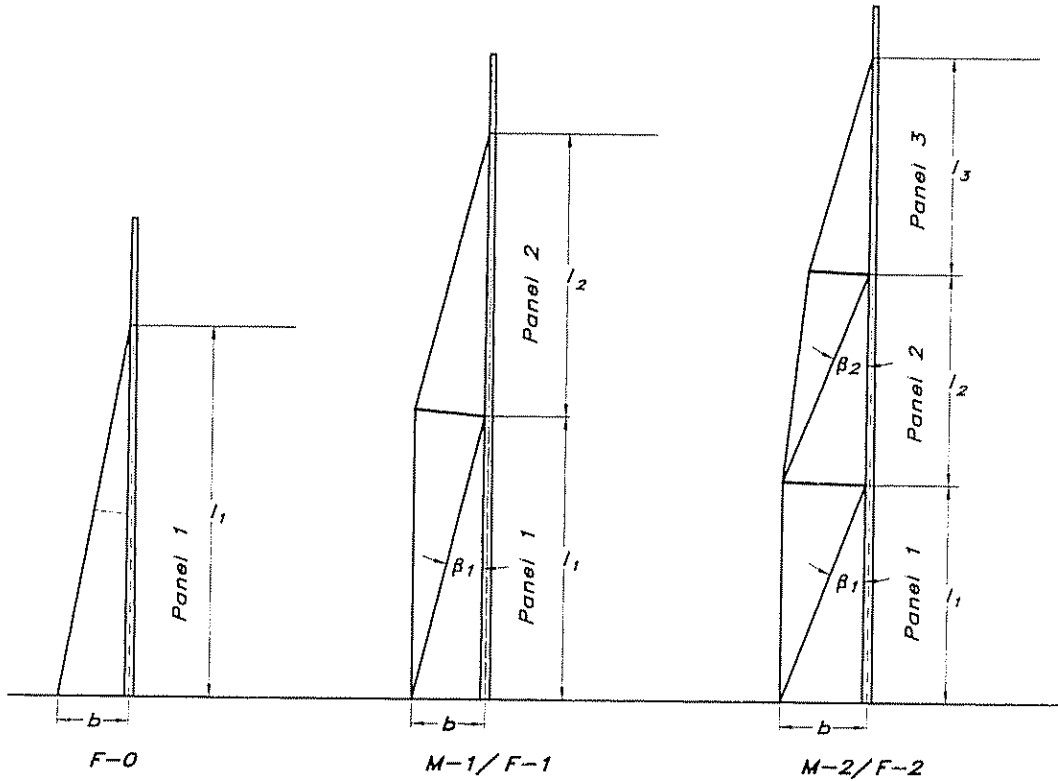
### *Handling*

Handling is better for wire compared to rod. It is possible to roll the wire into coils which have diameters of 0.5 – 0.8 m. Rod should not be coiled into smaller diameters than 200 times the rod diameter.

### *Price*

The price of a rod rig is 50% – 100% higher than for an equally strong wire rig.





Required transverse moment of inertia,  $I_x$ , for the mast :

$$I_x = k_f \cdot m \cdot PT \cdot l(n)^2 \text{ [mm}^4\text{]}$$

- $PT = 1.5 \cdot RM/b \text{ [N]}$
- $k_f =$  panel factor (see table below)
- $m = 1$  for aluminium
- $7.25$  for wood (Spruce)
- $70500/E$  for other materials
- $l(n) =$  actual panel length
- $k_3 = 1.35$  for deck stepped masts
- $1.00$  for keel stepped masts

When calculating  $I_x$  for panel 2 PT is decreased by:

$$D1 \cdot \cos \beta_1$$

When calculating  $I_x$  for panel 3 PT is decreased by:

$$D1 \cos \beta_1 + D2 \cos \beta_2$$

$D1$  is taken from Fig 11.6 for a single spreader rig.

$D1$  and  $D2$  are taken from Fig 11.7 for a double spreader rig.

Type of Rig	Panel Factor $k_f$	
	Panel 1	Panel 2 & 3
F-0	$2.4 \cdot k_3$	-
F-0 short spr.	$1.6 \cdot k_3$	-
M-1	$2.5 \cdot k_3$	3.50
F-1	$2.4 \cdot k_3$	3.35
M-2	$2.7 \cdot k_3$	3.80
F-2	$2.6 \cdot k_3$	3.60

Fig 11 9 Transverse mast dimensioning

**Transverse mast stiffness**

The tension in the shrouds and stays induces a compression in the mast, and in order not to bend or break, it has to have sufficient stiffness, ie enough transverse moment of inertia,  $I_x$ . The required stiffness depends on the load as well as on the length of the panel in question. In Fig 11.9 the formula for calculating the  $I_x$ - required is given. The formula is common to all rig types, the differences in the results coming from the fact that the panel lengths vary. Another factor that differs between the rig types is the panel factor  $k_1$  and the 'foot factor'  $k_3$ . By letting the mast go through the deck we are able to decrease the moment of inertia by 35%. PT is the design load, and once again it is calculated using the righting moment, this time divided by the horizontal distance between the mast centre and the chainplate for the shroud in question. The load thus arrived at is multiplied by 1.5 to handle the dynamic factors

**Longitudinal mast stiffness**

The design load, PT, is obviously the same as for the transverse stiffness, and so is the 'foot factor'  $k_3$ . Fig 11.10 gives the rest of the data needed and the formula to calculate the required longitudinal moment of inertia,  $I_y$ . Varying with the different rig and staying types as defined in Fig 11.6, is the staying factor  $k_2$ , shown in the table of Fig 11.10.

**Fractional mast top**

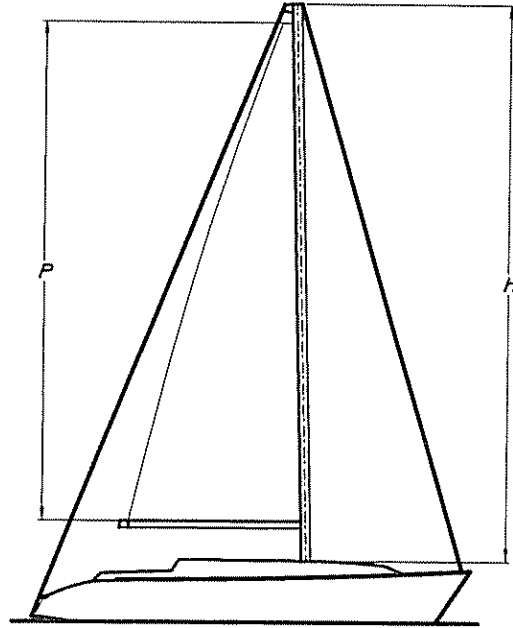
Special considerations for mast tops on fractional rigs are shown in Fig 11.11. Since there is no force from a foresail on the mast top, we are allowed to decrease the section modulus of the mast according to the formulae in the figure. We also see from the figure that if the distance from the top of the mainsail to the upper shrouds is less than 6% of the mast length ( $h$  in the figure), the rig is considered to be a masthead rig.

**Boom**

The boom is subjected to bending forces coming from the wind pressure on the mainsail which is counteracted by the sheet and kicking strap. This gives a vertical and horizontal force at the gooseneck, which has to withstand the forces  $F_v$  and  $F_h$  according to the formulae in the boom section of Fig 11.12. Once again the basis for the dimensioning force is the righting moment, in both cases the force is not to be less than 1000 N.

The bending forces that the boom has to withstand result in requirements for minimum section modulus, SM, as shown by the boxed formula in Fig 11.12. This section modulus is the vertical modulus, and the horizontal modulus is allowed to be half of the vertical. If we have a roller reefing boom, the section modulus must be that of the vertical modulus in all positions in which the boom can be locked. For the above formulae to be valid the sheet point on the boom is not allowed to be further from the end of the sail than 10% of the foot length. The attachment of the sheet must be able to withstand a force of at least the righting moment, RM, divided by the heeling arm, HA, with a minimum permissible value of 2000 N.

Fig 11.10 Longitudinal mast dimensioning



Required Longitudinal Moment of Inertia for the Mast ( $I_y$ ):

$$I_y = k_2 \cdot k_3 \cdot m \cdot PT \cdot h^2 \text{ [mm}^4\text{]}$$

$$PT = 1.5 \cdot RM/b \text{ [N]}$$

$k_2$  = staying factor (see table below)

$m$  = 1 for aluminium

7.25 for wood (spruce)

70500/E for other materials

$k_3$  = 1.35 for deck stepped masts

1.00 for keel stepped masts

$h$  = height above deck or superstructure to the highest sail carrying forestay

Type of Staying	Staying Factor $k_2$				
	F-0	M-1	F-1	M-2	F-2
1) Double Lowers	-	0.85	0.80	0.90	0.85
2) Single Lowers	-	0.80	0.75	0.85	0.80
3) Runners & i.f	-	-	0.85	-	0.80
4) Runners & c.s	-	1.00	0.95	0.95	0.90
5) Swept spreaders	-	-	1.00	-	0.95
6a) Short spreaders	1.05	-	-	-	-
6b) No spreaders	2.00	-	-	-	-

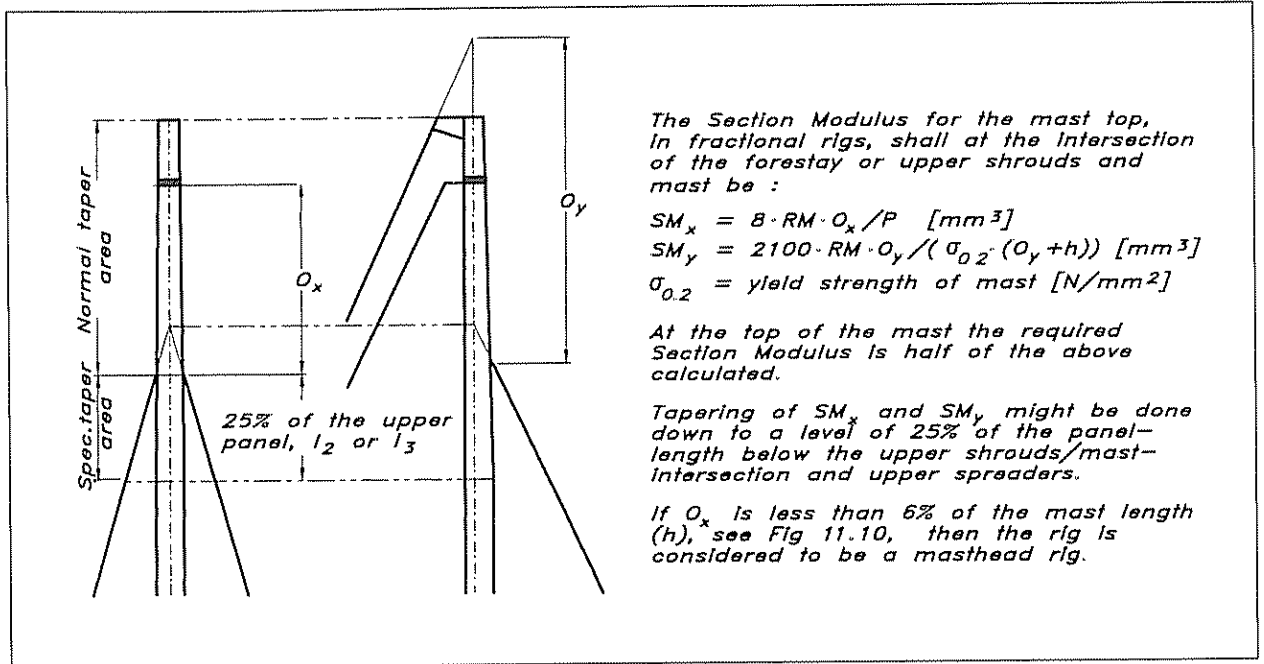


Fig 11.11 Fractional mast top

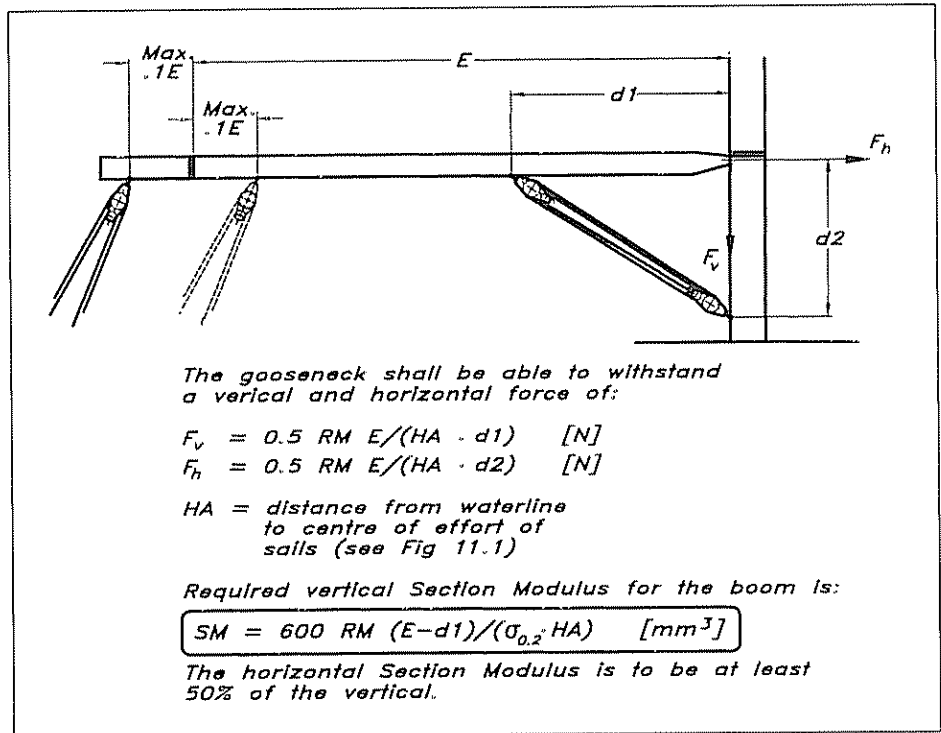


Fig 11.12 Boom requirements

**Spreaders**

Spreaders obviously are put in to diminish the free length of the mast tube. As we have shown earlier (Fig 11.9), the required moment of inertia for the mast to carry a certain load is proportional to the free length squared. So if we halve the free length then we need a mast with a section of just 1/4 of the moment of inertia. When installing the spreaders they should be set up in such a way that they cut the angle the shroud is

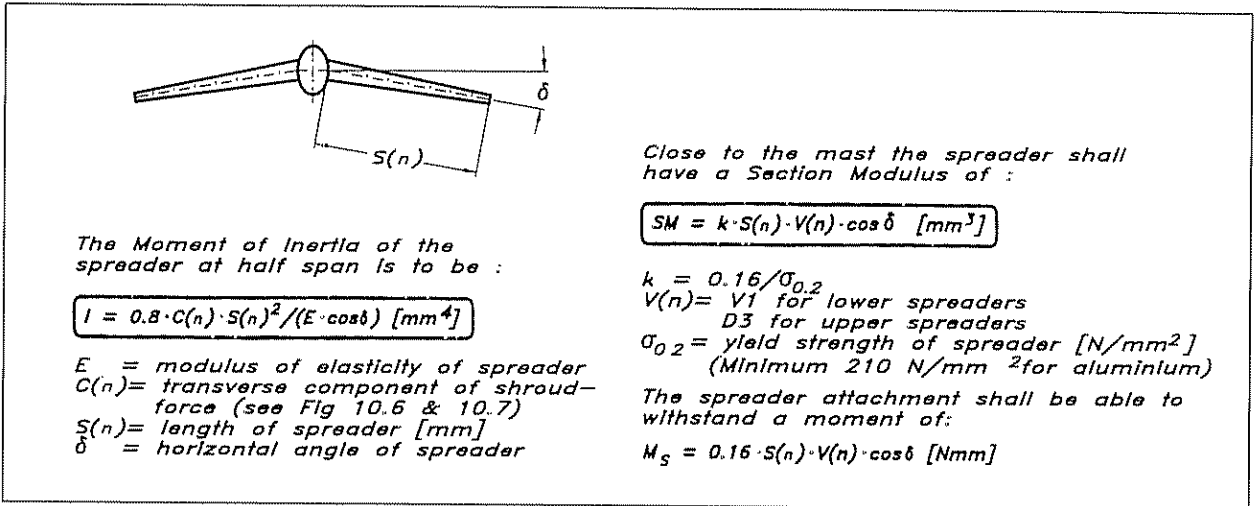
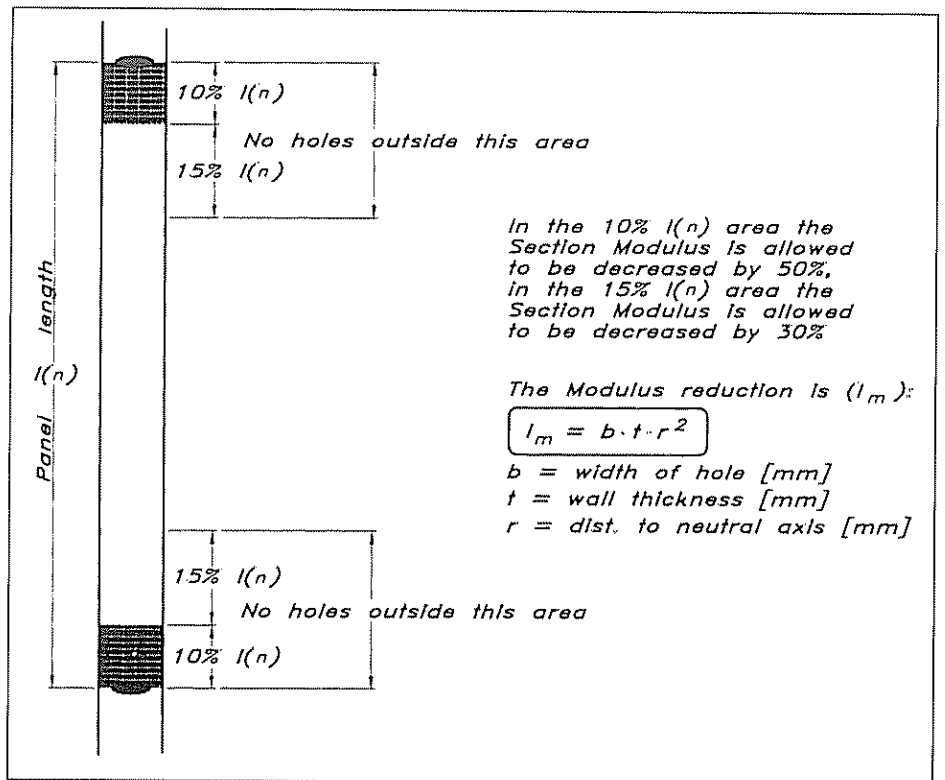


Fig 11.13 Spreader requirements

forming over the spreader tip into equal halves. This is easy to do on a one-spreader rig; on a two-spreader rig the intermediate and upper shroud come in at different angles. In this case, one has to make an intelligent adjustment, and take the mean angle the shrouds are forming above the spreader. The reason for all this is to ensure that the spreaders are put into pure compression and do not tend to slide up or down.

Fig 11.13 gives the formulae for dimensioning the spreaders. The dimensioning force is the transverse component of the shroud force,  $C$ , which can be found in Figs 11.6 and 11.7. Multiplying this force by 0.8 and the length of the spreader,  $S(n)$ , and then dividing the product with

Fig 11.14 Reduction of section modulus of mast



the modulus of elasticity and horizontal sweep angle of the spreader, the required moment of inertia at half span is found.

At the mast there is a requirement of a minimum section modulus, SM, as can be seen from the second boxed formula in Fig 11.13. Here the dimensioning force is the force of the  $V_1$  shroud for lower spreaders and of the  $D_3$  shroud for upper spreaders. The attachment of the spreader to the mast should furthermore be able to withstand a bending moment,  $M_s$ , according to the last formula in the figure. The reason for this is that by making the joint able to absorb a bending moment in the plane of the spreader, the longitudinal stability of the mast is enhanced.

### Holes in the mast

Holes in the mast are unavoidable. We need attachment points for stays, shrouds, winchpads etc and exits for halyards. Every hole means a weakening of the mast, and the moment of inertia we have calculated takes no account of holes.

As Fig 11.14 shows there are areas at the ends of each panel that are allowed to contain holes. Within 10% of the panel end we can reduce the section modulus by 50%, and for a further 15% of the panel length we are allowed to decrease the section modulus by 30%. The modulus reduction allowed is shown in the formula and is a function of the width of the hole, wall thickness of the mast and the distance to the neutral axis.

### The YD-40 rig

Fig 11.15 shows the type and dimensions of the YD-40 rig. We have chosen a masthead rig, which is easier to handle than a fractional one, but still gives good performance, especially when no rating rule has to be taken into account. The fore triangle is not excessively large, giving a good-sized, fully battened mainsail with plenty of drive in it.

The genoa is on a furler, concealed under the deck, and this is why the clew is slightly raised. Thanks to the raised clew you can roller reef the sail without changing the sheet position and, as a bonus, you will be able to see under the sail. Performance-wise, the genoa should go all the way down to the deck, but since it is a cruising yacht we are designing, other priorities than performance alone are also taken into account.

As can be seen from the figure the mast is keel stepped and equipped with double spreaders. In this way the mast weight is minimized and small sheeting angles for the foresail made possible, all of which enhance performance. Another factor which improves performance is the rake of the mast. Although not numerically proven, the rake of the mast together with the triangular planform gives a sweep back corresponding to an elliptical pressure distribution. And in terms of looks, this is how a mast traditionally should look.

To calculate the rig we start with the righting moment, RM, calculated to be 53,000 Nm at 30° of heel in fully loaded condition. Since the crew are onboard this is the correct RM to use in the rig calculations. From the formulae in Fig 11.3 we get the transverse load values of  $T_1 = 2920$  N,  $T_2 = 9100$  N,  $T_{\text{head}} = 3640$  N,  $T_{\text{boom}} = 3000$  N. The input values for the dimensioning forces are the upper- and lower-

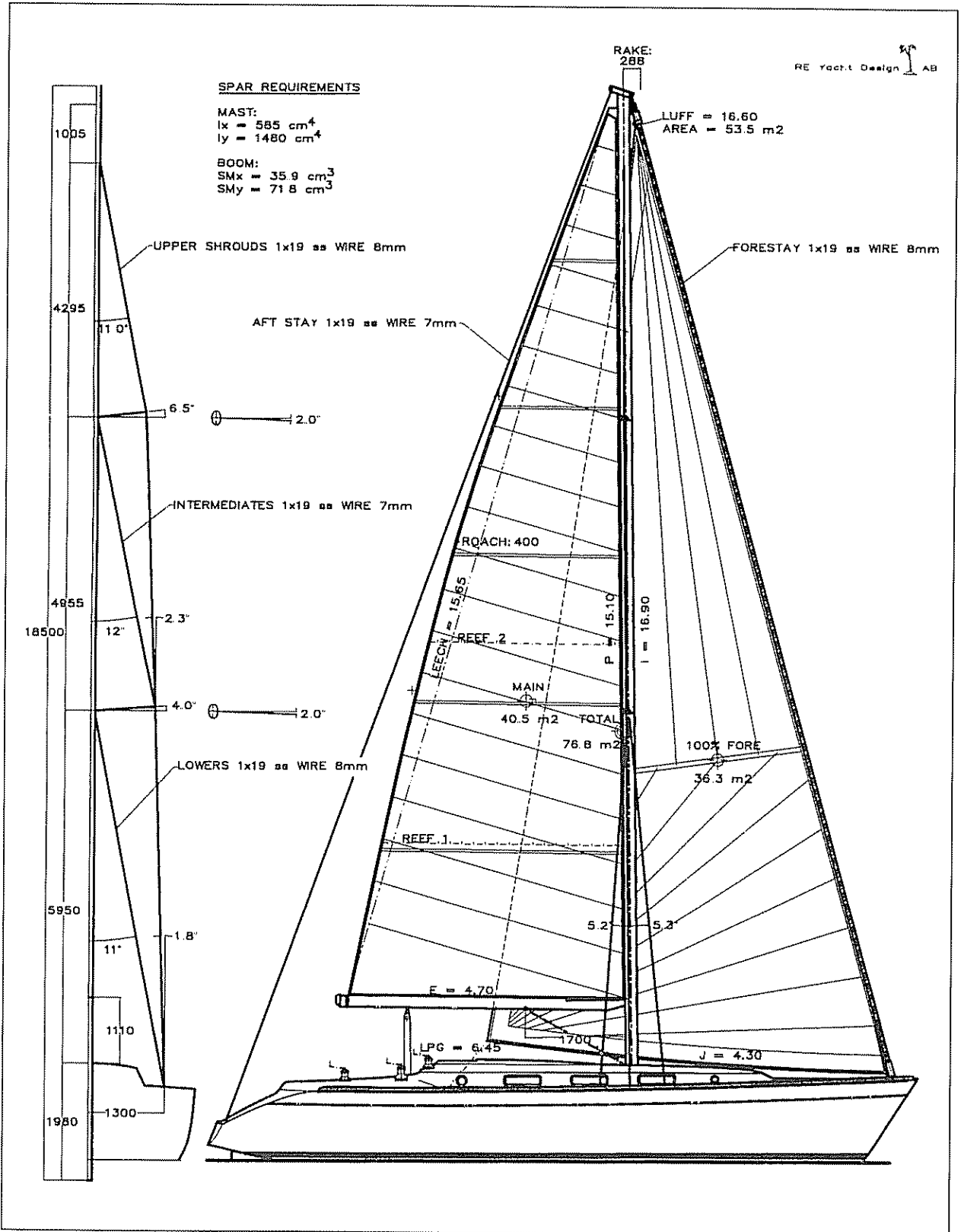


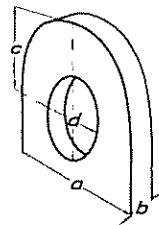
Fig 11.15 YD-40 rig

Typical properties for aluminium extrusions

Mast	Main Dim. (mm)	I <sub>y</sub> (cm <sup>4</sup> )	I <sub>x</sub> (cm <sup>4</sup> )	Wall Thkn. (mm)	Weight Kg/m	SM <sub>y</sub> (cm <sup>3</sup> )	SM <sub>x</sub> (cm <sup>3</sup> )
Oval Sect.	122/85	165	75	2.45	2.43	23.6	17.6
	130/93	215	100	2.50	2.71	29.0	21.5
	138/95	287	139	2.85	3.35	35.0	29.3
	155/104	413	191	3.05	3.69	45.9	36.7
	170/115	569	260	3.10	4.11	58.1	45.2
	177/124	725	345	3.40	4.75	74.7	55.6
	189/132	956	458	3.70	5.73	89.3	69.4
	206/139	1310	613	4.10	6.44	115	88.2
	224/150	1775	830	4.50	7.32	143	111
	237/162	2360	1120	4.85	8.76	176	138
274/185	3650	1650	4.90	10.32	232	178	
Delta Sect.	121/92	205	122	3.00	3.15	28.9	26.5
	129/100	292	175	3.50	3.74	38.9	35.0
	137/113	375	250	3.90	4.21	50.0	44.2
	146/112	508	310	4.40	5.05	61.9	55.3
Furl. Sect.	160/132	750	500	5.30	6.67	80.6	75.7
	190/94	580	200	3.00	4.69	55.4	42.5
	213/104	850	290	3.15	5.45	73.2	55.7
	235/116	1240	435	3.40	6.55	97.6	75.0
	232/126	1590	605	5.00	8.71	128	96
Boom Sect.	260/136	2400	900	5.75	10.36	176	132
	290/150	3520	1300	6.00	12.63	224	173
	86/59	60	23	1.80	1.67	14.0	7.8
	120/62	155	42	1.80	2.16	24.8	13.7
Spinn Pole Sect.	143/76	290	80	2.20	2.83	39.4	20.9
	162/125	615	330	2.80	4.75	76.0	53.0
	171/94	610	170	2.80	4.03	67.7	35.7
	200/117	1190	325	2.80	5.36	112	55.5
	250/140	2410	640	3.20	6.96	185	91.4
Pole Sect.	48/48	7.65	7.65	2.00	0.75		
	60/60	15.4	15.4	2.00	1.00		
	72/72	29.9	29.9	2.20	1.38		
	84/84	48.8	48.8	2.20	1.53		
Sect.	96/96	72.3	72.3	2.20	1.76		
	99/99	123	123	3.60	2.65		
	111/111	197	197	4.10	3.38		

Matching components made of stainless steel, type AISI-316

1x19 Wire			Rigging Screw		Chainplate lug (see fig.)			
Diam (mm)	Br.str (N)	Weight (kg/m)	Diam (in)	Br.str (N)	a (mm)	b (mm)	c (mm)	d (mm)
3	7700	0.040	1/4	14700	20.0	5.0	12.0	8.5
4	13800	0.073	5/16	22600	22.0	6.0	13.0	10.0
5	21600	0.113	3/8	33400	25.0	8.0	16.0	12.0
5.5	25700	0.139	7/16	46100	30.0	10.0	18.0	14.0
6	30000	0.165	7/16	46100	36.0	10.0	21.0	14.0
7	40900	0.225	1/2	66700	38.0	12.0	24.0	16.0
8	53500	0.327	5/8	93200	40.0	13.0	25.0	16.0
10	69100	0.475	3/4	123000	45.0	14.0	27.0	18.0
11	83500	0.648	3/4	123000	50.0	14.0	30.0	18.0
12	120200	0.820	7/8	167000	60.0	18.0	36.0	22.0
14	160100	1.000	1	218000	65.0	22.0	38.0	25.0



Chainplate lug  
 a = width  
 b = thickness  
 c = centre of hole to top of lug  
 d = diameter of hole

Fig 11.16 Typical rig dimensions and properties



mainsail head forces, and the upper mainsail boom force,  $T_{hu} = 3125 \text{ N}$ ,  $T_{hl} = 515 \text{ N}$ ,  $T_{bu} = 555 \text{ N}$

With these values we can enter Fig 11.4 and calculate the dimensioning forces  $F_1$ ,  $F_2$  and  $F_3$ . Since the rig is of the 2-spreader variety and  $BD+0.6P$  is less than  $l_1+l_2$ , we use the last row in the table of the figure, giving:  $F_1 = 0$ ,  $F_2 = 0$ ,  $F_3 = 2920 \text{ N}$  in Load Case 1, and  $F_1 = 1070 \text{ N}$ ,  $F_2 = 3125 \text{ N}$ ,  $F_3 = 0$  in Load Case 2.

Using the formulae in Fig 11.7, for a double-spreader rig we first calculate the tensions of the shrouds in Load Case 1, and by applying the relevant safety factors from the formulae we get the loads:  $P_{D1} = 27585 \text{ N}$ ,  $P_{V1} = 83025 \text{ N}$ ,  $P_{D2} = 26630 \text{ N}$ ,  $P_{V2} = 45100$ ,  $P_{D3} = 45600 \text{ N}$ .

Starting all over again with Fig 11.7 but using the forces of Load Case 2, we get:  $P_{D1} = 48910 \text{ N}$ ,  $P_{V1} = 47075 \text{ N}$ ,  $P_{D2} = 34570 \text{ N}$ ,  $P_{V2} = 0$ ,  $P_{D3} = 0$ .

Choosing the maximum values we get the dimensioning shroud forces:  $P_{D1} = 48910 \text{ N}$ ,  $P_{V1} = 83025 \text{ N}$ ,  $P_{D2} = 34570 \text{ N}$ ,  $P_{V2} = 45100$ ,  $P_{D3} = 45600 \text{ N}$ .

From Fig 11.8 we can see that our boat is of type I concerning the longitudinal staying, and from the formulae we get the dimensioning forces,  $P_{fo} = 43800 \text{ N}$  for the forestay, and  $P_a = 36500 \text{ N}$  for the aft stay.

Fig 11.9 leads on to the requirements for mast transverse stiffness. The dimensioning force,  $PT$ , is calculated to be  $61150 \text{ N}$  according to the formula in the figure. Knowing the material of the mast and the way it is stepped, material and panel factors can be applied, and the requirement for each panel's transverse moment of inertia can be calculated. For the YD-40 the dimensioning panel is the lower one giving a  $I_x$  – required of  $585 \cdot 10^4 \text{ mm}^4$ .

Doing the same calculations according to Fig 11.10 we can calculate the required longitudinal moment of inertia,  $I_y$ , which turns out to be  $1480 \cdot 10^4 \text{ mm}^4$ .

Entering values into Fig 11.12's formulae we get the requirement for the boom's section modulus. The vertical section modulus is not to be less than  $71.8 \cdot 10^3 \text{ mm}^3$  and the horizontal not less than  $35.9 \cdot 10^3 \text{ mm}^3$ .

Entering Fig 11.16 with all these values we can pick the relevant shrouds, stays and rig components. The upper table shows, in the shaded rows, the relevant mast and boom sections, and the lower one the required wire dimensions (with breaking strength), and the corresponding sizes for rigging screws and chain plates

The YD-40 ends up with a mast  $224 \cdot 150 \text{ mm}$  in diameter, weighing  $7.32 \text{ kg/m}$ , a boom measuring  $162 \cdot 125 \text{ mm}$ ,  $4.75 \text{ kg/m}$ , all shrouds and stays of  $8 \text{ mm } 1 \cdot 19$  stainless wire, except the intermediate shrouds and aft stay, which are  $7 \text{ mm}$ . With the wire dimensions go corresponding sizes of rigging screws and chain plate lugs,  $\frac{5}{8}$  in and  $\frac{1}{2}$  in rigging screws,  $13 \text{ mm}$  thick and  $12 \text{ mm}$  thick lugs respectively.

# 12

# HULL CONSTRUCTION

---

Is there really any need to calculate the strength of a boat? For centuries boats have been built from scantling rules that are based on experience, rules of thumb, guesswork and luck, with no actual strength or load calculations being made. The forces of the wind and sea are the same today as then, so reasons for the need to calculate boat strength must be sought elsewhere.

To begin with, modern boats of the 1990s have more highly loaded rigs compared with boats just 50 years ago. Aluminium spars, stainless stays and shrouds and sails from synthetic fibres deliver more power and need not be reefed as early as before, which lead to high loads from the rigging which must be absorbed by the hull.

Another factor working in this direction is today's more aggressive way of doing things, comparing ourselves and competing with our neighbour and consequently driving our boats harder.

With series production of boats the cost of production has become more important. Since the cost relates directly to the weight of the boat, the importance of not building too heavy plays an increasingly important role. Performance, on the other hand (almost always sought), is inversely proportional to the displacement, but still this has pushed the development towards lighter and lighter boats.

So, higher loads from the rig and an aggressive and competitive owner must be taken care of by an increasingly lighter hull structure. All this means that the margin of error gets smaller and that the need for accurate calculations of strength becomes more important.

Other factors that put higher demands on the structure are the development of increasingly shorter fin keels that increase the stress on the keel/hull joint, and separate rudders that are supported only by their own rudder shafts, or by a skeg so small that it hardly contributes to the strength.

Before calculating strength requirements one must know the loads, and this is perhaps the most uncertain part of it all. The loadings can be divided into two parts: global and local. Global loads affect the vessel as a whole, ie loadings from the rig when underway try to bend the hull girder, and the stresses and deflections can be calculated by means of simple beam theory (to be discussed later). Local loads can be divided into hydrostatic/dynamic loads imposed on the vessel by the sea and waves, and loads brought into the hull from chain plates, keel, rudder, winches, sheet blocks and tracks, stanchions etc.

In this chapter we will discuss the influence of different loads, global and local, and what deflections they induce. Then we will show how the

keel and rudder affect the hull structure, and finally survey different kinds of materials and their use, including exotic materials and sandwich construction. Details of the actual dimensioning of the YD-40 will be given in the next chapter.

### Concepts in structural mechanics

Although this is not meant to be a chapter on general structural mechanics, we will describe some basic concepts in structural design that are used in this chapter.

When we are talking of a material's stress, we mean the amount of force acting over the cross sectional area of the item in question, expressed in Newtons per square millimetre ( $\text{N}/\text{mm}^2$ ). The ultimate breaking stress represents the breaking stress, and the yield stress for metals means the maximum useful static stress.

Strain is the extension of the material per unit length when loaded, and it is expressed as a percentage. So if we have a piece of wood, steel, glassfibre etc, initially 100 mm long that when loaded becomes 103 mm long, the strain is said to be 3%. Obviously the lower the strain value the more brittle the material is.

The stiffness of a material is the ratio of stress to strain. If we compare two equal wires, one of nylon and the other one of stainless steel, both carrying the same load and stress, the stainless one will stretch just a little while the nylon will stretch quite a bit more, reflecting the different levels of strain. Dividing the stress by the strain you get a measure of the stiffness known as the modulus of elasticity:  $E = \text{stress}/\text{strain}$  [ $\text{N}/\text{mm}^2$ ]. This relationship is only true when the material is within its 'elastic region', which means that when the load is released the piece in question retains its original size. For metals this region is quite small. Typical permissible levels of strain are 0.2–0.3%. The level of stress at this point is called yield strength, as opposed to ultimate strength which describes when the material actually breaks.

When bending a beam or a panel one side will be subjected to compressional forces and the other side to tensional forces, both of them normal to the surfaces. Somewhere in between there will be a layer with no stress, called the neutral axis. In a homogeneous material this will pass through the geometrical centre of gravity for the cross-section. If the cross-section consists of parts of different moduli of elasticity, the cross-section is modified in the same proportion as the moduli of elasticity. If, for instance, one part has a 40% higher modulus of elasticity, this part is widened the same amount before calculating the centre of gravity for the cross-section.

The combined moment of inertia ( $I$ ) for a composite section is the sum of each part's own moment of inertia plus each part's distance from the total neutral axis squared, times its area. When calculating the resistance to bending for a beam or a panel, we need to know the section modulus ( $SM$ ), which, put simply, is the moment of inertia divided by the longest distance from the neutral axis to one of the surfaces.

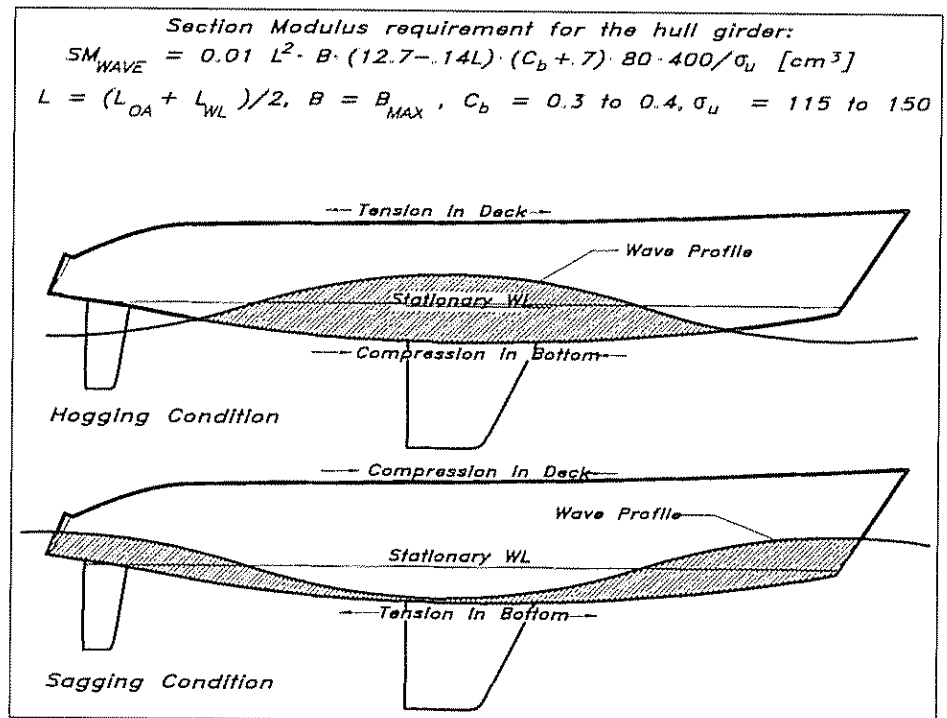
As stated earlier the bending force induces compressional and tensional forces on the surfaces, and also a transverse, or shear force

that is acting on the cross-section itself. This shear force also gives a shear stress along the beam or panel.

### Global loads

One case of global loadings primarily concerning ships and bigger yachts, are the bending-moment conditions of hogging and sagging: hogging when the wave crest is amidships and sagging when the wave trough is amidships with the crests at bow and stern. Normally hogging/sagging calculations are not performed on pleasure yachts below approximately 100 ft (30 m) (Fig 12.1).

Fig 12.1 Hull girder requirements (ABS)



The ABS (American Bureau of Shipping) guide for building and classing offshore racing yachts and the ISO 12215 Standard cover vessels up to 80 ft (24 m) and does not require the calculations of bending moments and hull girder strength, but the ABS rule for motor pleasure yachts stipulates a minimum hull girder section modulus SM at amidships varying with length, breadth and block coefficient. (See Fig 12.5 for how this is calculated for the YD-40.) This ABS formula is valid for yachts shorter than 45 m and made of fibre reinforced plastic with speeds below 25 knots. The beam (B) of the vessel is not to be greater than 2 times the depth of the canoe-body ( $D_c$ ).

The minimum ultimate strength of the hull material, tensile or compressive, is  $\sigma_u$ , whichever is less in N/mm<sup>2</sup>. L and B are length and beam in metres, and  $C_b$  is the block coefficient of the vessel. Typical values for the block coefficient are 0.35 to 0.42.

The other big villain which inflicts deformations is loading from the rig in sailboats. The loads come from the shroud tension to windward, and the tension in the fore-and-aft stays. The former is directly coupled

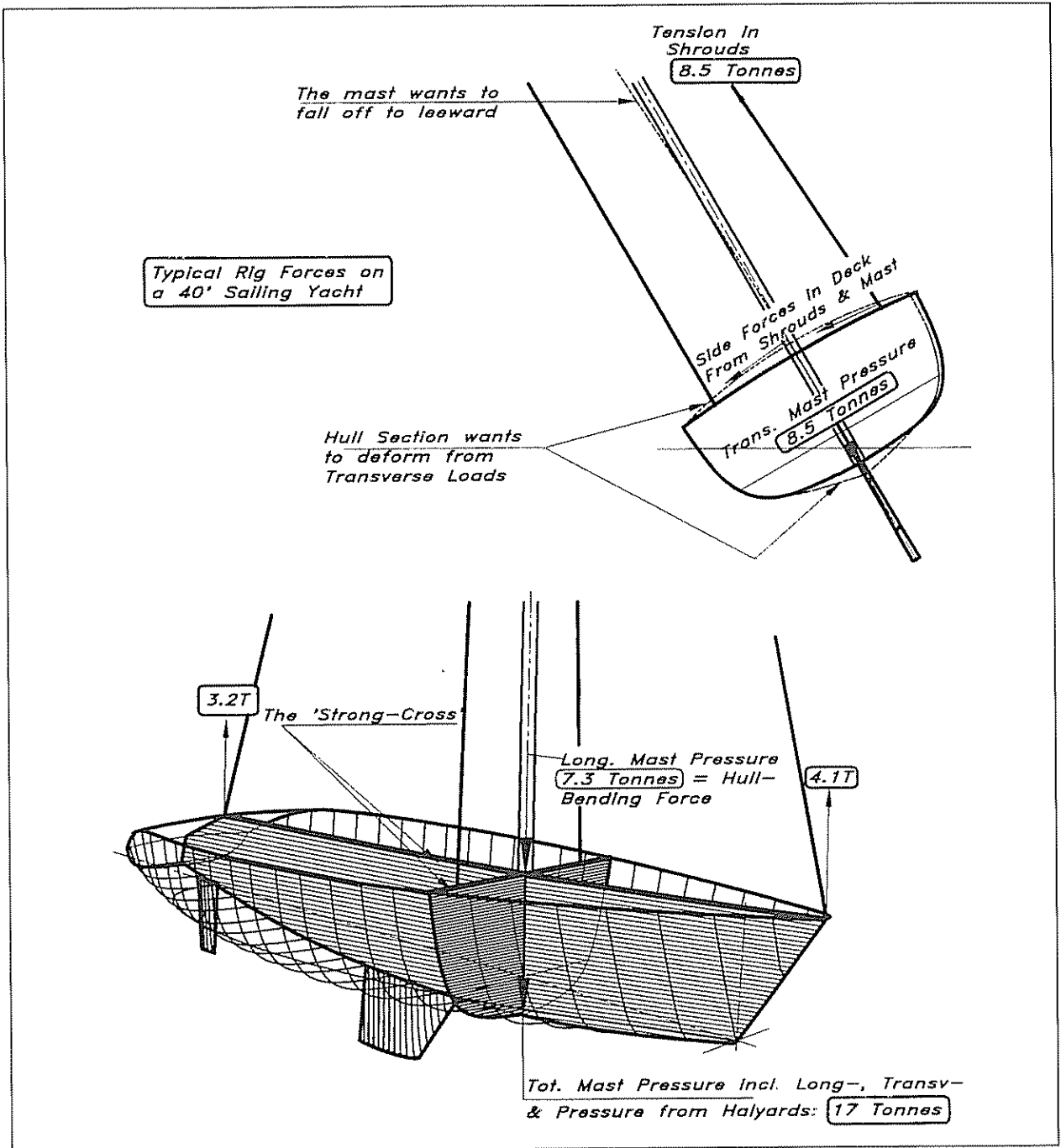


Fig 12.2 Forces from the rig

to the boat's righting moment and the latter to the need for a straight jibstay to get the best performance from the sails.

On a 'normal' ballasted sailing yacht the accumulated pressure on the mast foot, coming from stays, shrouds and halyard tension can reach a value of double the boat's displacement. Loadings from the shrouds are of the same magnitude as the displacement, and halyard tensions are approximately 15% of displacement. The tension in the fore-and-aft stay inducing a longitudinal bending moment in the hull girder, results in a

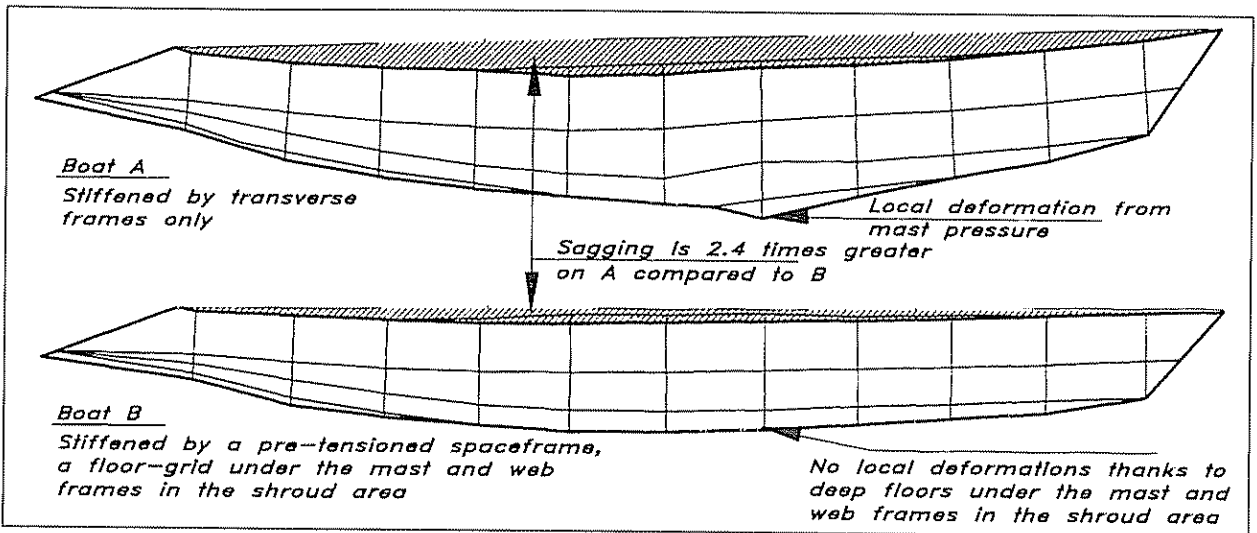


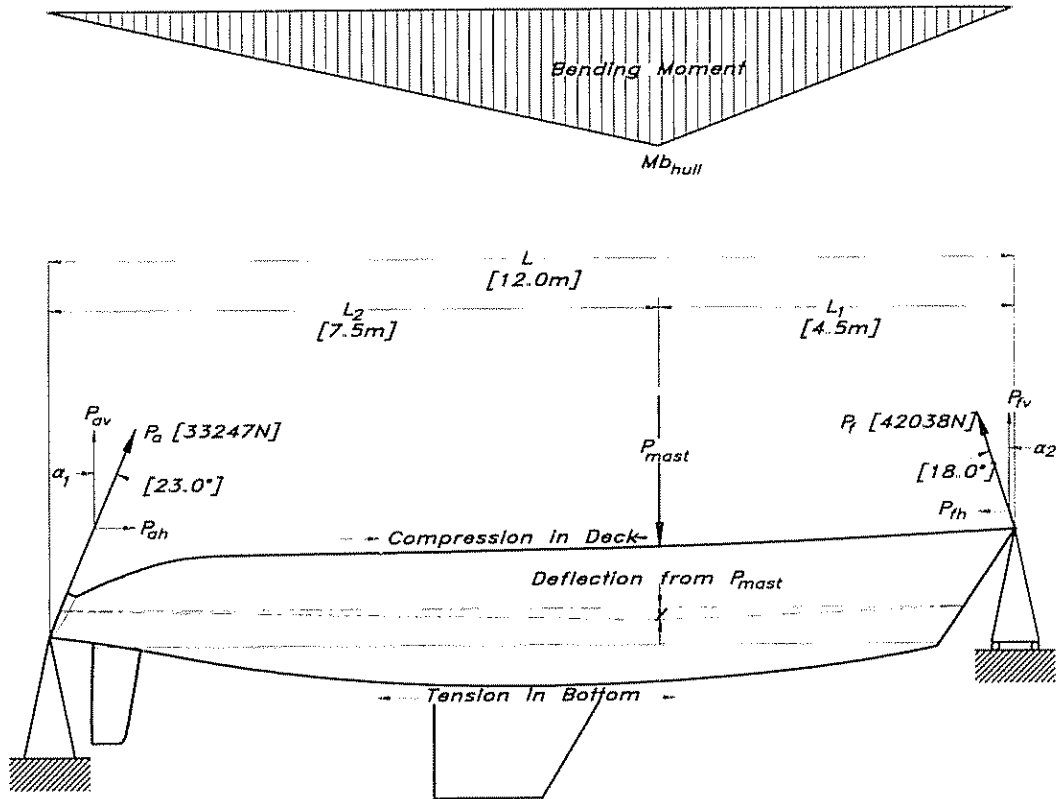
Fig 12.3 Longitudinal deformations from rigging loads

bending force of approximately 85% of the displacement, ie 7.3 tonnes on the YD-40 (a load that the hull girder must be able to absorb without undue deformations).

Transversely the hull section in the shroud area must be stiff enough not to lose its shape, so the mast falls off to leeward (Fig 12.2). To achieve this, the boat must have a 'strong cross' with the mast in its centre when seen from above. The hull for a proposed Whitbread maxi was computed by the Royal Institute of Technology (KTH) in Stockholm (see Fig 12.3) with regard to longitudinal deformations due to rigging loads. Boat 'A' is stiffened by frames, spaced 2 metres, but no longitudinal members, and the boat 'B' is stiffened by a pre-tensioned space frame. In both cases the hull is of sandwich construction, with a 40 mm PVC core and skins of S-glass in a vinyl-polyester matrix. As can be seen clearly it is not sufficient with just transverse frames to absorb the longitudinal rig-loadings, but a longitudinal stiffening system is needed. In the example shown it is in the form of a space frame, but a more usual approach today is to incorporate the stiffening system into the hull and deck structure, ie a monocoque type of structure. Most of the strength is put into the shell with this approach, with fewer internals and larger panels. The fibre orientation is crucial with the monocoque approach, and so is an analysis of the magnitude and direction of the forces involved. Boat size obviously plays an important role. Small vessels are almost self-supporting, ie monocoque, while the bigger ones need some sort of stiffeners, at least in specially loaded areas such as around the keel, mast, chain plates etc.

The 'rig-sagging' condition is the most severe one for a sailing yacht as it puts the deck into compression and the keel into tension, whereas these parts are better suited to the reverse condition. Light decks are not fully effective in compression, as there is a risk of buckling which is worsened by the presence of deck hatches and other openings. A simple technique to counteract this weakening of the deck due to openings, is to use the reinforcement that should have been in the hole as an extra strengthening to the edge of the opening.

Bending Moment Diagram:



$$\begin{aligned}
 P_{mast} &= 0.85 \text{-Displacement [ 71600 N ]} \\
 P_a &= P_{mast} / (\sin \alpha_1 / \tan \alpha_2 + \cos \alpha_1) \quad [ 33247 \text{ N } ] \\
 P_{ah} &= \sin \alpha_1 \cdot P_a \quad [ 12990 \text{ N } ] \\
 P_f &= P_a \cdot (\sin \alpha_1 / \sin \alpha_2) \quad [ 42038 \text{ N } ] \\
 P_{fh} &= \sin \alpha_2 \cdot P_f \quad [ 12990 \text{ N } ]
 \end{aligned}$$

Deflection of the Hull Girder :

$$y = ( P_{mast} \cdot L_1^2 \cdot L_2^2 ) / ( 3 \cdot E \cdot I \cdot L )$$

*E* = Young's Modulus ; *I* = Moment of Inertia for Hull Girder

Maximum Bending Moment (  $M_{b_{hull}}$  )  
of the hull occurs in the mast area:

$$M_{b_{hull}} = P_{mast} \cdot L_1 \cdot L_2 / L \quad [ 201375 \text{ Nm } ]$$

Fig 12.4 Longitudinal rig forces

With regard to the YD-40, with 7.3 tonnes pressure from the mast we can use a simplified model to estimate the required hull girder section modulus ( $SM_{hull}$ ). Considering the yacht to be a beam freely supported at its ends with the mast pressure trying to bend it, we will have a situation like that in Fig 12.4. The maximum bending moment occurs in the transverse section at the mast ( $M_{b_{hull}}$ ), so this is where we shall calculate the section modulus of the hull.

In order to establish the required section modulus we must take our hull section at the mast and simplify it to make it practical to calculate. In Fig 12.5 the actual hull and deck is drawn with a dashed line, and the simplified section with a bold line. The aim with the simplification is to reduce the section to rectangular parts oriented orthogonally to the boat's Y and Z axis. Having reduced the section thus, it is comparatively easy to calculate the section's moment of inertia (I), area (A) and neutral axis ( $X_0$ ), and from these results the hull girder's section modulus (as shown in Fig 12.5). For the sake of simplicity the modulus of elasticity is assumed to be equal in all parts, otherwise corrections of areas have to be performed for the different parts, corresponding to the ratios of the different moduli.

If an area correction is necessary, remember to make the increase only in width, never in height since this will change the part's moment of inertia in an incorrect way, ie it will be too high since height is in the formula with its cubed value. If, for example, the modulus of elasticity of the bottom panel is 50% greater than the other panels, the width of this panel is to be increased by 50% in the simplified section of the hull, before any computations are made. The thickness and vertical position are to be unaltered though.

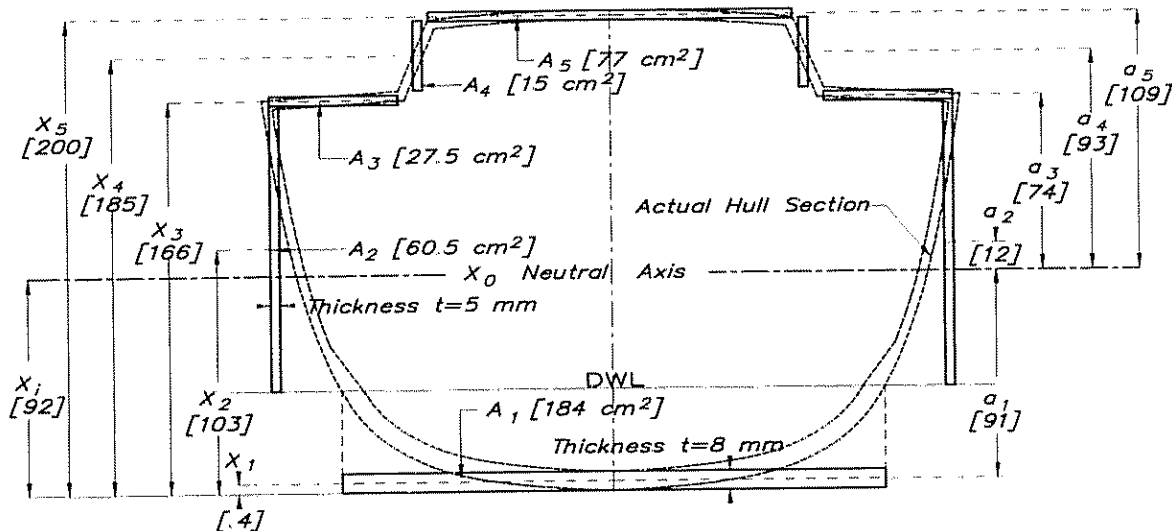
In this example, the section is divided into five parts ( $A_1 - A_5$ ) with all parts of thickness (t) except  $A_1$  which is 60% thicker. In order to determine the section's neutral axis ( $X_0$ ) you calculate the geometrical centre of gravity for the parts, as shown in the figure.

The individual moments of inertia for the parts are then calculated and added to the areas of the parts, and their respective distances from the section's neutral axis squared. The resulting section modulus for the hull section is the moment of inertia divided by the distance from the neutral axis to the deck and the bottom respectively. Use the smallest value to compare with the required modulus to withstand the mast pressure, which is: maximum bending moment ( $M_{b_{hull}}$  from Fig 12.4) divided by the ultimate compressive strength for the deck and the ultimate tensile strength for the bottom.

For the YD-40 the moment from the mast pressure of 71600 N leads to a required hull girder section modulus of 1632 cm<sup>3</sup> to take care of the longitudinal rig forces, and the actual boat has 29301 cm<sup>3</sup>. The ABS requirement for hull girder strength on a 12 m motor yacht is 17135 cm<sup>3</sup>, so the total required section modulus to handle all the forces becomes 17135 + 1632 = 18767 cm<sup>3</sup> which leaves us with a factor of safety of 1.6 overall, and 7.5 looking only at rig forces. This obviously is enough, but if not, more or better material must be used if the section is to be geometrically unchanged.

A check of the maximum compression forces in the deck is now easily done:  $P_{deck} = Mb_{hull}/(a_5 + 0.5t) + P_{hd}$  (=197738 N). The expression ( $a_5 + 0.5t$ ) is the distance from the top of the deck to the hull's neutral axis, see Fig 12.5.  $P_{hd}$  is the horizontal component of the fore and backstay tension, illustrated in Fig 12.4:  $P_{hd} = P_{th} = P_{ah}$ . Dividing this value with the deck cross-sectional area, we will see if the deck is strong enough to





Total sectional area ( $A_i$ ) : [ 467 cm<sup>2</sup> ]

$A_1$  to  $A_5$  = areas of the individual parts.

$$A_i = A_1 + 2 ( A_2 + A_3 + A_4 ) + A_5$$

Distance of neutral axis from bottom ( $x_i$ ) :

$$x_i = \frac{A_1 \cdot x_1 + 2 ( A_2 \cdot x_2 + A_3 \cdot x_3 + A_4 \cdot x_4 ) + A_5 \cdot x_5}{A_i}$$

Distances from the neutral axis for the different parts:

$$a_1 = x_i - x_1 \quad ( x_1 = t/2 )$$

$$a_2 = x_2 - x_i$$

$$a_4 = x_4 - x_i$$

$$a_3 = x_3 - x_i$$

$$a_5 = x_5 - x_i$$

Individual moment of inertia for each part ( in general form ) :

$$I_n = \frac{b \cdot h_n^3}{12}$$

where  $b$  is the horizontal, and  $h$  is the vertical measurement.

$$[ I_1 = 9.8 \text{ cm}^4 , I_2 = 72000 \text{ cm}^4 , I_3 = 0.6 \text{ cm}^4 , I_4 = 1070 \text{ cm}^4 , I_5 = 1.6 \text{ cm}^4 ]$$

The total moment of inertia for the hull section is the sum of each part's moment of inertia plus the sum of each area times its distance from the neutral axis squared ( $I_x$ ) :

$$I_x = I_1 + 2 ( I_2 + I_3 + I_4 ) + I_5 + A_1 \cdot a_1^2 + 2 ( A_2 \cdot a_2^2 + A_3 \cdot a_3^2 + A_4 \cdot a_4^2 ) + A_5 \cdot a_5^2$$

$$[ I_x = 3179207 \text{ cm}^4 \{ 3.18 \cdot 10^6 \text{ cm}^4 \} ]$$

The resulting Sectional Modulus is ( $SM_{sec}$ ) :

From $X_0$ to bottom : $SM_{sec} = \frac{I_x}{x_i}$	[29301 cm <sup>3</sup> ]
From $X_0$ to deckhead: $SM_{sec} = \frac{I_x}{x_5 - x_i + t/2}$	[34632 cm <sup>3</sup> ]

The required Section Modulus ( $SM_{req}$ ) : [18767 cm<sup>3</sup>]

$$SM_{req} = \frac{M b_{hull}}{\sigma_u} + SM_{wave}$$

$\sigma_u$  = the ultimate compression strength for the deck or  
 $\sigma_u$  = the ultimate tension strength for the bottom,  
 whichever is the smallest

$M b_{hull}$  from Fig 12.4 and  $SM_{wave}$  from Fig 12.1

Fig 12.5 Hull girder section modulus at mast

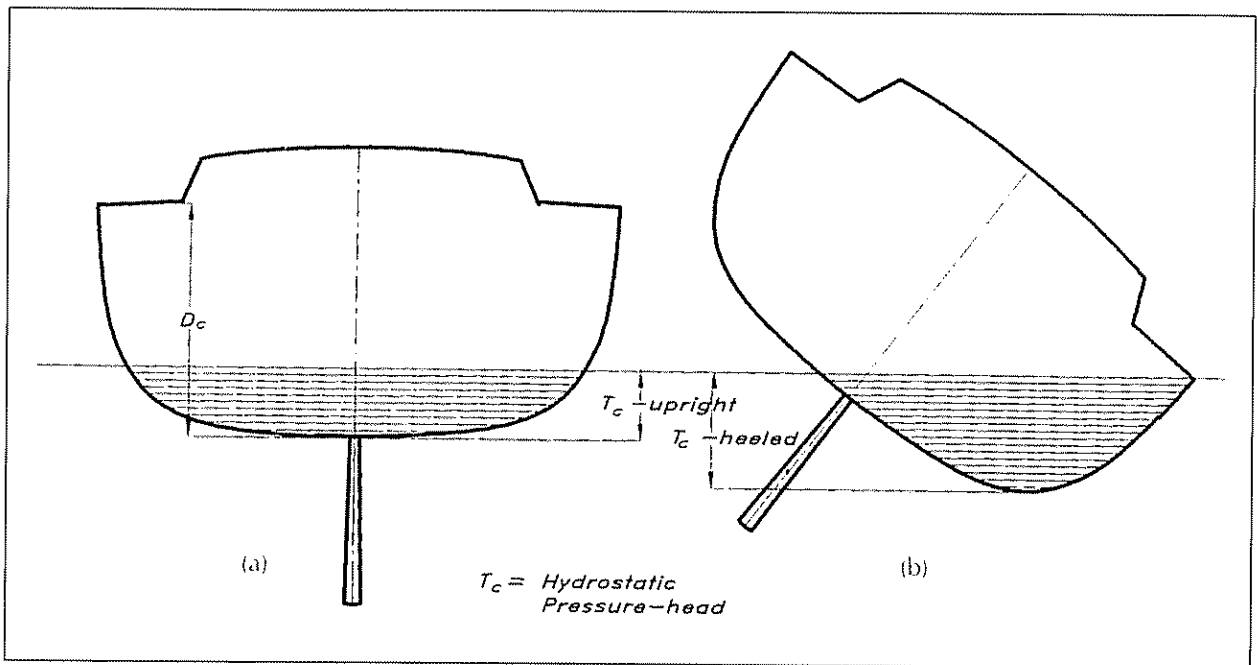


Fig 12.6 Hydrostatic pressures

absorb the compression forces. In our case the force in the deck leads to a compression stress of  $12.2 \text{ N/mm}^2$ , and with an ultimate allowable stress of  $117 \text{ N/mm}^2$  the safety margin is more than enough.

This might be considered the 'standard case'. A typical cruiser/racer dimensioned, by ISO 12215 or any other scantling rule, to withstand local pressure forces from the water, is strong enough to cope with the rigging forces. On extreme yachts though, with extraordinarily big rigs, low hull girder heights and built of 'exotic' materials with thin skins, it is wise to check the hull girder strength, and especially the compression stresses in the deck.

### Local hydrostatic loads

To establish a proper design load let us begin with the hydrostatic part. The simplest case is when the boat is at rest and upright in calm water. Then the hydrostatic pressure head is simply the depth of the underwater body. This is the dimension  $T_c$ . For a vessel operating in a wave-train it is not excessive to assume that the crest reaches the sheer line, and so the static pressure would become the  $D_c$  measurement (Fig 12.6(a)).

When under way and heeled in a rail-down condition, the immersed pressure head is approximately half of the full depth  $D_c$  (Fig 12.6(b)). In determining the hydrostatic pressure ISO uses 2.0. ' $T_c$ -upright', which on a 'normal' boat is somewhat in excess of  $D_c$ . Thus, there is a safety factor of approximately 2 built into the hydrostatic pressure.

### Local hydrodynamic loads

In the formula above no account is taken of speed, which naturally increases the pressure effects. It is commonly agreed that the pressure from speed varies with the speed squared, where speed is dealt with in terms of speed/length ratio. The ISO Standard takes the speed as an absolute function of length for sailing craft, which means that ISO assumes a fixed speed/

length ratio. This additional loading is added to the hydrostatic pressure together with a constant pressure head to arrive at a basic bottom pressure ( $P_b$ ). We will deal with this in more detail when discussing the ABS rule.

A vessel moving in a seaway is subjected to at least one more major load factor, that is, slamming. Several tests and measurements have been done to determine these loads, especially on planing power boats, where the slamming effects are the most severe. One of the best recognized methods to deal with the slamming loads is made by Heller and Jasper, and this method, used by the ISO Standard for power craft and fast sailing craft, gives a good fit for high speed vessels. The formula takes speed, length, bottom deadrise, displacement and running trim into consideration when defining the bottom pressure ( $P_b$ ).

For sailing boats the approach is slightly different. By starting with the previously achieved design pressure head, it is given a modifying 'slamming factor' depending on where on the boat bottom we are doing our calculations. Motor yachts are also subjected to a longitudinal 'slamming factor' but here it is incorporated in the original pressure formula (see Fig 12.7).

The work of Heller and Jasper has shown the primary slamming area to be in the forward sections of the boat, as can be seen from Fig 12.7. A word of caution though: on small fast boats with relatively high speeds ( $V(\text{knots})$  is greater than 10 times the square root of  $L(\text{m})$ ), the whole boat might be airborne in a big sea and land on the after part of the bottom, so it is wise to let the high pressure area be extended all the way to the transom on such a craft.

On the sailboat side Prof P N Joubert has calculated the bottom pressures for six sailing yachts that have been damaged by sea-forces but survived to be examined (Fig 12.8). The boats are:

- 1 *Odin*, a 39 ft steel yacht, buckled her bottom plating on a beat against a 25 m/s wind (50 knots). The deformed area was just ahead of the mast on one side between keel and  $L_{WL}$ .
- 2 *Pacha*, a 54 ft aluminium yacht, buckled a major part of the bottom in an area from the stem to the mast from keel to  $L_{WL}$ .
- 3 *Boomerang VII*, a 42 ft PVC-sandwich construction, delaminated in an area from stem to amidships from the keel up to some distance into the topsides.
- 4 *Destiny II*, a 42 ft plywood boat, got a transverse crack in her bottom where a structural bulkhead was attached.
- 5 *Magic Pudding*, a 37 ft cold moulded wooden boat, broke the same way as boat 4.
- 6 *Mary Blair*, a 41 ft aluminium boat, was injured in the same way as boat 2.

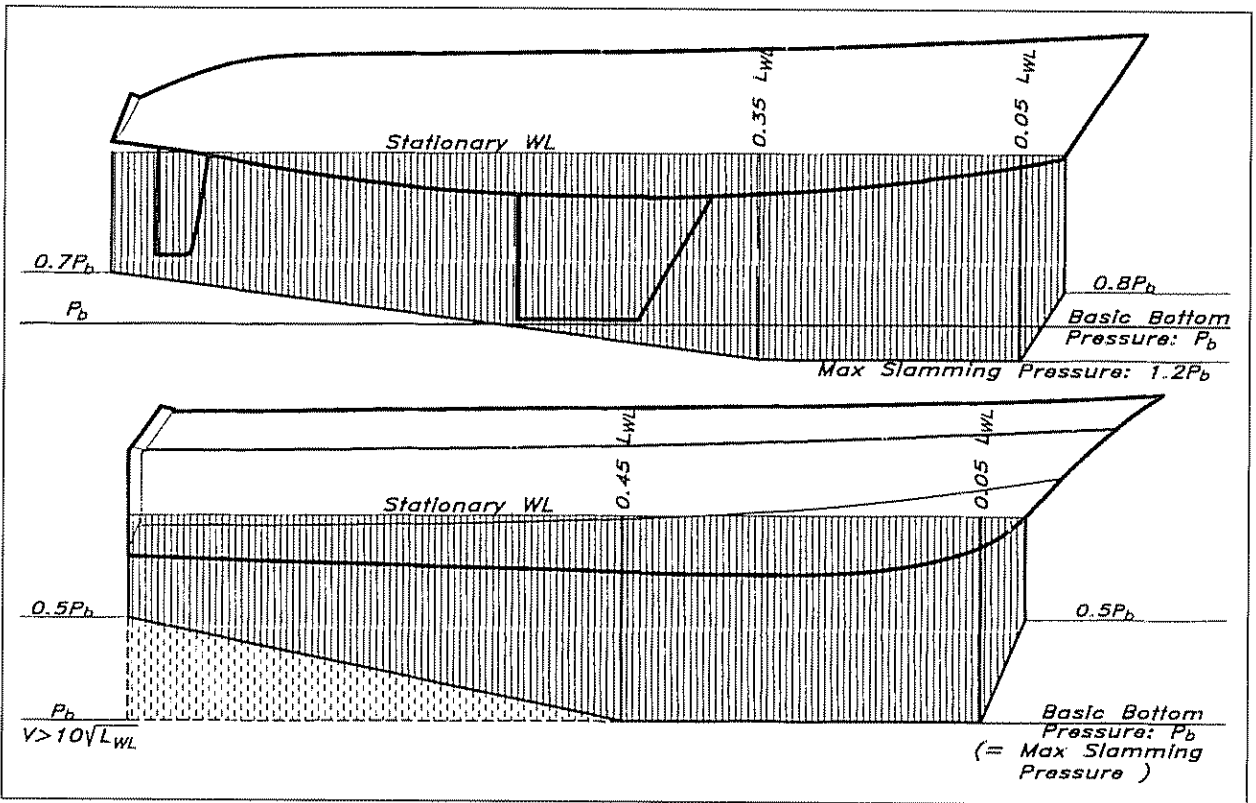


Fig 12.7 Longitudinal hydrodynamic loads (ABS)

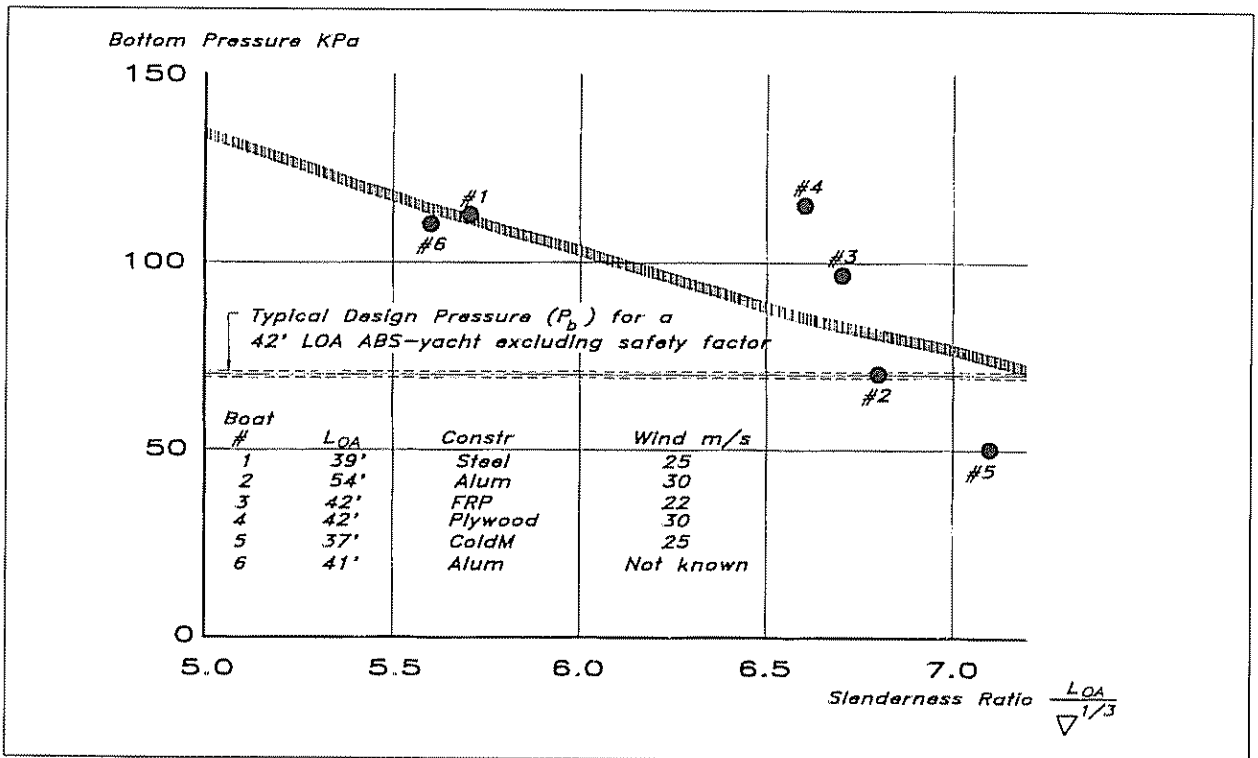


Fig 12.8 Calculated pressures from bottom failures (Joubert)

All these deformations, delaminations and cracks developed when the boats were on the wind. The reason for the failures were slamming loads, coming from the free falling of the boats from a crest down into the trough (a fall of 3 m (10 ft) or more).

The pressure loads on the shells of the boats have been calculated 'backwards' by knowing the construction of each vessel. Depending on the calculation method, ie using simple beam theory or taking membrane stresses etc into account, different pressures are reached. The more sophisticated calculation methods gives a much higher pressure before the collapsing of the skin than does the beam theory. Fig 12.8 shows the result using the beam theory, with the boats ordered after slenderness ratio ( $LOA/(\text{Displacement})^{1/3}$ ), and for comparison the ABS basic design head is represented by the dashed band.

### Transverse load distribution

So much for the bottom pressure, but what about the sides? The longitudinal distribution follows that of the bottom, but transversely the pressure diminishes the higher up the topsides you move. And there is a difference between sail and power. Relatively speaking, a sailboat that in some instances has her topsides completely buried is more loaded in the side plating, compared to a planing power boat which is more subjected to slamming on its bottom.

On a sailboat the topside pressure falls off to zero at about 1.5 the freeboard height from full bottom pressure at the waterline. On a planing motorboat the side pressure according to ISO is 20% of the bottom pressure plus a minimum static pressure head corresponding to half hull depth ( $0.5 \cdot D_c$ ).

Deck and superstructure design pressures are functions of boat length and a constant. We will give more details of this when showing an example of a calculation using the ISO rule. Fig 12.9 shows typical transverse load distributions for sailing and motor yachts.

### Local deformations

The Whitbread study of deformations made at KTH in Stockholm on different methods of stiffening a hull (Fig 12.10), shows that it is very important to have the forebody sufficiently stiffened. The hull is the same in all cases, with a different number of frames in the forward part. The hulls are basically stiffened by an inner space frame. The C boat has this space frame only, whereas the D boat has two additional stringers per side. In addition to this the E boat has one ring-frame before the mast, and the F boat has three ring-frames in the forebody.

The shaded areas in Fig 12.10 represent the deformed hull when subjected to slamming loads. As can be seen, the difference between the hull with only the space frame and the hull with stringers is not that great. The reason for this is that lacking transverse stiffeners the stringers get too long a span to effectively keep the deflections at a reasonable level.

By introducing a ring-frame into the forebody, ie frame spacing is 4.5 m, the deformations are diminished drastically, and by increasing the number to three the vessel starts to look like a boat even when under load (hull F in Fig 12.10). This ability to withstand slamming pressures

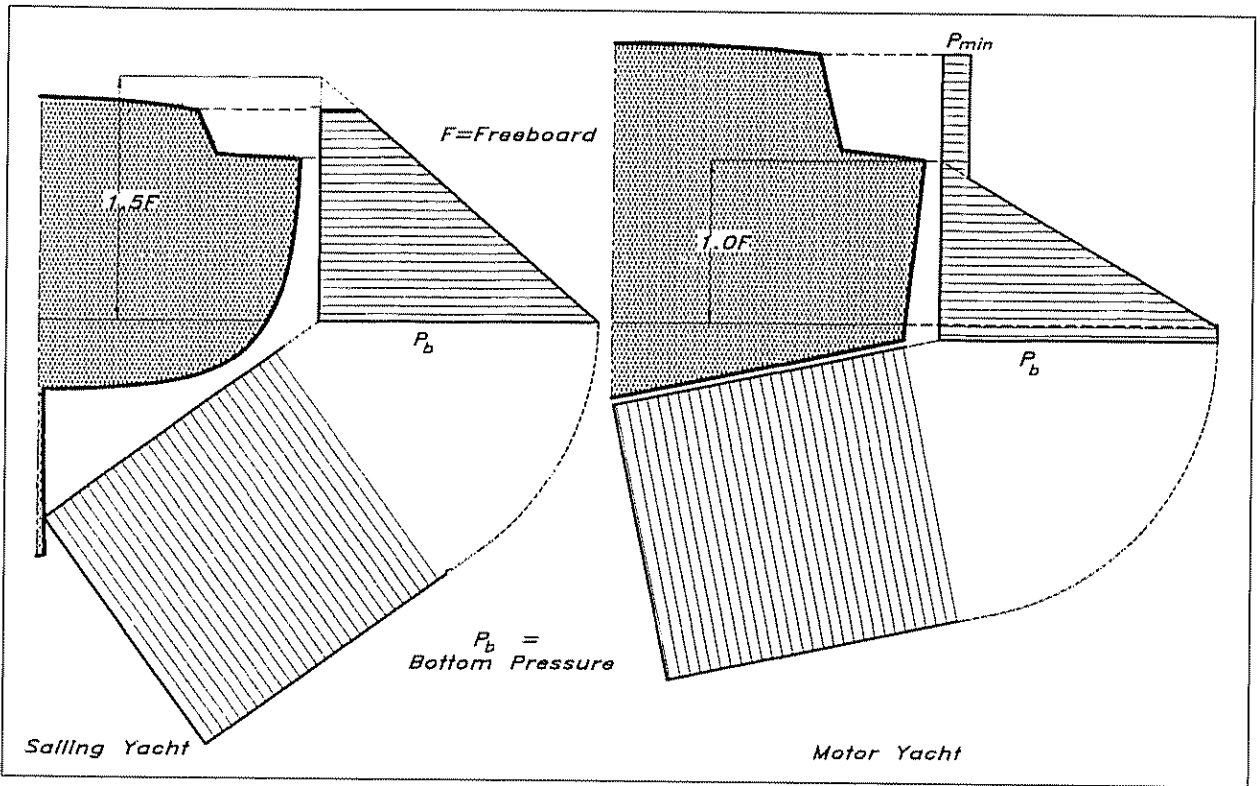


Fig 12.9 Transverse load distribution (NBS)

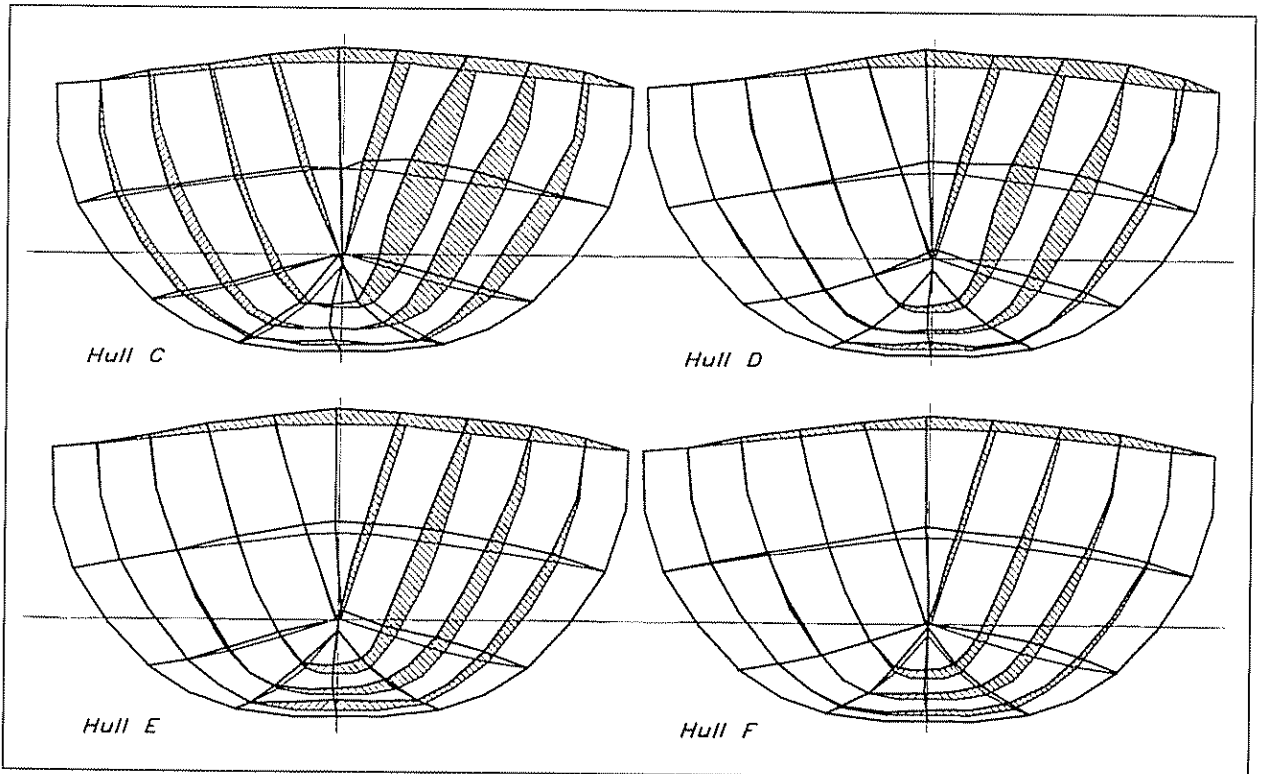


Fig 12.10 Deformations due to slamming (Hunyadi & Hedlund)

for the F hull shows roughly the same performance that a traditionally transversely frame-stiffened hull will give. As we have seen previously, the picture changes when dealing with longitudinal loadings. So, to summarize, the hull must be stiffened lengthwise as well as transversely to withstand the rigging and slamming forces. This can be done either by a separate stiffening system, by a monocoque structure or by a combination thereof.

### Forces from the keel

Fig 12.11 shows an example of a calculation for stresses from the ballast keel on the YD-40. The 'design-attitude' for the boat is 90° heeled over and situated totally in air. Regarding the hull as in the air and applying a factor of safety of 4 to 6 takes care of the added loadings from dynamics, which are not incorporated in the formulae

A simple calculation of moments around the keelbolts gives the transverse keel moment ( $M_{kt}$ ), and by dividing this moment with the distance between the windward keelbolts and leeward keel-edge ( $OF_{bolt}$ ) the keelbolt load ( $P_{ki}$ ) can be calculated (81156 N in our case).

The  $OF_{bolt}$  typically varies along the root chord of the keel, and to account for this it is reasonable to take a mean value of all  $OF_{bolt}$ s. Assuming the keel to have six pairs ( $n_{kb}$ ) of keelbolts, the loading on each bolt becomes ( $P_{kb} = P_{ki}/n_{kb}$ ) 13526 N. When calculating the required dimensions of the keelbolts it is the yield strength ( $\sigma_y$ ) of the material that shall be used, not the ultimate strength. The required diameter of the keelbolts ( $d_{kb}$ ), when using a safety factor of 5, becomes 21 mm, as can be seen from the formulae in Fig 12.11.

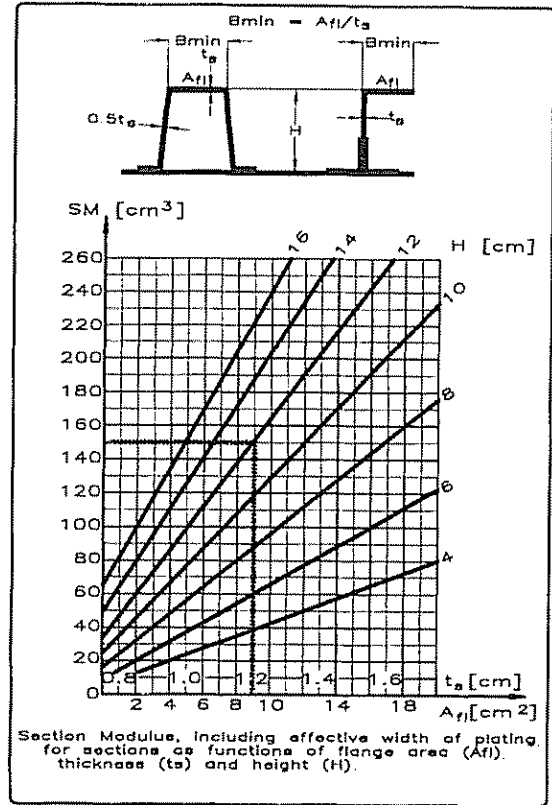
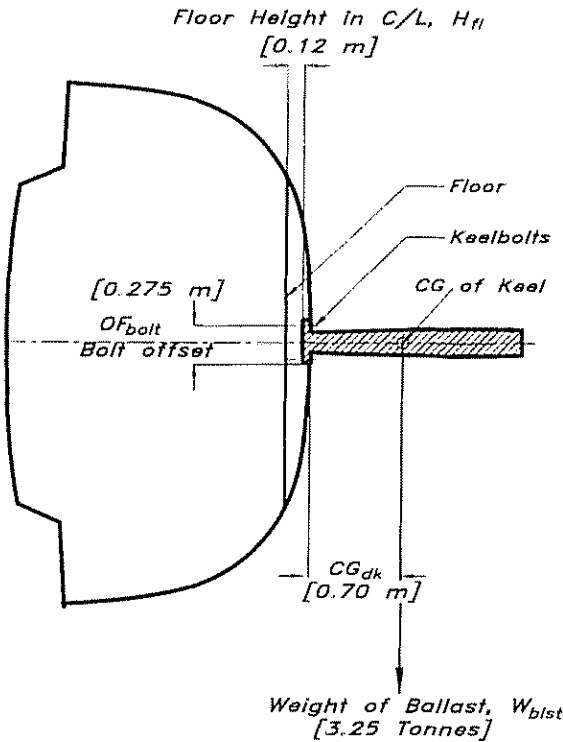
The yield strength used in the example above is 206 N/mm<sup>2</sup> which corresponds to stainless steel AISI-316. The diameter obtained is the minimum core diameter of the bolt, so the nominal bolt size will be a M26-bolt in the metric system or a 1 in bolt in the imperial system.

On the leeward side of the keel the tension in the keelbolts must be absorbed as a compression by the mating areas of the keel and hull. Since only the area nearest to the leeward edge is effective, it is reasonable to assume that 25% of the total area must be able to withstand a pressure corresponding to the total load on the bolts. The minimum required keel/hull area ( $A_{min}$ ) is 13873 mm<sup>2</sup>.

A typical ultimate strength in compression for a glassfibre laminate is 117 N/mm<sup>2</sup> in compression. The actual keel has a 25% area of approximately 150 000 mm<sup>2</sup>, so the factor of safety is considerable in this case.

Each pair of keelbolts is connected to a floor which has to absorb the moment induced by the tension in the windward keelbolt. The factor of safety for the floors is taken to be the same as for the keelbolts; in our example it is 5. So the bending moment working on each floor becomes the total transverse keel moment ( $M_{kt} \cdot 5$ ) divided by the number of floors, six in our example, which gives a bending moment ( $M_f$ ) of 18598 Nm.

The required section modulus ( $SM_f$ ) to withstand this moment is calculated by dividing the floor bending moment ( $M_f$ ) by the floor laminate's ultimate strength in tension, typically 125 N/mm<sup>2</sup> for a glassfibre laminate, and in this case it becomes 150 cm<sup>3</sup>. The result



Transverse Keel Moment ( $M_{kt}$ ) :  
 $M_{kt} = CG_{dk} \cdot W_{blst} \cdot g$  [ 22318 Nm ]

Total Keelbolt Load ( $P_{kt}$ ) :  
 $P_{kt} = \frac{M_{kt}}{OF_{bolt}}$  [ 81156 N ]

Required Keelbolt Diameter ( $d_{kb}$ ) :  
 $d_{kb} = 2 \cdot \sqrt{\frac{P_{kt} \cdot \eta_{kb}}{\sigma_y \cdot \pi}}$  [ 21 mm ]

Minimum Keel/Hull-Area ( $A_{min}$ ) :  
 $A_{min} = \frac{P_{kb} \cdot \eta_{kb} \cdot \eta_{kb}}{0.25 \cdot \sigma_{uc}}$  [ 13873 mm<sup>2</sup> ]

Required Section Modulus for Floors ( $SM_{fl}$ ) :  
 $SM_{fl} = \frac{M_{fl}}{\sigma_{ut}}$  [ 150 cm<sup>3</sup> ]

Keelbolt Tension ( $P_{kb}$ ) :  
 $P_{kb} = \frac{P_{kt}}{n_{kb}}$  [ 13526 N ]

$n_{kb}$  = number of keelbolts [6]  
 $\eta_{kb}$  = factor of safety; 4-6 [5]  
 $\sigma_y$  = yield strength for keelbolts (206 N/mm<sup>2</sup> for AISI-316)

Floor Bending Moment ( $M_{fl}$ ) :  
 $M_{fl} = \frac{M_{kt} \cdot \eta_{kb}}{n_{fl}}$  [ 18598 Nm ]

$n_{fl}$  = number of floors over keel [6]  
 $\sigma_{uc}$  = typical ultimate strength in compression for GRP (117 N/mm<sup>2</sup>)  
 $\sigma_{ut}$  = typical ultimate strength in tension for GRP (125 N/mm<sup>2</sup>)

Fig 12.11 Loadings from the keel



comes out in  $\text{cm}^3$  when using Nm for the moment and  $\text{N}/\text{mm}^2$  for the strength value.

Entering the diagram of Fig 12.11 with an SM-value of  $150 \text{ cm}^3$  and choosing a floor height (H) of 12 cm we need a flange area of  $9 \text{ cm}^2$  and a thickness of 1.2 cm. So the minimum floor breadth is  $(9/1.2) 7.5 \text{ cm}$ . If the keelbolts are passing through the floor, we must add their diameters to the breadth of the floor to achieve sufficient flange area, ie total breadth becomes 10 cm. These values are relevant for the floor section at the centreline; at the ends the required section modulus can be taken as half of that at the centreline,  $75 \text{ cm}^3$  for our boat. This leads to a section of 7.5 cm height, keeping the laminate thickness, breadth and flange area the same as at the centreline.

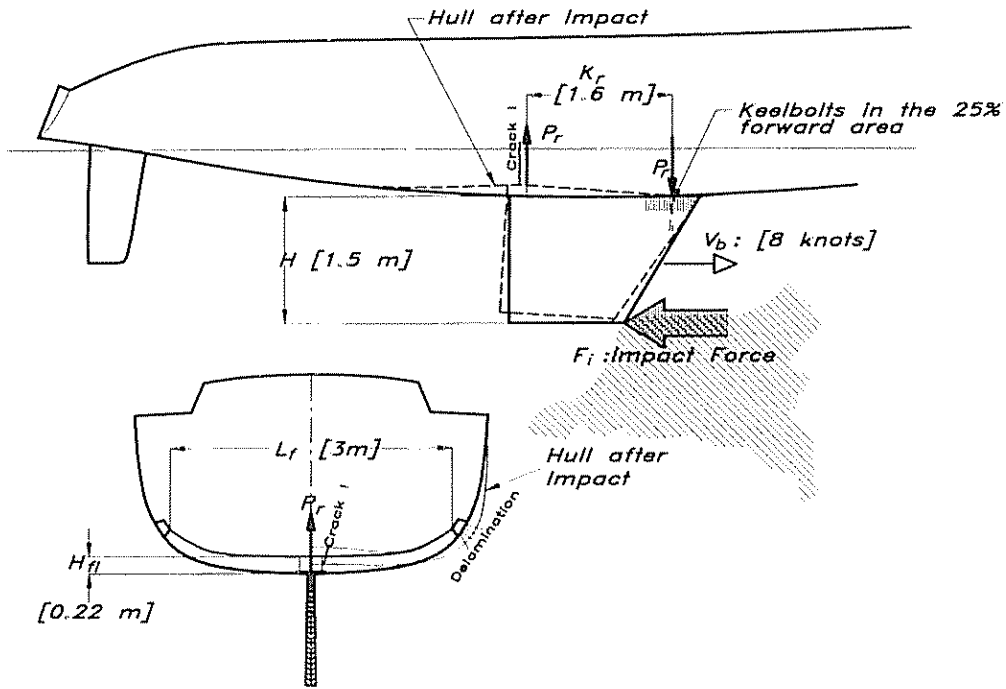
### Forces from grounding

It is not practical to calculate the impact force  $F_i$  exactly. It depends on the weight and speed of the vessel, as well as the shape of the seabed or rock (which governs the time of retardation) and the shape of the boat (which has great importance regarding the damping of the movement). For now it is sufficient to make some simplifications on the conservative side in order to guarantee the strength, since a slight increase of weight in this area seldom poses any substantial problems

From Fig 12.12 it can be seen that the impact force  $F_i$  gives a moment in the keel/hull area ( $M_{kl}$ ) of 200240 Nm. In order to arrive at this figure and to solve the equations of Fig 12.12, some assumptions have to be made. We assume the boat's speed to be 8 knots,  $V_s = 4.11 \text{ m/s}$ , and that the time to a full stop ( $t_s$ ) is 0.25 seconds. This equals a 'stopping-distance' of approximately half a metre (which is rather a sudden stop) and gives a retardation of  $a_r = V_s / t_s (= 16.44 \text{ m/s}^2)$ . Since the displacement of the vessel is 8120 kg this gives an impact force  $F_i = \text{Displ} \cdot a_r, 133493 \text{ N}$ . Now it is easy to calculate the impact moment,  $M_{kl}$  from the formula in the figure, and from this the resultant force  $P_r, 125150 \text{ N}$ , can be calculated by dividing the impact moment by the length of the keel. This force acts as a pressure on the aft part of the keel, and as tension on the forward part. As can be clearly seen from these equations, a short and/or deep keel gives much higher loadings on the hull when running aground.

The centre of rotation for the keel is very uncertain and depends on the stiffness of different parts of the keel/hull joint as well as the slope and/or the geometry of the joint. Since the keelbolts and the material in the joint are more deformed the further you get from the rotational centre, it is probable that only the most forward bolts are fully tensioned, and that the joint area is subjected to maximum pressure only in its aft part.

A reasonable way to calculate the required tensile strength ( $\sigma_{y25}$ ) for the most forward bolts, is to assume that the number of bolts situated within the forward 25% of the keel ( $n_{kb25}$ ) take care of the forces from the grounding ( $P_r$ ). In the YD-40 we have two bolts in the actual area, so the required tensile strength becomes  $181 \text{ N}/\text{mm}^2$ , as can be seen from the formula in Fig 12.12. Since the yield strength for AISI-316 stainless steel is  $206 \text{ N}/\text{mm}^2$  it is obvious that there is no risk of tearing



Impact Force ( $F_i$ ) :

$$F_i = m \cdot a_r$$

$$a_r = V_b / t_s; \text{retardation [ 16.44 m/s}^2\text{]}$$

$$V_b = \text{boatspeed [ 8 knots]}$$

$$V_b = 0.514 \cdot V_b; \text{speed [ 4.11 m/s]}$$

$$t_s = \text{time to full stop [ 0.25 s]}$$

Impact Moment ( $M_{kl}$ ) :

$$M_{kl} = F_i \cdot H \text{ [ 200240 Nm]}$$

Reaction Force ( $P_r$ ) :

$$P_r = \frac{M_{kl}}{K_r} \text{ [ 125150 N]}$$

Required Tensile Strength for Keelbolts In the 25% Forward Keel Area ( $\sigma_{y25}$ )

$$\sigma_{y25} = \frac{P_r}{n_{kb25} \cdot A_b} \text{ [ 181 N/mm}^2\text{]}$$

$n_{kb25}$  = Number of Bolts In the 25% Area  
 $A_b$  = Cross Sectional Bolt Area

Floor Bending Moment ( $M_{fl}$ ) :

$$M_{fl} = \frac{P_r \cdot L_f}{4} \text{ [ 93863 Nm]}$$

Required Floor Section Modulus ( $SM_{fl}$ ) :

$$SM_{fl} = \frac{M_{fl}}{\sigma_{ut}} \text{ [ 750 cm}^3\text{]}$$

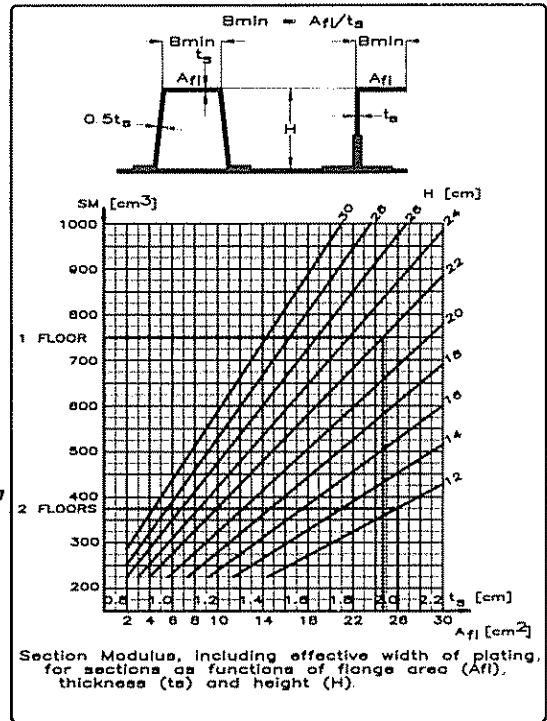


Fig 12.12 Loadings from grounding

the keelbolts apart by running aground with this boat. The most sensitive area is the aft part, where the keel meets the hull.

The maximum thrust from the grounding is  $P_r$  and occurs at the trailing edge of the keel. This force gives a bending moment in the floor supporting the aft part of the fin  $M_{kl}$  of 93863 Nm, and is calculated by multiplying the thrust by one quarter of  $L_r$ , where  $L_r$  is the length of the floor supporting the keel as illustrated in Fig 12.12.

This bending moment requires a section modulus,  $SM_{fl}$ , of the floor of 750 cm<sup>3</sup>. Entering the diagram in Fig 12.12 with this section modulus we read off a laminate thickness of 2 cm with the chosen floor height,  $H$ , of 22 cm. The minimum flange area is 25.4 cm<sup>2</sup> which leads to a floor width of 12.7 cm. One problem in real life with a shallow hull, is the lack of space between the sole and the bottom of the canoe body. It may not be possible to fit a floor of this height, and in that case we must use multiple floors in this area and divide the grounding force between them. By using two floors we can let the height remain 12 cm, as on the rest of them, resulting in a laminate thickness of 2.05 cm and a flange area of 26 cm<sup>2</sup> giving a floor width of 12.7 cm.

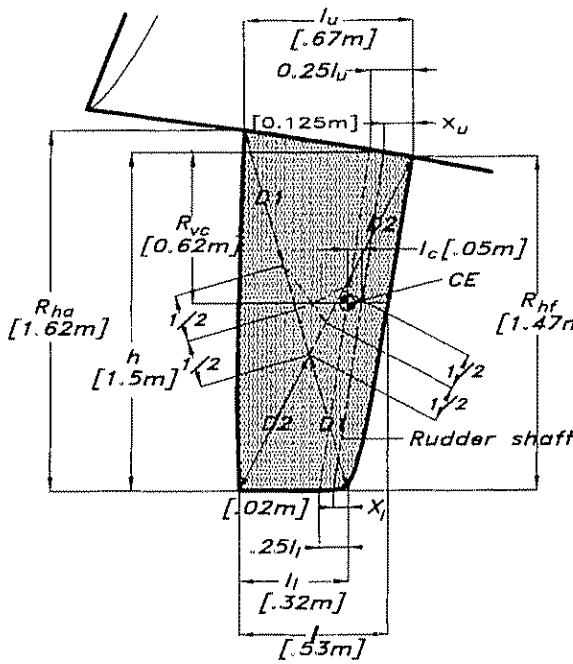
### Forces from the rudder

The rudder forces are developed when the rudder is producing a side force, ie when you are (a) turning the boat or (b) trying to counteract a turning moment. In the first case it is not necessary that the maximum force is developed, since the boat gives way for the side force by actually turning. In the second case it is more likely that maximum forces will develop. A typical case is when trying to counteract a broach when spinnaker reaching.

Fig 12.13 shows a typical spade rudder with values from the YD-40. In the following simplified calculations we have used double the geometric aspect ratio, the effective aspect ratio ( $AR_c$ ), which means that we do not take any ventilation into account and that the rudder is close to the boat bottom. This is hardly ever the case in reality, but it gives us an extra safety factor, because the forces are exaggerated this way.

The centre of effort for the rudder profile (NACA 0012) lies 25% aft of the leading edge ( $0.25l_u = 16.8$  cm &  $0.25l_l = 8$  cm). Vertically, the position can be calculated as indicated in Fig 12.13. By deducting the short parts (D1 & D2) from the full-length diagonals and triangulating the remaining parts (showed as dashed lines) we can accurately position the geometric centre of effort, but here we only use the vertical distance,  $R_{vc}$ . Normally this figure will be in the region of 45% of the total height. Knowing the CE position and the 25% line, the distance from the leading edge to the CE can be calculated easily. Also, knowing the position of the rudder shaft the corresponding distance (leading edge to CE,  $X_u = 12.5$  cm and  $X_l = 2$  cm) is easily determined. The difference between these figures gives the turning lever,  $l_c = 5$  cm in our example.

The effective aspect ratio,  $AR_c$ , is double the ratio between the average height and the average length of the rudder (6.2 for the YD-40). The lateral area  $A_{lr}$  of the rudder is obviously the average height times the average length, 0.765 m<sup>2</sup>. These values are used to



Effective Aspect Ratio ( $AR_e$ ) : [ 6.2 ]

$$AR_e = 2 \frac{R_{ha} + R_{hf}}{l_u + l_l}$$

Rudder Lift Coefficient ( $C_{lr}$ ) :

$$C_{lr} = c \cdot \alpha_0 \quad [ 1.5 ]$$

$$c = \frac{0.11}{1 + 2/AR_e} \quad [ 0.08 ]$$

$\alpha_0$  = angle of attack for max lift [18.75 deg]

Rudder Lateral Area ( $A_{lr}$ ) :

$$A_{lr} = 0.25 \cdot (R_{ha} + R_{hf}) \cdot (l_u + l_l) \quad [ 0.765 \text{ m}^2 ]$$

Rudder Sideforce ( $F_r$ ) :

$$F_r = 0.5 \cdot \rho \cdot V_a^2 \cdot A_{lr} \cdot C_{lr} \quad [ 9934 \text{ N} ]$$

Rudder Bending Moment ( $M_r$ ) :

$$M_r = R_{vc} \cdot F_r \quad [ 6159 \text{ Nm} ]$$

Rudder Torsional Moment ( $T_r$ ) :

$$T_r = l_c \cdot F_r \quad [ 497 \text{ Nm} ]$$

$R_{vc}$  = vertical dist. from top to CE

$l_c$  = horizontal dist. from shaft to CE

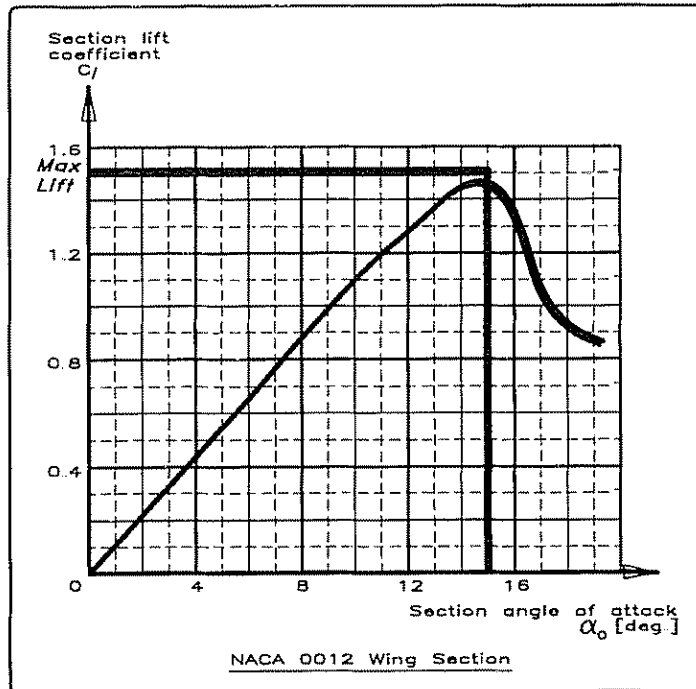


Fig 12.13 Loadings from the rudder

compute the lift coefficient and side force, according to the formulae and diagram in Fig 12.13.

As can be seen from the diagram in Fig 12.13 the maximum section lift coefficient,  $C_L$ , is 1.5 and occurs at a section angle of attack,  $\alpha_0$ , of  $15^\circ$ . The resulting lift coefficient of the entire rudder,  $C_{Lr}$ , can be approximated also to 1.5, and, according to the rudder lift coefficient equation,  $C_{Lr}$ , of Fig 12.13, the angle of attack will be  $18.75^\circ$ . The reason for this difference between the section angle of attack and the actual angle of attack is that the section coefficient assumes an infinite aspect ratio and consequently no end leakage and induced resistance.

The side force ( $F_r$ ) this rudder delivers, at a speed ( $V$ ) of 8 knots ( $V_s = 4.11$  m/s) is 9934 N for our YD-40. This side force is the load that determines the bending,  $M_r$ , and torsional,  $T_r$ , moments on the rudder shaft.  $M_r = 6159$  Nm and  $T_r = 497$  Nm for the YD-40.

This bending moment in the rudder shaft occurs at the hull bearing, and the torsional moment in the shaft at the attachment of the tiller arm, quadrant or tiller. The loading in the upper part of the rudder is a combination of these two moments, but in the lower part only the torsional moment is involved.

In the section on the ABS rule we will calculate the rudder shaft, but now let us see what demand the  $T_r$  puts on the steering mechanism. Assuming we are using an 8 in radius (0.2 m) rudder quadrant, the force in the steering cable will be  $497/0.2 = 2485$  N. The mechanical losses (friction etc) are approximately 20%, so the required force from the steering gear is 3106 N. The drive gear has a radius of 5 cm, which means that the steering moment is  $3106 \cdot 0.05 = 155$  Nm. With a wheel diameter of 1.2 m the force the helmsman must use becomes  $155/(1.2 \cdot 0.5) = 258$  N. The equivalent tiller length would be  $497/258 = 1.93$  m, quite a substantial tiller to match the wheel for power.

### Summary of loadings

Fig 12.14 shows the windward side of a sailing yacht beating into the wind. The shaded arrows indicate global loads imposed on the hull girder from the rigging forces. They are increased when the yacht is in hull sagging position, which is the case when travelling at hull speed in smooth water. As can be seen, the hull girder is subjected to bending which gives compression forces along the deck edge, tension along the bottom and shear forces in the topsides. On top of this there is transverse tension in the shroud area. Sailing in rough and steep seas might induce hull hogging also, not that the bending moment change sign (the rigging forces are too great to let that happen), but there will be pulsating compression and tension in the hull with the inherent risk of fatigue in the long run.

Furthermore, we have the local loadings, the hydrostatic pressure, with additional loadings from slamming in the forward part of the boat, which tries to buckle the plating and bend the stiffeners. These are the most important forces when calculating the thickness of the skin and scantlings of the stiffeners. As previously shown, the global strength of the vessel is sufficient if it is dimensioned to withstand hydrostatic and hydrodynamic loads, at least if it is of a 'non-extreme' type. Other local

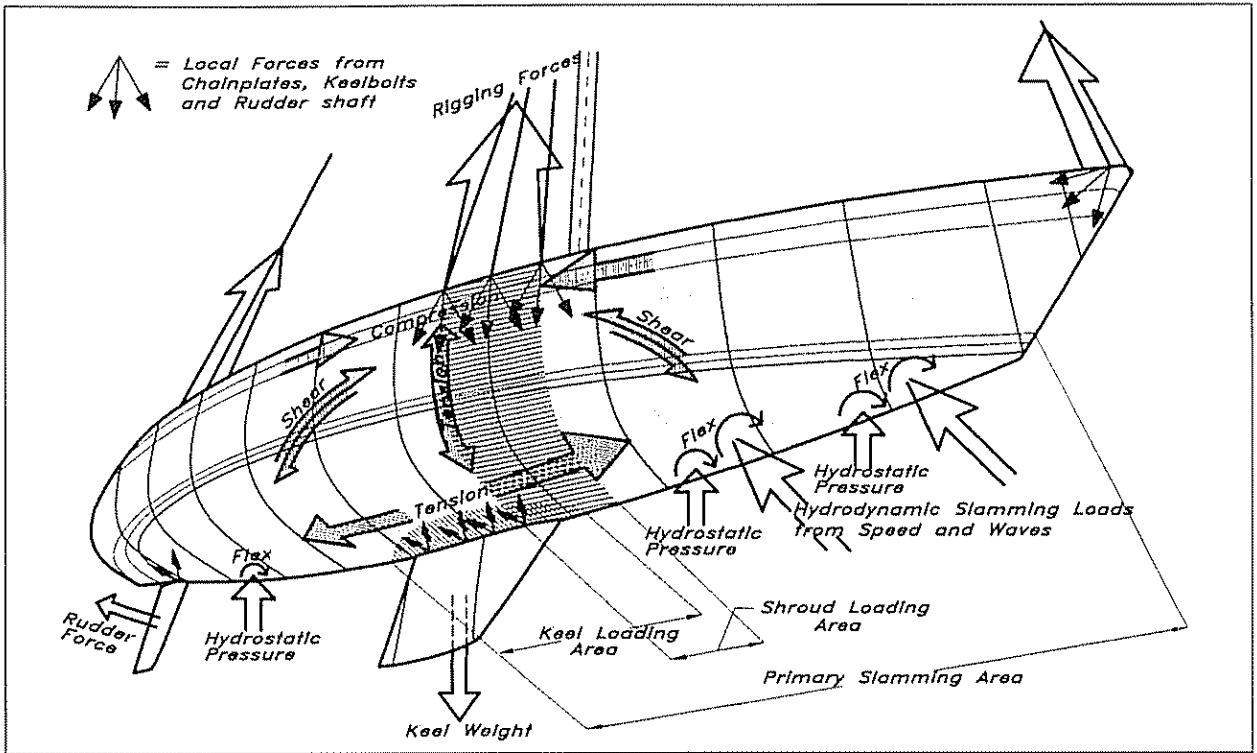


Fig 12.14 Forces on a sailing yacht

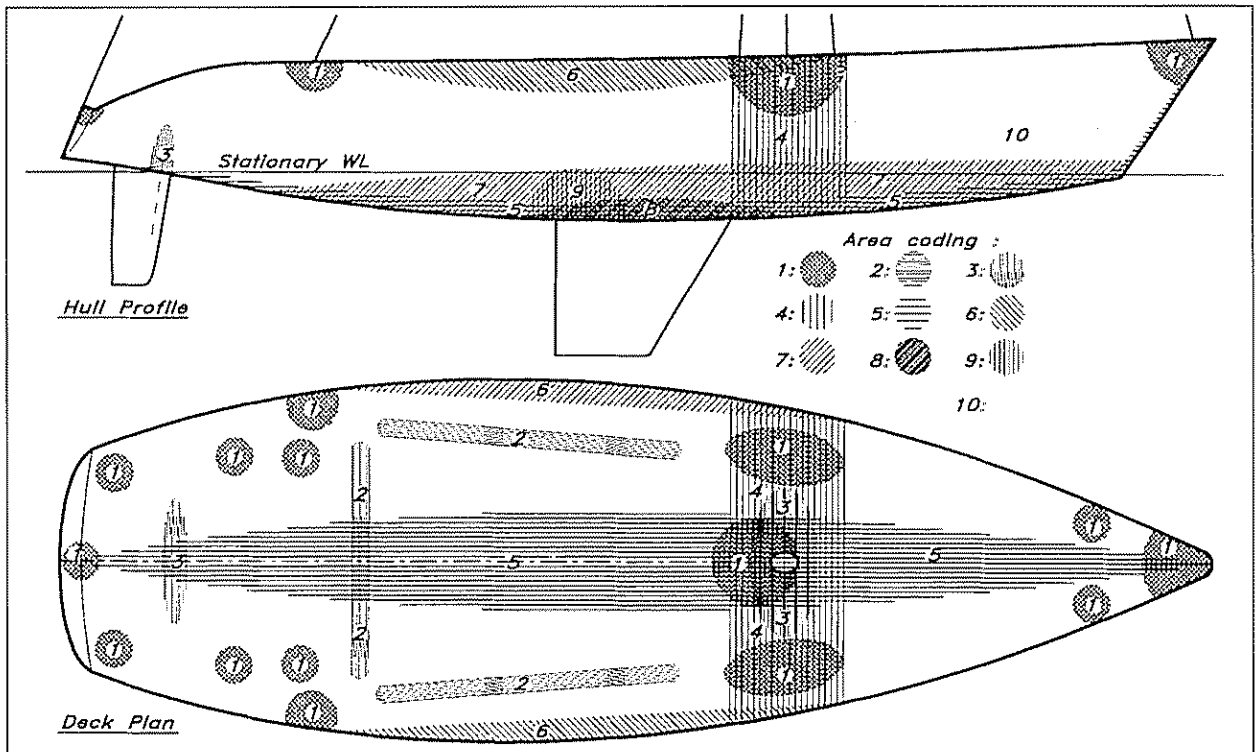


Fig 12.15 Loaded areas

loadings that must be taken into consideration are the ones that stem from attachments of shrouds and stays, keelbolts, rudder shaft, winches and other deck hardware.

Fig 12.15 shows the boat divided into primary 'concern areas' regarding loadings. A qualitative look into the consequences for the different areas when it comes to dimensioning and building gives us the following points:

### Loaded areas

- 1 Local loadings from attachments, ie chain plates, stay fittings, cleats, winches, stanchions etc. Demands on the laminate to be strengthened in order to cope with big, local loads. To help the laminate, this means large washers under bolts and in the case of a sandwich laminate, that the sandwich core is substituted for plywood, a very high density core or a single laminate. The last option, which might seem to be the most old-fashioned solution, actually has several advantages. First, regardless of core material (plywood or high density foam), the laminate in itself is better suited to withstand the compressional forces involved with through-bolting of deck fittings, and secondly, by going down into single laminate in these areas, the bolt heads or nuts will be countersunk into the core thickness, without disturbing the underdeck ceiling etc. It is wise though to increase laminate thickness and not leave it as just the combined inner and outer laminates. An increase of approximately 40% would not be out of order.
- 2 Basically the same comments as in area 1 are valid, but since these (2) areas concern primarily sheet tracks, with a more spread out load distribution the demands on the area concerned also mean that the extremely local bolt loads are less, and the increase in laminate thickness of 25% would be enough.
- 3 These areas are loaded by transverse forces from the mast and the rudder. The laminate must be able to withstand the edge-pressure, ie use a hard core or rather change to a solid beefed-up laminate.
- 4 This is an area extraordinarily loaded by rigging forces from the shrouds and the mast. The whole section in this area must be exceptionally stiff and resistant to torsional forces, so as not to collapse transversely. To achieve this, framing has to be increased, a structural bulkhead has to be fitted or a load-bearing space frame has to be fitted to absorb and distribute the loadings.

- 5 Longitudinal forces from the rig and waves mean that the deck might need to be strengthened with stringers to withstand the pressure and the hull in the bottom area in order to withstand the tension. The demands on the bottom to cope with loadings from the keel and slamming make it strong enough to absorb the global bending forces in most cases, but there is still the risk of the deck not being able to withstand the resultant compression forces if the hull girder is low or the rig exceptionally large.
- 6 This is an extra stressed area due to pulsating loads coming from the vessel working in waves. Special consideration might be necessary regarding the compression/tension properties of the laminate, but more likely the weak link is the deck to hull joint, which must be strong enough not to move or buckle, in order to avoid leakage. When the joint is not glassed over, but only fixed with bolts and a bedding compound, it is wise to use an aluminium toe rail at the deck edge, which will stiffen the edge section so that it does not open under load. Another way to obtain the same effect is to design the edge of the deck as a box (top-hat) girder.
- 7 The bottom panels in this area, ie forward of amidships and gradually tapering off towards the stern, are the most heavily loaded ones, with regard to hydrostatic and hydrodynamic loads. This puts a demand on the panels to be stronger and stiffer than on the rest of the bottom. When using a common lay-up over the entire bottom (which is the practice in series production), a 'strengthening effect' can be obtained by using a denser stiffening system in this area, thereby reducing the panel sizes.
- 8 An area that is loaded by the keel. The demands on this area require that the laminate be thick enough to withstand high local pressures from the keelbolts. Transversely the area must be stiff enough not to let the keel act like a pendulum when beating in a seaway.
- 9 The area in the aft part of the keel is most vulnerable when running aground. The grounding force must be spread over a larger area than the keel/hull joint itself.
- 10 This is the primary slamming area, putting extra heavy demand on the strength and stiffness of the panels involved. The forces from waves are much greater than when sailing in flat water.



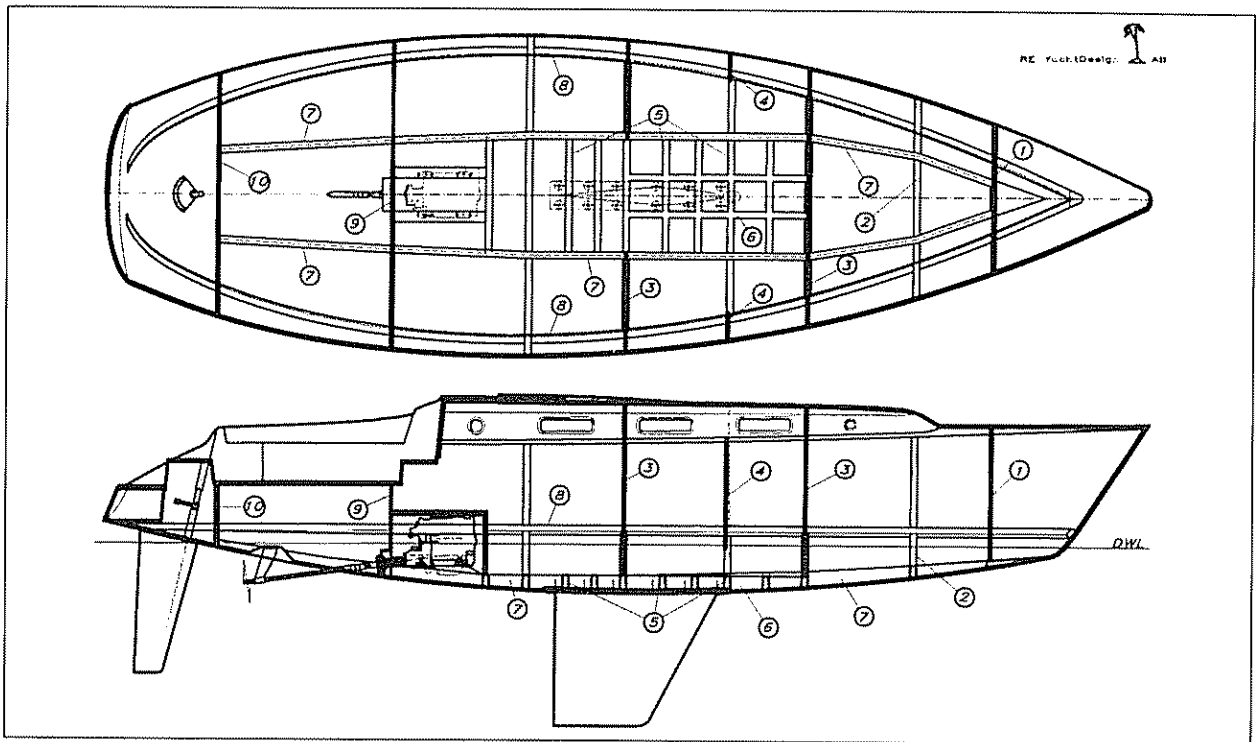


Fig 12.16 Stiffening system – YD-40 – single skin hull

Fig 12.16 shows the YD-40 which is stiffened according to the points above. Basically, the boat is stiffened by a system of longitudinal stringers, transverse frames and load carrying bulkheads. Looking at the system, starting from the bow, we have the following:

- 1 A watertight, structural collision bulkhead of sandwich construction which effectively strengthens this slamming area.
- 2 Extra floor in the forebody bottom to absorb slamming forces.
- 3 Structural sandwich bulkheads to strengthen the torsional rigidity of the hull/deck beam, to be stiff enough to resist the rig's transverse forces.
- 4 Extra webs in the shroud area.
- 5 A system of floors to distribute forces from the keel, the mast and from grounding.
- 6 Integrated mast-step girders spanning between area 3 bulkheads, in order to distribute the mast load longitudinally over a number of bottom floors.
- 7 Longitudinal bottom stringers from the collision bulkhead to the aftermost bulkhead. The bottom floors are connected to these stringers at their ends.
- 8 Side stringers that run the entire length of the boat and whose support points are the structural bulkheads.
- 9 A structural sandwich bulkhead carrying the propeller shaft thrust bearing, and also isolating the engine room from the accommodation, together with the engine casing.
- 10 The aftermost structural, watertight sandwich bulkhead, stiffening the aft body not to bend or flex from rudder forces.

Detailed calculations of the actual dimensions of the panels and stiffeners for the YD-40 are to be found in Chapter 14. We now turn to a discussion of materials.

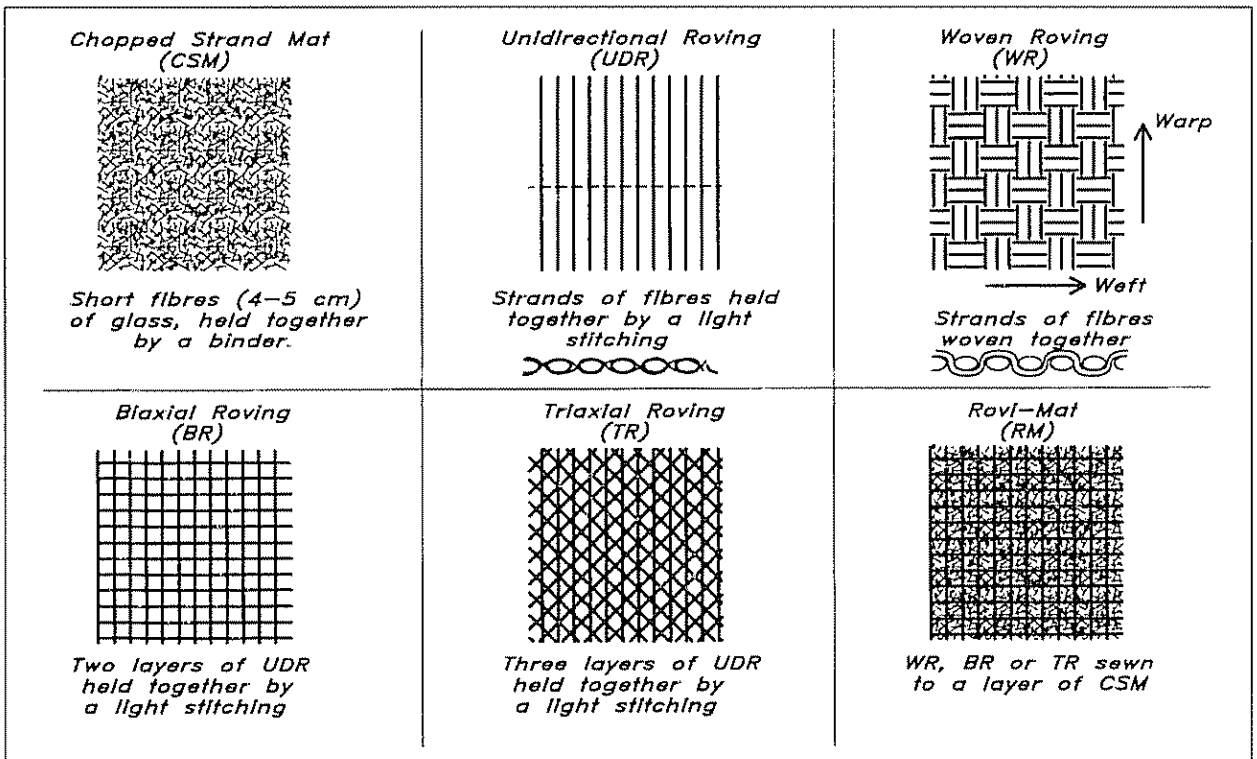
# 13

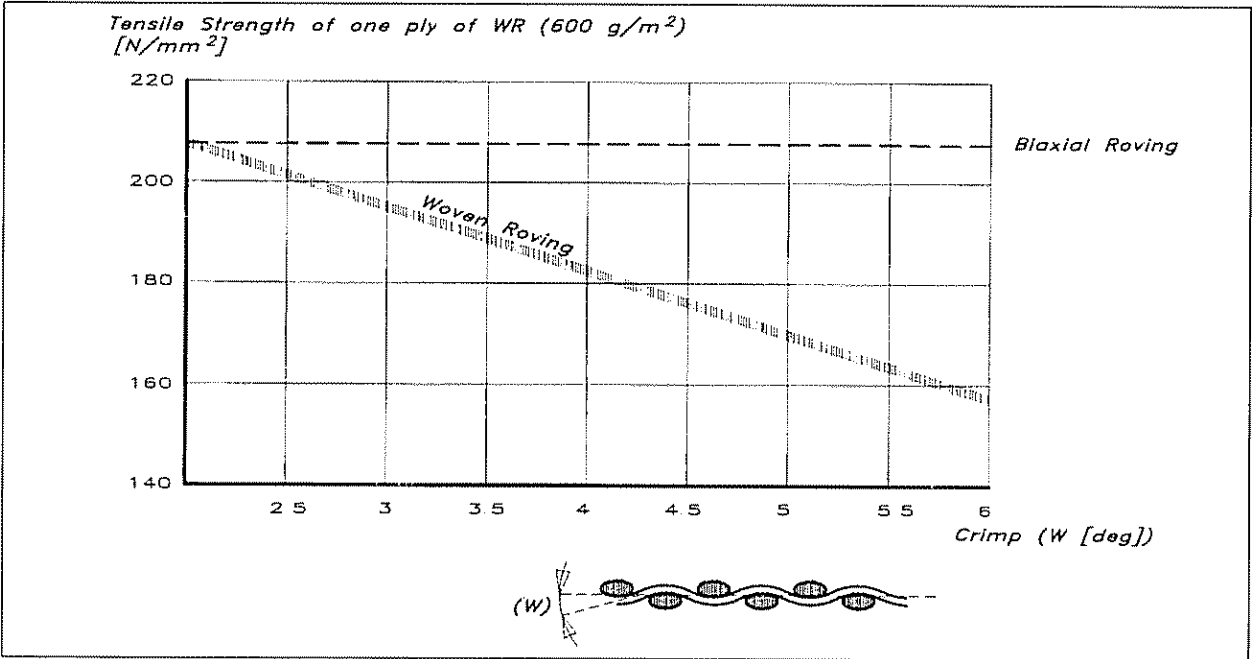
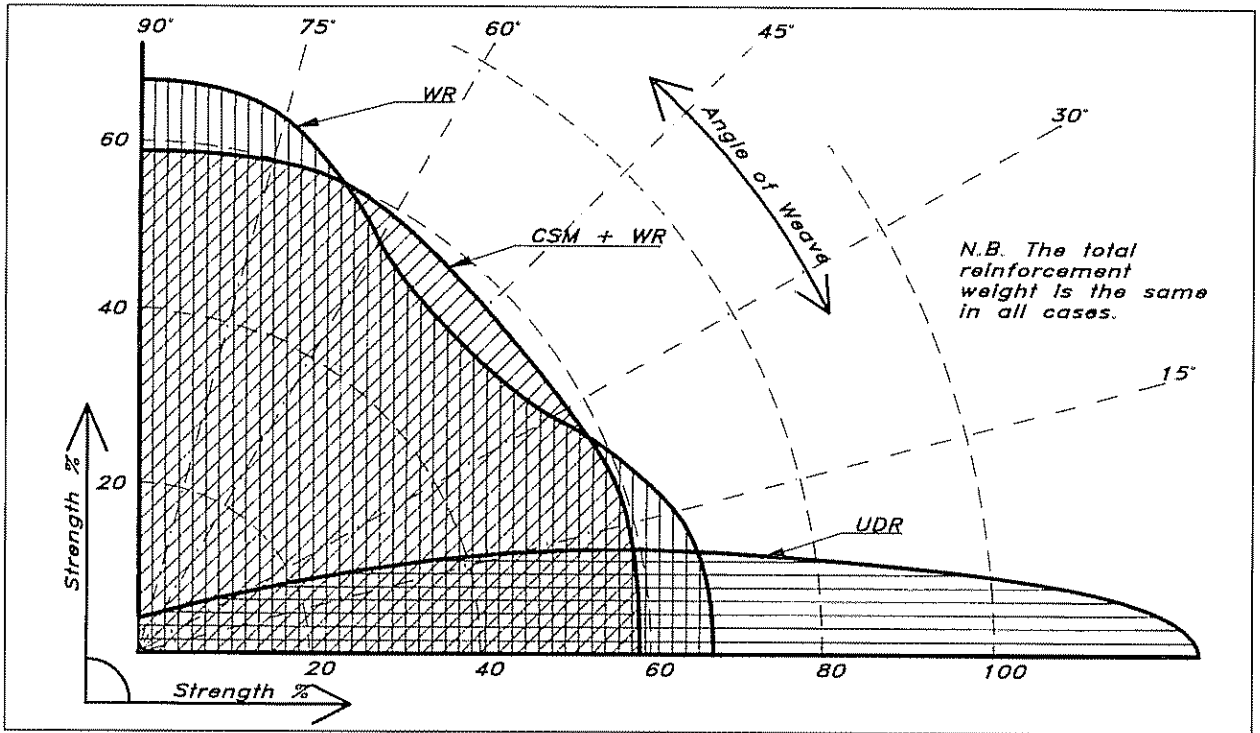
# MATERIALS

Fibre reinforced plastic (FRP) has been used widely in boat hulls and decks. Recently, interest in this material has grown among the other fields of the marine industry as well. One of the advantages of FRP in primary structures is the possibility of tailoring the strength properties of the laminate according to the need, and thus obtaining lighter but stronger structures. However, optimum solutions demand sophisticated calculation methods and material evaluations.

In contrast to steel, aluminium and to some extent wood, you build your own material when using resin and reinforcement to produce FRP laminate. It can be made in different ways and with different ingredients, so to give just one typical FRP strength value is not meaningful. You must know the actual lay-up in order to calculate its strength. The most important parameter that affects the strength is the form of the reinforcement and what it is made of. The most widely used reinforcement in the boat building industry is E-glass. There may be better materials strengthwise, but as yet the combined cost, strength and effectiveness of E-glass has not been equalled.

Fig 13.1 Reinforcement types





**Glass reinforcement**

Fig 13.2 (Top) Flexural strength vs angle of weave

Fig 13.3 Tensile strength vs crimp (Hildebrand & Holm)

Glass reinforcements come in a variety of shapes (as illustrated in Fig 13.1) The most commonly used type is chopped strand mat (CSM), which consists of short fibres, 4–5 cm long, evenly distributed and held together by a binder. The binder is of either an emulsion or powder type, which is dissolved by the styrene in the resin when wetting out the laminate. The emulsion type is slightly easier to work with because the powder type is more fragile and must be handled with care. One big

drawback with the emulsion type, however, is that it is prone to osmosis, so in the outer part of a laminate at least the powder type should be used.

While CSM is more or less isotropic (ie has the same strength in all directions), the other types are much more sensitive to the direction of load. This can become an advantage when building the lay-up, if one lines up the fibres with the primary load directions in order to take the best advantage of the available reinforcement materials. The use of rovings to take care of the primary loads is a good idea, but to ensure sufficient inter-laminar strength (strength between plies of reinforcement), the practice is to put in a layer of CSM between each roving layer. Manufacturers of glass reinforcement have noted this, and they have come up with a mat/roving combination: a roving sewn to a mat so that one can achieve the proper mix in one lay-up process. The most direction-sensitive type of reinforcement is the unidirectional type, which has virtually no strength in the 90° direction (see Fig 13.2).

The maximum slope of the fibres (crimp) in a woven roving (WR) has a strong influence on the tensile and compressive strength of the laminate, (see Fig 13.3). The tested laminate consists of two plies of 600 g/m<sup>2</sup> WR, and between them and also on the faces, one ply of 450 g/m<sup>2</sup> CSM. The fibre angle (W) is a measure of fibre curvature in degrees. The fibre curvatures in the warp and weft directions are not always the same in many woven roving products, so the tensile strength may vary up to 20% depending on direction. As can also be seen from Fig 13.3 a biaxial stitched roving has a higher tensile value, corresponding to a fibre slope of approximately 2°.

Another very important parameter regarding strength properties of the laminate is the fibre content, often expressed as a percentage by weight of the total laminate weight, (see Figs 13.4 and 13.5). Generally speaking the higher fibre content that can be reached the stronger the laminate becomes, as long as the fibres are wetted out and not subjected to resin starvation. In practice, it is not realistic to count a fibre content higher than 37%, and lower than 27% when using wet hand lay-up with a mat laminate. With a mix of mats and woven rovings in the laminate the fibre content usually varies from 35% to 45%, and with multidirectional material (rather than woven) up to 55%. The thickness of the cured laminate varies with fibre content as shown in Fig 13.6.

To calculate the strength properties of a glass mat/roving composite we can use the values from the mat-only and roving-only values. The combined properties can be approximated by calculating the average weight of the respective reinforcements as:

$$P_c = P_m \cdot X_m + P_r \cdot (1 - X_m)$$

where:

- $P_c$  = property of the mat/roving composite.
- $P_m$  = property of the mat portion, having the same fibre content as the mixed composite, Fig 13.4.
- $P_r$  = property of the roving portion, having the same fibre content as the mixed composite, Fig 13.5.
- $X_m$  = ratio of mat to the total mat/roving composite.

Fig 13.4  
CSM-polyester  
composite  
properties  
(Caprino & Teti)

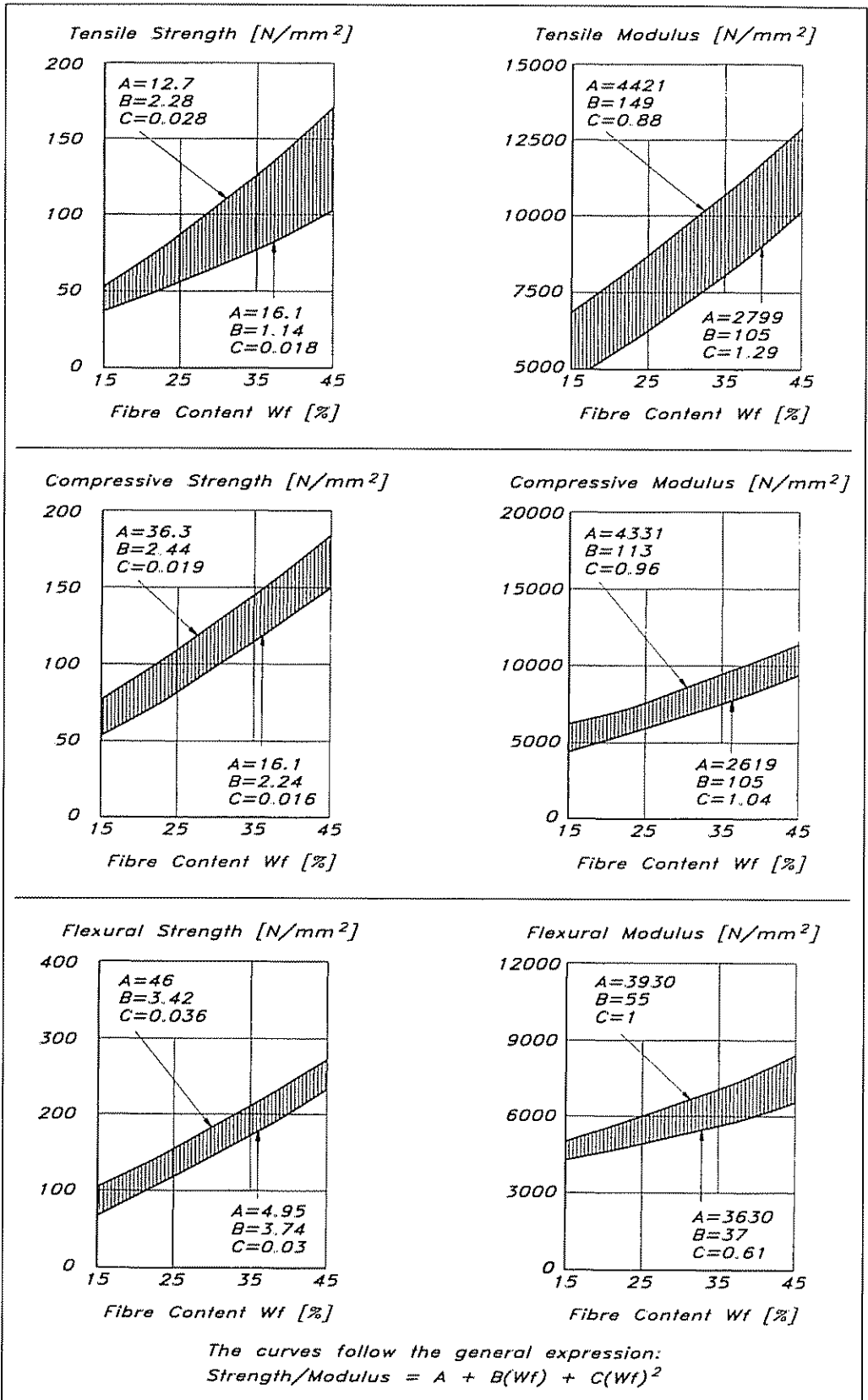
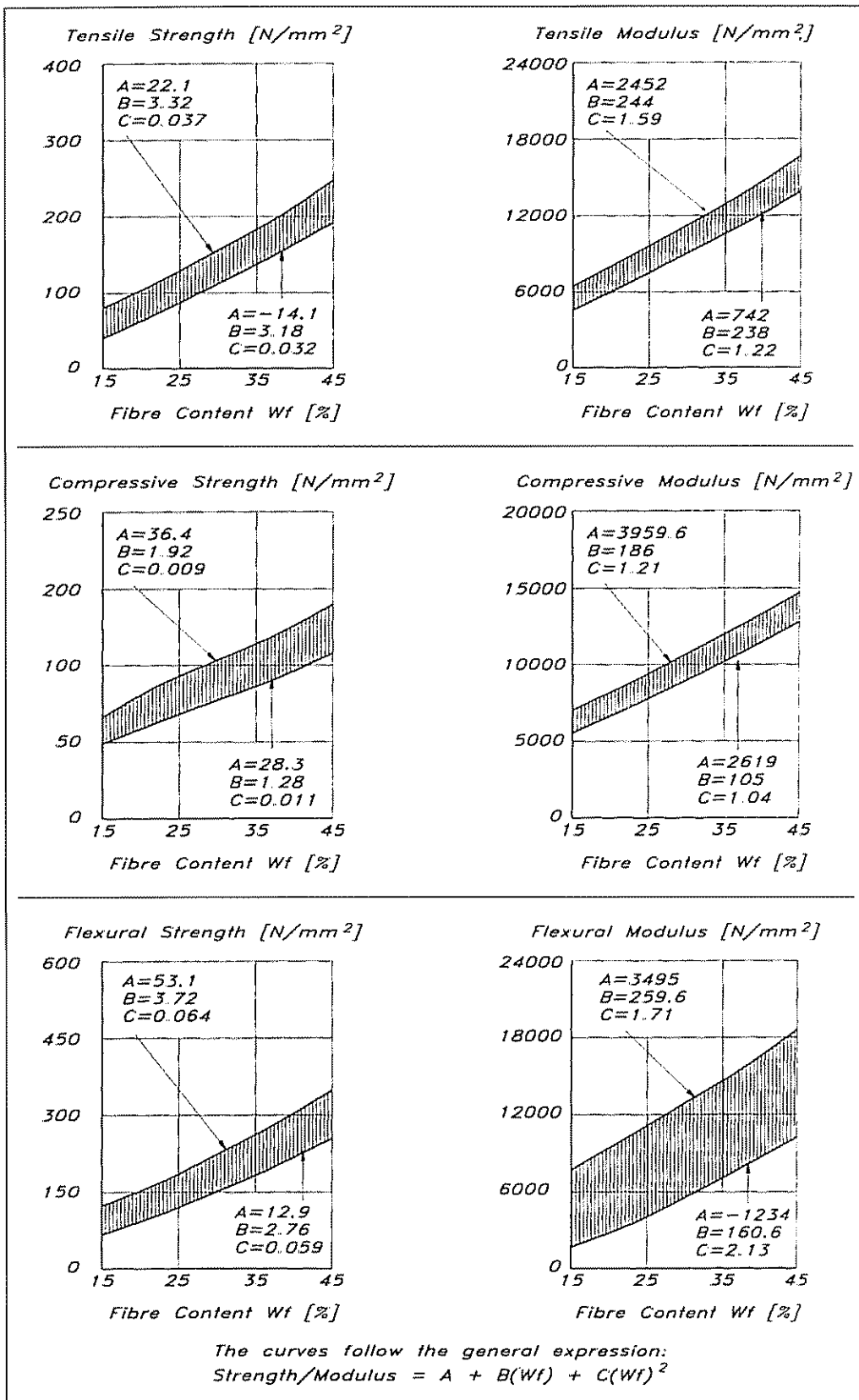


Fig 13.5  
WR-polyester  
composite  
properties  
(Caprino & Teti)



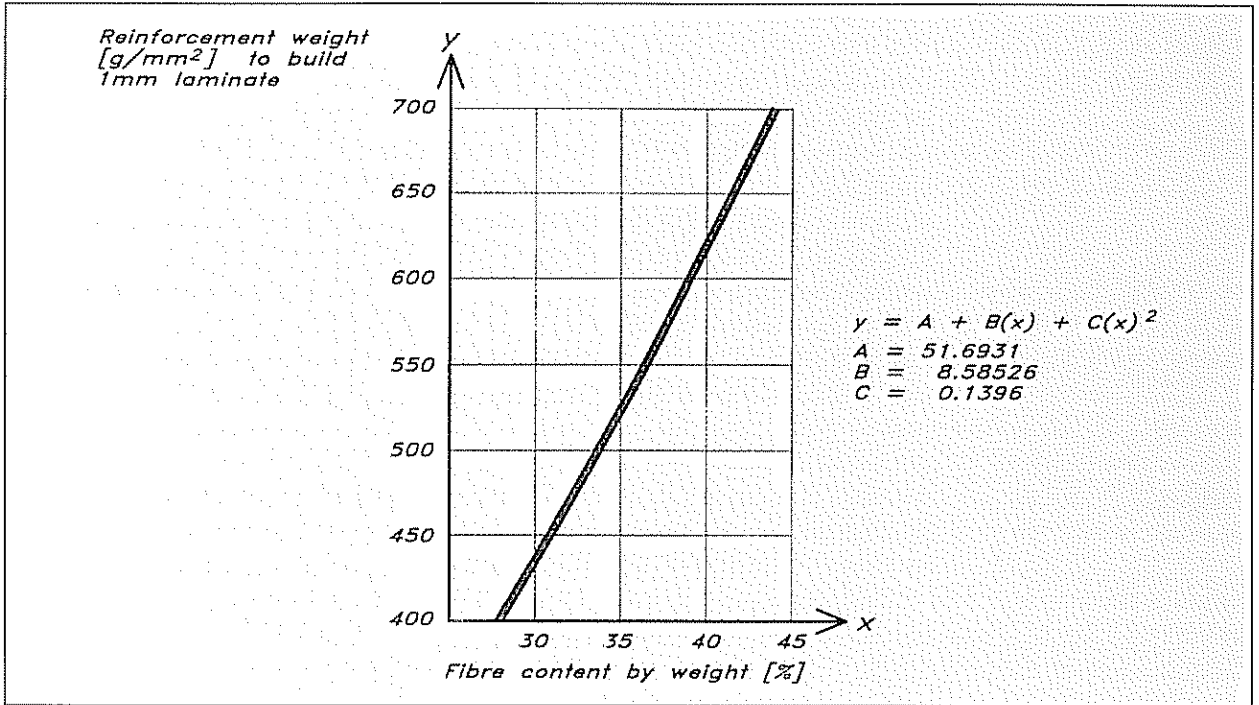


Fig 13.6 Thickness v fibre content (NBS)

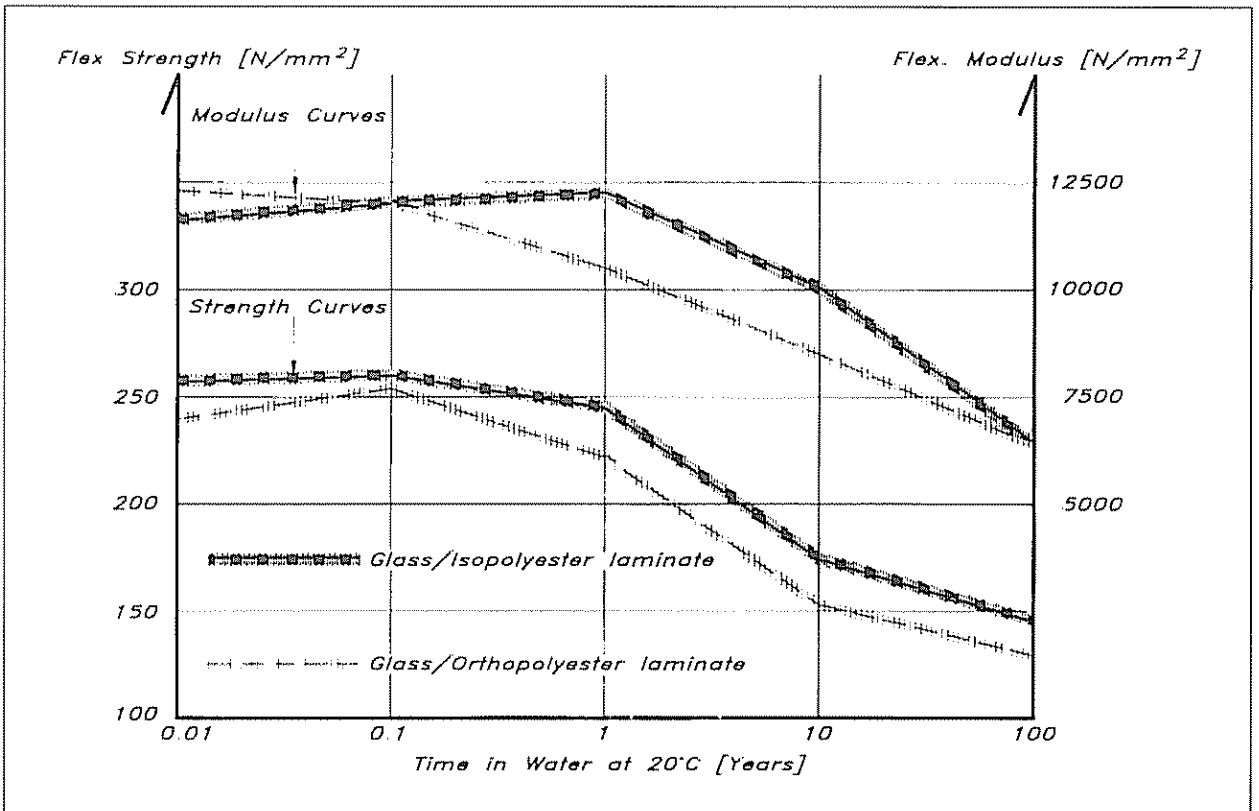


Fig 13.7 Strength and modulus in wet laminates

### Wet laminates

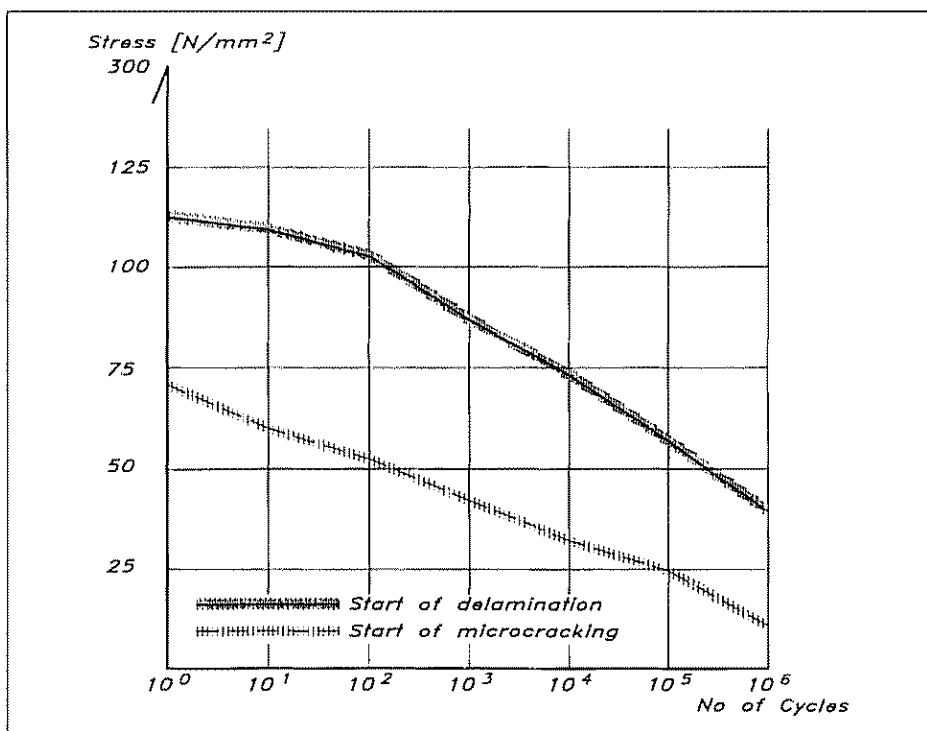
The values in Figs 13.4 and 13.5 are the ultimate strength and modulus values for dry laminates, but in practice this is not what can be expected from a boat laminate. The obvious reason is water, and the longer a laminate is submerged the weaker it becomes. Fig 13.7 shows the strength and elasticity properties for wet laminates as a function of time. The laminates are made of woven rovings with orthopolyester and isopolyester resin as a matrix. As can be seen the isopolyester laminate is not as apt to absorb water as the orthopolyester type. One thing to remember though, is that if you store the boat on land during winter and let the laminates dry out, the process effectively starts from year 0 when you relaunch the boat again. To guard against osmosis the isopolyester gives a better protection, and gelcoats should be of isopolyester or of an NCA or better type of resin.

### Fatigue

Another weakening factor for FRP laminates is fatigue. Yachts working in a seaway and with pulsating rig, keel and rudder loads are subjected to fatigue loadings. Fig 13.8 shows what happens to a CSM laminate.

The upper curve represents the failure of the laminate, and the lower curve corresponds to when microcracking first occurs. Microcracking is the first sign of laminate failure and it is obvious from the diagram that it takes place at a considerably lower level than the ultimate stress. What it means is that the resin, of orthopolyester type in this case, starts to develop cracks due to a low strain resistance: in other words it is too rigid. The strain level of this first failure is as low as 0.2% for an orthophthalic resin laminate compared to 2% matrix elongation before break.

Fig 13.8 Fatigue properties of a CSM laminate





Also obvious is the great fall in ultimate strength over stress cycles, from  $110 \text{ N/mm}^2$  to  $40 \text{ N/mm}^2$  after one million cycles, a reduction of 53%. This is something to bear in mind, especially when designing a yacht intended for long-range cruising over the oceans

As said previously, the diagram is valid for an orthopolyester CSM laminate; switching to a better resin and a roving-based reinforcement, the fatigue properties are improved.

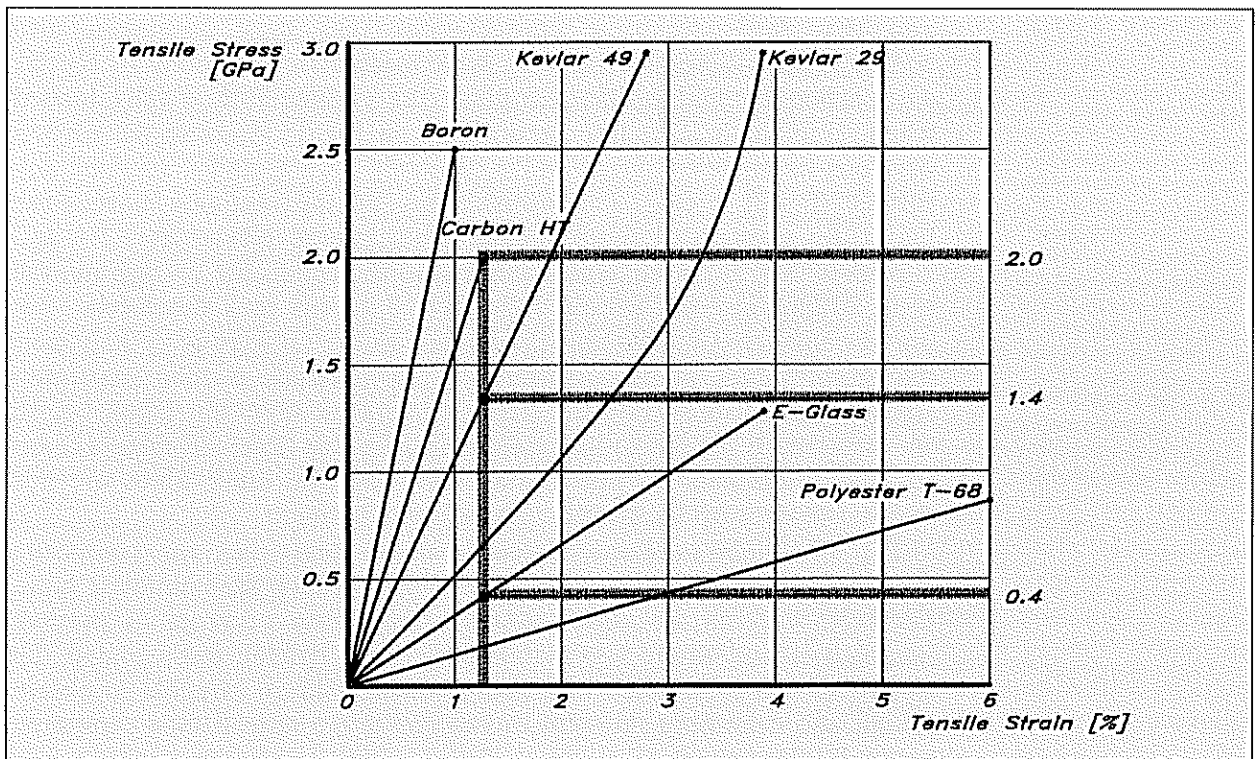
### Exotic laminates

To improve a laminate, ie to make it stronger, stiffer and lighter, we can substitute the ordinary E-glass for better fibres, and switch from wet hand lay-up techniques with orthopolyester to better resins and/or 'prepreg' materials.

Fig 13.9 shows the strength and strain properties for different reinforcement fibres. As we can see, the Kevlar 49 is the strongest one, while Boron is the stiffest one closely followed by carbon fibre. These figures show the values for the fibres themselves; put into a laminate they will be considerably lower.

As previously stated, it is very important to use a resin with a higher strain level than the fibre, to discourage the start of microcracking. Thanks to the high strength of these exotic fibres much higher demands on the resin's adhesive characteristics must be made. Ortho or isopolyester are not particularly good glues, whereas vinylester or, better still, an epoxy resin formulated for laminating is an excellent glue with high strain values, making it possible to utilize the high performance fibres to the full.

Fig 13.9 Fibre stress vs strain



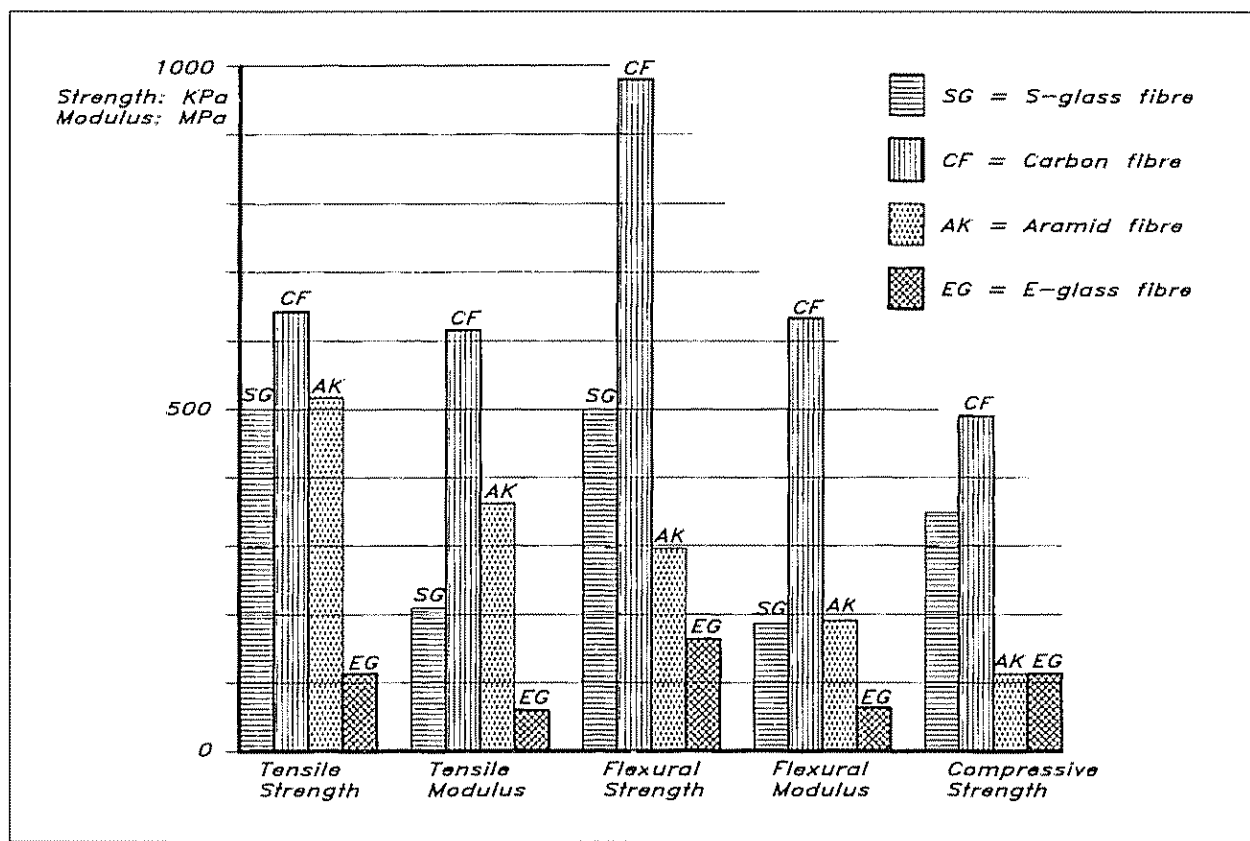
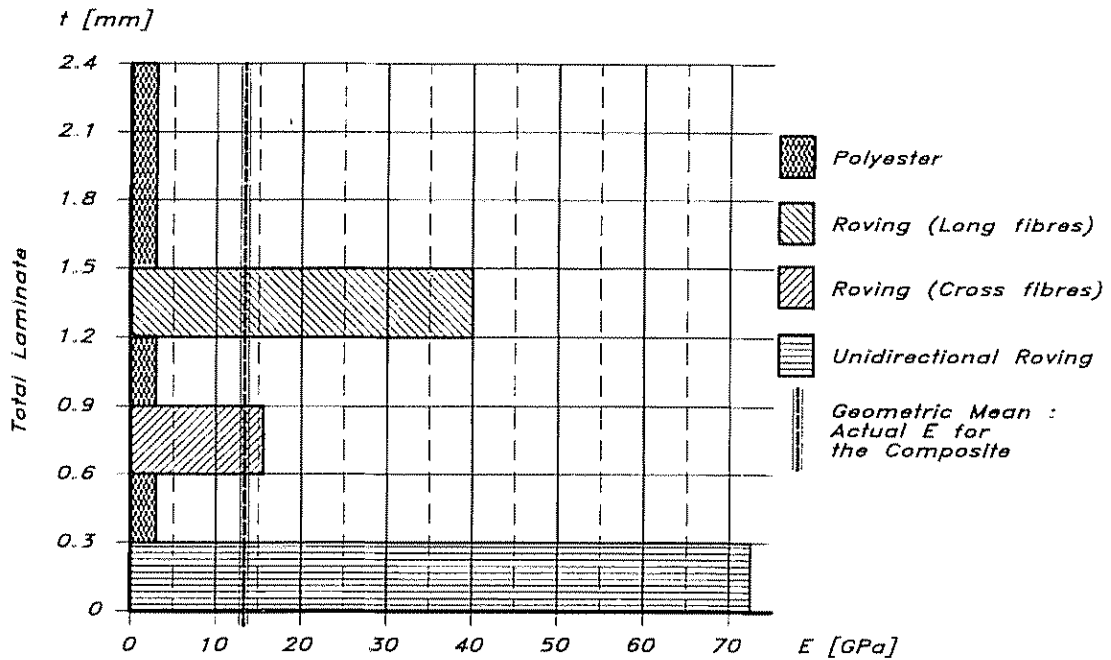


Fig 13.10 Typical composite properties

Usually the exotic fibres are used together with glass reinforcement and that leads to some consequences that must be taken into consideration. If, for instance, we have a laminate consisting of Kevlar 49, Carbon Ht and ordinary E-glass, the carbon fibre is fully loaded when strained to 1.2% (the vertical line in Fig 13.9). Here the carbon develops its highest strength value of nearly 2 GPa, and if strained any further it will break. The other fibres in the laminate have their maximum strength at much higher strain values: Kevlar at 2.7% and E-glass at 3.8%. To make all the fibres in the composite co-operate, the total strain must not exceed 1.2%, which means that the Kevlar can only be used to 1.2 GPa and the E-glass to 0.5 GPa, roughly half their maximum values. If we are using all the materials at their maximum strength and disregarding the strain, the stiffest fibre will break before the structure is loaded to its maximum, since this fibre will then take on too big a load. Or to put it the other way: the other fibres are not allowed to develop their assumed maximum strength.

Fig 13.10 shows some typical strength properties for composite laminates. The EG laminate is a common polyester/glass laminate hand laid wet, whereas the other laminates are Epoxy prepreps. A prepreg laminate is one where the manufacturer has already impregnated the fibre with a correct amount of resin, which makes it possible to obtain a high and even fibre ratio. In this example, the ratio is 60% compared to the EG laminate's 37%.



Actual E for the composite ( $E_{tot}$ ):

$$E_{tot} = \frac{E_{poly} \cdot t_{poly} + E_{wrl} \cdot t_{wrl} + E_{wrt} \cdot t_{wrt} + E_{ud} \cdot t_{ud}}{t_{tot}}$$

- $E_{tot}$  = E-modulus of the total composite  
 $E_{poly}$  = E-modulus of the resin used  
 $t_{poly}$  = total thickness of the resin in the composite  
 $E_{wrl}$  = E-modulus of long. fibres in the roving  
 $t_{wrl}$  = thickness of long. fibres in the roving  
 $E_{wrt}$  = E-modulus of transv. fibres in the roving  
 $t_{wrt}$  = thickness of transv. fibres in the roving  
 $E_{ud}$  = E-modulus of the unidirectional roving  
 $t_{ud}$  = thickness of the unidirectional roving

Fig 13.11 E-modulus in a composite laminate

The drawback with prepregs is that they are much more difficult to handle by the builder. He must store them at low temperatures so that they do not cure before they are used. When laminating, the tailored prepreg sheets are put into a mould, either male or female. This process is much more pleasant compared to wet lay-up because there are virtually no emissions, no sticky resin to handle and the available working timespan before it must be finished is much greater. When the prepregs are in place the whole moulded area is covered with a vacuum bag, and air is removed to solidify the laminate. In order to cure the prepregs heat is required, so the whole structure must be put into an

oven or covered with electric heat blankets. The temperature control is quite crucial regarding both heat and the length of heating. The best prepreg systems need a curing temperature of 60° Celsius.

To calculate the overall modulus of elasticity in a composite laminate we must know the individual modulus that the composite consists of. Fig 13.11 illustrates a way to determine the total modulus.

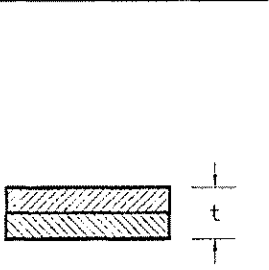
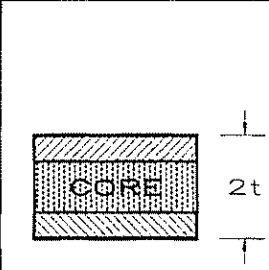
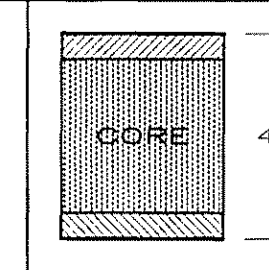
The laminate's total E-modulus,  $E_{tot}$ , is the weighted average of each component's modulus, with the weight equal to the thickness. By adding the product of each thickness and modulus and dividing the sum by the total thickness we get the total composite's modulus,  $E_{tot}$ . The fibre content in this example is 37.5%, ie directly proportional to the vertical axis (thickness). If it is possible to lessen the resin ratio, the total E-modulus will increase accordingly.

**Sandwich**

Basically there are three good reasons for building a yacht of sandwich construction.

- It gives a light building weight. However, practical considerations mean that the outer skin cannot be made too thin or else there will be insufficient strength to withstand docking, grounding and boatyard handling. The weight advantages for sandwich construction are therefore not so apparent in yachts below, say, 30 ft (9 m).
- Sandwich construction is able to utilize a stiffener free construction, making the whole hull totally self-supporting. In this case the scaling factors work in the reverse order. To build a boat of more than 25 ft (7.5 m) totally self-supported by its own hull panels, results in very high demands on the core material and skins.
- This method enables a boat to be built as a one-off where no moulds are available. This will be discussed in more detail later.

Fig 13.12 Strength and stiffness in sandwich vs solid

			
<i>Relative Stiffness</i>	100	700	3700
<i>Relative Strength</i>	100	350	925
<i>Relative Weight</i>	100	103	106

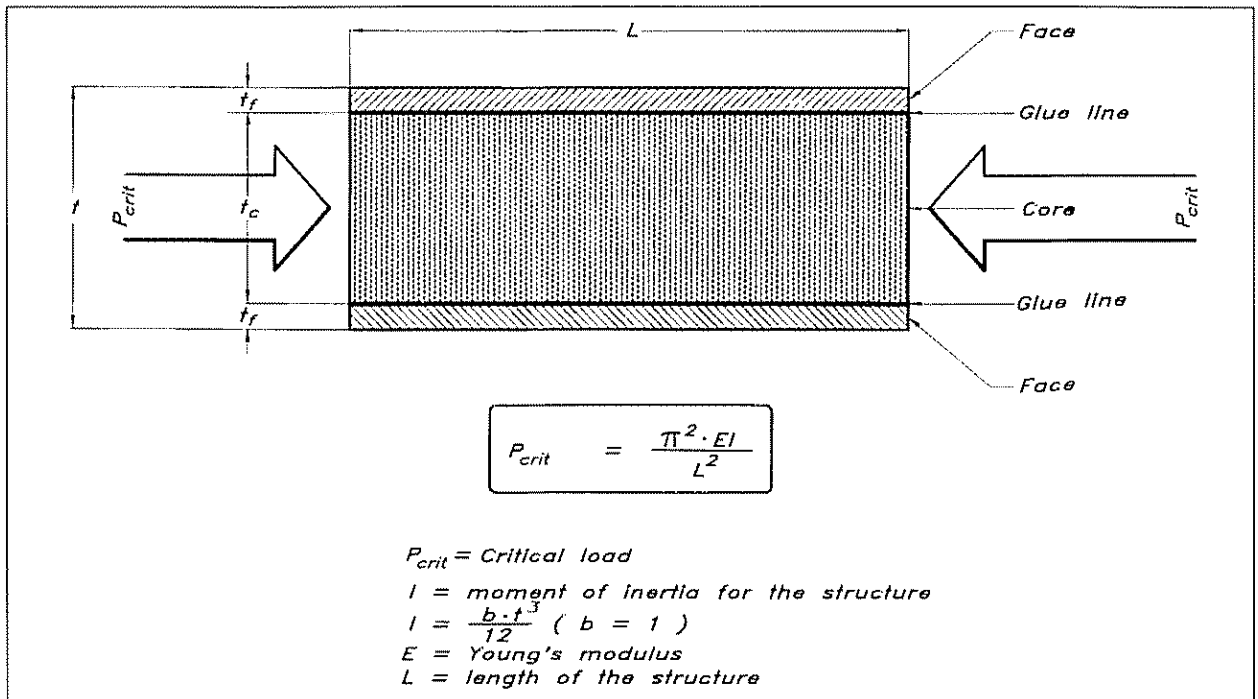


Fig 13.13 Critical load in a sandwich structure

The greatest advantage with sandwich construction compared to solid laminates, is that we can increase the strength and stiffness without a corresponding increase in the weight. Fig 13.12 shows clearly this advantage. By increasing the total thickness of the panel without increasing the total thickness of the laminates, the stiffness increases seven times for a doubling of the panel's thickness. By making the panel four times thicker the stiffness goes up 37 times compared to the solid laminate. The strength increases 3.25 and 9.25 times respectively, with the weight more or less equal. The core in this example is a honeycomb, with a foam or especially balsa core the weight would have increased slightly more. The reason for this drastic increase in strength and stiffness is illustrated in Fig 13.13.

The critical load that a structure can withstand,  $P_{crit}$ , is proportional to the modulus of elasticity of the composite and the moment of inertia of the cross-section, and inversely proportional to the length squared of the test specimen.

Comparing two panels of the same length,  $L$ , we see that the only way to increase  $P_{crit}$  is to get a material with a higher E-modulus,  $E$ , or change the section to obtain a higher moment of inertia,  $I$ . To increase only the E-modulus by using better materials has its practical limits, not to mention the economical aspects. A better way is to increase the I-value of the panel. Since the moment of inertia is proportional to the thickness raised to the third power, it is not difficult to increase the stiffness of the panel by making it thicker. But we do not want to increase the weight, and here the 'sandwich-principle' comes into play. By dividing the laminate into an outer and an inner face and filling the space in the middle with something that is light, but still fulfils its

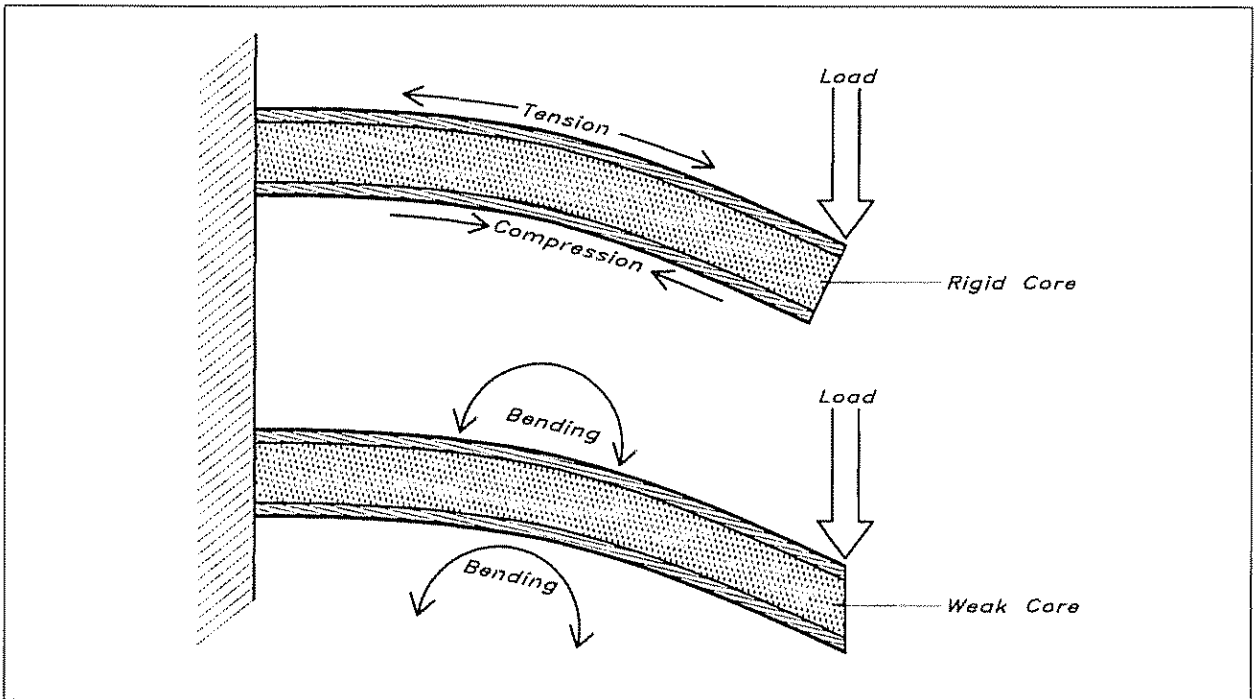


Fig 13.14 Comparison of cores that are rigid or weak

structural tasks, we will have the increase in total thickness without an excessive increase of weight.

The faces carry the tensile and compressive stresses in the sandwich. The local flexural rigidity of the faces is so small that for all practical purposes it can be ignored, and therefore laminates specifically designed to carry tensile and/or compression loads can be used. Faces also carry local pressure at fastenings etc, and where these pressures are high the face should be dimensioned for the shear force connected to it, so that we do not punch a hole in the face when applying the load.

The core has several important functions to perform. It has to be stiff enough to maintain a constant distance between the faces when the structure is loaded. It must also be so rigid in shear that the faces don't slide over each other. The shear rigidity of the core forces the faces to co-operate with each other. If the core is weak the faces do not co-operate, and the faces work as plates in bending, independent of each other. Since the local flexural rigidity is so small, the sandwich effect is lost and the structure collapses (see Fig 13.14). To keep the faces and the core co-operating with each other, the face/core joints must be able to transfer the shear forces between the faces and the core, but it is hard to specify numerically the demands on the joints. A simple rule is that the joints should be able to absorb the same shear stresses as the core.

This basic description of the sandwich principle shows that it is the sandwich structure as a whole that generates the positive effects. However, we should mention that the core has to fulfil the most complex demands. Strength in different directions and low density are not the only properties that it must have, but often there are special demands on buckling, insulation, absorption of moisture, fatigue, ageing resistance etc.

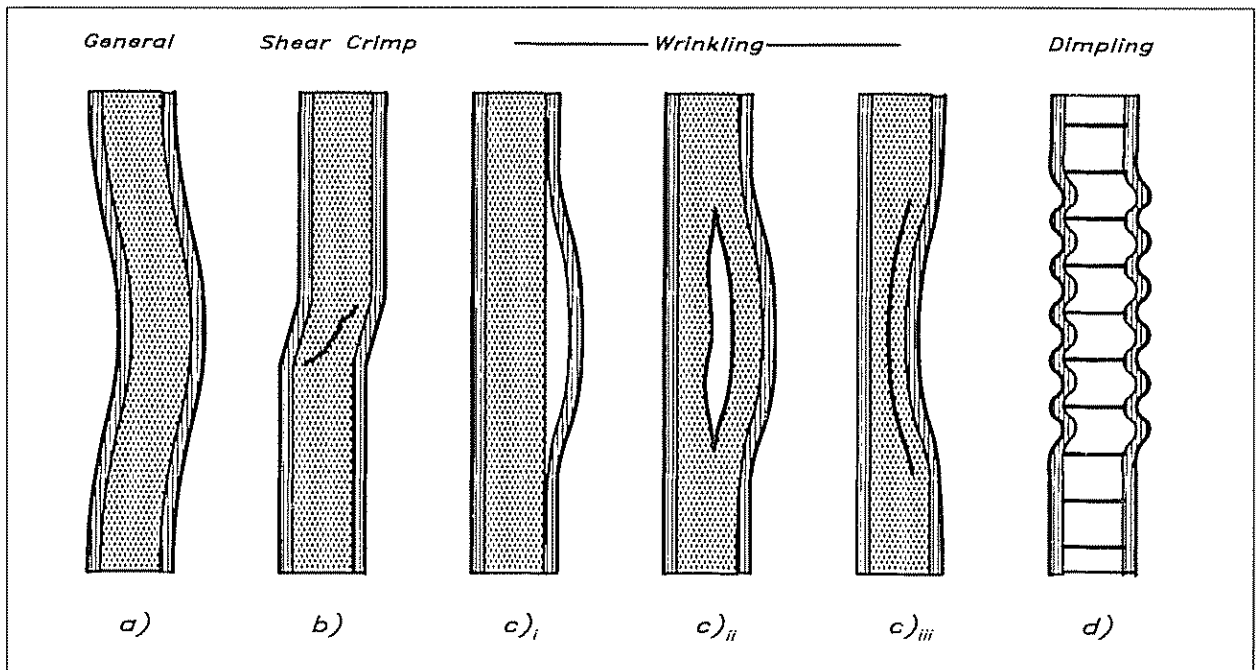


Fig 13.15 Sandwich buckling characteristics

Each part of the sandwich has its specific property, and together they act as a unit. It is important not to break the co-operation between the parts. If for example reinforcing frames are made, they should be made of a material with the same or less strength than the face material. Otherwise most of the stresses will be taken by the frame reinforcement, which it is not designed for. Cracks at attachments often result from a combination of sandwich structure and frame structure which has not been properly balanced.

### Typical sandwich buckling

A good understanding of a sandwich core's general qualities and the co-operation between faces and core can be obtained by carrying out a panel compression test. The panels are put into compression perpendicular to their plane, and the buckling characteristics are then studied. Possible results are depicted in Fig 13.15 as follows:

#### (a) General buckling

The core and the faces are co-operating well, but the panel is too slender, so the whole structure bends. If general buckling is feared, we can:

- use facings with a higher elastic modulus
- increase facing thickness
- use a core with a higher shear modulus
- increase core thickness.

#### (b) Shear crimping

The faces and the face/core joint are strong enough but the core fails in shear. To increase the total critical crimping load we can:

- increase core thickness
- use a core with a higher shear modulus.

#### (c) Wrinkling

The facings' buckling is prevented by the core which, when the facings

are subjected to compression, supports them laterally. If the compression stress on the facings exceeds a certain limit, the core will not be able to prevent their buckling. In the first case the bonding of the face to the core is not strong enough, in the second case the core is failing in tension while the third case shows a core that does not have enough compression strength. If local wrinkling is feared, we can:

- use a facing with a higher elastic modulus
- use a core with higher elastic properties.

#### (d) Dimpling

When the core is made of honeycomb, the bonding between faces and core only takes place at the honeycomb cells' edges. When the facings are subjected to a compressional force, they may therefore undergo buckling in the free spaces within the cells. When it is necessary to increase the critical dimpling stress, we can:

- use a facing with a higher elastic modulus
- use thicker facings
- use a core with smaller size cells.

#### Sandwich bending

The normal load conditions for panels in boats are in the bending mode. Fig 13.16 shows the distribution and levels of stresses in a sandwich beam. The index 'f' refers to the faces and 'c' to the core in the formulae. As we can see from the figure the faces are considered to take all normal forces and the core all shear forces.

Fig 13.16 Stresses in a sandwich beam

*Distribution of normal- and shear-stresses when  $E_c \ll E_f$  and  $t_f \ll t_c$   
The faces' own moment of inertia is small and can be ignored so:*

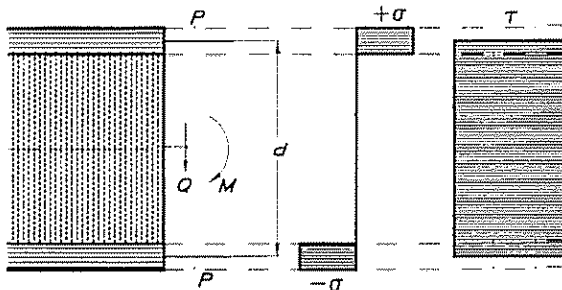
$$I_b = 2 \cdot b \cdot t_f \cdot \left( \frac{t_c}{2} + t_f \right)^2 = b \cdot t_f \cdot \frac{d^2}{2}$$

but  $b \cdot t_f = A_f = \text{Cross Section Area of the Face}$   
 $I_b = A_f \cdot \frac{d^2}{2}$ , and the normal stress becomes:

$$\sigma = \frac{M \cdot d \cdot 2}{A_f \cdot d^2 \cdot 2} = \frac{M}{A_f \cdot d} = \frac{P}{A_f}$$

*The shear stress is calculated from:*

$$\tau = \frac{Q \cdot b \cdot t_f \cdot d}{I_b \cdot 2 \cdot b} = \frac{Q}{b \cdot d}$$



$E_c$  = Elastic Modulus of Core  
 $E_f$  = Elastic Modulus of Face  
 $t_c$  = Thickness of Core  
 $t_f$  = Thickness of Face  
 $b$  = Width of Beam



The faces' own moment of inertia ( $I_0$ ) are very small and can be ignored. The resulting moment of inertia ( $I_b$ ) gives the total section's moment of inertia:  $I_b = A_f \cdot d^2 / 2$ , ie the resulting moment of inertia is proportionally dependent on flange area, or face thickness, and the square of the sandwich thickness.

Thanks to this simplification the normal stress in the faces ( $\sigma_f$ ) can be approximated to:  $\sigma_f = P / A_f$ , ie the load carrying capability is directly proportional to the flange area, or face thickness.

If the core is too weak to contribute significantly to the flexural rigidity of the sandwich, which can be safely assumed in most cases, the shear stress may be regarded constant over the thickness of the core. If, in addition, the flexural rigidities about their own axes are ignored ( $I_0 =$  small), the shear stress ( $\tau_c$ ) becomes:  $\tau_c = Q / (b \cdot d)$ , ie the shear stress is inversely proportional to the core thickness.

The approximations give a total error of 2–3% when the core is at least 5.77 times thicker than each facing and the modulus of elasticity of the faces is much greater than that of the core.

### Sandwich in practice

So far we have discussed the principles behind sandwich construction. Of a more practical nature is the choice of material. For the facings, since they are only subjected to tension or compression forces, and the thickness in itself is not of great importance, compared to that of a solid panel, it pays to use directional fibres or perhaps exotic ones in the laminates.

The core is subjected to a lot of, sometimes conflicting, demands. Fig 13.17 shows a table listing different demands versus ratings for some core materials. The ratings are not weighted, so we have to decide the priorities when making a selection of the core material. The most commonly used PVC core materials in boatbuilding are balsa and linear or cross-linked PVC foam. The best known linear type is Airex and the

Fig 13.17 Demands and ratings of core materials

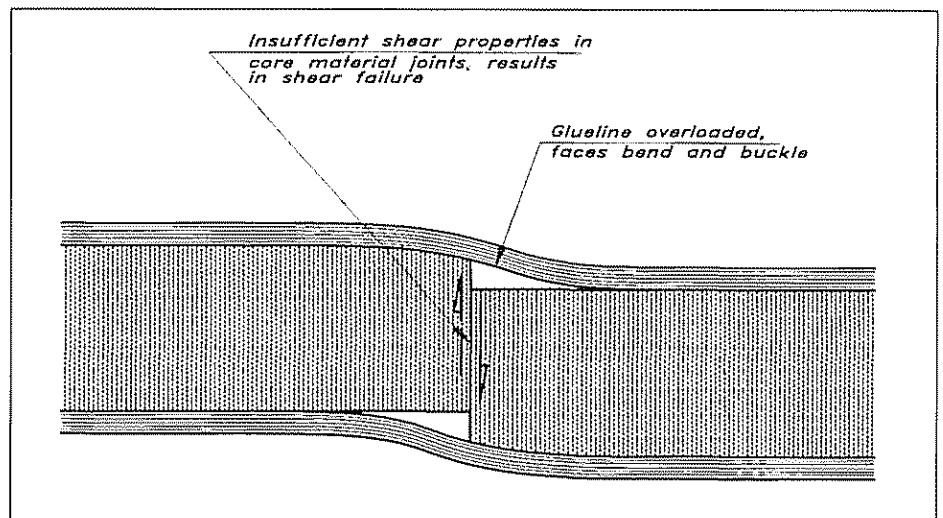
Demands	Plywood	Balsa	Poly Urethane	Linear PVC	Cross-Linked PVC
Light Weight	-1	2	2	2	2
Water Absorb.	0	-1	0	2	2
Shear Strength	2	2	0	1	1
Fatigue	2	2	-1	2	2
Impact Strength	2	1	-1	1	0
Adhesion	2	2	1	0	2
Heat Resist.	2	2	1	1	1
Therm.Insul.	1	2	2	2	2
Fire Resist.	-1	-1	0	2	2
Ageing, rot	-1	-1	2	2	2
Water Resist.	0	0	0	1	2
Repair	0	0	0	0	0
Economy	0	2	1	0	0
SUM	8	12	8	17	18

-1 = Poor  
 0 = Adequate  
 1 = Good  
 2 = Excellent

cross-linked types are Divinycell and Klegecell/Termanto. Recently there has been a development of the two types into a 'mixed linear/cross-linked' type which blends the linear's better impact properties with the cross-linked's better shear properties.

A problem that can arise when building a sandwich hull in a female mould is illustrated in Fig 13.18. In order to cover the curved mould the core material is divided into small cubes held together by a glass weave on one side. If the loose cubes are not glued together the shear properties of the core are drastically decreased: approximately 25% less than for the core material itself. It is not unusual for the builder to rely on the resin to fill the gaps between the 'core cubes' by itself and to glue them together. The drawbacks are many. First you cannot be sure whether the voids really are filled; secondly, you get hard spots between the faces which makes the panel considerably less resistant to impact forces; and thirdly, the weight is increased due to an excess of resin.

Fig 13.18 *Insufficient core joining*



One way to avoid this problem when laminating in a mould is to fill the voids with a microballoon filler that resembles the core material's strength and elasticity properties. To be sure that the voids are filled the core should be vacuumed down into the filler, which is spread over the already cured outer skin. Another method is to inject a filler into the core after both skins have been laminated and cured.

To be certain of a good bond between the core and the skins, the core should be primed with a fast setting resin that is left to cure partially before any laminating is made on top of it. This is to make sure that there will be no resin 'starvation spots' between laminate and core.

The shear properties of PVC foam are almost proportional to density. In Fig 13.19 this dependence for shear strength and shear modulus is shown. We can use these diagrams to choose a correct core when dimensioning a sandwich panel, a task we will perform in the next chapter on scantling determination.

Fig 13 19 Shear properties of cross-linked PVC-foam

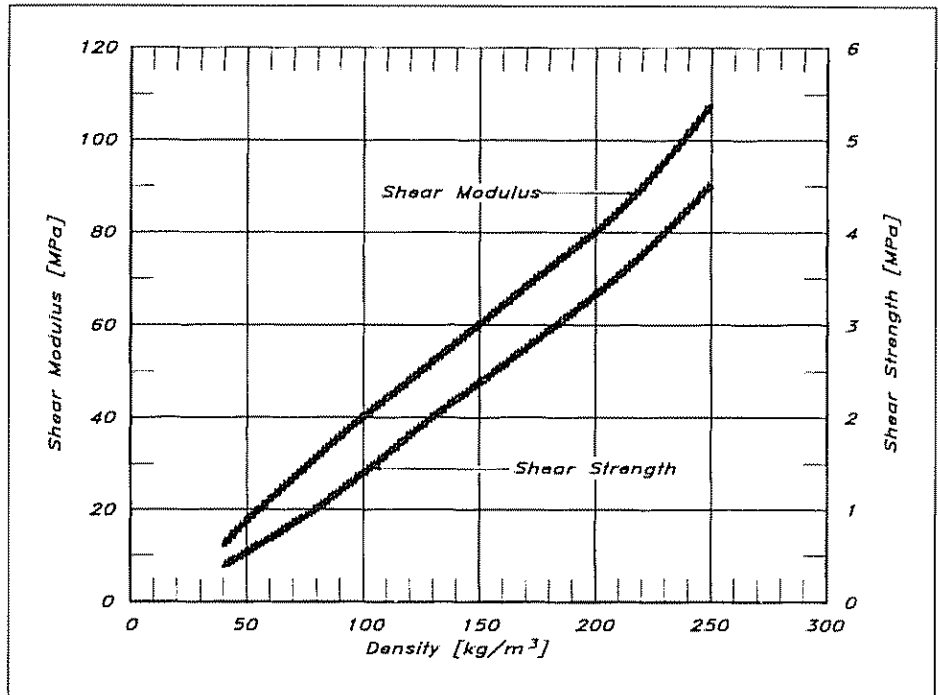
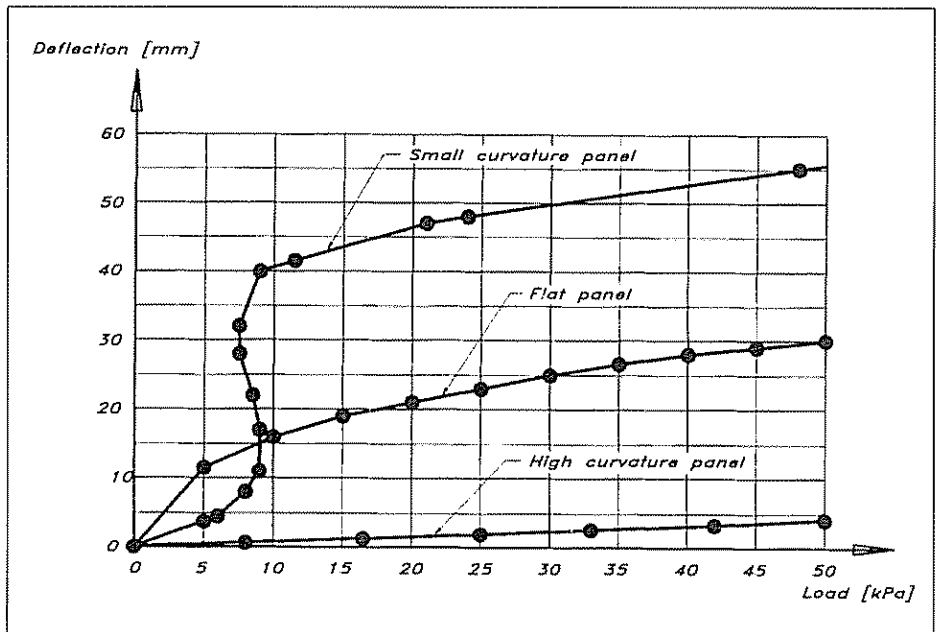


Fig 13 20 Bending behaviour for sandwich panels (Hildebrand)



### Final remarks

The simplified calculation methods outlined in this chapter, and in the ISO Standard, can be used successfully if the sandwich faces are thin, the panels not too curved and the deflections small. Recent tests have shown that the bending behaviour of a sandwich panel varies greatly with curvature. The core shear stresses decrease significantly with increasing curvature (up to 80% compared to a flat panel), so the simplified calculation methods give us an increased factor of safety. If the deflection of single-skin panels exceeds half of the plate thickness

(which is not uncommon for bottom panels) membrane effects must be expected and non-linear analysis applied, for which there are no simple rules of thumb. Fig 13.20 shows three different panels of the same lay-up but with different curvature, and their deflection behaviour under load. All panels are of sandwich construction and of a total thickness of 21.4 mm. The non-linear behaviour of the flat panel is quite clear, as is the 'snap-through', ie the deflection increases instantly without additional load, for the panel with a small curvature ( $A/s = 0.022$ ). The panel with higher curvature ( $A/s = 0.065$ ) shows an almost linear behaviour, with a stiffness substantially higher than the flat panel.

Another point to bear in mind is the non-exactness of the load assumptions that have to be made. As we shall see in the chapter on scantling determination, the size of the panels plays a significant role when deciding on what load to apply. Generally speaking we can reduce the load per unit area the larger the panel, since a big part of the design load relates to a slamming pressure that is limited in time and area, and consequently does not affect the entire panel with a constant pressure.

# 14

# SCANTLING DETERMINATION

---

In the previous chapter we discussed different loads on the boat and their consequences on the construction. Due to the very complex interactions between loads and strength requirements it is very difficult, by direct calculation, to determine the scantlings of the vessel. For this reason, the different classing societies – Lloyd’s, Veritas, ABS (American Bureau of Shipping) and others – have formulated scantling rules to follow in order to dimension a boat that will hold together, if used as intended. For pleasure boats, a new ISO Standard is being developed that will replace the classing societies’ standards for boats below 24 m in length. The Standard is not in its final format yet, but the structure of it is, largely based on two ABS Standards, the Ocean Racing Yacht guide (ORY 1994) and the High Speed Craft guide (HSC 1997), together with NBS–VTT extended rule (1997). The reason for this change is that the ISO Standard will be mandatory when harmonized by the European Union, if you want to sell boats below 24 m into the European Union, regardless of what the classification societies say in their rules. Having said that, it does not mean that the classing requirements are not valid, but to qualify to sell boats in Europe only the harmonized ISO Standard has to be met, not any classification society’s standard. In this chapter we will look at the proposed ISO Standard no. 12215–5. Not all aspects of the Standard will be dealt with since this would constitute a book of its own, but we will concentrate here on the parts dealing with glass reinforced plastics. Where there are details missing, or not yet finalized in the ISO Standard, we will use relevant parts from the ABS and VTT guides to make it possible to calculate proper scantlings for any boat built from fibre reinforced plastics. In certain areas, like the keel attachment, chainplates and rudders, there is no guidance in the ISO Standard, so here we will use the ABS ORY guidelines or good engineering practice.

## Structure of the ISO Standard

The ISO Standard is a modern one in that it clearly identifies the loads to consider, what material properties to use, and what safety factors to apply. Naturally, older rules also take these factors into consideration, but they are often hidden in constants or expressions so you do not really know what you are doing.

Fig 14.1 is a flow chart showing how to proceed through the Standard. The Standard consists of six parts. The first three parts consider materials and their minimum required properties. Part 4 sets requirements for the workshop conditions, material storage and handling, and requirements for the manufacturing of the craft. Part 5, the one we

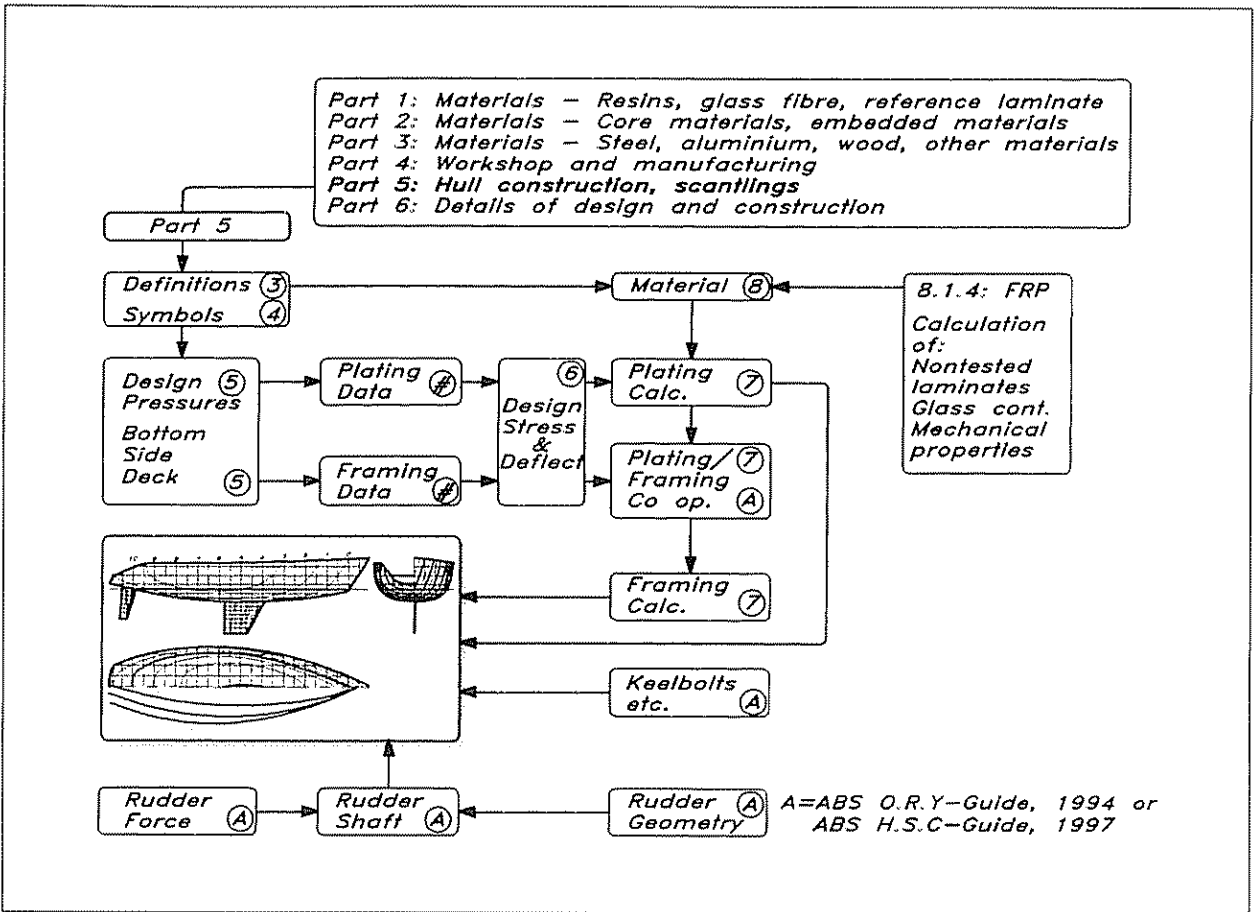


Fig 14.1 The ISO scantling Standard

will discuss, is called in full: 'Small craft – Hull construction/scantlings – Part 5: Design pressures, allowable stresses, scantling determination'. The first paragraph in Part 5 covers the scope: 'This part applies to determination of design loads, pressures, stresses, and to the determination of the scantlings, including internal structural members of small monohull craft, constructed of FRP, aluminium or steel, with a length of the hull ( $L_h$ ) up to 24 m'. Part 6 is not available yet, but will deal with details of design and construction. Where information is not available in the ISO Standard, we will use ABS, VIT or industry practice when dealing with these issues. So looking at Fig 14.1 and Part 5 we have the circled numbers in the boxes that refer to sections in the Standard and the #-marks that indicate data from the actual design. Where the letter A is circled, it means that the ISO Standard does not cover the issue, so we are using an ABS guide instead.

Although the Standard does not explicitly state what documentation is needed in the form of drawings, in general the plans listed opposite are essential, together with calculations, to show that the craft fulfils the scantling requirements. For a small boat this need for documentation is not that great due to the simplicity of the construction, but with increasing size, say from 10 m length upwards, the complexity increases

and, along with this, the need for proper documentation. A typical set of plans are as follows:

- Framing sections
- Bottom construction, floors, girders, etc
- Shell expansion
- Deck and cockpit
- Pillars
- Watertight and tank bulkheads
- Non-tight bulkheads, shelves, bunks which are glassed-in and used as structural supports
- Stern frame and rudder
- Keelbolt and chainplate connections
- Steering gear
- Cabin coach roof, sides and ends
- Closing appliances for hull, decks and superstructure

From here we move on to the definitions, Section 3, where the design category (A to D) and the size of the vessel is established. With that done, we choose our material properties from Section 8. The materials catered for are aluminium, steel and reinforced plastic. Section 8.1.4 (Fig 14.2) gives a method of calculation for mechanical properties of a non-tested glass laminate.

In Section 4 all symbols, coefficients and parameters that are used in the rule are listed. In this chapter we will list the relevant symbols, parameters etc in each figure where they are used, so you do not have to go back and forth when using the formulae.

Section 5 gives methods for determining the design pressures on different parts of the boat, sail or power.

Section 6 gives the allowable design stresses and deflections for different materials and also for the different parts of the boat.

Section 7 covers the actual scantling determination for the hull and deck panels. With plating sizes from our design in question and material properties from Section 8, we can calculate the thickness requirements according to Section 7.1.

After calculating the shell it is possible to do the framing calculations according to Section 7.2. Before calculating the stiffeners we must establish the interaction between plate and frames. This essentially means calculating the effective width of plating connected to a stiffener.

Since Part 6 of the Standard does not cover keels and rudders, we can instead turn to ABS to determine details such as keelbolts and rudder

Properties		ABS	ISO <sub>MIN</sub>	ISO <sub>CALC</sub>	
		N/mm <sup>2</sup>	N/mm <sup>2</sup>	N/mm <sup>2</sup>	
				Chopped (CSM)	(WR) and (MDR)
Tensile strength	$\sigma_{ut}$	124	80	$200 \cdot Wf + 25$	$400 \cdot Wf - 10$
Tensile modulus	$E_t$	6890	6350	$(15 \cdot Wf + 2) \cdot 10^3$	$(30 \cdot Wf - 0.5) \cdot 10^3$
Compressive strength	$\sigma_{uc}$	117	--	$150 \cdot Wf + 72$	
Compressive modulus	$E_c$	6890	---	$(40 \cdot Wf - 6) \cdot 10^3$	
Flexural strength	$\sigma_{uf}$	172	135	$502 \cdot Wf^2 + 106.8$	
Flexural modulus	$E_f$	7575	5200	$(33.4 \cdot Wf^2 + 2.2) \cdot 10^3$	
Shear strength perpen- dicular to warp	$\tau_{u PPW}$	75	50	$80 \cdot Wf + 38$	
Shear strength parallel to warp	$\tau_{u P/W}$	62	50	$80 \cdot Wf + 38$	
Shear modulus parallel to warp	$E_s$	3100	--	$(1.7 \cdot Wf + 2.24) \cdot 10^3$	
Interlaminar shear strength	$\tau_i$	17.3	15	--	
<i>Uni-directional (UD)</i>					
Tensile strength	$\sigma_{ut}$	--	--	$1800 \cdot Wf^2 - 1400 \cdot Wf + 510$	
Tensile modulus	$E_t$	--	--	$(130 \cdot Wf^2 - 104 \cdot Wf + 39) \cdot 10^3$	

Glass ply thickness, $t_i$ : [mm]	
$t_i = mf_i \cdot (Sf_i / Wf - (Sf_i - Sr_i)) / (1000 \cdot Sf_i \cdot Sr_i)$	
$mf_i$ = fibre weight, g/m <sup>2</sup>	
$Sf_i$ = glass spec.weight, kg/dm <sup>3</sup> :2.54-glass	
$Sr_i$ = resin spec.weight, kg/dm <sup>3</sup> :1.2-polyester	
$Wf$ = glass content by weight, ratio	

Reinforcement type	Glass content by weight $Wf$
Chopped sprayed up	0.28
CSM hand lay up	0.30
Woven Roving (WR)	0.48
Multidirectional (MDR)	0.55
Unidirectional (UD)	0.60

Fig 14.2 Properties of basic laminates

shafts. Two types of rudder are covered in the ABS ORY guide for sailing boats: spade rudders with no skegs, and semi-spade rudders with a skeg-hung pintle between the rudder tip and hull bottom. Planing power boat rudders are dealt with in the ABS HSC guide. Neither the ISO Standard nor the ABS guide say anything about the dimensioning of chainplates other than that they should be of sufficient strength. The reason for this might be that there are so many ways to do this that it is virtually impossible to cover all cases in a scantling rule. However, we will give an example in Fig 14.15.

**Hull definitions**

Fig 14.3 shows the measurements that must be taken to be able to determine the scantlings.

- $L_H$  = Length of hull, excluding bolted-on extensions such as bowsprits, stem fittings etc [m]
- $L_{WL}$  = Length of waterline at full load displacement [m]



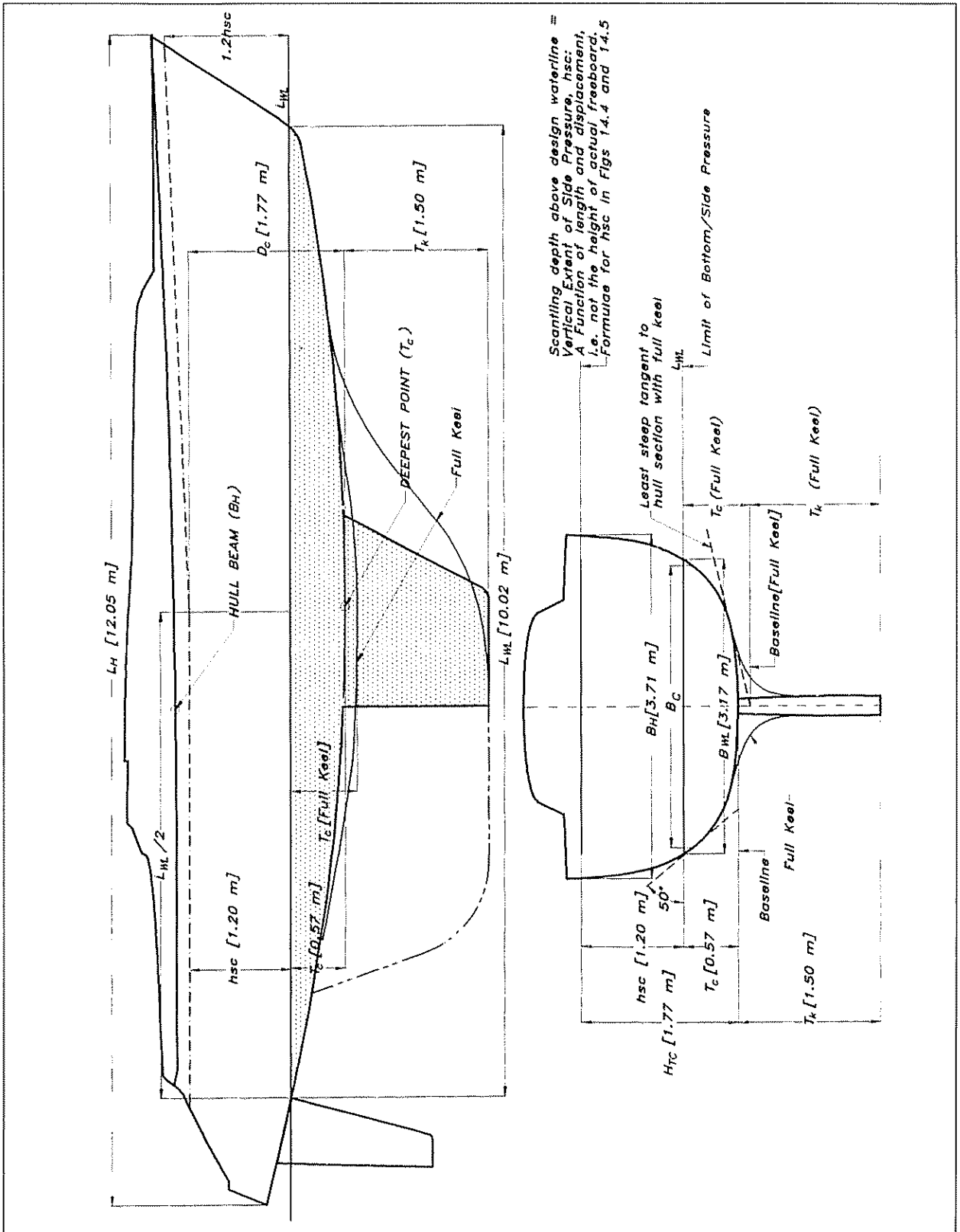


Fig 14 3 ISO hull definitions

- $B_H$  = Hull beam, excluding bolted-on extensions [m]
- $B_{WL}$  = Waterline beam [m]
- $B_c$  = Chine beam [m]
- $T_c$  = Immersed depth of canoe body measured vertically from the bottom of the hull at its deepest point at the centreline to the maximum estimated displacement waterline [m]
- $H_{Tc}$  = Scantling depth above baseline [m]
- $h_{sc}$  = Scantling height above design waterline [m]
- $T_k$  = Draft of keel below the canoe body [m]
- $m$  = Displacement mass [kg]
- $\nabla$  = Displacement volume [m<sup>3</sup>]

### Basic laminate

The basic laminate in real life normally consists of a polyester resin and alternate plies of fibreglass mat and fibreglass woven roving. The normal glass content is approximately between 30% and 35% by weight, ie there shall be at least 300g to 350 g reinforcement per 1000 g laminate. Fig 14.2 gives the minimum physical properties of the laminate used by ABS and ISO. The reason for the lower ISO values is that a pure chopped strand mat or spray-up laminate is allowed, while ABS requires a mat/roving-mix in the laminate. The last ISO column gives equations to calculate the actual properties in a laminate consisting of glass mat/roving and polyester provided a burn-out test is performed, to verify the glass content. If we are using a still better laminate, we might use the better values in the scantling equations, provided it is verified by tests. Also given in Fig 14.2 is a formula for calculating the thickness of a ply of a specific reinforcement type. If different types of reinforcements are used, which is normally the case, we calculate each layer's thickness and add them together to get the laminate's total thickness. This is the average thickness, given for design purposes, but the actual laminates may vary by as much as 15% above or below the average value. When measuring laminate thicknesses, the non-structural parts, as mentioned below, are not to be included.

Gel coats and surface reinforcement mats or cloths weighing less than 30 g per square metre are considered to be non-structural, and therefore are not to be included when calculating laminate scantlings.

If the laminate is assumed to have bidirectional woven roving in it, and if unidirectional reinforcing materials are employed, a sufficient balance of properties in the warp and weft directions is to be maintained to prevent laminate failure in any direction. For unidirectional laminates

the strength in the weft direction to the strength in the warp direction are to be not less than the following:

Member	Weft strength/Warp strength
Panel, aspect ratio = 1	0.80
Panel, aspect ratio > 2	0.61
Stiffening member	0.25

For aspect ratios between 1 and 2, the factors are to be obtained by interpolation.

### Design loads for the bottom

Fig 14.4 shows the magnitude and distribution of loads on the bottom panels for a power boat that we shall use for the calculation. Fig 14.5 shows the same thing for a sailing boat. The loads are expressed as design pressures in  $\text{kN/m}^2$  (kPa). To get a better feel for the loads it might be worth mentioning that 10 kPa gives a load of 1 tonne per square metre.

For the bottom of a power boat, or a planing sailing boat, the formulae in Fig 14.4 apply having taken some limits of application into consideration, ie length-beam ratios, length-displacement ratios, and speed-length ratios. Without going into details, the Standard covers all 'normal' boats with speeds above  $2.36 * (L_{WL})^{0.5}$ . The main formula in Fig 14.4 describes the bottom pressure  $P_{bl}$ . As can be seen, it consists of a term including displacement divided by length and width, ie a hydrostatic pressure.

To this hydrostatic pressure is then added a hydrodynamic factor,  $n_{cg}$ . This dynamic load factor is dependent on length, width, deadrise, trim, speed and displacement of the craft according to formula 2a. For smaller boats at high speeds, this  $n_{cg}$ -formula gives too high values, so formula 2b has been developed. This equation is just speed and length-dependent, and is used in order not to overestimate the dynamic load factor. The lesser value from formulae 2a and 2b should be used. The values in brackets, 5.65 and 4.78 respectively, are the results from the rescue boat described in Chapter 10, and the lower value is used when calculating the scantlings. In addition there are absolute minimum and maximum values as well as the  $n_{cg}$ -factor, as can be seen from the box in Fig 14.4. The absolute maximum is 6 and for boats below 12 m the minimum allowable factor is 2, decreasing to 1 for a 24 m boat. The  $n_{cg}$  values can be regarded as acceleration loads, expressed in Gs. Although this is not scientifically accurate, it does give a hint as to what kind of punishment the boat and its crew will suffer at a given speed in a seaway. It is worth mentioning that the unprotected human body normally loses consciousness at Gs of 6 to 7.

Equation 1 in Fig 14.4 includes additional factors  $k_{ar}$  and  $k_L$ , which are an area-reduction factor and a longitudinal impact distribution



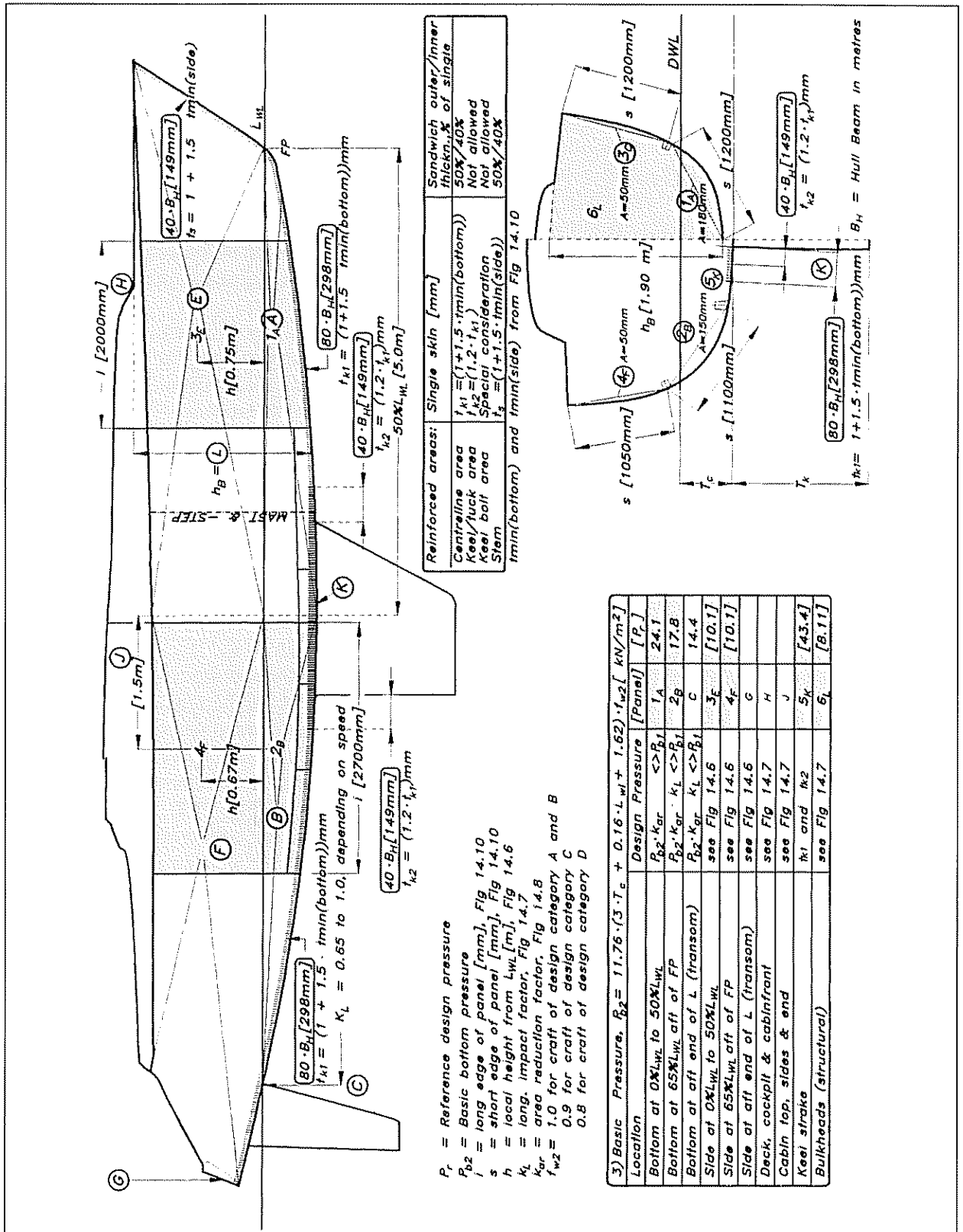


Fig 14 5 Sailing craft design pressures

factor respectively, which we will look at more closely after reviewing the sailboat design loads. In equation 2a there is a design category factor  $f_{w1}$  which is 1 for category A and B, 0.75 for category C, and 0.5 for category D, according to Fig 4.22.

To calculate the bottom pressures we start to calculate  $n_{cg}$  at the worst condition, ie highest speed with lightest displacement or highest displacement with a corresponding lower speed. Normally the worst case is with maximum displacement and corresponding speed. Maximum allowable deadrise is  $30^\circ$  and minimum allowable trim is  $4^\circ$  for motor craft and  $3^\circ$  for sailing craft. The worst condition  $P_{b1}$  pressure modified with  $k_{ur}$ ,  $k_L$  and  $f_{w1}$  is used as a reference pressure  $P_r$  when calculating the scantlings for the bottom.

The extent of the bottom is defined to meet the chine at the LCG position, if known, or at  $0.4 \cdot LWL$  forward of the transom if LCG is not known, as shown in Fig 14.6. In the case of a round bilged hull the chine position is established by drawing a tangent of  $50^\circ$  from the horizontal to the hull contour, as can be seen in Fig 14.3.

For sailing craft we calculate the basic bottom design pressure  $P_{b2}$  according to equation 3 in the boxed-in table in Fig 14.5. This pressure depends on the canoe body draft (hydrostatic pressure), a function of length (pressure from speed) and a constant.

In addition to this, we also have to calculate  $P_{b1}$ , and if this exceeds  $P_{b2}$  we have to use it (the greater one) as the reference pressure  $P_r$  for the sailing craft.

The extent of the bottom is defined as reaching the level of the stationary waterline at fully loaded displacement. Lengthways the craft is divided into four areas, as in our YD-40 case, A and B for the bottom, and E and F for the topsides. Areas A and E reach from the forward perpendicular (FP) to 50% of  $L_{WL}$  aft of the FP (see Fig 14.5), and here the panel pressure is at maximum. From this position to the transom, the pressure drops down to 65% minimum, depending on speed (see Fig 14.8). Just as for the motor craft, the pressure has to be modified by taking panel aspect ratio, longitudinal position and design area into consideration ( $k_{ur}$ ,  $k_L$  and  $f_{w2}$ ).

The canoe body draft used in the above calculations for sailing craft is not allowed to be less than  $0.062 \cdot L_{WL} - 0.26$ . In addition, to calculate  $P_{b2}$  for sailing craft, we also have to calculate  $P_{b1}$ , and the greater of the pressure  $P_{b1}$  or  $P_{b2}$  is to be used as reference pressure  $P_r$  for further calculations. The speed (in knots) shall be declared by the manufacturer or designer but not taken to be less than  $3(L_{WL})^{0.5}$ , minimum running trim is  $3^\circ$ , minimum deadrise is  $10^\circ$ , and maximum deadrise is  $30^\circ$ .

Around the centreline, area K, there is a reinforced area,  $t_{k1}$ , extending longitudinally over the entire bottom and each side of the centreline a distance equal to  $80 \cdot B_{H1}$  from the centreline as shown in Fig 14.5. The increase in thickness is to be 1.5 times the minimum bottom thickness plus 1 mm in this keel strake. The minimum thickness for bottom, side and deck we get from Fig 14.10. If the keel area is unprotected, ie not fitted with a separate protective keel (the case for most fast power boats), or if a ballast keel is attached to this bottom area, the keel

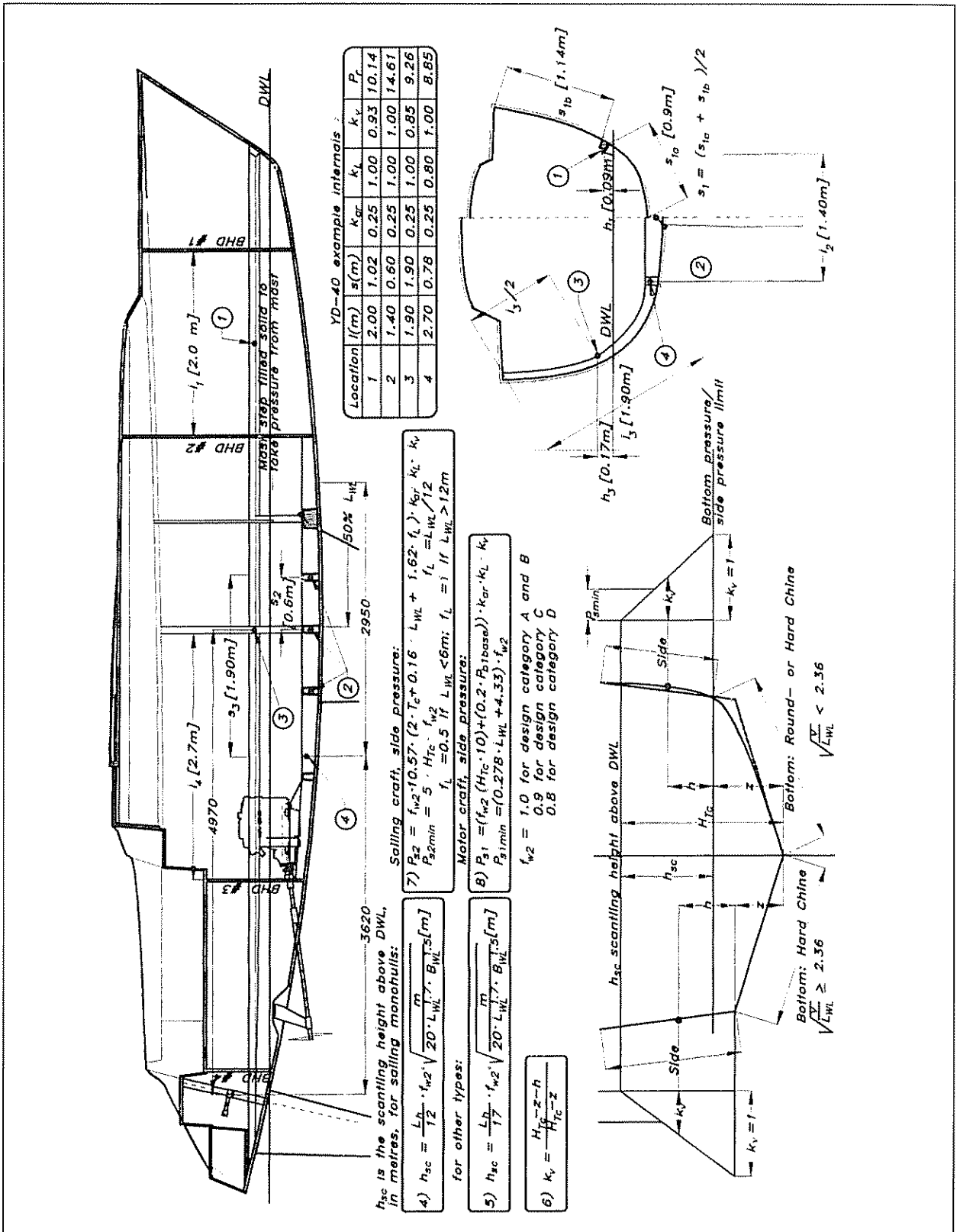


Fig 14.6 Design pressure for sides and internals

### Design loads for the topsides

strake closest to the centreline,  $t_{k2}$  ( $40 \cdot B_H$  from the centre), has to be 1.2 times thicker than the basic keel strake  $t_{k1}$ -thickness.

For the side panels we must decide at which height above the bottom/side limit the pressure acts to establish the correct design head. This height is called the scantling height,  $h_{sc}$  in Figs 14.4 and 14.6. To be able to define the panels we must have a stiffening system layout so we can identify each hull panel. The pressure acts on the geometric centre of the panel in question. In Fig 14.5 the panels marked  $3_E$  and  $4_F$  are two side panels of the YD-40 used as examples of the calculation. The shaded boxes in the table of the figure give the YD-40 values.

From Fig 14.5 we can also measure the different panel dimensions, length, span and curvature ( $l$ ,  $s$  and  $A$ ). These are not used in the design head calculations, but we will need them later when calculating the thickness of the panels

Fig 14.6 gives the equations to determine  $h_{sc}$  4 and 5, where it can be seen that sailing monohulls have a slightly higher value than other boats. The reason for this is the normal heeled position of this kind of boat when going upwind. A special vertical correction factor  $k_v$ , formula 6, applies to side pressures, and will be used for shell and strength members located above the loaded waterline or chine and below the scantling height,  $h_{sc}$ .

Equation 7 in Fig 14.6 gives the motor craft design side pressure. It consists of basically two terms: the first one, comprising  $H_{TC}$ , reflects a hydrostatic pressure, and the second term, 20% of a dynamic bottom pressure. The  $P_{blbase}$  is calculated from equation 1 in Fig 14.4 with factors  $k_{ar}$  and  $k_L$  taken as 1. The sailing craft side pressure is described in equation 8 and is constructed the same way as the bottom pressure in equation 3. There are minimum allowable values for both motor and sailing craft side pressures, which applies outside of  $h_{sc}$ .

### Design loads for the decks and bulkheads

The design pressure for the weather deck and cabin front, area  $H$ , is a direct proportion of boat length, and for the cabin top, sides and end, area  $J$ , it is set to  $P_{dmin}$  ( $\text{kN/m}^2$ ) according to the formulae 9 and 10 in Fig 14.7.

Watertight bulkheads and integral tank bulkheads are designed for a pressure according to equation 11 in Fig 14.7. Structural bulkheads that do not form part of a tank boundary are considered as stiffeners made up by a flat frame. The geometry of the resulting equivalent frame can be taken from equation 12.

### Design loads for the internals

The design loads for internals are taken from the design pressure, given in Figs 14.4, 14.5 or 14.6, at the appropriate location. This pressure is applied on the mid-length of the stiffener, and some YD-40 examples are shown, location #1 to #4, in Fig 14.6.

### Longitudinal impact distribution factor

As mentioned earlier, it is not necessary to apply the full pressure over the entire length of the boat. Fig 14.8 gives equations and a diagram



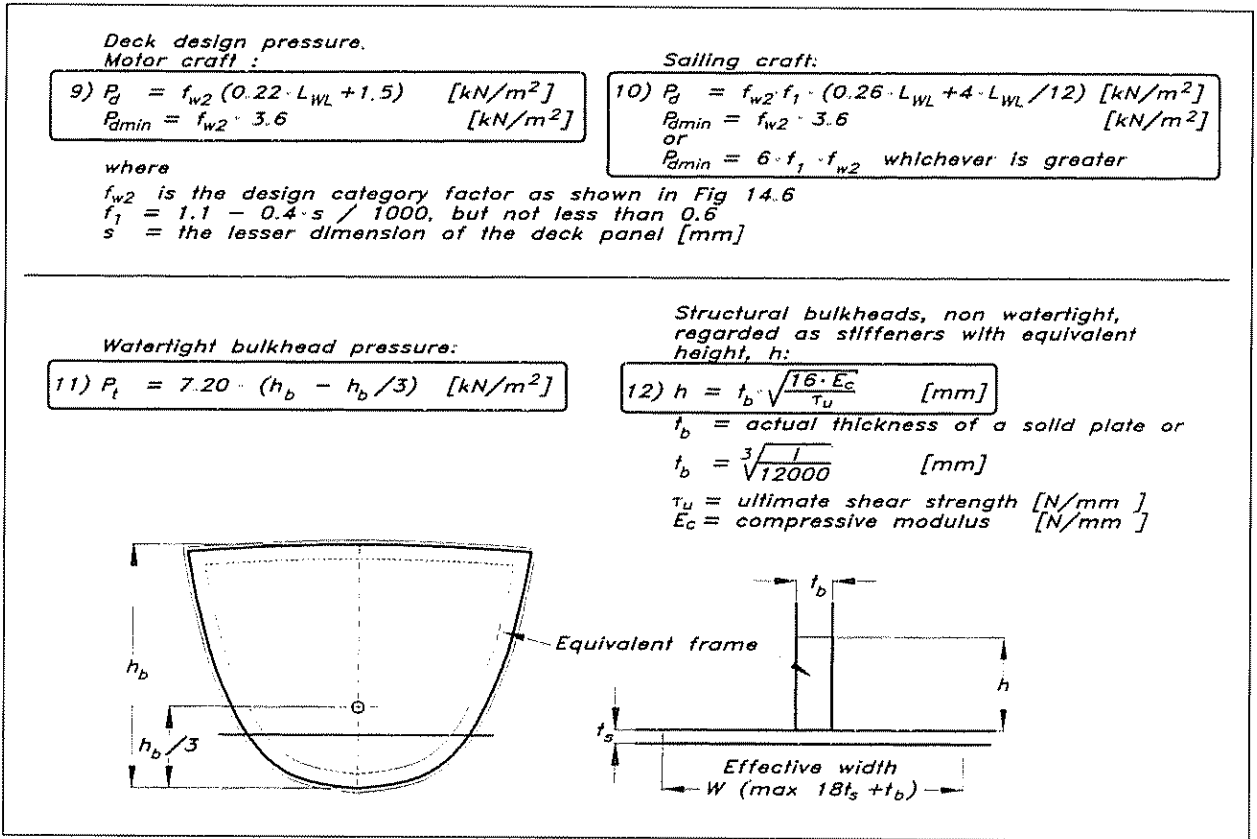


Fig 14 7 Design pressure for deck and bulkheads

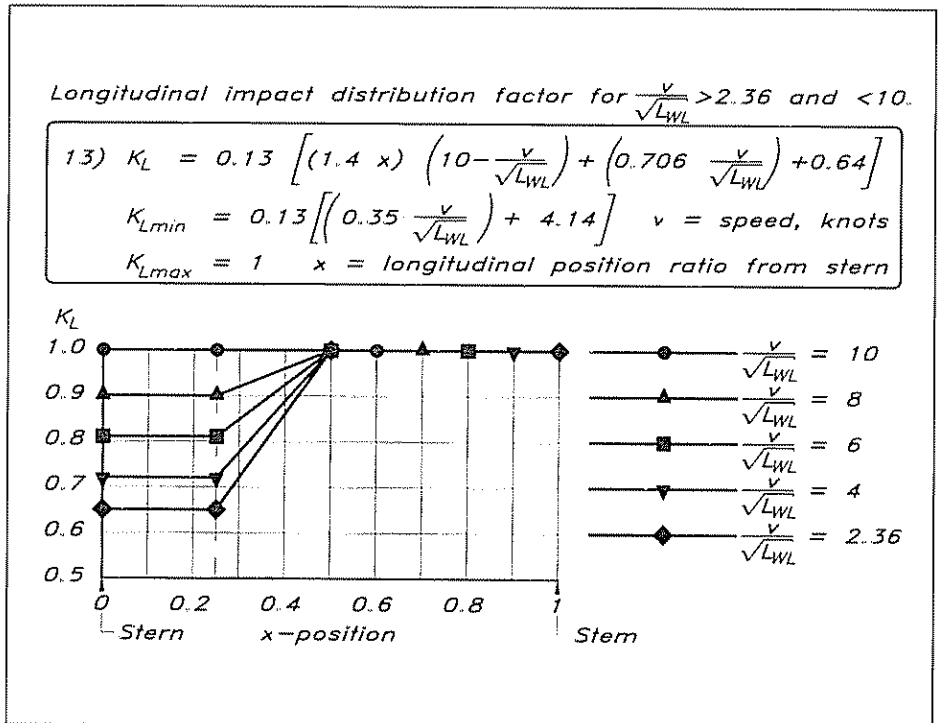


Fig 14.8 Longitudinal impact factor  $K_L$

that show how the pressure can be reduced aft of midships, depending on speed. Note that the speed is not an absolute number but expressed as a speed-length ratio. The stem position in the diagram means the forward end of  $L_{WL}$ . Areas affected by this factor are the bottom and topsides, but not the deck and superstructure.

### Area reduction factor

It might seem strange that there is a reduction factor for stiffeners of long lengths and panels of big sizes. The reason for this is that the

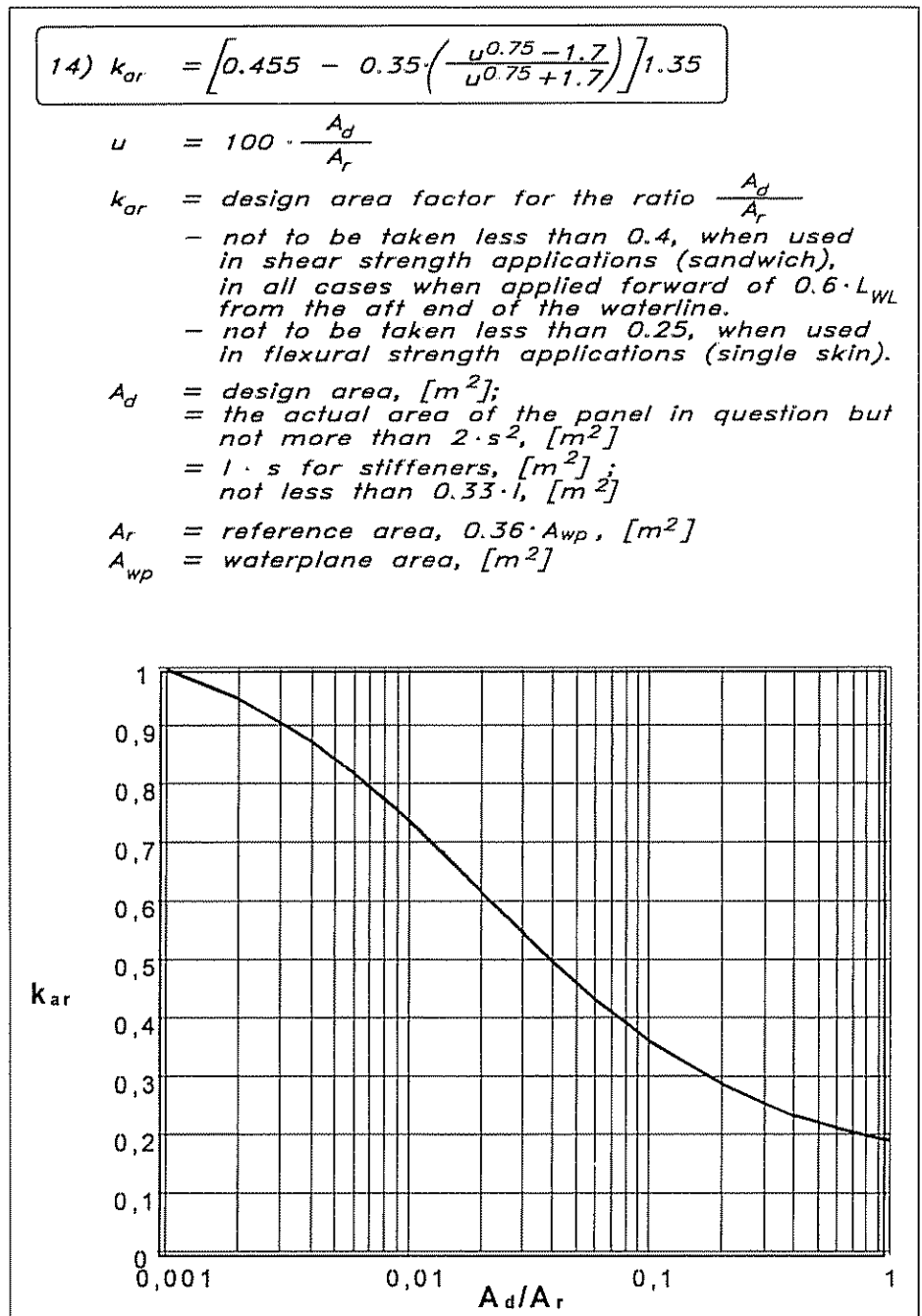
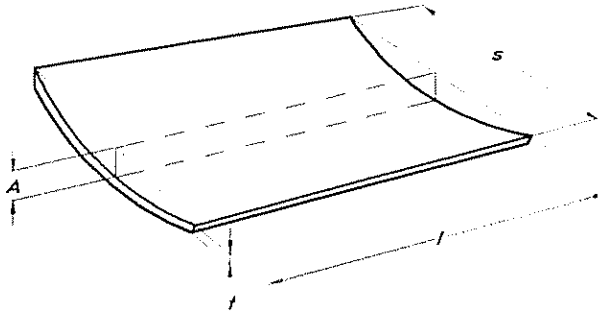


Fig 14.9 Area reduction factor

Thickness of hull, deck and bulkhead plating to be the greater of :

$$15a) \quad t = s \cdot f_k \sqrt{\frac{P_r \cdot k_2}{1000 \cdot \sigma_0}} \quad \text{or} \quad 15b) \quad t = s \cdot f_k \cdot \sqrt[3]{\frac{P_r \cdot k_3}{1000 \cdot k_1 \cdot E_F}} \quad [\text{mm}]$$

- $P_r$  = the reference pressure, given in Figs 14.4 14.5 and 14.6
- $s$  = the short span of the panel, in mm, given in Fig 14.5
- $k_1$  = allowable deflection coefficient, given in Fig 14.12
- $k_2$  = the aspect ratio factor, given in Fig 14.12
- $k_3$  = the aspect ratio factor, given in Fig 14.12
- $\sigma_0$  = minimum allowable design stress, in  $N/mm^2$ , given in Fig 14.11
- $E_F$  = minimum flexural modulus, in  $N/mm^2$ , given in Fig 14.3
- $f_k$  = curve correction, not to be less than 0.8 or greater than 1.0;  $f_k = 1.1 - 3A/s$
- $A$  = curve depth, in mm, as shown below



Minimum allowed thickness:

$$\begin{aligned}
 t_{min}(\text{bottom}) &= f_1 \cdot (3 + 0.5 \cdot L_H + 0.06 \cdot V_{max} + 0.2 \cdot m^{0.33}) \text{ mm} \\
 t_{min}(\text{side}) &= f_1 \cdot (3 + 0.5 \cdot L_H + 0.2 \cdot m^{0.33}) \text{ mm} \\
 t_{min}(\text{deck}) &= f_1 \cdot (2 + 0.2 \cdot L_H) \text{ mm}
 \end{aligned}$$

- $V_{max}$  = maximum speed in knots, not to be less than  $3 \cdot \sqrt{L_{WL}}$
- $m$  = displacement mass in kilograms
- $f_1$  = material reduction factor =  $\sqrt{130/\sigma_{uf}}$
- $\sigma_{uf}$  = ultimate flexural strength, MPa

Fig 14.10 Single skin panel calculation

Material	Structural members	Maximum allowable design stress $\sigma_a$ [ $N/mm^2$ ]
FRP single skin	Bottom and Side	$0.500 \sigma_{uf}$
	Deck	$0.330 \sigma_{uf}$
	Struct. bulkheads	$0.625 \sigma_{uf}$
	Watertight bulkheads	$0.625 \sigma_{uf}$
	Superstructures	$0.625 \sigma_{uf}$
FRP sandwich	Bottom and Side	$0.500 \sigma_{uf}$ or $0.500 \sigma_{uc}$
	Deck	$0.330 \sigma_{uf}$ or $0.330 \sigma_{uc}$
	Structural bulkheads	$0.625 \sigma_{uf}$ or $0.625 \sigma_{uc}$
	Watertight bulkheads	$0.625 \sigma_{uf}$ or $0.625 \sigma_{uc}$
	Superstructures	$0.625 \sigma_{uf}$ or $0.625 \sigma_{uc}$
FRP	Framing	$0.500 \sigma_{uf}$ or $0.500 \sigma_{uc}$
		Shear stress $T_o$ [ $N/mm^2$ ]
FRP	Framing	$0.5 T_o$
FRP sandwich	Core	$0.5 T_o$

$\sigma_{uf}$  = minimum ultimate flexural strength [ $N/mm^2$ ]  
 $\sigma_{ut}$  = minimum ultimate tensile strength [ $N/mm^2$ ]  
 $\sigma_{uc}$  = minimum ultimate compressive strength [ $N/mm^2$ ]  
 $T_u$  = minimum ultimate shear strength [ $N/mm^2$ ]

Fig 14.11 Allowable design stresses

design pressure is considered to be static, but the peak pressures the boat actually encounters are slamming loads of very short duration, acting over a very limited area. So the longer the stiffener or bigger the panel, the more the slamming pressure is spread out, so to speak.

Fig 14.9 shows the  $k_{ar}$  factor that applies to the stiffeners and the hull plating. The deck plating pressure does not incorporate an area reduction factor, since the deck is not subjected to slamming loads. The  $k_{ar}$  is not to be taken less than 0.4 for sandwich hull panels and not less than 0.25 for single skin panels.

**Panel calculation**

Fig 14.10 gives the formulae that calculate the required panel thickness. The 15a formula is a strength requirement and the 15b formula is a stiffness requirement. The greatest thickness is to be used. Normally for glass reinforced plastic the stiffness requirement is the dimensioning

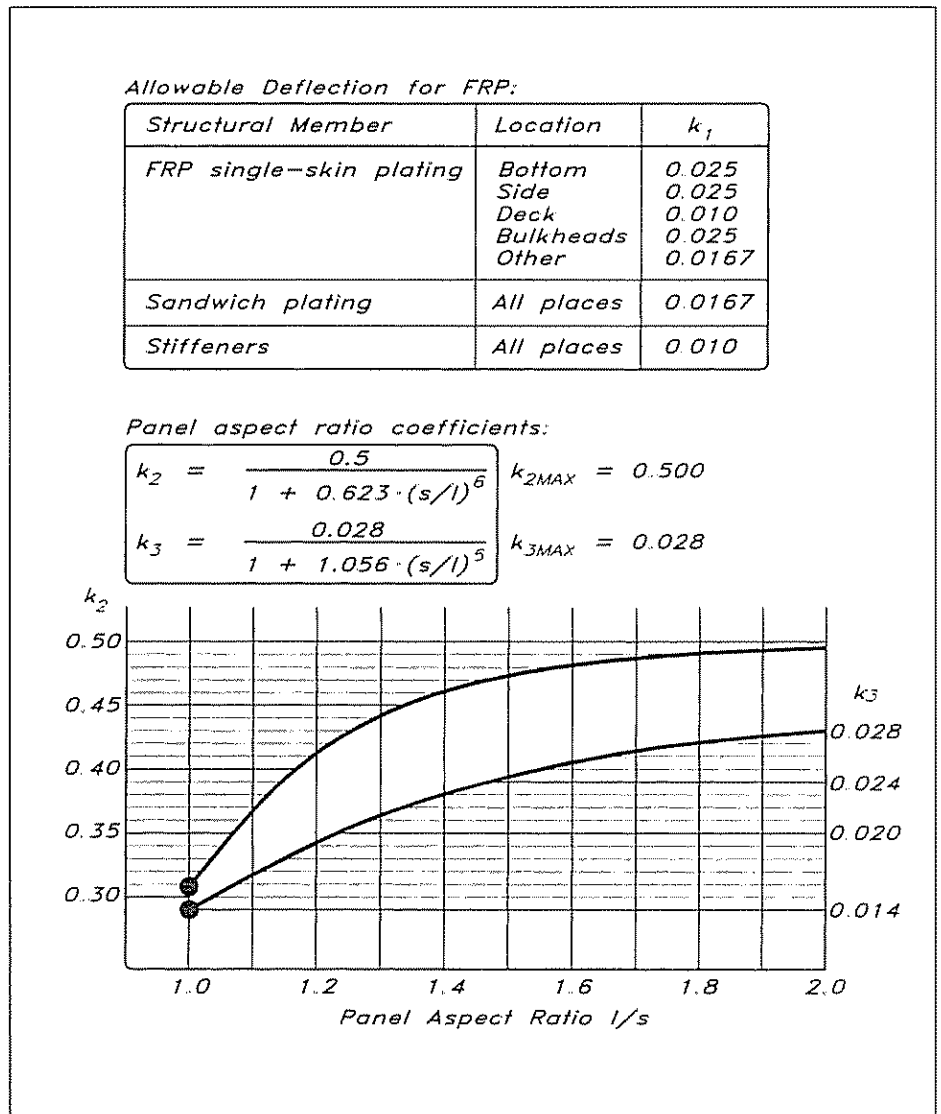


Fig 14.12 Deflection – and aspect ratio coefficients

factor due to the relatively low modulus of elasticity for this material.

Fig 14.10 shows all data we need: the short and long span,  $s$  and  $l$  – and the depth of the curvature in the short span direction,  $A$ . All of the measurements are to be in mm.

By entering Fig 14.12 with the panel aspect ratio,  $l/s$ , we get the aspect ratio reduction factors,  $k_2$  and  $k_3$ . These factors favour panels of low aspect ratios, since the short side and long side interact better the more quadratic the panel is.

Also from Fig 14.12 we get the allowable deflection factor,  $K_1$ . As can be seen, the allowable deflection for single skin plating is much greater than for sandwich panels. The obvious reason is that the single skin is so much more flexible than a sandwich one; it works like a membrane, in contrast to the sandwich, which works more like a stiff plate.

The design stress used in equation 15a in Fig 14.10 is a portion of the ultimate flexural stress given in Fig 14.2, varying with location according to Fig 14.11.

One last reduction factor to calculate is the curvature factor  $f_k$ , as given in Fig 14.10. Now we can plug in all data together with the design pressure into the Fig 14.10 equations and define the minimum thickness for our panels. It is necessary to do these panel calculations before calculating the stiffeners. The reason is that we must know our

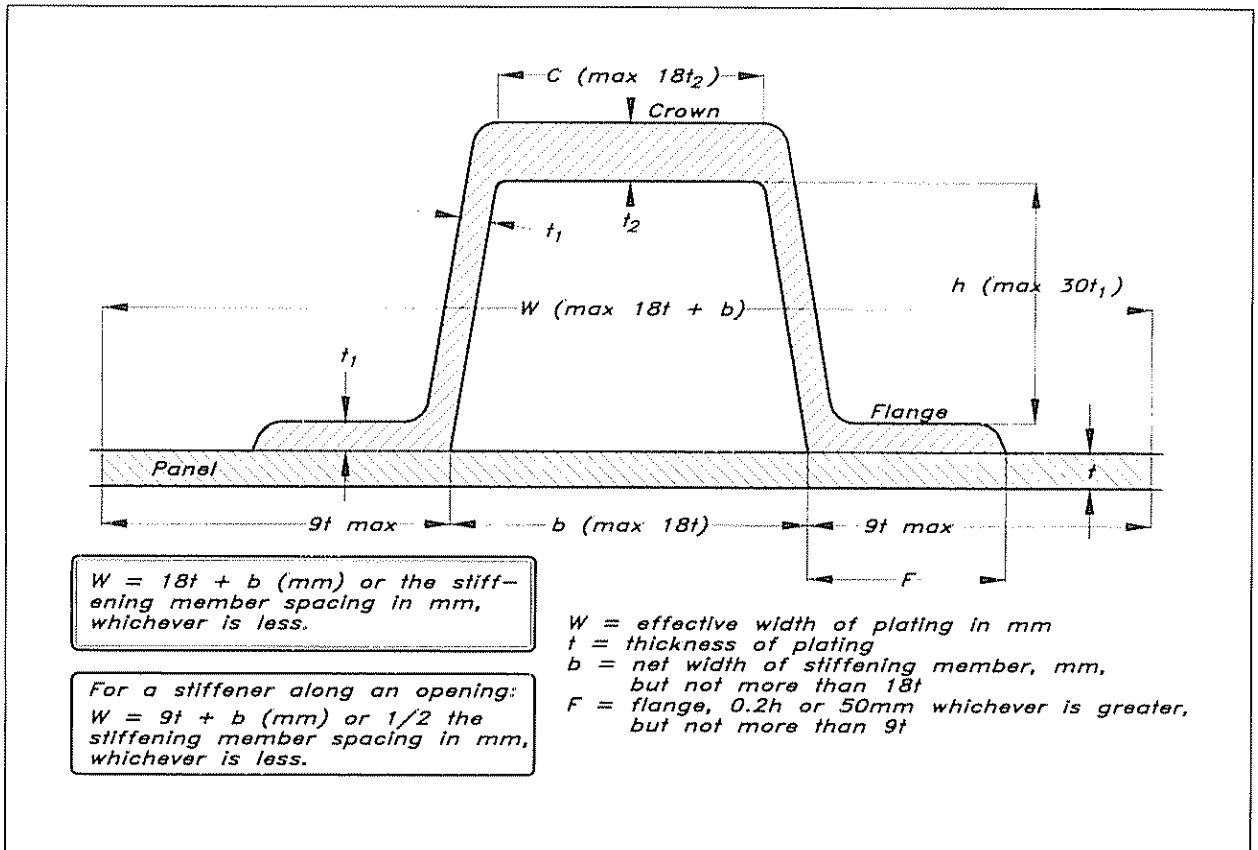


Fig 14.13 Stiffener details and effective width of plating

panel thickness in order to be able to calculate the effective width of plating in conjunction with the stiffener.

### Stiffener calculation

When dimensioning the stiffeners we do not reach the physical dimensions as a result of our calculations, but rather a strength and

The section modulus of each floor, frame, beam and longitudinal stiffening member, in association with the plating to which it is attached, is to be not less than given by the following formula :

$$16) \quad SM = \frac{C \cdot P_r \cdot s \cdot l^2}{\sigma_a} + SM_k \quad [cm^3]$$

$C = 183$  for floors at centreline on sailing craft

$C = 83.3$  for floors at the connection to frames, for girders, stringers, frames and beams

$P_r$  = reference design pressure  $[kN/m^2]$

$l$  = chord length between support points, in m

$s$  = the spacing of the stiffeners, for floors in way of frames is to be the greater of the floor or frame spacing, in m

$\sigma_a$  = the design stress, to be 0.5 times the minimum ultimate in  $N/mm^2$ , as given in Fig 14.2. To outer surface of shell, deck or bulkhead use tensile strength, to inner surface of crown or inner edge of internal, use compressive strength.

$$17) \quad SM_k = \frac{N \cdot W_k \cdot Y_k \cdot 9.8}{n \cdot \sigma_a} \quad [cm^3]$$

$SM_k$  = the required increase in section modulus, cm, for floors and frames in way of the ballast keel. For floors and frames clear of the ballast keel,  $SM_k = 0$

$N = 1.0$  at the centreline reducing linearly to 0.5 at 1/3 of the girth from the centreline to gunwale and not less than 0.5 from this point to the gunwale

$W_k$  = the weight of the ballast keel, in kg

$Y_k$  = vertical distance from mid depth of floor at centreline to vertical centre of gravity of ballast keel, in m

$n$  = number of floors in way of ballast keel, not less than three

The moment of Inertia for each floor, frame and beam, in association with the plating to which it is attached, is not to be less than given by the following formula :

$$18) \quad I = \frac{C_l \cdot P_r \cdot s \cdot l^3}{E_{TC}} \quad [cm^4]$$

$C_l = 57290$  for floors at the centreline on sailing craft

$C_l = 26040$  for floors at the connection to frames, for girders, stringers, frames and beams

$E_{TC}$  = the modulus of elasticity, in  $N/mm^2$ , where the shell and internal member laminates have different moduli of elasticity  $E$  is the base value used to calculate the moment of inertia of the combined shell and internal member, where the shell and internal member are of the same laminate  $E$  may be taken as the mean value of the tensile and compressive moduli

In way of the ballast keel the moment of Inertia  $I$ , in  $cm^4$ , is to be increased in proportion to the increase required in section modulus, where  $SM_k$  is obtained using  $N = 0.5$ .

Fig 14.14 Stiffener calculation

stiffness requirement, ie section modulus and moment of inertia requirements.

Fig 14.13 shows how big a part of the plating we are allowed to include in our stiffener. As can be seen, it is nine times the panel thickness each side of the stiffener. From the figure we also get other limitations of the stiffener geometry. The reason for restricting the width and height of the stiffener is to avoid local buckling of the stiffener parts.

Fig 14.14 gives equations and definitions for calculating the requirements of the stiffeners according to the ISO Standard. The formula 16 gives the required section modulus where the part  $SM_k$  is an additional requirement for floors located over the ballast keel on a sailing craft. Outside this area  $SM_k$  is zero, as well as on motor craft. The C-factor is always 83.33 for motor craft.

The second formula, 17, covers the calculation of  $SM_k$ , and also states that there shall be at least three floors over the ballast keel.

The third formula, 18, sets the requirement for the moment of inertia of the stiffeners. As for the section modulus requirement, the moment of inertia is to be increased in way of the ballast keel in proportion to the increase of the section modulus. The  $C_I$ -factor is always 26040 for motor craft, while it is 57290 for sailing craft at the centreline and 26040 at the connection to frames or girders.

Having established the minimum section modulus required, we could look at the graphs in Figs 12.11 or 12.12 to decide the actual dimensions.

Calculating the moment of inertia for the chosen section is not that easy. Fig 12.5 gives us a solution though. By dividing the stiffener into separate rectangular parts, we can calculate the location of the neutral axis, the parts' individual areas and moments of inertia, and their distances from the neutral axis. As can be seen from the figure, the total moment of inertia consists of the sum of all individual moments and the sum of all individual areas times their distances from the neutral axis squared.

### Spade rudder stock

The first thing to do with the rudder stock calculation is to geometrically define the rudder. Fig 14.15 gives the definitions and equations. In Fig 12.13 we can see the measurements needed by the equations 19, 20, 21 and 22. Basically we need the height and average length of the rudder to determine the rudder lateral area, as well as the location of the centre of pressure and the speed of the vessel.

By locating the rudder stock some way aft of the leading edge we are diminishing the turning lever and hence the torque on the shaft. It is a good rule of thumb not to place the centre of the shaft more aft than in a position that gives an area forward of the shaftline not more than 15% of the total projected area of the rudder. Balancing the rudder more could make the rudder 'steer by itself' in some conditions.

To start the calculation we first establish the sideforce the rudder is capable of delivering. This force  $F_r$  is dependent first of all on speed squared, which here is taken as  $L_{WL}$ , and rudder lateral area,  $A_{lr}$ . The lift coefficient is taken to 1.5 for rudders inside the design limits

The bending moment, torque and stock to be used for a spade rudder are given in the following formulae (ABS O.R.Y):

Rudder bending moment ( $M_r$ ): [ 782494 Ncm; 7825 Nm ]

$$19) M_r = F_r \cdot \left[ h_b - h + \frac{h(l_u + 2l_l)}{3(l_u + l_l)} \right]$$

Rudder torsional moment ( $T_r$ ):

$$20) T_r = F_r \cdot l_c \quad [ 56570 \text{ Ncm; } 566 \text{ Nm} ]$$

Rudder side force ( $F_r$ ):

$$21) F_r = 984 \cdot C_{lr} \cdot L_{WL} \cdot A_{lr} \cdot N \quad [ 11314 \text{ N} ]$$

$l_c = 0.33 l - x_{lc}$ ,  $l_c$  is not to be taken less than  $0.125 \cdot l$

$l$  = the horizontal length of the rudder, in cm, at the centroid of the projected area, as shown in Fig 12.13

$x_{lc}$  = the distance in cm at the same position, from the leading edge of the rudder to the centreline of the rudder stock, see Fig 12.13

$C_{lr} = 1.5$  for rudders having both  $h/l$  between 2 and 6 and  $t/l \geq 0.06$

$h, l_u, l_l$  are distances according to Fig 12.13 in cm

$A_{lr}$  = the total projected rudder area in  $m^2$

$t$  = maximum thickness of the rudder in cm at the centroid

$$N = 1 \text{ where ; } \frac{0.001 \cdot m}{(0.01 \cdot L_{WL})^3} \geq 4304 \quad [ 8071 ]$$

$$N = \frac{2.65 \cdot L_{WL}^2}{3 \sqrt{m^2}} \text{ where ; } \frac{0.001 \cdot m}{(0.01 \cdot L_{WL})^3} < 4304$$

$m$  = maximum estimated displacement in kilograms

$\sigma_c = \sigma_y$  or  $\sigma_u / 1.75$ , whichever is lesser, for metals

$\sigma_y$  = yield strength,  $\sigma_u$  = ultimate tensile strength in  $N/cm^2$  !!

Solid Rudder Stock Diameter ( $d$ ): [ 7 cm ]

$$22) d = \sqrt[3]{\frac{32}{\pi \cdot \sigma_c} (0.5 \cdot M_r + 0.5 \cdot \sqrt{M_r^2 + 4 T_r^2})}$$

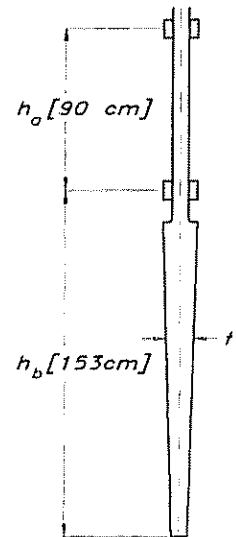


Fig 14.15 Spade rudder stock of metal

imposed, aspect ratio between 2 and 6, and a thickness ratio of more than 0.06, which in practice covers all normal rudders.

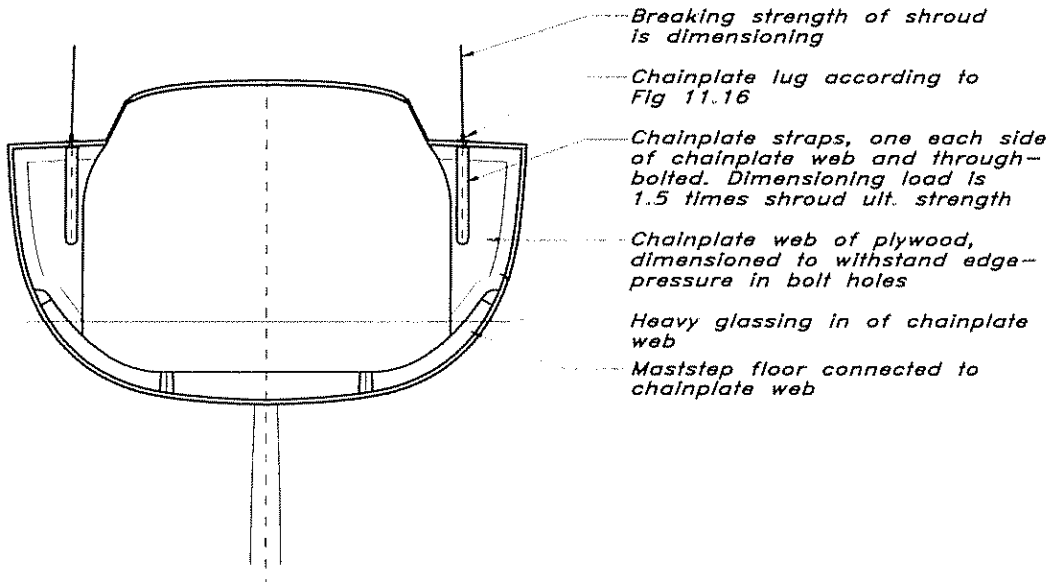
The factor  $N$  in the force formula is there to increase the dimension of rudder stocks in light boats. The reason for this is that they simply are faster than heavy boats, especially when reaching in strong winds, and this puts great strains on the rudder shaft.

Now we can easily calculate the bending and torsion moments,  $M_r$  and  $T_r$ . Entering the equations with units according to ABS, ie N, knots, cm etc, we get our results in N, Ncm and cm. In Fig 14.15 the equivalent SI-system units are shown, N and Nm, so it is easier to compare the results with those of Fig 12.13. In Fig 12.13 the speed in the calculations is set to 8 knots, and by taking the greater force and moments from Fig 14.15, it is easy to 'calculate backwards' that the speed the ABS guide uses for a 10 m wl boat is 8.8 knots, which corresponds to a Froude number of 0.46, ie slightly above displacement speed.

When calculating the rudder stock diameter it is the yield stress of the stock material we shall use, or the ultimate tensile stress divided by



Typical chainplate dimensioning

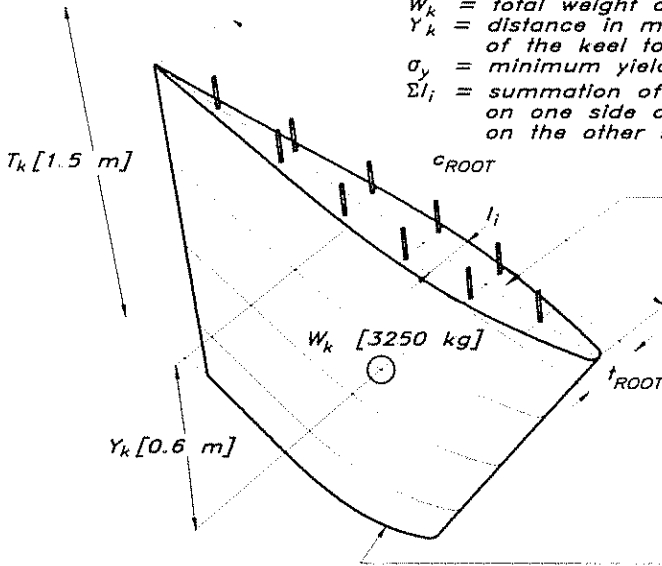


ABS Keelbolt dimensioning

Minimum diameter of each keelbolt at the bottom of the thread:

$$23) d_{kb} = \sqrt{\frac{2.55 \cdot W_k \cdot Y_k}{\Sigma l_i \cdot \sigma_y}} \quad [ 21 \text{ mm } ] \text{ ABS O.R.Y}$$

- $W_k$  = total weight of ballast keel [kg]
- $Y_k$  = distance in mm from the centre of gravity of the keel to the top of the keel
- $\sigma_y$  = minimum yield strength of bolt material [kg/mm<sup>2</sup>]
- $\Sigma l_i$  = summation of distances from the centre of bolts on one side of the keel to the edge of the keel on the other side [mm]



Root area ( $A_R$ ): [0.230 m<sup>2</sup>]  
 $A_R = c_{ROOT} \cdot t_{ROOT} \cdot 0.62$

Keel volume ( $V_k$ ): [0.288 m<sup>3</sup>]  
 $V_k = \frac{T_k \cdot (A_R + \sqrt{A_R \cdot A_T} + A_T)}{3}$

Keel CG-dist ( $Y_k$ ): [0.6 m]  
 $Y_k = \frac{T_k \cdot (A_R + 2 \cdot \sqrt{A_R \cdot A_T} + 3 \cdot A_T)}{4 \cdot (A_R + \sqrt{A_R \cdot A_T} + A_T)}$

Tip area ( $A_T$ ): [0.158 m<sup>2</sup>]  
 $A_T = c_{TIP} \cdot t_{TIP} \cdot 0.62$

Fig 14.16 Keelbolts and chainplates

1.75, whichever is lesser, in  $\text{N/cm}^2$ . All these calculations lead to a solid rudder stock diameter of 7 cm or more, conveniently expressed 70 mm, when using stainless steel type 316 for the stock.

### Chainplates and keelbolts

As previously stated, neither the ISO Standard nor ABS give any specific guidance regarding chainplate dimensions. Generally speaking, approved materials are mild steel, stainless steel, monel or aluminium. Where aluminium is used, stainless steel sleeves are to be fitted in the boltholes. The chainplates are to be effectively attached to bulkheads, webs or brackets. The deck structure is also to be reinforced in way of the chainplate in the form of bulkheads or web frames.

One (but not the only) method of chainplate construction is shown in Fig 14.16. By starting with the wire's ultimate strength we choose a suitable chainplate lug from Fig 11.16. Chainplate straps under the deck are bolted to this lug and to each other through a plywood web. To ensure that the shroud attachment does not give way if the rig is overloaded, the chainplates are dimensioned for a force 1.5 times greater than the breaking load for the wire to which it is attached.

Fig 14.16 also shows what dimensions and other data we need to calculate the keelbolts. One measure that cannot readily be taken from the drawings is the centre of gravity for the keel,  $Y_k$ , below the keel root. A simplified way of calculating this value is shown, which holds true for trapezoidal plan forms with 'normal' wing sections. This calculation also gives the volume of the keel so the weight,  $W_k$ , can easily be calculated. The density for cast iron in practice is  $7300 \text{ kg/m}^3$  and the lead  $11300 \text{ kg/m}^3$ .

The resulting diameters of the keelbolts are to the bottom of the threads so the nominal size is bigger to account for this.

### Sandwich construction

Fig 14.17 gives the relevant equations given by the ISO Standard to determine the dimensions for the skins and core of a sandwich panel.

The equations 24a and 24b are strength requirements and give the required section modulus for the panel, to the outer skin and to the inner skin respectively counted from the neutral axis, which is in the middle of the section if outer and inner skins are equal. If not, the neutral axis has to be computed. When determining the outer skin, the tensile strength of the laminate is to be used, and for the inner skin the compressive strength is to be used. This might seem a bit odd when looking at it at first, since a panel is flexing inwards when loaded by the sea, and consequently the inside is put under tension. The reason that the ISO and ABS take an approach the other way around is that they consider the panels to be fixed at their edges, ie over the stiffeners or bulkheads defining them (the edges). Then we have a situation where the bending moments are greatest at the edges and with their signs inverted compared to the moments in the panel field. This is a simplification since in real life it can be debated whether the edges are fixed or not, the stiffeners and bulkheads bend or not, or if the whole yacht is in fact flexing. To solve all this is not possible by simple beam

The section modulus and the moment of Inertia of the skins about the neutral axis of a strip of sandwich panel 1 cm wide are to be not less than given by the following formulae :

$$24a) SM_o = \frac{s^2 \cdot f_k^2 \cdot P_r \cdot k_2}{6 \cdot 10^5 \cdot \sigma_{ot}} \quad \text{or} \quad 24b) SM_i = \frac{s^2 \cdot f_k^2 \cdot P_r \cdot k_2}{6 \cdot 10^5 \cdot \sigma_{oc}} \quad [cm^3]$$

$$25) I = \frac{s^3 \cdot f_k^3 \cdot P_r \cdot k_3}{12 \cdot 10^6 \cdot ETC \cdot k_1} \quad [cm^4]$$

- $SM_o$  = required section modulus to outer skin from the neutral axis
- $SM_i$  = required section modulus to inner skin from the neutral axis
- $I$  = required moment of inertia of the skins about the neutral axis
- $s$  = short edge of panel, Fig 14.10
- $f_k$  = correction factor for curvature, Fig 14.10
- $\sigma_{oo}$  = design stress of outer skin, Fig 14.11
- $\sigma_{oi}$  = design stress of inner skin, Fig 14.11
- $P_r$  = reference pressure for the location in question  $[kN/m^2]$
- $E_F$  = minimum flexural modulus, in  $kg/mm^2$ , used in Fig 14.3 or 13.4 & 13.5
- $k_1$  = deflection ratio coefficient, Fig 14.12
- $k_2$  = panel aspect ratio coefficient, Fig 14.12
- $k_3$  = panel aspect ratio coefficient, Fig 14.12
- $ETC = 0.5 (E_T + E_C)$ , Fig 14.3

The thickness of the core and skins are to be not less than given by the following formulae :

$$26) \frac{d_o + d_c}{2} = \frac{V \cdot 0.001 \cdot P_r \cdot s}{T_o} \quad [mm]$$

- $d_o$  = overall thickness of sandwich, in mm
- $d_c$  = core thickness, in mm
- $V$  = aspect ratio factor, given in the table below

Panel Aspect Ratio	V	Panel Aspect Ratio	V
>2	0.500	1.5	0.484
2	0.500	1.4	0.478
1.9	0.499	1.3	0.466
1.8	0.499	1.2	0.455
1.7	0.494	1.1	0.437
1.6	0.490	1.0	0.420

$$27) T_u = \frac{2 \cdot V \cdot 0.001 \cdot P_r \cdot s}{0.5 \cdot (d_o + d_c)} \quad [N/mm^2]$$

- $T_o$  = design stress, in  $N/mm^2$
- 0.50 times the ultimate shear strength of the core material, given by manufacturer, or in Fig 13.19
- $T_u$  = ultimate stress, in  $N/mm^2$

Skin buckling criteria:  
The skin buckling stress,  $\sigma_c$  :

$$28) \sigma_c = 0.6 \sqrt[3]{E_s \cdot E_c \cdot G_c}$$

is in general to be not less than  $2.0 \cdot \sigma_{oo}$  and  $2.0 \cdot \sigma_{oi}$

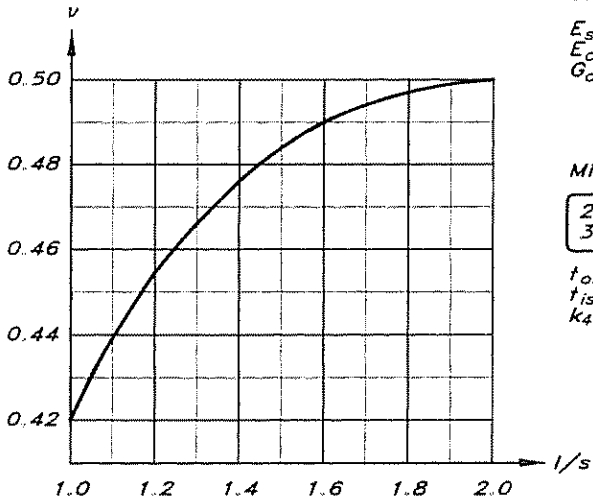
- $E_s$  = compressive modulus of skins  $[kPa]$
- $E_c$  = compressive modulus of core  $[kPa]$
- $G_c$  = shear modulus of core  $[kPa]$

Minimum skin thickness: (ABS H.S.C)

$$29) t_{os} = 0.35 \cdot k_4 \cdot (3.2 + 0.26 \cdot LH)$$

$$30) t_{is} = 0.25 \cdot k_4 \cdot (3.2 + 0.26 \cdot LH)$$

- $t_{os}$  = thickness of outer skin,  $[mm]$
- $t_{is}$  = thickness of inner skin,  $[mm]$
- $k_4 = 1.1$  for bottom shell
- $= 1.0$  for side shell and deck



$$V = 1.95038 - 6.10417 \cdot (1/s) + 8.98536 \cdot (1/s)^2 - 6.2205 \cdot (1/s)^3 + 2.08115 \cdot (1/s)^4 - 0.27244 \cdot (1/s)^5$$

Aspect Ratio (1/s) Reduction Factor V

Fig 14.17 Sandwich construction

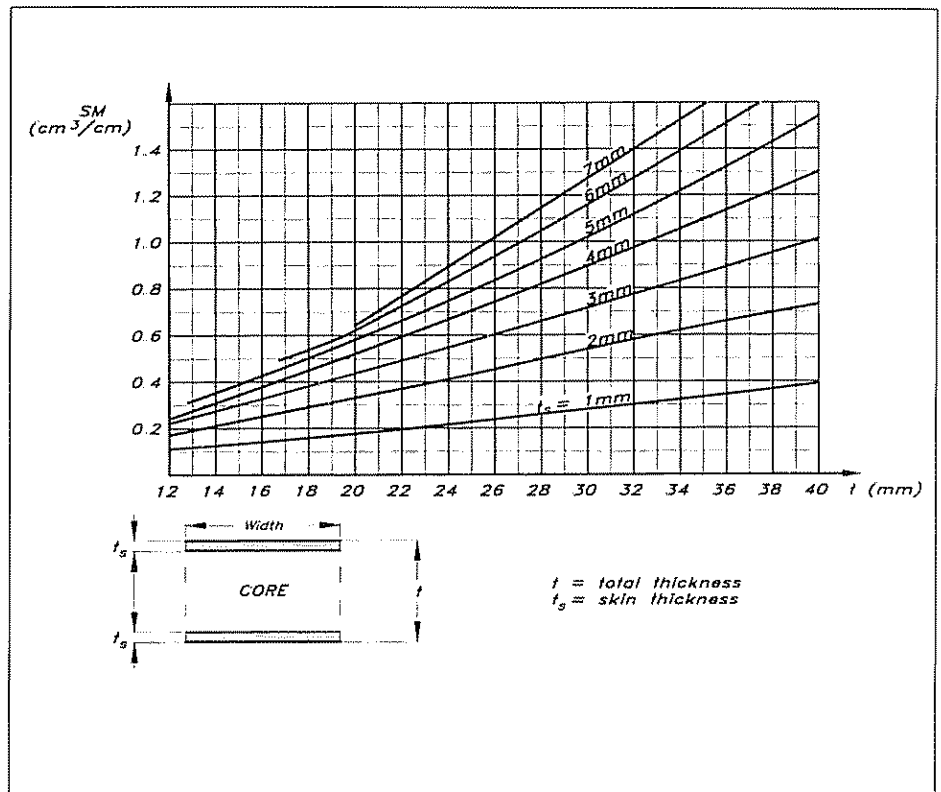


Fig 14.18 Section modulus for sandwich panels

theory, but instead we must do it by finite element analysis, which is far beyond the scope of this book. Anyhow, the ABS guide has proven to provide adequate results over the years, so obviously the simplifications work.

The equation 25, the moment of inertia requirement, is a stiffness requirement and the modulus of elasticity for the skins used are the average of the tensile and compressive modulus.

The first thing we do when determining the sandwich scantlings is to define the panel dimensions and material properties. By using the strength requirements of equations 24a and 24b we get the section modulus requirements, and by using the stiffness requirement of equation 25 we get the moment of inertia requirement for the panel.

Then we check that the core stands up to what is expected from it. From equation 27 in Fig 14.17 we calculate the required shear strength for the core. Remember that the design value is half of the ultimate shown in Fig 14.19.

Fig 14.16 gives the reduction factors for aspect ratio for sandwich panels, which are used in the formulae 24 to 27.

Fig 14.18 shows how the section modulus for different sandwich laminates vary with overall thickness and skin thickness. It is valid only for panels with inner and outer skins being equal.

So far we have looked at the proposed ISO Standard and ABS guides in general, and as a last effort in this chapter we will apply them on the YD-40.

<i>Core material</i>	<i>Density</i>	<i>Min. ult. shear strength</i>
	<i>kg/m<sup>3</sup></i>	<i>N/mm<sup>2</sup></i>
<i>Balsa, end-grain</i>	128	1.9
<i>Balsa, end-grain</i>	144	2.1
<i>PVC, cross-linked</i>	80	1.0–1.2
<i>PVC, cross-linked</i>	100	1.4–1.5
<i>PVC, linear</i>	80 – 96	1.2

Fig 14.19 Typical core properties

### The YD-40 scantlings

The stiffening system as indicated in Fig 14.5 is modified compared to the one in Fig 12.16, in that the panels are greater. The reason for this is that we will dimension the YD-40 to be built with sandwich panels that are much stiffer than single-skin panels, and consequently are able to carry much greater spans without too much deflection

Figs 14.20–14.22 give the calculations for one hull panel, one structural bulkhead, one frame and one keel-loaded floor

We start by acquiring material properties from Fig 14.2, or if we have an idea of the lay-up from Figs 13.20 and 13.21. The lay-up we are going to use consists of 50% CSM and 50% WR with a fibre content of 40%, so we can calculate our material properties.

From Figs 14.5, 14.6 and 14.7 we get our design loads and panel dimensions, from Figs 14.8 and 14.9 the reduction factors, and from Fig 14.10 the equations to calculate the single-skin thickness. The reason for calculating the single-skin requirement is to establish the skin thickness that allows us to calculate the effective width of plating in conjunction with stiffeners, Figs 14.7 and 14.13. Working through the formulae of Fig 14.17 we can calculate the sandwich requirements, and from Fig 14.18 the dimensions.

The deck panels and structural bulkheads follow the same calculations with the loads acquired from Fig 14.7.

For dimensioning of the internals we start with Fig 14.6 to get the dimensions and design heads of the internals. Fig 14.14 gives the equations to calculate the requirements, and by using the graph in Fig 12.11 we can determine the actual dimensions to fulfil the section modulus requirements. To calculate the required moment of inertia, we must start with a trial section and calculate it according to the simplified method described in Fig 12.5.

As can be seen from the results, the equivalent single-skin laminate will be 13.2 mm thick weighing 20.5 kg/m<sup>2</sup> compared to the sandwich's 9.5 kg/m<sup>2</sup>. At the same time the stiffening system is not as dense, which is also illustrated in Fig 12.16, which contributes to a lighter structure. The skins of the sandwich are 2.5 mm thick, and this might be regarded

LAMINATE : 50% CSM + 50% WR ;  $W_f = 39\%$  Values from Fig 13.4 & 13.5

$$\begin{aligned} \sigma_{ut} &= (120 + 190) / 2 = 155 \text{ N/mm}^2 & \sigma_o &= 77.5 \text{ N/mm}^2 \\ E_T &= (10300 + 13200) / 2 = 11750 \text{ N/mm}^2 \\ \sigma_{uc} &= (195 + 113) / 2 = 154 \text{ N/mm}^2 & \sigma_o &= 77.0 \text{ N/mm}^2 \\ E_C &= (9300 + 12500) / 2 = 10500 \text{ N/mm}^2 \\ \sigma_{uf} &= (215 + 253) / 2 = 234 \text{ N/mm}^2 & \sigma_o &= 117 \text{ N/mm}^2 \\ E_F &= (6800 + 12400) / 2 = 9600 \text{ N/mm}^2 \end{aligned}$$

PANEL #1<sub>A</sub> from Fig 14.5

$$P_f = 24.1 \text{ kPa} ; l = 2000 \text{ mm} ; s = 1200 \text{ mm} ; A = 180 \text{ mm}$$

Reduction factors from Fig 14.9

$$k_{ar} = 0.267 < 0.4 \text{ (min)}$$

Reduction factors from Fig 14.12

$$k_1 = 0.025 ; k_2 = 0.485 ; k_3 = 0.026$$

Single skin calculation according to Fig 14.10

Curve correction,  $k_c = 0.80$

$$a) t = 1200 \cdot 0.800 \cdot \sqrt{\frac{24.1 \cdot 0.485}{1000 \cdot 234 \cdot 0.5}} = 9.6 \text{ mm}$$

$$b) t = 1200 \cdot 0.800 \cdot \sqrt[3]{\frac{24.1 \cdot 0.0259}{1000 \cdot 0.025 \cdot 9600}} = 13.2 \text{ mm}$$

Trial sandwich panel : Equal skins with  $t_f = 2.5 \text{ mm}$  and  $t_c = 15 \text{ mm}$

Minimum outer skin thickness = 2.44 mm, equation 29)

Minimum inner skin thickness = 1.74 mm, equation 30)

Sandwich panel requirements according to Fig 14.17

Actual panel section modulus, Fig 14.18 and moment of Inertia (calculated)

$$a) SM_i = \frac{1200^2 \cdot 0.8^2 \cdot 24.1 \cdot 0.485}{600000 \cdot 154 \cdot 0.5} = 0.234 \text{ cm}^3$$

$$a) SM_i = 0.35 \text{ cm}^3/\text{cm} \text{ OK !}$$

$$b) SM_o = \frac{1200^2 \cdot 0.8^2 \cdot 24.1 \cdot 0.485}{600000 \cdot 155 \cdot 0.5} = 0.232 \text{ cm}^3$$

$$b) SM_o = 0.35 \text{ cm}^3/\text{cm} \text{ OK !}$$

$$c) I = \frac{1200^3 \cdot 0.8^3 \cdot 24.1 \cdot 0.026}{12000000 \cdot 11125 \cdot 0.0167} = 0.249 \text{ cm}^4$$

$$c) I = 0.39 \text{ cm}^4/\text{cm} \text{ OK !}$$

$$E_{TC} = (11750 + 10500) / 2 = 11125 \text{ N/mm}^2$$

All requirements are exceeded with the panel suggested.

The skin buckling stress,  $\sigma_c = 243 \text{ N/mm}^2 > 2 \cdot \sigma_{oi}$  and  $2 \cdot \sigma_{oo} \text{ N/mm}^2$

The shear strength requirement for the core is calculated from the equation 27) and using aspect ratio factor  $\nu$  in Fig 14.17

$$\nu = 0.492$$

$$\tau_u = \frac{2 \cdot 0.492 \cdot 0.001 \cdot 24.1 \cdot 1200}{(20 + 15) \cdot 0.5} = 1.42 \text{ N/mm}^2$$

The requirement gives a PVC-core of  $100 \text{ kg/m}^3$  according to Figs 13.19 or 14.19 with a total panel thickness of 20 mm and a core of 15 mm.

The trial panel is satisfactory if 20 mm thick, shear strength of core is dimensioning.

Fig 14 20 Calculation of the hull panel for YD-40

**Watertight BULKHEAD #2 from Figs 14.5 and 14.6**

$h = 8.1 \text{ kPa}; l = 2450 \text{ mm}; s = 1800 \text{ mm}$

Reduction factors from Fig 14.12

$k_1 = 0.0167; k_2 = 0.272; k_3 = 0.022$

Trial sandwich panel : Equal skins with  $t_f = 1.5 \text{ mm}$  and  $t_c = 20 \text{ mm}$

Sandwich panel requirements according to Fig 14.17

$$a) SM_i = \frac{1800^2 \cdot 8.1 \cdot 0.272}{600000 \cdot 154 \cdot 0.5} = 0.17 \text{ cm}^3$$

$$b) SM_o = \frac{1800^2 \cdot 8.1 \cdot 0.272}{600000 \cdot 155 \cdot 0.5} = 0.17 \text{ cm}^3$$

$$c) I = \frac{1800^3 \cdot 8.1 \cdot 0.022}{12000000 \cdot 11125 \cdot 0.0167} = 0.47 \text{ cm}^4$$

$$E_{TC} = (11750 + 10500)/2 = 11125 \text{ kg/mm}^2$$

All criteria are fulfilled with the panel suggested.

Actual panel section modulus, Fig 14.18 and moment of Inertia (calculated)

$$a) SM_i = 0.40 \text{ cm}^3/\text{cm} \text{ OK !}$$

$$b) SM_o = 0.40 \text{ cm}^3/\text{cm} \text{ OK !}$$

$$c) I = 0.49 \text{ cm}^4/\text{cm} \text{ OK !}$$

The shear strength requirement for the core is calculated from the last equation 27), using aspect ratio factor  $V$  in Fig 14.17

$$V = 0.476$$

$$\tau_u = \frac{2 \cdot 0.476 \cdot 0.001 \cdot 8.1 \cdot 1800}{(24 + 20) \cdot 0.50} = 0.63 \text{ N/mm}^2$$

The requirement gives a PVC-core of  $60 \text{ kg/m}^3$  according to Fig 13.19 with a total panel thickness of 24 mm and a core of 20 mm.

Fig 14.21 Calculation of sandwich bulkhead for YD-40

as a practical minimum thickness for the boat not to be too sensitive to impact forces and crowded docking manoeuvres. To increase impact resistance we can make the outer skin slightly thicker than the inner. If we keep the ratio of inner skin thickness to outer skin thickness to be at least 0.75, and keep the total skin thickness to 5 mm, we reach 2.8 mm for the outer and 2.2 mm for the inner skin. Of course we can use better fibres, S-glass, Kevlar, carbon, etc, and then it is possible to get enough strength and stiffness with thinner skins and lower weights, which is satisfactory, and indeed desirable, if the design is meant for high-level racing, but it is not necessarily true from a practical point of view for a cruiser or cruiser/racer.

**INTERNAL #1 from Fig 14.6 ( side stringer )**

$$P_r = 10.14 \text{ kPa}; l = 2.0 \text{ m}; s = 1.02 \text{ m}; \sigma_a = 77.5 \text{ N/mm}^2$$

Stiffener requirements  
according to Fig 14.14

$$SM = \frac{83.33 \cdot 10.14 \cdot 1.02 \cdot 2^2}{77.5} = 44.5 \text{ cm}^3$$

$$I = \frac{26040 \cdot 10.14 \cdot 1.02 \cdot 2^3}{10000} = 215 \text{ cm}^4$$

Dimensions from Fig 12.11 for SM-req.  
and moment of inertia (calculated)

$$H = 70 \text{ mm}; t_s = 10 \text{ mm}; B = 50 \text{ mm}$$

$$I = 459 \text{ cm}^4 \quad \text{OK!}$$

Dimensions according to Fig 14.13 :  $W = 264 \text{ mm}; t = 11.9 \text{ mm}$   
 $F = 50 \text{ mm}; h = 55 \text{ mm}; t_1 = 5 \text{ mm}; C = 50 \text{ mm}; t_2 = 10 \text{ mm}$

**INTERNAL #2 from Fig 14.6 ( 1 of 3 keel bearing floors )**

$$P = 14.61 \text{ kPa}; l = 1.4 \text{ m}; s = 0.6 \text{ m}; \sigma_a = 77.5 \text{ N/mm}^2; N = 1$$

Stiffener requirements  
according to Fig 14.14

$$SM = \frac{183 \cdot 14.61 \cdot 0.6 \cdot 1.4^2}{77.5} = 40.7 \text{ cm}^3$$

$$SM_k = \frac{9.8 \cdot 3250 \cdot 0.6}{3 \cdot 77.5} = 82.3 \text{ cm}^3 + SM = 123 \text{ cm}^3 \text{ ( SM-req )}$$

Increase of  $I$  in way of ballast keel :  $( 0.5 \cdot 82.3 + 40.7 ) / 40.7 = 2.01$  ;  $( N = 0.5 )$

$$I = \frac{57290 \cdot 14.61 \cdot 0.6 \cdot 1.4^3}{11125} \cdot 2.01 = 249 \text{ cm}^4$$

Dimensions from Fig 12.11 for SM-req.  
and moment of inertia (calculated)

$$H = 140 \text{ mm}; t = 10 \text{ mm}; B = 50 \text{ mm}$$

$$I = 2250 \text{ cm}^4 \quad \text{OK!}$$

Dimensions according to Fig 14.13 :  $W = 275 \text{ mm}; t = 12.5 \text{ mm}$   
 $F = 50 \text{ mm}; h = 122 \text{ mm}; t_1 = 5 \text{ mm}; C = 50 \text{ mm}; t_2 = 10 \text{ mm}$

Fig 14.22 Calculation of internals for YD-40



# 15

# LAYOUT

---

The term 'layout' covers a wide area, and in this chapter we will discuss accommodation, cockpit, deck, instruments, hatches, ventilation and safety equipment. These different matters will be dealt with in general terms, but we will use the solutions used in YD-40 to show one way of meeting the demands.

## Generic space requirements

Before using the boat there are some general requirements that must be met, in order to make the vessel practical and comfortable to sail and live aboard. Fig 15.1 shows some important dimensions concerning the space required for a man standing, sitting and lying. The 'module-man' we are using is 1.8 m tall. Optimizing for a bigger or smaller person is done by interpolating the values according to size.

When standing up (Fig 15.1(A)), the reach forward measurement is meant to show the practical maximum to reach controls when movement forward is restricted. The eye height shown is just that; in order to see over an obstruction (the deckhouse for example), this height has to be decreased by at least 100 mm. The seat/wheel gap in the figure is the minimum comfortable; a greater distance makes it more comfortable to stand but on the other hand more difficult to reach the wheel when sitting down.

The seat height and depth shown in (B) is for a rather upright seating position, for instance when eating or sitting by a navigation table. For a more relaxed sitting the depth can be increased by 80 mm but at the same time the height is reduced by the same amount, to keep the sum of height and depth to 900 mm which produces a comfortable sitting geometry. The angle of the backrest can vary between 5° and 15° from vertical.

Fig 15.1(C) shows the width requirements when sitting down. It is worth noting that when the seat is beside a bulkhead the width required is greater than when it is free-standing.

The picture in Fig 15.1(D) shows the minimum measurements for a comfortable seagoing berth. The narrowing of the ends are not necessary but this often happens due to the form of the hull. If the berth is a dedicated sea berth these measurements are adequate, but if the berth is also to be used in harbour it might feel a bit cramped. Widening it by 100 mm will remedy this and doubling it will produce a usable double berth for harbour use, with a width of 1300 mm. If the double berth is free-standing with the sides not 'walled in' the width should be increased to 1400 mm minimum. A standard length of a berth is 2000 mm, but to tailor a berth for a specific body length, you need to add at least 50 mm to this body length at each end.

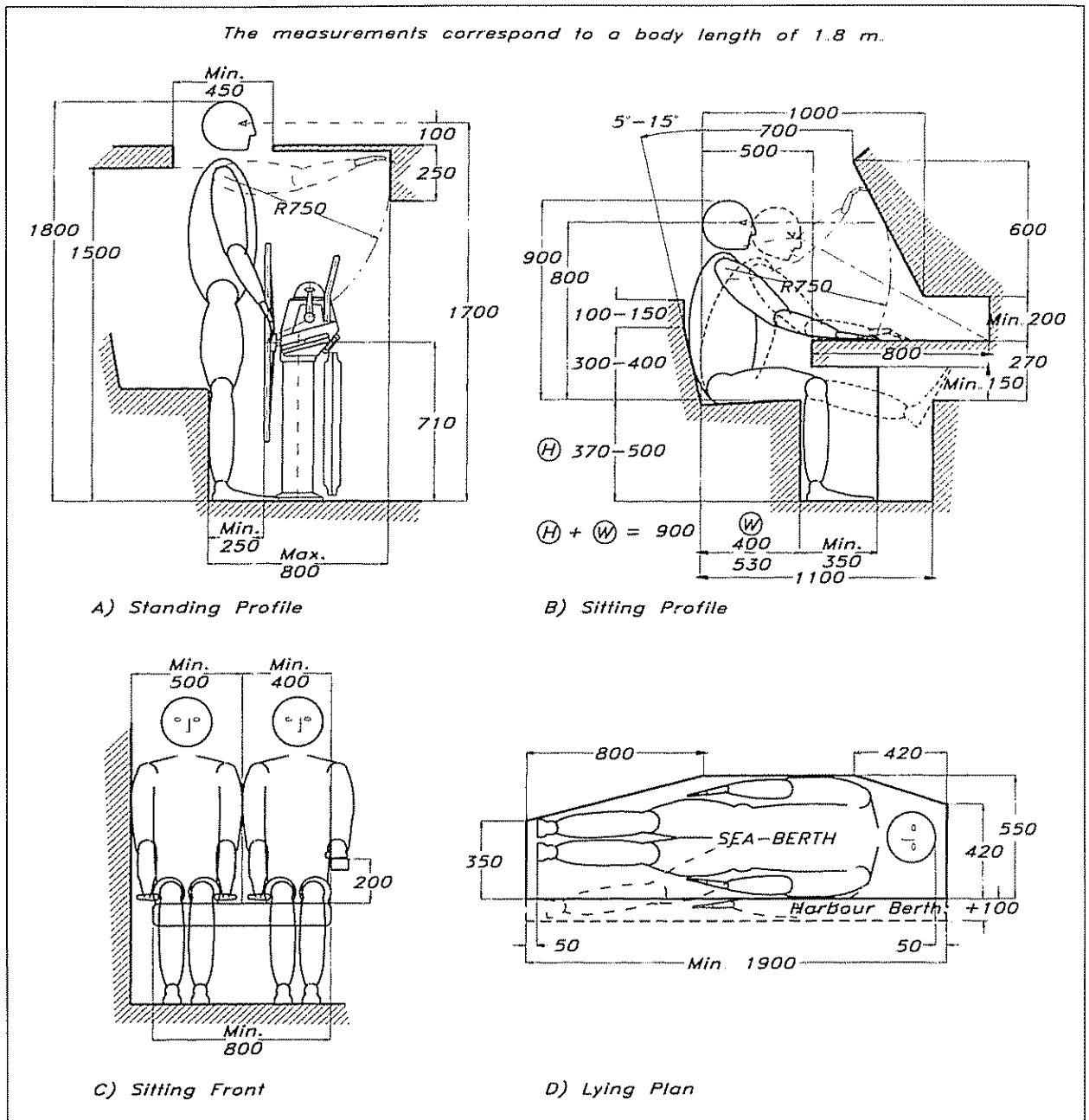


Fig 15.1 The human figure

**Accommodation**

Looking at the YD-40's accommodation (Fig 15.2), there are some general features to consider. Basically the layout follows the principle that the activity areas are situated near the centre of motion of the boat, so that they can be used when under way. The lounging and sleeping areas, as well as stowage areas, are grouped forward and aft. As we have discussed previously, the aim with this design is to produce a comfortable offshore yacht for four persons, so we do not have to fill the boat to its extreme ends with bunks and accommodation. The numbers below (1-13) refer to the circled numbers in Fig 15.2.

- 1 Looking in more detail we start with the forepeak. This part is entirely given to deck stowage for items like extra sails, fenders, lines etc. By burying the headsail furler here we get a clear foredeck with the genoa tack low down. Since this space has nothing to do with the rest of the accommodation the bulkhead to the forward cabin can easily be made watertight.
- 2 Another advantage of not pushing the accommodation too far forward is the position of the anchor windlass and chainlocker. They can be placed comparatively far back so as not to hamper the rough weather performance. Such heavy items placed far from the pitching centre play quite an important role in forming the gyradius of the boat.
- 3 This far back we are in the forward cabin. This is laid out as a cabin for harbour use, and that is why the double berth is placed here, a berth type that cannot easily be converted to a comfortable sea-berth. To achieve an acceptable width the berth is raised, and since this is too high to sit on, a separate seat is included. To make a cabin like this habitable, there is a hanging locker, a dresser and a general stowage space for personal belongings, so they do not have to occupy the more public areas.
- 4 Moving further aft to the saloon there are some other points to consider. There must at least be enough space around the table that all people who can sleep on the boat can also eat onboard. This is no problem for the YD-40, but on boats with an exceptionally large number of berths it might be. The saloon settees must be long enough (in our case) to sleep on, since the forward double berth is unusable at sea. This dual function means that the backrests must fold up in order to have the berths wide enough to sleep on, while retaining a proper sitting depth while folded down. On a boat with a shallow hull like this one it might be a problem to locate water tanks big enough, so here we use the space under the settees for tankage.
- 5 Thanks to the offset opening of the door to the forward cabin, the L-settee on the port side is deep enough to contain a big fixed table, while leaving a wide passageway to starboard. Making the table fixed also allows us to install a proper locker underneath with a door, instead of the more usual small opening top. For big-scale dining there is a drop-leaf on the starboard side of the table, so it is possible to use the starboard settee as well.
- 6 Especially in boats under about 10 m (33 ft) it is often hard to fit in a full-size chart table and seat. Big charts may be 1300 x 800 mm when opened out, so the table top should ideally be this size. In the YD-40 this is possible by aligning the table along the hull side. If this is not possible we should at least strive for an area of 800 x 650 mm, ie a big chart folded once. For the navigator to be able to brace himself when the boat heels over 30° the seat must have a sturdy backrest (when aligned the way it is in the YD-40), or have a concave sitting area (when aligned athwartships). Fig 15.3 shows clearly what it is like when sailing at a heel angle. Another thing to bear in mind when designing the interior is the narrowing of the boat the further down you get, and the effect of thickness of hull and other items. The circled area in Fig 15.3 shows just this. It is not sufficient just to deduct the sole width according to the relevant waterline on the lines plan without further deducting the hull and sole thickness. In this case they amount to a further deduction of 80 mm compared to the hull waterline.  
Further demands on a good navigation station require it to contain plenty of stowage space as well as bulkhead areas for books and electronic

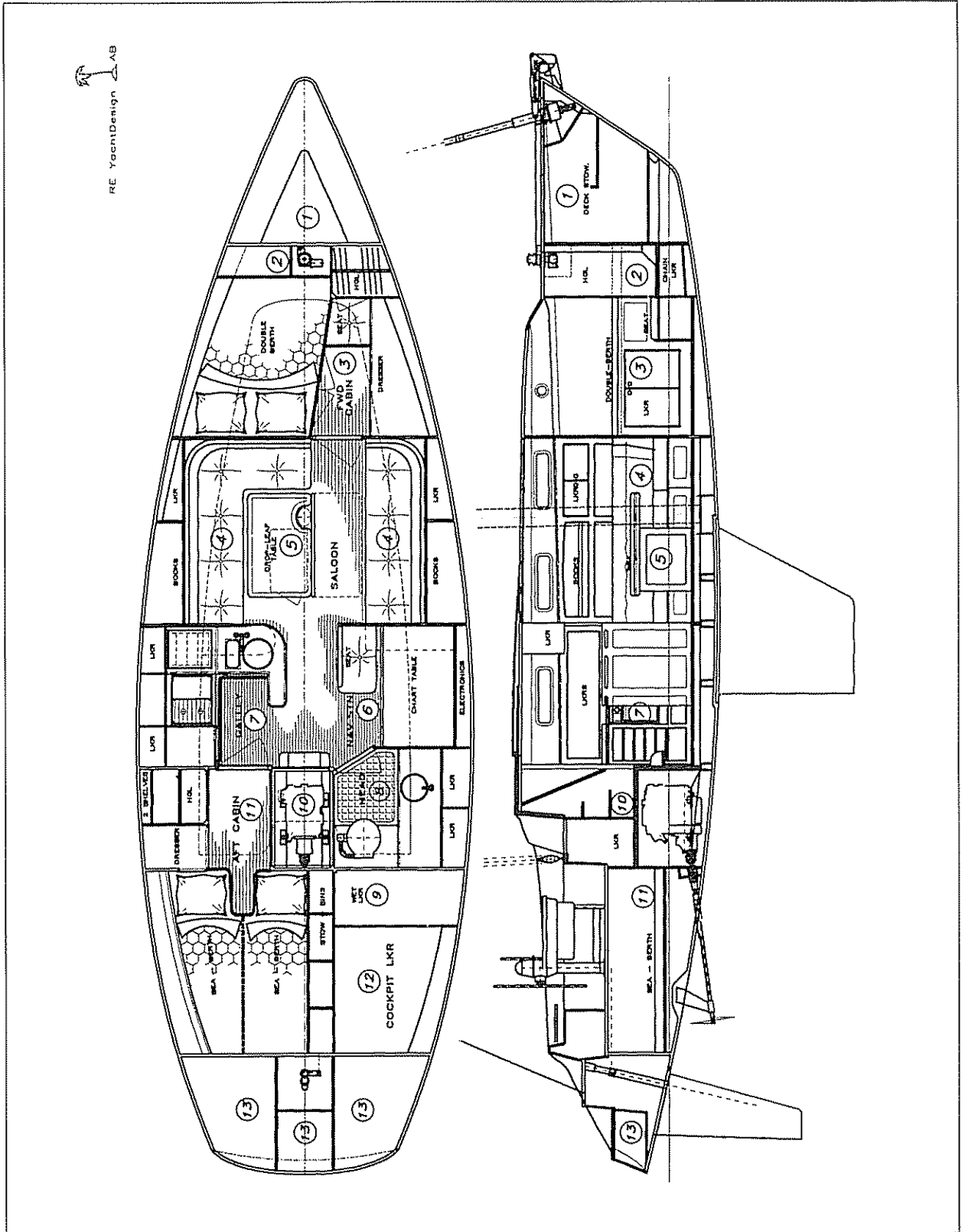


Fig 15 2 Accommodation layout – YD-40

instruments. A stowage bin under the working area is a good place to keep the charts flat, and by making it 50 mm deep it is possible to stow up to 200 charts unfolded, or, if the area is not enough, 100 charts folded once can be stowed per 50 mm depth. The best place for an overhead bookshelf is on an athwartship's bulkhead, so the books in it can be handled on either tack without falling out when removing the retaining fiddle.

Space requirements for electronic instruments will vary depending on owner preferences and the intended use of the boat. The single most important instrument that any boat should have is the compass. The primary one should not be electronic, but independent of the boat's electrical system, and it should be placed up in the cockpit to steer by. Instruments in the navigation area can be divided into three groups:

- (a) *Navigation* instruments (compass, speed and distance meters, depth sounder, Loran-C or Decca receiver, satellite navigator, chart plotter and radar).
- (b) *Weather and communications* instruments (barometer, wind speed and direction, air and water temperature, multiple band radio receiver, weather fax, VHF and other radio transmitters).
- (c) *Boat performance* instruments (with the raw data gathered from instruments in (a) and (b), added to data such as heel angle, course and speed over ground from a satellite navigator, the processing unit in the boat-performance instrument package can calculate VMG, leeway, direction and strength of current, time and distance to the next mark or waypoint, and calculate polar curves for the boat in actual conditions).

Most of these instruments are quite small and can generally be surface-mounted. Since many of them need input from the operator they must be placed within easy reach of the navigator. Radars and high resolution chart plotters are bulky, since the screens they use are quite deep, heavy and hungry for electrical power. Flat screens are now coming on the market (1994), but their resolution remains on the low side; for chart plotters the image should be in colour so that they are more readable and on a par with paper charts.

- 7 Galleys in the past could be placed almost anywhere in the boat, forward, along one side of the saloon, or aft. Today, the common location for galleys is next to the aft companionway, and there are good reasons for this. This is the area where the violent pitching motions are smallest, the cook is not isolated from the rest of the crew, the ventilation through the companionway hatch is good and food may be passed to the cockpit easily.

In the YD-40 the galley is placed to port of the companionway, and thanks to the size of the boat it is sufficiently off-centre not to place the cook in the general traffic between the cockpit and saloon. The planform is J-shaped, with the 'hook' of the J forming a bracing for the cook when the boat heels. As we can see from Fig 15.3 it is important that the distance from this 'bracing-hook' to the stove be great enough to allow the cook to take up the boat's heel angle. The heel angle shown is 30° which is certainly greater than the normal sailing angle, but temporarily, in squalls for example, it is not an exceptionally large angle. Another way of keeping the cook in place is by using a restraining belt. The disadvantage with this method is that the cook is strapped in and cannot escape if an accident, such as a boiling pot falling over, occurs.

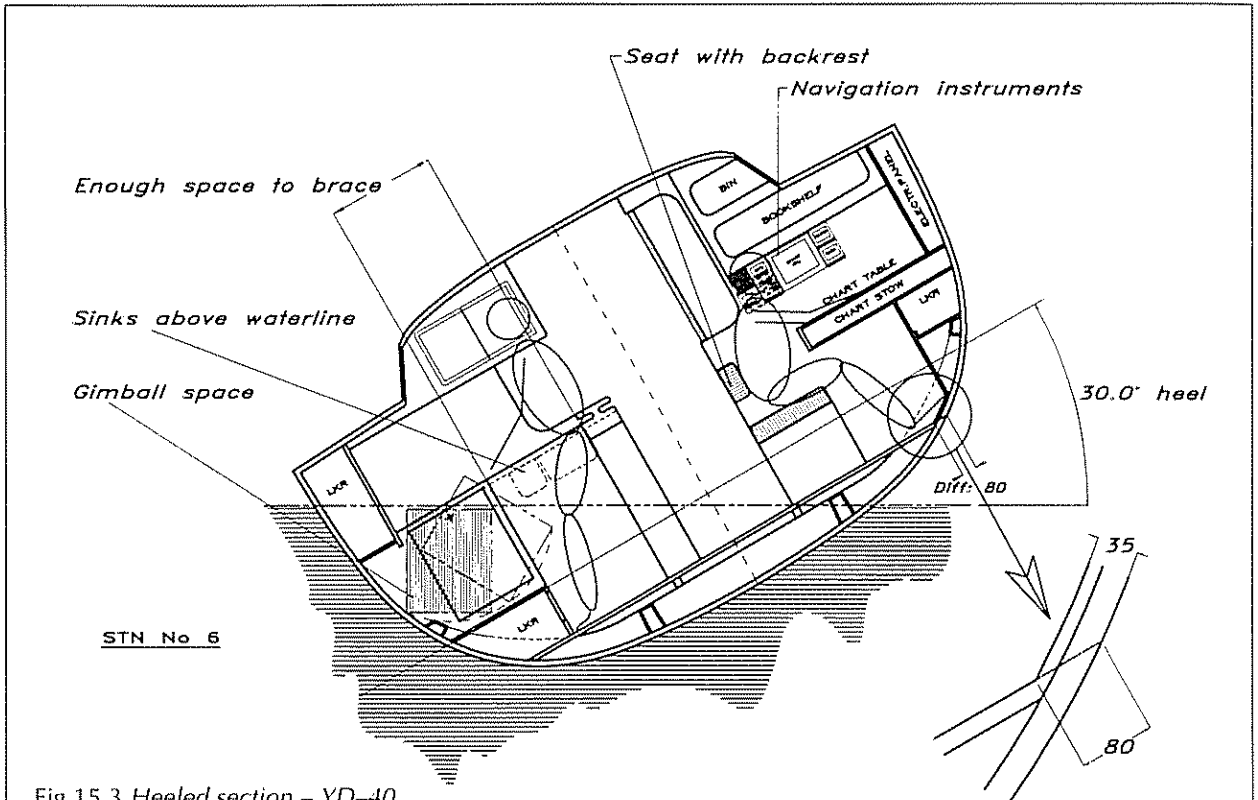


Fig 15.3 Heeled section – YD-40

As an added safety factor a crashbar should be set across the stove front to keep the cook from accidentally falling on to the burners. Another vital feature to bear in mind when designing the galley is to make sure that there is enough space behind and in front of the stove to gimbal freely over approximately  $60^\circ$ .

There are many stoves on the market, but generally the following features are desirable:

- Stainless steel construction
- Removable top gratings, for easy cleaning
- A high fiddle rail around the burners with pot-holders, to keep pots from falling over
- Sturdy gimbals positioned for good dynamic balance when the boat is rolling
- An oven

- A lock on the oven door, to keep things inside it in rough weather.

Several stove fuels are available:

- (a) *Alcohol* has the coolest flame and therefore cooks the slowest. It is fairly safe, with no risk of explosion, and a fire can be put out with water. It has a tendency to smell sometimes to the point that crew members may be sick.
- (b) *Kerosene* has the hottest flame. It was once the most common stove fuel, but it is becoming increasingly more difficult to obtain, and is getting more expensive as well. It requires a vaporizing priming procedure to be lit, and tends to smell bad.

(c) *LPG* (liquefied petroleum gas) is the second hottest in flame heat. It is stored in liquid form and automatically vaporizes as it is released, so it can be lit just like household gas. The big drawback with *LPG* is that it is heavier than air, and mixed with air it forms an explosive mix. If it escaped inside the hull and settled in the bilge this could be highly dangerous. Therefore, it must be stored and handled with care:

- Stow *LPG* bottles in separate airtight compartments that drain overboard.
- Install a cut-off valve that is situated in the galley, and preferably an electric solenoid valve in the bottle stowage compartment, also operable from the galley.
- Install a leak-warning system in case of leakage into the bilges.
- Install a stove with a flame-out safety shut-off in the oven as well as on the top burners.

(d) *CNG* (compressed natural gas), unlike *LPG*, is lighter than air. Therefore, if it leaks, it will rise and can be ventilated away. It is not as widely available as *LPG*, however, and it is more expensive.

The sink must be deep enough not to spill even with a half-load of dishwater, which means a depth of at least 180 mm. Having two sinks is a good idea, one for washing dishes and the other for rinsing and emptying cooking water etc. By making the bigger sink round we make the most of the volume, ie we use a smaller amount of water to fill the sink up to a given level. As can be seen from Fig 15.3, the sinks in the YD-40 are placed high enough and sufficiently inboard to allow them to drain when the boat is heeled over.

Some sort of refrigeration is essential, because ice is increasingly expensive

and difficult to find (not to mention the awkward handling). Even small boats carry refrigeration in the form of insulated boxes cooled at home, and plugged into the boat's 12-volt system. On bigger boats like the YD-40, however, we need a permanent refrigeration system. To start with we need an efficient box or cabinet to hold the refrigerator. By far the most important component is the insulation. There must be at least 100 mm of insulation all round the compartment. A very good insulating material is polyurethane or PVC-foam. The door to the refrigerator can be either side or top-opening, with the latter considered to be more thermally efficient (since cold air does not pour out when opening the box). However, you often need items from the bottom of the box and to reach them you have to rearrange some food on the box top, where it will be warmed up during the search process. A way around this problem is to make the top opening as big as the box itself, and equip the box with 'modular inserts', stacked beside each other, containing food sorted by type, meal rations or any other system that is suitable, so that the entire contents of the box do not have to be disturbed when looking for a specific item.

Finally, there should be adequate counter space with high sturdy fiddles, with work areas on both sides of the stove. Having the stove directly against a bulkhead is not a good idea, since it is an uncomfortable place to stand in, and the process of preparing a meal benefits from having an area each side of the stove.

- 8 Like the galley, the head area traditionally has been placed almost anywhere in the vessel. Today just two areas are preferred: between the saloon and forward cabin, or (as in the case of the YD-40) close to the companionway. The advantage of the latter position is the same as for the

galley: the motion of the boat is least felt here, so the head can be used underway in rough weather. As can be seen the WC is aligned fore-and-aft. This is the proper orientation for use at sea regardless of heel direction, provided the distance between the surrounding counter and bulkhead is not less than 650 mm and not greater than 750 mm. Anything smaller will render the WC useless, and if made greater the ability to offer good bracing is reduced.

One disadvantage of placing the WC this way is that the wash-basin is forced outboard, and will not self-drain on a port tack in fresh weather. Two solutions are given: either we install a holding tank, or pump out the waste water via a loop that goes up under the sidedeck.

The free area in front of the wash basin and WC should be approximately 700 x 700 mm to be useful as a washing and showering area. It is not necessary, though, that the sole be completely flat: the hull might still show, especially if the head is placed aft in the boat since the hull lines are rather shallow in this area.

Having the head situated between the saloon and forepeak does prevent it from being used comfortably in a seaway, but since it is possible to use the full width of the boat here, it might be the only place to locate it in order to get enough elbow space, especially in smaller yachts. It also puts the saloon further back in the boat, where space is greater.

- 9 Foul weather gear is troublesome to stow. Not only is it bulky but also dampened by salt water. Therefore it is essential to have a separate wet gear locker. In the YD-40 it is situated directly aft of the head, so this compartment is used to take the wet gear without wetting the rest of the interior. There is also a hatch on top of the locker leading directly to the cockpit so that people do not have to come down to get their foul

weather suits. To make it possible to dry clothes stored here, there is a hot air outlet from the heating system into this locker.

- 10 A 'landing platform' is formed by the top of the engine compartment, situated just two steps down from the cockpit. Enclosed by the longitudinal bulkheads to the head and aft cabin this gives a very secure companionway entrance. The locker behind the step is very useful for stowage of boots, tools, flares etc.

- 11 It is a good idea to place the sea-going berths in the aft part of the boat, as there is less motion here compared to the forward part. In smaller boats where it is impossible to fit a proper aft cabin there is usually room for a quarter-berth at least. In the YD-40 we have a proper cabin containing sufficient stowage and hanging locker space for two persons. There are some features in the berth area worth considering. To begin with, there is a notch in the head of the berth, because this makes entering and leaving the berth easier, especially when two people are using it. To be suitable as a double sea-berth, there is a solid, fold-up dividing bunk board, stowed under the cushion when not in use. Lee cloths are good, but only when used on single berths. To separate effectively two sleepers in a double-berth we need a substantial divider. At the centreline along the berth there is a row of stow bins. It would have been possible to extend the berth into this area, but by not doing so the berth is not completely under the cockpit sole, where a claustrophobic feeling might have been experienced. At the same time we gain some stowage bins, of which there can never be too many.

- 12 Extra sails, lines, fenders, fuel and water jerrycans, inflatable, outboard engine, cleaning compounds, lubricants etc. are just a few things that most cruisers carry, in



addition to the personal gear and food for the crew. This type of accessory does not belong in the accommodation, but should be placed in a cockpit stowage space. On the YD-40 it is situated under the starboard cockpit seat. This is quite large, but in real life it should be subdivided with fiddles and dividers so as not to become a giant gear-mixer when the going gets rough.

**13** The aftermost part of the boat (the lazarette) contains the steering mechanism, stowage for the liferaft, LPG bottles and lighter items such as fenders. The compartment just aft of the steering quadrant on the YD-40 contains a folding boarding ladder, integrated with the transom platform, and by being at this low level it is possible to reach it from the water.

### Deck layout

To design a deck layout that suits all types of boats and people is impossible. Like the accommodation, the intended use of the yacht has a profound influence on the layout. On a cruising boat the priorities are different compared to those of a racer. The racing deck is a working platform that has to perform efficiently for a well-defined crew with specific tasks. In contrast, the cruiser's deck must work with a smaller crew, offer space to sunbathe, protection from bad weather, and at the same time not be in conflict with the interior arrangement. On top of this we must not forget the performance side of it. The YD-40 is intended to be a performance-oriented cruiser, and looking at the deck more closely we can see what compromises are made in comparison to a pure racer. The numbers below (14-33) refer to the circled numbers in Fig 15.4.

**14** Originally, forward-raking sterns like this one were developed on racing yachts to minimize deck weight, or to reduce the rated length under the IOR rule. It is interesting to note that on yachts designed to race under the IMS system (which does not measure the length in the same way as IOR), the transoms do not rake forward as heavily, since cockpit space can be gained this way.

On a cruiser we can take advantage of the forward-raking type of stern by recessing a transom platform into it. This creates a good deck to board the yacht from a dinghy or floating dock. It also makes it easier to recover a person who has fallen overboard, eases stern anchor handling and makes a nice showering and towelling area after a bath.

**15** The cockpit itself must be long enough to lie down in, even under way. This can be achieved even in quite small boats if considered in the early design stages. It might not be possible to have a long enough cockpit together with a heavily raked transom on a small yacht, and in this case the cockpit length should be given priority. On a racer it is not the lying-down requirement that dictates the length, but rather the number of crew that shall be working in the cockpit, and the layout of the sail handling gear. On the YD-40 the benches are over 2 m long, and on the starboard side the bench contains hatches to the cockpit stowage space and the wet locker.

**16** Generally speaking a steering wheel

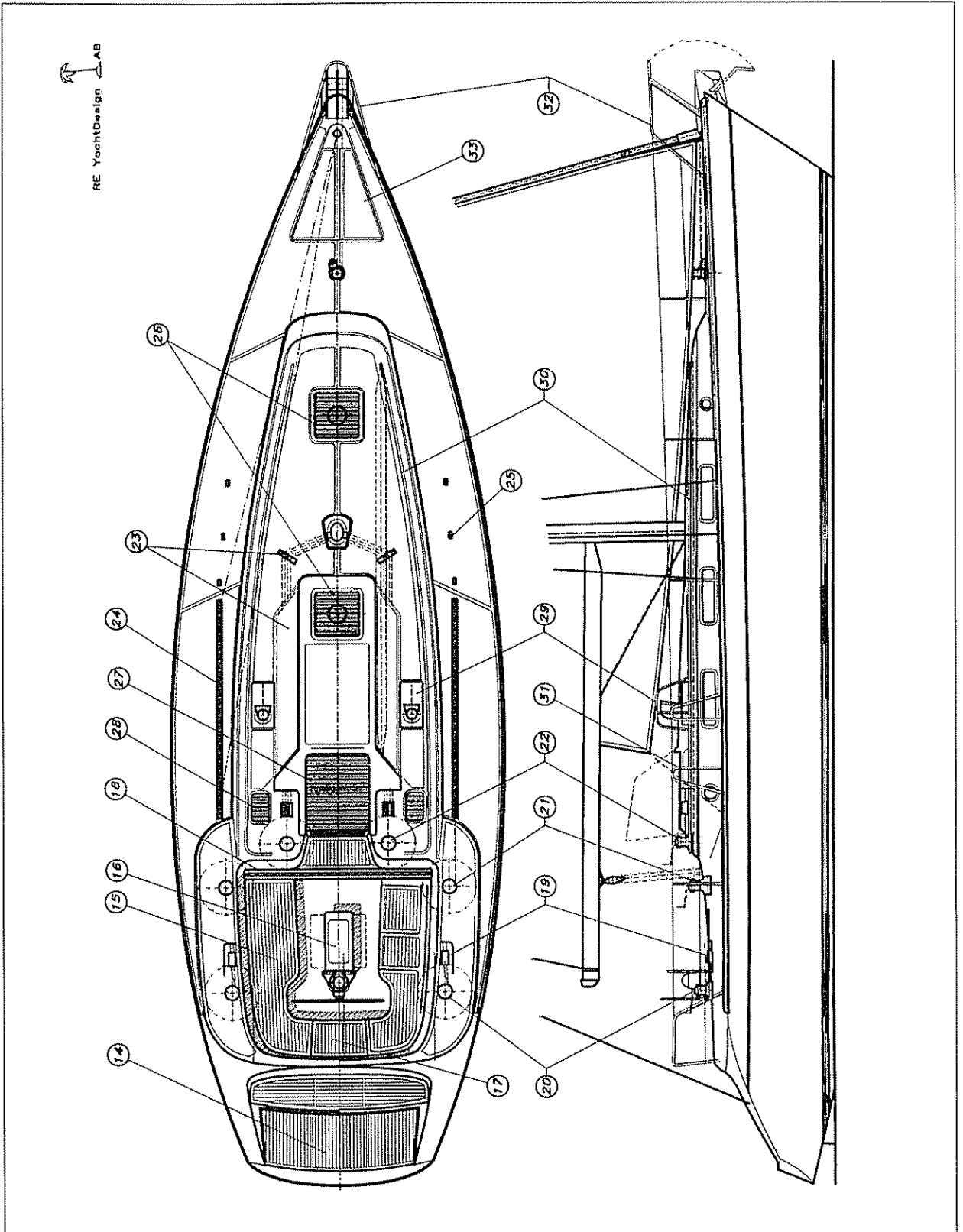


Fig 15.4 Deck layout – YD-40

takes up less space when under way than a tiller, but the opposite is true when at anchor. The feel of the boat is better with a tiller, and course adjustments can be made more quickly, which is especially important broad reaching in heavy weather, when broaching is most likely to happen. The disadvantage with a tiller is most obvious on a larger yacht. As we have shown in Chapter 12, in the discussion of rudder forces, the tiller length has to be almost 2 m to equal the wheel-steering power on the YD-40. This makes it highly impractical on this cockpit design. To achieve a quick enough rudder action the number of turns from hard over port to hard over starboard should not exceed two on a performance-oriented boat, while on a heavy slow-reacting cruiser the number of turns may be allowed to reach three.

On a cockpit as wide as that of the YD-40, it is impossible to brace oneself against the opposite cockpit seat when the boat heels. Therefore the steering pedestal is extended forward to contain a cockpit table with a stowage space and a foot rest.

**17** To give the helmsman a chance to remain behind the wheel, an arched helmsman's seat should be fitted. For the same reason the cockpit sole each side of the wheel should be angled approximately 20°. On the YD-40 the helmsman's seat is removable, and there is a door in the aft cockpit coaming to enhance the accessibility of the transom platform.

**18** Mainsheet handling systems often collide with other cockpit requirements on cruisers. Therefore, it is becoming common to employ a mid-boom sheeting system for the main, with the sheet coming to a winch on the coachroof. In

this way there will be virtually no lines in the cockpit. The disadvantage of the system is that the sheet loads will be much greater compared to an end-boom sheeting system, and the position of the mainsheet winch will be out of reach of the helmsman.

**19 and 20** The system we have used consists of a mainsheet track recessed into the aft edge of the bridgedeck, with the sheet and traveller control lines led into the coamings and aft via sunken rope clutches to winches which can be reached by the helmsman. The sheet is double-ended so that it can be operated from either side of the boat. The coamings are wide, and angled to be comfortable to sit on when the boat heels.

**21** The primary winches are situated well forward in the cockpit, to give a free coaming area as large as possible. The sizing of winches can be taken from most winch manufacturers' catalogues. Fig 15.5 gives another way of determining the sheet loads from the main and foresails. The genoa winches for the YD-40 should be at least of size 52, but preferably size 54. The mainsheet winch working through a tackle of 3:1 ratio should be of size 24.

**22** On a cruising boat it is desirable to have the sail control lines (such as reefing lines, outhauls, halyards and kicking strap) which lead to the cockpit. For this reason the utility winches are placed either side of the companionway hatch, where they are easily reached from the cockpit. This tight grouping of winches is not necessarily the best on a racing boat, where different crew members might get in each other's way when operating the boat.

Foresail sheet load ( $F_F$ ):

$$F_F = 3.45 \cdot V^2 \cdot A_F \quad [ 3.45 \cdot 10^2 \cdot 53.5 = 18458 \text{ N} ]$$

Main sheet load ( $F_M$ ):

$$F_M = 3.45 \cdot \frac{E \cdot P^2 \cdot V^2}{L_L \cdot T_R} \quad [ 3.45 \cdot \frac{4.70 \cdot 15.1^2 \cdot 10^2}{15.65 \cdot 3} = 7875 \text{ N} ]$$

$F_F$  = Foresail sheet load [N]  
 $F_M$  = Mainsail sheet load [N]  
 $V$  = Windspeed [m/s]  
 $A_F$  = Foresail area [m<sup>2</sup>]  
 $E$  = Mainsail foot [m]  
 $P$  = Mainsail luff [m]  
 $L_L$  = Mainsail leech [m]  
 $T_R$  = Mainsail tackle ratio

Winch power ratio ( $P_W$ ):

$$P_W = \frac{F_F}{F_C} \text{ or } \frac{F_M}{F_C} \quad [ \frac{18458}{350} = 52.7 \quad \frac{7875}{350} = 22.5 ]$$

$F_C$  = Crew power on handle, 200 – 500 [N]

Fig 15.5 Calculation of winch size (Marshall)

- 23 Leading sail control lines to the cockpit via turning blocks on the coachroof, puts the roof under tension and exerts lifting pressure. Therefore, it is important to install tie rods between deck and hull in the mast area. Line organizers are used to direct the different lines to the cockpit. It is a good idea to extend the companionway hatch garage to cover these lines as well, since stepping on exposed lines on the deck can be very dangerous.
- 24 On a racing yacht we usually have the opportunity to place the genoa tracks at an optimum location. This means a foresail sheeting angle of between 7.5° and 10°. The sheeting angle obtained on the YD-40 varies between 10° and 12°, with the greater angle in the foremost sheeting position, since the tracks are parallel to the centreline. This is not bad, because this is the sheeting position for a small headsail, used in hard weather, and by being sheeted slightly outboard it does not backwind the main.
- 25 As we can see from the deck plan the genoa tracks might be moved slightly inwards, especially in the forward end, as long as attention is paid to the coachroof. The position of the chain plates is dictated by the rig calculation. To move them inwards would mean higher rigging loads due to a narrower staying base. This in turn would require a heavier mast section and stronger standing rigging. It is an iterative process to find the proper geometry that fits the available mast sections, wire/rod and intended deck layout. By using a three-spreader rig we might have succeeded in moving the chain plates inward to the deckhouse, but then they would have interfered with the saloon accommodation. It is difficult to please everybody.
- 26 Light and ventilation are needed below, and the deck is the obvious place to let both of them in. When a skylight hatch is open it ventilates and no other ventilation is needed. Ventilation is

required, however, when the hatch is closed. The obvious place to put a ventilator is in the hatch itself. A standard 100 mm diameter clam shell ventilator is easy to fit, and is sufficient to ventilate a cabin for two people in temperate climates.

- 27** Making the companionway hatch of smoke-tinted acrylic lets the light in but privacy is maintained. It should be possible to lock the hatch in an open position, so that it does not slide back and forth in a seaway. Installing a dodger over the companionway increases the ventilation; in fact it is the main factor in the boat's ventilation system. When the wind is forward it acts as a huge exhaust, and when the wind is aft it scoops in great amounts of air.

When sailing with the companionway hatch open it is extremely important that wash boards may be secured so that they do not fall out if the boat is knocked down. It is a good idea to carry two sets of wash boards: one good-weather set of lighter construction with built-in ventilation openings, and the other a heavy-weather set up, built solidly and tight.

- 28** As a general principle each compartment in the vessel should have its own ventilation. Quarter-berths or aft cabins in particular can become hot and uncomfortable if not properly ventilated. For obvious reasons the head also needs good ventilation. On the YD-40 these requirements are taken care of by two ventilation skylights each side of the companionway.

- 29** One very common, and good, ventilator is the dorade type. It consists of a scoop-

type ventilator placed on top of a baffled water trap. By direction the scoop into or from the wind it can act either as an exhaust or an intake ventilator. By placing the ventilators high on the roof and as close to the centreline as possible, as on the YD-40, they can be left open during rather rough weather without letting in water. To prevent lines being snagged, guards should be installed around them; these also serve as handholds.

To determine the total ventilation area needed we must start with the amount of fresh air that is needed below. For each person there should be a minimum air supply of 0.3 cubic metres per minute (CMM) and preferably 0.4 CMM. Fig 15.6 shows how much ventilation a certain size of vent provides, varying with wind-speed. It is in rough weather sailing with the hatches closed that the ventilators must provide all intake and exhaust air. If we consider a six-person crew the required fresh air is  $6 \times 0.4$  CMM = 2.4 CMM. The two 100 mm dorade vents on the YD-40 provide 2.8 CMM at a windspeed of 6 m/s. The exhaust area must at least equal the intake area, and we have two 100 mm exhaust vents in the skylight hatches that take care of that.

- 30** The first and most important safety factor to consider on deck is the danger of falling overboard. A vital item is a full-length grab rail, so that you can move from the cockpit to the foredeck and have something to hold on to all the way. This rail also makes a good attachment for the safety harness. On the YD-40 this rail is bent inwards at the cockpit so that it is possible to clip on the harness before leaving the cockpit.

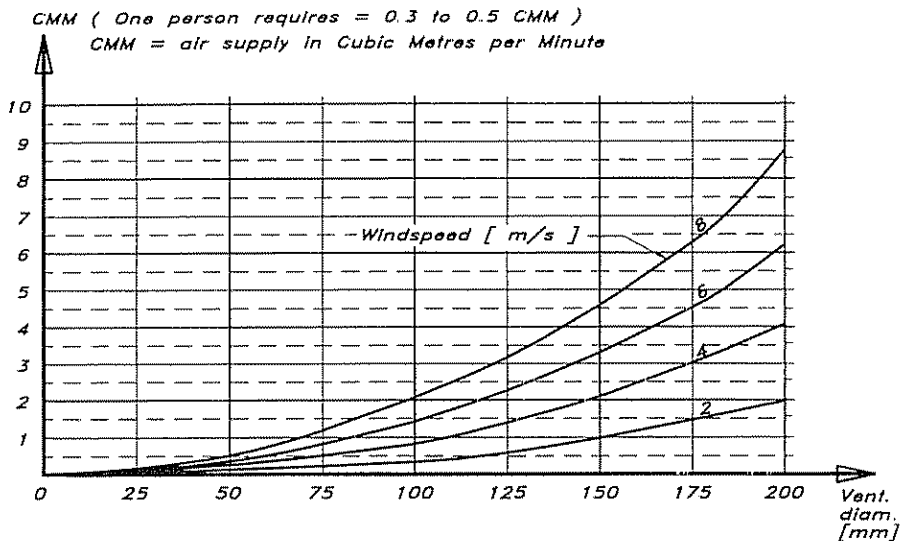


Fig 15.6 Airflow through ventilators

For boats with sail-handling systems (reefs, halyards, lifts etc) on the mast it is a good idea to incorporate a mast pulpit.

**31** The last chance of rescue before hitting the water rests with the lifelines. Their height is often a compromise between looks and function. To be safe the height should be at least 750 mm but the desire for good looks combined with efficiency has established a height of 600 mm, with double lifelines. For small boats of lengths below 8.5 m even 450 mm is accepted by the Nordic Boat Standard. As can be seen from the profile drawing the YD-40 has a lifeline gate at the maximum beam. This is very convenient when boarding the boat lying alongside a dock or when boarding from a dinghy. The demands on the stanchions supporting the lifelines are quite high. They must be throughbolted, but even so they cannot be trusted to be strong points for the safety harness because a human body thrown against the lifelines during a violent roll can reach a force of 10 000 N (one tonne).

**32** The bow is an area where the combination of heaving and pitching movements is the greatest, so here it is essential to have something to hold on to, ie the pulpit. Being a wrap-around structure it is possible to design it to be strong enough to bear the load from a falling body. A disadvantage of being wrapped around is that it is an obstacle when boarding the boat over the bow, from a dock or shore when moored stem to. By making the forward part folding down we can have both good accessibility to the foredeck when folded down, and strength and security when folded up.

**33** To have access to the forward deck stowage we must ensure that the deck hatch can be opened when the anchor is down and the chain is crossing the deck. In practice this means that the hatch must be offset or divided at the centreline. Thanks to the recessed foresail furler the deck is clear and unobstructed to aid anchor handling.

# 16

# DESIGN EVALUATION

---

A basic aim of this book has been to provide the reader with the tools required for evaluating a design, not only qualitatively, but also in a quantitative way. Detailed formulae have been provided, enabling the designer to compute the performance characteristics of the yacht. In combination with the statistical information presented it is also possible to compare a proposed design with an existing fleet of yachts.

This chapter summarizes the use of non-dimensional parameters, composed of the main data, for quick estimates of the performance properties of the design. These parameters have all been defined in earlier chapters but they are collected here, and their usefulness in evaluating the total concept is discussed.

We then describe one of the most important tools available to the professional yacht designer today, namely the Velocity Prediction Program (VPP). This computer program predicts the speed, heel, leeway, apparent wind and many other quantities for a yacht under all possible wind conditions. By systematically changing the program input, while specifying the yacht, the designer may optimize his design with respect to different qualities.

The formulae given in this book are largely based on empirical information available from tests of different kinds. The hydrodynamic part, for instance, relies very much on the extensive series of yacht tests at the Delft University of Technology, while much of the aerodynamics comes from wind-tunnel tests and full-scale experiments. These kinds of results have been statistically evaluated to obtain the useful formulae in the book. The same kind of formulae are used in the VPPs.

If more exact information is required on a specific design the traditional way has been to model-test it. This, however, is quite expensive, and is done only in connection with large projects like the America's Cup or Whitbread races, or perhaps for very expensive luxury yachts. We will describe briefly how this testing is done.

A modern way to study a new design in detail is to carry out numerical flow calculations, ie using a technique known as Computational Fluid Dynamics (CFD). This technique has become possible through the rapid development of computers over the last few decades which enables very detailed studies of the flow and resistance properties of the design to be made. Its advantage is that it is faster and cheaper than model-testing, but the technique is still under development and must, so far, be considered less reliable than the tests. We will give a brief account of the status of CFD applied to yacht hydrodynamics at the end of this chapter.

### Non-dimensional parameters

The main data relevant to a yacht's speed potential are the length, displacement, wetted area and sail area. To estimate stability the heeling arm and metacentric height are also required. For judging seaworthiness the beam, hull draft and some information on the righting moment at large heel angles are also required.

Since the sail area is a measure of the driving force, and friction is the predominant resistance component at low speeds, the sail area/wetted area,  $S_A/S_W$ , is the most important speed parameter in light airs. This value should be above 2.0, otherwise the yacht will be very slow under these conditions. High performance will be obtained for ratios above about 2.5. Note that the sail area is defined here as the sum of the main and fore triangles.

In stronger winds the situation is much more complex. Not only the resistance, but also the sail carrying capability come into play. As for the resistance, we have seen that the component due to the generation of a wave system becomes increasingly important when the speed increases. In fact, it is so important that most hulls will never be able to leave the displacement speed regime at  $F_n = 0.45$ . The parameter of interest in this respect is the length/displacement ratio,  $L_{WL}/\nabla^{1/3}$  (or the English equivalent, displacement/length ratio: see Fig 5.21). For a hull to reach the semi-planing region it has to have a ratio larger than around 5.7 (smaller than 150), which is very rare. Dinghies, of course, are well above this limit and so are the Ultra-Light Displacement Boats (ULDBs), like the Whitbread 60 footers and the America's Cup yachts. Production boats can seldom reach higher values than 5.2 (smaller than 200), and most yachts are well below this value if the real sailing displacement is used.

The vast majority of cruising and racing yachts thus operate in the displacement speed region, in which the wave resistance at a given Froude number is essentially proportional to the displacement. A parameter often used for the medium to strong wind performance is therefore the sail area/displacement ratio,  $S_A/\nabla^{2/3}$ . This parameter is also a measure of the yacht's acceleration ability. It should be above 15 for reasonably good sailing performance. Very good performance may be expected for ratios of 20–22. It should be noted that the sail area/displacement ratio says nothing about the influence of length on speed. The ratio indicates the ability to reach a certain Froude number. If this is given the speed varies as the square root of the length.

A simple and reasonably accurate way of checking the stability is to compute the Dellenbaugh angle (as described in Chapter 4). Inserting the sail area, heeling arm, displacement and metacentric height into the formula of Fig 4.21 the heel angle in a breeze of approximately 8 m/s is estimated. The figure yields the variation between tender and stiff yachts.

The seakeeping qualities of the yacht are best checked by computing the stability index (STIX), as explained in Fig 4.22. This takes into account the proportions of the hull, the sail area and the righting moment curve. For ocean sailing, STIX values above 32 are recommended, while 23 should be enough for offshore cruising and



racing. Inshore, DSF should be above 14, while values above 5 are sufficient in sheltered waters.

### The Velocity Prediction Program (VPP)

The most important module of a VPP is a routine for solving the equations for equilibrium, discussed in Chapter 5. Returning to Fig 5.1, we see that when the yacht is in equilibrium, ie moves on a straight course at constant speed, the forces and moments in each of the three main directions cancel each other. More specifically, the following relations hold:

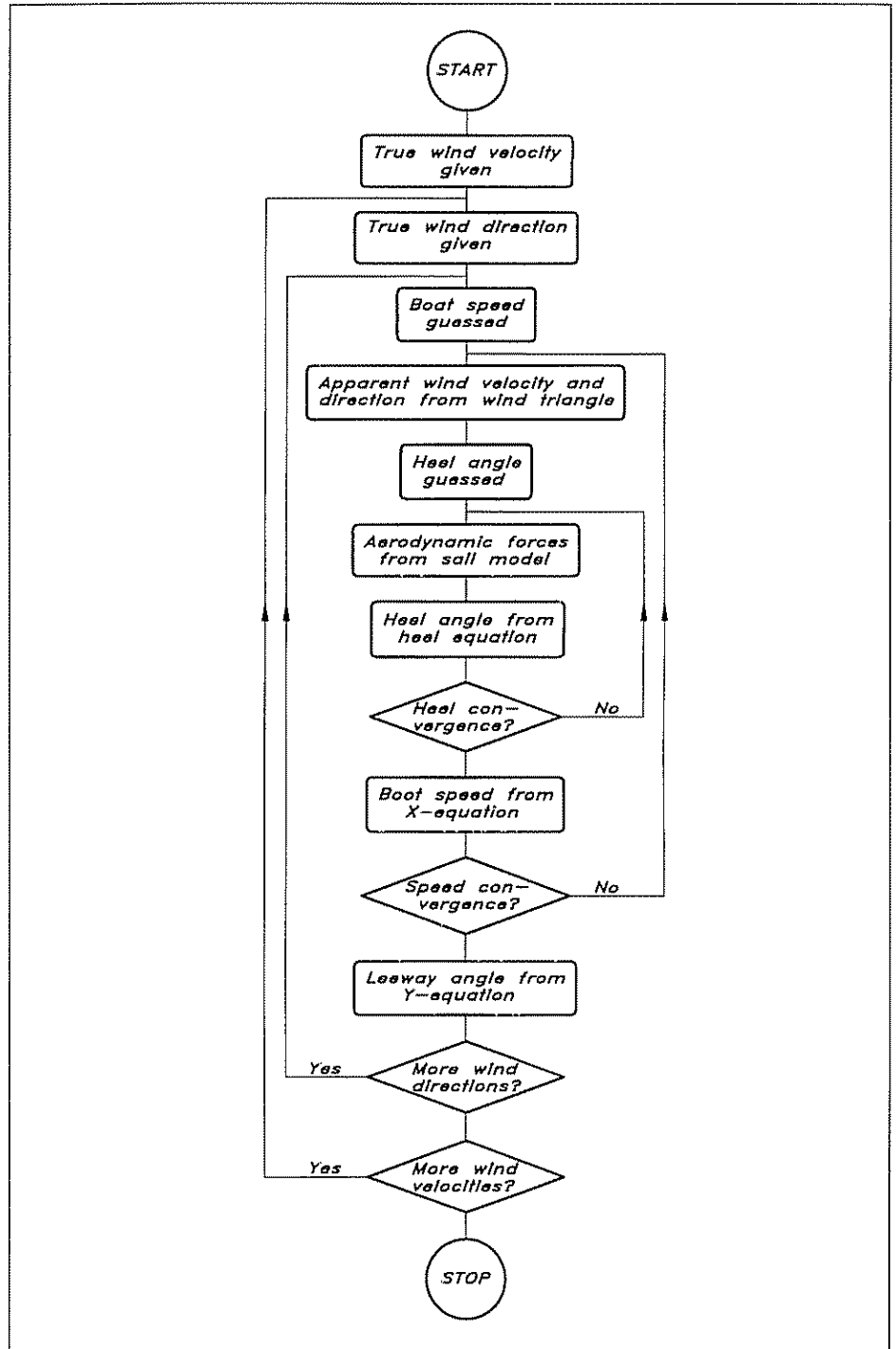
- 1 Along the direction of motion the driving force from the sail is equal to the total resistance.
- 2 At right angles to the direction of motion in the horizontal plane the side force from the sail is equal to the side force from the underwater body.
- 3 Vertically, the buoyancy force is equal to the gravity force and the vertical components of the keel and sail forces are assumed to cancel each other.
- 4 The heeling moment from the sails is equal to the righting moment from the hull.
- 5 The pitching moment from the sails is equal to the restoring moment from the hull.
- 6 The total yawing moment is zero, since the hydro and aerodynamic forces act along the same line in the horizontal plane. (See Chapter 8.)

These are the equilibrium conditions in all six degrees of freedom. In practice the vertical force balance (3) is assumed automatically satisfied, and so is the balance of the pitching moment (5). Very few programs include the yawing balance (6) in their equations, but the most advanced ones have a model for non-zero rudder angles and may therefore consider this relation.

Most VPPs thus take into account only the longitudinal and transverse forces, and the moment around the longitudinal axis, ie relations 1, 2 and 4. As for the first relation, formulae for the resistance components are required, and those most commonly used are given in Chapter 5. The aerodynamic driving force is normally computed as shown in Chapter 7. Relevant formulae for the hydrodynamic side force are given in Chapter 6, and the opposing aerodynamic force in Chapter 7. The moment equation can be formulated using the stability relations of Chapter 4, together with the heeling forces from Chapter 7. Thus the formulae required in a VPP have already been presented. In fact, they are the ones used in the VPP developed by one of the authors.

Using the formulae of Chapters 4, 5, 6 and 7 relations 1, 2 and 4 may be formulated mathematically. The method for solving them is not obvious, however. It is necessary to use an iterative procedure. Thus,

Fig 16.1 VPP flow diagram



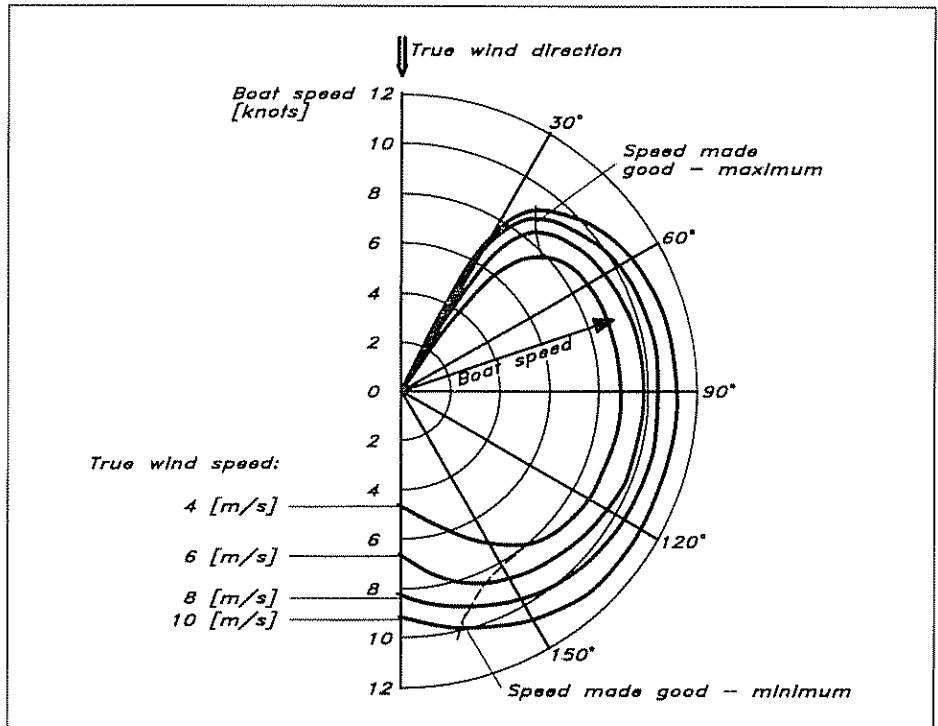
the value of some variables have to be guessed at the start. Based on these values a solution is obtained, which includes new values of the quantities guessed. These may now be used as a new start and the process is repeated. If the procedure is convergent the computed values in each iteration get closer and closer to the initial ones, ie those obtained in the previous iteration, and when they are close enough the

solution is considered converged. Some care is needed in the present case to obtain convergence, but the general sequence of operations is given in Fig 16.1.

The program moves systematically through a set of given true windspeeds and for each speed a set of given wind directions is considered. These variations correspond to the two outer loops of Fig 16.1. For a given combination of true windspeed and direction the procedure starts with a guess of the boat speed. The apparent windspeed and direction may then be obtained from the wind triangle, (see Fig 5.2). Now the heel angle has to be guessed, and this angle, together with the apparent wind, yield the aerodynamic forces from Figs 7.19, 7.21 and 7.22. The heeling moment may be computed and the heel angle found from the heel equation (4). If the computed angle is not close enough to the guessed one, the latter is updated and the process repeated with new aerodynamic forces. This is the innermost loop of the diagram. When the heel angle has converged, a speed may be found that gives a resistance which is equal to the known aerodynamic driving force. Equation 1 is thus employed. The guessed speed may now be updated, a new apparent wind computed, etc. This is the outer loop to the right in the figure. Upon convergence of the speed the leeway may be solved from the side force equation (2).

The result of the VPP calculation is often presented in the form of a polar plot (see Fig 16.2). Each curve represents a certain wind velocity, and the yacht speed may be found as the length of an arrow from the centre to the curve. The angle between the arrow and the vertical is the true wind angle. Points of special interest are the upper- and lowermost

Fig 16 2 Polar plot



ones of each curve, since these represent the best upwind and downwind performance of the yacht. The arrows to these points thus give the optimum pointing angles upwind and downwind. The latter information is particularly valuable, since it is normally very difficult for the helmsman to find the best course downwind.

A polar plot is of interest not only to the designer, who can evaluate different alternatives rapidly, but also to the racing yachtsman. Apart from the information on the best course to sail, recommendations on the best setting of the sails may be obtained, and a target speed for all possible conditions may be computed. The size of the sail area and the optimum flattening of the sails are normally computed in the program, based on the reefing and flattening functions mentioned in Chapter 7. Due to its ability to evaluate performance VPPs are also becoming useful in the handicapping rules. The International Measurement System (IMS) is based on a program very similar to the one described here, and this system has become the natural successor to the IOR rule.

The weakest feature of all VPPs is their ability to predict the performance in waves. This is because no simple methods are available for estimating the effect of waves on sailing hydro- and aerodynamics. The most promising work in this area is that of Professor Gerritsma and his co-workers at the Delft University of Technology, described briefly in Chapter 5. It is likely that general formulae for the added resistance in waves will become available soon and this will certainly improve the predictions. A problem that is still unresolved is the effect of the motions on the aerodynamics, even though interesting studies of this effect have been made at Massachusetts Institute of Technology, where most of the early research on VPPs was carried out.

### **Towing tank testing**

There are principally two different techniques for testing sailing yachts in towing tanks. The apparently most natural way is to tow the yacht at the correct centre of effort of the sails and, by means of an active rudder, let it attain its equilibrium heel and yaw angles. Each measured point in such a test represents a realistic sailing condition, so the number of test points may be kept to a minimum.

In the other technique the hull is kept fixed in all degrees of freedom, except heave and pitch, and the towing force, side force and their moments are registered for systematically varied speeds, heel angles and yaw angles. To evaluate such a test a special VPP is required. Rather than using the empirical formulae of the standard VPP, the measured forces and moments are introduced into the program. In this way the evaluation will be specialized for the hull in question and the results may be expected to be more exact. The process is not straightforward, however, since the means for interpolating the measured data to any possible speed/heel/yaw combination must be developed.

The first technique is called free-sailing and the second one semi-captive. Obviously, more test points are required in the latter, but the equipment required is less complicated and the results are independent of the stability of the model, since the heel is fixed. Different stabilities

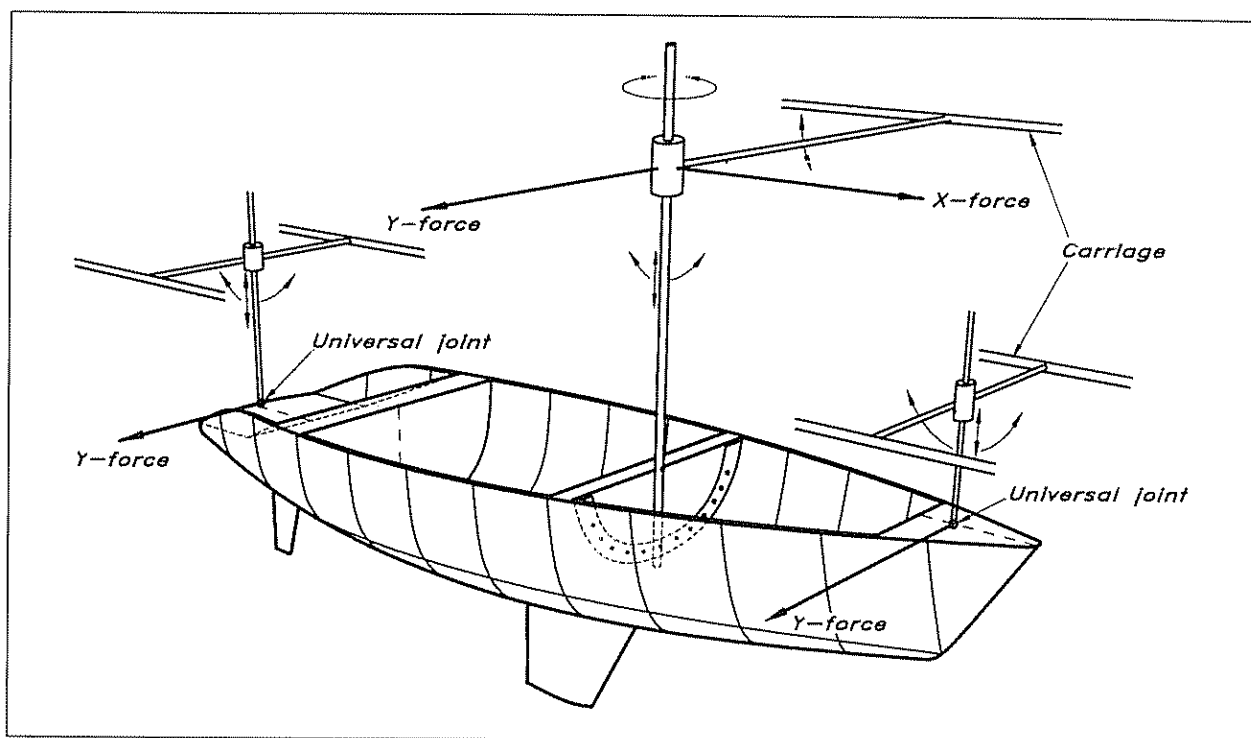


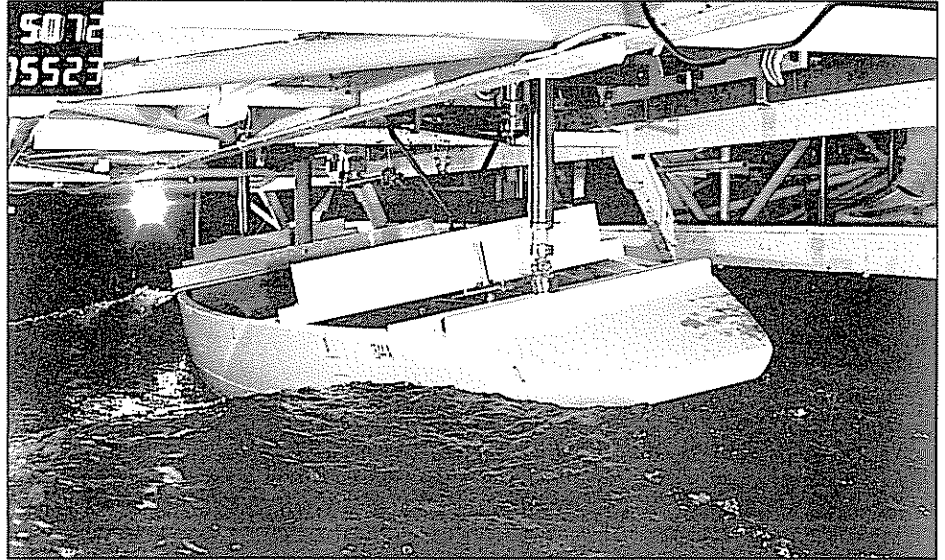
Fig 16.3 SSPA's yacht dynamometer (principle)

may be evaluated in the VPP. The free-sailing technique also calls for more expensive models, since a lead keel is required and the vertical centre of gravity has to be correct. At present, the semi-captive technique is by far the most common one in towing tanks all over the world.

In Fig 16.3 the test rig used at SSPA Maritime Consulting in Gothenburg, Sweden, is shown. The towing force is applied to a mast approximately at the height of the CE via a transverse bar from the carriage. The bar is hinged at both ends to allow the mast to move vertically. At the point of attachment to the mast the longitudinal (X) and transverse (Y) forces are measured. The mast is always kept vertical, and when the hull heels it pivots around an axis through the mast at deck level. The foot of the mast may be locked at any sideways position to fix the heel angle. To enable rapid yaw changes the mast is free to rotate at the point of attachment to the transverse bar.

Fore and aft there are posts, free to move vertically and longitudinally, but locked in the transverse direction. They are attached to the hull by universal joints, and the side force at each joint is measured. A major advantage of this equipment is that it is stiff. Exact settings of the yaw and heel angles may be made, and they do not change under load. A disadvantage is that the side force is applied horizontally, rather than at right angles to the mast, so there is a vertical component missing. This is compensated for by weights, which can be determined beforehand. Since the weights constitute only a small correction to the displacement, there is no need to know them very accurately. Fig 16.4 shows a 12 m hull under test at SSPA.

Fig 16.4 12 m hull under test at SSPA



### Computational Fluid Dynamics (CFD)

There are two main types of methods used in naval architecture. In the simplest approach, called potential flow theory, the viscosity of the water is neglected. This enables calculations of the wave resistance, as well as the induced resistance and the side force, to be carried out rapidly on a workstation or even a PC.

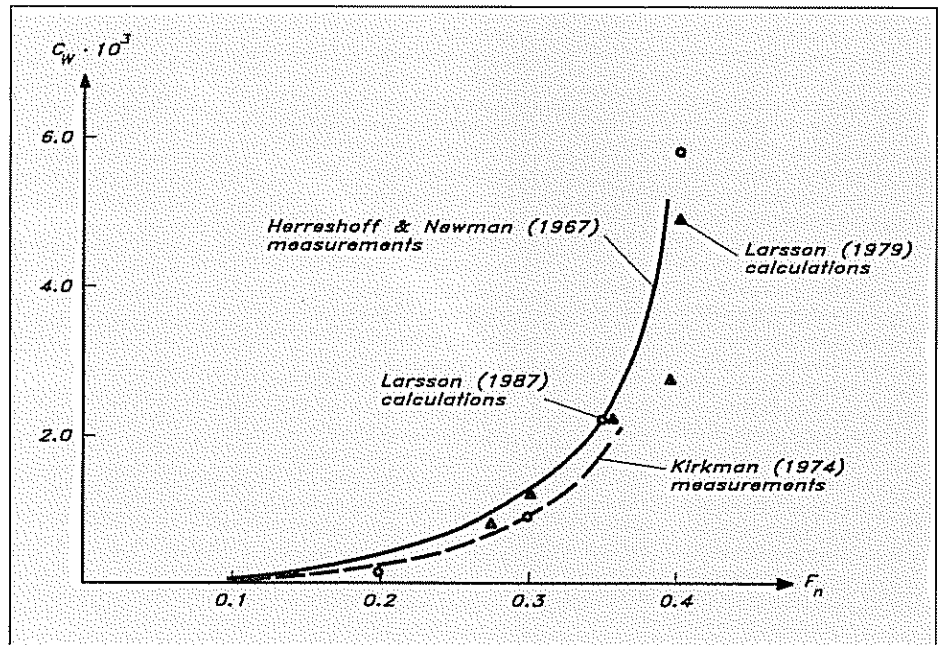
In the second type either the fundamental equations of fluid mechanics, the Navier-Stokes equations, are solved, or a simplification known as boundary layer theory is employed. As explained in Chapter 5, the boundary layer is the thin region of water surrounding the hull, where the velocity relative to the hull changes from zero on the surface to approximately the yacht speed at the outer edge. By assuming that this layer is thin relative to the hull length the Navier-Stokes equations can be much simplified, but the assumption breaks down under certain circumstances, such as in the hull/keel or keel/bulb junction. For most ships the boundary layer assumption also breaks down in the stern region, but yachts are normally sufficiently slender that the theory may be used all the way to the stern. Bustles or skegs may complicate the flow, however, particularly if separation occurs.

Referring again to Fig 5.4, the frictional and roughness resistance components may be obtained using boundary layer theory, while normally the full Navier-Stokes equations are required for the viscous pressure component. Wave and induced resistance may be found from potential flow theory, while the heel resistance is irrelevant in CFD, since the calculations are carried out for the heeled hull. The added resistance in waves, finally, may be obtained from unsteady potential flow theory. It is thus possible to compute all components of the total resistance, as well as the side force, so the output from the calculations is the same as that from the tank. To evaluate the results a VPP is required, where the CFD output is introduced in the same way as the results from the tank.

As stated above, two advantages of CFD are that it is faster and cheaper than the tank. Another advantage is that very detailed information may be obtained on the flow everywhere around the hull. Pressure distributions, streamlines and velocity vectors are normally produced by the CFD programs, and especially interesting regions may be zoomed in. To obtain all this information from the tank would be extremely expensive. On the other hand, the CFD technique is new and experience so far limited. The approximations involved also tend to make the results less accurate than those from the tank. Therefore, CFD at present is a tool to be used when optimizing a design. Absolute accuracy is then not necessary, but the method must be able to rank alternatives in the right order. Furthermore, the detailed flow information may guide the designer in the search for a better alternative.

SHIPFLOW is a CFD program developed especially for hydrodynamics problems by one of the authors and his co-workers. It includes a potential flow module, as well as both kinds of viscous flow methods: one based on boundary layer theory and one solving the Navier-Stokes equations. Although its major use is in ship design, the code has been used also for several yacht projects. Most results are confidential, but Figs 16.5–16.8 present some calculations.

Fig 16.5 Calculated and measured wave resistance – *Antiope*



In the figures the computed wave resistance, induced resistance and side force of the 5.5 m yacht *Antiope* are shown. This is a standard test case in yachting hydrodynamics and the measured data are also included in Figs 16.5–16.7 for comparison. As for the wave resistance in Fig 16.5 there are two sets of measurements, and the computed results seem to lie between the two, except at the lowest speed. The side

Fig 16 6 Calculated and measured lift coefficients on Antiope

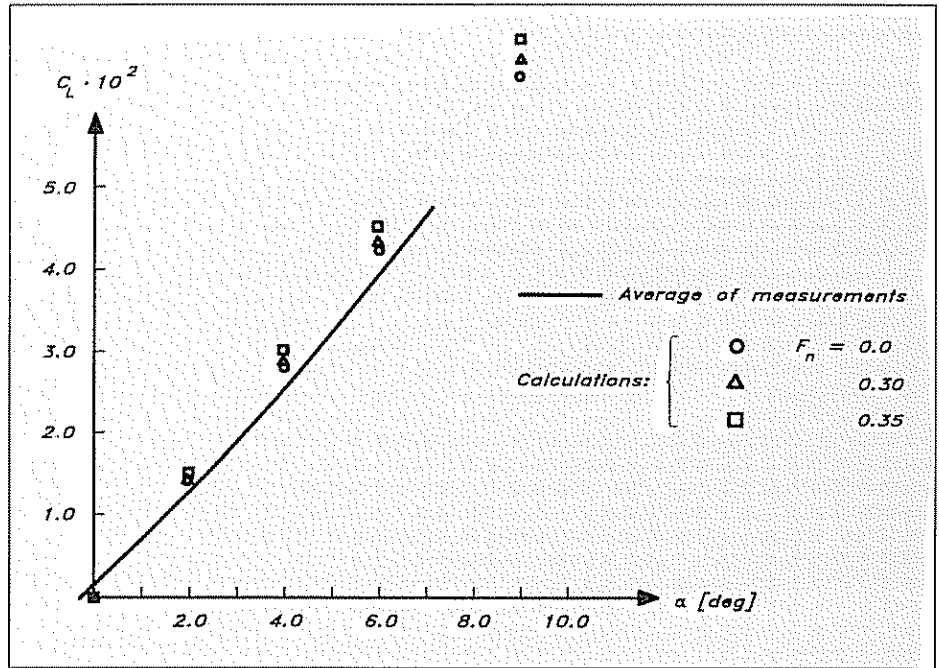
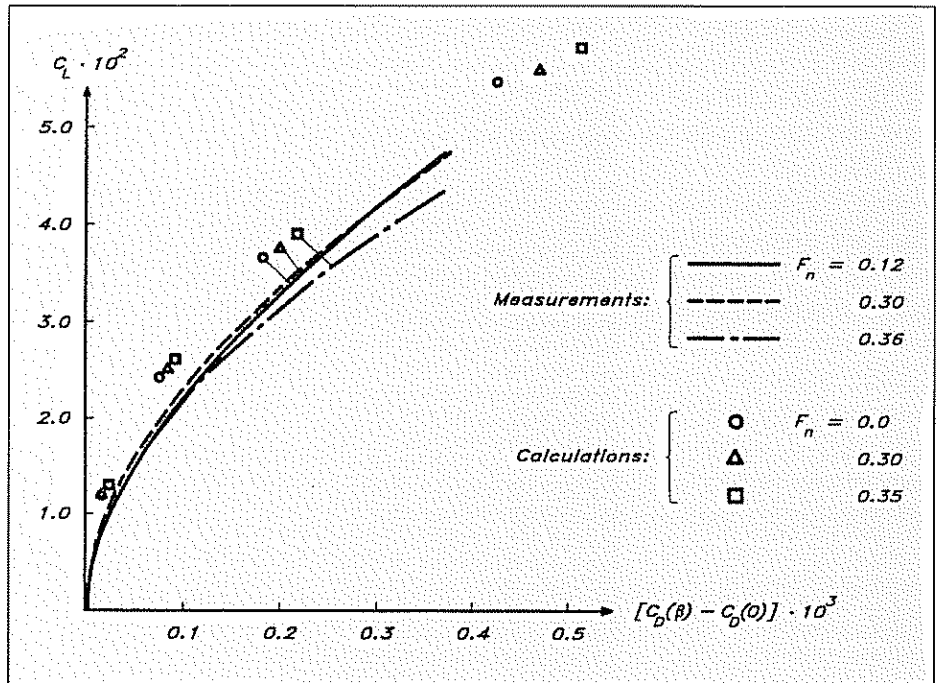


Fig 16 7 Calculated and measured lift-drag polars on Antiope



force and induced resistance of Figs 16 6 and 16 7 are somewhat overpredicted, which is to be expected, since these results are from the potential flow module. The neglected viscosity should reduce the values to some extent. There are no measured data in Fig 16 8, but it is interesting to see the computed results for a systematic variation of both speed and leeway angle. It appears that the lift increases slightly with Froude number for a given leeway.



Fig 16.8 Computed lift-drag polars for varying Froude numbers – Antiope

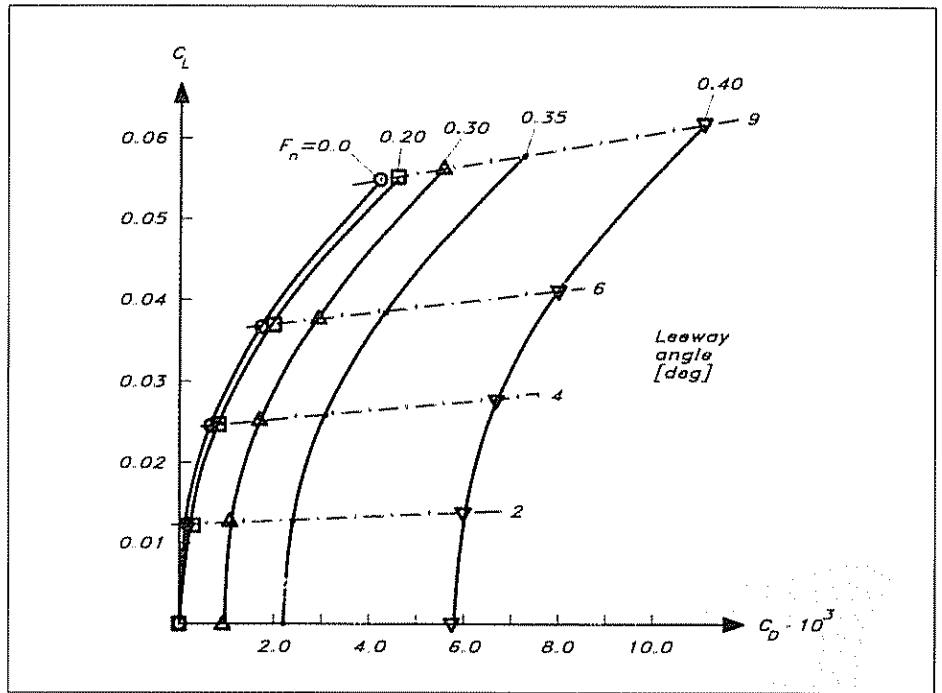


Fig 16.9 Pressure distribution on a sailing yacht computed by SHIPFLOW. (Copy of a colour photo, where each colour corresponds to a pressure interval)

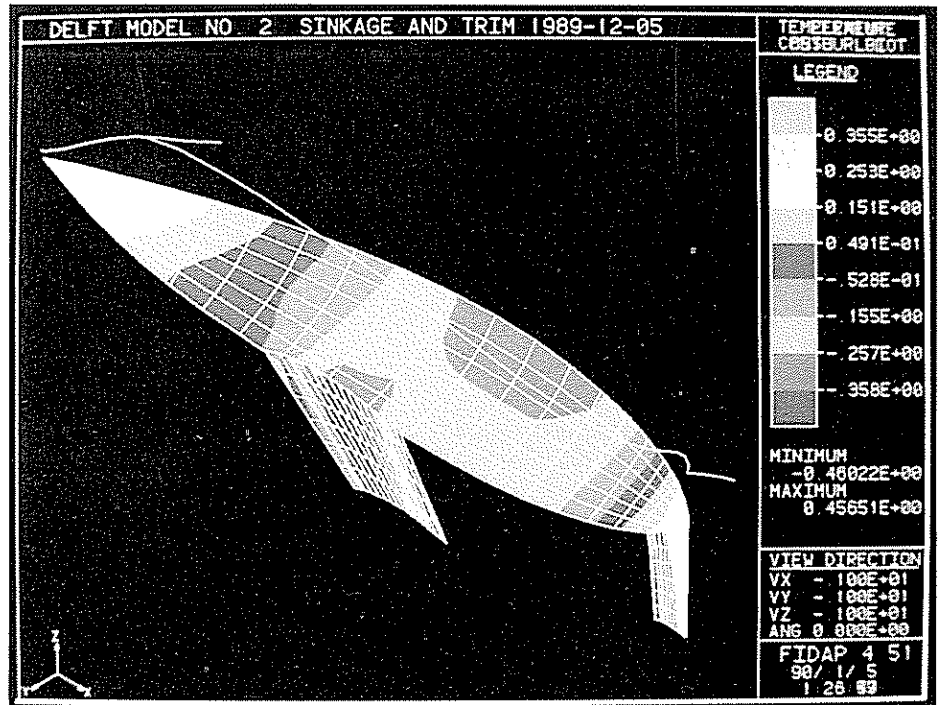


Fig 16.9 shows the pressure distribution on a yawed and heeled hull. This is the type of plot used for detailed studies of the flow. Normally it is plotted in colour, which gives a good presentation to the results, but this has not been possible in this book.

## APPENDIX 1

# Main particulars of the YD-40

Refer to List of Symbols on page x

	<i>Half-loaded displacement.</i>	<i>Light displacement.</i>
• $L_{OA}$	= 12.05 m	12.05 m
• $L_{WL}$	= 10.02 m	9.85 m
• $B_{MAX}$	= 3.71 m	3.71 m
• $B_{WL}$	= 3.17 m	3.12 m
• $T_C$	= 0.57 m	0.54 m
• $T$	= 2.07 m	2.04 m
• $\nabla_C$	= 7.63 m <sup>3</sup>	6.95 m <sup>3</sup>
• $m_C$	= 7.82 t	7.12 t
• $SW_C$	= 25.2 m <sup>2</sup>	24.4 m <sup>2</sup>
• $SW$	= 30.9 m <sup>2</sup>	30.1 m <sup>2</sup>
• $\Delta$	= 8.12 t	7.25 t
• Blst	= 3.25 t	3.25 t
• $I$	= 16.9 m	16.9 m
• $J$	= 4.3 m	4.3 m
• $P$	= 15.1 m	15.1 m
• $E$	= 4.7 m	4.7 m
• $SL$	= 16.6 m	16.6 m
• $SMW$	= 7.75 m	7.75 m
• $SAF$	= 36.3 m <sup>2</sup>	36.3 m <sup>2</sup>
• $SAM$	= 35.5 m <sup>2</sup>	35.5 m <sup>2</sup>
• $SA$	= 71.8 m <sup>2</sup>	71.8 m <sup>2</sup>
• $C_{ku}$	= 1.85 m	1.85 m
• $C_{kl}$	= 1.05 m	1.05 m
• $T_k$	= 1.50 m	1.50 m
• $C_{ru}$	= 0.68 m	0.68 m
• $C_{rd}$	= 0.32 m	0.32 m
• $T_r$	= 1.47 m	1.47 m
• $\wedge_k$	= 21°	21°
• $\wedge_r$	= 14°	14°
• LCB	= -3.5%	-3.5%
• $C_p$	= 0.56	0.56
• $SA/SW$	= 2.3	2.4
• $SA/\nabla_C^{2/3}$	= 18.5	19.7
• $L_{OA}/B$	= 3.25	3.25
• $L_{WL}/T$	= 4.84	4.83
• $L_{WL}/T_C$	= 17.6	18.2
• $L_{WL}/\nabla_C^{1/3}$	= 5.09	5.16
• $L_{OA}/L_{WL}$	= 1.20	1.22
• $F_r/L_{WL}$	= .142	.144
• $F_r/F_u$	= 1.22	1.22
• Blst Rto	= 0.40	0.45

APPENDIX 2

# WEIGHT CALCULATION

The mass of the different weights onboard the hull are given in kilograms and distances in metres.

LCG is measured from the forward end of the waterline and positive in the aft direction, denoted 'a' in the table, with negative values forward of the waterline, 'f'.

ICG is measured from the centreline with

positive values to starboard, denoted 's' in the table and negative to port, 'p'.

VCG is measured from the waterline with positive values above and negative values below the waterline.

Vessel Name: YD-40

Condition: Half loaded

<b>Group 1 Structure</b>				
<i>Item name</i>	<i>Mass</i>	<i>LCG</i>	<i>TCG</i>	<i>VCG</i>
Hull gelcoat	45 000	5.37a	0.00	0.18
Hull GRP	450 000	5.37a	0.00	0.18
Hull sandwich core	87 000	5.37a	0.00	0.18
Hull sandwich filler	50 000	5.37a	0.00	0.18
Keel strake extra	47 000	5.18a	0.00	0.29
Deck flange extra	46 000	5.69a	0.00	1.24
Deck gelcoat	16 000	6.08a	0.00	1.35
Deck GRP	100 000	6.08a	0.00	1.35
Deck sandwich core	17 000	6.08a	0.00	1.35
Deck sandwich filler	11 000	6.08a	0.00	1.35
Coamings GRP	40 000	8.20a	0.00	1.39
Roof GRP	105 000	4.80a	0.00	1.52
Roof sandwich core	12 000	4.80a	0.00	1.52
Bilge stringer	95 000	4.89a	0.00	0.16
Bottom stringer	55 000	4.90a	0.00	-0.44
Mast step	55 000	4.00a	0.00	-0.40
#1 to #4 floor	37 000	5.00a	0.00	-0.41
Engine bed	50 000	7.15a	0.00	-0.37
#1 bulkhead	15 000	0.85a	0.00	0.74
#2 bulkhead	34 000	3.00a	0.00	0.68
#3 bulkhead	15 000	6.55a	0.00	0.68
#4 bulkhead	11 000	9.75a	0.00	0.35
GRP taping	75 000	4.65a	0.00	0.37
Misc	120 000	4.90a	0.00	0.40
<b>Group total</b>	<b>1588 000</b>	<b>5.30a</b>	<b>0.00</b>	<b>0.41</b>

<b>Group 2 Forepeak</b>				
<i>Item name</i>	<i>Mass</i>	<i>LCG</i>	<i>TCG</i>	<i>VCG</i>
Sole 15 ply	5 000	0.40a	0.00	0.24
Shelf 12 ply	6 000	0.00	0.00	0.80
Furler housing	14 000	0.50f	0.00	1.00
Misc	3 000	0.15a	0.00	0.55
<b>Group total</b>	<b>28 000</b>	<b>0.16f</b>	<b>0.00</b>	<b>0.77</b>

<b>Group 3 Forward Cabin</b>				
<i>Item name</i>	<i>Mass</i>	<i>LCG</i>	<i>TCG</i>	<i>VCG</i>
Berth top 12 ply & framing	20 000	2 15a	0 70p	0 60
Berth front	5 000	2 35a	0 17s	0 05
Overhead locker	9 000	1 07a	0 33p	1 08
Hanging locker	17 000	1 38a	0 49s	0 67
Seat	8 000	1 85a	0 50s	-0 01
Chain locker	10 000	1 38a	0 00	0 00
Dresser	14 000	2 25a	0 74s	0 65
Sole 15 ply	7 000	2 49a	0 60s	-0 27
Berth cushion	13 000	2 15a	0 70p	0 63
Seat cushion	3 000	0 00	0 00	0 00
Roof liner	5 000	2 00a	0 00	1 45
Side liner	5 000	1 60a	0 00	0 90
Saloon door	6 000	3 02a	0 39s	0 65
Misc	13 000	2 02a	0 05s	0 56
<b>Group total</b>	<b>135 000</b>	<b>1 89a</b>	<b>0 03s</b>	<b>0 53</b>

<b>Group 4 Saloon</b>				
<i>Item name</i>	<i>Mass</i>	<i>LCG</i>	<i>TCG</i>	<i>VCG</i>
Port settee tops & fronts	22 000	3 80a	0 90p	0 10
Stbd settee tops & fronts	15 000	4 07a	1 05s	0 10
Bookshelves & lockers	27 000	4 35a	0 00	0 90
Chain plate knees	25 000	3 80a	0 00	0 90
Table	15 000	4 25a	0 15p	0 10
Sole 15 ply	33 000	4 20a	0 15s	-0 26
Roof liner	8 000	4 25a	0 00	1 52
Side liner	8 000	4 25a	0 00	1 00
Port cushion	13 000	3 80a	0 90p	0 10
Stbd cushion	10 000	4 07a	1 05s	0 10
Misc	15 000	3 97a	0 03s	0 26
<b>Group total</b>	<b>191 000</b>	<b>4 07a</b>	<b>0 01p</b>	<b>0 37</b>

<b>Group 5 Nav Station</b>				
<i>Item name</i>	<i>Mass</i>	<i>LCG</i>	<i>TCG</i>	<i>VCG</i>
Nav table top 12 ply	8 000	5 75a	1 25s	0 65
Nav table fronts	10 000	5 75a	0 95s	0 05
Nav table seat	7 000	5 50a	0 45s	0 10
Nav table bookshelf	7 000	6 30a	1 15s	1 05
Nav table electr panel	7 000	5 75a	1 62s	0 90
Sole	15 000	5 85a	0 55s	-0 26
Roof liner	3 000	5 70a	0 90s	1 60
Side liner	4 000	5 70a	1 78s	0 95
Cushion	3 000	6 22a	0 60s	0 12
Misc	7 000	5 80a	1 05s	0 50
<b>Group total</b>	<b>71 000</b>	<b>5 82a</b>	<b>0 98s</b>	<b>0 40</b>

<b>Group 6 Galley</b>				
<i>Item name</i>	<i>Mass</i>	<i>LCG</i>	<i>TCG</i>	<i>VCG</i>
Counter tops 12 ply	10 000	5 50a	0 91p	0 65
Counter fronts & shelves	12 000	5 60a	0 80p	0 30
Overhead locker	7 000	5 90a	1 05p	1 30
Side locker	12 000	5 22a	1 65p	0 90
Drawers	7 000	6 38a	1 33p	0 29
Icebox liner & insulation	15 000	5 30a	1 33p	0 31
Sinks	5 000	5 38a	0 70p	0 38
Taps & plumbing	10 000	5 20a	0 70p	-0 11
Stove	22 000	5 88a	1 30p	0 47
Sole 15 ply	15 000	6 01a	0 25p	-0 26
Roof lining	3 000	5 85a	1 03p	1 60
Side lining	4 000	5 85a	1 82p	1 02
Misc	10 000	5 62a	1 00p	0 39
<b>Group total</b>	<b>132 000</b>	<b>5 65a</b>	<b>1 05p</b>	<b>0 43</b>

<b>Group 7 Head</b>				
<i>Item name</i>	<i>Mass</i>	<i>LCG</i>	<i>TCG</i>	<i>VCG</i>
Wash basin countertop 12 ply	5 000	7 15a	1 32s	0 56
Wash basin counterfront & shelf	6 000	7 06a	1 04s	0 15
Side locker	7 000	7 02a	1 56s	0 97
Fwd bulkhead	12 000	6 44a	1 24s	0 65
Door	6 000	6 58a	0 54s	0 64
Side bulkhead	12 000	7 15a	0 22s	0 69
Aft bulkhead	12 000	7 75a	0 88s	0 65
WC base	5 000	7 41a	0 60s	-0 12
Wash basin & plumbing	5 000	6 88a	1 21s	0 29
WC & plumbing	15 000	7 39a	0 64s	0 08
Sole	8 000	7 01a	0 73s	-0 26
Roof liner	2 000	7 21a	1 04s	1 60
Side liner	1 000	7 09a	1 65s	0 90
Misc	10 000	7 03a	0 88s	0 45
<b>Group total</b>	<b>106 000</b>	<b>7 10a</b>	<b>0 87s</b>	<b>0 44</b>

<b>Group 8 Aft Cabin</b>				
<i>Item name</i>	<i>Mass</i>	<i>LCG</i>	<i>TCG</i>	<i>VCG</i>
Hanging locker & dresser	12 000	7 37a	1 40p	0 72
Berth top	15 000	8 81a	0 66p	0 06
Berth front	7 000	7 98a	0 55p	-0 09
Fwd bulkhead	9 000	6 63a	1 15p	0 73
Door	6 000	6 63a	0 70p	0 75
Stow bins	4 000	8 72a	0 12s	0 45
C/L bulkhead	15 000	8 81a	0 32s	0 31
Sole	10 000	7 26a	0 75p	-0 26
Roof liner	7 000	7 96a	0 70p	1 00
Side liner	5 000	8 88a	1 40p	0 73
Cushions	14 000	8 81a	0 56p	0 13
Misc	10 000	8 10a	0 59p	0 33
<b>Group total</b>	<b>114 000</b>	<b>8 07a</b>	<b>0 64p</b>	<b>0 35</b>

<b>Group 9 Cockpit Stow and Lazarette</b>				
<i>Item name</i>	<i>Mass</i>	<i>LCG</i>	<i>TCG</i>	<i>VCG</i>
Locker sole 15 ply	15 000	8 52a	0 80s	-0 15
Locker bulkhead	8 000	8 25a	0 94s	0 10
Lazarette sole 15 ply	20 000	10 09a	0 00	0 05
Lazarette bulkhead	25 000	9 98a	0 00	0 45
Lazarette hatches	8 000	9 95a	0 00	0 85
Misc	7 000	9 47a	0 28s	0 24
<b>Group total</b>	<b>83 000</b>	<b>9 53a</b>	<b>0 26s</b>	<b>0 23</b>

<b>Group 10 Installations</b>				
<i>Item name</i>	<i>Mass</i>	<i>LCG</i>	<i>TCG</i>	<i>VCG</i>
Engine	207 000	7 04a	0 00	-0 06
Prop shaft	12 000	7 80a	0 00	-0 37
Shaft sleeve	6 000	8 25a	0 00	-0 33
Shaft coupling	3 000	7 52a	0 00	-0 25
Propeller	4 000	9 42a	0 00	-0 50
P bracket	4 000	9 20a	0 00	-0 30
Fuel filter	2 000	7 40a	0 20p	0 18
Water filter	2 000	7 44a	0 25s	0 18
Water intake & piping	2 000	7 26a	0 29s	-0 34
Fuel piping	2 000	6 60a	0 28p	0 15
Shore power	12 000	7 85a	1 05p	-0 10
Batteries	100 000	8 04a	0 25p	-0 25
Wiring	75 000	7 10a	0 00	0 40
Nav stn instr	19 000	5 22a	1 25s	1 00
Cool compressor & piping	13 000	5 30a	1 30s	-0 10
Heater & ducting	10 000	8 31a	0 40s	0 30
Rubber blade	26 000	10 31a	0 00	-0 50
Rudder shaft	29 000	10 14a	0 00	-0 07
Rudder sleeve	8 000	10 09a	0 00	0 06
Rudder quadrant	3 000	10 08a	0 00	0 44
Rudder linkage	8 000	9 32a	0 00	0 40
Rudder wheel	4 000	8 78a	0 00	1 50
Steering pedestal	17 000	8 65a	0 00	1 05
Pedestal instr	4 000	8 54a	0 00	1 62
Fuel tank & piping	33 000	8 70a	0 40s	-0 15
Water tank & piping	38 000	4 72a	0 00	-0 13
Holding tank & piping	11 000	7 30a	1 40s	0 20
Misc	71 000	7 32a	0 00	0 01
<b>Group total</b>	<b>725 000</b>	<b>7 54a</b>	<b>0 05s</b>	<b>0 02</b>

<b>Group 11 Deck Equipment</b>				
<i>Item name</i>	<i>Mass</i>	<i>LCG</i>	<i>TCG</i>	<i>VCG</i>
Pulpit	15 000	0 65f	0 00	1 80
Stanchions	12 000	4 95a	0 00	1 31
Pushpit	10 000	9 70a	0 00	1 45
Lifelines	10 000	4 70a	0 00	1 65
Sheer rail	28 000	4 75a	0 00	0 00
Bollards	4 000	4 70a	0 00	1 50
Mast turn blocks	3 000	3 93a	0 00	1 65
Genoa tracks & cars	6 000	5 50a	0 00	1 30
Genoa foot blocks	2 000	8 45a	0 00	1 20
Rope clutches	3 000	6 50a	0 00	1 60
#1 winches	35 000	7 90a	0 00	1 39
#2 winches	22 000	8 90a	0 00	1 37
#3 winches	15 000	6 85a	0 00	1 80
Main tracks & blocks	4 000	8 50a	0 00	1 15
Chain plates	8 000	3 90a	0 00	1 20
Bow roller	12 000	1 00f	0 00	1 39
Bow anchor	20 000	1 03f	0 00	1 35
Anchor windlass	25 000	1 04a	0 00	1 35
Anchor chain	70 000	1 12a	0 00	0 00
Aft stay attachment	4 000	10 38a	0 00	0 85
Fwd deck hatch	4 000	0 60a	0 00	1 36
Fwd cabin deck hatch	5 000	2 50a	0 00	1 60
Saloon deck hatch	5 000	4 30a	0 00	1 60
Companionway hatch	10 000	6 50a	0 00	1 65
Companion garage	16 000	5 80a	0 00	1 65
Deckhouse windows	7 000	4 66a	0 00	1 37
Deck ventilators	3 000	5 15a	0 00	1 65
Misc	40 000	4 04a	0 00	1 06
<b>Group total</b>	<b>398 000</b>	<b>3 98a</b>	<b>0 00</b>	<b>1 06</b>

<b>Group 12 Rig &amp; Sails</b>				
<i>Item name</i>	<i>Mass</i>	<i>LCG</i>	<i>TCG</i>	<i>VCG</i>
Mast & spreaders	124 000	4 15a	0 00	8 92
Boom	23 000	6 42a	0 00	2 70
Stays 7 or 8 mm	12 000	5 68a	0 00	9 40
Shrouds 8 mm	10 000	4 15a	0 00	12 00
Shrouds 8 mm	17 000	4 10a	0 00	4 60
Runn rigging	12 000	4 06a	0 00	9 40
Spinn pole (on deck)	13 000	2 15a	1 10p	1 45
Rigg screws & toggles	9 000	3 87a	0 00	0 00
Jib furler	18 000	1 08a	0 00	8 62
Winches & stoppers on mast	7 000	3 90a	0 00	2 16
Genoa hoisted	15 000	3 50a	0 00	6 80
Main hoisted	15 000	5 80a	0 00	7 80
Rodkick & blocks & lines	6 000	4 85a	0 00	1 70
Mast top fittings	3 000	4 20a	0 00	18 60
Misc	35 000	4 16a	0 05p	7 28
<b>Group total</b>	<b>319 000</b>	<b>4 16a</b>	<b>0 05p</b>	<b>7 28</b>

**Group 13 Ballast**

<i>Item name</i>	<i>Mass</i>	<i>LCG</i>	<i>TCG</i>	<i>VCG</i>
Keel	3250 00	4.96a	0.00	-1.27
<b>Group total</b>	<b>3250 00</b>	<b>4.96a</b>	<b>0.00</b>	<b>-1.27</b>

**Group 14 Payload**

<i>Item name</i>	<i>Mass</i>	<i>LCG</i>	<i>TCG</i>	<i>VCG</i>
Helmsman	80 000	9.10a	0.00	1.75
2 crew	160 000	6.00a	0.00	0.70
Forepeak gear	60 000	0.60a	0.00	0.80
Fwd cabin gear	65 000	1.80a	0.60p	0.10
Saloon gear	35 000	4.00a	0.50p	0.08
Nav stn gear	40 000	5.95a	1.35s	0.75
Galley gear	85 000	6.20a	1.40p	0.50
Head gear	15 000	7.20a	1.30s	0.05
Aft cabin gear	25 000	7.20a	1.30p	-0.10
Cockpit lkr gear	80 000	8.90a	0.90s	0.35
Lazarette gear	50 000	10.00a	0.00	0.45
1/2 water	175 000	4.72a	0.00	-0.15
1/2 fuel	50 000	8.70a	0.40s	-0.13
1/2 holding tank	60 000	7.30a	1.40s	0.20
<b>Group total</b>	<b>980 000</b>	<b>6.07a</b>	<b>0.04s</b>	<b>0.42</b>
<b>TOTAL ALL GROUPS</b>	<b>8120.000</b>	<b>5.36a</b>	<b>0.00s</b>	<b>0.00</b>



APPENDIX 3

# STIX CALCULATION

BOAT		YD 40			
<b>Intended Cat. A-B-C-D</b>		<b>A</b>	<b>A</b>		<b>= PASS !</b>
LH (m)	12.05	VC (m3)	1.25		
LWL (m)	9.96	FM (m)	1.15		
BH (m)	3.71	HD (m)	1.30		
BWL (m)	3.15	Min Hd (m)	0.71	<b>PASS !</b>	
Tc (m)	0.56	T (m)	2.05		
<b>CREW LIMIT (#pers)</b>	<b>8</b>	<b>(To be on Builder's Plate !)</b>			
GZ-90 (m)	0.56				
ASP (m2)	72.00				
HCE (m)	7.28				
HLP (-m)	0.82				
Angle of downflooding (A <sub>DH</sub> )	120.00		Min A <sub>DH</sub>	<b>PASS !</b>	
Angle of vanishing stab (A <sub>VS</sub> )	129.00		Min A <sub>VS</sub>	<b>PASS !</b>	
Area under GZ-curve to A <sub>DH</sub> (m deg)	69.80				
Area under GZ-curve to A <sub>VS</sub> (m deg)	70.10				
<b>LIGHT SHIP CONDITION</b>		<b>Mass(kg)</b>	<b>X (m)</b>	<b>Z (m)</b>	
<b>LIGHT SHIP MASS (MLcc) (kg)</b>	<b>7250.00</b>	<b>5.20</b>	<b>37700</b>	<b>-0.10</b>	<b>-725</b>
<b>MINIMUM SAILING CONDITION</b>					
LIGHT SHIP (kg)	7250	5.20	37700	-0.10	-725
CREW (min.kg)	150	8.70	1305	1.40	210
LIFERAFT (kg)	39	9.00	351	0.90	35
BASIC EQUIPMENT (kg)	356	6.50	2314	0.60	214
<b>MIN. SAILING MASS (Mmsc)</b>	<b>7795</b>	<b>5.35</b>	<b>41670</b>	<b>-0.03</b>	<b>-266</b>
<b>MAXIMUM LOAD CONDITION</b>		<b>Mass(kg)</b>	<b>X (m)</b>	<b>Z (m)</b>	
LCC (kg)	7250	5.20	37700	-0.10	-725
CREW (#pers)	450	7.00	3150	0.70	315
CREW (min kg)	150	8.70	1305	1.40	210
LIFERAFT (kg)	39	9.00	351	0.90	35
BASIC EQUIPMENT (kg)	356	6.50	2314	0.60	214
STORES (kg)	285	5.00	1425	0.00	0
WATER (kg)	175	4.00	700	-0.15	-26
WATER (kg)	175	4.00	700	-0.15	-26
WATER (kg)	0	1.00	0	1.00	0
FUEL (kg)	100	7.00	700	-0.15	-15
HOLD (kg)	120	5.00	600	0.20	24
PERSONAL GEAR (kg)	200	6.00	1200	0.20	40
<b>LOADED DISPL.MASS (MLdc)</b>	<b>9300</b>	<b>5.39</b>	<b>50145</b>	<b>0.00</b>	<b>45</b>
LOADED VOLUME (m3)	9.16				
MAXIMUM LOAD (ML) (kg)	2050				
<b>Max Load ex. FUEL,WATER (kg)</b>	<b>1600</b>	<b>(To be on Builder's Plate !)</b>			
<b>STIX 12217-2 DIS (Jan-99)</b>					
FDS	1.27			LBS	10.66
FIR	1.07				
FKR	1.22			FR	4.16
FDL	0.99			FL	0.99
FBD	1.03			FB	1.99
FWM	1.00				
PDF	1.25				
<b>STIX</b>	<b>46</b>				

# REFERENCES

---

The literature on sailing theory and yacht design is extensive. For a comprehensive list of references, see the annual reviews by Larsson and Milgram below. The following list contains essentially the references referred to in the book.

- Abbott, I H, von Doenhoff, A E 1949. *Theory of Wing Sections*. New York: McGraw-Hill.
- ABS 1991. *Guide for Building and Classing Motor Pleasure Yachts*. American Bureau of Shipping, New York.
- ABS 1994. *Guide for Building and Classing Offshore Racing Yachts*. American Bureau of Shipping, New York.
- ABS 1997. *Guide for Building and Classing High Speed Craft*. American Bureau of Shipping, New York.
- AIAA Symposium on the Aero/Hydraulics of Sailing. Held annually since 1969. Western Periodicals Company, North Hollywood.
- Allen, H G 1969. *Analysis and Design of Structural Sandwich Panels*. Oxford: Pergamon Press.
- Cannell, D, Leather, J 1976. *The Design of Sailing Yachts*. London: Adlard Coles Nautical.
- Caprino, G, Teti, R 1989. *Sandwich Structures Handbook II*. Prato – Pelf SpA, Padua.
- Chesapeake Sailing Yacht Symposium. Held bi-annually since 1974. Society of Naval Architects and Marine Engineers, New York.
- Claughton, A R, Wellicome, J F, Sheno, R A 1998. *Sailing Yacht Design – Theory*. Harlow: Addison Wesley Longman.
- Claughton, A R, Wellicome, J F, Sheno, R A 1998. *Sailing Yacht Design – Practise*. Harlow: Addison Wesley Longman.
- DIAB 1991. *Divinycell Technical Manual H-Grade*. Divinycell International AB, Laholm.
- Dyne, G, Widmark, C 1998. *On the Efficiency of Water Jet Systems*. International Conference on Water Jet Propulsion – Latest Developments, Amsterdam 22–23 October.
- Gentry, A E 1971. *The Aerodynamics of Sail Interaction*. 2nd AIAA Symposium on the Aero/Hydraulics of Sailing.
- Gerritsma, J, Keuning, J A 1985. 'Model Experiments with Yacht Keels'. *Seahorse Magazine*, March/April 1985. pp 23–26.
- Gerritsma, J, Keuning, J A, Onnink, R 1992. *Sailing Yacht Performance in Calm Water and in Waves*. 12th Symposium on Developments of Interest to Yacht Architecture, Amsterdam.
- Gerritsma, J, Onnink, R, Versluis, A 1981. 'Geometry, Resistance and Stability of the Delft Systematic Yacht Series'. *International Shipbuilding Progress* 28(328): 276–97.
- Gutelle, P 1984. *The Design of Sailing Yachts*. London: Nautical Books.
- Hammitt, A G 1975. *Technical Yacht Design*. London: Adlard Coles Nautical.
- Hazen, G S 1980. *A Model of Sail Aerodynamics for Diverse Rig Types*. New England Sailing Yacht Symposium.
- Henry, R G, Miller R T 1963. *Sailing Yacht Design – An Appreciation of a Fine Art*. Transactions Society of Naval Architects and Marine Engineers, New York.
- Herreshoff, L E 1974. *The Common Sense of Yacht Design*. New York: Caravan-Maritime Books.
- Hildebrand, M, Holm, G 1991. *Strength Parameters of Boat Laminates* (in Finnish). Technical Research Centre of Finland, Research Notes No 1289, Helsinki.
- Hildebrand, M 1991. *On the Bending and Transverse Shearing Behaviour of Curved Sandwich Panels*. Technical Research Centre of Finland, Research Notes No 1249, Helsinki.
- Honey, R A 1983. *Fibre Reinforcement Plastics in Boatbuilding*. University of Auckland, Department of Mechanical Engineering, Auckland.

- Hunyadi, B, Hedlund, P 1983. *Strength Comparison of Two Constructional Concepts for a 25 Metres Racing Yacht* (in Swedish) The Royal Institute of Technology (KTH), Department of Lightweight Structures, Publication No. 83-16, Stockholm
- ISO/TC 188/WG 18 ISO/CD 12215-5 17. *Small Craft-Hull Construction/Scantlings – Part 5: Design Pressures, Allowable Stresses, Scantling Determination*. International Standards Organization – SIS/SMS, Stockholm
- Joint Committee on Safety from Capsizing 1985. Final Report of the Directors United States Yacht Racing Union, Newport and Society of Naval Architects and Marine Engineers, New York.
- Joubert, P N 1982 'Strength of Bottom Plating of Yachts'. *Journal of Ship Research*, Vol. 26, No 1, March 1982, pp 45-49.
- Kay, H F 1971 *The Science of Yachts, Wind and Water* London: G T Foulis
- Kinney, F S 1973 *Skene's Elements of Yacht Design*. New York: Dodd, Mead & Co.
- Lackenby, H 1978 *ITTC Dictionary of Ship Hydrodynamics* Marine Technology Monographs Royal Institute of Naval Architects, London
- Larsson, L 1990. 'Scientific Methods in Yacht Design'. *Annual Review of Fluid Mechanics*, Vol 22, pp 349-85
- Lewis, E V, ed 1988 *Principles of Naval Architecture* Society of Naval Architects and Marine Engineers, New York.
- Lloyd's 1978-1993 *Rules and Regulations for the Classification of Yachts and Small Craft*. Lloyd's Register, Yacht and Small Craft Department, Southampton.
- Marchaj, C A 1979 *Aero-Hydrodynamics of Sailing* London: Adlard Coles Nautical.
- Marchaj, C A 1982 *Sailing Theory and Practice*. London: Adlard Coles Nautical
- Marchaj, C A 1986 *Seaworthiness, The Forgotten Factor*. London: Adlard Coles Nautical.
- Marshall, R 1980 *Race to Win* New York and London: W W Norton & Company
- Marshall, R 1990. *Designed to Cruise*. New York and London: W W Norton & Company
- Marshall, R 1979. *Designed to Win*. London: Adlard Coles Nautical
- Milgram, J H 1971 *Sail Force Coefficients for Systematic Rig Variations*. Technical Report No. 10, Society of Naval Architects and Marine Engineers, New York.
- Milgram, J H 1998 'Fluid Mechanics for Sailing Vessel Design' *Annual Review of Fluid Mechanics*, Vol. 30, pp. 613-653.
- Miller, R T, Kirkman, K L 1990. *Sailing Yacht Design – A New Appreciation of a Fine Art* Annual Meeting, Society of Naval Architects and Marine Engineers, New York.
- NBS 1990 *Nordic Boat Standard* Det Norske Veritas Classification A/S, Oslo.
- Nomoto, K, Tatano, H 1979 *Balance of Helm Sailing Yachts – a Ship Hydrodynamics Approach on the Problem* 6th Symposium on Development of Interest to Yacht Architecture, Amsterdam, pp 64-89
- Obara, C J, van Dam, C P 1987 *Keel Design for Low Viscous Drag*. 8th Chesapeake Sailing Yacht Symposium
- Olofsson, N 1996 *Force and Flow Characteristics of a Partially Submerged Propeller* PhD Thesis, Chalmers University of Technology, Department of Naval Architecture and Ocean Engineering, Gothenburg
- Phillips-Birt, D 1966 *Sailing Yacht Design* London: Adlard Coles Nautical.
- Poor, C L 1986. *The International Measurement System* Offshore Racing Council, London
- Rousmaniere, J eds 1987. *Desirable and Undesirable Characteristics of Offshore Yachts* New York and London: W W Norton & Company.
- Sponberg, E W 1986. 'Carbon Fibre Sailboat Hulls: How to Optimize the Use of an Expensive Material' *Marine Technology*, Vol. 23, No. 2, April 1986, pp 165-174
- Street, D M 1973 and 1978. *The Ocean Sailing Yacht, Vol 1 & 2* New York and London: W W Norton & Company
- Symposium on Developments of Interest to Yacht Architecture Held bi-annually since 1969 HISWA, Amsterdam
- VTT 1997. *VTT-NBS Extended Rule* Technical Research Centre of Finland, Technical Report VTT VALB172, Helsinki

# INDEX

---

- ABS (American Bureau of Shipping)  
rules 8, 228
- accommodation 14, 298–305
- aerodynamic force 56, 57, 156
- aerodynamics, model for 147–53
- alternative propulsion devices  
199–200
- aluminium, properties for  
extrusions 224
- America's Cup 111
- angle of attack 124–5
- apparent wind 153
- appendage resistance 190
- Archimedes Principle 32–3, 183
- area reduction factor 282–4
- areas, calculation of 30
- aspect ratio, keel 100–5
- aspect ratio, sail 135–8
- assessment of seaworthiness 53
- attitude 43
- balance 155–63  
rudder 162–3
- ballast ratio 94
- Barkla, H M 11
- base length factor 53
- basic laminate 274–5
- beam 16
- beam displacement factor 53
- beam/draft ratio 82
- beam of waterline 17
- Bergstrom & Ranzen 138
- bilge factor 32
- biplane theory 111, 157
- block coefficient 18, 19
- boat type, choice of 10
- body plan 20, 21
- boom 218
- boom requirements 220
- bottom, design loads for 275
- boundary layer 60, 62, 63, 118, 144
- breaking strength of wire/rod rigging  
214
- bulb (keel tip shape) 106–7
- buoyancy, centre of, 19, 34, 37, 81
- Burrill diagram 179
- buttocks 197–8
- calculation of areas 30–2
- camber 139–42
- canard wings 111–113
- cant angle 109
- cardboard method to find centre of  
gravity 36–7, 44
- cavitation 179–80, 199–200
- centre of buoyancy 19, 34, 37, 81
- centre of effort (CE) 157–61
- centre of gravity 19, 35–6  
methods of finding 36
- centre of lateral resistance (CLR)  
157–60
- centreboard keel 115
- centrifugal force 50
- checklist of design considerations 15
- chopped strand mat (CSM) 251–4
- chord 99–100
- coefficient  
block 18  
prismatic 18  
sail 149, 151
- Computational Fluid Dynamics  
(CFD) 311, 318–21
- Computer Aided Design (CAD) 7–9,  
27–9
- Connell, D 2
- Contessa 32 46
- conversion factors xvi
- Copenhagen ship curves 25
- corrosion in wire/rod, resistance to  
215
- cost 13–14
- curvature of lines 27–8
- damping 46–9
- Davidson Laboratory, New York  
107, 146
- deadrise 187–8
- deck layout 305–310
- deep-V hull 193
- definitions 16–22,  
ISO hull 272–4
- deformations, studies of hull 237–9
- Delft parent models 73–4
- Delft keels 115
- Dellenbaugh angle 52, 83, 312
- depth 17
- design  
checklist 15  
evaluation 311–21  
loads 280  
loads for bottom 275–79  
methodology 5–9
- parameters 12–11  
pressures (motor craft and fast  
sailing craft) 276, 277, 279  
spiral 5–6  
waterline (DWL) 38–9
- dimensioning forces for shrouds 210
- dimensions 11–13  
definitions 17
- displacement 17, 43, 32–4, 76–8
- displacement length factor 53
- downflooding factor 55
- draft 17, 92
- drag 120, 121, 126–7, 146–50  
induced 149  
viscous 149, 150
- driving force 135, 136
- ducks 24
- dynamic stability 53, 197–8
- dynamometer 317
- effort, centre of (CE) 157–61
- e-glass 250
- elliptical force distribution 99, 103
- elliptical keels 103
- elongation of wire/rod 215
- engine 164–82
- equilibrium trim angle 192
- exotic laminates 257–60
- fairing fillet between keel and hull  
110
- Fastnet Race 1979 45, 5
- fatigue in FRP 256
- fatigue, rigging 215
- fibre reinforced plastic (FRP) 250
- fillet at junction of keel and hull 110
- flattening factor 150
- flare 19, 20
- flotation, centre of 40
- flow  
around hull 60–1  
around sails 132  
around a wing 96–7
- forces and momentum 56–8  
grounding 241  
keel 239  
rig 229  
rudder 243  
shrouds 208–212  
stays 212–14
- fractional mast top 218

- freeboard 19  
   height 94  
 frequency of encounter 47, 84  
 frictional resistance 61–4  
 Froude number 71–2  
 FRP 250  
   fatigue in 256
- Gentry, A E 134  
 Gerritsma, Professor J 73, 88, 159  
 ghost transom 20  
 glass reinforcement 251  
 global loads 228  
 gravity, centre of 16  
   methods of finding 36  
 Grimalkin 45, 46, 51  
 grounding, forces from 240  
 gyradius 85–90
- Hadler procedure 191–2  
 half breadth plan 20, 21  
 Hazen's model 147, 148  
 heel resistance 83  
 heel, effect of 155–7  
 heeled waterline 43  
 Heller and Jasper slamming factors 235  
 high speed hydrodynamics 183–204  
 high speed rescue vessel 200–4  
 hogging 49  
 hull  
   buttocks 197–8  
   construction 226–49  
   definitions, ISO 272–4  
   design 26, 27, 56–95  
   forces on a turning 197  
   form parameters 74  
   frictional resistance calculation 189  
   geometry 16–29  
   girder requirements 228, 233  
   statistics 90  
 humps and hollows, wave 72  
 hydrodynamic  
   lift components 184  
   loads 234–7  
   high speed 183–204  
 hydrostatic loads 234  
 hydrostatics and stability 30–55
- inertia  
   calculation of mass moment 84, 85  
   transverse moment  
     hull 39–40  
     mast 218  
 International Towing Tank Conference (ITTC) 4  
 inverse taper 110–11  
 inversion recovery factor 53  
 ISO hull definitions 272–4  
 ISO Standard 269–74
- junction angle 109  
 keel and rudder design 96–131  
 keel  
   bolts and chainplates 289, 290  
   elliptical 103  
   forces 239  
   loadings 240  
   planform, definition of 99–100  
   tandem 113  
   tip shape 105–7  
   winged 107–110  
 Kelvin wave system 69  
 Kirkman, K L 153  
 knockdown recovery factor 53
- laminar flow 60, 61–3  
 laminate  
   basic 274–5  
   exotic 257–60  
 layout 297–310  
 lead 161  
   definition 161  
   between perpendiculars 16  
 length  
   waterline 16  
   waterline/canoe body 92  
   waterline/draft 92  
   overall 16  
   overall/length of waterline 94  
   overall/max beam 91  
 length/beam and beam/draft ratio 82–3  
 length/displacement ratio 78, 93  
 length/weight ratio 11  
 lift 122, 147–53  
   coefficient 149, 320  
 lifting line theory 100–3  
 loaded areas 247–8  
 loadings 245–9  
   from shrouds 229  
   from the keel 240  
 loads  
   bottom 275–79  
   decks and bulkheads 280  
   internals 280  
   topsides 280  
 longitudinal impact distribution factor 280–2
- Maple leaf 194  
 MARIN 171, 172, 193  
 Marchaj, C A 137  
 mast  
   dimensioning 205–14  
   disturbances (airflow) 143–6  
   holes in 222  
   interference (airflow) 142–3  
   longitudinal 219  
   tests 145, 146  
   through deck 208  
   top, fractional 218, 220
- transverse 217  
   master curves 7, 27  
   masthead rig 138–9  
   materials 250–68  
   maximum area section 17  
   metacentre  
     transverse 40–1  
     longitudinal 42  
   midship section 17  
 Milgram, Professor 136, 137  
 Miller, R T 153  
 minimum sailing condition 55  
 modulus  
   elasticity 215, 227, 232–5  
   section for boom 218  
   section for mast top 220  
 moment 189, 191  
   inertia calculations 38, 39
- NACA sections 116–18, 128  
 Navier-Stokes equations 318  
 Netherlands Ship Model Basin 171  
 Nomoto, Professor 159  
 Nordic Boat Standard (NBS) 205
- orbital motion 50  
 osmosis 256
- panel calculation 283, 284–6  
 particle motion 51  
 perpendiculars 16  
 pitching 84, 86  
 planform concepts (keels) 113  
 planform design 107  
 planform, sail 134–9  
 planimeter 25  
 planing 183–5  
 planing hull, forces on 190  
 polar plot 315  
 pressure and velocity distribution  
   beneath a planing flat plate  
   principle 184  
 pressure, bottom 236–7, 275–79  
 pressure distribution 64–6, 119, 321  
 prismatic coefficient 17, 18, 78–80  
 profile plan 20  
 propeller 164–82  
   blade area 179–80  
   characteristics 169–71, 177–8  
   design 171–74  
   pitch 169  
   performance 174–8  
   resistance 181  
   surface piercing 200  
   tangential component 169  
   torque 170  
   4-bladed 193  
 proportions versus size calculation (Barkla) 11–12  
 propulsion devices, alternative 199–200

- rake, mast 222, 223  
 rated length 16  
 rescue vessel, high speed 200–4  
 residuary resistance 74–5, 165  
 resistance 165–8  
   appendage 190  
   components 58–60  
   to corrosion in wire/rod 215  
 Reynolds number 63, 129  
 rig  
   breaking strength 214  
   calculation 222–5  
   construction 205–25  
   dimensions and properties 224  
   double spreader 212  
   streamlining 146  
   transverse loads on shrouds 209  
   types 207  
   weight 216  
   wind resistance 216  
   YD-40 222–5  
 rigging loads 229–232  
 rigging, wire and rod comparison 214–16  
 righting moment 42, 206  
   influence of waves on 49–51  
 rolling 46–9  
 roughness 66–9  
 rudder  
   balance 162–3  
   configuration 112  
   loadings 244  
   forces from 240  
   forward 111–113  
  
 sagging 49  
 sail and rig design 132–54  
 sail camber 139–42  
 sail statistics 153–4  
 sails, air flow around 132–4  
 sandwich construction 260–8, 290–3  
 Sativsky's formula 185–7, 188  
 scale factor 20  
 scantling determination 269–96  
 Scheel keel 114  
 seakeeping 84, 88–90  
 seakindliness 89  
 section  
   characteristics 118–28  
   design 128–9  
   modulus for mast top 220  
   shape 124–5  
 sectional area calculation 34  
 separation 61  
 sheer line 19, 28  
 SHIPFLOW 63, 319–21  
 shroud load 209, 211–12  
 shrouds and stays  
   drag 147  
   dimensioning forces for 210  
   transverse loads on 209  
   wind resistance of 216  
 Simpson's Rule 31–2, 39–40  
 single skin panel calculation 283  
 skin friction 63–4  
 slamming factor 235  
 space requirements 297  
 spade rudder stock 287–90  
 speed  
   length ratio 73  
   parameters 312  
   spray rails 193–5  
   spreaders 207, 220–2  
   spreaders, number of 207  
   SSPA Maritime Consulting test rig stability 312  
   index 54  
   statistics 52  
   transverse and longitudinal 40–6  
 stall, types of 122  
 standing rigging, breaking strength 214–5  
 stays, forces on 212–14  
 stepped bottoms 193  
 stress in hull materials 227  
 stiffener calculation 286–7  
 stiffness, transverse and longitudinal mast 218  
 STIX computation 53, 54, 55, 329  
 streamlining rig 146  
 structural mechanics 227  
 Sunshine 85–6, 87  
 symbols x–xv  
  
 tandem keels 113  
 tangential component, propeller 169  
 tank testing 316–18  
 taper ratios 110–111  
 tools 22–5  
 towing tank testing 316–18  
 transom flaps 193, 196  
 transverse  
   load distribution 237, 238  
   loads on rig 209  
   mast dimensioning 217  
   metacentre (M) 40–1  
 trapezoidal keel 114  
 trim tabs 123, 124  
 Troost propeller series 171–3  
 tumble home 19  
 turning hull, forces on 197  
 types of rig 207–8  
  
 van de Stadt & Partners model 74  
 Velocity Prediction Program (VPP) 6, 86, 311, 313–16  
  
 velocity triangle 58  
 ventilators, airflow through 310  
 venturi effect 134  
 vertical position of the centre of buoyancy (VCB) 37–8  
 V-shape hull 194  
 vibration 127–8  
 viscous pressure resistance 64–6  
 viscous resistance 60–1  
 volume displacement calculation 35  
 vortices 59  
  
 water jets 203  
 water plane area 38–40  
 waterline length 92  
 wave motion 84  
 wave resistance 69–73, 167–8, 319  
 wave systems 70–3  
 weather helm 162  
 weight calculation 323–28  
 weight of rig 216  
 wet laminates 255, 256  
 wetted surface calculation 32–3  
 Whitbread Study of Deformations 237–9  
 winch size calculation 308  
 wind moment factor 55  
 wind resistance of shrouds and stays 216  
 windage, estimation of 166  
 wing, flow around 96–7  
 wing theory 100–3  
 winged keels 107–110  
 winglet keel 114  
 wire and rod rigging comparison 214–16  
 work plan 26  
  
 YD-40 (Yacht Design 40 footer) 3–4  
   checklist 15  
   genoa 139  
   keel area 130–1  
   lines drawing 20–22  
   main particulars 322  
   mast 143  
   masthead rig 138  
   maximum speed 68  
   optimum propeller 174–8, 180  
   perspective view 29  
   preliminary layout 14  
   propeller resistance 181–2  
   resistance curve 58  
   righting moment 222  
   rig 222–5  
   sail area/wetted surface ratio 154  
   scantlings 293–7  
   specification 322  
   stiffening system 249